

Oil & Natural Gas Technology

DOE Award No.: DE-FC26-05NT15549

Final Report

Produced Water Management and Beneficial Use

Primary Authors: Terry Brown
Carol D. Frost
Thomas D. Hayes
Leo A. Heath
Drew W. Johnson
David A. Lopez
Demian Saffer
Michael A. Urynowicz
John Wheaton
Mark D. Zoback

Project Managers: Lee L. Landkamer
Geoffrey Thyne

Editorial Assistance: Jenny J. Reinke
Normandy Roden
George William Sherk

Report Prepared By: Colorado Energy Research Institute
Dag Nummedal, Director
Colorado School of Mines
1500 Illinois St.
Golden, CO. 80401

Report Prepared For: United States Department of Energy
National Energy Technology Laboratory

Report Period: 29 April 2005 to 31 October 2007

Report Date: January 2009



Office of Fossil Energy



DISCLAIMER

This report was prepared as an account of work sponsored by an agency of the United States Government. Neither the United States Government nor any agency thereof, nor any of their employees, makes any warranty, express or implied, or assumes any legal liability or responsibility for the accuracy, completeness, or usefulness of any information, apparatus, product, or process disclosed, or represents that its use would not infringe privately owned rights. Reference herein to any specific commercial product, process, or service by trade name, trademark, manufacturer, or otherwise does not necessarily constitute or imply its endorsement, recommendation, or favoring by the United States Government or any agency thereof. The views and opinions of authors expressed herein do not necessarily state or reflect those of the United States Government or any agency thereof.

ABSTRACT

Large quantities of water are associated with the production of coalbed methane (CBM) in the Powder River Basin (PRB) of Wyoming. The chemistry of co-produced water often makes it unsuitable for subsequent uses such as irrigated agriculture. However, co-produced waters have substantial potential for a variety of beneficial uses. Achieving this potential requires the development of appropriate water management strategies.

There are several unique characteristics of co-produced water that make development of such management strategies a challenge. The production of CBM water follows an inverse pattern compared to traditional wells. CBM wells need to maintain low reservoir pressures to promote gas production. This need renders the reinjection of co-produced waters counterproductive. The unique water chemistry of co-produced water can reduce soil permeability, making surface disposal difficult.

Unlike traditional petroleum operations where co-produced water is an undesirable by-product, co-produced water in the PRB often is potable, making it a highly valued resource in arid western states. This research project developed and evaluated a number of water management options potentially available to CBM operators. These options, which focus on cost-effective and environmentally-sound practices, fall into five topic areas: Minimization of Produced Water, Surface Disposal, Beneficial Use, Disposal by Injection and Water Treatment.

The research project was managed by the Colorado Energy Research Institute (CERI) at the Colorado School of Mines (CSM) and involved personnel located at CERI, CSM, Stanford University, Pennsylvania State University, the University of Wyoming, the Argonne National Laboratory, the Gas Technology Institute, the Montana Bureau of Mining and Geology and PVES Inc., a private firm.

TABLE OF CONTENTS

Disclaimer	i
Abstract	ii
Executive Summary	xii
Minimization of Produced Water	xiii
Surface Disposal	xv
Beneficial Use	xx
Disposal by Injection	xxii
Water Treatment	xxiii
Preface	xxvi

Topic Area: Minimization of Produced Water

Chapter 1	<i>Membrane-Enhanced Coalbed Methane to Minimize Produced Water</i>	1-1
	Authors: Drew W. Johnson and Theodore A. Cramer	
	Executive summary	1-1
	Introduction	1-2
	Approach	1-3
	Membrane Modules and Configurations	1-3
	Model Development	1-5
	Model verification, apparatus and procedures	1-7
	Results and discussions	1-12
	Liquid Film Coefficients	1-12
	Model Verification	1-13
	Model Predictions	1-16
	Conclusions	1-18
	Recommendations for future research	1-18
	Nomenclature	1-19
	Dimensionless Parameters	1-20
	Greek Letters	1-20
	Subscripts	1-20
	References	1-20
Chapter 2	<i>Coal Pore Structure and Enhanced Recovery of Coalbed Methane using CO₂: Coal Characterization and the Effects of Sorption/Desorption within Intact Cores</i>	2-1
	Authors: Richard Pribyl and Michael Urynowicz	
	Executive Summary	2-1
	Introduction	2-1
	Coal-bed Natural Gas	2-1
	Gas Storage Capacity of Coal	2-2
	The Powder River Basin	2-2
	Produced Water	2-3
	Enhanced Coal-bed Natural Gas Production	2-3
	Exchange ratios	2-3

Field tests	2-3
Scope of Research	2-4
Objectives	2-4
Sample Origins	2-4
Sample Properties	2-5
Proximate and ultimate analyses	2-5
Hydraulic conductivity	2-6
Density	2-6
Porosity	2-6
Microporosity Experiment	2-7
Introduction	2-7
Coal porosity	2-7
Conventional techniques for quantifying porosity	2-8
Water adsorption isotherms	2-8
Experimental	2-8
Procedure	2-8
Adsorption isotherms	2-10
Results and discussion	2-11
Comparison of samples	2-14
Time limitations	2-15
Conclusions and recommendations	2-15
Transport Properties of Intact Cores	2-16
Introduction	2-16
Transport in coal seams	2-16
Dual porosity and permeability	2-16
Factors affecting coal permeability	2-16
Research on saturated intact coal	2-17
Experimental	2-17
Development of experimental apparatus	2-17
Procedure	2-18
Sorption isotherms	2-21
Results and Discussion	2-21
Coal permeabilities for nitrogen, carbon dioxide, and methane	2-21
Sorption isotherms	2-26
Limitations	2-27
Conclusions and Recommendations	2-27
Summary and Conclusions	2-28
Summary of Experimental Results	2-28
Conclusion	2-28
Recommendations for Future Research	2-29
Modeling (model matching to collected data)	2-29
Continuation of microporosity research	2-29
Porosity characterization by conventional methods	2-30
Quantify swelling (implementation of strain gauges)	2-30
X-ray image analysis	2-30

	References	2-31
Chapter 3	<i>Hydraulic Fracture Growth from Water Enhancement Tests in the Powder River Basin, Wyoming: Implications for Coalbed Methane Water Management</i>	3-1
	Authors: Mark D. Zoback, Hannah E. Ross and L. B. Colmenares	
	Executive Summary	3-1
	Goals and Objectives	3-1
	Introduction	3-2
	Calculating the Least Principal Stress and Hydraulic Fracture Orientation from Water-Enhancement Tests	3-5
	Water-Enhancement Tests from Cordilleran Compliance Services	3-6
	Relationship Between Water Production and Orientation of Hydraulic Fractures	3-7
	Relationship Between Water Production and Normal Faults	3-8
	Implications for CBM Water Disposal and CBM Wellbore Completion Practices in the Powder River Basin	3-12
	Recommendations for Future Research	3-13
	References	3-13

Topic Area: Surface Disposal

Chapter 4	<i>Surface Disposal and Minimization of Produced Water: Isotopic Ratios as Tracers of CBM Water</i>	4-1
	Authors: Carol D. Frost, Catherine Campbell and E.L. Brinck	
	Executive Summary	4-1
	Introduction	4-1
	Experimental Methods	4-2
	Results, Discussions and Conclusions	4-4
	Subtask 3.1	4-4
	Results	4-7
	Strontium isotope results	4-7
	Water quality results	4-11
	Discussion	4-13
	Geochemical evolution	4-13
	Binary mixing	4-14
	Mobilization of salts	4-16
	Conclusions: Subtask 3.1	4-18
	Subtask 3.2	4-19
	Introduction	4-19
	Samples	4-19
	Results	4-26
	Water quality results	4-26
	Strontium isotope results	4-29
	Discussion	4-30

	Trends in water quality and Sr isotopic composition in the Gillette-Schoonover area	4-30
	Comparison of Gillette-Schoonover area to the northeastern part of the Powder River Basin: Possible influence of faulting	4-32
	Geographic and temporal variability due to depositional systems and sediment provenance	4-33
	Correlation of Sr isotopic compositions to water enhancement and resulting fracture patterns	4-34
	Conclusions: Subtask 3.2	4-35
	Subtask 3.3	4-36
	Introduction	4-36
	Samples	4-37
	Results	4-37
	Discussion	4-38
	Conclusions: Subtask 3.3	4-41
	Recommendations for Future Research	4-42
	References	4-42
Chapter 5	<i>Regional Siting Concerns for Coalbed Methane Infiltration Ponds in the Powder River Basin</i>	5-1
	Authors: John Wheaton, Elizabeth Brinck Meredith, Shawn Kuzara and Jay Hanson	5-1
	Executive Summary	5-1
	Introduction	5-3
	Anticipated Water Quality Changes	5-4
	Methods	5-5
	Coal Creek Study Site	5-6
	Background	5-6
	Water Levels	5-7
	Water Budget	5-7
	Ground Water Model	5-11
	Saturated Paste Extract Analyses	5-13
	Water Quality	5-17
	Results of laboratory analyses	5-17
	Water quality modeling	5-18
	Beaver Creek Study Site	5-19
	Results	5-21
	Upper Well Site	5-21
	Middle Well Site	5-21
	Lower Well Site	5-22
	Projected Trends	5-22
	Leonardite Tests	5-23
	Remote Sensing Evaluation	5-27
	Conclusions	5-28
	Recommendations for Future Research	5-29

	Acknowledgements	5-30
	References	5-30
	Appendix 5.A: Monitoring Site Information	5-32
	Appendix 5.B: Water Budget for the Coal Creek CBM Infiltration Pond near Ucross, Wyoming.	5-34
	Appendix 5.C-1: Water Quality for the Coal Creek Sites	5-36
	Appendix 5.C-2: Water Quality for the Beaver Creek Sites	5-48
	Appendix 5.D: Coal Creek Water Quality Modeling	5-60
	Appendix 5.E: Column Leach Trials	5-63
	Plate 5.1: Geologic Cross-sections of the Coal Creek Site	5-71
	Plate 5.2: Specific Conductivity, Water Depth, SAR and Major Ion Chemistry Changes with Time And Distance Down-Gradient at the Coal Creek Research Site.	5-72
	Plate 5.3: Specific Conductivity, Water Depth, SAR and Major Ion Chemistry Changes with Time And Distance Down-Gradient at the Coal Creek Research Site.	5-73
	Plate 5.4: Specific Conductivity, Water Depth, SAR and Major Ion Changes with Time And Distance Downstream at the Beaver Creek Research Site.	5-74
Chapter 6	<i>Controls on the Fate of CBM Co-Produced Waters and Impacts to Shallow Aquifer Levels</i>	6-1
	Authors: Demian Saffer and Kurt McCoy	
	Executive Summary	6-1
	Specific Tasks	6-1
	Introduction	6-1
	Overview of Project and Results	6-1
	Experimental Methods	6-3
	SubTask 1: Evaluate and Quantify Controls on Fate of Discharged Waters. Generate Both Time-Averaged and Time Series of Water Budgets.	6-3
	Subtask 2: Formulate and Calibrate Models of Groundwater Flow and Surface Runoff at the Local (Km) Scale Using Field Observations.	6-5
	Subtask 3: Evaluate Proxies for Predicting the Fate of CBM Waters, including Rainfall-Runoff Analyses and Infiltration Tests.	6-6
	Infiltration tests	6-6
	Rainfall runoff models	6-7
	Results and Discussions	6-8
	SubTask 1: Evaluate and Quantify Controls on Fate of Discharged Waters. Generate Both Time-Averaged and Time Series of Water Budgets.	6-8

Subtask 2: Formulate and Calibrate Models of Groundwater Flow and Surface Runoff at the Local (Km) Scale Using Field Observations.	6-12
Subtask 3: Evaluate Proxies for Predicting the Fate of CBM Waters, including Rainfall-Runoff Analyses and Infiltration Tests.	6-14
Rainfall runoff models	6-14
Infiltration tests	6-16
Conclusions	6-18
References	6-19

Topic Area: Beneficial Use

Chapter 7	<i>Agricultural Application of Untreated CMB Waters</i>	7-1
	Author: Terry Brown	7-1
	Executive Summary	7-1
	Introduction	7-2
	Subtask 1: Application of Untreated Powder River Basin CBM Water to Soil	7-3
	Subtask 1.1: Collect Baseline Soil Chemistry, Soil Hydraulic Properties and Produced Water Chemistry at the WJ Irrigation Site	7-3
	Initial site evaluation	7-3
	Experimental design and baseline development	7-5
	Subtask 1.2: Installation and Operation of Lysimeter and Temperature, Soil Water and EC Probes	7-5
	Subtask 1.3: Treatment Application and Irrigation at the WJ Irrigation Study Site	7-8
	Application of amendments	7-8
	Installation of two pivot irrigation systems	7-9
	Subtask 1.4. Monitoring Results	7-10
	Results	7-10
	Conclusions: Subtask 1	7-15
	Subtask 2: Modeling-Irrigation Modeling	7-16
	Soil Water Salinity Model: Pre-irrigation Conditions	7-16
	Soil Water Salinity Model: Post-irrigation Conditions	7-24
	Results	7-25
	Subtask 3: Soil Fertility Evaluations	7-25
	Plant Nutritional Issues Related to Elemental Toxicity	7-25
	Conclusions of this study	7-31
	Plant Nutritional Issues Relating to Soil Buffer Capacity Losses	7-31
	Conclusions of this study	7-32
	Greenhouse Study: Alfalfa Production Using CBM Co-Produced Water and Soil Amendments.	7-34
	Conclusions of this study	7-36

Subtask 4: Use of Amendments to Reclaim Sites Impacted by CBM Co-Produced Water	7-38
Conclusions of This Study	7-39
Recommendations for Future Research	7-40
Management of Coal-Bed Natural Gas Produced Water	7-40
Appendix 7.1: Results of Pre-irrigation Soil Sample Analysis from the WJ Irrigation Site	7-45
Appendix 7.2: Baseline-Soil Chemistry Data for the Research Plots	7-47
Appendix 7.3: Soil Chemistry Data Collected from Treated Subplots Located at the Eight Research Plots after One Season of Irrigation.	7-54
Appendix 7.4: Soil Chemistry Data Collected from Treated Subplots Located at the Eight Research Plots after Two Seasons of Irrigation.	7-61
Appendix 7.5: ANOVA Evaluations for Data Collected from the WJ Amendment Plots after One and Two Years of Irrigation.	7-70
Appendix 7.6: Greenhouse Study - ANOVA Evaluations for Plant Production Data Collected from the North and South Pivot Area Fertility Plots	7-72

Topic Area: Disposal by Injection

Chapter 8	<i>Sub-Hydrostatic Pore Pressure in Aquifers of the Powder River Basin, Wyoming, and Implications for Disposal of Coalbed Methane Water Through Injection</i>	8-1
	Authors: Mark D. Zoback and Hannah E. Ross	
	Executive Summary	8-1
	Goals and Objectives	8-1
	Introduction	8-2
	Powder River Basin Hydrogeology	8-4
	Powder River Basin Geology	8-4
	Water Level Data	8-6
	Calculating Pore Pressure	8-6
	Pore Pressure Analysis: Present Day Sand and Coal Pore Pressure Magnitudes in the Powder River Basin	8-7
	Groundwater System Before CBM Production in the Powder River Basin	8-8
	Initial Pore Pressure Magnitudes from the BLM Database	8-10
	Hydraulic Communication Between Sands and Coalbeds in the Powder River Basin	8-11
	Wyoming	8-11
	Montana	8-15
	Implications for Injection of CBM Water into Sand Aquifers	8-16
	Modeling CBM Water Injection into Sand Aquifers	8-16

	Characteristics of the Confining Unit between Coalbeds and Aquifers in the PRB	8-25
	Conclusions	8-27
	Recommendations for Future Research	8-28
	References	8-28
Chapter 9	<i>Coalbed Methane Produced Water Disposal by Injection</i>	9-1
	Authors: David A. Lopez and Leo A. Heath	
	Executive Summary	9-1
	Introduction	9-3
	Goals	9-3
	Objectives	9-3
	Project Location	9-3
	Background	9-4
	Water Issues	9-4
	Geology of the Montana Portion of the Powder River Basin	9-5
	Structural Geology	9-5
	Stratigraphy	9-6
	Depositional Settings of the Ft. Union Formation	9-6
	Geologic Assessment of Injection Targets	9-7
	Engineering Discussion and Injection Design	9-12
	Down-hole Water-Gas Separation	9-12
	Water Injection Expected Performance	9-12
	Rate and pressure performance	9-12
	Expected Reservoir Conditions	9-13
	Rate and Pressure Performance Correlations	9-15
	Water Volume Expected Performance	9-16
	Injection System Design	9-16
	Wellbore Design	9-16
	Injection Water Handling Design	9-17
	Injection Pump Design	9-19
	Summary and Conclusions	9-20
	Recommendations for Future Research	9-21
	References	9-21
	Appendix 9.A: Powder River Basin Typical CBM Water Disposal Well Sketch	9-24
	Appendix 9.B: Technical Discussion	9-25

Topic Area: Water Treatment

Chapter 10	<i>Electrodialysis Process Development for the Demineralization of Coalbed Methane Produced Water</i>	10-1
	Authors: Thomas Hayes and Paula Moon	
	Executive Summary	10-1
	Introduction	10-2
	Approach	10-8

	Experimental Methods	10-9
	Produced Water Characterization	10-9
	Laboratory Prototype Treatment Train	10-11
	Laboratory Scale Electrodialysis Prototype Testing	10-12
	Part I: Comparison of CMX versus CM10-S membranes	10-12
	Part II: Back-diffusion studies	10-13
	Part III: Post-demineralization treatment	10-14
	Part IV: Membrane stability evaluation	10-14
	Results	10-15
	Produced Water Characterization	10-15
	Laboratory Scale Electrodialysis Prototype Testing	10-17
	Part I: Comparison of CMX versus CM10-S membranes	10-17
	Part II: Back-diffusion studies	10-18
	Part III: Post-demineralization treatment	10-19
	Part IV: Membrane stability evaluation	10-20
	Discussion	10-22
	Part I: Comparison of CMX versus CM10-S Membranes	10-22
	Part II: Back-Diffusion Studies	10-23
	Part III: Post-Demineralization Treatment	10-24
	Part IV: Membrane Stability Evaluation	10-24
	Economic Analysis	10-25
	Conclusions	10-30
	Recommendations for Future Research	10-31
	Acknowledgments	10-31
	References	10-32
	Publications to Date	10-33
	Conferences	10-33
Chapter 11	<i>Standardized Testing of Coalbed Methane Water-Treatment Systems</i>	11-1
	Authors: John Wheaton and Shawn Kuzara	
	Executive Summary	11-1
	Purpose	11-2
	Background	11-2
	Description of Field Laboratory	11-3
	Laboratory and trailer	11-3
	Flow measuring instruments	11-5
	Field chemistry instrumentation	11-11
	Plans for Deployment	11-12
	References	11-16
	Appendix 11.A: Ground-Water Information Center Water Quality Reports	11-17

Appendix A: Statement of Tasks Performed

EXECUTIVE SUMMARY

Large quantities of water are associated with the production of coalbed methane (CBM) in the Powder River Basin (PRB) of Wyoming. The chemistry of co-produced water often makes it unsuitable for subsequent uses such as irrigated agriculture. However, co-produced waters have substantial potential for a variety of beneficial uses.

Achieving this potential requires the development of appropriate water management strategies. There are several unique characteristics of co-produced water that make development of such management strategies a challenge. The production of CBM water follows an inverse pattern compared to traditional wells. CBM wells need to maintain low reservoir pressures to promote gas production. This need renders the reinjection of co-produced waters counterproductive. The unique water chemistry of co-produced water can reduce soil permeability, making surface disposal difficult. Unlike traditional petroleum operations where co-produced water is an undesirable by-product, co-produced water in the PRB often is potable, making it a highly valued resource in arid western states.

This research project developed and evaluated a number of water management options potentially available to CBM operators. These options, which focused on cost-effective and environmentally sound practices, are reflected in the ten tasks undertaken by the research project:

- Task 1 Membrane-Enhanced CBM to Minimize Produced Water
- Task 2 Electrodialysis Treatment of Produced Water
- Task 3 Isotopic Evaluation of CBM-Produced Waters
- Task 4 Reservoir Geomechanics and the Effectiveness of Wellbore Completion Methods in Coalbed Methane Wells in the Powder River Basin
- Task 5 Evaluating the Use of Produced Water Generated During Coal Bed Methane Extraction for Land Application in the Powder River Basin
- Task 6 Regional Siting Criteria for CBM Infiltration Ponds
- Task 7 Controls on the Fate of CBM Co-Produced Waters and Impacts to Shallow Aquifer Groundwater Quality
- Task 8 Field Laboratory and Standard Method of Testing Performance of Water Quality Treatment Systems
- Task 9 Water Treatment by Injection

Task 10 Regulations/Technology Consistency.

This task was undertaken by the Argonne National Laboratory. It involved regulatory analysis and an initial briefing of technology developers regarding regulatory requirements as well as updates regarding changes in those requirements. Argonne also briefed federal and state agencies having relevant regulatory authority regarding technology developments. Argonne's efforts under Task 10 have not been included in the present report.

The subtasks associated with each of the tasks are detailed in General Appendix A: Statement of Tasks Performed.

The research project, which was managed by the Colorado Energy Research Institute (CERI) at the Colorado School of Mines (CSM), involved personnel located at CERI, CSM, Stanford University, Pennsylvania State University, the University of Wyoming, the Argonne National Laboratory, the Gas Technology Institute, the Montana Bureau of Mining and Geology and PVES Inc., a private water management consulting firm. The results of the research project fall into five topic areas:

- Minimization of Produced Water (Tasks 1 and 4);
- Surface Disposal (Tasks 3, 6 and 7);
- Beneficial Use (Task 5);
- Disposal by Injection (Task 9); and,
- Water Treatment (Tasks 2 and 8).

MINIMIZATION OF PRODUCED WATER

This topic area included Tasks 1 and 4. The objective of Task 1 was to minimize CBM water production using gas permeable membranes to recover methane. Wellbore completion practices were evaluated in Task 4 to determine if there are ways to produce less CBM water and still achieve adequate depressurization for gas production.

The objectives of Task 1 were addressed by Johnson and Cramer (Chapter 1: *Membrane-Enhanced Coalbed Methane to Minimize Produced Water*) and by Pribyl and Urynowicz (Chapter 2: *Coal Pore Structure and Enhanced Recovery of Coalbed Methane using CO₂: Coal Characterization and the Effects of Sorption/Desorption within Intact Cores*). The objectives of Task 4 were addressed by Zoback, Ross and Colmenares (Chapter 3: *Hydraulic Fracture Growth from Water Enhancement Tests in the Powder River Basin, Wyoming: Implications for Coalbed Methane Water Management*).

Johnson and Cramer investigated the feasibility of membrane degassing technology for the recovery of methane from coal seams without dewatering the aquifer. One proposed approach involved placing membrane fibers directly within the saturated coal seam and supplying a CO₂ sweep gas to the membrane lumens providing simultaneous CO₂ sequestration and CH₄ recovery.

A mass balance study conducted on an infinitesimal fiber element provided the basis for development of a system of differential equations from which the gas composition within the fiber lumen could be determined as a function of fiber length. The limits of effective recovery were determined by normalizing model predictions to an average conventional well producing $1.56 \times 10^4 \text{ m}^3 \text{ day}^{-1} \text{ CH}_4$ (550,000 scf/d). Using this approach, it was estimated that $4.11 \times 10^5 \text{ m}^3$ of CO_2 would be sequestered daily, while the produced gas composition would be 95% CH_4 , 4.4% CO_2 , and 0.6% H_2O vapor. A total of 16.8% of the dissolved CH_4 in the formation water would be removed during a single pass. Increasing groundwater flow velocity resulted in a decrease in required membrane surface area for equivalent recovery with diminishing effect. Increasing pore pressure resulted in fewer required membranes for equivalent recovery.

For a hypothetical coal seam 36.6 m thick located at an average depth of 107 m with a corresponding average pore pressure of $1.05 \times 10^3 \text{ kPa}$ and a lateral groundwater velocity of 100 cm/day, Johnson and Cramer determined that 290,000 m^2 of membrane surface area would be required (corresponding to a hypothetical “curtain” of fibers 7.73 km wide spanning the height of the coal seam assuming a single layer of fibers spaced one diameter apart). A coal seam at 457 m with a pore pressure of 4.48 MPa would require only 7728 m^2 of membrane surface area (0.206 km wide curtain), 97% fewer fibers as compared to the hypothetical coal seam located at 107 m. These calculations were made assuming the presence of methane in the coalbed water at the saturation limit with no free gas phase present.

Johnson and Cramer noted that additional research is needed to improve model predictions and to determine how the model represents the physical coal-seam environment. Despite the fact that mobile, free gas pockets may also exist, the model as currently developed only considers dissolved methane. They suggested that a model incorporating free gas pockets in conjunction with dissolved methane might (a) better represent the physical environment and (b) significantly reduce the required membrane surface area for equivalent conventional recovery.

Johnson and Cramer concluded that the placement of membrane fibers in the proposed configuration would be a challenge as either a series of wells or an excavated trench would be required. They noted that horizontal drilling could also be employed to place fibers in the lateral extent. Though they did not conduct an economic analysis, they suggested that the costs associated with an approximate 7.73 km installation of fiber fabric at a depth of a hundred meters would most likely negate the environmental benefits of the approach.

Initially, Pribyl and Urynowicz noted that enhanced recovery methods involving CO_2 and N_2 injection have the potential to decrease the volume of co-produced water. In order to evaluate this potential in the PRB, characterization of the coal microstructure and gas transport kinetics was required in order to predict coal-gas interactions. Intact cores, preserving both the coal matrix and fracture system, from two coal seams in the Powder River Basin were collected. Water adsorption isotherms were used to obtain pore size distributions. The pore size distribution was found to be as follows:

- 17.7 – 19.5% of the total porosity was classified as microporosity.
- 17.0 – 19.2% exists in mesopores.
- The remaining fraction was made up of macropores.

Experimental apparatuses were developed for exploring gas permeabilities of the intact cores and measuring gas adsorption isotherms. Mass flowrates through intact cores were found to be fairly constant for CH₄, CO₂ and N₂ injection. Coal permeabilities ranged from 0.1 – 7.9 Darcy.

In order to determine if there were ways for CBM operators to produce less CBM water, Zoback, Ross and Colmenares evaluated CBM wellbore completion methods in the PRB. They found that CBM operators routinely carried out water-enhancement on their wells, where water-enhancement procedures were used to connect the coal cleats to the wellbore to increase gas production.

Zoback, Ross and Colmenares analyzed ~200 water-enhancement tests from CBM wells in the PRB in order to determine the magnitude of the least principal stress and the orientation of hydraulic fracture growth. They found that both horizontal and vertical hydraulic fractures were created and that some wells with vertical hydraulic fractures produce excessive volumes of CBM water.

They noted that the creation of both vertical and horizontal hydraulic fractures implied that the magnitude of the least principal stress varied throughout the basin. This observation led them to define three different stress states in the PRB:

- Areas that had active normal faults (extensional stress regimes).
- Areas that were slightly more compressive (either normal or strike-slip stress regimes).
- Areas with reverse faulting (compressional stress regimes).

They observed that for the Big George coal, wells with excessive water production are within normal faulting areas. This suggested to them that vertical hydraulic fractures in communication with normal faults may play a role in the water production.

SURFACE DISPOSAL

Tasks 3, 6 and 7 are included in this topic area. The objectives of Task 3 were to develop an understanding of the fate of CBM co-produced water following discharge and to determine locations where coal seams were isolated from adjacent aquifers. The objectives of Task 6 were to (a) verify and improve assessment methods for identifying infiltration pond sites in the PRB, (b) evaluate concepts for sequestering sodium and controlling salt migration from infiltration ponds and (c) test remote-sensing techniques for identifying good and poor infiltration pond sites. The objectives of Task 7 were to (a) evaluate/quantify the factors controlling the exchange of CBM discharge to shallow groundwater, (b) calibrate numerical models of groundwater flow (and chemical transport) and (c) develop numerical models which will be transferable to other regions.

The objectives of Task 3 were addressed by Frost, Campbell and Brinck (Chapter 4: *Surface Disposal and Minimization of Produced Water: Isotopic Ratios as Tracers of CBM Water*). The Task 6 objectives were addressed by Wheaton, Meredith, Kuzara and Hanson (Chapter 5: *Regional Siting Concerns for Coalbed Methane Infiltration Ponds in the Powder River Basin*)

with the objectives of Task 7 being addressed by Saffer and McCoy (Chapter 6: *Controls on the Fate of CBM Co-Produced Waters and Impacts to Shallow Aquifer Levels*).

Frost, Campbell and Brinck used stable isotopic environmental tracers along with standard water quality data to accomplish three subtasks:

- To monitor the infiltration and dispersion of CBM co-produced water into the shallow subsurface.
- To determine locations where coal seams are isolated from adjacent aquifers and co-produced waters were limited to coal seams.
- To evaluate what information may be provided by isotopic analyses of carbon, oxygen, and hydrogen in CBM-co-produced waters.

To accomplish the first subtask, Frost, Campbell and Brinck used the Sr isotopic ratio, $^{87}\text{Sr}/^{86}\text{Sr}$, to trace the infiltration of co-produced water and to show a connection between changes in water quality and strontium concentration at an on-channel CBM disposal site. They suggested that on-channel discharge showed promise for future disposal in that there were fewer salts in existing channels due to annual flushing. However, they noted the amount and duration of CBM discharge may exceed the water mounding caused by annual flooding in which case stream bank salts may be mobilized.

Research conducted to accomplish the second subtask suggested that the Upper Wyodak coal zone aquifer in the Gillette and Schoonover areas was a well-confined combined sand and coal aquifer unit but that the Wyodak Rider coal zone aquifers were only partially confined allowing interactions between sandstone and possibly other coal aquifers with the Wyodak Rider aquifer. Frost, Campbell and Brinck noted that faults in the northeastern part of the Powder River basin affect aquifer connectivity, either by acting as seals or conduits. They concluded that the Sr isotopic ratio is not well-correlated to fracture patterns developed during the well enhancement process because there are many factors in addition to fracture pattern that control interactions between aquifers.

With regard to subtask 3, Frost, Campbell and Brinck showed that the fractionation in oxygen and hydrogen isotopes caused by evaporation of light-element isotopes can be used to identify watersheds that have been infiltrated by CBM holding ponds. This indicator could be useful when infiltration rates are uncertain. Their initial carbon isotopic results demonstrated that $\delta^{13}\text{C}$ of dissolved inorganic carbon (DIC) and DIC concentration in co-produced CBM water were distinct from shallow ground water and surface water in Powder River Basin. They concluded that this may be a very useful indicator of the presence of CBM co-produced waters in the near-surface environment.

With regard to Task 6, research undertaken by Wheaton, Meredith, Kuzara and Hanson was intended:

- To verify and improve methods used to evaluate proposed coalbed methane infiltration pond sites by evaluating changes in ground water conditions at specific sites.
- To evaluate the mineral leonardite as a tool to sequester sodium and reduce salt loading associated with infiltration of CBM co-produced water.
- To evaluate multi-spectral satellite data as a tool to assess candidate infiltration pond sites with the intent of identifying sites that may not be appropriate for infiltration ponds due to mineral species of concern.

Initially, Frost, Campbell and Brinck noted that improper design and siting of discharge ponds may lead to unacceptable impacts such as changes in shallow groundwater quality. They found that design considerations should include (a) the materials that make up the sides and bottom of the impoundment, (b) the duration of use, (c) the size and number of ponds in an area, (d) the depth of excavation, (e) the mineralogy of the soil profile and in the shallow subsurface, (f) aquifers which underlie the impoundment, (g) the distance to outcrop and (h) reclamation.

They also noted that infiltration ponds provide an economical means of managing CBM co-produced water and that water infiltrating from these ponds may recharge shallow aquifers, potentially enhancing ground-water resources. However, as the infiltrating water moves through the previously unsaturated material, a series of geochemical reactions may occur that increase TDS and the concentration of other constituents. They asserted that predicting these changes is an important step in successfully designing and siting infiltration ponds.

Data from a five-year study at the Coal Creek off-channel site showed that about 64% of the total water discharged to the pond actually helped recharge shallow aquifers. However, reduced rates of infiltration over time at CBM ponds can be expected, especially at off-channel sites. They note that sodium in the CBM-production water appears to cause dispersion of the clays in the pond floor and walls, thus decreasing infiltration over a period of time. Vertical hydraulic conductivity at the Coal Creek infiltration pond site was estimated to have decreased by one order of magnitude from approximately 0.1 to 0.01 feet/day, apparently in response to dispersion of clays.

Wheaton, Meredith, Kuzara and Hanson observed that groundwater levels beneath and adjacent to ponds rise in direct response to infiltration and decrease as the pond bottoms seal or as the pond is allowed to dry when it no longer receives CBM co-produced water. Total dissolved solids (TDS) loads in the underlying and adjacent shallow aquifers increase, then decrease as available salts are flushed from the system. Both water levels and water quality were observed to have returned to near baseline conditions in monitoring wells around the perimeter of the pond. Directly beneath the pond TDS concentrations remained high as the groundwater mound slowly dissipated. Wheaton, Meredith, Kuzara and Hanson anticipated that the mobilized salts would eventually be sequestered as the decreased permeability of the pond floors reduced groundwater flow.

Drill cuttings and cores were collected through the Coal Creek pond floor both prior to filling the pond with CBM co-produced water and again after the pond had dried out when discharges of co-produced water ended. Data from these samples provided insight to the fate of the mobilized salts. Saturated paste extract (SPE) data indicated the salts originated from material between the pond floor down to a depth of 10 feet (ft) and migrated no further than 10 to 15 feet vertically to depths between 15 and 25 ft below the pond floor. Groundwater quality data from monitoring wells indicated the salts had moved horizontally about 200 ft beyond the pond perimeter.

A second study site (the Beaver Creek site) consisted of two on-channel infiltration ponds on a stream channel that was originally ephemeral and changed to intermittent. Infiltration through the pond floors and along the stream channel recharged the alluvial aquifer creating a thicker profile of saturated soil. Salts within this newly saturated soil profile could then be dissolved and mobilized by the ground water.

Downstream from the upper pond, data from monitoring wells showed an initial increase in calcium, magnesium, sodium and sulfate concentrations. Frost, Campbell and Brinck observed that over time these concentrations generally dropped back to baseline or below. They concluded that the increase was likely due to the dissolution of salts such as gypsum which were then flushed through the system. They also concluded that increases in sodium and bicarbonate in the alluvial water likely reflected mixing with CBM co-produced water.

At a lower well site, downstream of both infiltration ponds, increases in calcium, magnesium, sodium and sulfate in the alluvial aquifer were due to dissolution of salts. The increase in sulfate concentrations (from 30 meq/L to 80 meq/L) and very little change in alkalinity and chloride concentrations suggested that the majority of the salts dissolved were sulfate salts. They noted that the high concentration of bicarbonate in CBM co-produced water results in very low solubility of carbonate salts. They also noted that the oxidation of pyritic materials may contribute to the increased SO₄ levels.

Leonardite is a weathered form of coal that is used primarily to improve sodic soils. In laboratory tests, Wheaton, Meredith, Kuzara and Hanson tested leonardite as a possible treatment to reduce Na in produced water. The sodium adsorption ratio (SAR) was reduced in test samples, though they concluded that this was due primarily to increases in Mg and Ca. They observed that the reduction in SAR was accompanied by an increase in TDS and a decrease in pH. They concluded that applications for using leonardite for reducing SAR of managed water appear to be limited.

Multispectral satellite data were evaluated to determine if specific mineral species in the soils could be identified and associated with salt loading in groundwater beneath the Coal Creek pond. Analysis of ASTER data indicated dominance of epsomite (MgSO₄*7H₂O) in soils at the Coal Creek site. Frost, Campbell and Brinck noted that this is consistent with water-quality changes measured beneath the pond. They concluded (a) that ASTER data may provide a useful tool to assess possible pond sites but that further evaluation is needed and (b) that remote sensing data interpretations should be confirmed by soils analyses on the site.

Wheaton, Meredith, Kuzara and Hanson also concluded that predictions of groundwater quality impacts and identification of possible problem sites was feasible using site-specific

hydrogeologic investigations, SPE and remote sensing data but that actual impact identification requires on-site monitoring through the life of the pond.

With regard to Task 7, Saffer and McCoy used a detailed case study to characterize the fate and transport of CBM co-produced waters. Specific project activities focused on evaluating and quantifying the factors controlling the exchange of CBM discharge to shallow groundwater through field data collection, calibration of infiltration and flow models and transfer of models to the watershed scale. Their research focused on four fronts:

- Maintaining and downloading data from remote hydrologic field data collection stations.
- Developing water budgets for in-channel impoundments and analyzing temporal trends in the water budgets.
- Using the field data to project watershed-scale surface water flows for a range of development scenarios.
- Evaluating the utility of proxies for infiltration as a tool to predict the fate and transport of CBM discharge *a priori*.

During the course of their research, Saffer and McCoy recorded data from weirs, shallow aquifer/alluvial monitoring wells and rain gauges at the Beaver Creek Site. The full dataset extended from July, 2003 through the end of 2006. The water budget datasets were limited to non-winter months from 2003-2005. Well hydrograph data were available for the full 3-year period.

Analysis of well water level data by Saffer and McCoy indicated a continuing trend of groundwater mounding beneath the stream channel. The rate of mounding was observed to decrease over time. Two well nests at different distances downstream of in-channel discharge sites exhibited water level increases (referenced to a control site) of 2.6 ft and 3.3 ft from July 2003-2004, and rises of 0.9 ft and ~1.2 ft from July 2004-2005. From fall 2005 through October, 2006, the relative water levels increased by ~0.8 ft.

Though variability over time was observed to be substantial, water budget analysis by Saffer and McCoy showed that conveyance losses in the channel and ponds themselves account for ~50% of the discharged water. The remainder of discharged water flowed down-channel out of the study area as artificial surface runoff. Based on infiltration rates deduced from water budget analyses, they projected that runoff leaving the study site will fully infiltrate within two miles of stream length. The full time series of water budgets showed that water losses in ponds had decreased systematically over the study period. In contrast, conveyance losses in stream channels had increased. Seasonal variation had also increased as vegetation cover and transpiration increased.

The temporal trends in the water budget indicated (a) significantly increased peak transpiration losses in the channels over time resulting from vegetation growth and (b) decreased infiltration rates in the ponds, most likely caused by disruption of clays and/or silting. Saffer and McCoy considered these to be key findings.

Watershed routing models showed that for the entire Beaver Creek watershed, surface water loading at the confluence with the Powder River was most sensitive to soil type. Discharge on a per-pond basis had a secondary effect. Incorporation of temporal variability in conveyance losses into surface water routing models illustrated that projected loading to the Powder River from the Beaver Creek watershed should exhibit strong seasonality. Flows during the late fall through early spring will be significantly larger than those during the summer. Saffer and McCoy noted that the long-term trend toward increased transpiration did not affect projected winter flow but did decrease the summer flow with each year since initial development. In evaluating impacts of co-produced waters on surface water flows and water budgets, they concluded that it is critical to consider the range of expected flows rather than a single average value. They also noted that more realistic and complex models, which include spatial heterogeneity in soils, are necessary to fully understand and estimate flows in future development scenarios.

Analysis of rainfall-runoff response in the study area indicated that the watershed behaved predictably to storm events. Forward models of the rainfall-runoff response were consistent with observations only if (a) there was little dependence on antecedent moisture and (b) the soils had a high infiltration capacity. Saffer and McCoy noted that this is broadly consistent with field observations and suggested that similar analyses of gauged watersheds prior to development may be a useful tool for estimating or predicting spatially averaged conveyance losses. Direct measurements of infiltration were consistent with the basic trend of higher infiltration rates in channel reaches than within the ponds, but the magnitude of the directly measured rates is far higher (~10 times larger) than those inferred from the water budget analysis. Consequently, Saffer and McCoy suggested that direct infiltration tests are of only limited use for predicting impacts in undeveloped watersheds.

BENEFICIAL USE

The objectives of Task 5 were to determine how co-produced waters might affect the physical and chemical nature of PRB soils and to study the interaction between water quality (conductivity, TDS, SAR and alkalinity) and soil types. These objectives were addressed by Brown (Chapter 7: *Agricultural Application of Untreated CBM Waters*) who examined both the effect of untreated co-produced waters on PRB soils and ways to mitigate associated soil damage. Four different studies were undertaken:

- An irrigation site was established to study the physical and chemical changes to soil when using untreated CBM water for irrigation, both with and without the use of soil amendments intended to prevent soil damage.
- A U.S. Department of Agriculture soil salinity model (FAO-SWS) was calibrated for use in the Powder River Basin and was used to predict the effects of untreated CBM water and soil amendments for a 10 year period.
- Soil fertility studies were performed to assess the impact of untreated CBM water and soil amendments on crop productivity.
- A study was conducted to examine the efficacy of using applications of gypsum to reclaim soils impacted by untreated CBM water.

With regard to the first study, the field site was first instrumented with probes and data loggers to measure soil moisture, solution salt content and temperature during the irrigation season. In addition, a lysimeter was placed below an intact, vegetated soil monolith to measure water infiltration rate. Soil samples were collected and analyzed so that baseline soil chemistry and hydraulic properties could be evaluated preceding the installation of two center-pivot irrigation systems. Various amounts of gypsum and sulfur, known to alleviate soil damage from sodic water containing carbonate, were applied to test plots and then co-produced water was applied by the center-pivots for an abbreviated first season followed by a full second irrigation season. Soil samples were collected and analyzed following both irrigation seasons. Visual evaluation of the test plots following the first irrigation season indicated that the amendments were successful in maintaining soil permeability while untreated plots suffered reduced permeability as evidenced by ponding and crusting of soil. The conditions of the soil at the end of the second irrigation period were noticeably deteriorated compared to the previous year. The soil surfaces for all treatments were dispersed. Brown concluded that the primary reason for the dispersion could be attributed to the fact that the amendments were depleted during the second irrigation season due to dissolution. This indicated that more amendments needed to be applied for continued soil protection.

An irrigation model was completed during the second study using baseline conditions to simulate projected soil conditions over a 10-year period. The data collected from the research plot were compared to the results of the model to determine whether additional calibration was needed for Wyoming and Montana climatic conditions. After two irrigation seasons, the data collected at the field irrigation site appeared to support the initial model calibration.

Soil fertility evaluations were conducted during the third study to determine the impact of soil amendments and co-produced water on the production of alfalfa. The research was conducted at two center-pivot sites located north of Sheridan, Wyoming and in a greenhouse study conducted at Colorado State University. Brown concluded that adverse impacts to soil fertility could be attributed to phosphorous deficiency and low soil pH. The phosphorous deficiency was likely due to the addition of gypsum (added to decrease soil SAR) which caused the precipitation of calcium phosphate minerals (e.g., hydroxyapatite). This finding shows that fertilizer applications will be required at some irrigation sites. The low soil pH was caused by the application of sulfur as an amendment to remove carbonate from the co-produced water. Brown also concluded that ag-lime could be added to increase soil pH and buffering capacity. These results illustrate the need to closely manage the application of amendments based on soil conditions throughout the irrigation period.

The fourth study addressed the potential to reclaim sodic soil sites impacted by co-produced water. Two tons of gypsum were applied per acre at the surface without incorporation. One year after amendment application, soil evaluations showed a decrease in the average SAR value. The decline in SAR values at the site translated into a less dispersed soil. Reclamation was achieved with no supplemental irrigation. Brown concluded that application of gypsum had reestablished soil conditions as needed to support productive plant growth under climatic conditions existing in northern Wyoming.

DISPOSAL BY INJECTION

Task 9 focused on the disposal of co-produced waters by injection. Research addressing this practice was conducted by Zoback and Ross (Chapter 8: *Sub-Hydrostatic Pore Pressure in Aquifers of the Powder River Basin, Wyoming, and Implications for Disposal of Coalbed Methane Water Through Injection*) and by Lopez and Heath (Chapter 9: *Coalbed Methane Produced Water Disposal by Injection*).

Zoback and Ross focused on the injection of co-produced waters into aquifers as one means of disposal of such waters. For injection to be feasible, they concluded that the porosity and permeability of the sands need to be high, the pore pressure would ideally be sub-hydrostatic and the aquifer could not be in hydraulic communication with coalbeds or aquifers used for irrigation.

In order to determine if pore pressures in the aquifers were low enough to allow for significant CBM water injection and to determine whether the coals and sands were in hydraulic communication with each other, Zoback and Ross determined pore pressures in 250 wells that monitor water levels in coalbeds and adjacent sands within the PRB. All 250 wells had pore pressures below hydrostatic pressure, suggesting that injection of CBM water should be feasible. However, by analyzing pore pressure changes with time for both the coals and their overlying/underlying sands, Zoback and Ross found after 8 to 13 years of water level monitoring that ~60% of the sands less than 200 ft from producing coals appear to be in hydraulic communication with the coalbeds. In contrast, sands further than 200 ft from producing coalbeds showed no changes in pore pressure over the 8 to 13 year time period. Zoback and Ross recommended that injection of CBM water should be carried out in sands further than at least 200 ft from adjacent coalbeds to be sure that the disposed water did not migrate over time into producing coalbeds.

Zoback and Ross also ran fluid flow simulations to determine the rates at which CBM water could be injected into shallow (~300 ft) and deep (~1000 ft) aquifers. They found that for the shallow sand model they could inject water at a rate of ~160 bbl/day whereas for the deeper sand, whose pore pressures are lower than the shallow sand, the rate was ~435 bbl/day. Both these rates were higher than ~100 bbl/day, which is the average water production rate from CBM wells in the PRB. With regard to deep aquifer injection sites, these results allowed Zoback and Ross to infer that it would take only one injection well to dispose of the water production from approximately four CBM wells.

The focus of research conducted by Lopez and Heath was to identify specific potential injection targets in the Tongue River Member of the Fort Union Formation. A complicating factor for disposal by injection in the Tongue River Member was that potential shallow injection zones were water saturated. Injectivity into these zones was not as great as deeper injection zones such as limestone beds in the Mississippian Madison Group.

Lopez and Heath hypothesized that channel sandstones were probably the best targets for injection because they have more favorable porosity and permeability and because injecting into coal beds may conflict with future CBM development. To test this hypothesis, six channel

sandstone units were identified in the Tongue River Member and were informally named ‘A’ through ‘F’ in ascending order. Isopach maps indicated clearly that these channels were widely distributed and that potential injection targets would not be available in every location where an injection might be desired.

Due to the uncertainty inherent in the mapping of channels, the design of an injection well was based on an existing well with excellent channel sandstone development rather than being based solely on channel isopach mapping. The well chosen was the International Nuclear Corporation, State MT Minerals #1, in Sec 28, T9S, R44E, Big Horn County, Montana. This injection well encountered well-developed channel sandstones in the ‘A,’ ‘C’ and ‘D’ intervals and had good resistivity and sonic logs.

Production from CBM wells in the PRB typically starts with significant water rates, in excess of 200 B/D, and low gas rates. Over time water rates decrease to smaller volumes and gas rates increase to their maximum values. This requires the handling of variable water volumes and supports the central gathering of water from multiple wells for combined disposal or treatment.

Data from four active water disposal wells completed in Wasatch and Ft. Union sand aquifers in the northern PRB showed reasonable injection rates (200 – 4500 B/D) depending on formation sand thicknesses completed. These data also showed well pressures that did not exceed an estimated fracture gradient of 0.70 psi/ft. Disposal well histories over a period of 2 to 16 months indicated no change or increase in well pressures for injected volumes of 36,000 to 600,000 BW. These data corresponded to an average effective formation permeability of 31.5 md, which did not require stimulation treatment to achieve reasonable injection rates. This experience confirmed data and calculations derived from analysis of the International Nuclear Corporation well.

Lopez and Heath noted that well completion designs for new drilled injection wells of approximately 2000 ft depth would reasonably assume injection down production casing. The casing would be cemented fully to surface and perforated with at least 4 holes per foot in target sands totaling 100 ft to 300 ft of net pay thickness.

The analysis undertaken by Lopez and Heath indicated that significant, but limited, volumes of water could be injected into zones identified in the Tongue River Member of the Ft. Union Formation. Because of the difficulties in locating well-developed channel sandstones and because the target zones were already at least partly water saturated, Lopez and Heath concluded that a combination of water disposal methods (e.g., surface discharge, infiltration ponds, direct agricultural and domestic use, treatment, and injection) would yield both the most feasible disposal plans and a balance between environmental goals and economic constraints.

WATER TREATMENT

This topic included Tasks 2 and 8. The objective of Task 2 was to develop electro dialysis for reliable, low cost treatment of co-produced waters. The objective of Task 8 was to establish the industry standard for evaluating treatment technologies that are offered for reducing sodium content of coalbed-methane-production water.

Hayes and Moon (Chapter 10: *Electrodialysis Process Development for the Demineralization of Coalbed Methane Produced Water*) addressed the objective of Task 2 by developing a simplified, modular, electrodialysis-based, processing train for the conversion of coalbed methane produced water into a water stream suitable for beneficial use. Their “Evaluation of a Laboratory Prototype” included:

- Identification of energy industry partners to provide access to active CBM production fields.
- Characterization of co-produced water samples taken from CBM fields in the PRB.
- Determination of treatment goals to achieve beneficial use criteria for water suitable for agricultural applications.
- Design and construction of a treatment train to meet treatment goals and provide reliable operation.
- Testing the performance and reliability of an electrodialysis process train capable of achieving treatment goals.

Energy industry partners (Marathon Oil and Anadarko) allowed access to selected CBM sites in the PRB and provided water samples and water aliquots during the project. Based on an analysis of samples of co-produced water taken from four locations in the PRB of Wyoming, Hayes and Moon determined that PRB co-produced water does not typically exhibit the problems of significant concentrations of oils and greases and high levels of soluble organic compounds (e.g. volatile acids). Following this and other analyses, Hayes and Moon established the following goals for achieving a quality of water suitable for agricultural beneficial use:

- Product Water Recovery Efficiency > 90%
- Brine Volume Reduction > 90%
- Sodium Absorption Ratio (SAR) < 6
- Total Dissolved Solids levels reduced to the range of 1,000 to 2,000 mg/l (Conductivity < 1,500 $\mu\text{S}/\text{cm}$)

A laboratory prototype was constructed consisting of prefiltering for suspended solids removal, followed by electrodialysis (ED), followed by equilibration of the product water stream with a calcium-bearing mineral. Results indicated that a low-cost configuration for the ED system could consist of a non-selective membrane as the cation membrane, a sodium bicarbonate concentrate stream maintained at over 50,000 mg/l TDS and a current density of 4.00 mAmps/cm². In a number of runs, approximately 90% desalination was achieved with modest energy inputs of 0.18 kWh/lb of NaCl removed or less. This was observed when the conductivity of the co-produced water was reduced to very low levels (< 300 $\mu\text{S}/\text{cm}$). Where only partial desalination was required to achieve a treatment endpoint of 1,000 to 1,500 $\mu\text{S}/\text{cm}$, the required energy input could be reduced to levels as low as 0.11 kWh/lb of NaCl removed. Post treatment that employed passive equilibration with calcium carbonate in the form of powder or limestone was able to reduce SAR values from over 55 to below 6, without significantly raising the conductivity of the final water product.

In terms of ease of use and cost effectiveness, passing the water stream over a bed of limestone was the recommended post treatment method. Using this pretreatment process, the laboratory ED unit operated on actual CBM co-produced water and showed minimal degradation to the membranes of the stack cells over an extended 20-hour run before any cleaning was applied. In terms of overall performance, the laboratory ED process showed good stability in treating actual co-produced waters. All performance goals were achieved. Hayes and Moon concluded that ED technology could be considered a viable option for future scale-up and field piloting within the PRB to achieve economical processing of co-produced waters to allow for the subsequent beneficial use of those waters. They estimated that total breakeven system processing costs were less than 12 cents/bbl.

The primary objective of Task 8 was to provide CBM operators with objective, comparable data to allow an accurate evaluation of produced-water treatment equipment. This objective was addressed by Wheaton and Kuzara (Chapter 11: *Standardized Testing of Coalbed Methane Water-Treatment Systems*). Initially, Wheaton and Kuzara observed that operating costs for CBM producers will decrease and options for utilization of co-produced water will increase if viable treatment systems can be designed and deployed successfully. They also observed that:

- Water-treatment technologies that are being proposed for reducing sodium concentrations in co-produced water include ion exchange, electro-dialysis, membrane filtration and distillation.
- Numerous techniques with varying claims for treatment of co-produced water are being advertised currently and additional systems will no doubt be introduced.
- CBM operators need objective, comparable data to accurately evaluate and select a treatment option.
- Water-treatment companies need to be able to test and refine their methods under field conditions.
- Treatment methods will become a valuable option for the management of co-produced water if those methods are economically viable, produce the target water quality and create waste that is within acceptable limits.
- The actual performance of advertised treatment systems needed to be documented to allow CBM operators to compare and choose the best option for their particular setting.

Based on these observations, Wheaton and Kuzara designed and built a field laboratory unit to test water-treatment systems. They note that several companies have voiced interest in using the unit. One company was preparing to test a high-pressure reverse osmosis system. Another company was ready to test an ion-exchange system and was planning to utilize this field laboratory for the first test.

Though Wheaton and Kuzara originally planned to use the unit solely to evaluate co-produced water treatment systems, other water-management applications have become apparent. For example, the unit could be deployed to provide water-budget monitoring for irrigation applications. They noted that one company, having developed a downhole separator and pump, has made a commitment to test the field laboratory unit if funding becomes available.

PREFACE

Large quantities of water are associated with the production of coalbed methane (CBM) in the Powder River Basin (PRB) of Wyoming. The chemistry of co-produced water often makes it unsuitable for subsequent uses such as irrigated agriculture. However, co-produced waters have substantial potential for a variety of beneficial uses.

Achieving this potential requires the development of appropriate water management strategies. There are several unique characteristics of co-produced water that make development of such management strategies a challenge. The production of CBM water follows an inverse pattern compared to traditional wells. CBM wells need to maintain low reservoir pressures to promote gas production. This need renders the reinjection of co-produced waters counterproductive. The unique water chemistry of co-produced water can reduce soil permeability, making surface disposal difficult. Unlike traditional petroleum operations where co-produced water is an undesirable by-product, co-produced water in the PRB often is potable, making it a highly valued resource in arid western states.

This research project developed and evaluated a number of water management options potentially available to CBM operators. These options, which focused on cost-effective and environmentally-sound practices, are reflected in the ten tasks undertaken by the research project:

- Task 1 Membrane-Enhanced CBM to Minimize Produced Water
- Task 2 Electrodialysis Treatment of Produced Water
- Task 3 Isotopic Evaluation of CBM-Produced Waters
- Task 4 Reservoir Geomechanics and the Effectiveness of Wellbore Completion Methods in Coalbed Methane Wells in the Powder River Basin
- Task 5 Evaluating the Use of Produced Water Generated During Coal Bed Methane Extraction for Land Application in the Powder River Basin
- Task 6 Regional Siting Criteria for CBM Infiltration Ponds
- Task 7 Controls on the Fate of CBM Co-Produced Waters and Impacts to Shallow Aquifer Groundwater Quality
- Task 8 Field Laboratory and Standard Method of Testing Performance of Water Quality Treatment Systems
- Task 9 Water Treatment by Injection

Task 10 Regulations/Technology Consistency

This task was undertaken by the Argonne National Laboratory. It involved regulatory analysis and an initial briefing of technology developers regarding regulatory requirements as well as updates regarding changes in those requirements. Argonne also briefed federal and state agencies having relevant regulatory authority regarding technology developments. Argonne's efforts under Task 10 have not been included in the present report.

The subtasks associated with each of the tasks are detailed in General Appendix A: Statement of Tasks Performed.

The research project, which was managed by the Colorado Energy Research Institute (CERI) at the Colorado School of Mines (CSM), involved personnel located at CERI, CSM, Stanford University, Pennsylvania State University, the University of Wyoming, the Argonne National Laboratory, the Gas Technology Institute, the Montana Bureau of Mining and Geology and PVES Inc., a private firm. The results of the research project fall into five topic areas:

- Minimization of Produced Water (Tasks 1 and 4);
- Surface Disposal (Tasks 3, 6 and 7);
- Beneficial Use (Task 5);
- Disposal by Injection (Task 9); and,
- Water Treatment (Tasks 2 and 8).

TOPIC AREA: MINIMIZATION OF PRODUCED WATER

CHAPTER 1:
Membrane-Enhanced Coalbed Methane to Minimize Produced Water

Drew W. Johnson¹
Theodore A. Cramer²

EXECUTIVE SUMMARY

The purpose of this study was to investigate the feasibility of membrane degassing technology for the recovery of methane from coal seams without dewatering the aquifer. One proposed approach involves placing membrane fibers directly within the saturated coal seam and supplying a CO₂ sweep gas to the membrane lumens providing simultaneous CO₂ sequestration and CH₄ recovery.

A mass balance conducted on an infinitesimal fiber element provided the basis for development of a system of ordinary differential equations from which the gas composition within the fiber lumen can be determined as a function of fiber length. The limits of effective recovery were determined by normalizing model predictions to an average conventional well producing $1.56 \times 10^4 \text{ m}^3 \text{ day}^{-1}$ CH₄ (550,000 scf/d). Using this approach, it was estimated that $4.11 \times 10^5 \text{ m}^3$ of CO₂ would be sequestered daily, while the produced gas composition would be 95% CH₄, 4.4% CO₂, and 0.6% H₂O vapor. A total of 16.8% of the dissolved CH₄ in the formation water would be removed during a single pass. Increasing groundwater velocity results in a decrease in required membrane surface area for equivalent recovery with diminishing effect. Increasing pore pressure results in fewer required membranes for equivalent recovery. For a hypothetical coal seam 36.6 m thick located at an average depth of 107 m with a corresponding average pore pressure of 1.05×10^3 kPa and a lateral groundwater velocity of 100 cm day^{-1} , 290,000 m² of membrane surface area would be required (corresponding to a hypothetical “curtain” of fibers 7.73 km wide spanning the height of the coal seam assuming a single layer of fibers spaced one diameter apart). A coal seam at 457 m with a pore pressure of 4.48 MPa would require only 7728 m² of membrane surface area (0.206 km wide curtain), 97% fewer fibers as compared to the hypothetical coal seam located at 107 m. These calculations were made assuming methane is present in the coalbed water at the saturation limit with no free gas phase present.

Additional research is needed to improve model predictions and how the model represents the physical coal-seam environment. The model as currently developed, only considers dissolved methane; however, mobile, free gas pockets may also exist. Therefore, a model that incorporates free gas pockets in conjunction with dissolved methane may better represent the physical environment and significantly reduce the required membrane surface area for equivalent conventional recovery. Placement of membrane fibers in the proposed configuration would be a challenge as either a series of wells or an excavated trench would be required. Horizontal drilling could also be employed to place fibers in the lateral extent. While no economic analysis was

¹ Department of Civil and Environmental Engineering, University of Texas at San Antonio, BSE Bldg 1.318, One UTSA Circle, San Antonio, TX 78249. Correspondence: drew.johnson@utsa.edu.

² Department of Civil & Architectural Engineering, University of Wyoming, 1000 E. University Avenue, Laramie, WY 82071.

conducted, costs associated with an approximate 7.73 km installation of fiber fabric at hundred meters of depth would most likely negate the environmental benefits of the approach unless a less costly installation method is devised.

Funding from this research supported a graduate student thesis: Cramer, Theodore A., “Membrane Gas Transfer of Methane and Carbon Dioxide in Submerged Coal Deposits”, M.S., Department of Civil and Architectural Engineering”, University of Wyoming, August 2007.

Results of the work were presented at the North American Membrane Society Annual Conference, Orlando FL, May 2007: Cramer, Theodore A., and Drew W Johnson, “Membrane Gas Transfer of Methane and Carbon Dioxide in Submerged Coal Deposits”

A manuscript describing the research and significant findings has been submitted for publication in a peer review journal. Cramer, T. A., Johnson, D. W. and Urynowicz, M. A., “Membrane Gas Transfer of Methane and Carbon Dioxide in Submerged Coal Deposits”, Environmental Technology, submitted, November (2007)

INTRODUCTION

The current economical CBM recovery approach requires several wells to be drilled throughout the seam from which to pump the water that saturates the deposit. As the dewatering process continues, the hydrostatic pressure within the gas-bearing coal seam is reduced until the methane is released from the coal and migrates to the well. Well spacing and extent of dewatering vary depending on the hydrologic character of the coal seam; where, the rate of recharge may prevent a regional aquifer from being easily dewatered for increased methane extraction. On average, stable methane production occurs after one to six months of dewatering and is sustained for 12 to 24 months before declining at an annual rate of approximately 20%. As noted in the Ruckelshaus Institute of Environment and Natural Resources, *Water production from coalbed methane development in Wyoming: A summary of quality, quantity and management options*. 2005, University of Wyoming: Laramie. p. 1-77, through the course of recovering Wyoming’s total estimated methane reserves by dewatering, 8.63 billion m³ of water would be co-produced.

The purpose of this study was to investigate the feasibility of membrane degassing technology for the recovery of methane from coal seams. Membrane degassing technology can be used to recover dissolved methane without dewatering the aquifer. The proposed approach involves placing well-spaced membrane fibers directly within the saturated coal seam where a CO₂ sweep gas is supplied to the membrane lumens providing simultaneous CO₂ sequestration and CH₄ recovery. The research objectives were to develop a model for CH₄ and CO₂ gas transfer through a membrane within a submerged coal deposit, verify this model experimentally, and utilize it to further evaluate the feasibility of the method as compared to conventional methane recovery

APPROACH

Membrane Modules and Configurations

Membranes are typically manufactured as either flat sheets or hollow fibers. Sheet membranes have been used for reverse osmosis, volatile organic compound (VOC) such as trichloroethylene (TCE) removal from water (Czerwinski et al., 2004; Duan et al., 2001), and to simplify the study of membrane materials for full-scale application with hollow fiber membranes (HFM). However, sheet membranes are limited to parallel fluid flow along the membrane surface. Reverse osmosis is a pressure driven, membrane separation process that utilizes non-porous, water permselective, sheet membranes to separate water from a salt solution typically for residential sized drinking water applications (Wijmans and Baker, 1995; Van Der Bruggen et al., 2003). Under normal osmosis (dialysis), water permeates through the membrane from the pure-water side to the less concentrated water or salt side (Wijmans and Baker, 1995). By applying high pressure to the salt side while maintaining the pure-water side near atmospheric pressure (Greenlaw et al., 1977), the osmotic pressure can be overcome and result in movement of water from the salt side to the pure-water side (Wijmans and Baker, 1995).

Hollow fiber membranes (HFM), or tubes on the order of 100 μm in diameter, are typically used when a very large surface area per unit volume is required (Johnson et al., 1997; Peng et al., 2003). Furthermore, HFM are very flexible in their configuration (Tan et al., 2005). Closed-end operation entails sealing one end of the fiber so that either a positive or negative pressure can be applied to the inside or fiber lumen. Flow-through operation utilizes a sweep gas or alternative fluid that wicks the permeate from the surface of the membrane on either the shell or lumen side of the membrane. By utilizing shell-side liquid flow, high pressure drops through the membrane leading to large energy requirements for pumping are avoided and the fluid can flow either parallel or normal to the fibers (Tan et al., 2005; Korin et al., 1996); although, the pressure drop of gases flowing through a membrane fiber was found to be less than 1% (Quinones-Bolanos et al., 2005). Shell-side feed results in lower transfer kinetics and shorter membrane-fluid residence times (Abou-Nemeh et al., 2001), where the former can be increased by introducing turbulence into the feed stream (Peng et al., 2003). The fluid flowing within the fiber lumens is parallel and laminar due to the small hydraulic diameter of the fibers (Peng et al., 2003; Korin et al., 1996).

Individual hollow fibers can also be woven into a fabric that permits either parallel or normal shell-side flow (Fang et al., 2002). In 2002, a study by Fang et al. utilized HFM fabric and membrane bundles for in-situ transfer of hydrogen gas into a shallow aquifer to stimulate biodegradation of a plume of chlorinated solvents. The membrane fabric, composed of thousands of evenly spaced gas-permeable, hollow-fiber membranes, was installed normal to groundwater flow; while, the membrane bundles were placed in closely spaced wells throughout the aquifer. The porosity of the fabric was similar to the porosity of the aquifer, approximately 33%, resulting in minimal resistance to lateral groundwater flow (Reynolds number ranging from 10^{-3} to 10^{-4}) while providing a large area for gas transfer (Fang et al., 2002). The membrane bundles were advantageous due to their relatively simple installation and lower cost resulting from using existing wells and established drilling techniques (Fang et al., 2002).

Hollow fiber modules, furthermore, can be left unconfined to float freely in the shell-side fluid or packed into bundles (Johnson et al., 1997). The unconfined orientation is limited to closed-end operation, where the inlet of the fibers is fixed and the individually sealed ends are left unconfined. As bundles, either flow-through or closed-end operation is possible; however, normal fluid flow through tightly packed membranes results in headloss and potential fouling, which increases headloss and decreases mass transfer performance (Johnson et al., 1997). Also, fiber to fiber contact reduces the effective, active surface area of the membrane (Johnson et al., 1997) and often results in bubble formation during gas transfer applications. To reduce the formation of bubbles, the fiber surface may be sealed within three inches of any fixed end, where contact is most likely to occur (Ahmed et al., 2004). Depending on the module, if a failure occurs in an individual fiber, the whole module must be replaced unless the defective fiber can be sealed (Peng et al., 2003).

Closed-end configuration is applicable for oxygenation of water with microporous HFM. To avoid the formation of bubbles, in one study, pure oxygen was supplied to the polypropylene fibers at a pressure no greater than 13.8 kPa; although, other studies indicated the bubble point of microporous membranes to be as high as 68.9 kPa (Ahmed et al., 2004; Ahmed and Semmens, 1992). Solid or composite membranes would be desirable for this application so that higher oxygen feed pressures may be applied without the formation of bubbles (Ahmed and Semmens, 1992). A composite PDMS membrane used for gas transfer was pressurized to 414 kPa without the formation of bubbles; although, the liquid film along the membrane surface became supersaturated at low water velocities resulting in bubble formation (Ahmed et al., 2004). Additionally, at low feed pressures, the back diffusion of other dissolved gases significantly affects the rate and uniformity of gas transfer by decreasing the partial pressure of oxygen in the membrane (Fang et al., 2004). At the closed-end of the membrane, the partial pressure of each dissolved component, not excluded by the membrane, will approach equilibrium with the concentration of that dissolved species in the bulk liquid (Tan et al., 2005). For atmospheric systems, nitrogen gas is most prominent due to its high atmospheric partial pressure in equilibrium with the water (Ahmed and Semmens, 1992). However, back diffusion of water vapor has also resulted in poor performance of closed-end membranes for bubbleless aeration of water (Abou-Nemeh et al., 2001; Ahmed and Semmens, 1992). Water vapor will continuously diffuse into the membrane, supersaturating the gas phase and lead to condensation as the feed diffuses into the water (Fang et al., 2004). Placement of hydrophilic membrane material at the sealed end of the membranes allows accumulated condensate to diffuse back into the liquid phase while the lumen pressure exceeds that of the surrounding water (Fang et al., 2004) or by utilizing a flow-through approach, the water vapor is rapidly swept away by the sweep stream (Abou-Nemeh et al., 2001; Fang et al., 2004).

Flow-through configuration has been used to deliver hydrogen gas to ground water with HFM. To maintain a similar concentration of hydrogen throughout the length of each fiber, a high gas flow rate (7mL/min) was used (Fang et al., 2004). With flow-through configuration, however, transfer efficiency nears one hundred percent only at extremely low gas flow conditions. Alternatively, at low transfer efficiencies, wasting of the feed gas and any stripped contaminants occurs at the outlet end (Fang et al., 2004); in the case of hydrogen, this may lead to explosive conditions at the outlet (Fang et al., 2004). Therefore, means to capture and separate vented components should be included at the outlet. To avoid changes in gas composition within the

fibers from back diffusion during low gas flow conditions, which results in non-uniform gas delivery, the contents of the membrane can be regularly flushed with a pulse of gas equal to the internal volume of the membranes, refilling them with pure gas (Fang et al., 2004). Operating conditions included maintaining the feed pressure of hydrogen just above atmospheric, pressurizing the water to approximately 27.6 kPa or 3 meters of hydrostatic pressure, and pumping the water normal to the membranes to better simulate a groundwater environment (Fang et al., 2002). To measure the amount of water vapor back diffusing into flow-through modules, several researchers have utilized a liquid-nitrogen water trap at the outlet end of the module (Fang et al., 2004; Dutta and Sikdar, 1999). Overall, membrane modules “must be designed to encourage the discharge of condensate as it forms” (Fang et al., 2004). One method suggested installing the membrane modules vertically so that condensate would flow to the bottom as the gas was fed counter-currently, flowing to the top of the modules (Fang et al., 2004)

Model Development

Other investigations have led to the development of membrane gas transfer models in water systems (Tan et al., 2005; Fang et al., 2002; Fang et al., 2004; Ito et al., 1998). Fang et al. developed a model for a two component system where hydrogen was supplied to the membrane lumens for bubbleless gas transfer into groundwater (Fang et al., 2004).

Augmenting the Fang et al. model (Fang et al., 2004), gas transfer of CO₂, CH₄, and H₂O vapor through a single hollow fiber element can be depicted as in **Figure 1.1**, where individual fibers are placed perpendicular to groundwater flow and CO₂ is supplied to the fiber lumen.

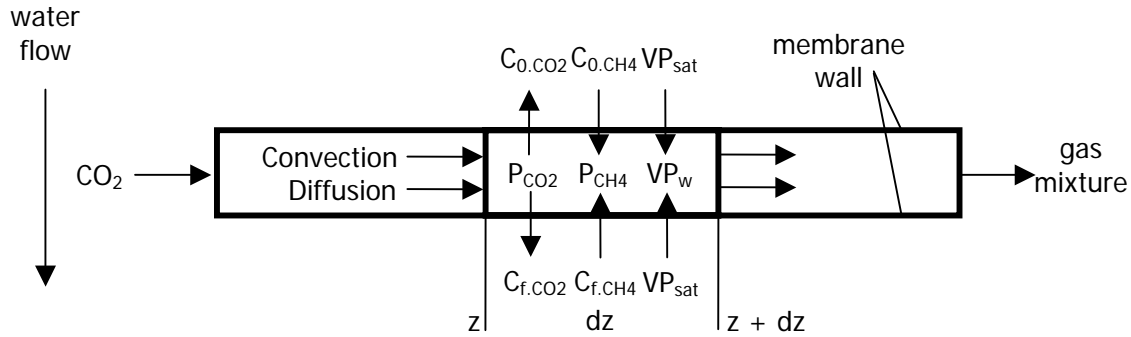


Figure 1.1: Mass balance of an infinitesimal fiber element.

A mass balance conducted on an infinitesimal fiber element of length dz provides the basis for development of a system of ordinary differential equations (ODEs) from which the gas composition and molar flow rate within the fiber lumen can be determined as a function of fiber length as shown by Eqns. i - iv.

$$\frac{dN_{CO_2}}{dz} = K_{o.CO_2} \left(\frac{C_{o.CO_2} + C_{f.CO_2}}{2} \frac{P \left(\frac{N_{CO_2}}{N_{CO_2} + N_{CH_4} + N_w} \right)}{Hc_{CO_2}} \right) 2\pi R_o \quad (i)$$

$$\frac{dN_{CH_4}}{dz} = K_{O,CH_4} \left(\frac{C_{o,CH_4} + C_{f,CH_4}}{2} - \frac{P \left(\frac{N_{CH_4}}{N_{CO_2} + N_{CH_4} + N_w} \right)}{Hc_{CH_4}} \right) 2\pi R_o \quad (ii)$$

$$\frac{dN_w}{dz} = (K_C(P_w - P) + K_D(VP_{sat} - P \left(\frac{N_w}{N_{CO_2} + N_{CH_4} + N_w} \right))) 2\pi R_m \quad (iii)$$

$$\frac{dP}{dz} = - \frac{128(N_{CO_2}\mu_{CO_2} + N_{CH_4}\mu_{CH_4} + N_w\mu_{w,g})RT}{\pi(2R_{in})^4 P} \quad (iv)$$

The first two differential equations (Eqns. i and ii) simulate axial mass transfer (N) of CO₂ and CH₄ assuming that the dissolved concentration of each species changes as the water flows past the membrane and can be represented by an arithmetic average of the concentration before the fiber (C_o) and after the fiber (C_f). Concentrations of CH₄ and CO₂ before the fiber are specified based upon model input parameters. Concentration after the fiber is calculated based upon the change in axial gas flow rate over the length of fiber from the inlet at z = 0 to the end of the fiber at z = L and the liquid flow rate past the fiber (Q_w) as shown by Eqn. v for both CH₄ and CO₂ species (i).

$$C_{f,i} = C_{o,i} - \frac{N_{z=L} - N_{z=0}}{Q_w} \quad (v)$$

Equations i- iv are based upon liquid phase concentrations. Henry's constant values (Hc) (Sander, 1999) are used to relate gas pressure in the fiber to equivalent liquid phase concentrations. The equations incorporate mass transfer coefficients for describing the rates of gas and water vapor exchange between the water and the fiber lumen. The overall liquid phase mass transfer coefficients (K_{O,CO₂}, K_{O,CH₄}) in Eqns. i and ii are calculated from the liquid film and membrane mass transfer coefficients, K_L and K_M, respectively, through use of the resistance-in-series model (Eqn. vi). The gas film mass transfer coefficient, K_{G,i}, is assumed negligible and neglected from the equation (Fang et al., 2002).

$$K_{O,i} = \frac{K_{L,i} \frac{Ha}{\tanh Ha} K_{M,i}}{K_{L,i} \frac{Ha}{\tanh Ha} + K_{M,i}} \quad (vi)$$

The Hatta number (Eqn. vii) is used to augment K_L to account for the chemical reaction of CO₂ with water in Eqn. i. As CO₂ diffuses into the water, it reacts to form carbonic acid (H₂CO₃), bicarbonate (HCO₃⁻), and carbonate (CO₃²⁻), thus increasing the gas flux through the membrane. The rate constant (k_{acid}) is for the rate determining step of the chemical reaction, namely the formation of carbonic acid (Portielje and Lijklema, 1995).

$$Ha = \frac{(D_{CO_2} k_{acid})^{0.5}}{K_{L,CO_2}} \quad (vii)$$

For rapid reaction rates, or those characterized by a Hatta number greater than three, the effect of chemical reaction is significant. Hatta numbers less than 0.3 characterize slow reactions, where the effect of chemical reaction is negligible (Kinnan and Johnson, 2002). For model verification, Ha remained above three for all conditions, while for model scale-up, Ha ranged between 1.5 and 2.5. Therefore, the effect of chemical reaction is included in all analyses.

Water vapor transfer is represented by Eqn. iii, where trans-membrane total pressure (P_w) and saturated vapor pressure (VP_{sat}) contribute to an overall driving force and K_C and K_D are water vapor transfer coefficients for convective and diffusive transport as described by Jou et al. (Jou et al., 1999). Saturated vapor pressure is temperature dependent and calculated from an empirical equation developed by Wagner and Pruss (Wagner et al., 1993).

The final differential equation (Eqn. iv) simulates lumen pressure as a function of fiber length. For laminar flow conditions within the fiber lumen, the equation is derived from the Hagen-Poiseuille Equation and is based upon the Ideal Gas Law. Although alternative equations are available for turbulent flow conditions within the fiber, calculations indicated flow conditions would never enter the turbulent range for this application. The Ideal Gas Law is generally applicable for pressurized systems up to 1.01 MPa. Above this pressure, intermolecular forces are no longer negligible requiring use of the Van Der Waals Equation as a modification to the Ideal Gas Law. For model predictions, a coal seam at an average depth of 107 m below the surface of the ground water table was considered to maintain approximate pore and lumen pressures below this threshold, simplifying the analysis.

The derived differential equations each require an initial condition for analysis. Initial conditions are for the inlet of the fiber or at $z=0$. Since pure CO_2 is applied to the fibers, the initial condition for N_{CO_2} is the molar flow rate of CO_2 supplied per fiber and the initial condition for P is the applied lumen pressure of CO_2 ; all other initial condition values are zero at the fiber inlet. The system of differential equations (Eqns. i – iv) and Eqn. v can be solved iteratively with the Bulirsch-Stoer method by Mathcad computational software (Mathcad version 13.1, MathSoft, Inc., Cambridge, MA).

MODEL VERIFICATION, APPARATUS AND PROCEDURES

The membranes used for model verification were composite hollow fiber membranes (Model MHF 200 TL) manufactured by Mitsubishi Rayon, New York, NY. They incorporated a 1 μm thick, non-porous urethane, selective layer laminated between two microporous, hydrophobic polyethylene layers. The outside diameter of the fibers was 281 μm with 30 μm wall thickness. Membrane mass transfer coefficients (K_M) and water vapor diffusion coefficients (K_C , K_D) utilized in the model were determined previously (Cramer 2007) for this membrane. For the respective gases, K_M is CO_2 : $2.48 \times 10^{-5} \text{ m s}^{-1}$, CH_4 : $2.56 \times 10^{-4} \text{ m s}^{-1}$, and O_2 : $1.91 \times 10^{-4} \text{ m s}^{-1}$, while $K_C = 1.27 \times 10^{-8} \text{ mol Pa}^{-1} \text{ m}^{-2} \text{ s}^{-1}$ and $K_D = 1.01 \times 10^{-6} \text{ mol Pa}^{-1} \text{ m}^{-2} \text{ s}^{-1}$.

Flow-through, 32-fiber membrane bundles were formed by sealing the ends of the membranes into an external shell composed of 0.635 cm OD steel, rigid copper, or nylon tube. Alumilite (regular urethane casting resin, Alumilite Corp., Kalamazoo, MI) was used to form an air tight seal between the shell side of the membranes and the inside wall of the tubing. The excess Alumilite was trimmed flush with the outside end of the tubing to expose the fiber lumen to the gas supply.

For the model verification studies, a 15.2 cm ID stainless steel, cylindrical vessel housed two 32-fiber membrane module bundles that could be operated independently in either flow-through or closed-end mode. An aluminum ring (average dimensions: 15.0 cm ID; 3.81 cm tall; 0.318 cm wall) placed at the bottom of the vessel supported a 14.0 cm average diameter steel mesh around its perimeter. Glass spherical media, average diameter 14.5 mm, was placed, randomly, on top of the mesh to distribute liquid flow evenly within the vessel. This packing occupied approximately 0.305 m of the vessel's 0.457 m total height. The inlet and outlet ends of the one meter long fiber modules were secured to the bottom of the vessel with stainless steel, straight adapters (DMC Series, 0.635 cm tube (OD) x 0.635 cm male pipe (ID), Tylok International Inc., Euclid, OH). Whitey ball and needle valves (Swagelok Co., Solon, OH) at the inlet and outlet ports to the membrane modules enabled the flexibility in mode of operation. A recycle line was connected through a variable speed pump (Masterflex L/S 77300 pump and controller; 7518-10 pump head; 6429-14 tygon tubing, Cole-Parmer Instrument Co., Vernon Hills, IL) and sampling port (631204 Mininert termination valve, VICI, Houston, TX) to the top and bottom of the vessel. At the top connection of the recycle line, a pressure transmitter and inlet methane gas supply was also connected. Although the orientation of the fiber bundles allowed for cross-flow conditions over a majority of their length, the one meter fibers were not well spaced and overlapped randomly due to the confines of the vessel. Carbon dioxide was applied to the inlet side of the membranes through a mass flow controller and pressure transmitter. The downstream ends of the modules were connected sequentially through another pressure transmitter, whitey needle valve, Mininert sampling port, temperature controller (Series EW-89000, $\pm 0.1\%$ accuracy, Cole-Parmer Instrument Co., Vernon Hills, IL), and volumetric flow meter before being vented through a fume hood. A schematic diagram of the experimental apparatus is shown in **Figure 1.2**. All instruments interfaced with LabVIEW software through a CB-27 connector block (National Instruments, Austin, TX).

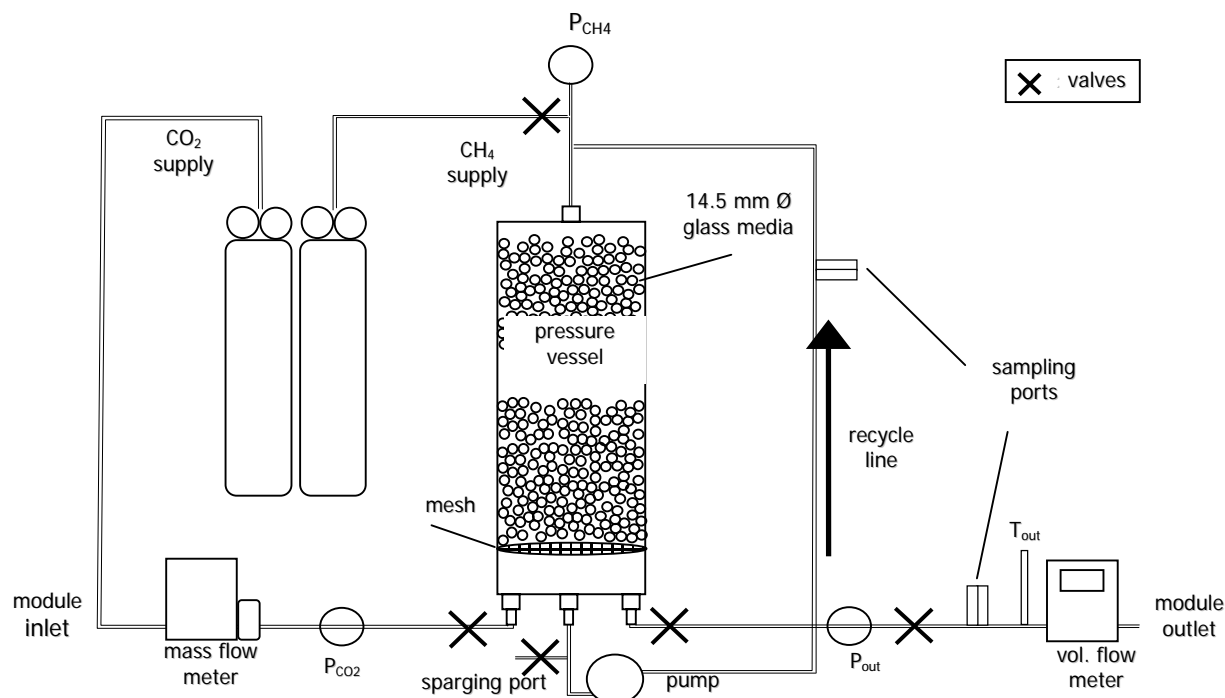


Figure 1.2: Experimental setup for CH₄/CO₂ model verification.

To ensure lumens remained open during module construction and gas exchange could occur within the constructed vessel, initial tests involved only gases on either side of the membranes. Methane was applied to the bottom of the vessel while carbon dioxide was applied to the membrane modules such that the trans-membrane pressure was maintained near zero for gas pressures of 30 kPa and 379 kPa. Methane pressure and flow rate through the vessel was controlled by adjusting the regulator and the valve at the vessel outlet. A three hour equilibration period followed initial stabilization of trans-membrane pressure and individual flow rates. Following this period, a 30 μ L gas sample was withdrawn from the module sampling port and analyzed with a gas chromatograph (GC), (Clarus500 Series, Perkin Elmer, Waltham, MA) with a thermal conductivity detector (TCD), where CH₄ and CO₂ column residence times were approximately 3.1 and 4.6 minutes, respectively. To confirm steady-state conditions existed, two consecutive samples were analyzed at approximately 8-minute increments and compared. Method parameters were developed from a similar method published by Kraemer and Bagley (Kraemer and Bagley, 2006). Specific method parameters and procedures for standard preparation, sample injection, and headspace analysis for liquid samples are described by Cramer (Cramer 2007).

A modified version of the experimental apparatus shown in **Figure 1.2** was used to determine the liquid film transfer coefficient of the membranes. A correlation for liquid film mass transfer coefficients was developed experimentally to account for membrane orientation and fiber-to-fiber contact within a bench-scale vessel. Modifications to the apparatus included supplying the membranes with oxygen, closing the valve immediately downstream of the outlet pressure transmitter to operate the membranes in closed-end mode, pumping distilled water from a reservoir, through the vessel, and to an outlet constant head device, and measuring the change in

dissolved oxygen (DO) between the inlet reservoir and wasting stream from the constant head device with a DO meter (Series 52 meter; Series 5739 probe, YSI Incorporated, Yellow Springs, OH). The DO meter was calibrated in air at 100% relative humidity, as described in the YSI 52 manual, preceding each set of tests. Oxygen was supplied to both modules at 240 kPa and diffusion through the membranes into the water was measured with the mass flow meter. Water flow rate was measured at the outlet flask by timing the collection of water into a graduated cylinder and weighing the water to obtain a volume measurement. Dissolved oxygen measurements were taken at the inlet tube within the reservoir and at the outlet flask once the mass flow reading had stabilized and the hydraulic residence time had been exceeded for the particular water flow rate which ranged from 7 to 105 mL min⁻¹.

The experimental method resulted in an overall mass transfer coefficient for oxygen. The liquid film mass transfer coefficient for oxygen was calculated from the previously determined membrane permeability value for oxygen and the resistance-in-series model. To obtain the liquid film coefficient for other gases, a correlation was developed from the plot of the ratio of Sherwood number over Schmidt number versus Reynolds number on a log-log scale, where the y-intercept and slope of the linear regression represents the constants a and b, respectively (Eqn. viii).

$$Sh_i = a Re^b Sc_i^{1/3} \quad \text{(viii)}$$

For model predictions, the liquid film transfer coefficient was calculated from the Fang et al. correlation for Sherwood number (Eqn. viv), which assumed membrane fibers were well spaced as intended for in-situ scale-up (Fang et al., 2002).

$$Sh_i = 0.730 Re^{0.379} Sc_i^{1/3} \quad \text{(viv)}$$

Kinematic viscosity, used to determine the Reynolds number of the flowing water, was calculated through use of dynamic viscosity and water density. Since each of these components is dependent on temperature, tabulated values for viscosity and an empirical formula for density published by the National Physical Laboratory were used to obtain the values associated with the temperature of the system (Peggs, 1995; Watson, 1995). Based upon the definition of the Sherwood number, liquid film coefficients can be calculated (Eqn. x).

$$K_{L,i} = \frac{Sh_i D_i}{2R_o} \quad \text{(x)}$$

After K_L and K_M were calculated, the overall mass transfer coefficients for CO₂ and CH₄ used in the model were then obtained through the resistance-in-series model (Eqn. vi).

Subsequent tests involved analyzing the outlet gas stream while methane-saturated water was circulated through the vessel at various flow rates. Limitations of the pump and tubing resulted in flow conditions between 2 and 130 mL min⁻¹ through the vessel, encompassing potential coal seam flow rates. The vessel was filled with distilled water, and was sparged with CH₄ for at least one hour to achieve gas saturation of the water. After completing the sparging, the valves to the vessel were closed to maintain the dissolved concentration of CH₄ while the gas supply lines

were reconnected to the vessel as shown in **Figure 1.2**. Additionally, a liquid sample was collected from the recycle line to determine, through GC headspace analysis, the initial liquid-phase concentrations of CH₄ and CO₂. Carbon dioxide was applied to the membrane modules by adjusting the regulator slightly above atmospheric pressure and throttling the downstream module valve to provide back pressure while maintaining a small flow rate across the sampling port. Adjustments to the downstream module valve and regulators for both gas cylinders were made to obtain a zero trans-membrane pressure within the accuracy of the pressure transmitters. To track the stabilization of pressure, all instruments were logged every two seconds.

Model verification involved solving the model for the conditions used during the GC measurements and comparing gas composition determined from the GC and model results. The verified model was then used to compare membrane-enhanced CBM recovery to established recovery methods. Daily CO₂ sequestration and CH₄ recovery rates per fiber were calculated by Eqns. xi and xii, which represent total changes in gas volume flow rate within the fiber lumens over fiber length (L). MV is the associated molar volume of the gases.

$$\text{CO}_2 \text{ sequestered} = (N_{\text{CO}_2 z=0} - N_{\text{CO}_2 z=L})MV_{\text{CO}_2} \quad (\text{xi})$$

$$\text{CH}_4 \text{ recovered} = (N_{\text{CH}_4 z=L} - N_{\text{CH}_4 z=0})MV_{\text{CH}_4} \quad (\text{xii})$$

The number of membrane fibers (n) required to obtain a daily total CH₄ recovery rate equal to conventional recovery methods was determined by dividing the total conventional recovery by the predicted recovery per fiber. The total volume of CO₂ sequestered per day was found by multiplying the required number of fibers by the CO₂ sequestration rate per fiber. After specifying fiber spacing, the linear distance required to place all membrane fibers could be calculated. The percent of CH₄ removed from the methane-saturated water flowing across the membranes was then calculated from the change in CH₄ flow rate through the membrane fiber, the water flow rate past the membranes (Q_w), and the CH₄ concentration in the water (C_{sat.CH4}) (Eqn. xiii).

$$\%_{\text{CH}_4, \text{removed}} = n \frac{(N_{\text{CH}_4 z=L} - N_{\text{CH}_4 z=0}) * 100}{Q_w C_{\text{sat.CH}_4}} \quad (\text{xiii})$$

RESULTS AND DISCUSSIONS

Liquid Film Coefficients

The liquid film oxygen transfer coefficient (K_{L,O_2}) for the membrane fibers within the bench-scale vessel was determined with respect to cross-flow velocity and compared to literature values for well-spaced membranes (Fang et al., 2002) as shown in **Figure 1.3**.

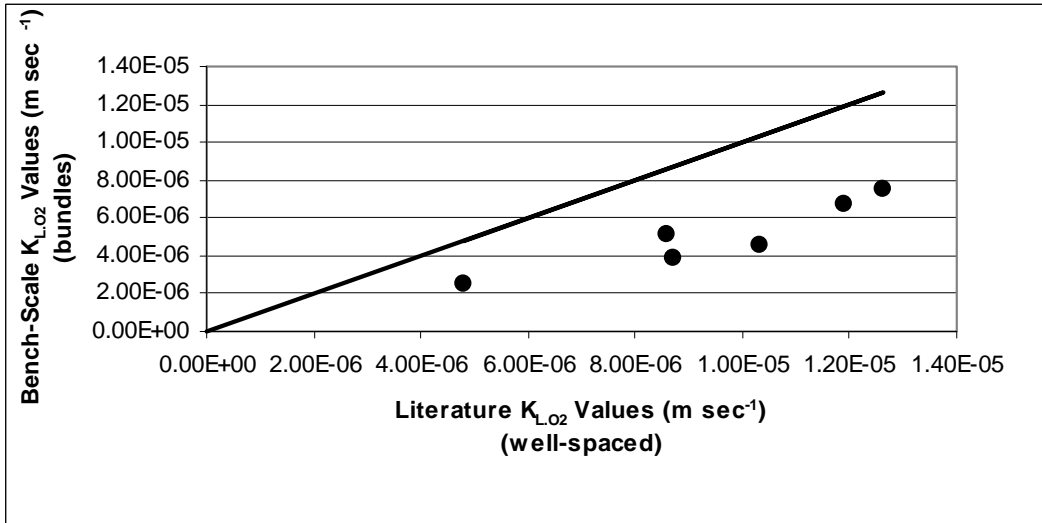


Figure 1.3: Parity plot of literature and bench-scale O_2 liquid film mass transfer coefficients.

The parity plot indicates the liquid film mass transfer coefficient for the fibers is reduced by a factor of approximately four for membrane bundles, which may be due to fiber-to-fiber contact and orientation to the liquid flow. Decreased transfer coefficients for fiber bundles relative to well-spaced fibers have been observed in other studies (Johnson et al., 2003) as well. The correlation used to determine the liquid film mass transfer coefficient for CO_2 and CH_4 is provided in Eqn. xiv as shown in **Figure 1.4**.

$$Sh_i = 0.093 Re^{0.215} Sc_i^{1/3} \quad (xiv)$$

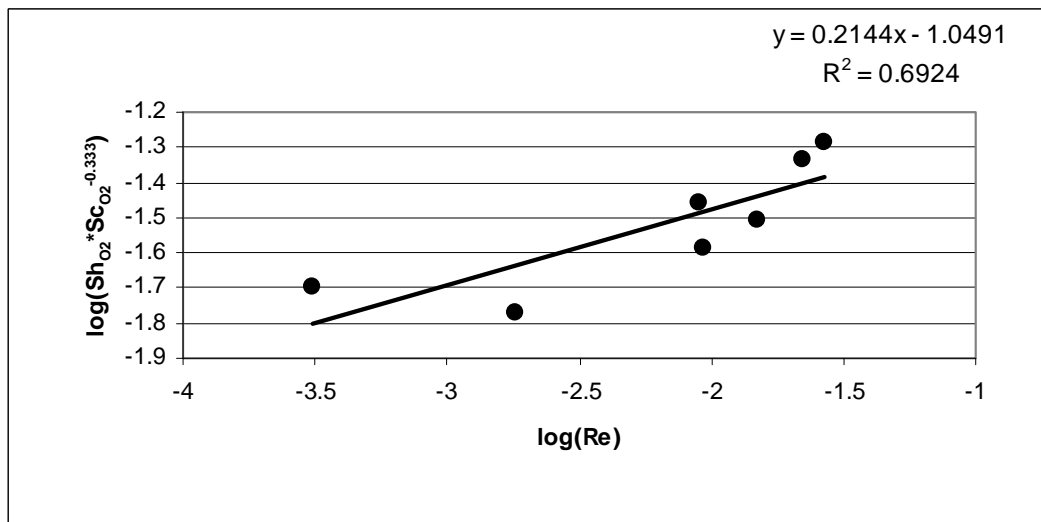


Figure 1.4: Correlation for determining $K_{L,i}$ for CO_2 and CH_4 .

The resulting $K_{L,i}$ values for these two gases, determined from Eqn. v, were CO_2 : $2.06 \times 10^{-6} \text{ m s}^{-1}$ and CH_4 : $2.05 \times 10^{-6} \text{ m s}^{-1}$. Since the K_M values were greater by one to two orders of magnitude of the K_L values, the more significant liquid film transfer coefficients were dominant in the overall mass transfer coefficient equation.

Model Verification

Initial testing utilizing methane and carbon dioxide gas on opposite sides of the membrane indicated potential recovery gas composition near one hundred percent CH_4 at the outlet end of the membranes. As shown in **Figure 1.5**, the gas composition of the recovery stream is strongly dependent on the lumen-side, sweep-gas flow rate, where low flow rates and high gas pressures result in CH_4 being the predominant gas exiting the module. From these tests, module construction and gas exchange feasibility were verified.

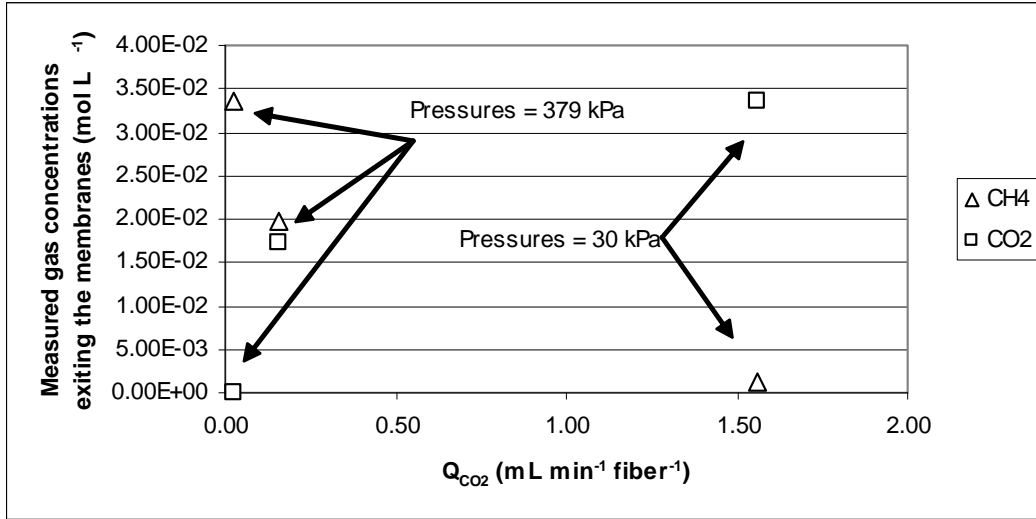


Figure 1.5: Measured recovery over varying lumen flow rates for gas phase diffusion.

The effect of shell-side water flow rate and lumen flow rate on gas composition at the outlet of the membranes was determined with the bench-scale vessel. As depicted in **Figure 1.6 and 1.7**, CH₄ recovery increases with increasing cross-flow water velocity and decreases with increased lumen-side CO₂ flow rate. Therefore, the optimal recovery approach would involve a high natural or induced groundwater velocity across the membranes while a low CO₂ sweep-gas flow rate per fiber (<1 mL min⁻¹) is maintained.

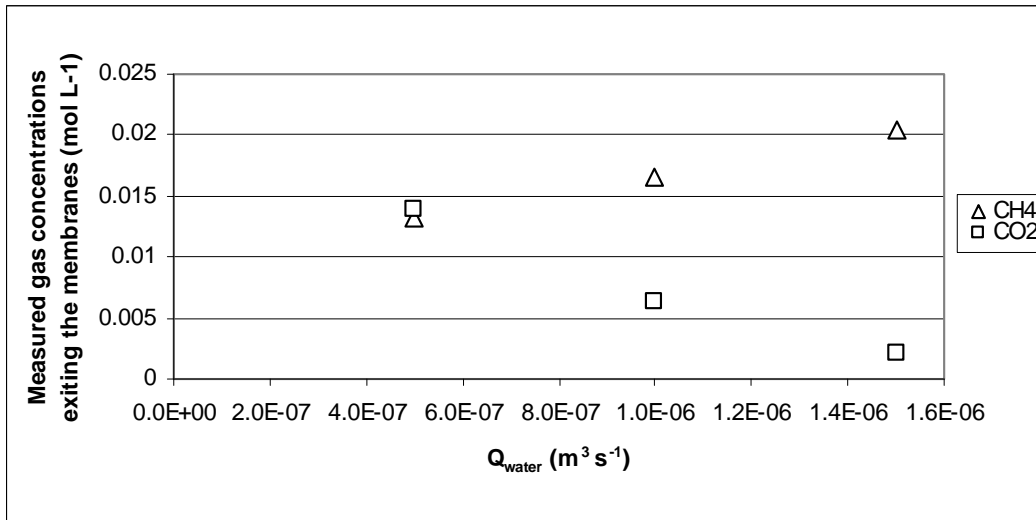


Figure 1.6: Dependence of outlet gas composition on liquid flow rate.

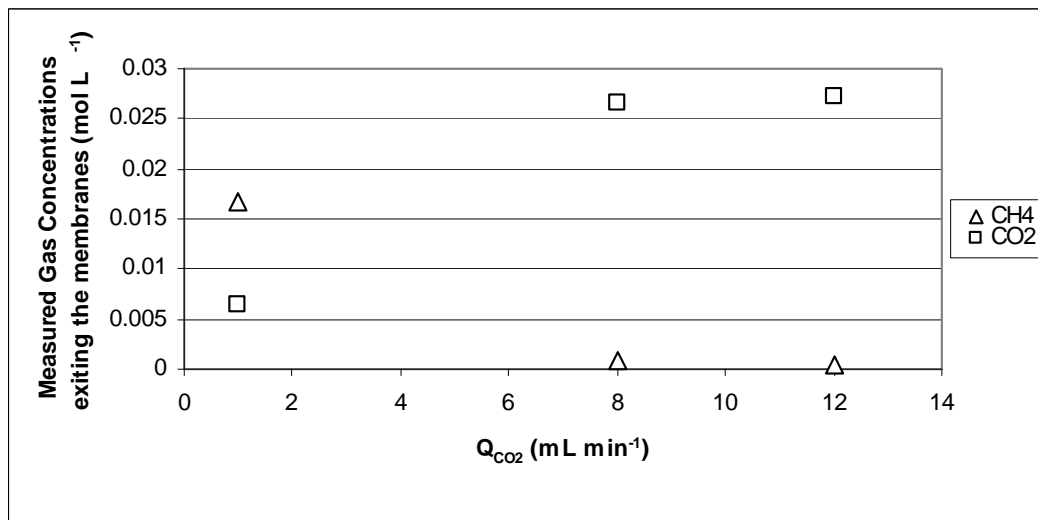


Figure 1.7: Dependence of outlet gas composition on CO₂ flow rate.

Verification of the model was based on the extent of agreement between experimentally measured and model predicted values. For model predictions, two analyses were conducted, one using K_L values determined specifically for the bench-scale apparatus and the other, K_L values obtained from correlations in the literature (Fang et al., 2002). Measured values are compared to each set of predicted values through parity plots (**Figures 1.8 and 1.9**).

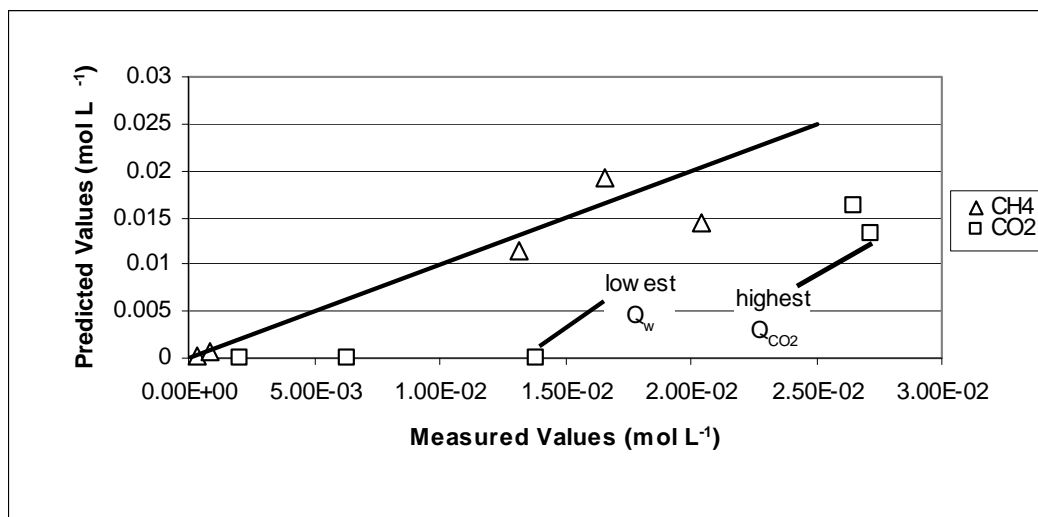


Figure 1.8: Parity plot for model verification using bench-scale K_L values.

For broader application, required active membrane surface area was predicted in terms of various groundwater velocities and pore pressures (**Figures 1.10 and 1.11**).

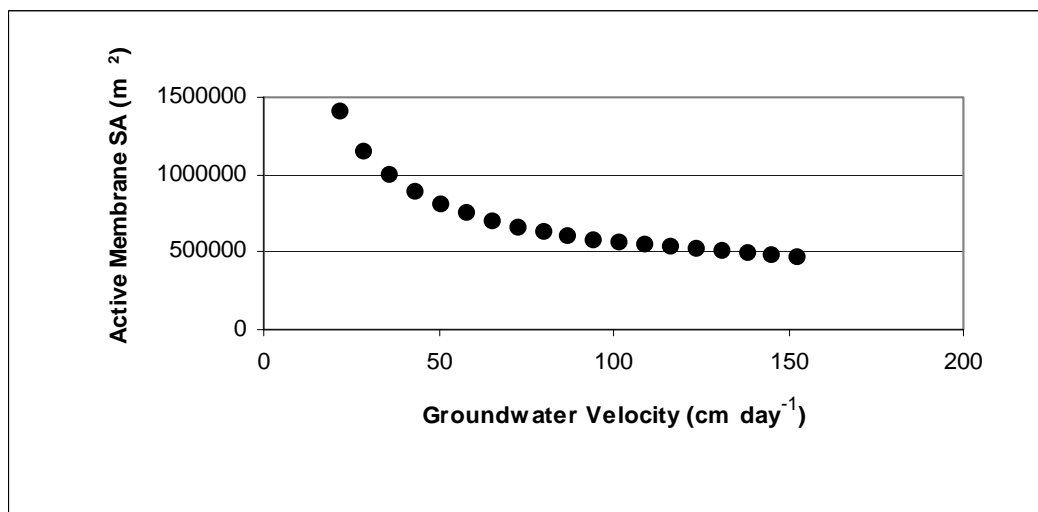


Figure 1.10: Required membrane surface area for varying groundwater velocities.

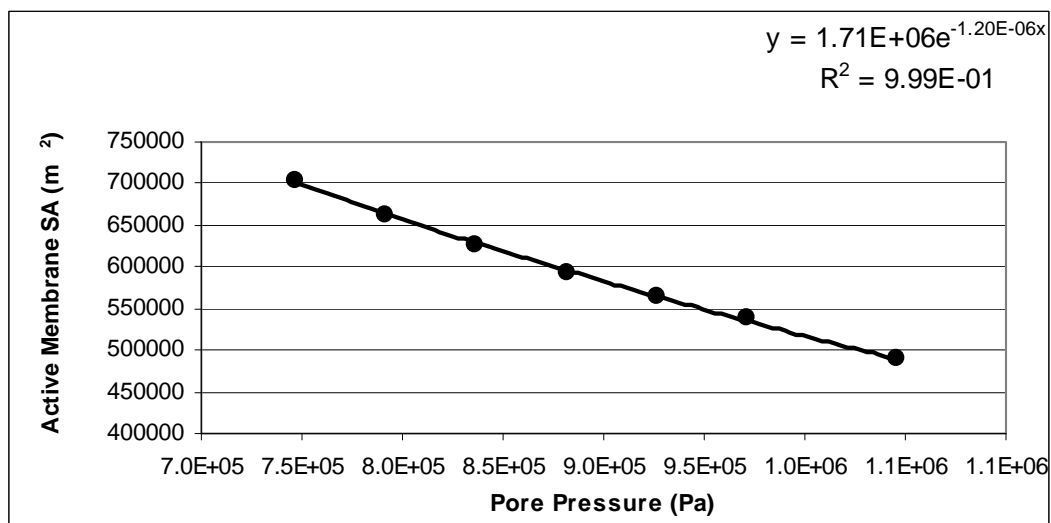


Figure 1.11: Required membrane surface area for varying pore pressures, within Ideal Gas Law applicability.

Constraints for the analysis included 97% CH₄ gas composition at the outlet and CH₄ recovery of 1.56 x 10⁴ m³ day⁻¹. As depicted in **Figure 1.10**, increasing groundwater velocity results in a decrease in required membrane surface area with diminishing effect. Groundwater velocities within the shallow subsurface are not typically greater than 100 cm day⁻¹ (Fang et al., 2002) and velocities above 100 cm day⁻¹ do not significantly reduce the required surface area. **Figure 1.11** indicates increasing pore pressure, and CO₂ supply pressure to maintain zero trans membrane

pressures, results in fewer required membranes for equivalent recovery. The exponential regression of the data is a good approximation for deeper seams with larger associated pore pressures. Using this approximation, a coal seam at 457 m with a pore pressure of 4.48 MPa would require 97% fewer fibers and only 0.206 km of membrane fabric as compared to the hypothetical coal seam located at 107 m.

CONCLUSIONS

The research objectives were to develop a model for CH₄ and CO₂ gas transfer through a membrane within a submerged coal deposit, verify this model experimentally, and utilize it to further evaluate the feasibility of the method as compared to conventional methane recovery. A mass balance conducted on an infinitesimal fiber element provided the basis for development of a system of ordinary differential equations from which the gas composition within the fiber lumen can be determined as a function of fiber length. To verify the model, a bench-scale vessel was used. Overall, agreement appears reasonable for CH₄ recovery; however, agreement for CO₂ recovery declines as liquid flow decreases and lumen flow rate increases. Experimental testing indicated a near one hundred percent CH₄ gas composition at the fiber outlet was possible under conditions of high groundwater velocities and low lumen-side CO₂ flow rates. The limits of effective recovery were determined by normalizing model predictions to the average rate of CH₄ recovery for a conventional well. Using this approach, it was estimated that $4.11 \times 10^5 \text{ m}^3$ of CO₂ would be sequestered daily, while the outlet gas composition would be 95% CH₄, 4.4% CO₂, and 0.6% H₂O vapor. A total of 16.8% of the dissolved CH₄ would be removed during the single pass. These values could be expected immediately after fiber installation within the seam.

For broader application, required active membrane surface area was predicted in terms of various groundwater velocities and pore pressures. Increasing groundwater velocity results in a decrease in required membrane surface area for equivalent recovery with diminishing effect. Although groundwater velocities within a shallow subsurface are not typically greater than 100 cm day^{-1} , higher velocities do not significantly reduce the required surface area. Increasing pore pressure results in fewer required membranes for equivalent recovery. A coal seam at 457 m with a pore pressure of 4.48 MPa would require only 0.206 km of membrane fabric and 97% fewer fibers and as compared to the hypothetical coal seam located at 107 m.

A model representing a multiple-pass system should be explored to increase the percent of dissolved methane removed. The model only considers dissolved methane; however, mobile, free gas pockets may also exist. Therefore, a model that incorporates free gas pockets in conjunction with dissolved methane may better represent the physical environment and significantly reduce the required membrane surface area for equivalent conventional recovery.

RECOMMENDATIONS FOR FUTURE RESEARCH

Additional research is needed to improve model predictions and how the model represents the physical coal-seam environment. The model as currently developed, only considers dissolved methane; however, mobile, free gas pockets may also exist. Therefore, a model that incorporates free gas pockets in conjunction with dissolved methane may better represent the physical environment and significantly reduce the required membrane surface area for equivalent

conventional recovery. Detailed information describing the extent and distribution of free gas phase methane within coals seams does not exist and obtaining this information though future research would be necessary to incorporate this aspect into the model calculations.

NOMENCLATURE

a,b	liquid film correlation constants
C_0	upstream liquid concentration (mol m^{-3})
C_f	downstream liquid concentration (mol m^{-3})
$C_{\text{sat,CH}_4}$	saturated liquid concentration for methane (mol m^{-3})
d	characteristic length scale (m)
D	diffusion coefficient of species into water ($\text{m}^2 \text{s}^{-1}$)
dz	fiber element length (m)
Hc	Henry's constant ($\text{Pa m}^3 \text{mol}^{-1}$)
k_{acid}	rate constant for CO_2 reaction (s^{-1})
K_C	convective mass transfer coefficient ($\text{mol Pa}^{-1} \text{m}^{-2} \text{s}^{-1}$)
K_D	diffusive mass transfer coefficient ($\text{mol Pa}^{-1} \text{m}^{-2} \text{s}^{-1}$)
K_G	gas-film mass transfer coefficient (m s^{-1})
K_L	liquid-phase mass transfer coefficient (m s^{-1})
K_M	membrane mass transfer coefficient (m s^{-1})
K_O	overall mass transfer coefficient (m s^{-1})
MV	molar volume ($22.414 \text{ L mol}^{-1}$ at STP)
n	number of membrane fibers
N	axial mass transfer (mol s^{-1})
P	total pressure (Pa)
P_i	partial pressure (Pa)
Q_w	liquid flow rate ($\text{m}^3 \text{s}^{-1}$)
R	gas constant ($\text{m}^3 \text{Pa mol}^{-1} \text{K}^{-1}$)
R_{in}	inside fiber radius (m)
R_m	log-mean fiber radius (m)
R_o	outside fiber radius (m)
T	temperature (K)
v	velocity of fluid (m s^{-1})
VP_{sat}	saturated vapor pressure (Pa)
L	fiber length (m)

Dimensionless Parameters

Ha	Hatta number
Re	Reynolds number = vd/ν
Sc	Schmidt number = ν/D
Sh	Sherwood number = $K_L d/D$

Greek Letters

μ	dynamic viscosity (Pa s)
ν	kinematic viscosity ($\text{m}^2 \text{s}^{-1}$)
π	pi
ρ	density (kg m^{-3})

Subscripts

CH ₄	methane
CO ₂	carbon dioxide
i	species: CO ₂ or CH ₄
O ₂	oxygen
w	water
w.g	water vapor
z	axial location within the fiber

REFERENCES

- Abou-Nemeh, I., S. Majumdar, A. Saraf, K. K. Sirkar, L. M. Vane, F. R. Alvarez, L. Hitchens, 2001.** "Demonstration of pilot-scale pervaporation systems for volatile organic compound removal from a surfactant enhanced aquifer remediation fluid II. Hollow fiber membrane modules," *Environmental Progress*, 20(1): p. 64-73.
- Ahmed, T. and M.J. Semmens, 1992.** "Use of independently sealed microporous hollow fiber membranes for oxygenation of water: model development," *Journal of Membrane Science*, 69(1-2): p. 11-20.
- Ahmed, T., M.J. Semmens, and M.A. Voss, 2004.** "Oxygen transfer characteristics of hollow-fiber, composite membranes," *Advances in Environmental Research*, 8(3-4): p. 637-646.
- Cramer, T.A., 2007.** "Membrane Gas Transfer of Methane and Carbon Dioxide in Submerged Coal Deposits, in *Civil & Architectural Engineering*," University of Wyoming: Laramie. p. 93.
- Czerwinski, W., et al., 2004.** "Siloxane-urethane membranes for removal of volatile organic solvents by pervaporation," *Desalination*. 163(1-3): p. 207-214.

- Duan, S., A. Ito, and A. Ohkawa, 2001.** “Removal of trichloroethylene from water by aeration, pervaporation and membrane distillation,” *Journal of Chemical Engineering of Japan*, 34(8): p. 1069-1073.
- Dutta, B.K. and S.K. Sikdar, 1999.** “Separation of volatile organic compounds from aqueous solutions by pervaporation using S-B-S block copolymer membranes,” *Environmental Science and Technology*, 33(10): p. 1709-1716.
- Fang, Y., et al., 2002.** “Passive dissolution of hydrogen gas into groundwater using hollow-fiber membranes,” *Water Research*, 36(14): p. 3533-3542.
- Fang, Y., et al., 2004.** “Condensation studies in gas permeable membranes,” *Journal of Membrane Science*, 231(1-2): p. 47-55.
- Fang, Y., et al., 2004.** “Membrane gas transfer under conditions of creeping flow: Modeling gas composition effects,” *Water Research*, 38(10): p. 2489-2498.
- Greenlaw, F.W., et al., 1977.** “Dependence of diffusive permeation rates on upstream and downstream pressures. I. Single component permeant,” 2(2): p. 141-151.
- Ito, A., et al., 1998.** “Removal of dissolved oxygen using non-porous hollow-fiber membranes,” *Journal of Membrane Science*, 145(1): p. 111-117.
- Johnson, D.W., C. Yavuzturk, and J. Pruis, 2003.** “Analysis of heat and mass transfer phenomena in hollow fiber membranes used for evaporative cooling,” *Journal of Membrane Science*, 227(1-2): p. 159-171.
- Johnson, D.W., M.J. Semmens, and J.S. Gulliver, 1997.** “Diffusive transport across unconfined hollow fiber membranes,” *Journal of Membrane Science*, 128(1): p. 67-81.
- Jou, J.-D., W. Yoshida, and Y. Cohen, 1999.** “A novel ceramic-supported polymer membrane for pervaporation of dilute volatile organic compounds,” *Journal of Membrane Science*, 162(1-2): p. 269-284.
- Keller, A.A. and B.G. Bierwagen, 2001.** “Hydrophobic hollow fiber membranes for treating MTBE-contaminated water,” *Environmental Science and Technology*, 35(9): p. 1875-1879.
- Kinnan, C.M. and D.W. Johnson, 2002.** “Iron fouling in membrane gas transfer applications,” *Journal of Membrane Science*, 205(1-2): p. 45-71.
- Korin, E., I. Ladizhensky, and E. Korngold, 1996.** “Hydrophilic hollow fiber membranes for water desalination by the pervaporation method,” *Chemical Engineering and Processing*, 35(6): p. 451-457.
- Kraemer, J.T. and D.M. Bagley, 2006.** “Supersaturation of dissolved H₂ and CO₂ during fermentative hydrogen production with N₂ sparging,” *Biotechnology Letters*, 28(18): p. 1485-1491.

- Montgomery, S.L., 1999.** "Powder River basin, Wyoming: An expanding coalbed methane (CBM) play," AAPG Bulletin, 83(8): p. 1207-1222.
- Peggs, S.L., 1995.** "Tables of Physical & Chemical Constants," [Webpage] [cited 2006; 16:] Available from: http://www.kayelaby.npl.co.uk/general_physics/2_2/2_2_1.html.
- Peng, M., L.M. Vane, and S.X. Liu, 2003.** "Recent advances in VOCs removal from water by pervaporation," Journal of Hazardous Materials, 98(1-3): p. 69-90.
- Portielje, R. and L. Lijklema, 1995.** "Carbon Dioxide Fluxes Across the Air-Water Interface and Its Impact on Carbon Availability in Aquatic Systems," Limnology and Oceanography, 40(4): p. 690-699.
- Quinones-Bolanos, E., et al., 2005.** "Water and solute transport in pervaporation hydrophilic membranes to reclaim contaminated water for micro-irrigation," Journal of Membrane Science, 252(1-2): p. 19-28.
- Sander, R., 1999.** "Compilation of Henry's Law constants for inorganic and organic species of potential importance in environmental chemistry." Max-Planck Institute of Chemistry: Mainz, Germany. p. 1-107.
- Tan, X., G. Capar, and K. Li, 2005.** "Analysis of dissolved oxygen removal in hollow fibre membrane modules: Effect of water vapour," Journal of Membrane Science, 251(1-2): p. 111-119.
- Van Der Bruggen, B., et al., 2003.** "A review of pressure-driven membrane processes in wastewater treatment and drinking water production," Environmental Progress, 22(1): p. 46-56.
- Wagner, W. and A. Pruss, 1993.** "International Equations for the Saturation Properties of Ordinary Water Substance. Revised According to the International Temperature Scale of 1990. Addendum to J. Phys. Chem. Ref. Data [bold 16], 893 (1987)," Journal of Physical and Chemical Reference Data, 22(3): p. 783-787.
- Watson, W.T.R., 1995.** "Tables of Physical & Chemical Constants," [Webpage] [cited 2006; 16:] Available from: http://www.kayelaby.npl.co.uk/general_physics/2_2/2_2_3.html.
- Wijmans, J.G. and R.W. Baker, 1995.** "The solution-diffusion model: a review," Journal of Membrane Science, 107(1-2): p. 1-21.

CHAPTER 2:
Coal Pore Structure and Enhanced Recovery of Coalbed Methane using CO₂:
Coal Characterization and the Effects of Sorption/Desorption within Intact Cores

Richard Pribyl and Michael Urynowicz¹

EXECUTIVE SUMMARY

Coal-bed methane (CBM) is natural gas trapped within coal seams under hydrostatic pressure. Conventional methods of methane extraction require partial dewatering of the coal seams to reduce formation pressure. The volume of the extracted water can be substantial. Enhanced recovery methods involving CO₂ and N₂ injection can potentially decrease the volume of produced water. In order to evaluate the potential for enhanced CBM in the Powder River Basin, with the desired effect of minimizing produced water, characterization of the coal microstructure and gas transport kinetics is required in order to predict coal-gas interactions. Intact cores, preserving both the coal matrix and fracture system, from two coal seams in the Powder River Basin were collected. Water adsorption isotherms were used to obtain pore size distributions. The pore size distribution was determined as follows: 17.7-19.5% of the total porosity was classified as microporosity, 17.0-19.2% exists in mesopores and the remaining fraction was made up of macropores. Experimental apparatuses were also developed for exploring gas permeabilities of the intact cores and measuring gas adsorption isotherms. Mass flowrates through intact cores were found to be fairly constant for CH₄, CO₂ and N₂ injection, with coal permeabilities ranging from 0.1-7.9 Darcy.

INTRODUCTION

Coal-bed Natural Gas

Coal-bed natural gas, also known as coal-bed methane (CBM), is natural gas trapped in underground coal seams. CBM is composed primarily of methane, usually varying between 88% and 98% of total composition, with heavier hydrocarbons and carbon dioxide making up the remainder (White et al., 2005). Usually the underground coal beds lie below the local hydrological surface, which provides pressure that effectively traps the coal-bed gases within the coal seam, as well as driving the gases to sorb to the coal matrix. Due to the porous structure of coal, substantial amounts of gas can be stored in coal through adsorption to the coal matrix surfaces and absorption into pores within the coal matrix. Collectively, these two processes are termed sorption.

CBM wells are typically constructed in relatively shallow coal beds, although in some cases it has been feasible to develop seams over 5000 feet in depth (Wolf et al., 2001). Conventional CBM extraction techniques require partial dewatering of the targeted coal seams in order to relieve the pressure and augment gas flow to production wells. Dewatering typically occurs from the same production wells, with gases being separated from the water at the well surface. Water

¹ Department of Civil and Architectural Engineering, University of Wyoming, 1000 E. University Avenue, Laramie, WY 82071. Correspondence: murynowi@uwyo.edu.

production is highest at the onset of production, but declines steadily thereafter. Gas production usually increases as water extraction drops and overburden pressure is reduced.

There are multiple factors that make CBM an appealing source of energy. Coal seams targeted for CBM production are often considered “unmineable,” due to depth, geographical location, safety concerns or other factors. Therefore, natural gas can be recovered from coal deposits that would not otherwise be utilized. Additionally, there is a growing body of evidence that suggest that methane within these coals seams can be actively regenerated (Budwill, 2003; Budwill et al., 2001). This provides the potential for coal seams to provide a renewable source of secondary biogenic CBM. In addition, CBM is a much cleaner source of energy than coal or oil, with fewer toxic and greenhouse gas emissions. The past two decades have seen a dramatic increase in the extraction of CBM. Due to increased understanding of geological conditions favoring CBM production and improvements in the efficiency of extraction technology, the expansion of CBM development has been substantial. The amount of CBM extracted in 2000 was fifteen times that produced in 1989.

Gas Storage Capacity of Coal

Estimates have shown anywhere from 400 to 700 trillion cubic feet (TCF) available for production from coal seams in the Unities States, with roughly 150 TCF being economically viable utilizing the current methods for CBM extraction. CBM proved reserves in the United States were estimated to be 8.9% of the total proved reserves of natural gas in 2000 (White et al., 2005).

Multiple factors have been shown to influence the gas storage capacity of coals. Coal rank and maceral types, depth, temperature and moisture content all determine in part the amount of CH₄ sorbed within the coal structure. More than 95% of the gas found in a coal seam is sorbed within the coal matrix. Therefore, adsorption isotherm data provides the most telling data for estimating gas storage capacities within coal. Adsorption isotherms express the amount of a gas species that can be stored through sorption in a substance at a specific temperature and pressure. Gravimetric, volumetric, and chromatographic techniques are utilized to quantify the amounts of methane that may be stored in the porous structure of coal.

The Powder River Basin

During the past decade, and especially in recent years, the Powder River Basin (PRB) of northeast Wyoming and southeast Montana has experienced a boom in CBM production. The PRB covers 12,000 square miles and consists of the Anderson, Wyodak and Big George coal seams, which contain low-grade subbituminous coal. The majority of the coal seams are less than 2,500 feet from the surface. Conservative estimates of CBM reserves in the PRB are around 10 TCF, although some estimates have been as high as 40 TCF (EPA 2004). In 2006, more than 24,000 CBM wells had been drilled, with an additional 50,000 permitted (Casper Star-Tribune 2006). As more potential gas stores are explored and located in underground coal seams, it is likely that CBM production will continue to increase.

Produced Water

Increasing development of CBM plays nationwide has brought about several challenges in regards to the handling and disposing of produced water. Many of these challenges have become especially visible during the fast-paced development of the Powder River Basin. Some of the issues associated with CBM-produced water have included water quality degradation, erosion and flooding due to large amounts of discharged water, and the lowering of local water tables (White et al., 2005). The most pressing issues have typically involved the vast quantity of water produced and disposal practices.

More than 1.5 million barrels per day are extracted from the PRB as a result of CBM production. Typical disposal of produced water includes surface discharge and reinjection. Coal-bed waters often have high concentrations of salts, including NaCl and bicarbonate, as well as other dissolved solids that may require costly treatment before disposal (Nummedal 2004). The saline and sodic qualities of the water also limit their ability to be used for agricultural purposes. The subsurface geological properties often limit the effectiveness of reinjection. As a result, an attractive solution for dealing with the problems associated with produced water is to decrease the amount of water extracted to the surface.

Enhanced Coal-bed Natural Gas Production

Enhanced coal-bed methane (ECBM) production is an innovative option for increasing methane recovery while decreasing the volume of produced water (Cui and Bustin, 2005; Gunter et al., 2004; Shi et al., 2004). ECBM involves injecting carbon dioxide, nitrogen gas, or a combination of the two into coal seams targeted for natural gas production. The injected gases enhance methane production by displacing methane sorbed within the coal matrix. Theoretically, this will allow for increased methane production with decreased pre-production dewatering of the seam. Additionally, ECBM utilizing CO₂ is a potential method of sequestering carbon dioxide with the value-added product of natural gas production. In order to further evaluate the feasibility of utilizing ECBM recovery, it is necessary to understand the microstructure of the targeted coal and its interaction with methane, carbon dioxide, and nitrogen gases.

Exchange ratios

Coal generally has a preference for sorbing CO₂ over CH₄. Research has shown the sorptive capacity of CO₂ in coal to be anywhere from two to ten times that of CH₄ (Gunter et al., 2004). The exchange ratio between CO₂ and CH₄ is dependent on the coal rank, with low-grade subbituminous coals typically having a larger CO₂:CH₄ exchange ratio than high-grade coals (Reeves, 2003). As Powder River Basin coals are low-grade subbituminous in rank, it is generally accepted that PRB coals will exhibit relatively high exchange ratios.

Field tests

There have been few ECBM field demonstrations. In 1993, BP-Amoco injected CO₂ at the pilot scale in Colorado's San Juan Basin. The results of this test were promising, and in 1996 Burlington Resources initiated CO₂-ECBM production from deep coal seams in the San Juan

Basin. The Fenn-Big Valley in Alberta, Canada was also targeted for CO₂-ECBM production in 1997. The results of these field tests show that ECBM production is a potentially viable method of increasing methane production, reducing extracted water, and sequestering greenhouse gases (White et al., 2005; Gunter et al., 2004; Reeves 2001; Reeves 2001).

SCOPE OF RESEARCH

Objectives

The current research discussed in this paper is an effort to further characterize intact coal samples collected from the Powder River Basin. In order to accomplish this, two different experimental procedures were developed. In the first, water adsorption isotherms were carried out on triplicate samples of Canyon and Smith coals. This paper will discuss two experimental trials, using initially dry and initially saturated samples of each coal. Pore size distributions were determined for the sampled cores, making it possible to determine the fraction of total porosity made up of micropores, mesopores, and macropores for saturated, intact coals representative of the PRB. In the second, an experimental apparatus was constructed for examining the transport kinetics of gas injected through intact cores. Mass flow rates and permeabilities were measured for PRB coals, and a procedure was developed for performing gravimetric adsorption isotherms on the coal specimens. The objectives of the current work are listed below.

- Quantify the relative pore structure of intact coal cores.
- Characterize the water-gas-coal interactions.
- Compare the competitive adsorption/desorption of methane, carbon dioxide and nitrogen across intact coal cores.
- Develop counter-diffusion breakthrough curves for methane, carbon dioxide and nitrogen.
- Determine the relative effect of changes in gas type and content on coal permeability.

As part of characterizing the sampled coals, preliminary experiments were carried out in order to obtain general properties of the samples. The origins and general characteristics of the sampled coals are summarized in the following subsections.

Sample Origins

Coal samples from two different sites in the Powder River Basin were collected for this experiment. These sites consist of coal-bed methane (CBM) wells drilled by the Montana Bureau of Mines and Geology (MBMG) on Montana state land. The two wells, SL-3 and SL-5, are located 18 miles and 31 miles, respectively, west of the Powder River along the Montana-Wyoming state line. The first site, SL-3, is positioned above the Smith Aquifer. The coordinates for this well are 45.00792° North and 106.53133° West. The Smith coal samples were collected on April 29, 2005, from a depth ranging between 349 feet and 358 feet. The second site, SL-5, targeted the Canyon Aquifer, with sample depths ranging between 408 feet and 431 feet. The Canyon coal was collected on June 10, 2005. SL-5 is located at 45.01189° North and 106.27149° West. Both of the sampled coal seams lie in the Upper Wyodak Formation.

The wells were first drilled down to the coal seams in the desired aquifer and lined with 5-inch diameter steel casing. The coal samples were then collected from the underlying coal seam using a 3-inch diameter split spoon tube. A core liner was not employed in collecting the samples. Once the split spoon was retrieved to the surface, the split spoon was laid on its side and opened. A quick description of the core was made, including length and physical state, and then the samples were carefully placed into storage containers. Some of the coal samples were placed inside a rigid PVC tube, which was subsequently filled with CBM water from a tanker truck on site. The PVC tube, roughly 5.5 feet in length, was then closed shut from a valve at the end. The remaining coal cores were placed in plastic sample bags and sealed shut with strapping tape. The samples were then transported to the University of Wyoming, in Laramie, WY, where they were stored in a cold room at a temperature of 3° C (37° F).

Sample Properties

Proximate and ultimate analyses

As a basis of characterizing the sampled coals, Wyoming Analytical Laboratories in Laramie, Wyoming performed proximate and ultimate analyses on samples of Canyon coal and Smith coal. The analyses were conducted in accordance with ASTM standards D-5142 and D-3176. The results of the proximate analysis are shown in **Table 2.1**, and the results of the ultimate analysis are shown in **Table 2.2**.

Table 2.1: Proximate Analysis of Sampled Coals

Canyon Coal			Smith Coal		
Moisture	31.09	wt. %	Moisture	26.95	wt. %
Ash	2.69	wt. %	Ash	4.43	wt. %
Volatile Matter	28.75	wt. %	Volatile Matter	29.32	wt. %
Fixed Carbon	37.47	wt. %	Fixed Carbon	39.3	wt. %
Total	100.00	wt. %	Total	100.00	wt. %
Heating Value	8277	Btu/lb	Heating Value	8782	Btu/lb

Table 2.2: Ultimate Analysis of Sampled Coals

Canyon Coal			Smith Coal		
	As Received (wt. %)	Moisture Free (wt. %)		As Received (wt. %)	Moisture Free (wt. %)
Moisture	31.09		Moisture	26.95	-
Hydrogen	2.67	3.87	Hydrogen	0.11	0.15
Carbon	48.15	69.88	Carbon	51.72	70.80
Nitrogen	3.84	5.57	Nitrogen	1.08	1.48
Sulfur	0.15	0.21	Sulfur	0.55	0.75
Oxygen	11.41	16.56	Oxygen	15.16	20.75
Ash	2.69	3.90	Ash	4.43	6.06
Total	100.00	100.00	Total	100.00	100.00

These values are indicative of low-grade a coal, which is expected as the PRB contains almost exclusively subbituminous coals, and agree with published data (Kloubek, 1994).

Hydraulic conductivity

The hydraulic conductivity of a Canyon coal core was determined in order to establish a basis for mass transport through saturated, intact coal. A triaxial soil permeameter, manufactured by the Trautwein Soil Testing Company, was used for the experiment. A saturated, intact core measuring 9.6 inches in length and 3 inches in width was placed into the permeameter. A rubber sleeve was placed around the core to prevent sidewall leakage. The permeameter was filled with water and then pressurized to provide overburden pressure. A confining pressure of 50 psi was established on the core, and water was injected at pressures of 1 psi and 10 psi during two experimental trials. Flow rates through the core ranged from 2×10^{-4} to 4×10^{-3} for injection pressures of 1 and 10 psi, respectively. Calculated from Darcy's Law, the hydraulic conductivity while injecting at 1 psi was on the order of 10^{-6} cm/s, and the hydraulic conductivity increased to the order of 10^{-5} at an injection pressure of 10 psi. This equated to core permeability on the order of 1 md. Due to limited numbers of Smith coal samples, hydraulic conductivities of the Smith coal were not determined.

Density

In order to determine the density of the saturated coal samples, coal plugs were cut from the original sample cores to known dimensions and a volume was calculated. Triplicate samples were used for the Canyon and Smith coals. To ensure that the samples were saturated, the plugs were placed into a flask and covered with deionized water. A vacuum was applied to the flask until no visible air bubbles could be detected on the coal surface, a process that took roughly three days. The samples were then weighed and the densities calculated. Both the Canyon coal and Smith coal were found to have a density of 1.29 g/cm^3 .

Porosity

Before pore size distributions were quantified for the two coal samples, the overall porosity of the saturated, intact cores had to be determined. To accomplish this, triplicate samples of known volume for both the Canyon and Smith coals were cut from the original cores. Again, the samples were placed in deionized water under vacuum to ensure saturation. The samples were weighed, and then placed in an oven at 105 degrees Celsius for three days. The samples were weighed again, and the difference in weight was attributed to lost water. It was assumed that the volume of water lost was equal to the total pore volume. With the density of water equal to 0.998 g/cm^3 at ambient conditions, the pore volume was determined for each sample. The total porosity was then determined by dividing the initial saturated volume into the total core volume. The Canyon coal was found to have a saturated porosity of 39.6% by volume, and the Smith coal had a saturated porosity of 38.5% by volume.

Based upon the results of the proximate analysis, it was also possible obtain a theoretical value for the initial saturated porosity in order to confirm the above calculations. Using the reported

moisture contents, 31.09% and 26.95% respectively for the Canyon and Smith coal samples, it is possible to convert weight percent of water to volume through the coal density. Doing so resulted in a porosity of 40.4% by volume for Canyon coal and 35.1% by volume for Smith coal, which are in good agreement with the values determined experimentally. Using the values of 31.09% and 26.95% for the Canyon and Smith coals, the total pore volume equates to a total pore volume of 0.31 cm³/g for Canyon coal and 0.27 cm³/g for Smith coal. These values are an order of magnitude higher than values reported in the literature for similar coals (Clarkson and Bustin, 1999), which reported total pore volumes ranging from 0.021-0.043 cm³/g. However, these values were obtained from dried, crushed, and sieved samples and cannot be directly compared to the total pore volumes of intact coals, which contain a significant cleat system and are saturated with coal-bed water.

MICROPOROSITY EXPERIMENT

Introduction

Coal porosity

Coal is a highly porous medium, with varying pore sizes. Coal is often described as having a dual porosity, composed of the microporosity and macroporosity. It is also common to see the term mesoporosity included, which is a transition between the two (Fischer et al., 2005). The subclassifications for porosity are based on the differing physical processes that occur at varying pore sizes. Macroporosity is made up of the larger cleats and fractures through which fluids generally move in laminar, Darcy flow. To evaluate long-distance transport of gases through a coal seam, such as to a production well, it is necessary to look at the macroporosity of the coal. The mesoporosity is the region of pores where capillary condensation occurs and transport occurs by diffusion (Bossie-Codreanu et al., 2004). Microporosity consists of the smallest pores in the coal matrix, and at this scale sorptive processes dominate. Prior research has shown that nearly all of the surface area present within a coal matrix is found in the micropores (White et al., 2005). The microporosity of coal has been shown to be the most important factor affecting gas sorption and desorption (Clarkson and Bustin, 1999) and is sometimes termed the primary porosity.

Varying classifications of porosity are seen in coal characterization research. Although the different classifications are generally fairly agreeable, this can lead to confusion. In this paper, pore sizes will be defined in agreement with IUPAC, which classifies micropores as having a pore radius < 2.1 nm (21 Å), mesopores as having a pore radius between 2.1 and 53 nm (21 – 530 Å) and macropores as having a pore radius > 53 nm (530 Å).

The porosity and pore size distribution of coal are often related to the coal rank. Coals of high rank typically have a lower porosity than less mature coals, although the porosity is typically composed of micropores. Low rank coals, conversely, often have much higher porosities, but the porosity is composed primarily of meso- and macropores. Some research, however, has disputed these results, indicating the majority of porosity in subbituminous coal is composed of micropores (Stanton et al., 2001). Thus, it is essential to understand the pore size distribution of a

specific coal in order to make adequate predictions of sorptive capacities and transport characteristics for a seam targeted for CBM production.

Conventional techniques for quantifying porosity

The three general characteristics that are typically utilized for quantifying and understanding coal porosity are pore volume, pore size distribution, and surface area. Gas and liquid adsorption are the most common methods for determining coal porosity. Helium and mercury displacement are highly utilized techniques for evaluating pore volumes. Mercury porosimetry has been used to quantify pore size distribution. BET surface area, based upon the Brunauer-Emmett-Teller equation and utilizing N₂ or CO₂ adsorption, is the typical method employed to determine surface areas. The detailed methodology and experimental results of these techniques has been described elsewhere (White et al., 2005; Clarkson and Bustin, 1999; Reucroft et al., 1987; Kloubek, 1994).

It should be noted that the conventional methods of analysis are typically carried out on dried, crushed coal samples. As CBM is extracted from intact coal, often water-saturated, there are obvious limitations in applying porosity characteristics determined through these methods to CBM applications. Additionally, it is recognized that adsorption of CO₂ causes swelling within coal structures, leading to increased error when using CO₂ for determining BET surface areas (Larson, 2004; Romanove et al., 2006). As it is understood that changes in moisture content and sorptive and desorptive processes have a direct influence on coal structure, it is therefore imperative that new techniques be explored for quantifying the pore structure of water-saturated, intact coal samples.

Water adsorption isotherms

Water adsorption isotherms, although less commonly utilized, are another method of determining pore size distributions. Water adsorption isotherms are simply a gravitational method for determining the amount of water sorbed by a sample at varying relative humidities. The method has been traditionally used for determining the pore size distributions of limestone and sandstone formations targeted for oil production (Fischer et al., 2005; Melrose, 1998). The use of water adsorption isotherm has two major advantages over traditional methods of determining pore size distributions. The method is extremely simple experimentally and does not involve the use of toxic or corrosive substances. Additionally, the use of mercury porosimetry or pressurized gas may damage the delicate microstructure of coal, resulting in biased data (Fischer et al., 2005; Kloubek, 1994). Previous research utilizing water adsorption isotherms on sandstone and limestone have shown highly accurate results that are agreeable with data obtained from other methods.

Experimental

Procedure

The experimental procedure for this experiment was adopted from work performed on sandstone and limestone by Fischer et. al. in 2005 (Fischer et al., 2005). Water adsorption isotherms were

determined by subjecting the samples to varying relative humidities and recording the change in mass associated with each relative humidity. Solutions of high-purity glycerol and distilled water were used to establish a controlled relative humidity (relative vapor pressure) within a sealed container. Glycerol is safe to handle, mixes completely with water at any proportion, and has negligible vapor pressure at ambient conditions, making it an ideal candidate for use in this experiment. Relative humidities of 20, 40, 60, 70, 80, 85, 90, 93, and 98% were used in this experiment. The weight percent of glycerol and corresponding relative vapor pressures are shown in **Table 2.3**.

Table 2.3: Relative Humidities and Weight Percent Glycerol

Relative Humidity (%)	Glycerol (wt. %)
0	100
20	94.9
40	86.0
60	73.6
70	64.8
80	51.8
85	42.9
90	31.7
93	23.6
96	14.4
98	7.4
100	0.0

Two experimental trials were carried out in this experiment, using initially dry coal and initially saturated coal. Triplicate samples of Canyon and Smith coal were used for each trial. Intact pieces of saturated coal weighing in a range of 15 to 25 grams were taken from the original core samples and saturated with deionized water under vacuum. The samples were then weighed. The coal to be used for the initially dry trial was then dried in an oven at 105°C until there was no change in mass. The initially dry samples were placed in a small dish and situated above the glycerol-water solution in a closed vessel at a relative humidity of 20%. The samples were weighed on a weekly basis until equilibrium was reached, equilibrium being defined as a change in weight of less than 0.05%. The process was then repeated at the next higher relative humidity. Likewise, the initially saturated samples were placed in a vessel with a relative humidity of 98%. After the samples reached a constant mass, the humidity was lowered to next lower humidity, and the process was repeated. A photograph of the experimental setup is shown below in **Figure 2.1**.



Figure 2.1: Experimental Setup for Water Adsorption Isotherms

The experiment was carried out at an ambient room temperature of 20 °C. Before starting the experiment, the small dish and airtight container were treated with Lysol™ Mold and Mildew Killer to prevent mold from growing on the samples, especially when subjected to high relative humidities. In order to ensure accurate relative vapor pressures within the experimental containers, the densities of the water-glycerol solutions were checked periodically. A PAAR Densitymeter DMA 48 was used for this purpose. Additional water or glycerol was added to the solution as necessary to correct any changes from the originally established densities. The time required to reach equilibrium moisture content at each relative humidity varied from several weeks to several months, depending on the size of the sample and the relative vapor pressure. Typically, samples took longer to reach a constant mass at the higher relative humidities.

Adsorption isotherms

Adsorption isotherms are calculated by relating the mass of water adsorbed at each relative humidity to the capillary pressure through the general Kelvin equation (Fischer et al., 2005; Melrose 1998). The general Kelvin equation is shown below.

$$RT \ln(p/p^0) = -P_c \cdot v$$

where: R = universal gas constant (0.0821 L-atm/mol-K)

T = temperature (K)

(p/p⁰) = relative vapor pressure

P_c = capillary pressure (MPa)

v = molar volume, H₂O (18.05 cm³/mol)

The capillary pressure, in turn, can be expressed as a pore size radius as shown below.

$$P_c = 2\sigma/r_m$$

where: P_c = capillary pressure (MPa)

σ = surface tension (dyn/cm)

r_m = mean radius of curvature (cm)

This makes it possible to determine the size of the pores into which water is sorbing at each relative vapor pressure, and subsequently the pore volume comprised of those pore sizes. By comparing the change in mass of the sample at each relative humidity to the change in mass between totally saturated and totally dry values (the total porosity) an accurate pore size distribution is determined. Of special note are the pore sizes related to relative humidities of 60 and 98%. A relative humidity of 60% is the dividing point between microporosity and mesoporosity, while 98% relative humidity is the division between sorption in mesopores and macropores (Fischer et al., 2005). The relative vapor pressures used in this experiment, along with their corresponding capillary pressures and the related pore sizes is shown in **Table 2.4**.

Table 2.4: Capillary Pressure and Pore Size at Utilized Relative Humidities

Relative Humidity (%)	P_c (MPa)	P_c (psi)	Pore Size (nm)
0			< 0.6
20	217.32	31520	0.6
40	123.72	17944	1.2
60	68.98	10005	2.1
70	48.16	6985	3
80	31.13	4515	5
85	21.94	3182	6.5
90	14.23	2064	9.5
93	9.8	1421	19
96	5.51	799	40
98	2.73	396	53
100	0	0	> 53

Results and discussion

Adsorption isotherms were obtained for the initially dry samples for relative humidities of 20 to 80%. The adsorption isotherms for the initially saturated samples cover a range of relative humidity from 70 to 98%. By combining the initially dry trials with the initially saturated trials, complete adsorption isotherms for the Canyon and Smith coal samples were obtained. The Canyon coal adsorption isotherm is shown in **Figure 2.2**, and the Smith coal adsorption isotherm is shown in **Figure 2.3**.

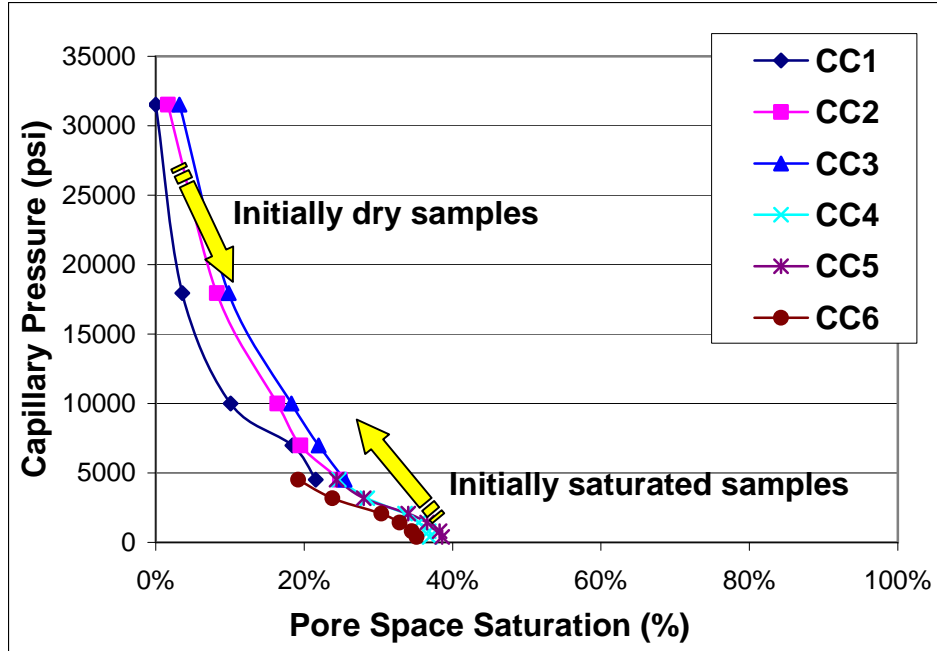


Figure 2.2: Canyon Coal Water Adsorption Isotherms

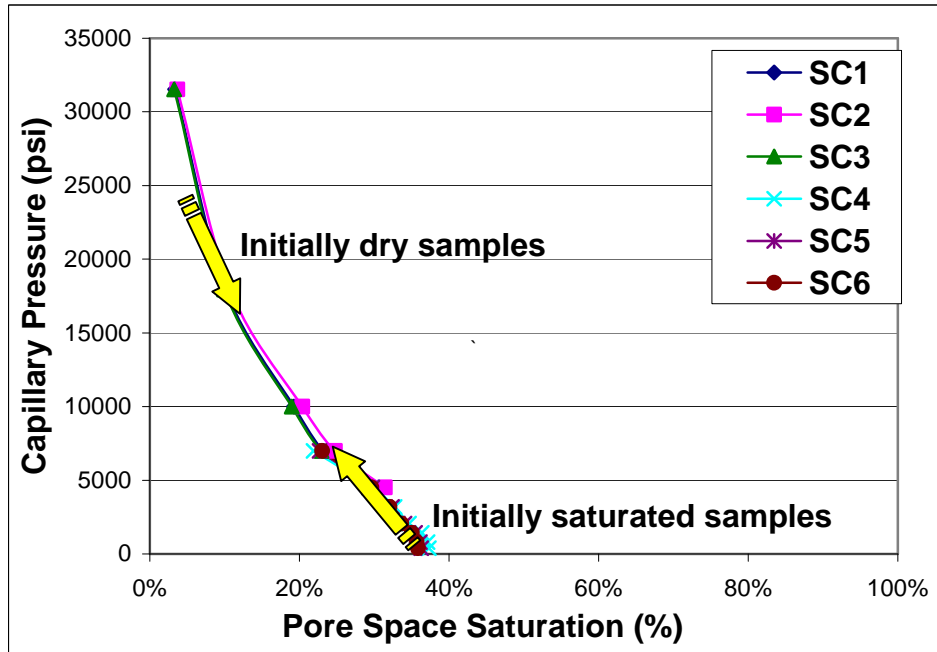


Figure 2.3: Smith Coal Water Adsorption Isotherms

Figure 2.4 shows the average of the Canyon and Smith coal data, expressed in terms of relative humidity against sorption. Figure 2.5 expresses the adsorption data in terms of a pore size distribution.

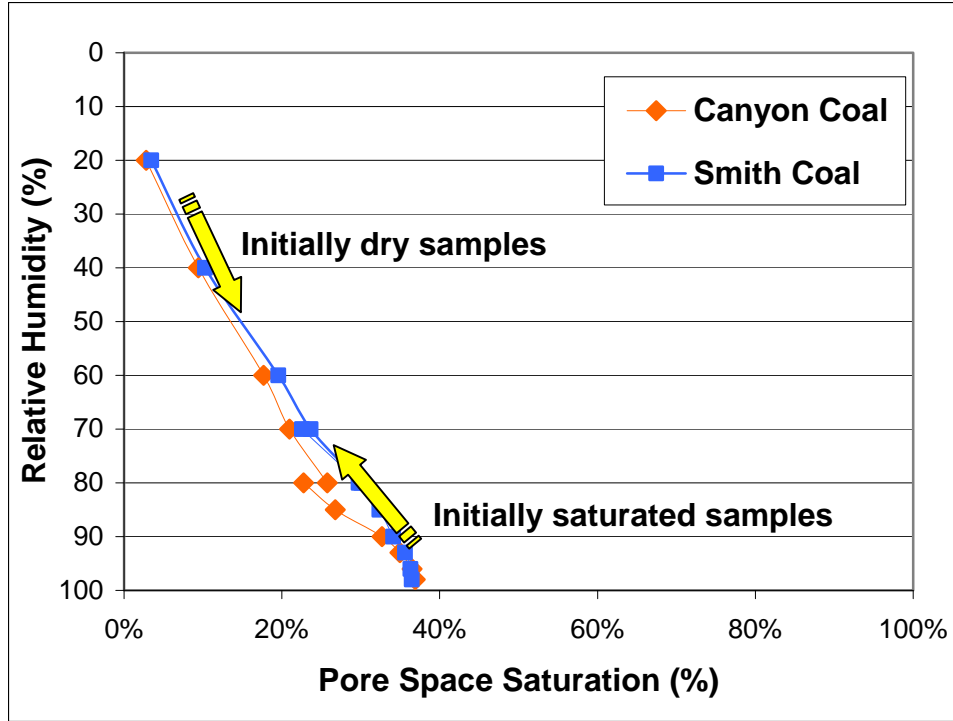


Figure 2.4: Sorption versus Relative Humidity for Canyon and Smith Coal Samples

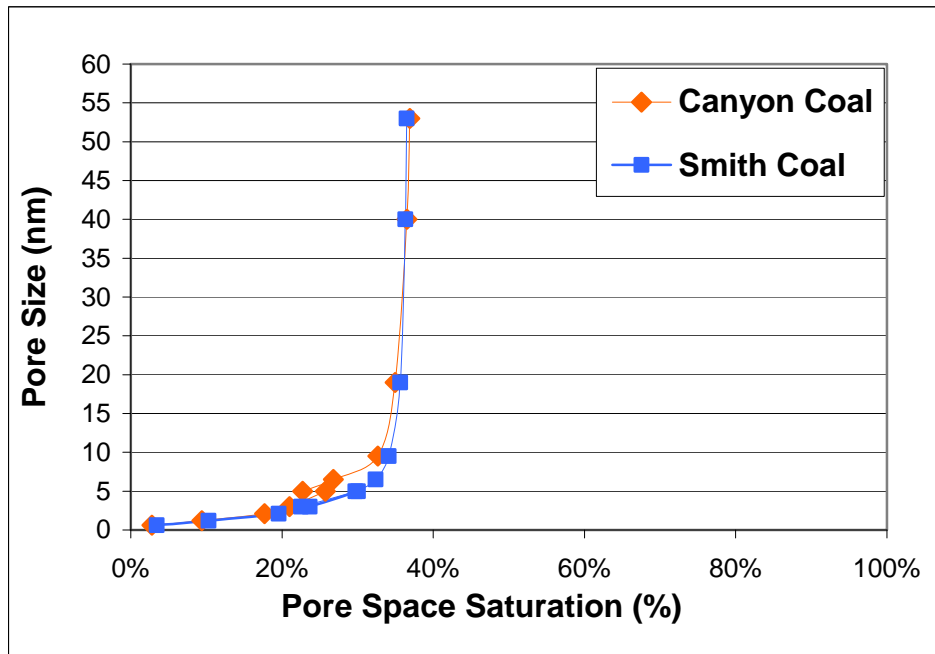


Figure 2.5: Pore Size Distribution of Canyon and Smith Coals

Data collected at a relative humidity of 60%, which relates to a pore size of 2.1 nm, may provide the most telling data. A pore size of 2.1 nm is the cut-off between microporosity and

mesoporosity, and defines the transition from surface adsorption upon the coal matrix and capillary condensation within the fracture spaces. In effect, this provides the microporosity of the coal, which as has been stated above, is extremely important in predicting sorption capacities of coal. It should also be noted that the highest relative humidity utilized is 98%, which defines the cut-off from mesoporosity to macroporosity. The macroporosity is therefore determined as the remaining total porosity not saturated at a relative humidity of 98%.

Comparison of samples

The results of the water adsorption experiment show that the porosity of the Canyon coal samples can be broken down as 17.7% microporosity, 19.2% mesoporosity and 63.1% macroporosity. A similar breakdown of the Smith coal samples results in 19.5% microporosity, 17.0% mesoporosity, and 63.5% macroporosity. The complete pore size distribution as determined from this research is shown below in **Table 2.5**.

Table 2.5: Pore Size Distribution of Canyon and Smith Coals

Pore Size Distribution (% Total Porosity)		
Pore Size (nm)	Canyon Coal	Smith Coal
0.6	2.8%	3.4%
1.2	6.6%	6.8%
2.1	8.3%	9.3%
3	3.3%	3.5%
5	3.3%	6.8%
6.5	2.5%	2.5%
9.5	5.9%	1.7%
19	2.3%	1.5%
40	1.6%	0.7%
53	0.4%	0.2%
> 53	63.1%	63.5%

Review of the water adsorption isotherms shows strong consistency between the triplicate samples, with slightly greater variation in the Canyon coal samples. It is not surprising that the pore size distributions of the samples from the Canyon and Smith are in strong agreement, due to the two coals being similar in rank and originating from the same geographical formation.

Although both the Canyon and Smith coals have a high porosity in the saturated intact state, 39.6% and 38.5% respectively, the percentage of microporosity is relatively low. In both samples, the microporosity contributed less than 20% of the total porosity while the macroporosity was greater than 60%. Therefore, this data is in agreement with previous research suggesting that the porosity of low-grade coals consists primarily of macropores as previously discussed. It would follow, theoretically, that the methane storage capacities of the Canyon and Smith coals might be significantly lower than high-grade, more thermally mature coal seams. Additionally, the high macroporosity is indicative of an extensive fracture network within the

coal matrix, which could suggest high permeabilities and the possibility of substantial mass transport through the Canyon and Smith coal seams.

Time limitations

It was originally planned to measure complete adsorption isotherms for both the initially saturated and initially dry samples for comparison. To the authors' knowledge, this experimental method had not been used on intact coal samples previously, and the length of time necessary for the samples to reach mass equilibrium at each relative vapor pressure was unknown. Due to the considerable time necessary for the samples to reach equilibrium, it became impractical to complete adsorption isotherms for both trials. It was decided to match the data from the initially dry and initially saturated samples once data for overlapping relative vapor pressures had been collected. This process alone took more than two years to complete.

Conclusions and recommendations

Water adsorption isotherms were successfully measured for Canyon coal and Smith coal samples collected in the Powder River Basin. The procedure was found to be straightforward, minimizing potential sources of error. Experimental results show the Canyon coal to have a microporosity of 17.7%, mesoporosity of 19.2% and macroporosity of 63.1%, and the Smith coal to have a microporosity of 19.5%, mesoporosity of 17.0%, and macroporosity of 63.5% (percentage of total porosity). Thus, the fracture system within the coal matrix makes up the vast majority of the total porosity of the sampled subbituminous coals. The microporosity, which is the primary factor affecting gas sorption capacities, is relatively low at less than 20%. This data agrees with trends found in other research that show microporosity to be related to coal rank. From the data collected, the Canyon and Smith coals can be expected to have relatively low methane storage capacity, due to the small microporosity fraction. The high macroporosity suggests an extensive cleat system, which suggests the possibility of relatively high permeabilities in the in-situ coal seams.

It is the authors' recommendation that water adsorption isotherms continue to be measured for the Canyon and Smith coals so that complete pore size distributions can be gathered for both the initially dry and initially saturated samples. This would allow comparison between the two and a check on the validity of the experimental results. Research on sandstone and limestone suggests that a hysteresis is expected between the initially dry and initially saturated samples (Fischer et al., 2005). The initially saturated samples are expected to have slightly higher pore space saturations at each relative vapor pressure. The reason for this is believed to be the trapping of water molecules in larger pores by water molecules sorbed in smaller pores, creating a bottleneck effect. It is also recommended that this experimental process be repeated for the same coals, in order to examine the reproducibility of the results. Sound judgment should be exercised in choosing sample sizes for additional experiments. Smaller samples would result in faster mass equilibrium at each relative vapor pressure. However, reducing sample size too much may cause a bias in regards to accurately representing the cleat porosity.

TRANSPORT PROPERTIES OF INTACT CORES

Introduction

Transport in coal seams

In order to adequately predict transport processes within underground coal seams that will determine the production of gases and water during CBM extraction, it is necessary to have a thorough understanding of the coal structure itself. The difficulty in characterizing coal is due to the fact that coal is very complex. Coal is a highly heterogeneous three-dimensional structure composed of organics and inorganics, the composition of which can vary greatly from seam to seam and even within individual seams. Additionally, the process of sorbing and desorbing gases can substantially change the composition and structural orientation of the coal matrix that directly influence transport properties of the coal seam. On top of this, transport through the coal structure is also dependent on rank, maceral content, depth, temperature and moisture content (White et al., 2005).

Dual porosity and permeability

Due to the dual porosity structure of coal, transport of gases through coal seams also occurs through two pathways. Although the term permeability is often used for describing transport kinetics, there are in fact two permeabilities that affect the movement of coal-bed gases through a coal seam. Coal-bed gases and water typically move throughout the seam by way of the fracture network. Therefore, the fracture permeability of the seam is typically the major factor controlling gas transport over large distances, such as to production wells (Wolf et al., 2004). The process of cleat flow is typically understood to be laminar flow and is described by Darcy's Law. The second method of gas transport is the diffusion of gas particles through the coal matrix, which is dependent on the coal's intrinsic permeability and is described by Fick's Law. Diffusion into the coal matrix is the major factor affecting the rate of gas sorption into and desorption out of the coal structure.

In order for CBM gas to be extracted at a producing well, the sorbed gas must first desorb from the coal matrix and move through the coal matrix via diffusion until reaching the cleat system. Desorption of the gas is typically caused through depressurizing of the coal matrix through the extraction of water. The gas then moves, typically in a free state although some gas is dissolved in water, through the seam fractures to the collecting well. Depending on the specific characterizations of the seam, either diffusion through the coal matrix or laminar flow through the cleat system can be the rate-limiting step ultimately determining the rate of gas production.

Factors affecting coal permeability

There are other seam properties that also have a direct impact on transport kinetics. The moisture content of coal has a direct impact on the permeability of a seam. Typically, as water is removed from the seam, the coal matrix shrinks and results in fracturing within the matrix. As a result, the seam permeability generally increases (White et al., 2005). It can be concluded that drying of the coal matrix, and the subsequent shrinking thereof, will result in higher permeabilities. Research

also indicates that many low ranks coals have a strong preference to sorb water over methane, which indicates sorption of water also affects the gas storage capacity of a seam.

The overburden pressure acting upon a coal seam also has direct consequences on the effective permeability. Increased confining pressure typically causes compression within the coal seam, leading to closure of the cleat system and dramatic reductions in permeabilities. Prior research has shown that there is an exponential decline in permeability as confining pressure is increased (White et al., 2005). Additionally, evidence suggests that the stress history of a coal seam also affects cleat permeability.

There is evidence suggesting that coal rank influences permeability, with high-rank coals typically having lower permeabilities than low-rank coals (White et al., 2005). Low-grade subbituminous coals, such as those found in the PRB, are considered high permeability coals due to extensive cleat formations present within the coal matrix.

Research on saturated intact coal

A great deal of the current research on coal properties and gas sorption and transport is being carried out on dried, crushed coal (Shimada et al., 2005; Clarkson and Bustin, 2000; Clarkson and Bustin, 1997). As has been discussed above, the sorptive and transport properties of a coal seam are dependent on the moisture content of the coal. Drying coal therefore changes the structure of the coal matrix, which can have a significant impact on quantifying transport kinetics and gas storage capacities. Additionally, crushing the experimental samples destroys the fracture system that determines the cleat permeability and affects long-distance transport through a coal seam.

To date, there is an extremely limited amount of data that has been collected from intact coal samples. However, the currently published work shows that there is a substantial difference in the properties of intact coal specimens compared to data obtained from dried, crushed coal. Sasaki and Fujii (Sasaki and Fujii, 2005) examined CO₂ adsorption in crushed and intact coal samples from the same seam and found that the adsorption capacity of the intact coal was one half or less that of the crushed coal. Wolf et. al. (Wolf et al., 2004) conducted multiphase flow experiments through partially saturated intact coals and found that the exchange ratios of CO₂ and CH₄ differed substantially with changes in water saturation. Clarkson and Bustin (Clarkson and Bustin, 2000) also found evidence that the moisture content has a far greater influence on gas sorption selectivity of coal than coal rank. These trends suggest that in order to more accurately represent conditions existing in underground coal seams, it is necessary to examine larger, intact pieces of core that have not been allowed to dry after sampling.

Experimental

Development of experimental apparatus

The design of the system used in this research was an ongoing process that evolved over the course of two years. The conceptual design was based primarily on the work of Wolf et. al (Wolf et al., 2001; Wolf et al., 2000), who used a pressurized coal holder to explore gas permeabilities

and CO₂ to CH₄ exchange ratios in Dutch coals. The experimental procedure is based on obtaining a mass balance on gas and water entering and exiting the sample, an intact coal core. A triaxial soil permeameter, manufactured by Trautwein Soil Testing Equipment, was retrofitted to provide injection of pressurized gas into a saturated, intact coal core. The entire core holder was placed on a balance for measuring changes in mass. For this reason, it was important to use a balance with an adequately high precision in order to detect mass change within the core. An inline flow meter was used to measure the flow rate of the gas during injection, as well as to confirm the injection pressure. Following the flow meter was a hydration vessel, the purpose of which was to saturate the injection gas before reaching the coal in order to minimize drying within the core. After passing through the sample, the effluent could be vented or collected for subsequent analysis.

Procedure

During the course of this research, addressing equipment malfunctions and reducing sources of error led to several iterations in methodology. Ultimately, the following procedure was developed for measuring gas transport kinetics during the final experimental trials.

The first step in the experimental procedure was to prepare a core for mounting in the core holder. The cores were three inches in diameter and varied in length from two to ten inches. The ends of the core had to be cut flat so that the end plates of the permeameter would sit flush against the sample. Initially a high-speed, water-cooled rock saw was selected for preparing the cores. However, the saw imparted significant stress that often fractured the sample before completing a smooth cut. Additionally, the water used for cooling the saw was tap water and might potentially change the core chemistry. As a result, a hacksaw was used for preparing subsequent samples. Using a hacksaw allowed for minimal application of stress, as well as the ability to periodically submerge the sample in CBM water in order to maintain saturation. The cores were cut by frequently rotating the sample, so that the cores were gradually cut towards the center of the core. This way, if the sample fractured nearing the end of the cut, the overall shape of the core was generally maintained. Following cutting, the cores were measured and weighed. Next, they were rinsed in CBM water and the ends of the core were lightly brushed to remove fouling of the pores and cleat system.

After preparing a core, the next step in the procedure was to setup the experiment and apply confining pressure to the sample. The sample core was placed in an elastomer sleeve and mounted in the permeameter. The permeameter was then filled with water, allowing for easy identification of any system leaks at the connection fittings and minimizing any safety hazards due to over pressurization. Confining pressure was then applied from a compressed air tank through FlowLine nylon tubing. The permeameter was situated on an Acculab VA-12KG digital balance, having a precision of 0.2 grams. Confining pressure was stepped up in 10 psi increments over the course of an hour in order to examine the system for leaks, and to prevent tearing of the elastomer sleeve or equipment failure due to pressure shock. After mounting the core, data collection was initiated and ambient conditions were recorded.

During the experimental trials, the injection gas was supplied from a compressed cylinder and administered through a two-stage regulator. The regulator was used to control the injection

pressure, with the flow meter providing confirmation. For all trials of the flow through experiments, the outlet pressure was equal to atmospheric pressure. The gas flow rate was measured with an Alicat Scientific mass flow meter having a range of 0 to 100 standard cubic centimeters per minute (sccm). The gas density was used to convert standard cubic centimeters per minute to grams per minute. The injection gas then traveled through a needle valve before reaching a hydration vessel consisting of a column of gravel saturated with deionized water. After passing through the hydration vessel, the gas was injected through the coal core, under the established overburden pressure within the permeameter. The effluent gas and water were either collected in Tedlar Bags, where it could be stored for future analysis, or vented to a laboratory hood. The data from the mass flow meter and balance were automatically logged in a computer, which recorded data at fifteen-minute intervals. The logged data was entered into an Excel™ spreadsheet for analysis.

A schematic of the experimental apparatus is shown below in **Figure 2.6**. **Figure 2.7** provides a detail schematic of the coal core within the permeameter. An image of a completed system is shown in **Figure 2.8**. Three experimental systems were constructed for this research. However, shortly after completion, the outer cylinder of one of the permeameters failed and the system was afterwards inoperable. It is believed that the cause of the failure was simply age and fatigue, resulting in fracturing.

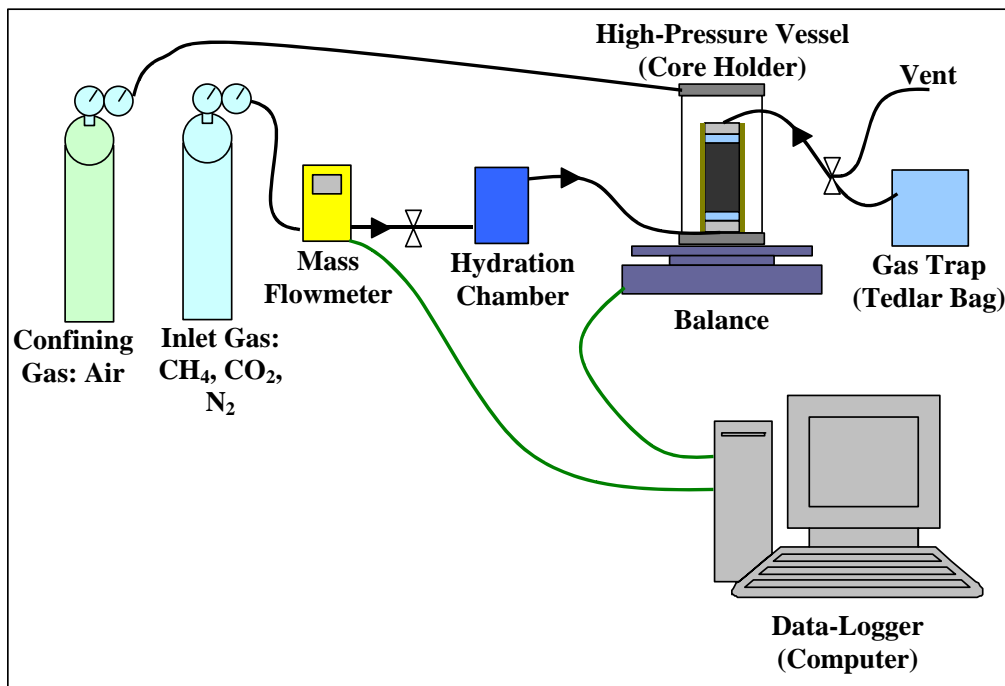


Figure 2.6: Schematic of the Experimental Apparatus

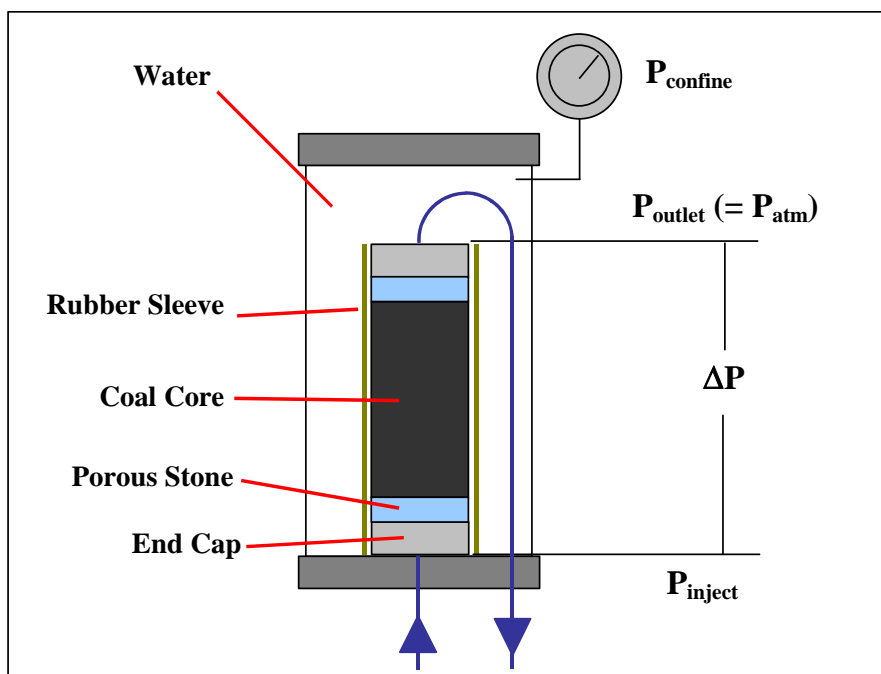


Figure 2.7: Detailed Schematic of the Core Holder

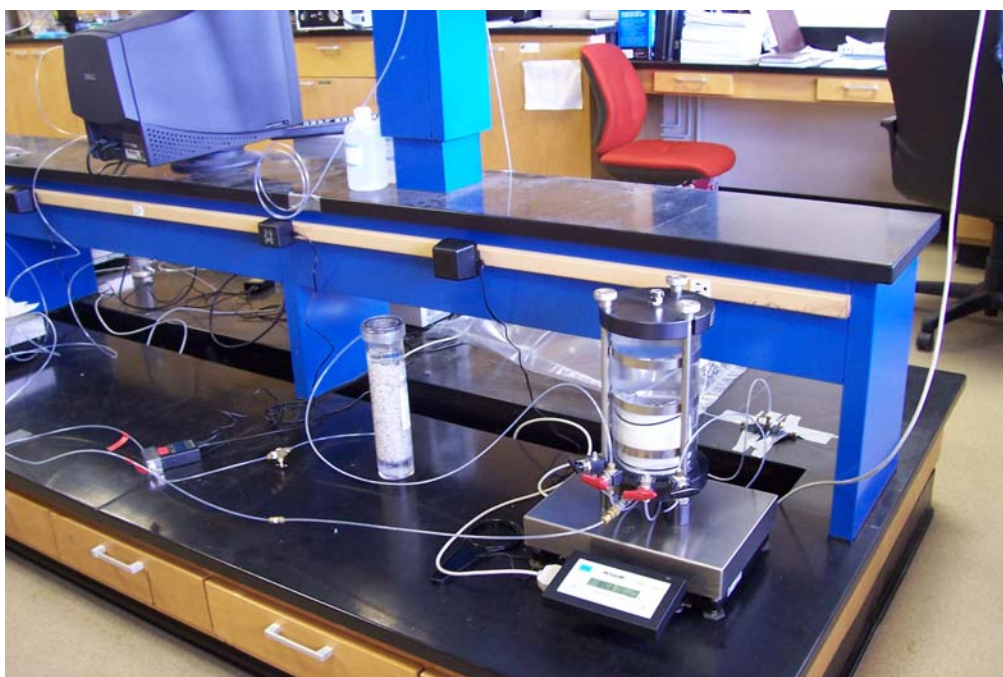


Figure 2.8: One of Two Operational Experimental Apparatuses

Nitrogen gas was injected first through coal samples in order to establish initial coal gas permeability. Due to the inert nature of N_2 and the low affinity for sorption to coal, brief nitrogen injection provided gas permeability data with minimal sorption and desorption effects. During the developmental period of this apparatus, nitrogen also provided negligible safety concerns if

leaks were encountered. In following experimental trials, methane and carbon dioxide were injected through coal samples, including cores previously tested with nitrogen and cores fresh from storage in CBM-produced water. All experiments were carried out at an ambient temperature of 20 °C. Confining pressures utilized during experimental trials ranged from 25-80 psi, with injection pressures ranging from 1-70 psi. In some cases, before gas could be injected at a lower pressure (1-20 psi), initial injection had to be at notably higher pressures in order to force water through the coal before gas flow could be initiated. This period of dewatering usually took one to three hours. The majority of the permeability data was collected from Canyon coal cores, due to core availability. Limited trials were completed on Smith coal.

Sorption isotherms

Experimental trials were completed with the purpose of measuring gas adsorption isotherms for the intact coal samples. During the adsorption trials, CH₄, CO₂ or N₂ gas was injected into a core at 10 psi until the increase in mass, directly representing the adsorbed gas, reached a relatively constant value. The injection pressure was then increased to 20 psi and the core was again allowed to reach equilibrium. This process was continued in 10-psi increments up to a final pressure of 70 psi (10 psi below the maximum applied confining pressure of 80 psi). Prior to starting an adsorption isotherm, it was often necessary to subject the core to increased injection pressures (40-70 psi) in order to force water to exit the core and initiate gas flow through the sample. Once flow was established, injection pressures were immediately reduced and the collected water was quantified.

Results and Discussion

A total of twenty-one experimental trials were carried out using the developed gas injection apparatus. The experimental trials took anywhere from a couple of days to several weeks to complete, depending on flow rates through the cores and experimental objectives. Trials 1-6 measured permeability to N₂ in Canyon coal cores. Trial 7 measured the N₂ permeability of a Smith coal core. Trials 9 and 10 collected permeability data for CH₄ and CO₂ in Canyon coal. Trials 11, 12, and 19 were aborted due to mechanical failures with the flow meters and no meaningful data was collected. During the course of the research, it was found that the differential sensors within the flow meters were easily damaged due to pressure shock. Despite efforts to minimize rapid changes in pressure, the flow meters still incurred damage and had to be repaired. Trials 13, 14, 16 and 18 were aborted due to an apparent inability to inject gas through the core samples. These cores were deemed “impermeable” at the operating pressure of the experimental apparatuses. Trials 15, 17, 20 and 21 were adsorption isotherm experiments. However, due to numerous power outages as a result of electrical storms, much of the data for Trial 21 was lost and the results cannot be adequately interpreted. The results of the successful trials are summarized below.

Coal permeabilities for nitrogen, carbon dioxide, and methane

Examples of collected data during N₂ injection experiments are shown below in **Figure 2.9** and **Figure 2.10**.

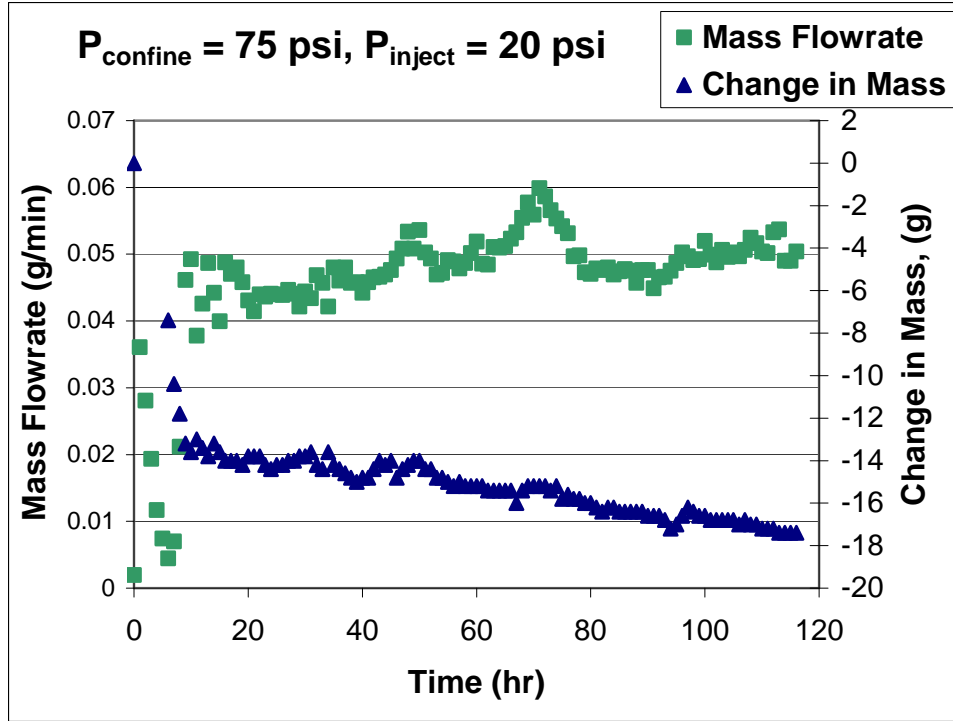


Figure 2.9: Gas Injection Data for N₂ through Canyon Coal Core CC1

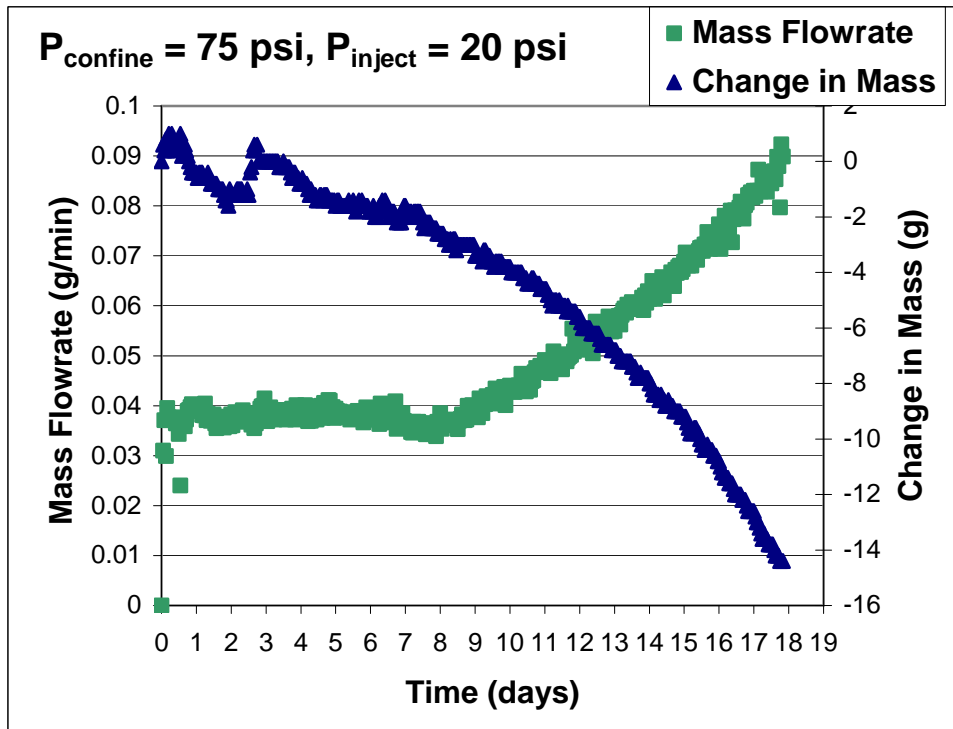


Figure 2.10: Gas Injection Data for N₂ through Canyon Coal Core CC2

The collected data indicates that drying was occurring within the core at high flow rates, resulting in a corresponding increase in mass flow rates. Notice in **Figure 2.10**, the flow rate is fairly constant for eight days, before suddenly increasing at a near linear rate. At this same time period, the mass of the core begins to decrease at an increasing rate. It is believed this change in flow behavior was due to excessive drying within the core. A water balance was maintained by collecting effluent moisture in order to ensure that decreases in core mass were contributed to water loss, which was confirmed to be the case for this trial. This provides strong evidence that moisture content has a direct relationship on the mass transfer rate of gas through intact coal. In order to observe changes in mass due to gas sorption and desorption, it was subsequently necessary to reduce the effects of drying. This was attempted through lowering injection flow rates, by decreasing injection pressure, and adequately hydrating the injection gas before reaching the core.

A summary of the mass flow data for nitrogen through Canyon coal samples, collected at two confining pressures and an injection pressure of 20 psi, is shown in **Table 2.6**. **Table 2.7** lists the corresponding data for the Smith coal sample. Note that the flow rates and permeability for the Smith coal sample are several orders of magnitude higher than those measured for the Canyon coal samples. Although this significant difference may be in part due to the different coal origins, it is the authors' opinion that a more likely reason for the difference is the inherent heterogeneity of coal, including the presence of fractures that may act as preferential flow paths. This stresses the importance of testing multiple coal samples before attempting to characterize an entire coal seam.

Table 2.6: Summary of N₂ Flow Characteristics in Canyon Coal Samples

Confining Pressure:	50	75	psi
Mass Flow Rate:	0.09-0.11	0.03-0.05	g/min
Mass Flux:	28-35	9-16	kg/day-m ²
Permeability:	6.9-7.9	2.3-3.7	Darcy

Table 2.7: Summary of N₂ Flow Characteristics in Smith Coal Sample

Confining Pressure:	50	psi
Mass Flow Rate:	0.12-0.14	g/min
Mass Flux:	99-115	kg/day-m ²
Permeability:	5.9-6.5	Darcy

In subsequent trials, methane, carbon dioxide and nitrogen were injected in succession through one Canyon coal core in order to compare mass flow rates of the three gases. The collected mass flow data is show in **Figure 2.11**. A summary of the flow characteristics for the multi-gas injection is shown below in **Table 2.8**. By normalizing to water loss from the core, the adsorption of gas within the coal was also successfully quantified, as shown in **Figure 2.12**.

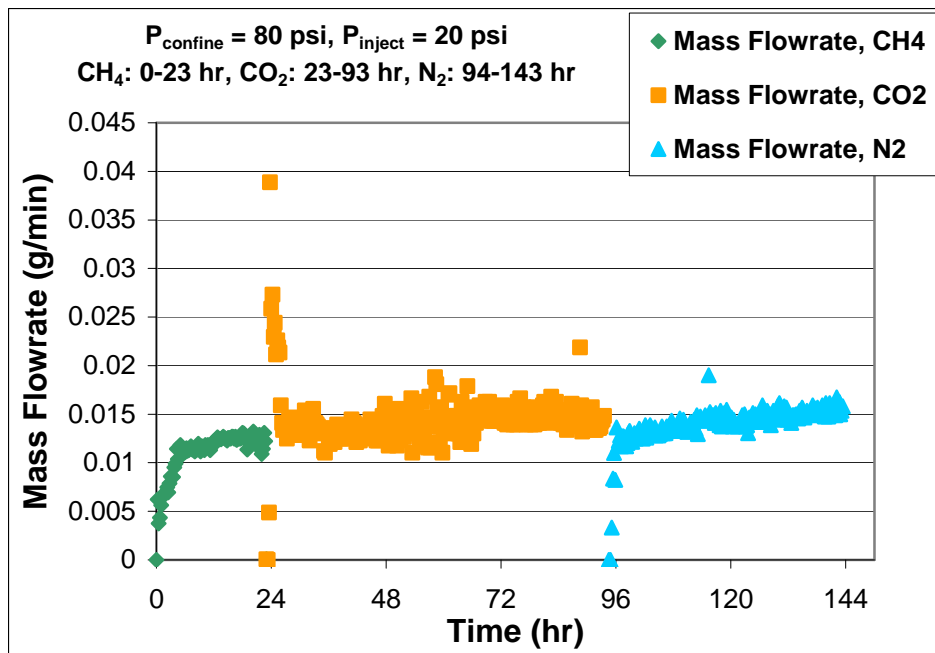


Figure 2.11: Flow Injection Data for CH₄, CO₂, and N₂ through Canyon Coal Core CC1

Table 2.8: Summary of Multi-Gas Flow Characteristics in Canyon Coal Sample

Gas:	CH ₄	CO ₂	N ₂	
Confining Pressure:	80	80	80	psi
Mass Flow Rate:	0.007-0.012	0.012-0.016	0.012-0.015	g/min
Mass Flux:	3.1-4.2	3.9-5.2	3.8-5.1	kg/day-m ²
Permeability:	0.09-0.11	0.32-0.39	0.39-0.42	Darcy

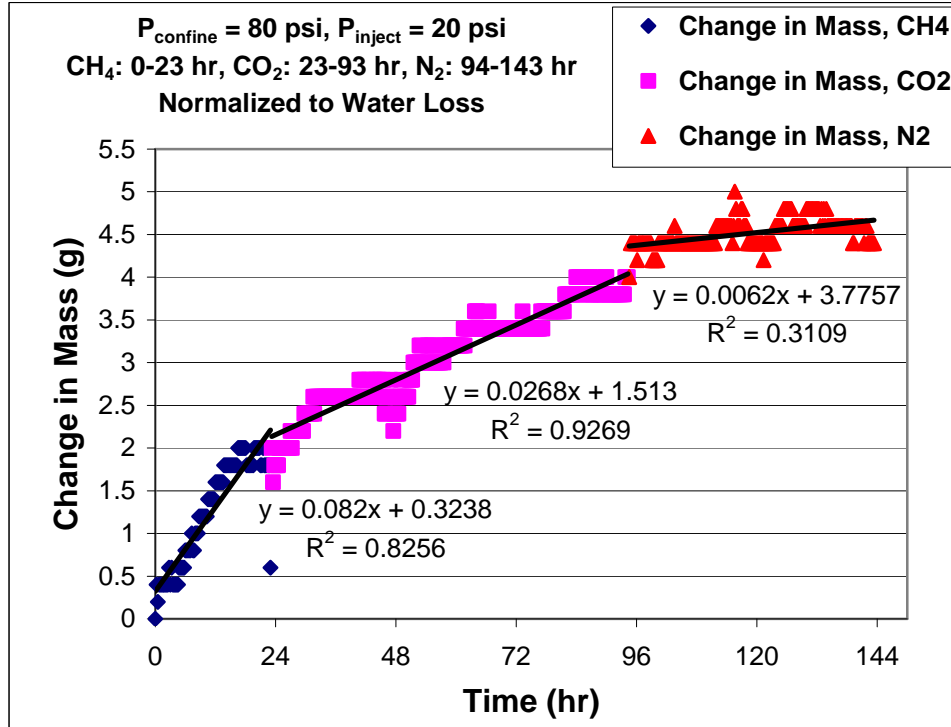


Figure 2.12: Gas Sorption Data for CH₄, CO₂, and N₂ in Canyon Coal Core CC1

As can be seen in **Figure 2.11** and **Table 2.8**, the mass flow rate through the core remained fairly constant between the three injected gases. However, the mass flow rate of CH₄ and the corresponding coal permeability were slightly lower than those measured with CO₂ and N₂. It should also be noted that all the values are roughly one-tenth of those collected during previous experiments, showing the inherent heterogeneity between different cores. Comparisons to available literature show the experimentally determined values to be several orders of magnitude higher than expected. Research on Japanese coal cores resulted in permeabilities ranging from 0.2-15 md (Sasaki and Jujii, 2005). However, these experiments were completed at significantly higher confining pressures, suggesting that the lower overburden pressures of the present work, and the subsequent opening of coal cleats, may explain increased permeabilities. Permeability data determined from field conditions by Gunter et al. (Gunter et al., 2004) was also reported in the range of 0.1-100 md. This suggests that the current research apparatus may not be directly applicable to in-situ conditions until data at higher pressure regimes are collected.

The data in **Figure 2.12** suggests that there is a substantial difference in the rate of adsorption between the three gases. This shows that the developed experimental system has the precision to measure gas sorption, assuming that drying effects are properly managed. It is difficult to draw direct results from this data, however, as it is expected that methane is leaving the core during the carbon dioxide and nitrogen injections, which would result in a lower increase in mass during this time period. From this data, it was realized that it would be necessary to analyze the composition of the effluent gas in order to more fully understand any exchange taking place within the coal. It was decided to use a gas chromatograph (GC) to analyze the effluent stream at periodic intervals during subsequent experiments. Unfortunately, follow-up flow-through

experiments did not result in successful data due to mechanical failure of the flow meters and the impermeable nature of several of the sample specimens at the applied injection pressure.

Sorption isotherms

Experimental trials were completed with the purpose of measuring gas adsorption isotherms for the intact coal samples. During the first adsorption trial, methane gas was injected into a Canyon coal core at 10 psi until the increase in mass, directly representing the adsorbed gas, reached a relatively constant value. The injection pressure was then increased to 20 psi and the core was again allowed to reach equilibrium. This process was continued in 10-psi increments up to a final pressure of 70 psi (10 psi below the confining pressure of 80 psi). Following the CH₄ adsorption isotherm, CO₂ was injected into the same core, beginning again at an injection pressure of 10 psi with subsequent increases as 10-psi steps. The gravimetric adsorption isotherms for these trials are shown in **Figure 2.13**.

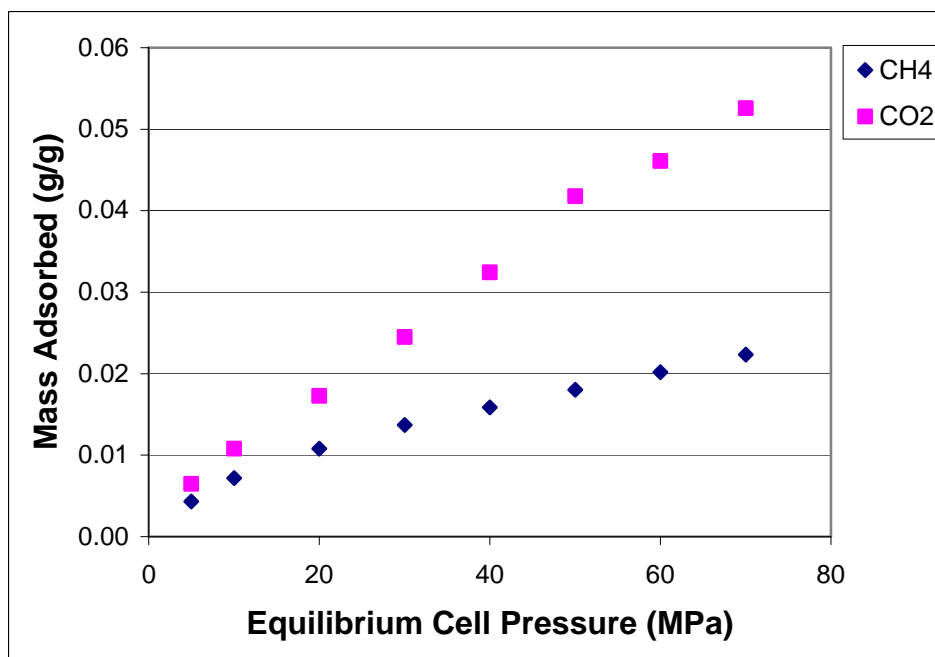


Figure 2.13: Gravimetric Adsorption Isotherm for CH₄ and CO₂ in Canyon Coal

Figure 2.13 shows that, on a mass per mass basis, CO₂ was adsorbed at a greater rate than CH₄, which agrees with results expected from the current body of knowledge on coal sorption. The amount of carbon dioxide adsorption on a mass basis was slightly more than twice that of methane. This is unexpected, as it is well known that subbituminous coals generally show a strong preference for sorption of CO₂ over CH₄, with ratios of CO₂ to CH₄ as high as 10 to 1. At this time, numerical models have not been matched to the collected data. As such, the results are inconclusive regarding sorption capacities of the sampled coals. Effluent samples were collected during the adsorption isotherm experiments at periodic intervals, typically coinciding with the increasing of the injection pressure. However, the results of the GC analysis are also inconclusive, showing no apparent trends regarding the exchange of CO₂ and CH₄ within the

samples. The reason for this is believed to be inadequate sampling rates during the duration of the experiment.

Limitations

Permeability data obtained from the current research is inherently on the low end of permeabilities that could be expected from the sampled coal seams as a direct result of the methodology imposed. In order to place a specimen within the core holder, the core had to be intact enough to be cut to shape and mounted within the permeameter. As a result, more fractured samples were not tested due to the fact they were not large enough to be situated in the core holder. The larger pieces of coal typically had fewer fractures than the more fragmented smaller pieces, and since permeability is dependent on the cleat system, there is a bias in the experiment results due to the sample size.

The Trautwein permeameters used in this research had a pressure limitation of roughly 100 psi. As a result, examination of the transport kinetics of intact coal was not completed at pressures above 80 psi due to fear of equipment failure. Additionally, imperfections in the coal cores tended result in rips in the confining rubber sleeve at upper end pressures. Despite this pressure limitation, the resulting data is still considered an accurate representation of in-situ conditions that may exist in shallow coal seams within the PRB. However, it will be necessary to develop a new core holder for this apparatus in order to examine higher pressures more relevant to deeper coal seams. Additionally, the permeability of several cores examined in this research was so low that flow could not be established through them at the working pressures of the developed device. Therefore, in order to measure permeabilities of a wider range of cores, including highly intact cores with minimal fractures present, the experimental system will need to be modified in order to apply higher injection pressures.

Conclusions and Recommendations

The measurement of gas transport kinetics provided limited results that can be applied to characterizing Powder River Basin coal. Coal permeabilities measured with the flow-through apparatus ranged from 0.09 to 7.9 Darcy, which is considerably higher than separately reported values. The mass transfer rates of CH₄, CO₂ and N₂ were found to be relatively constant across individual coal cores. Additionally, gas adsorption isotherms confirmed that coal has a preference for adsorbing CO₂ over CH₄, although not to the degree expected.

During the course of this research period, it was attempted to construct an apparatus that could accurately and consistently measure gas flow rates, and corresponding coal permeabilities, of intact coal cores. Additionally, it was conceived that this device could be used to measure gravimetric adsorption isotherms. In meeting these objectives, the results are mixed. Permeability results from this research are significantly higher than expected from data published elsewhere regarding low-grade coals. However, results between individual trials show strong consistency. At the low pressure regimes in which these experimental trials were completed, it is not unreasonable to assume the reported data to be representative of the sampled coals. Due to limited quantities of sampled cores, and several mechanical failures of testing equipment that

resulted in unusable data, it was not possible to check the consistency of these results to an adequate degree.

SUMMARY AND CONCLUSIONS

Summary of Experimental Results

The total porosity of intact, water-saturated coal cores from Canyon coal seam and Smith coal seam in the Powder River Basin were found to be 39.6% and 38.5%, respectively. This can be expressed as a total pore volume of 0.31 cm³/g for Canyon coal and 0.27 cm³/g for Smith coal. The results of the water adsorption isotherms obtained from glycerol-water solutions in a controlled environment indicate that the pore volume of the Canyon coal can be subdivided into 17.7% microporosity, 19.2% mesoporosity and 63.1% macroporosity. Similarly, the Smith coal total porosity is made up of 19.5% microporosity, 17.0% mesoporosity, and 63.5% macroporosity.

Data collected using the developed flow-through apparatuses for injecting CO₂, CH₄ and N₂ while maintaining a mass balance on intact core coals showed that mass transfer rates of the three gases were relatively constant across individual coal cores. Coal permeabilities ranged from 0.09 to 7.9 Darcy. The results of gas adsorption isotherms, as well as analysis of the effluent stream, were inconclusive.

Conclusion

Using glycerol-water solutions to determine the pore size distribution of coal samples, and subsequently the microporosity composition, was found to be a simple but effective experimental procedure. The method has the advantages of involving no toxic or corrosive substances, as well removing the potential for damage to the delicate micropore structure that is possible with gas and mercury intrusion techniques. Due to the unforeseen length of time required to complete the experiment, however, repeated trials could not be completed to test the reliability of the procedure for additional samples. There was significant consistency between the triplicate samples used for the Canyon and Smith coals, suggesting minimal error in the methodology.

Despite the limited amount of data collected from the coal permeameter apparatuses, there is considerable promise that significant amounts of meaningful data can be collected from these devices. In order for this to be accomplished, several issues will need to be addressed. The delivery method of the injection gas must be rethought so as to prevent damage to the differential sensors in the flow meter, which ultimately deemed much of the collected data unusable. The ability to apply higher injection pressures, as well as to increase the pore pressure within the core holder needs to be adequately addressed. Additionally, it is recommended that effluent gas be analyzed in-line during the entire course of the experimental trials in order to gain an accurate picture of the exchange of gases occurring within the coal specimens. Despite these shortcomings, the developed apparatuses have been proven capable of measuring gas kinetic characteristics and sorption/desorption processes within intact coal cores. In order to more fully understand in-situ gas-water-coal interactions at the field scale, it is imperative that research be

continued on intact coal that maintains the extensive fracture network and moisture content present at field scale.

Recommendations for Future Research

There is no short path to understanding the highly variable, extremely complicated substance that is coal. Nor is there an easy solution with regards to characterizing and predicting the physical and chemical processes that occur within coal during CBM extraction. As one question is answered, many more arise. Despite the considerable amount of research currently underway, there are still many unknowns regarding coal and CBM production. This paper has explored new methods for quantifying gas permeabilities in intact coal and examining the microstructure of the coal matrix. Yet this research has merely opened the door to numerous research possibilities and directions. Below is a short summary of several topics that could, and quite probably should, be pursued in the near future.

Modeling (model matching to collected data)

The ability to collect meaningful data is only the first step in understanding the complicated phenomena that occurs in underground coal seams during CBM production and gas transport. In order to ultimately predict gas storage capacities, methane and water production, reinjectivity of produced water and potential CO₂ sequestration, accurate models must be matched to experimentally collected data. Modeling provides a means of extrapolating laboratory data in the first steps towards pilot and field scale applications. Langmuir-type models have previously been matched to laboratory and field scale data with considerable accuracy (Shimada et al., 2005; Clarkson et al., 1997). Other research suggests that the extended Langmuir model or IAS theory of Myers and Prausnitz (1965) may provide more accurate means of modeling adsorption data (Clarkson and Bustin, 2000). Now that an experimental apparatus has been developed that has the potential for characterizing a great deal of intact coal samples, modeling of that data is the logical next step towards understanding the gas-water-coal interactions.

Continuation of microporosity research

Water adsorption isotherms have been shown to be a valuable tool for characterizing the microstructure of coal samples. However, time limitations prevented confirmation of the reported data as well as completion of full adsorption/desorption cycles for initially dry and initially saturated samples. It is recommended that this line of research be completed, as well as additional trials initiated for the purpose of examining repeatability. The use of smaller samples may result in decreased procedural time requirements; however, adequate care and judgment should be utilized to ensure the sample sizes are reasonable representations of the varying coal structure. The development of an air exchange system that would force increased airflow of the humidity-controlled environment across the coal samples may also lead to decreased trial lengths.

Porosity characterization by conventional methods

The use of water adsorption isotherms obtained from controlled humidity environments is a fairly unconventional method for examining the micropore structure of coal. Additionally, it has the potential advantage of being less destructive than traditional techniques. However, traditional analysis of the same samples subjected to water adsorption isotherms in the present work could potentially provide useful correlations that could ultimately be used to derive improved pore size distributions from the wealth of data currently existing. Nitrogen BET surface area, mercury porosimetry, and helium displacement would all help to further understand the pore volume, pore size distribution and surface area of PRB coals, as well as providing a basis for comparing data collected from the water adsorption technique illustrated in this work. The detailed procedures and correlations between measured data from coal samples have been described in detail by many authors (White et al., 2005; Fischer et al., 2005; Clarkson and Bustin, 1999; Reucroft et al., 1987; Kloubek 1994; Clarkson et al., 1997).

Quantify swelling (implementation of strain gauges)

It is well known that the sorption and desorption of different gases causes swelling and shrinking of the coal matrix (White et al., 2005). There is research suggesting that permeability decreases due to depressurizing of a coal seam, due to subsequent cleat closure, may be lessened by the shrinking of the coal matrix caused by methane desorption (Cui and Bustin, 2005). Other research suggests that the swelling caused by CO₂ injection is considerably greater than the shrinking caused by CH₄ desorption within intact coal samples, leading to net decreases in permeability [P10]. Strain gauges have been successfully utilized in experimental trials to quantify the extent of swelling and shrinking that occurs within intact coal samples during gas sorption and desorption (Cui and Bustin, 2005; Wolf et al., 2004; Wolf et al., 2000; Xue and Ohsumi, 2004). The inclusion of strain gauges into gas injection experiments has the potential to help quantify the extent of swelling/shrinking during exposure to CO₂, CH₄ and N₂. Data of this nature could also help explain changes in flow rates and permeability that occur during gas transport.

X-ray image analysis

New technologies are continuing to emerge that can be applied towards characterizing coal properties and gas-coal interactions. Research involving the use of transmission electron microscopy and CT-scans for examining the cleat system of intact coal cores has shown promising results (Bossie-Codreanu et al., 2004; Wolf et al., 2004; Karacan and Okandan, 2001). Internal imaging techniques can prove an invaluable method of examining the matrix and cleat composition of intact coal samples. Ultimately, it may be possible to incorporate such a technology into an experimental gas injection apparatus in order to obtain a complete picture of changes within coal structure during sorption, desorption, and gas injection.

REFERENCES

- Bossie-Codreanu, D., Wolf, K.H.A.A., and Ephraim, R., 2004.** “A New Characterization Method for Coal Bed Methane.” *Geologica Belgica*, 7/3-4, pp. 137-145.
- Budwill, K., Bustin, M., Muehlenbachs, K. and Gunter, B., June 2001.** “Biogenic Methane Production from Coal with Implications for Carbon Dioxide Sequestration.” Proceedings from Rock the Foundation Convention, 18-22, Canadian Society of Petroleum Geologists.
- Budwill, K., Nov. 2003.** Alberta Research Council, Edmonton, Canada. “Microbial Methanogenesis and its Role in Enhancing Coalbed Methane Recovery.” CSEG Recorder, pp. 41-46.
- Clarkson, C.R. and Bustin, R.M., 1999.** “The Effect of Pore Structure and Gas Pressure Upon the Transport Properties of Coal: A Laboratory and Modeling Study. 1. Isotherms and Pore Volume Distributions.” *Fuel*, 78, pp. 1333-1344.
- Clarkson, C.R. and Bustin, R.M., 2000.** “Binary Gas Adsorption/Desorption Isotherms: Effect of Moisture and Coal Composition upon Carbon Dioxide Selectivity over Methane.” *International Journal of Coal Geology*, 42, pp. 241-271.
- Clarkson, C.R., Bustin, R.M. and Levy, J.H., 1997.** “Application of the Mono/Multilayer and Adsorption Potential Theories to Coal Methane Adsorption Isotherms at Elevated Temperature and Pressure.” *Carbon*, Vol. 35, pp. 1689-1705.
- Cui, X., and Bustin, M., Sep. 2005.** “Volumetric Strain Associated with Methane Desorption and Its Impact on Coalbed Gas Production from Deep Coal Seams.” *AAPG Bulletin*, v.89, no.9, pp. 181-1212.
- EPA 816-R-04-003, June 2004.** “Attachment 5 the Powder River Basin.” Evaluation of Impacts to Underground Sources of Drinking Water by Hydraulic Fracturing of Coalbed Methane Reservoirs.
- Fischer, H., Morrow, N.R., and Mason, G., May 26-28, 2005.** “Water Adsorption/Desorption Isotherms for Characterization of Microporosity in Sandstones and Carbonate Rocks.” Proceedings of the 7th International Symposium on the Characterization of Porous Solids (COPS-VII), Aix-en-Provence, France, pp. 295-302.
- Gunter, W.D., Mavor, M.J., and Robinson, J.R., Sep. 5-9, 2004.** “CO₂ Storage and Enhanced Methane Production at Fenn-Big Valley, Alberta, Canada, with Application.” Proceeding of the 7th International Conference on Greenhouse Gas Control Technologies, Vancouver, Canada.
- Karacan, C.O. and Okandan, E., 2001.** “Adsorption and Gas Transport in Coal Microstructure: Investigation and Evaluation by Quantitative X-Ray CT Imaging.” *Fuel*, v.80, pp. 509-520.

- Kloubek, J., 1994.** “Investigation of Porous Structures Using Mercury Reintrusion and Retention.” *Journal of Colloid and Interface Science*, v.163, pp. 10-18.
- Larsen, J.W., 2004.** “The Effects of Dissolved CO₂ on Coal Structure and Properties.” *International Journal of Coal Geology*, v. 57, pp. 63-70.
- Melrose, J.C., Aug. 1998.** “Use of Water-Vapor Desorption Data in the Determination of Capillary Pressures at Low Water Saturations.” *SPE Reservoir Engineering*, pp. 913-918.
- Nummedal, D., April 19, 2004.** “CERI/CSM Proposal No.: 7310 in Response to DOE-NETL Solicitation No.: DE-PS26-04NT15460-02 Produced Water Management and Beneficial Use Area of Interest 2.”
- Reeves, S., July 14, 2003.** “Enhanced CBM Recovery, Coalbed CO₂ Sequestration Assessed.” *Oil & Gas Journal*, pp. 49-53.
- Reeves, S., Sep. 30–Oct. 3, 2001.** “Geological Sequestration of CO₂ in Deep, Unmineable Coalbeds: An Integrated Research and Commercial-Scale Field Demonstration Project.” *SPE 71749, Proc. Annual Tech. Conference and Exhibition*.
- Reucroft, P.J. and Sethuraman, A.R., 1987.** “Effect of Pressure on Carbon Dioxide Induced Coal Swelling.” *Energy & Fuels*, Vol.1, pp. 72-75.
- Romanov V.N., Goodman A.L. and Larsen J.W., 2006.** “Errors in CO₂ Adsorption Measurements caused by Coal Swelling.” *Energy & Fuels*, Vol.20, No.1, pp. 415-416.
- Sasaki, K. and Fujii, T., 2005.** “Adsorption Characteristics of CO₂ Gas Permeability of Coal Samples for CO₂ Sequestration into Japanese Coal Seams”, *Proc. Of 7th Int. Conf. On Green House Gas Control Technology (GHGT7)*, Elsevier, pp.2257-2261.
- Shi, J.Q., Durucan, S. and Syhrial, E., 2004.** “Reservoir Depletion Induced Changes in Coalbed Permeability and Implications for Enhanced CBM Recovery Using CO₂ Injection.” *Geologica Belgica*, 7/3-4, pp. 123-127.
- Shimada, S., Li, H., Oshima, Y. and Adachi, K., 2005.** “Displacement Behavior of CH₄ Adsorbed on Coals by Injecting Pure CO₂, N₂, and CO₂-N₂ Mixture.” *Environ Geol*, 49, pp. 44-52.
- Stanton, R., Flores, R., Warwick, P.D., Gluskoter, H., and Stricker, G.D., May 14-17, 2001.** “Coal Bed Sequestration of Carbon Dioxide.” *Proceedings from the 1st National Conference on Carbon Sequestration*, National Energy Technology Laboratory, Washington D.C.
- The Casper Star-Tribune, March 19, 2006.** “By the Numbers: Wyoming and Montana.” Online.

- White, C.M., Smith, D.H., Jones, K.L., Goodman, A.L., Jikich, S.A., LaCount, R.B., DuBose, S.B., Ozdemir, E., Morsi, B.I., and Schroeder, K.T., May-June 2005.** “Sequestration of Carbon Dioxide in Coal with Enhanced Coalbed Methane Recovery – A Review.” *Energy & Fuels*, v.19, no.3, pp. 659-724.
- Wolf K.H.A.A., Barzandji, O.H.M., Bertheux, W. and Bruining, J., Aug. 13-16, 2000.** “CO₂-Sequestration in the Netherlands. CO₂-Injection and CH₄-Production as Related to the Dutch Situation: Laboratory Experiments and Field Simulation.” *Proc. 5th Int. Conf. on Greenhouse Gas Control Technologies*, Cairns, Australia, pp. 1-6.
- Wolf, K.H.A.A., Barzandji, O.H.M., Bruining, J., and Ephraim, R., May 2001.** “CO₂ Injection in and CH₄ Production from Coal Seams: Laboratory Experiments and Image Analysis for Simulations.” *Proceedings of the 1st National Conference on Carbon Sequestration*, 15-17, Washington DC.
- Wolf, K.H.A.A., Bossie Codreanu, D., Ephraim, R. and Siemons, N., 2004.** “Analyzing Cleat Angles in Coal Seams Using Image Analysis Techniques on Artificial Drilling Cuttings and Prepared Coal Blocks.” *Geologica Belgica*, 7/3-4, pp. 105-113.
- Wolf, K.H.A.A., Siemons, N. and Bruining, J., 2004.** “Multiphase Flow Experiments in Order to Understand the Behavior of (Partly) Saturated Coals as a Gas Reservoir: Examples.” *Geologica Belgica*, 7/3-4, pp. 115-121.
- Xue, Z., and Ohsumi, T., Sep. 5-9, 2004.** “Coal Matrix Swelling caused by Adsorption of Carbon Dioxide and its Impact on Permeability.” *Proc. 7th Int. Conf. on Greenhouse Gas Control Technologies*. Vancouver, Canada, pp. 2253-3356.

**CHAPTER 3:
Hydraulic Fracture Growth from Water Enhancement Tests
in the Powder River Basin, Wyoming: Implications
for Coalbed Methane Water Management**

Mark Zoback, Hannah E. Ross and L. B. Colmenares¹

EXECUTIVE SUMMARY

Large quantities of water are associated with the production of coalbed methane (CBM) in the Powder River Basin (PRB), Wyoming, and this water has high saline and sodium contents, making it unsuitable for agricultural use and environmentally damaging. In order to determine if there are ways for CBM operators to produce less CBM water we have evaluated CBM wellbore completion methods in the PRB. We have found that CBM operators in the PRB routinely carry out water-enhancement on their wells, where water-enhancement procedures are used to connect the coal cleats to the wellbore to increase gas production. Operators in the PRB are routinely fracturing the coal through this water-enhancement process (Colmenares and Zoback, 2007). We analyzed ~200 water-enhancement tests from CBM wells in the PRB in order to determine the magnitude of the least principal stress and the orientation of hydraulic fracture growth. We find that both horizontal and vertical hydraulic fractures are created and that some wells with vertical hydraulic fractures produce excessive volumes of CBM water.

The creation of both vertical and horizontal hydraulic fractures implies that the magnitude of the least principal stress is varying throughout the basin and this has lead us to define three different stress states in the PRB: areas that have active normal faults, areas that are slightly more compressive (either normal or strike-slip stress regimes) and finally, areas with reverse faulting regimes. We observe that for the Big George coal, wells with excessive water production are within normal faulting areas, suggesting that vertical hydraulic fractures in communication with normal faults may play a role in the water production.

GOALS AND OBJECTIVES

The goals of this research are to better understand the way in which wellbore completion practices affect the quantity of coalbed methane (CBM) waters that are co-produced with CBM in the Powder River Basin. To determine if water enhancement activities carried out routinely as part of wellbore completion practice cause hydraulic fracturing of overlying strata, data from about 500 wells will be examined. The objectives are to determine with certainty whether well completion practice induces hydraulic fracturing of the adjacent strata (and hence water production from adjacent formations).

¹ Department of Geophysics, Mitchell Building Room 347, Stanford University, Stanford, CA 94305-2215. Correspondence: zoback@stanford.edu.

INTRODUCTION

Coalbed methane (CBM) production in the Powder River Basin (PRB) is accompanied by the production of large volumes of CBM water (**Figure 3.1**). In 2006, ~590 million barrels (bbl) of CBM water were produced (an average of ~100 bbl/well/day) (WOGCC, 2006). The water quality is generally sufficient for drinking and livestock use, however the saline and sodium contents are too high for agricultural use (Wheaton and Donato, 2004; Bartos and Ogle, 2002; The Ruckelshaus Institute of Environment and Natural Resources, 2005). The high saline and sodium content of the CBM water causes a reduction in soil permeability because the ions precipitate out of solution and are deposited within the soil. This in turn reduces the productivity of the soil and can cause soil erosion and ultimately damage to wildlife habitats (Wheaton and Donato, 2004). At present, most of the produced water is discharged into evaporation/infiltration ponds or reservoirs (The Ruckelshaus Institute of Environment and Natural Resources, 2005). However, in the eastern part of the PRB, where water quality is reasonably high, CBM water is used for irrigation or discharged directly into streams (The Ruckelshaus Institute of Environment and Natural Resources, 2005).

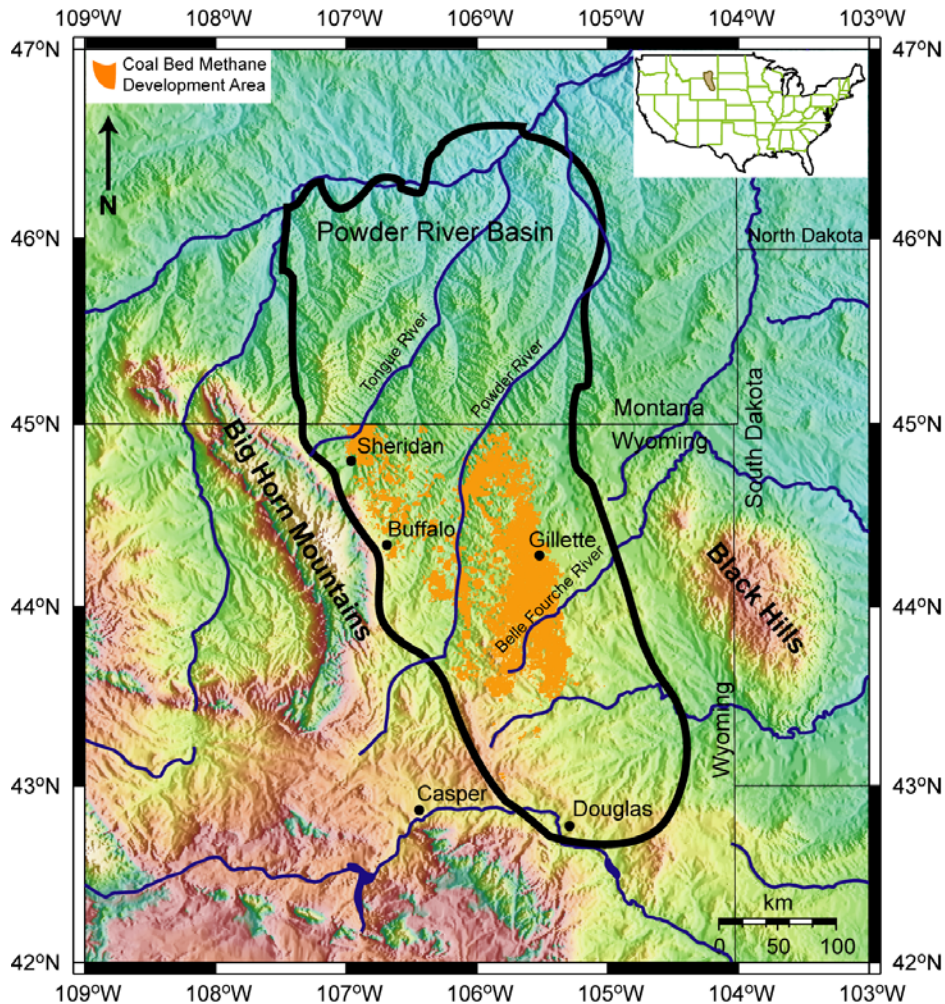


Figure 3.1: Location map of the Powder River Basin, Wyoming (modified from Colmenares and Zoback, 2007). Orange dots correspond to CBM wells.

The goals of this study are to evaluate CBM wellbore completion methods in the PRB to determine if there are ways to produce less CBM water, while still achieving adequate coal depressurization for CBM production. To achieve these goals we have extended the study conducted by Colmenares and Zoback (2007), using water-enhancement tests to map stress across the basin and to understand why water production from some wells is excessive (>7,000 bbl/month), whereas in other parts of the basin water production is manageable.

Colmenares and Zoback (2007) found that CBM operators in the PRB routinely carry out water-enhancement on their wells. Water-enhancement procedures are used to connect the coal cleats to the wellbore to increase gas production, as well as to wash away any drilling fines generated during drilling that may block gas flow to the well. As it turns out, CBM operators in the PRB routinely fracture the coal through water-enhancement. Colmenares and Zoback (2007) analyzed water-enhancement tests from CBM wells to determine which wells had been hydraulically fractured. Using the flow rate and wellhead pressure recorded during water-enhancement they were able to calculate the magnitude of the least principal stress (S_3) in 372 CBM wells and determine the orientation of hydraulic fracture propagation.

Colmenares and Zoback (2007) found that in some areas the hydraulic fractures were propagating horizontally, whereas in other areas the fractures were propagating vertically. In addition, they found that many of the wells with vertical fractures produced excessive volumes of CBM water (~7,000 bbl/month) and little to no methane (CH_4). In the Big George coal, ~70% of all the water produced is from only one third of the total number of wells, all of which are characterized by vertical hydraulic fractures. In contrast, some of the wells with vertical hydraulic fracture propagation produce small volumes of water (<7000 bbl/month) and are very good gas producers (with some delay in gas production). Wells with horizontal hydraulic fractures typically produce small volumes of water but are poor gas producers. Colmenares and Zoback (2007) hypothesize that the vertical fractures associated with the production of large volumes of water actually penetrate overlying sand aquifers. Hence, the operators are draining the aquifers rather than the coals and are unable to efficiently depressurize the coal for CH_4 production.

Colmenares and Zoback (2007) investigated reasons for the apparent correlation between hydraulic fracture orientation and water production. They looked at stratigraphy, coal thickness and coal depth, but found no correlation with any of these factors. Colmenares and Zoback (2007) also tried to understand why S_3 varies throughout the basin (**Figure 3.5** in Colmenares and Zoback (2007)) and concluded that perhaps coal thickness plays a role, as the ratio of S_3 to the overburden stress (S_v) appears to be smaller in thicker coals than in thinner coalbeds. However, this correlation seems to be only truly apparent in the Big George coal, which incidentally contains the largest water producing wells (greater than 20,000 bbl/month) analyzed by Colmenares and Zoback (2007).

We have obtained additional water-enhancement tests from CBM wells in the PRB, to supplement those analyzed by Colmenares and Zoback (2007), in order to better understand why the stress varies throughout the basin and why some wells produce excessive volumes of CBM water (**Figure 3.2**). In this report we outline the method used to determine the orientation of

hydraulic fracture propagation and then report on the fracture orientations obtained from our water-enhancement tests. We also look at the relationship between fracture orientation and gas and water production, where we observe a similar correlation as Colmenares and Zoback (2007). Following this, we define three stress states that we observe to exist in the PRB and show that active normal faults may play a role in fluid migration.

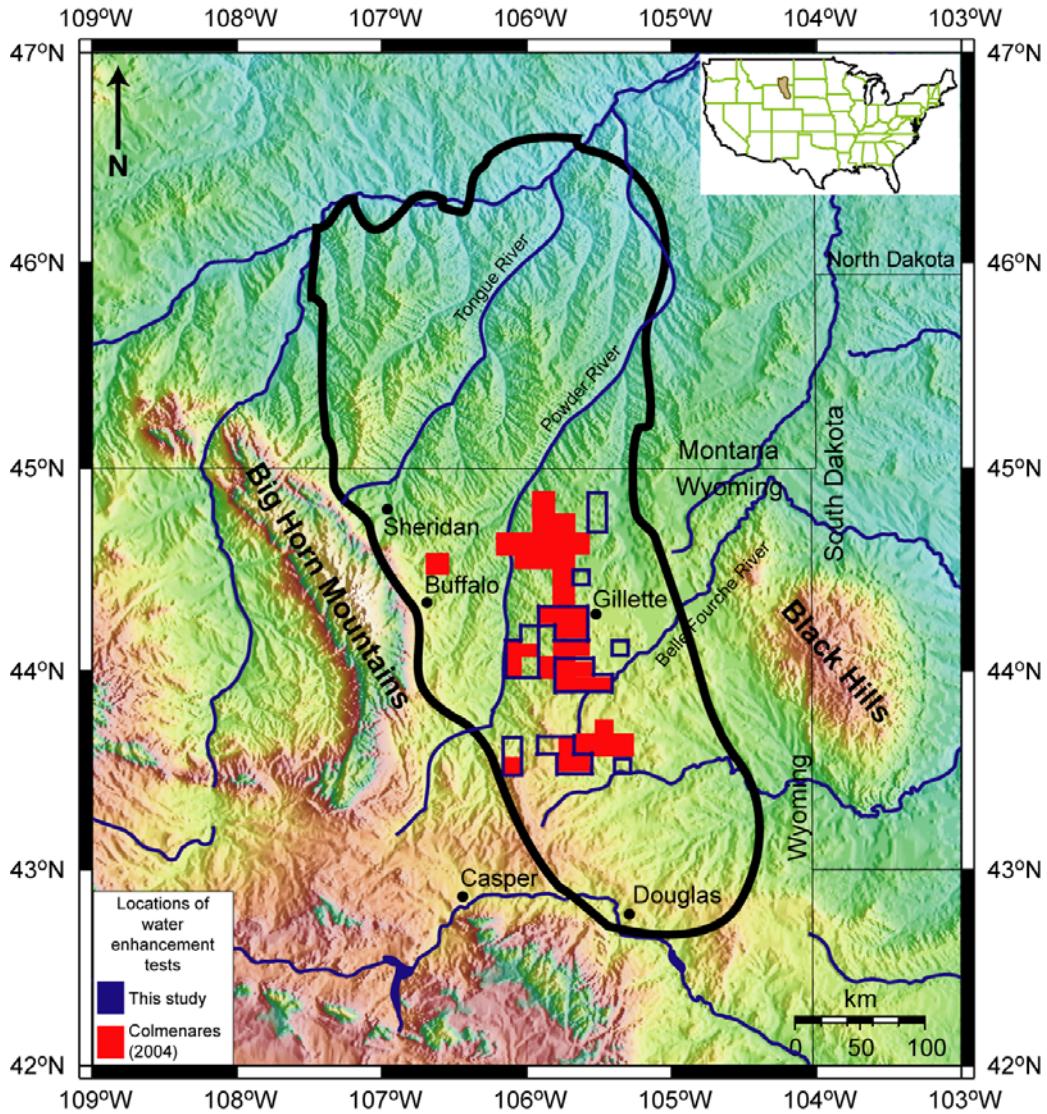
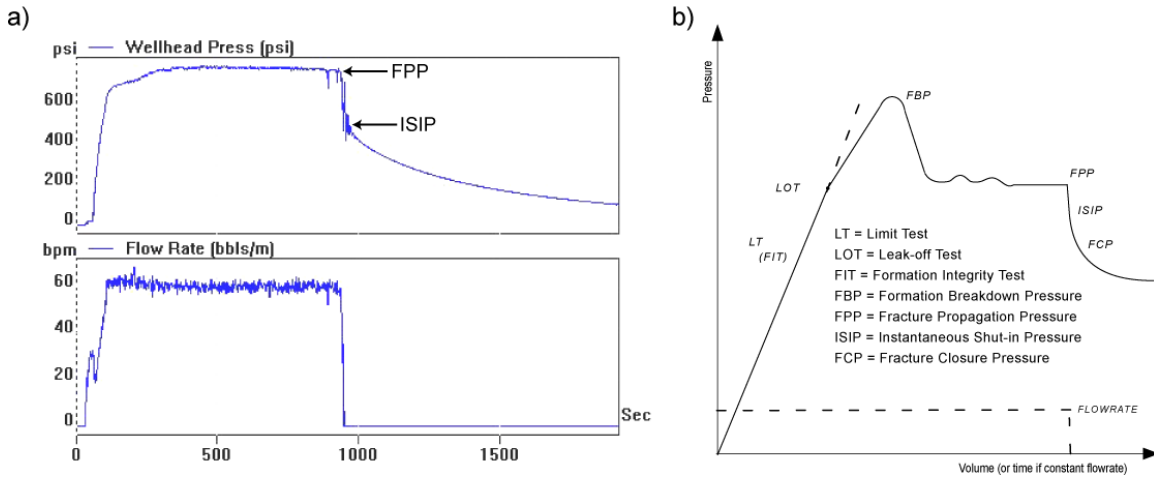


Figure 3.2: Township and range locations of wells with water-enhancements tests analyzed for both this study, in blue, and by Colmenares (2004) and Colmenares and Zoback (2007), in red.

Calculating the Least Principal Stress and Hydraulic Fracture Orientation from Water-Enhancement Tests

During water-enhancement the operators typically pump water into the well at a rate of ~60 barrels per minute (bpm) for approximately 15 minutes. The flow rate and wellhead pressure are measured during the procedure and if the wellhead pressure stays at a constant value, even though a constant rate of water is being pumped into the coal, this indicates that a hydraulic fracture has formed (**Figure 3.3a**) (Colmenares and Zoback, 2007).



Figures 3.3a and 3.3b: a) Water-enhancement test from a CBM well in the PRB. b) Schematic diagram of an extended leakoff test (Zoback et al., 2003). The dashed line diverging from the leakoff test would be the pressure path if no fracture is created. Modified from Colmenares and Zoback, 2007.

Water-enhancement tests from the PRB have similar pressure-time history as extended leak-off tests (Zoback et al., 2003), which means that we can calculate the magnitude of S_3 using the same principals applied to extended leak-off tests. To calculate the magnitude of the least principal stress (S_3) at depth, we take the instantaneous shut-in pressure at the surface and add the pressure from the weight of the column of fluid in the wellbore (**Figure 3.3b**) (Zoback et al., 2003). After obtaining the magnitude of S_3 , we can then determine the orientation of fracture propagation. Hydraulic fractures will open in the direction of S_3 and propagate perpendicular to the orientation of S_3 (Hubbert and Willis, 1957). If S_3 corresponds to the minimum horizontal stress (S_{hmin}) then the fracture will propagate in the vertical plane. However, if S_3 is equal to the overburden stress (S_v), the fracture will propagate in the horizontal direction. To calculate the magnitude of S_v , rock densities are integrated from the surface to the depth of interest, z , where:

$$S_v = \int \rho(z) g dz \cong \bar{\rho} g z \quad (1)$$

and $\rho(z)$ is the density as a function of depth, g is the gravitational acceleration and $\bar{\rho}$ is the mean overburden density. Because density logs are not available for any of the CBM wells analyzed we used a mean overburden density of 2.3 g/cc, which is a reasonable average for the lithological units above the coal in the PRB (interbedded shales and sands).

To determine whether S_3 corresponds to S_v we compare the magnitude of S_3 with the magnitude of the expected overburden stress for the depth of the coal interval in question. In **Figure 3.4** we show the overburden stress gradient and the hydrostatic pore pressure gradient as black and grey lines respectively. If S_3 plots on the overburden line it means that S_3 is equal in magnitude to S_v and horizontal hydraulic fractures have formed. If S_3 plots below the overburden line then the magnitude of S_3 is equal to S_{hmin} and vertical hydraulic fractures have formed. For the wells shown in **Figure 3.4**, vertical hydraulic fractures were created through water-enhancement tests.

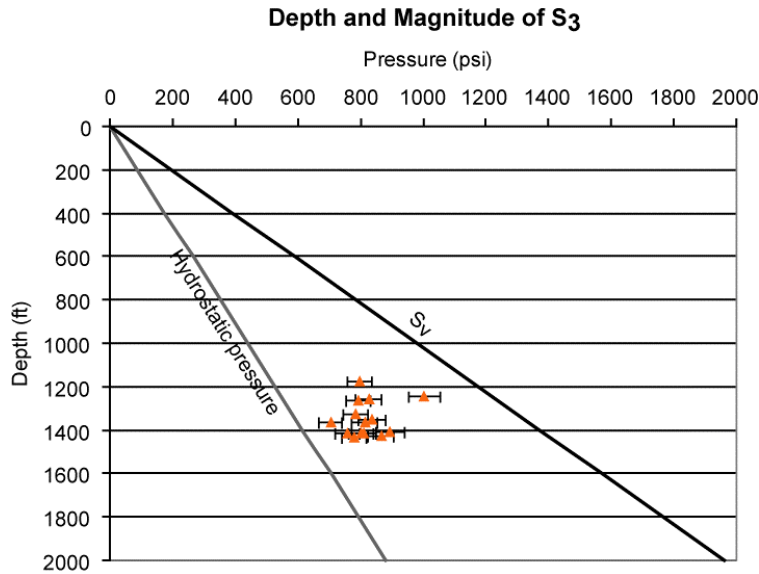
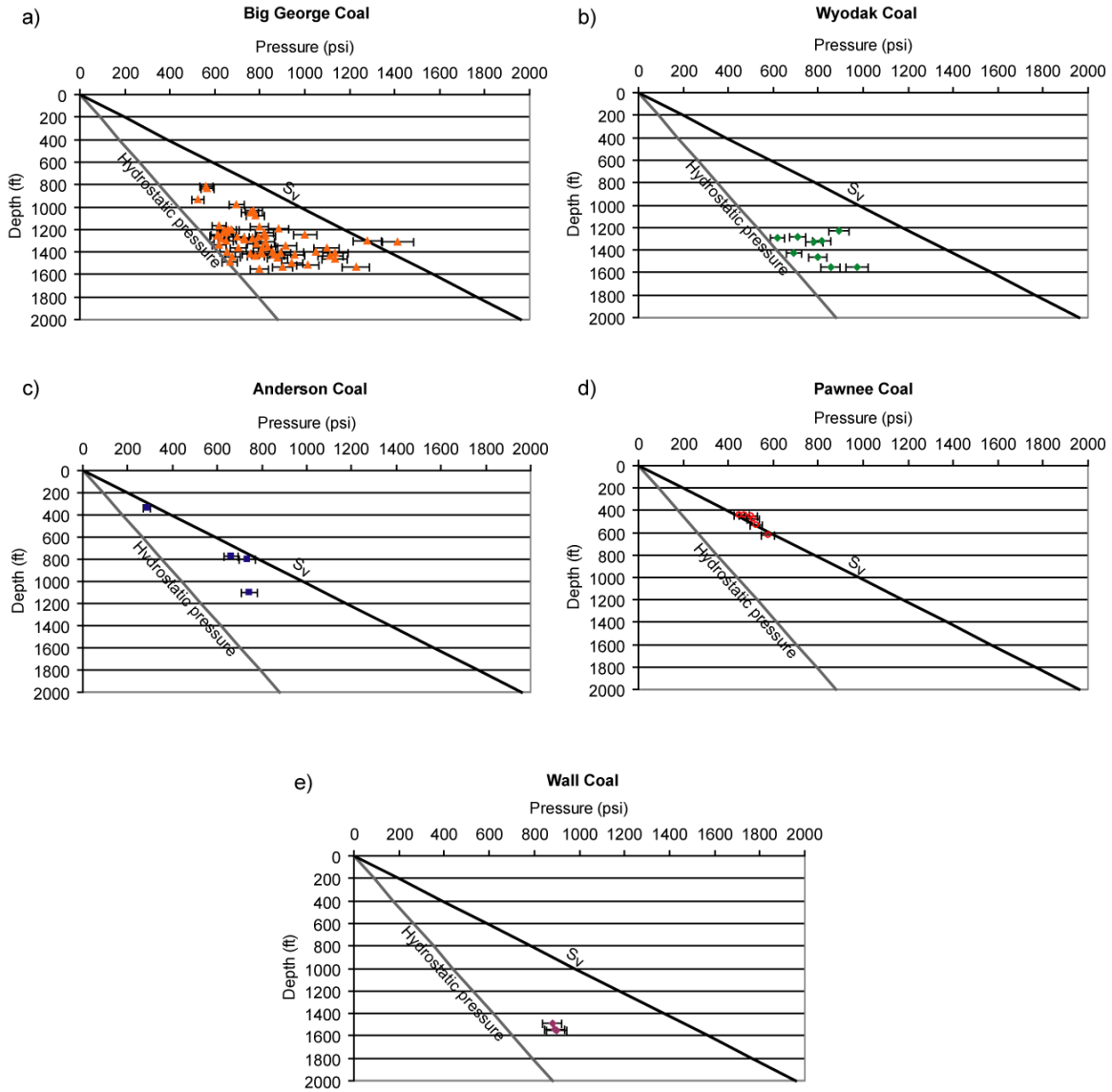


Figure 3.4: Depth versus pressure plot showing the magnitude of S_3 (orange triangles) for the Big George coal. Note that S_3 is less than the overburden stress (S_v) implying that hydraulic fractures created through water-enhancement are vertical. The hydrostatic pore pressure gradient is ~ 0.44 psi/ft.

Water-Enhancement Tests from Cordilleran Compliance Services

We obtained 198 water-enhancement tests from Cordilleran Compliance Services that supplement tests previously available to Colmenares and Zoback (2007) (**Figure 3.5**). An analysis of the 198 wells suggests that 87 were hydraulically fractured during the water-enhancement process and of those 87 wells, 89% have vertical fractures and 11% horizontal fractures (**Figure 3.5**).

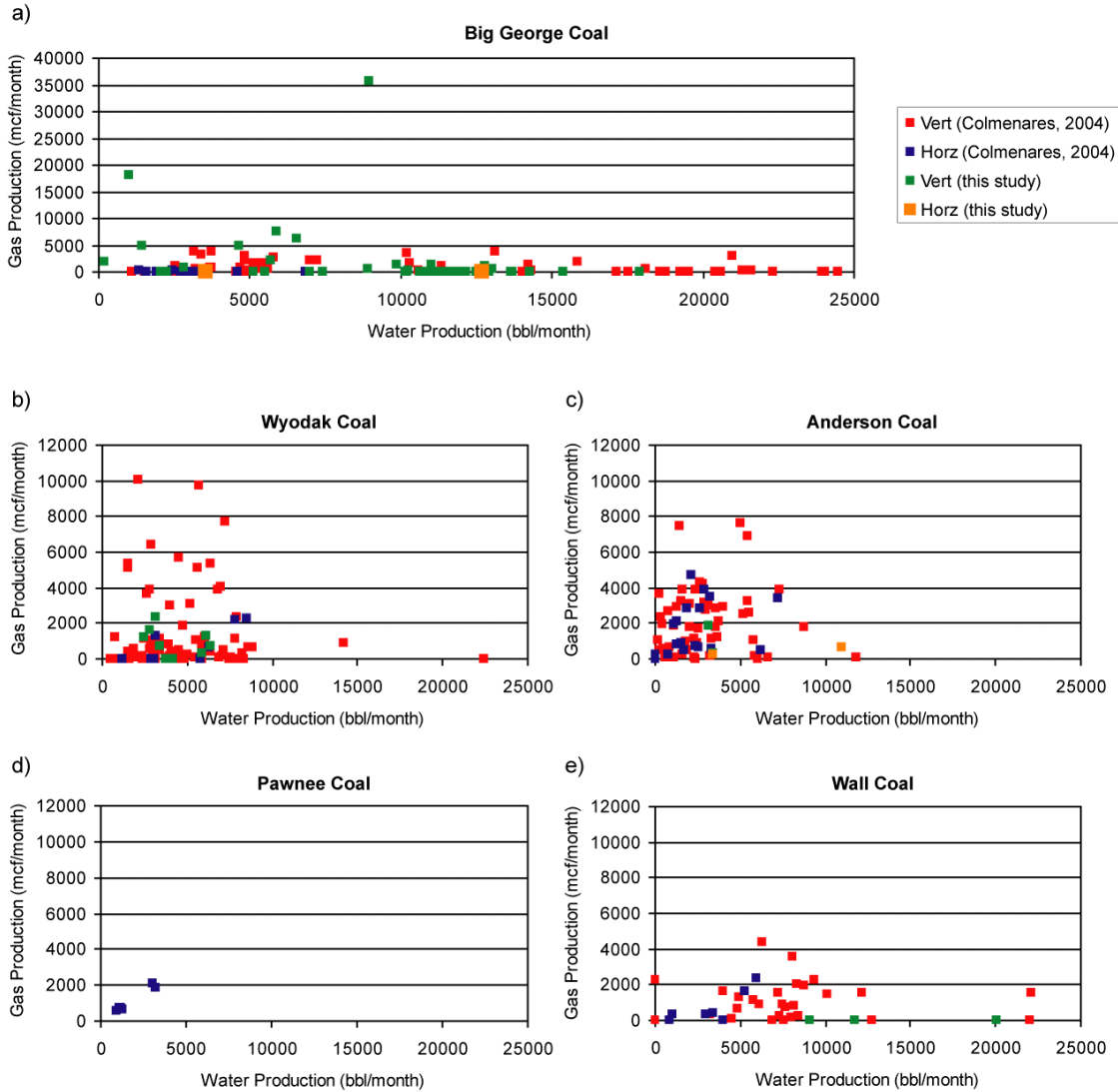


Figures 3.5a through 3.5e: Magnitude of S_3 plotted on pressure versus depth profiles for the a) Big George, b) Wyodak, c) Anderson, d) Pawnee and e) Wall coals. The black line corresponds to the overburden stress (S_v) and the dark grey line corresponds to the hydrostatic pore pressure gradient.

Relationship Between Water Production and Orientation of Hydraulic Fractures

We carried out a similar analysis as Colmenares and Zoback (2007) to see if hydraulic fracture orientation was correlated with CBM water and gas production. We obtained gas and water production data from the Wyoming Oil and Gas Conservation Commission (WOGCC, 2006) for the same CBM wells that we analyzed water-enhancement tests. Our conclusions are similar to Colmenares and Zoback (2007) (**Figure 3.6**), where they found that some CBM wells with vertical fractures produced large volumes of CBM water (~7,000 bbl/month) and little to no gas, whereas CBM wells with horizontal hydraulic fractures produced small volumes of both water and gas. They also found that some CBM wells with vertical fractures produced large volumes of

gas with manageable volumes of water. Our analysis supports their findings, although we do find that three wells with horizontal hydraulic fractures in our data set produce over 7,000 bbl/month (Figures 3.6a and 3.6c). In addition, one of our wells producing from the Big George coal has excessive water production (~9,000 bbl/month), but also produces extremely large volumes of gas (~35,500 mcf/month) (Figure 3.6a).



Figures 3.6a through 3.6e: Gas production versus water production for the a) Big George, b) Wyodak, c) Anderson, d) Pawnee and e) Wall coals. Vert corresponds to wells with vertical hydraulic fractures and horz corresponds to wells with horizontal hydraulic fractures. Points in blue and red come from Colmenares (2004) and Colmenares and Zoback (2007). Points in green and orange are from this study.

Relationship Between Water Production and Normal Faults

We have used Anderson, Coulomb and Byerlee faulting theory (Zoback, 2007) to look at the magnitude of S_3 in relation to the critical magnitude of S_{hmin} required for normal faults to slip.

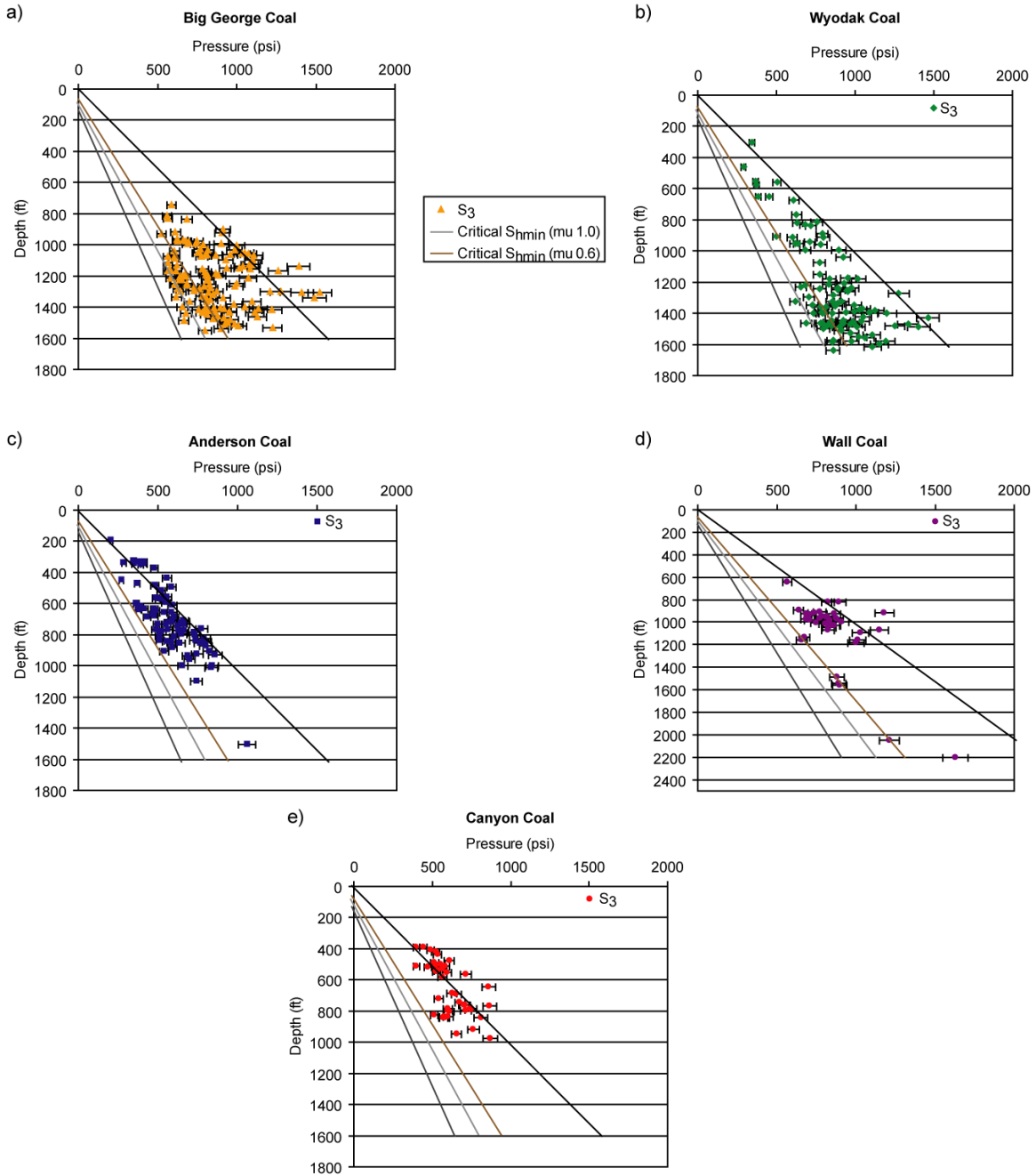
Horizontal hydraulic fractures tell us that S_3 is equal to the overburden stress and according to Anderson faulting theory; we are in a reverse faulting stress regime wherever we have determined that horizontal fractures have formed in the PRB. However, vertical hydraulic fractures tell us that S_3 is less than S_v and therefore we are in either a strike-slip or normal faulting regime. We can use Coulomb faulting theory and Byerlee's law to calculate the magnitude of S_{hmin} that will cause normal faults to slip. The following equation is used in the calculation:

$$\frac{S_v - P_p}{S_{hmin} - P_p} \leq \left[\sqrt{\mu^2 + 1} + \mu \right]^2 \quad (2)$$

where μ is the coefficient of friction, S_v is the overburden stress, S_{hmin} is the minimum horizontal stress and P_p is the pore pressure.

We calculated S_v using equation 1 and determined the P_p from our pore pressure analysis of coals in the PRB in Chapter 4. **Figures 3.7a-e** show S_3 plotted against depth for the Big George, Wyodak, Anderson, Wall and Canyon coals. We can see that for the Big George, Wyodak and Wall coals, some of the wells have least principal stresses that fall within the critical S_{hmin} lines, indicating that normal faults are present and likely to slip in the areas where these wells are located. However, for wells with least principal stresses that fall between the critical $0.6S_{hmin}$ and S_v lines, they could be part of either normal or strike-slip faulting regimes. For the Canyon and Anderson coals there are no normal faults likely to slip in the areas analyzed (**Figures 3.7c and 3.7e**).

This has lead us to define three different stress states in the PRB, areas that have active normal faults, areas that are slightly more compressive (either normal or strike-slip stress regimes) and finally, areas with reverse faulting regimes. **Figure 3.8** is a location map showing the stress state and the coalbed for which this stress state has been determined. We can see from **Figure 3.8** that normal, compressive and reverse stress regimes exist very close to each other within the lower half of the study area, but to the north we see only compressive and reverse regimes. It appears that the magnitudes of the horizontal stresses are changing within coalbeds in the PRB, and that in general the horizontal stresses are decreasing toward the south and west.



Figures 3.7a through 3.7e: Magnitude of S_3 plotted on pressure versus depth profiles for the a) Big George, b) Wyodak, c) Anderson, d) Pawnee and e) Wall coals. The black line corresponds to the overburden stress (S_v), the dark grey line corresponds to the pore pressure gradient, the light grey line corresponds to the critical normal faulting line using a coefficient of friction of 1.0 and the brown line corresponds to the critical normal faulting line using a coefficient of friction of 0.6. When S_3 falls between the critical normal faulting lines it means that those wells are in active normal faulting areas.

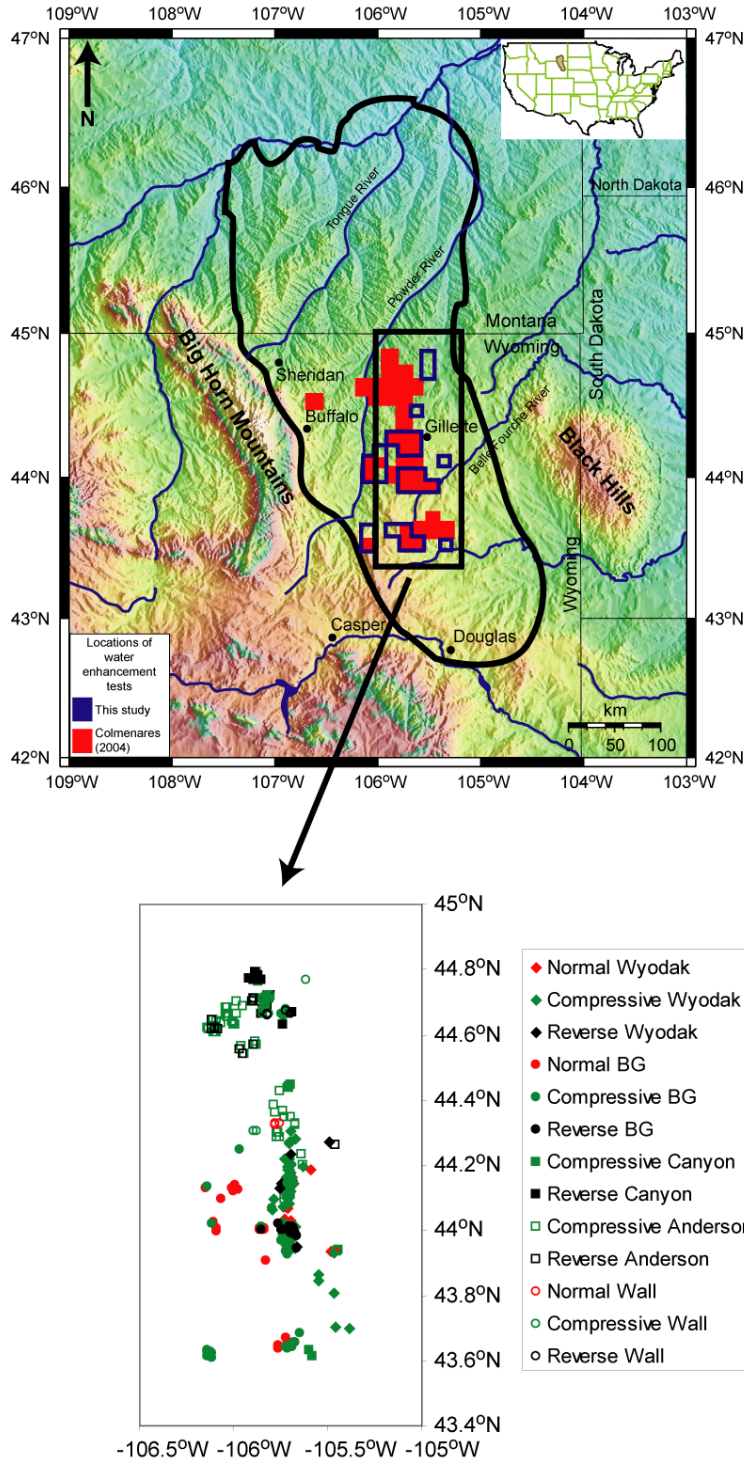


Figure 3.8: Location map showing the stress state and the coalbed for which this stress state has been determined. Points in red correspond to wells in active normal faulting areas, green, to wells in compressive areas (normal/strike-slip) and black, to wells in reverse faulting areas. Wyodak stands for the Wyodak coal, BG for Big George coal, Canyon for Canyon coal, Anderson for Anderson coal and Wall for Wall coal.

When we compare S_3/S_v with water production for wells from Colmenares and Zoback’s (2007) study, as well as the current study, we find a correlation in the Big George coal between active normal faulting areas and wells with vertical hydraulic fractures that produce very large volumes of water ($> 25,000$ bbl/month) (**Figure 3.9**). Water production from other coalbeds does not reach 25,000 bbl/month, so we do not observe the same relationship as in the Big George coal.

Figure 3.9 implies that active normal faults in communication with vertical hydraulic fractures may play a role in CBM wells with very large water production, where the faults may act as permeable conduits for fluid migration to the producing coalbed.

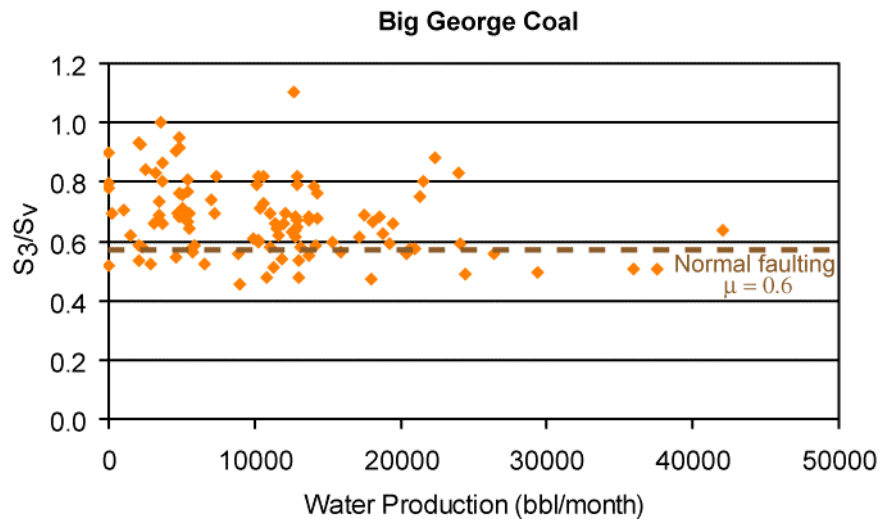


Figure 3.9: The ratio of $S_3:S_v$ plotted against water production for the Big George coal. $S_3/S_v < 0.58$ means that the well is in an active normal faulting regime.

Implications for CBM Water Disposal and CBM Wellbore Completion Practices in the Powder River Basin

In this study we have analyzed 198 water-enhancement tests in order to extend the research carried out by Colmenares and Zoback (2007), who analyzed ~500 tests to understand CBM operating procedures in the PRB. Like Colmenares and Zoback (2007), we find that in some areas of the basin the operators are creating vertical hydraulic fractures through water-enhancement, whereas in other areas they are creating horizontal hydraulic fractures. In addition, we find that some of the wells with vertical hydraulic fractures produce excessive volumes of CBM water, $>7,000$ bbl/month, and when the Big George coal is located in areas of active normal faulting, water production from CBM wells can be in excess of ~25,000 bbl/month. We hypothesize that active normal faults in communication with vertical hydraulic fractures may act as permeable conduits for water migration and give rise to production rates in excess of 25,000 bbl/month.

We also recommend that operators follow the procedures outlined in Colmenares and Zoback (2007) to help minimize CBM water production. Colmenares and Zoback recommended that

operators create minifrac (~2 bbl/min for ~ 2 min) to determine the magnitude of S_3 before carrying out normal water-enhancement procedures. The minifrac will allow the operator to determine if they are in an area where horizontal hydraulic fractures will form or in an area where vertical fractures will form. If they are in an area where horizontal hydraulic fracture will form the operators can then water enhance at any rate and duration they choose. However, if they are in an area where vertical fractures will form, it is best if water-enhancement is kept to a minimum to ensure that the fractures do not propagate into overlying aquifers or come into communication with active normal faults.

RECOMMENDATIONS FOR FUTURE RESEARCH

While both the field data and flow simulations show the potential for limiting the amount of water production during CBM water production in the PRB and for CBM water injection into selected aquifers, appreciable additional research needs to be done. With approximately 15,000 CBM wells having been drilled in the PRB, the magnitudes of the least principal stress and pore pressure has to be documented more broadly throughout the region through analysis of additional water enhancement tests and pressure monitoring.

REFERENCES

- Advanced Resources International, Inc., 2002.** Powder River Basin coalbed methane development and produced water management: DOE/NETL-2003/1184.
- Applied Hydrology Associates, Inc. and Greystone Environmental Consultants, Inc., 2002.** Groundwater modeling of impacts associated with mining coal bed methane development in the Powder River Basin: Technical Report Powder River Basin Oil and Gas Environmental Impact Statement, U.S. Bureau of Land Management, Buffalo Field Office, <http://www.blm.gov/wy/st/en/info/NEPA/bfodocs/prb_eis/prb-feis.html>.
- Ayers, W., 2002.** Coalbed gas systems, resources, and production and a review of contrasting cases from the San Juan and Powder River basins: AAPG Bulletin, 86, 1853-1890.
- Bartos, T. T., and K. M. Ogle, 2002.** Water quality and environmental isotopic analyses of ground-water samples collected from the Wasatch and Fort Union Formations in areas of coalbed methane development — implications to recharge and ground-water flow, Eastern Powder River Basin, Wyoming: U.S. Geological Survey Water-Resources Investigations Report 02-4045.
- Colmenares, L. B., 2004.** Rock strength under true triaxial loading, seismotectonics of Northern South America and geomechanics and Coal Bed Methane Production in the Powder River Basin: unpublished PhD Thesis, Stanford University, Stanford, California.
- Colmenares, L. B., and M. D. Zoback, 2007.** Hydraulic Fracturing and Wellbore Completion of Coalbed Methane (CBM) Wells in the Powder River Basin, Wyoming: Implications for Water and Gas Production: AAPG Bulletin, 91, 51-67.

- Daddow, P. B., 1986.** Potentiometric-surface map of the Wyodak-Anderson coal bed, Powder River structural basin, Wyoming, 1973-84: U.S. Geological Survey Water-Resources Investigations Report 85-4305, 1 sheet, Scale 1:250,000.
- De Bruin, R. H., R. M. Lyman, R. W. Jones, and L. W. Cook, 2004.** Coalbed Methane in Wyoming: State of Wyoming Geological Survey Information Pamphlet 7, Laramie, Wyoming.
- Deutsch, C. V., 2002.** Geostatistical reservoir modeling: Oxford University Press.
- Environmental News Network, 2001.** Coalbed methane boom in Wyoming's Powder River Basin: <<http://www.enn.com/archive.html?id=25012&cat=archives>>, accessed April 2007.
- Flores, R. M., 2004.** Coalbed methane in the Powder River Basin, Wyoming and Montana: An assessment of the Tertiary-Upper Cretaceous coalbed methane total petroleum system: U.S. Geological Survey Digital Data Series, DDS-69-C, chapter 2.
- Flores, R. M., and L. R. Bader, 1999,** Fort Union coal in the Powder River Basin, Wyoming and Montana: A synthesis: U.S. Geological Survey Professional Paper, 1625-A, PS8-PS29.
- Freeze, R. A., and J. A. Cherry, 1979.** Groundwater: Prentice-Hall.
- GEM, 2004.** GEM 2004.10 User's Guide: Computer Modelling Group Ltd., Calgary, Alberta, Canada.
- GEM, 2005.** GEM 2005.15 User's Guide: Computer Modelling Group Ltd., Calgary, Alberta, Canada.
- Hower, T. L, J. E. Jones, D. M. Goldstein, and W. Harbridge, 2003.** Development of the Wyodak coalbed methane resource in the Powder River Basin: SPE 84428, presented at the SPE Annual Technical Conference and Exhibition, Denver, Colorado, October 5-8.
- Hubbert, M. K., and D. G. Willis, 1957.** Mechanics of hydraulic fracturing: Petroleum Transactions of the American Institute of Mining Metallurgical and Petroleum Engineers, 210, 153-163.
- Montana Board of Oil and Gas Conservation (MBOGC), 2007.**
<<http://bogc.dnrc.state.mt.us/>>, accessed March 2007.
- Ross, H. E., 2007.** Carbon dioxide sequestration and enhanced coalbed methane recovery in unmineable coalbeds of the Powder River Basin, Wyoming: unpublished PhD Thesis, Stanford University, Stanford, California.

The Ruckelshaus Institute of Environment and Natural Resources, 2005. Water production from coalbed methane development in Wyoming: A summary of quantity, quality and management options: Final report prepared for the Office of the Governor, State of Wyoming, <<http://www.uwyo.edu/enr/ienr/cbm.asp>>, accessed February 2007.

Wheaton, J., and J. Metesh, 2002. Potential Ground-Water Drawdown and Recovery from Coalbed Methane Development in the Powder River Basin, Montana: Project Completion Report to the U.S. Bureau of Land Management, Montana Bureau of Mines and Geology Open File Report 458, <<http://www.mt.blm.gov/mcfo/cbm/eis/CBM3DGWReport.pdf>>, accessed March 2007.

Wheaton, J., and T. Donato, 2004. Coalbed-methane basics: Powder River Basin, Montana: Montana Bureau of Mines and Geology Information Pamphlet 5, <www.mbm.g.mtech.edu/pdf/ip_5.pdf>, accessed March 2007.

Wyoming Oil and Gas Conservation Commission (WOGCC). <<http://wogcc.state.wy.us/>>, accessed between 2004 and 2007.

Zoback, M. D., C. A. Barton, M. Brudy, D. A. Castillo, T. Finkbeiner, B. Grollmund, D. B. Moos, P. Peska, C. D. Ward and D. J. Wiprut, 2003. Determination of stress orientation and magnitude in deep wells: International Journal of Rock Mechanics and Mining Sciences, 40, 1049–1076.

Zoback, M. D., 2007. Reservoir geomechanics: Cambridge University Press.

TOPIC AREA: SURFACE DISPOSAL

CHAPTER 4:
Surface Disposal and Minimization of Produced Water:
Isotopic Ratios as Tracers of CBM Water

Carol D. Frost, Catherine Campbell and E.L. Brinck¹

EXECUTIVE SUMMARY

Task 3 used stable isotopic environmental tracers along with standard water quality data to accomplish three subtasks: 1) to monitor the infiltration and dispersion of coalbed methane (CBM)-produced water into the shallow subsurface, 2) to determine locations where coal seams are isolated from adjacent aquifers and co-produced water will be limited to coal, and 3) evaluate what information may be provided by isotopic analyses of carbon, oxygen, and hydrogen in CBM-co-produced waters.

In subtask 1 we used the Sr isotopic ratio, $^{87}\text{Sr}/^{86}\text{Sr}$, to trace the infiltration of product water and show a connection between changes in water quality and strontium concentration at an on-channel CBM disposal site. We suggest that on-channel discharge shows promise for future disposal in that there are fewer salts in existing channels due to annual flushing. However, the amount and duration of CBM discharge may exceed the water mounding caused by annual flooding, in which case stream bank salts may be mobilized.

In subtask 2 we suggest that the Upper Wyodak coal zone aquifer in the Gillette and Schoonover areas is a well-confined combined sand and coal aquifer unit but that the Wyodak Rider coal zone aquifers are only partially confined allowing interactions between sandstone and possibly other coal aquifers with the Wyodak Rider aquifer. Faults in the northeastern part of the Powder River basin affect aquifer connectivity, either by acting as seals or conduits. The Sr isotopic ratio is not well-correlated to fracture pattern developed during the well enhancement process because there are many factors in addition to fracture pattern that control interactions between aquifers.

In subtask 3 we show that the fractionation in oxygen and hydrogen isotopes caused by evaporation of light-element isotopes can be used to identify watersheds that have been infiltrated by CBM holding ponds. This indicator could be useful when infiltration rates are uncertain. Our initial carbon isotopic results demonstrate that $\delta^{13}\text{C}$ of dissolved inorganic carbon (DIC) and DIC concentration in co-produced CBM water is distinct from shallow ground water and surface water in Powder River Basin. This may be a very useful indicator of the presence of CBM produced waters in the near-surface environment.

INTRODUCTION

The objective of Task 3 was to develop an understanding of the fate of coalbed methane (CBM) co-produced water following discharge, as well as locations where coal seams are isolated from adjacent aquifers and where, therefore, water production will be limited to the coal. These goals require fingerprinting of the produced water so that it may be traced through the hydrogeologic

¹ Department of Geology and Geophysics, University of Wyoming, 1000 University Avenue, Laramie WY 82071. Correspondence: frost@uwyo.edu.

environment. The isotopic ratio of stable isotopes 87-strontium to 86-strontium was used to distinguish waters from different parts of the basin, as well as water from coal and sandstone aquifers.

Task 3 is composed of three subtasks:

- Subtask 3.1: Use Sr isotopic measurements to monitor infiltration and dispersion of produced water into the shallow subsurface at two field sites; Beaver Creek and Coal Creek located in Wyoming.
- Subtask 3.2: Identify locations in the Powder River Basin where coal seams are isolated from adjacent aquifers and hence water production will be limited to the coal. This work was performed in conjunction with colleagues completing Task 4, and integrated results based upon Sr isotopic ratios with information about fracture patterns associated with individual wells.
- Subtask 3.3: Evaluate the potential of additional environmental isotopic tracers of co-produced waters and water-rock interaction. Specifically, we measured stable isotopes of oxygen, hydrogen and carbon of water samples from the Beaver Creek site to determine if these can distinguish produced water from local meteoric water and therefore if they can be used as a tracer as produced water infiltrates.

EXPERIMENTAL METHODS

Monitoring well samples were collected after two well-casing volumes of water were removed. Water samples from CBM wellheads and discharge points, the ponds and streams were collected using rinsed 2L containers. Temperature and pH were measured in the field; samples were filtered through a 0.45 um filter and kept cool and dark until laboratory analysis. Half of each sample was acidified to pH 2 for major ion analysis.

Strontium was isolated from a 3 ml aliquot of each un-acidified water sample using Teflon columns filled with Eichrom® Sr-Spec resin and the strontium isotopic composition determined by thermal ionization mass spectrometry at the University of Wyoming. The internal precision of $^{87}\text{Sr}/^{86}\text{Sr}$ isotope ratio measurements is ± 0.00001 . 76 analyses of NBS 987 strontium standard measured during the course of this study gave an average value of $^{87}\text{Sr}/^{86}\text{Sr} = 0.71026 \pm 0.00002$ (2 standard deviations). All analyses were normalized to an $^{86}\text{Sr}/^{88}\text{Sr}$ ratio value of 0.1194. Analytical blanks were less than 0.2 ng, negligible compared to sample sizes of at least 0.1 microgram strontium. An additional 1-ml aliquot of each sample was spiked with an ^{84}Sr -enriched tracer and strontium concentration determined by isotope dilution. Strontium concentrations are reproducible at the 1% level. Replicates collected in January 2003 show that $^{87}\text{Sr}/^{86}\text{Sr}$ ratios are reproducible within the error expected from the precision of the instrument, but strontium concentrations vary more than would be expected due to error associated with the analytical processes. These samples were collected while the monitoring wells were being pumped and suggest either that strontium concentration varies as a function of the amount of water pumped from the well, or that strontium is not remaining in solution during transport and storage prior to analysis (**Table 4.1**).

Table 4.1: Sr Reproducibility

		January 2003	
		Sr ppm	⁸⁷ Sr/ ⁸⁶ Sr
MT	BC-4	2.29	0.71262
WY	BC-4	1.88	0.71260
MT	BC-6	1.59	0.71343
WY	BC-6	0.67	0.71344
MT	BC-11	4.97	0.71269
WY	BC-11	3.35	0.71271
MT	BC-14	3.47	0.71282
WY	BC-14	3.59	0.71282
<p>Samples labeled MT were taken to Billings, MT before being mailed to Laramie, WY for Sr analysis.</p> <p>Samples labeled WY were taken directly to Laramie, WY.</p>			

Major ion concentrations were measured for the CBM production wells and Beaver Creek samples. Major cations and trace elements were measured by ICP-MS, sodium (Na) by flame atomic absorption, anions by ion chromatography and alkalinity by potentiometric titration at the University of Wyoming. TDS was calculated by summing the major ionic constituents and converting bicarbonate into equivalent carbonate (Drever, 1997).

Water samples were collected with plastic syringe, filtered with Cameo 0.45 mm nylon filters to prevent the inclusion of organic matter that can interfere with isotopic analysis and placed in 20 ml glass vials. To prevent evaporation, containers were completely filled with water, capped and sealed with layer of parafilm. Values of d¹⁸O were determined by CO₂-H₂O direct equilibration method using a Finnigan Gas Bench III device online with a Finnigan Delta Plus XP mass spectrometer. For dD analysis the samples were prepared using offline Zn reduction method and were analyzed on an Optima dual inlet mass-spectrometer. Isotopic analysis was carried out at the Stable isotope Facility at University of Wyoming. Internal standards were analyzed after every 8 samples and the analytical uncertainty for d¹⁸O and d D is better than 0.05 and 1 ‰ respectively. The d¹⁸O and d D values are reported in per mil relative to V-SMOW.

Samples collected for dissolved inorganic carbon isotopic analyses were passed through a Cameo 0.45 micron nylon pre-filter attached to 60 cc Luer-lock syringe. The water sample was then transferred in 30 ml Wheaton glass serum vials with teflon septa and sealed with Al caps using a crimper. Few drops (2-3) of benzalkonium chloride were added to each vial before filling it with water to halt any metabolic activity. Samples were analyzed for d¹³C_{DIC} on a GasBench-II device coupled to a Finnigan DELTA plus mass spectrometer in the central Stable Isotope Facility at the

University of Wyoming. The reproducibility and accuracy was monitored by replicate analysis of samples and internal lab standards and was better than ± 0.1 ‰. The $d^{13}C_{DIC}$ values are reported in per mil relative to V-PDB.

Water quality was modeled with Visual MINTEQ (Allison and Brown, 1992). This model incorporates complete analytical data including major cation, major anion, and trace element concentrations, pH, and alkalinity. The calculated outputs include the charge balance, ionic strength, chemical speciation, and saturation indices (McBeth et al., 2003). The saturation index is defined as the log of the quotient of the ion activity product (IAP) and solubility product (K_{sp}). A solution in equilibrium has saturation indices equal to zero. A saturation index greater than zero implies a species that is oversaturated, whereas a negative saturation index implies undersaturation (Drever, 1997).

RESULTS, DISCUSSIONS AND CONCLUSIONS

Subtask 3.1

The objective of this subtask was to use strontium isotopic tracing to study the fate and impact of CBM product waters on shallow aquifers and the hyporheic zone. Our study looked at two on-channel CBM produced water disposal ponds in the ephemeral upper reaches of the Beaver Creek area, approximately 80 kilometers southwest of Gillette, Wyoming. This site was chosen due to the aforementioned measurable difference in strontium isotope ratios, as well as the ability to start water sampling within two months after CBM produced water discharge began in November, 2002. We use strontium isotope and concentration data to:

1. Distinguish CBM water from surface and shallow ground water.
2. Trace the infiltration of CBM water through the hyporheic zone and near surface aquifers.
3. Monitor the dissolution of local salts and their mobilization into the ground water.
4. Detect geochemical changes as the atmospherically isolated CBM water is discharged into the on-channel impoundments.

This study, which is published in Brinck and Frost (2007), was performed in an area of increasing CBM production in the head waters of the Beaver Creek watershed, a tributary to the Powder River. This ephemeral drainage is approximately 80 kilometers south-west of Gillette, Wyoming (**Figure 4.2**). Within a 2-kilometer stretch of this ephemeral drainage two ponds were excavated within the tributary including the widening and deepening of an existing stock pond to create the up-gradient pond (herein referred to as the upper pond). Water production from CBM wells began to be discharged into the upper pond on November 20, 2002, while the larger, down-gradient pond (the lower pond) began filling ten days earlier on November 10, 2002. After the upper pond filled (around Dec. 8, 2002; (Payne, 2004), water began flowing down the once ephemeral, now perennial stream channel. Water piped from several (up to 5) natural gas wells are combined and discharged from a central pipe at each pond. The specific wells discharging into these ponds vary based on the gas and water production history of each well in addition to the production company's specific goals. All CBM wells in this area are completed in the Big George Coal. The strontium isotope ratio for the CBM water has varied with time from 0.71388

to 0.71457, perhaps due to varying combinations of wells or fluctuations in pumping rates. However, the $^{87}\text{Sr}/^{86}\text{Sr}$ ratio of the produced water is distinct from water from near surface aquifers despite these temporal variations in strontium isotope ratio.

The soil in this part of the Powder River Basin is classified under the Cambria-Theedle-Kishona association. These medium textured soils are moderately deep (50 to 100 cm) and very deep (over 150 cm over bedrock). They have formed on gently sloping to moderately steep (3 to 30 percent) alluvial fans, ridges and hills. The soil overlies soft shale and interbedded sandstone and shale. Cambria soils are fine-loamy, mixed, superactive, mesic Ustic Haplargids whereas Theedle and Kishona soils are fine-loamy, mixed, superactive, calcareous, mesic Ustic Torriorthents. All soil profiles in this area are characterized by Bk (calcareous) horizons (NRCS, 2004).

Three sets of nested monitoring wells were installed by the Western Research Project Cooperative at the Beaver Creek site in the Powder River Basin of Wyoming (**Figure 4.1**; Payne and Safer, 2005). The first set of wells is up-gradient from both of the CBM water impoundments (the upper well site), the second set is between the two impoundments (the middle well site), and the third set is down-gradient from both impoundments (the lower well site). The upper wells site (ambient ground water) allows seasonal sampling of ground water unaffected by the infiltrating CBM water. The middle well site was placed within the ephemeral channel itself, allowing the investigation of CBM water's interactions with the hyporheic zone and shallow aquifer below the streambed. The lower well site is slightly off-channel on the floodplain, enabling the investigation of the interaction of CBM water with the floodplain soils and off-channel ground water. Additionally, four weirs were installed within the streambed, two of which were used for sampling (**Figure 4.2**).

Water sampling of the two CBM produced waters, the two ponds, two of four installed weirs, and two wells from each of the three sets of wells began in January 2003, one month after the upper pond filled. Sampling continued approximately every three months for three years. In each of the well locations samples were collected from two depths – the alluvial layer (approximately 5 meters below the ground surface) and the underlying Wasatch Formation (approximately 10 meters below the ground surface). The weir samples were collected from the weirs directly below each pond.

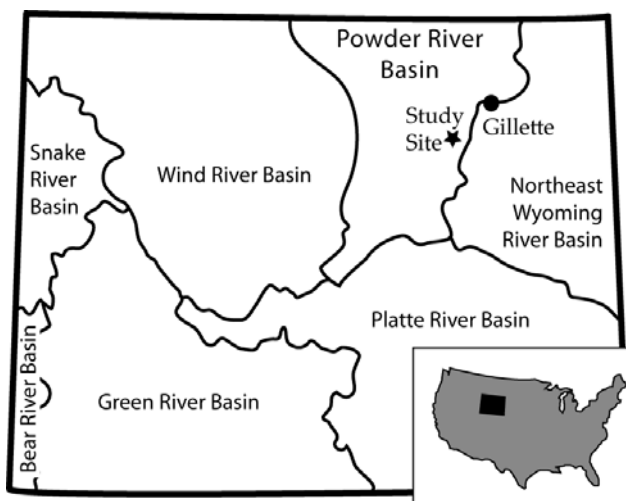


Figure 4.1: Wyoming river basins including the starred location of the study site (from Wyoming State Water Plan). Inset is the location of Wyoming within the continental United States.

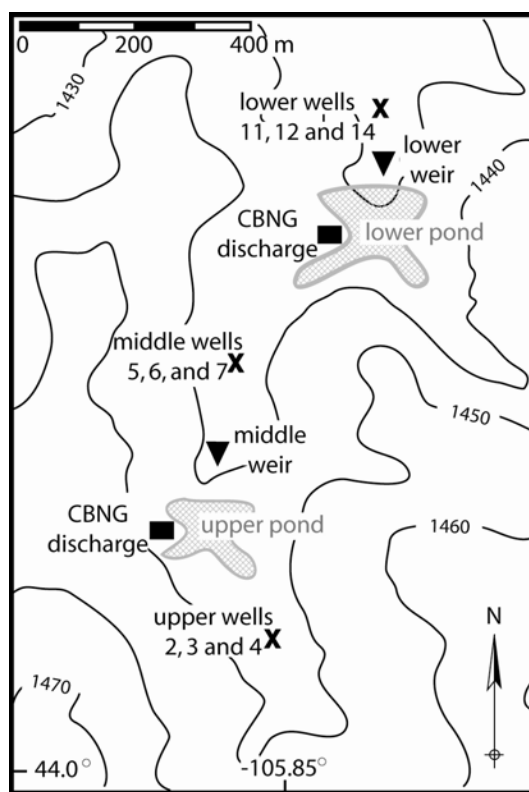


Figure 4.2: Topographic map of Beaver Creek study site showing the location of the nested well sites (crosses), CBM discharge points (squares) and the weirs (triangles) from which samples were taken (from Payne and Saffer, 2005). Contours are labeled in meters above sea-level. Location within Wyoming is marked with a star on **Figure 4.1**.

Results

Strontium isotope results

Water samples were collected on 13 different dates over a period of 35 months at the Beaver Creek study site (**Table 4.2**). The strontium concentration and $^{87}\text{Sr}/^{86}\text{Sr}$ ratio of the CBM product water (black squares) and the local ground water monitored at the upper well site (open squares), has remained relatively constant throughout the monitoring period (**Figure 4.3a-d**). The $^{87}\text{Sr}/^{86}\text{Sr}$ ratio of the CBM water ranges from a minimum of 0.71388 to a maximum of 0.71457, whereas the local alluvial and Wasatch formation ground water ranges from a minimum of 0.71255 to a maximum of 0.71279. These values are easily distinguished by thermal ionization mass spectrometry. This distinguishable fingerprint results from the waters' interaction with stratigraphically separated aquifer material of very different composition (coal and alluvium) and allows us to follow the infiltration of the CBM water.

Table 4.2: Beaver Creek Sr (ppm) and ⁸⁷Sr/⁸⁶Sr for CBNG Discharge, Ponds, Streams and Wells

Table 2 Beaver Creek Sr (ppm) and ⁸⁷ Sr/ ⁸⁶ Sr for CBNG Discharge, Ponds, Streams, and Wells																
Stream Location	ID	Depth (m)	January 2003		April 2003		August 2003		October 2003		December 2003		February 2004		May 2004	
			Sr (ppm)	⁸⁷ Sr/ ⁸⁶ Sr	Sr (ppm)	⁸⁷ Sr/ ⁸⁶ Sr	Sr (ppm)	⁸⁷ Sr/ ⁸⁶ Sr	Sr (ppm)	⁸⁷ Sr/ ⁸⁶ Sr	Sr (ppm)	⁸⁷ Sr/ ⁸⁶ Sr	Sr (ppm)	⁸⁷ Sr/ ⁸⁶ Sr	Sr (ppm)	⁸⁷ Sr/ ⁸⁶ Sr
Upper	Up-CBNG		1.36	0.71401	0.97	0.71411	1.40	0.71388	1.23	0.71391	1.21	0.71391	1.19	0.71402	1.09	0.71397
	Up-pond	0	0.87	0.71397	0.69	0.71402	0.75	0.71394	0.75	0.71394	0.74	0.71393			0.63	0.71397
	BC-2	5.5	1.32	0.71276	2.48	0.71255	1.54	0.71278	1.38	0.71278	1.77	0.71260			1.34	0.71276
	BC-4	9.6	1.88	0.71260	1.63	0.71271	1.90	0.71260	1.80	0.71259	1.10	0.71274			1.88	0.7125B
	M-weir	0			1.28	0.71380	0.68	0.71388	0.58	0.71390	0.85	0.71374			0.60	0.71342
	BC-5	11.6	1.70	0.71312					0.85	0.71324	1.02	0.71312			0.95	0.71323
	BC-6	7.9	0.67	0.71344	0.94	0.71346			0.69	0.71329						
Lower	BC-7	7.6						1.19	0.71311	1.09	0.71311			0.93	0.71311	
	L-CBNG		1.29	0.71411	0.89	0.71417	1.36	0.71422	1.20	0.71420	1.08	0.71423	1.14	0.71423	1.22	0.71436
	L-pond	0	0.99	0.71403	0.70	0.71410	0.63	0.71415	0.71	0.71416	0.78	0.71416			0.74	0.71428
	L-weir	0			1.02	0.71344	0.75	0.71392	0.65	0.71381	0.91	0.71370			0.62	0.71392
Middle	BC-11	11.6	3.35	0.71271	1.37	0.71274	2.30	0.71278	2.01	0.71276	1.94	0.71271			193	0.71273
	BC-14	4.6	3.59	0.71282	3.57	0.71233	5.2a	0.71289	6.35	0.71287	6.58	0.71289	6.45	0.71287	7.07	0.71239
Upper	Up-CBNG		1.15	0.71415	1.17	0.71420			1.21	0.71402	1.22	0.71399			1.16	0.71400
	Up-pond	0						0.79	0.71405	0.69	0.71396	0.79	0.71401	0.72	0.71398	
	BC-2	5.5	1.40	0.71275			1.16	0.71277	1.37	0.71275	1.30	0.71277	1.35	0.71275		
	BC-4	9.6	1.75	0.71260			1.57	0.71260	1.73	0.71260	3.74	0.71258	1.87	0.71260		
Middle	M-weir	0						1.77	0.71330	3.09	0.71299					Dry
	BC-5	11.6	1.03	0.71316			1.15	0.71309	1.10	0.71312	1.06	0.71307	0.95	0.71307		
	BC-7	7.6	0.98	0.71310			0.95	0.71307	0.80	0.71305	1.03	0.71305	1.14	0.71311		
Lower	L-CBNG		1.26	0.71441	1.29	0.71457			1.19	0.71432	1.21	0.71442	1.13	0.71437		
	L-pond	0						0.90	0.71438	0.99	0.71434	0.90	0.71436	0.95	0.71437	
	L-weir	0	0.44	0.71382			0.97	0.71372	0.80	0.71384	0.43	0.71381				Frozen
	BC-11	11.6	1.92	0.71272			1.71	0.71274	1.86	0.71272	1.94	0.71273	1.96	0.71272		
BC-14	4.6	7.38	0.71293	6.93	0.71293	7.00	0.71291	7.27	0.71294	7.35	0.71293	6.77	0.71294			

Note: Sample identification terms beginning with BC represent monitoring wells. Wells 2 and 4 are in the upper well set, wells 5, 6, and 7 are in the middle well set, and wells 11 and 14 are in the lower well set. Prefixes Up-, M-, and L- represent the sample location within the study of upper, middle, and lower.

The on-channel ponds (circles in **Figure 4.3a**) in which the CBM water is collected before it is allowed to run overland shows a decrease in strontium concentration from the discharged CBM water. The stream samples (diamonds in **Figure 4.3b**) were collected at two weirs in the stream channel below both ponds. Most of these samples have similar concentrations as the CBM discharged water, but a slightly lower $^{87}\text{Sr}/^{86}\text{Sr}$ ratio.

Ambient water collected from the upper wells has had a constant strontium isotope ratio throughout the three-year sampling period. However, from the time of the first sampling in January 2003, the middle well site water samples (open triangles) have yielded $^{87}\text{Sr}/^{86}\text{Sr}$ ratios intermediate between the ambient ground water ratio and the CBM water ratio (**Figure 4.3c**). The increasing water levels at well 6 indicate that the aquifer at the middle site had been influenced by CBM water prior to the January 2003 sampling date; therefore this intermediate strontium value does not reflect baseline conditions.

The two lower wells, well 11 (X) and well 14 (+), are displayed separately due to their distinct strontium characteristics. Lower well 14 has shown a steady increase in strontium concentration away from both ambient conditions and CBM values (**Figure 4.3d**, **Figure 4.4a**) over time, accompanied by a slight but significant shift in $^{87}\text{Sr}/^{86}\text{Sr}$ ratio towards that of the CBM water (**Figure 4.4b**). Well 11 does not display this trend, but rather stays near ambient conditions. Possible reasons for this difference include the difference in depth of well 14 (at 4.5 meters deep) and well 11 (at 11.6 meters deep). Additionally, well 14 is 5.5 meters off the main stream channel, whereas well 11 is 14 meters off the stream channel (Payne and Saffer, 2005). Strontium concentrations and $^{87}\text{Sr}/^{86}\text{Sr}$ ratios in water samples from all other monitored wells have remained consistent since sampling began (**Figure 4.4a and 4.4b**).

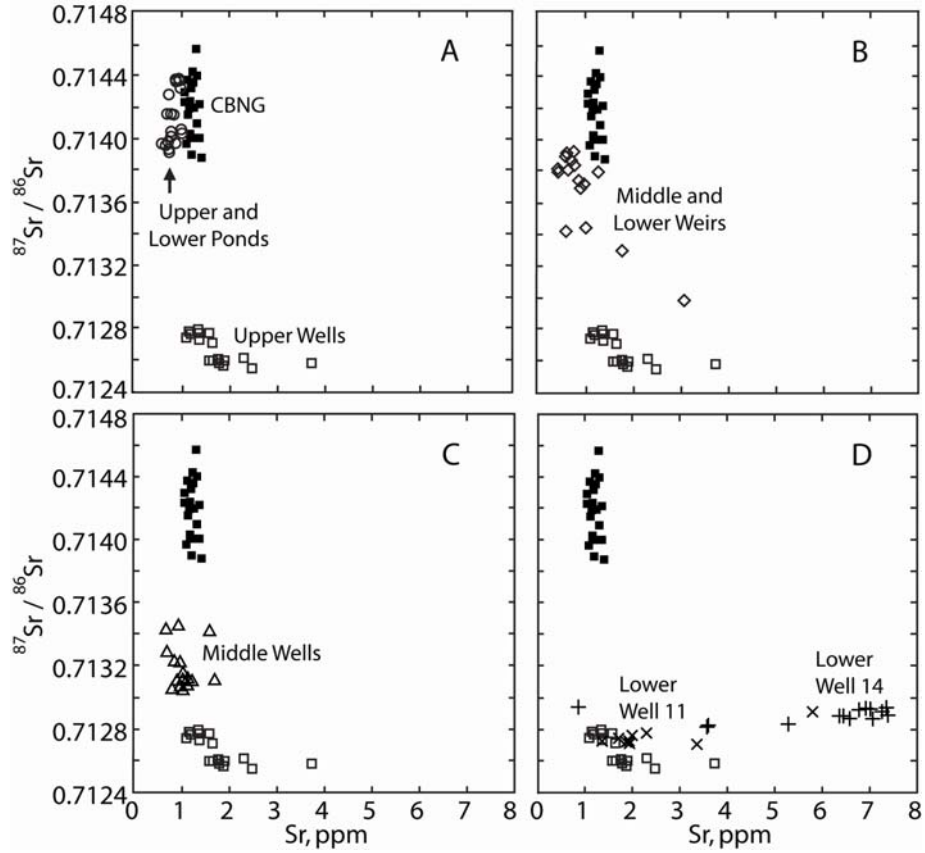


Figure 4.3a through 4.3d: Summary of Sr isotopic and concentration data. The CBM produced water (black squares) and the upper wells that monitor the local ground water (open squares) are included in graphs A through D for reference. In addition to the upper wells and CBM water samples, graph A shows the upper and lower CBM collection ponds (open circles), graph B shows the stream water sampled at the middle and lower weirs (open diamonds), graph C shows the middle well site (open triangles) and graph D shows lower wells 11 (X) and 14 (+).

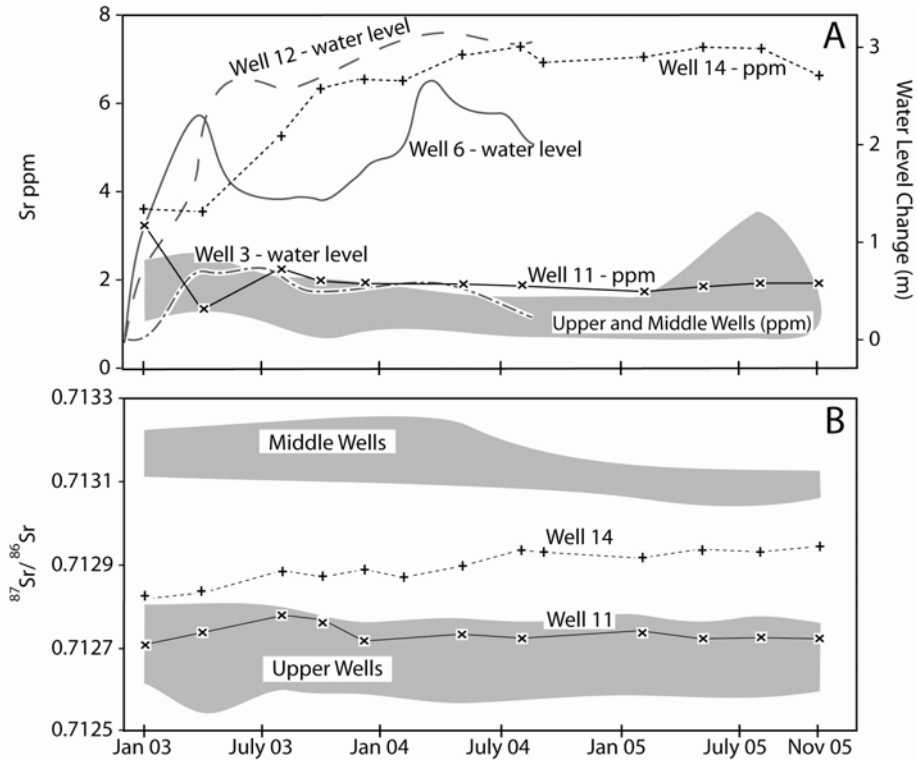


Figure 4.4a and 4.4b: (a) Change in Sr ppm with time for lower wells 11 (X) and 14 (+). The Sr concentrations for the upper and middle wells are generalized in the shaded area. Also included on the secondary Y axis is water level data (Payne and Saffer, 2005) for one well at each of the three monitoring well sites (measured for the first 20 months). Well 3 is in the upper well site, well 6 is in the middle well site, and well 12 is in the lower well site. Well 12 is the same depth and distance from the stream bed as well 14. (b) Strontium isotope ratios for lower monitoring wells 11 (X) and 14 (+). Strontium isotope ratios for the upper and middle well sites are generalized in the shaded areas. The average CBM strontium isotope ratio is off axis at 0.714.

Water quality results

CBM product water is characterized by high concentrations of TDS, sodium (Na), potassium (K) and alkalinity (as HCO_3), and low concentrations of calcium (Ca) and magnesium (Mg) as compared to the local ground water in this area measured at the upper well site (**Table 4.3**). Additionally, compared to local water, CBM water has a low concentration of the trace element manganese (Mn) and high levels of the trace elements boron (B) and barium (Ba). The usefulness of Ba as a tracer of CBM water is limited by the precipitation of BaSO_4 (McBeth et al. 2003), as seen by the decrease in Ba concentration from the CBM discharge to the pond to the middle wells. The pond water has similar levels of TDS, Na, HCO_3 , Mg, K, and B as CBM water. However the pond water has lower concentrations of Ca, Mn, Sr, and Ba and a higher concentration of Al. The concentrations in the stream water are similar to the pond water except for higher sulfate (SO_4) and Mn and lower Ba values.

Table 4.3: Beaver Creek Water Quality

		Table 3 Beaver Creek Water Quality																
		Cations								Anions			Trace Elements					
Sample Date	ID	pH	TDS mg/L	Na ppm	Mg ppm	Si ppm	K ppm	Ca ppm	Fe ppm	ALK mg/L	Cl ppm	SO4 ppm	B ppb	Al ppb	Mn ppb	Sr ppb	Ba ppb	U ppb
Upper Wells	8/6/2003 BC-2	7.29	791.05	74.9	41.9	5.0	1.7	132.5	4.3	415.42	4.1	321.8	27.2	443.5	192.6	1150.6	32.7	22.6
	8/6/2003 BC-4	6.79	1038.78	121.7	41.8	5.9	4.3	173.2	12.2	318.25	3.5	519.2	23.9	18.5	361.1	1463.4	14.3	1.1
	8/21/2004 BC-2	7.35	788.34	77.2	44.1	5.4	1.8	142.6	4.7	303.94	3.2	359.4	33.6	462.5	171.9	1240.0	27.0	22.6
	8/21/2004 BC-4	7.20	1085.14	123.3	42.7	5.8	4.4	180.5	13.1	325.48	2.9	551.7	28.8	33.8	429.0	1524.2	35.6	1.0
	2/5/2005 BC-2	6.69	771.07	69.9	46.7	4.2	1.5	125.2	0.6	398.37	2.9	323.6	36.0	71.3	130.3	1155.4	48.8	
	2/5/2005 BC-4	6.85	1142.20	127.8	49.3	5.8	4.2	173.5	2.2	386.35	2.9	586.0	34.2	19.5	444.0	1572.2	31.9	
	8/9/2005 BC-2	7.50	742.11	57.6	38.5	3.9	1.9	120.8	2.1	434.55	4.4	298.6	36.1	83.5	176.3	1053.0	28.3	20.3
	8/9/2005 BC-4	7.00	1151.99	116.1	40.9	5.1	4.5	173.4	10.9	417.33	3.7	591.6	39.7	46.0	442.2	1461.9	22.4	1.0
CBNG Water	8/6/2003 Up-CBNG	7.20	1411.03	483.3	18.4	4.7	8.0	43.9	3.3	1705.74	8.1	<0.2	90.0	4.5	18.4	1038.6	929.6	0.0
	8/6/2003 L-CBNG	7.65	1346.20	459.6	18.4	4.7	8.2	49.0	4.9	1608.25	8.0	0.1	87.4	22.9	43.6	1011.3	969.5	0.0
	8/21/2004 Up-CBNG	7.41	1445.42	502.2	18.7	5.2	8.5	47.4	3.2	1726.06	8.6	0.2	98.6	15.5	26.1	1037.1	907.7	0.2
	8/21/2004 L-CBNG	7.26	1385.09	481.6	18.3	4.8	8.3	54.1	2.8	1634.69	8.3	0.5	92.7	34.8	53.3	1089.4	937.6	0.1
	2/5/2005 Up-CBNG	7.28	1399.38	528.0	22.2	5.8	8.6	48.9	0.5	1551.98	7.0	12.8	112.6	9.1	28.2	1115.2	950.6	
	2/5/2005 L-CBNG	7.23	1282.56	479.9	20.3	4.8	8.3	47.3	0.5	1446.05	6.3	1.8	100.7	10.2	40.5	1053.1	982.7	
	8/9/2005 Up-CBNG	6.90	1438.37	484.9	19.5	4.8	8.0	44.4	2.3	1742.40	13.8	1.1	116.9	6.1	19.2	980.8	871.0	0.0
	8/9/2005 L-CBNG	7.30	1360.53	458.0	17.1	4.7	8.0	50.7	4.0	1639.26	8.9	0.5	83.7	14.3	56.2	1047.1	876.3	0.0
Pond Water	8/6/2003 Up-pond	8.63	1393.68	486.1	16.9	2.7	8.6	17.1	0.7	1716.82	8.7	6.0	88.0	130.8	4.6	559.9	288.9	0.5
	8/6/2003 L-pond	8.97	1394.66	488.6	18.1	4.1	9.2	19.4	0.7	1704.49	9.0	4.7	92.6	126.3	4.6	631.2	376.8	0.4
	2/5/2005 Up-pond	7.98	1225.46	483.0	20.1	3.2	8.6	17.8	0.2	1377.56	7.1	5.9	108.4	144.8	5.6	785.1	456.5	
	2/5/2005 L-pond	8.65	1218.07	478.5	20.3	0.9	8.1	24.4	0.1	1365.17	6.3	6.1	95.5	14.4	<2.9	895.3	687.7	
	8/9/2005 Up-pond	8.70	1769.45	629.2	19.9	1.2	10.5	10.4	1.1	2188.87	12.8	4.6	140.2	311.6	4.8	668.3	268.1	0.8
	8/9/2005 L-pond	8.40	1535.10	548.8	20.2	4.6	10.7	15.5	0.0	1868.22	11.8	1.9	103.3	44.4	6.6	778.7	507.2	0.0
	8/6/2003 M-weir	9.20	1433.62	502.6	17.1	2.6	9.4	17.1	0.8	1758.14	9.2	7.5	89.1	130.5	6.2	486.5	153.6	0.9
	8/6/2003 L-weir	8.52	1304.83	447.6	20.5	3.3	8.4	25.0	0.6	1557.72	8.5	22.4	88.5	42.1	18.2	578.9	256.9	2.0
Stream Water	8/21/2004 L-weir	8.76	1406.87	496.6	22.9	1.4	7.8	15.8	0.4	1626.37	9.4	50.2	93.7	13.5	4.7	386.6	99.8	3.5
	2/5/2005 M-weir	7.42	1936.97	441.8	70.7	3.3	6.1	181.7	0.9	1004.39	10.6	726.5	78.5	27.7	223.3	1771.7	180.0	
	2/5/2005 L-weir	7.31	1268.46	415.3	32.6	2.2	5.7	75.6	0.4	1142.05	6.7	166.7	84.6	8.7	127.3	972.8	411.4	
	8/9/2005 L-weir	8.30	1438.18	490.7	21.9	2.7	8.3	15.2	-0.3	1641.46	9.4	80.5	93.8	13.7	5.0	384.7	141.5	4.9
	8/6/2003 BC-7	7.49	778.78	136.7	38.6	6.7	3.8	193.8	4.2	655.97	7.9	63.5	70.3	178.7	13.1	942.4	80.9	15.3
	8/21/2004 BC-5	7.33	760.33	88.8	38.2	5.0	2.8	151.9	6.4	393.93	7.0	265.8	24.6	74.7	128.9	911.3	35.1	9.2
	8/21/2004 BC-7	7.20	1161.94	304.2	34.7	6.5	3.1	175.6	3.7	892.52	10.2	183.8	90.4	129.8	6.6	872.1	76.9	28.5
	2/5/2005 BC-5	6.69	1018.52	97.2	49.3	4.9	3.0	172.6	1.7	392.26	8.5	487.9	25.9	136.2	152.3	1147.4	42.7	
L-Well 11	2/5/2005 BC-7	6.51	932.25	155.0	38.4	6.5	2.9	171.0	0.7	855.77	7.4	128.2	51.9	65.8	8.4	947.9	80.6	
	8/9/2005 BC-5	6.90	884.66	92.3	36.6	4.1	2.8	147.7	4.7	379.85	11.3	397.8	23.3	41.1	120.5	881.6	28.3	9.8
	8/9/2005 BC-7	6.90	920.09	169.9	34.6	6.0	3.0	181.8	3.2	677.68	8.5	178.9	48.2	91.7	7.5	887.6	73.5	22.6
	8/6/2003 BC-11	6.93	1489.56	156.6	73.1	6.5	3.5	250.4	14.1	261.18	4.8	851.7	28.1	667.2	237.3	1702.2	15.4	6.6
	8/21/2004 BC-11	7.37	1486.88	157.8	69.4	4.9	3.1	239.5	10.5	311.20	4.6	843.6	28.8	23.0	236.5	1628.0	12.5	5.4
	2/5/2005 BC-11	6.50	1556.13	154.6	77.4	5.1	3.2	229.0	2.0	411.82	4.5	877.1	32.2	54.1	231.2	1710.8	33.2	
	8/9/2005 BC-11	7.30	1505.41	154.8	70.5	5.7	4.3	237.8	11.6	370.97	6.2	831.5	34.6	529.7	230.6	1635.5	44.7	7.9
	Lower Well 14	1/21/2003 BC-14	7.05	2132.89	136.1	144.1	4.8	1.3	322.1	1.7	216.62	4.4	1411.6	49.6	0.2	4.3	3593.3	17.7
4/9/2003 BC-14		7.40	2095.97	131.1	138.9	4.4	1.2	336.6	1.7	271.47	4.8	1343.3	40.5	10.7	<2.9	3572.3	28.9	
8/6/2003 BC-14		6.83	2880.36	150.0	173.9	5.1	1.6	495.7	2.0	418.88	6.0	1839.5	67.2	35.2	67.2	5277.9	30.5	
10/5/2003 BC-14		7.73	4060.87	326.4	261.0	4.9	2.4	542.7	2.2	413.17	5.8	2711.6	107.1	76.3	38.6	6347.4	24.6	
2/13/2004 BC-14		7.23	4598.59	462.2	351.6	3.9	1.8	481.5	2.4	388.87	5.3	3098.2	95.9	42.6	7.1	6448.7	55.2	
5/15/2004 BC-14		7.64	5135.06	556.5	397.0	3.7	1.5	473.7	2.2	403.61	6.6	3494.7	96.8	38.1	7.2	7068.3	23.3	
8/21/2004 BC-14		7.50	5750.91	713.6	461.9	4.1	1.7	458.6	2.3	449.59	7.9	3878.9	144.1	18.5	36.4	7375.9	36.8	
9/18/2004 BC-14		7.96	5335.76	666.4	424.5	4.3	5.5	425.9	2.2	448.26	10.5	3575.4	142.5	21.7	36.4	6925.1	42.8	
2/5/2005 BC-14		6.64	4786.97	483.1	398.0	4.0	0.9	447.4	2.3	508.17	6.7	3193.8	106.4	33.8	20.1	7004.0	30.1	
5/7/2005 BC-14		8.66	4779.28	524.4	376.3	3.4	0.9	446.6	7.4	580.63	8.7	3125.3	115.2	5.6	20.4	7270.0	15.3	269.2
8/9/2005 BC-14		7.30	4864.84	528.0	371.5	4.3	1.0	449.9	8.9	666.80	9.8	3162.6	150.7	104.1	84.2	7350.2	25.0	276.5
11/4/2005 BC-14	7.70	4285.01	361.8	348.0	4.9	0.9	451.1	8.4	738.03	9.9	2735.9	153.6	172.8	80.5	6769.1	26.9	263.5	

The middle well site has lower Na, K, B and Ba and higher Mg, Ca and SO₄ compared to the pond and stream water. However, the concentrations of Na, Mg, K, Ca, are similar to the upper wells. Ba is higher and SO₄ lower in the middle wells than the upper wells. TDS concentrations at the middle well site are initially much higher than the ambient conditions, then decrease.

Well 11 in the lower well site is similar in composition and concentration to the upper well site but has higher Ca, and SO₄ values. Well 14 in the lower well site has rising concentrations of

TDS, Na, Mg, Ca, SO₄, B, and Sr with time and all these species are higher in concentration in well 14 than in the upper wells and the CBM water. Manganese values however, in well 14 are lower than those in well 11 and the upper wells. Concentrations of uranium (U) were measured for the last three samples taken from well 14. All three values are higher than both the upper well site and the CBM water.

Variations in ion concentrations can be seen between wells at different depths within the same nested well site. Wells 2 and 4 in the upper well site are 5.5 m and 9.6 m below the ground surface respectively. Well 2 has consistently higher concentrations than well 4 in Al and U whereas well 4 has consistently higher concentrations of Na, Ca, SO₄, Mn, and Sr. Wells 7 and 5 in the middle well site are 7.6 m and 11.6 m deep respectively. Well 7 has consistently higher alkalinity, Na, B, and U whereas well 5 has consistently higher SO₄ and Mn.

Discussion

Geochemical evolution

In the ephemeral tributary of Beaver Creek, the CBM produced water (black squares) has a higher ⁸⁷Sr/⁸⁶Sr ratio than the local ground water (open squares) and is easily distinguished from ambient shallow ground water and surface water by the ⁸⁷Sr/⁸⁶Sr ratio (**Figure 4.5a-4.5d**). The ⁸⁷Sr/⁸⁶Sr ratio of the CBM water ranges from 0.71388 to 0.71457 and is therefore easily distinguished from the shallow ground water ⁸⁷Sr/⁸⁶Sr ratios ranging from 0.71255 to 0.71279.

Strontium concentration is higher in the CBM discharge points (black squares) than in the collection ponds (circles) to which they discharge (**Figure 4.5a**). Using the major ion concentrations for the upper and lower CBM discharge points and pond samples collected in December 2003 (Montana Bureau of Mines and Geology) and February 2005, and the water quality model Visual MINTEQ, the saturation indices were calculated for the upper and lower discharge points and ponds. Aragonite (CaCO₃), calcite (CaCO₃), dolomite (CaMg (CO₃)₂), strontianite (SrCO₃) and vaterite (CaCO₃) are all near saturation (saturation indices near zero) or oversaturated (have saturation indices greater than zero) in the CBM discharge water. The saturation indices of all these species increase in the associated collection ponds. The introduction of the atmospherically isolated CBM water to the holding ponds causes the pH to increase from an average of 7.28 in the CBM discharge water to an average of 8.55 in the associated ponds (**Table 4.3**). This more alkaline pH reduces the ability of the pond water to hold calcium carbonate in solution, increasing the likelihood of precipitation. The increase in pH from CBM to pond was also observed by Patz et al. (2006) and McBeth et al. (2003). In addition to precipitating as strontianite, the chemical similarity of strontium to calcium allows strontium to substitute into calcium carbonate minerals. The precipitation of these species causes the concentration of strontium to be lower in the collection ponds than the CBM water (**Figure 4.5a**).

The increase in Al and decrease in Ba and Mn concentrations from CBM discharge to the ponds was also noted by Patz et al. (2006) and McBeth et al. (2003). They proposed these changes were due to the increase in pH which increases the mobility of Al due to the formation of anionic Al complexes in alkaline pH, and causes the precipitation of BaSO₄ and MnCO₃.

Additional evidence that may indicate the precipitation of strontium is found in the stream samples. The stream samples collected from weirs below both ponds were found to have, in general, a slightly lower $^{87}\text{Sr}/^{86}\text{Sr}$ ratio than the CBM water (**Figure 4.5b**). This lower $^{87}\text{Sr}/^{86}\text{Sr}$ ratio is not expected to result from the addition of local groundwater because baseflow is unlikely in a loosing stream such as Payne and Saffer (2005) predict for this reach of Beaver Creek (**Figure 4.6**). However, if the lower $^{87}\text{Sr}/^{86}\text{Sr}$ ratio was from the dissolution of salts, one would predict an increase in strontium concentration – a condition not supported by the data. This downward shift in the $^{87}\text{Sr}/^{86}\text{Sr}$ ratio without a corresponding increase in strontium concentration is interpreted as either evidence of the precipitation and re-dissolution of strontium-bearing salts along the length of the stream bed or cation exchange with clays present in the soil. Cation exchange would contribute a lower the strontium isotope ratio to the water without changing the concentration.

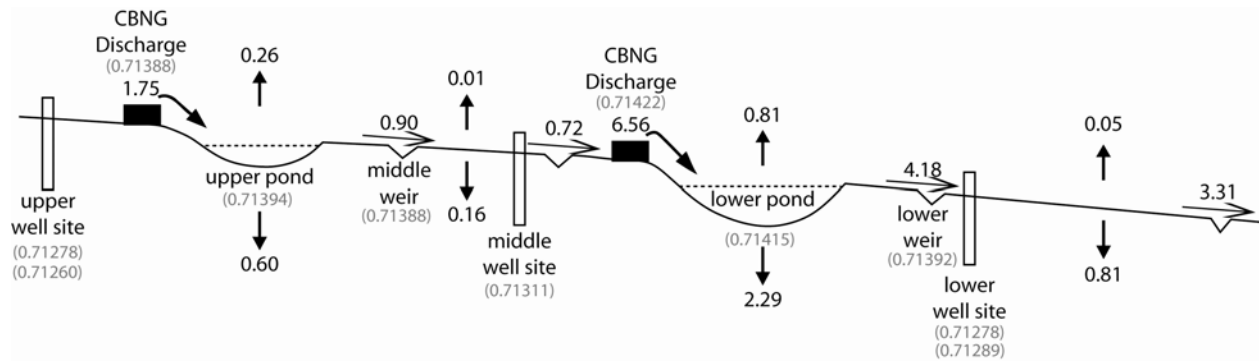


Figure 4.6: Beaver Creek water budget for the week of August 5-11, 2003. Values are in liters per second. Downward, upward and horizontal arrows represent infiltration, evaporation and surface flow respectively (Payne and Saffer, 2005). Parenthetical values in grey are the $^{87}\text{Sr}/^{86}\text{Sr}$ ratios for the sample set collected in August 2003.

Binary mixing

The middle well site wells (open triangles in **Figure 4.5c**) are between the two on-channel ponds and within the stream channel. The $^{87}\text{Sr}/^{86}\text{Sr}$ ratios at this site are intermediate between the upper pond and local groundwater (upper well) values, interpreted to represent mixing of strontium from these two end-members. The average strontium concentrations of the upper pond water, upper well site, and middle well site are 0.74, 1.69, and 1.01 respectively. The average $^{87}\text{Sr}/^{86}\text{Sr}$ ratios for the upper pond, the upper well site and the middle well site are 0.71398, 0.71267 and 0.71316 respectively. To determine the fraction of strontium in the middle well samples contributed by the upper CBM produced water collection pond we use a binary mixing equation (Equation 1a) (Faure, 1998):

$$\frac{{}^{87}\text{Sr}}{{}^{86}\text{Sr}}_{\text{Middle}} = \left(\frac{{}^{87}\text{Sr}}{{}^{86}\text{Sr}}_{\text{Pond}} \right) f_{\text{Pond}} \frac{(\text{Sr}_{\text{Pond}})}{(\text{Sr}_{\text{Middle}})} + \left(\frac{{}^{87}\text{Sr}}{{}^{86}\text{Sr}}_{\text{Upper}} \right) (1 - f_{\text{Pond}}) \frac{(\text{Sr}_{\text{Upper}})}{(\text{Sr}_{\text{Middle}})} \quad (1a)$$

The two end members in this mixing equation are the pond water and the upper well water. The resulting mixture is the middle well water. The terms “ $^{87}\text{Sr}/^{86}\text{Sr}$ ” in the equation refer to the $^{87}\text{Sr}/^{86}\text{Sr}$ ratio of water samples in the upper pond, upper wells and middle wells as indicated by the subscripts “Pond”, “Upper” and “Middle”. The quotient terms in the equation (Sr) refer to the concentration of strontium in the water samples indicated by the subscripts. This equation is solved for the unknown “f”, which is the fraction of water in the middle well water that is contributed by the pond. Substituting the average concentrations and $^{87}\text{Sr}/^{86}\text{Sr}$ ratios into this equation results in:

$$0.71316 = (0.71398)f \frac{0.74}{1.01} + (0.71267)(1 - f) \frac{1.69}{1.01} \quad (1b)$$

This equation is solved for the fraction of water from the pond (f):

$$f = 0.72 \quad (1c)$$

The CBM pond water contributes roughly 70% of the water in the middle wells and 30% is contributed by the local ground water. This calculation assumes that strontium concentrations of pond and CBM produced water are constant. If strontium from local sources enters the CBM produced water, either through dissolution of local salt or through cation exchange, the fraction of water contributed by CBM water could actually be much higher. Observations of the stream samples as described earlier indicate it is unlikely that the pond water infiltrated to the depth of the middle wells without interaction with the local strontium. The 70% estimate was calculated using the average values for the three sources of water samples. By adding and subtracting one standard deviation from the average values we estimate the potential range in the fraction of water supplied by the pond water. Using the variation within the data, a minimum of 65% and a maximum of nearly 100% were calculated using equation 1a. It is unlikely that all the water in the well originated from the CBM produced water, so this calculation is probably an artifact of averaging seasonal variation.

Because the $^{87}\text{Sr}/^{86}\text{Sr}$ ratio has remained unchanged from this intermediate value since the first collection, made 32 days after the upper pond began to fill, the data indicate that CBM water has either infiltrated to 11.5 meter-depths within this time frame or flowed through the alluvial aquifer from the pond to the middle well site. Thirty-two days, therefore, represents a maximum time for subsurface flow and infiltration to the water table.

This estimate agrees well with the hydrological measurements made by Payne and Saffer (2005) (**Figure 4.6**). Evidence of mixing as observed in intermediate strontium isotope values is corroborated by hydrologic monitoring of middle well 6 which shows increased ground water levels due to the infiltration of CBM water (**Figure 4.4a**) (Payne and Saffer, 2005). The water level in well 6 increased by 2 meters by May 2003, a rise attributed to CBM water infiltration. This rise was followed in the summer by a decrease of 1 meter, perhaps due in part to increased transpiration rates in the spring and summer retarding CBM infiltration and/or a change in water management by the CBM production company, which minimized overland flow. The water level increases again to 2.5 meters above the baseline from January 2004 to May 2004 followed again

by a decrease in water level during the growing season to the end of the monitoring period (August 2004).

There is a slight decrease in the $^{87}\text{Sr}/^{86}\text{Sr}$ ratio in the middle wells beginning July 2004 (**Figure 4.4b**). The timing of this decrease corresponds roughly to a change in water management. Minimal overland flow from the upper pond was allowed after this date, and the middle stream site was found to be dry during the August 2004, August 2005, and November 2005 sampling dates. However, the slight changes in average strontium concentration for the upper pond, upper wells and middle wells before August 2004 (0.738, 1.669, and 1.003) and after August 2004 (0.747, 1.724, and 1.019) results in the same percentage of strontium contribution from CBM using the binary mixing equation (Equation 1a). Although there was no surface flow in August 2004, 2005 and November 2005 there was the same percent contribution of CBM water to the middle wells. This implies that there is a significant CBM contribution to the water in the middle wells through subsurface flow.

Mobilization of salts

The addition of water to semi-arid soils has the potential to mobilize the salts that accumulate over time. Salts in soil originate from a number of sources including *in situ* weathering, atmospheric deposition, and the fossil salts associated with sedimentary rocks (Essington, 2004). Because strontium is chemically similar to calcium, changes in strontium concentration closely follow changes due to precipitation or dissolution of calcium bearing salts. The soil in this area is calcium-carbonate buffered (NRCS, 2004) so strontium should be a good indicator of mobilization of Beaver Creek salts. Additionally, some of the soils classified in this area are gypsum-rich including the Lismas series (found in T79N, R71W) partially composed of a Cy horizon with masses of gypsum throughout. Whereas the soil classifications in the drainage studied here do not include specific gypsum horizons, this mineral is common in Powder River Basin soils (NRCS, 2004).

The crosses in Figures 3.1.3D, 4A and 4B represent wells 11 (X) and 14 (+) in the lower well site, a set of nested wells that are below both ponds and slightly off-channel. Over time, well 14 has shown only modest increases in strontium isotope ratio upward towards that of the CBM input water (**Figure 4.4b**) but has shown strontium concentrations much greater than that of CBM water (**Figure 4.4a**). We interpret the increase in strontium concentration in well 14 to indicate the dissolution of salts in the previously unsaturated alluvial material as CBM water infiltrates. The increase in strontium concentration without a large increase in the $^{87}\text{Sr}/^{86}\text{Sr}$ ratio implies the mobilization of local salts, not the presence of salts originating in the CBM water. The local ground water as measured in the upper wells acquires its $^{87}\text{Sr}/^{86}\text{Sr}$ ratio from the soil and alluvium with which it interacts; therefore the local soil and alluvium must have an $^{87}\text{Sr}/^{86}\text{Sr}$ ratio of 0.7127. The high concentration of strontium derived from local sources in well 14 water keeps the overall strontium isotope ratio in well 14 from increasing to the higher $^{87}\text{Sr}/^{86}\text{Sr}$ ratio of CBM produced water despite the addition of CBM water indicated by the increase in water level in lower well 12 (**Figure 4.4a**) (Payne and Saffer, 2005). Cation exchange may play a role in maintaining a strontium isotope ratio in well 14 water near to that of the local ratio. However, the increase in strontium concentration implies a larger role is played by the dissolution of salts.

The increase in strontium concentration and slight increase in strontium isotope ratio in well 14 were not observed in well 11. We attribute this discrepancy to the greater depth of well 11 and the greater distance from the CBM produced water source in the streambed. These strontium data can constrain the extent of the water mounding predicted by the single soil layer SUTRA model of Payne (2004). Well 11 is out of the range of impact of the water mounding under the stream bed whereas well 14, being closer to the stream bed and shallower, is within the zone impacted by the CBM water. Using the strontium data from wells 11 and 14 we are able to verify the potential accuracy of this model and help constrain future, more detailed water mounding models.

The 2-fold increase in strontium concentration in lower well 14 and the relative absence of such changes in concentration at the middle well site may be related to the locations of the wells relative to the channel. The middle site wells are screened in the aquifer directly below the stream channel itself. This is a location that normally experiences annual to semi-annual flushing of soluble salts in the soil profile during spring run-off. These annual to semi-annual saturated flow events prevent the accumulation of soluble salts within the ephemeral channel. Therefore when CBM water is introduced to the channel there is no appreciable increase in strontium concentration and other water quality indicators such as TDS. In contrast, the lower site monitoring well 14 lies 5.5 meters off the stream channel on a terrace over a meter above the channel and is screened 4.5 meters below the surface. Annual spring flows persist only as long as the snowmelt, which most likely does not result in water mounding to the extent seen in lower well 12 (**Figure 4.4a**). Prior to the introduction of CBM water, this stream bank soil built up soluble salts between rare flooding events. The lower well site at well 14 is now experiencing saturated conditions due to ground water mounding related to CBM discharge (Payne, 2004; Payned and Saffer, 2005). The water mounds to a greater extent at the lower site than the middle well site due to higher surface flows (**Figure 4.6**) and possibly more subsurface flow due to the larger size of the lower pond compared to the upper pond. The water mounding at the lower well site impacts a larger volume of soil that is rarely saturated in contrast to the middle well site where CBM water infiltrates well flushed soil. We infer that the water at the lower well site is dissolving some of these soluble salts, leading to the observed increased concentrations of strontium and other major ions seen at the lower well site and not at the middle well site.

The composition (**Table 4.3**) of water in well 14 shows that Na, Ca, Mg, and SO₄ concentrations increase and then decrease with time and the concentrations are higher compared to both the upper wells and the CBM water. By using the water quality model MINTEQ, the saturation indices of calcite and gypsum were calculated for the twelve well 14 samples. Calcite is oversaturated implying it is unlikely to dissolve in this water, whereas gypsum is undersaturated implying it would likely dissolve if present. Dissolution of gypsum yields Ca ions which, due to the oversaturation of calcite, the Ca ions may then precipitate with carbonate as calcite. This re-precipitation of cations may explain why the concentration of SO₄ increases by 2500 ppm (52 meq/L) while Ca only increases by 200 ppm (10 meq/L). Additionally, SO₄ ions may also be contributed by the dissolution of MgSO₄, as indicated by the increase in Mg concentration in well 14.

If we use the upper wells as an indication of what salts may be present in local soil and alluvium, we see that the concentration of calcium (in meq/L) exceeds that of alkalinity. When this water

evaporates in the soil, the alkalinity in the upper well water would first be taken up as calcite leaving the remaining Ca and Mg to form sulfate salts. These sulfate species are far more soluble than calcite (Drever, 1997). The introduction of CBM water to soils containing these salts would first mobilize these sulfate species, resulting in the increase in SO_4 we see in lower well 14. The change in concentration of Mg and Na is nearly balanced (in meq/l) by the change in SO_4 . This fits the stoichiometry of bloedite ($\text{Na}_2\text{SO}_4 \cdot \text{MgSO}_4 \cdot 4\text{H}_2\text{O}$) which may be an ephemeral phase formed by evaporation in the vadose zone (Drever, 2006). While the Na increase may be explained by bloedite, the high solubility of sodium species would imply an even greater concentration of Na than is seen in well 14. In arid and semi-arid areas, it has been shown that Na and Cl are the first to dissolve (Drever and Smith, 1978). This apparent discrepancy may be the result of prior mobilization of Na species by flooding events.

It would be useful to predict how long soil and alluvium must be flushed before the pulse of high TDS water has been removed from the system. At Beaver Creek well 14 the concentration of a number of ions peaked within 9-18 months: the concentration of Ca peaked in October 2003, Na, Mg and SO_4 peaked in August 2004. Strontium also peaked in August 2004, but the concentration has not dropped significantly in the year following. We suggest that it is premature to make predictions about when water quality may improve on the basis of this limited monitoring history. Accurate predictions of ground water quality will require a longer monitoring period and a detailed soil chemistry investigation.

Conclusions: Subtask 3.1

We have used strontium isotopes in conjunction with strontium concentration to:

1. Fingerprint water from distinct aquifers.
2. Trace the interaction of water discharged during CBM production as it interacts with the surface, hyporheic zone and near-surface aquifers. Strontium isotope data from the middle well site illustrate that fractions of water from different sources can be estimated at sites irrespective of the effects of evaporation or precipitation.
3. Identify the mobilization of local soil-based salts. The Sr concentration and $^{87}\text{Sr}/^{86}\text{Sr}$ ratio of lower well 14 indicate that increasing ion concentrations in the water is due to mobilization of local salts in the soil.
4. Corroborate other geochemical data in explaining water quality changes due to precipitation and dissolution of salts.

The fundamental characteristic that allows this tracer to be applied is that the $^{87}\text{Sr}/^{86}\text{Sr}$ ratio of CBM water is markedly different than that of the surface and near surface waters in the Powder River Basin. However, the strontium isotope technique utilized here can be of use in other hyporheic zone investigations where amount and direction of water movement is of concern. In situations where the $^{87}\text{Sr}/^{86}\text{Sr}$ ratios are measurably different in surface and ground water the volume of contributed water can be estimated using simple mixing calculations. Introduced water such as roadway run-off is also a good candidate for strontium isotope tracing due to its interaction with asphalt, hydrocarbons, road salt and gravel. Additionally, agricultural inputs such as fertilizer, pesticides and herbicides make irrigation run-off an equally appealing candidate for strontium isotope tracing. The chemical and isotopic composition of mine drainage,

springs and geothermal water have a good possibility of being distinguishable from surface and near surface water chemistry and may therefore also be good candidates for strontium isotope tracing.

We have used this tool to trace the infiltration of product water and show a connection between changes in water quality and strontium concentration at an on-channel CBM disposal site. We suggest that on-channel discharge shows promise for future disposal in that there are fewer salts in existing channels due to annual flushing. However, the amount and duration of CBM discharge may exceed the water mounding caused by annual flooding, in which case stream bank salts may be mobilized. Additionally, the change in vegetation species and biomass that occurs due to the creation of a perennial stream may be of concern to landowners if the local vegetation, adapted to semi-arid conditions, is out-competed by undesirable riparian vegetation or by a floral community that is not stable when the source of water is removed (Stearns et al., 2005). The conclusions drawn here that existing ephemeral channels have fewer soluble salts than the associated floodplain imply that ponds excavated off existing channels (off-channel) may also experience the mobilization of local salts. Further work on salt mobilization from soils and the duration of ground water degradation in CBM situations is needed. The strontium isotope ratio may be used to fingerprint salts in off-channel situations as well. Additionally, in situations where CBM product water is used for irrigation, strontium isotopes are a good candidate for following changes to the calcium cycle caused by the high sodium levels in the CBM water.

Subtask 3.2

Introduction

The objective of this subtask was to identify locations in the Powder River Basin where coal seams are isolated from adjacent aquifers and hence water production will be limited to the coal. This task built upon the preliminary Sr isotopic data from CBM wells presented by Frost et al. (2002a) and the M.S. thesis of B.N. Pearson (2002). That work suggested that coal and sand aquifer systems may have distinct Sr isotopic compositions, and intermediate ratios may indicate incomplete aquifer isolation, hence wasteful excess water production. The initial work focused on the eastern area of the Powder River Basin in the vicinity of Gillette and Wright, Wyoming. These studies did not differentiate individual coal zones. Hence the additional work performed for this subtask had the following goals:

1. Can different coal zones be identified by distinct Sr isotopic compositions?
2. Do the trends identified in the Gillette area apply across the basin?
3. Do Sr isotopic compositions correlate to fracture patterns associated with individual wells as identified by Task 4?

Samples

The 189 ground water samples interpreted in this subtask include 30 from Frost et al. (2002a), 90 from Pearson (2002) and 69 new analyses (Campbell, 2007). The new water samples were obtained with the assistance of Coal Bed Methane Associates of Laramie, the Casper office of the Bureau of Land Management, Welldog Inc. with the cooperation of RMT Williams

Production Company and Black Diamond Production Company. These include 19 water samples from wells completed in sandstone aquifers. The 170 coal aquifer samples include water produced from the Eocene Wasatch Formation Lake DeSmet and Felix coal zones, and from the Upper Paleocene Fort Union Formation Wyodak Rider, Upper Wyodak, Lower Wyodak and Knobloch coal zones. The samples extend the geographic coverage of the previous studies (see map, **Figure 4.7**). We obtained water quality and Sr isotopic data for each sample (**Table 4.4**).

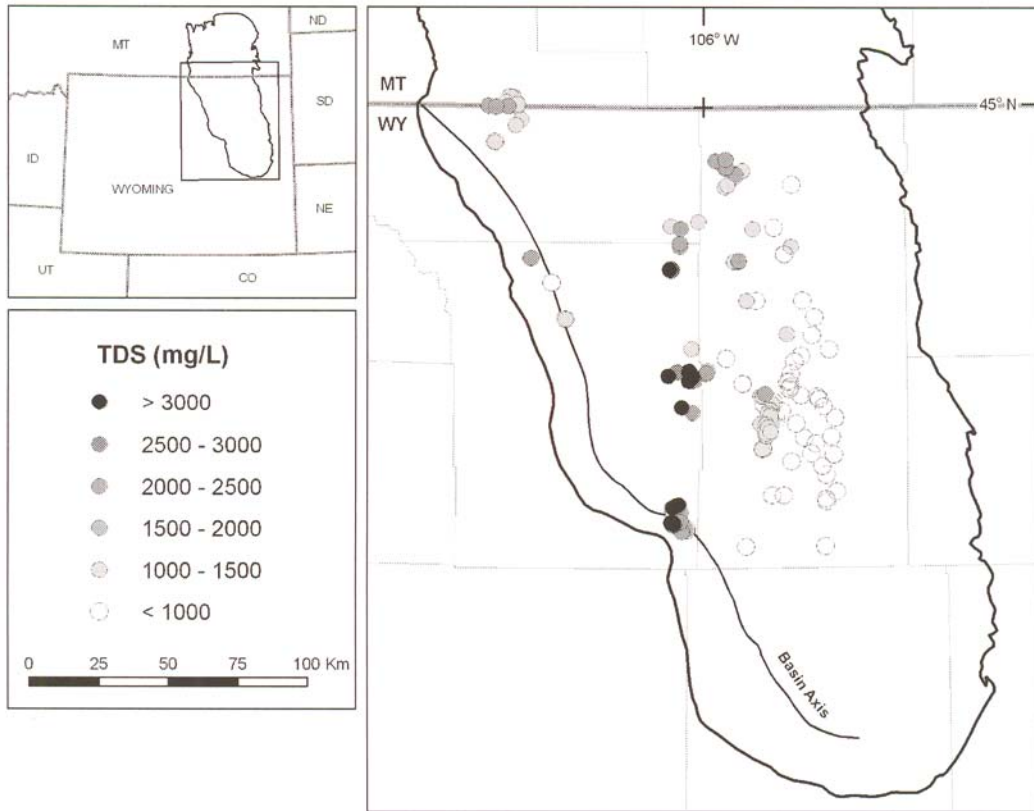


Figure 4.7: Map showing location of co-produced water samples used in this study. The circles are coded according to the TDS of the water. The highest TDS samples are located along the Johnson/Campbell county line.

Table 4.4: Sr Isotopic and Selected Water Quality Data for CBNG Co-produced Water Samples, Powder River Basin, Wyoming

Table 4. Sr isotopic and selected water quality data for CBNG co-produced water samples, Powder River Basin, Wyoming.

Sample Name	API Number	Well Name	Coal Name	Coal Zone	Depth (ft) (km)	Longitude	Latitude	87Sr/86Sr	TDS	SO4	SAR	Data Source
B1LD	1921166	Texaco 13U 31-32	Ucross	Lake De Smet	205	-106.788	44.520	0.71414	-	-	-	Pearson, 2002
B2LD	1921198	Texaco 43HE-123	Ucross	Lake De Smet	223	-106.784	44.506	0.71376	1,586	-	-	Pearson, 2002
B3F	1921269	LDEC 21BC1-212	Bull Creek	Felix	763	-106.691	44.425	0.71239	595	83.6	83.6	Pearson, 2002
B4F	1921270	LDEC 21BC2-212	Felix	Felix	905	-106.691	44.425	0.71149	535	7.46	7.46	Pearson, 2002
B5F	1921436	CrossH 32UF-1701	Upper Felix	Felix	945	-106.627	44.305	0.71193	547	18.1	18.1	Pearson, 2002
B6LD	1921437	Cross H 32U-1701	Ucross	Lake De Smet	397	-106.626	44.305	0.71256	1,071	8.2	8.2	Pearson, 2002
B7LD	1921505	Texaco 33BC-123	Bull Creek	Lake De Smet	695	-106.787	44.505	0.71275	1,138	68	68	Pearson, 2002
B8S	NA	JM Huber Gutz #1	Sand	Sand	190	-106.845	44.925	0.71005	703	14	27.18	Pearson, 2002
D52S	NA	JM Huber Beauty Gulch Pasture #1	Sand	Sand	4	-106.896	44.954	0.70829	1,900	23	26.06	Pearson, 2002
B9S	NA	JM Huber Paterson Well #2	Sand	Sand	40	-106.852	44.894	0.70960	-	-	-	Pearson, 2002
B10S	NA	Dunning #3 JM Huber LPD BWQ [SPRING?]	Sand	Sand	300	-106.902	44.948	0.70884	-	-	-	Pearson, 2002
B11S	NA	JM Huber S and J Paterson #1	Sand	Sand	140	-106.851	44.928	0.71044	706	12	26.67	Pearson, 2002
B12S	NA	JM Huber LPD BWQ Dunning Home #2	Sand	Sand	40	-106.908	44.973	0.71008	-	-	-	Pearson, 2002
B13S	NA	JM Huber Dunning Barn #1	Sand	Sand	40	-106.906	44.973	0.71080	-	-	-	Pearson, 2002
BD1BL	1926349	Landrey 22-20-5277C	Cook	Lower Wyodak	1,577	-106.153	44.469	0.71547	1,757	1.9	18.3	Campbell, 2007
BD2BU	1926350	Landrey 22-20-5277D	Anderson	Upper Wyodak	1,202	-106.153	44.469	0.71404	3,046	2.3	35.4	Campbell, 2007
BD3BU	1926351	Landrey 42-20-5277D	Anderson	Upper Wyodak	1,075	-106.145	44.470	0.71333	2,343	1.8	36.3	Campbell, 2007
BD4BL	1926357	Landrey 31-20-5277C	Cook	Lower Wyodak	1,515	-106.148	44.473	0.71483	2,714	0.3	37.6	Campbell, 2007
BD5BU	1926353	Landrey 31-20-5277D	Anderson	Upper Wyodak	1,200	-106.148	44.473	0.71249	2,609	0.4	33.1	Campbell, 2007
BD7BL	1926358	Landrey 33-20-5277C	Cook	Lower Wyodak	1,451	-106.148	44.466	0.71517	1,841	0.5	19.1	Campbell, 2007
BD8AU	1926352	Landrey 33-20-5277B	Anderson	Lower Wyodak	1,060	-106.146	44.469	0.71475	2,362	0	52.5	Campbell, 2007
BD9AL	1926354	Landrey 42-20-5277B	Wall	Lower Wyodak	1,649	-106.146	44.469	0.71475	1,123	14.1	16	Campbell, 2007
BD10BL	1926359	Landrey 42-20-5277C	Cook	Lower Wyodak	1,442	-106.146	44.470	0.71506	2,544	1.1	26.8	Campbell, 2007
BW1W	1923370	Moore Land Federal 41-14-4277	Big George	Wyodak Rider	1,235	-106.071	43.617	0.71218	1,193	0	6.01	Campbell, 2007
BW2W	1923392	Moore Land Federal 12-11-4277	Big George	Wyodak Rider	1,330	-106.086	43.628	0.71536	1,351	0	8.15	Campbell, 2007
BW3W	1923393	Moore Land Federal 21-11-4277	Big George	Wyodak Rider	1,462	-106.080	43.631	0.71213	1,348	0	5.71	Campbell, 2007
BW4W	1923394	Moore Land Federal 23-11-4277	Big George	Wyodak Rider	1,332	-106.081	43.624	0.71211	1,662	0.2	7.07	Campbell, 2007
BW5W	1923400	Moore Land Federal 43-11-4277	Big George	Wyodak Rider	1,322	-106.071	43.625	0.71221	1,266	0	6.43	Campbell, 2007
BW6W	1924199	BCU Dry Fork 21-27-4377	Big George	Wyodak Rider	1,583	-106.103	43.676	0.71806	2,010	0	8.16	Campbell, 2007
BW7W	1924888	BCU Dry Fork 34-17-4377	Big George	Wyodak Rider	1,489	-106.136	43.692	0.71203	3,033	0.1	12.1	Campbell, 2007
BW8W	1924891	BCU State 41-16-4377	Big George	Wyodak Rider	1,443	-106.112	43.703	0.71314	4,467	0.1	21.2	Campbell, 2007
BW9W	1924897	BCU State 12-16-4377	Big George	Wyodak Rider	1,604	-106.125	43.700	0.71222	1,844	0.1	9.37	Campbell, 2007
BW10W	1924914	BCU Dry Fork 21-20-4377	Big George	Wyodak Rider	1,536	-106.142	43.689	0.71210	1,419	0.1	8.69	Campbell, 2007
BW11W	1925029	BCU 32-28-4377	Big George	Wyodak Rider	1,607	-106.117	43.671	0.71260	1,144	0	6.23	Campbell, 2007
BW12W	1925038	BCU 32-15-4277	Big George	Wyodak Rider	1,438	-106.096	43.614	0.71200	1,690	0	9.57	Campbell, 2007
BW13W	1925050	BCU 34-33-4377	Big George	Wyodak Rider	1,450	-106.116	43.650	0.71300	2,263	0	12.1	Campbell, 2007
BW14W	1925054	BCU 14-34-4377	Big George	Wyodak Rider	1,604	-106.108	43.650	0.71259	912	0	6.4	Campbell, 2007
BW15W	1925061	BCU 34-5-4277	Big George	Wyodak Rider	1,434	-106.136	43.635	0.71143	2,334	0	10.4	Campbell, 2007
BW16W	1925073	BCU 32-5-4277	Big George	Wyodak Rider	1,485	-106.136	43.643	0.71175	3,170	0	14.9	Campbell, 2007
BW17W	1925080	BCU 43-5-4277	Big George	Wyodak Rider	1,490	-106.131	43.639	0.71217	4,020	0	30.9	Campbell, 2007
BW18W	1925086	Bullhacker Creek UN 32-3-4277	Big George	Wyodak Rider	1,479	-106.097	43.643	0.71283	1,364	0	7.38	Campbell, 2007
BW19W	1925087	Bullhacker Creek UN 23-3-4277	Big George	Wyodak Rider	1,493	-106.101	43.639	0.71239	1,012	0	8.42	Campbell, 2007
BW20W	1925088	Bullhacker Creek UN 21-3-4277	Big George	Wyodak Rider	1,517	-106.101	43.647	0.71438	2,160	0.1	9.7	Campbell, 2007

Final Report: Produced Water Management and Beneficial Use

Sample Name	API Number	Well Name	Coal Name	Coal Zone	Depth (ft) zone (km)	Distance from east recharge	Longitude	Latitude	87Sr/86Sr	TDS	SO4	SAR	Data Source
BW21W	1925099	BCU 12-5-4277	Big George	Wyodak Rider	1,484		-106.146	43.643	0.71055	3,161	0	12.6	Campbell, 2007
BW22W	1926313	BCU 32-29-4377	Big George	Wyodak Rider	1,553		-106.136	43.671	0.71266	1175	0	7.21	Campbell, 2007
G1U	530473	Lynde Trust 15-34	Wyodak	Upper Wyodak	482	12.5	-105.487	44.056	0.71294	382	0.1	6	Frost et al., 2002a
G2U	530802	Thrush 5-44	Wyodak	Upper Wyodak	275	5.8	-105.405	43.987	0.71287	644	0.1	8	Frost et al., 2002a
G3U	530949	Mankin 14-23	Wyodak	Upper Wyodak	612	10.3	-105.477	44.048	0.71319	530	0	7	Pearson, 2002
G4U	530994	Leo CG 41-30	Wyodak	Upper Wyodak	399	6.7	-105.477	44.048	0.71315	625	0.1	7	Frost et al., 2002a
G5U	531229	John Miller 5-32-15	Wyodak	Upper Wyodak	270	10.1	-105.496	44.315	0.71268	720	0.08	8.4	Frost et al., 2002a
G6U	531234	Durham Ranch 3-31-20-4571	Wyodak	Upper Wyodak	457	13.8	-105.412	43.867	0.71339	660	0	6.3	Frost et al., 2002a
G7U	531384	Durham Ranch 5-33-3	Anderson	Upper Wyodak	661	14.6	-105.493	43.903	0.71333	571	0.1	7	Frost et al., 2002a
G8U	531494	Durham Ranch 8-42-11	Anderson	Upper Wyodak	570	14	-105.468	43.893	0.71305	-	0.01	6.9	Frost et al., 2002a
G9U	531760	Durham State 34-16	Anderson	Upper Wyodak	715	20.9	-105.513	43.870	0.71419	510	0.03	7.3	Frost et al., 2002a
G10U	531900	MM 24-7	Fort Union	Upper Wyodak	853	16.3	-105.560	44.059	0.71380	620	0.73	6.9	Pearson, 2002
G11U	531934	Tripp 41-2	Wyodak	Upper Wyodak	842	20.7	-105.589	44.171	0.71354	888	0.1	8	Pearson, 2002
G12K	532105	Haight 22-25	Pawnee/Cache	Knobloch	1,411	8.2	-105.457	44.023	0.71242	270	0.04	10.28	Pearson, 2002
G13U	532860	W. Fork Floechni 43-42	Wyodak	Upper Wyodak	879	16.3	-105.445	43.801	0.71396	480	0.75	6.1	Pearson, 2002
G14U	532910	Lang 14-14	Fort Union	Upper Wyodak	901	20.5	-105.605	44.132	0.71379	840	0	8.1	Pearson, 2002
G15U	531711	Bog State 2-36	Wyodak	Upper Wyodak	765	10.9	-105.450	43.569	0.71370	395	0.1	6	Frost et al., 2002a
G16U	533031	Swanson 13-14-49-72	Anderson	Upper Wyodak	531	10.9	-105.487	44.220	0.71244	-	-	-	Pearson, 2002
G17U	533115	Durham Ranch 13-36	Wyodak	Upper Wyodak	746	5.9	-105.464	43.830	0.71393	390	0.82	6.1	Frost et al., 2002a
G18U	533307	Bluebird CS State #1	Big George	Upper Wyodak	1,094	38.1	-105.822	44.098	0.71420	900	4.34	-	Pearson, 2002
G19U	533964	Laney 9-19-49-71A	Anderson	Upper Wyodak	450	6.7	-105.430	44.209	0.71276	620	4	7.1	Frost et al., 2002a
G20U	533975	Moser 14-35	Wyodak	Upper Wyodak	1,014	21.4	-105.606	44.089	0.71417	660	0	7.3	Pearson, 2002
G21U	533977	Moser 43-27	Wyodak	Upper Wyodak	1,066	24.1	-105.611	44.107	0.71355	697	0.9	7	Frost et al., 2002a
G22U	534071	Wagensen 11-32-4671	Wyodak	Upper Wyodak	397	8.4	-105.421	43.926	0.71358	509	0.25	-	Frost et al., 2002a
G23U	534083	Heiland 42-3-4773	Wyodak	Upper Wyodak	992	22.5	-105.612	44.081	0.71386	710	1.9	7	Frost et al., 2002a
G24U	534118	Persson 12-33	Wyodak	Upper Wyodak	1,315	24.3	-105.647	44.009	0.71429	700	0.89	7.8	Pearson, 2002
G25U	534171	Schlautmann 9-10-45-74BG	Canyon	Upper Wyodak	1,432	38.2	-105.731	43.884	0.71414	900	12	9.3	Frost et al., 2002a
G26W	534174	Schlautmann 16-10-45-74WY	Anderson	Wyodak Rider	1,225	38	-105.731	43.887	0.71320	970	5.1	11	Pearson, 2002
G27W	534176	Schlautmann 15-10-45-74BG	Anderson	Wyodak Rider	1,146	39	-105.736	43.884	0.71367	1120	1.5	12	Pearson, 2002
G28W	534249	Heiland 24-27-4873	Wyodak	Wyodak Rider	775	22	-105.621	44.104	0.71338	680	0.1	6	Frost et al., 2002a
G29U	534735	Rourke 8-18-48-71A	Anderson	Upper Wyodak	490	6.5	-105.427	44.139	0.71304	-	-	-	Pearson, 2002
G30U	535359	Lindsey 21-13-4673	Wyodak	Upper Wyodak	1,044	20.2	-105.580	43.968	0.71403	777	0.03	-	Frost et al., 2002a
G31U	535985	Steinboedel 5-7-49-71	Anderson	Upper Wyodak	326	8.3	-105.446	44.242	0.71261	-	-	-	Pearson, 2002
G32U	536125	Meserve 5-3-49-72A	Anderson	Upper Wyodak	498	12.7	-105.507	44.256	0.71287	770	0.07	7.6	Pearson, 2002
G33W	536791	McBeth 41-7-4673BG	Big George	Wyodak Rider	1,008	26.8	-105.671	43.983	0.71372	772	0.039	-	Frost et al., 2002a
G34U	537482	Milne 15-30-49-72A	Anderson	Upper Wyodak	911	17.7	-105.558	44.189	0.71327	800	0.06	8	Pearson, 2002
G35U	538804	Bluebird CS State #19	Wyodak	Upper Wyodak	1,375	38	-105.822	44.098	0.71597	897	3.32	-	Pearson, 2002
G36U	539087	Throne 14-23-4774	Wyodak	Upper Wyodak	1,514	29.1	-105.727	44.033	0.71473	907	0	-	Pearson, 2002
G37U	539139	Geer 43-24-4774	Wyodak	Upper Wyodak	1,368	28.8	-105.692	44.030	0.71430	1,195	0.25	-	Campbell, 2007
G38U	539435	Durham Ranch 23-26-4573	Wyodak	Upper Wyodak	1,040	27.6	-105.601	43.844	0.71510	810	1.8	7.1	Frost et al., 2002a
G39U	540399	Hayden 23-11-4774	Wyodak	Upper Wyodak	1,510	26.5	-105.722	44.064	0.71435	1,578	1.94	8.39	Campbell, 2007
G40U	540415	Geer 21-15-4774	Wyodak	Upper Wyodak	1,590	28.2	-105.741	44.056	0.71509	1,214	0.07	8.58	Campbell, 2007
G41W	540416	Geer 32-15-4774BG	Big George	Wyodak Rider	1,286	27.1	-105.737	44.053	0.71372	-	0.15	-	Campbell, 2007

Final Report: Produced Water Management and Beneficial Use

Sample Name	API Number	Well Name	Coal Name	Coal Zone	Depth (ft)	Distance from east recharge zone (km)	Longitude	Latitude	87Sr/86Sr	TDS	SO4	SAR	Data Source
G42U	540418	Hayden 41-15-4774	Wyodak	Upper Wyodak	1,584	27.1	-105.731	44.057	0.71460	1,266	1.65	8.26	Campbell, 2007
G43W	541776	Persson 43-12-4674 BG	Big George	Wyodak Rider	1,175	29.3	-105.692	43.975	0.71343	1,349	2	11.5	Campbell, 2007
G44U	541784	State 41-36-4774 BG	Big George	Upper Wyodak	1,091	28.1	-105.693	44.012	0.71376	1,109	0	10.4	Campbell, 2007
G45U	541788	State 21-36-4774 BG	Big George	Upper Wyodak	1,077	28.1	-105.702	44.012	0.71452	1,343	2.45	9.48	Campbell, 2007
G46U	541789	State 14-36-4774 BG	Big George	Upper Wyodak	1,180	28.9	-105.707	44.001	0.71444	1,262	1.43	7.85	Campbell, 2007
G47W	541935	Geer 34-1-4674BG	Big George	Wyodak Rider	1,164	30.1	-105.697	43.986	0.71351	1,402	6.91	11	Campbell, 2007
G48W	541938	Geer 32-1-4674BG	Big George	Wyodak Rider	1,080	32	-105.697	43.994	0.71355	1,284	0.08	11.3	Campbell, 2007
G49U	542226	Geer 22-19-4773	Wyodak	Upper Wyodak	1,356	26.5	-105.683	44.038	0.71423	883	0.54	8.05	Campbell, 2007
G50W	543933	Persson 41-15-4674BG	Big George	Wyodak Rider	1,230	34.4	-105.732	43.967	0.71357	1,378	1.19	11.7	Campbell, 2007
G51W	543939	Persson 21-15-4674BG	Big George	Wyodak Rider	1,308	36.6	-105.742	43.967	0.71278	1,407	1.64	12.3	Campbell, 2007
G52W	543943	McBeth 21-25-4674BG	Big George	Wyodak Rider	1,070	33.1	-105.702	43.938	0.71403	1,192	9.82	11.9	Campbell, 2007
G53W	543944	McBeth 34-26-4674BG	Big George	Wyodak Rider	1,010	32.4	-105.717	43.927	0.71372	1,201	0.06	11.9	Campbell, 2007
G54U	543946	McBeth 34-26-4674	Wyodak	Upper Wyodak	1,365	32.7	-105.717	43.927	0.71464	1,046	2.88	10.6	Campbell, 2007
G55W	543952	McBeth 23-23-4674BG	Big George	Wyodak Rider	1,085	35.6	-105.721	43.945	0.71358	1,186	2.33	12	Campbell, 2007
G56W	543957	Ruby 32-14-4674BG	Big George	Wyodak Rider	1,225	35.7	-105.717	43.964	0.71392	1,361	1.96	11	Campbell, 2007
G57W	543959	McBeth32-26-4674BG	Big George	Wyodak Rider	1,080	32.7	-105.717	43.935	0.71376	1,215	0.27	11.7	Campbell, 2007
G58W	543981	McBeth 14-13-4674BG	Big George	Wyodak Rider	1,122	34.1	-105.707	43.956	0.71397	1,330	0.07	10.4	Campbell, 2007
G59U	547297	Flying T 12-32-4672	Canyon	Upper Wyodak	1,028	18.9	-105.545	43.921	0.71332	997	0.81	7.82	Campbell, 2007
G60W	543969	McBeth 34-24-4674BG	Big George	Wyodak Rider	975	35.7	-105.697	43.942	0.71407	1,306	0	10.3	Campbell, 2007
G61U	532140	Little Thunder Edwards 43-124372	Wyodak	Upper Wyodak	675	14	-105.445	43.714	0.71366	396	1.8	6	Frost et al., 2002a
G62U	533187	Thunder Edwards 21-7	Wyodak	Upper Wyodak	606	12.3	-105.446	43.722	0.71333	470	17	5.7	Pearson, 2002
G63W	534517	Pine Tree Draw CS State #1	Big George	Wyodak Rider	1,075	27.6	-105.807	43.567	0.71378	649	2.95		Pearson, 2002
G64U	534524	Stuart 12-33	Wyodak	Upper Wyodak	620	9.3	-105.399	43.747	0.71363	494	-		Frost et al., 2002a
G65W	535476	Moore CS #60	Big George	Wyodak Rider	925	32.8	-105.688	43.735	0.71387	671	0.05		Pearson, 2002
G66W	543698	Groves CS #21	Big George	Wyodak Rider	980	28.8	-105.637	43.735	0.71457	571	0.29		Pearson, 2002
G67S	NA	Monitoring	Sand	Sand	80	10.6	-105.487	44.123	0.71263	4290	2410		Frost et al., 2002a
G68S	NA	Martens and Peck Sec. 22 CBM Sand Monitoring	Sand	Sand	400	10.6	-105.486	44.123	0.71265	587	99.7		Frost et al., 2002a
G69S	NA	Monitoring	Sand	Sand	185	10.6	-105.487	44.123	0.71271	3650	2140		Frost et al., 2002a
G70S	NA	Barlow BWO Glenn Barlow #4 Permit 166	Sand	Sand	400	42.5	-105.869	44.189	0.71214	588	296		Pearson, 2002
G75S	NA	Barlow BWO Glenn Barlow #2 Permit 164	Sand	Sand	400	42.5	-105.869	44.189	0.71214	588	296		Pearson, 2002
G71S	NA	Throne 11-26-4774 MS	Sand	Sand	1,450	43	-105.874	44.176	0.71179	322	-		Pearson, 2002
G72S	NA	BRC FED 33-31A	Sand	Sand	300	10.6	-105.430	43.657	0.71304	1580	983		Pearson, 2002
G73S	P128990W	All Night Creek Sand Barrett State 13-36-4374 MS	Sand	Sand	860	25.9	-105.714	43.660	0.71228	281	1.1		Pearson, 2002
G74S	NA	CBM-MON-1W	Sand	Sand	860	29.6	-105.687	44.255	0.71258	1010	10	13	Frost et al., 2002a
G54C	NA	CBM-MON-2	Wyodak-upper	Upper Wyodak	905	22.8	-105.621	44.260	0.71349	1030	1	9	Frost et al., 2002a
N1U	529839	Walls Fee 74-7	Wyodak	Upper Wyodak	480	6.3	-105.551	44.368	0.71308	990	0.81	7.7	Pearson, 2002
N2U	531001	Hall 33-2633	Canyon	Upper Wyodak	299	0	-105.602	44.545	0.71335	1,040	0.7	8	Frost et al., 2002a
N3L	532869	Soukup Draw State #1	Lower Canyon	Lower Wyodak	528	3.4	-105.633	44.522	0.71366	894	0.17		Pearson, 2002
N4L	534205	Parks Longhorn 6-14-55-73W	Pawnee	Lower Wyodak	545	0	-105.598	44.749	0.71393	800	3	11	Pearson, 2002
N5L	534424	L-X Bar LXFEE 14-35A	Anderson	Upper Wyodak	543	21.8	-105.854	44.775	0.71314	1,320	1.2	23	Pearson, 2002
N6L	534425	LXFEE 3-2C	Canyon	Lower Wyodak	805	21.8	-105.854	44.782	0.71175	1,600	1.6	23	Pearson, 2002
N7U	534475	West 12-28CA	Canyon	Upper Wyodak	645	25.8	-105.901	44.800	0.71238	1,550	0.92	22	Pearson, 2002
N8L	534690	LX-State-1-36C	Canyon	Lower Wyodak	687	19.4	-105.824	44.793	0.71404	1,050	0.16	22	Pearson, 2002

Final Report: Produced Water Management and Beneficial Use

Sample Name	API Number	Well Name	Coal Name	Coal Zone	Depth (ft) zone (km)	Distance from east recharge	Longitude	Latitude	87Sr/86Sr	TDS	SO4	SAR	Data Source
N9U	535333	LX-State 1-36ALC	Anderson	Upper Wyodak	390	19.4	-105.824	44.794	0.71362	1,390	1.9	18	Pearson, 2002
N10L	535352	West 16-13CO	Cook	Lower Wyodak	1,020	30.9	-105.946	44.825	0.71463	2,000	0.16	32	Pearson, 2002
N11U	535416	Floyd 10-28-51-74A	Anderson	Upper Wyodak	812	22.4	-105.760	44.367	0.71449	540	0.78	13	Frost et al., 2002a
N12U	535851	Floyd 10-30-51-74A	Anderson	Upper Wyodak	963	26.3	-105.803	44.368	0.71399	1,306	1.2		Frost et al., 2002a
N13K	536006	WEST 6-28-56-75CO	Wall/Pawnee	Knobloch	603	25.2	-105.894	44.804	0.71256	1,550	0.07	32	Pearson, 2002
N14U	538294	Spotted Horse CS State #13	Upper Canyon	Upper Wyodak	603	25.2	-105.901	44.739	0.71332	1,331	0.83		Pearson, 2002
N15L	538300	Spotted Horse CS State #6	Wall	Lower Wyodak	775	24	-105.891	44.746	0.71414	1,350	1.22		Pearson, 2002
N16L	539040	Stevens 5-4-53-74A	Anderson	Lower Wyodak	1,085	12.3	-105.776	44.605	0.71418	-	-		Pearson, 2002
N17L	540220	Soukup Draw CS State #7	Wall	Lower Wyodak	811	3.4	-105.633	44.522	0.71343	593	0.04		Pearson, 2002
N18U	540502	Kline Draw CS State #12	Upper Canyon	Upper Wyodak	360	28	-105.900	44.830	0.71213	1,443	0.46		Pearson, 2002
N19L	540518	Kline Draw CS State #28	Cook	Lower Wyodak	615	28	-105.900	44.830	0.71218	1,362	0.58		Pearson, 2002
N20L	540534	Kline Draw CS State #44	Wall	Lower Wyodak	701	28	-105.900	44.830	0.71486	1,624	1.07		Pearson, 2002
N21L	541229	Stevens 5-4-53-74CO-R	Cook	Lower Wyodak	1,120	12.3	-105.775	44.604	0.71481	1,004	0.27		Pearson, 2002
N22U	541695	BC 07CK-05-53-73	Cook	Upper Wyodak	661	3.4	-105.664	44.606	0.71427	-	9.52		Pearson, 2002
N23U	542974	BC 01CN-06-53-73	Canyon	Upper Wyodak	492	4	-105.679	44.609	0.71456	715	6.32		Pearson, 2002
N24U	3321346	Kuhn Ranch 1-3-53-77A	Anderson	Upper Wyodak	904	38.4	-105.104	44.604	0.71065	1,741	0.92		Pearson, 2002
N25U	554969	Laramore 5275-10-43CA	Canyon	Upper Wyodak	720	25.2	-105.862	44.495	0.71322	1,029	1.9	11.9	Cambell, 2007
N26K	554972	Laramore 5275-11-43WA	Cook	Knobloch	1,725	23.4	-105.841	44.496	0.71468	1,617	3.9	12.6	Cambell, 2007
N27L	554973	Laramore 5275-10-43MO	Wall	Lower Wyodak	1,460	25.2	-105.862	44.495	0.71336	1,489	0.9	15.3	Cambell, 2007
N28U	554976	Laramore 5275-11-41LA	Anderson Lower	Upper Wyodak	589	22.1	-105.837	44.499	0.71321	1,642	5.8	16.4	Cambell, 2007
N29W	554978	Laramore 5275-10-43LA	Anderson Lower	Wyodak Rider	508	22.1	-105.862	44.496	0.71357	1,445	0.6	18.6	Cambell, 2007
N30K	1921558	Kuhn Ranch 7-27-53-77W	Wall	Knobloch	1,667	40	-105.108	44.545	0.71495	1,549	0.04		Pearson, 2002
N31W	1921910	Kuhn Ranch 7-22-53-77A	Anderson	Wyodak Rider	978	38.7	-105.108	44.556	0.71293	1,698	1.63		Pearson, 2002
N32U	3320335	Floyd 9-29A	Anderson	Upper Wyodak	656	32.3	-105.023	44.626	0.71312	1,240	0.12	24	Pearson, 2002
N33U	3321101	Tietjen 15-29-5477A	Anderson	Upper Wyodak	917	42.1	-105.149	44.612	0.71166	1,446	1.6		Pearson, 2002
N34S	NA	Arvada/BWO Gallimore #1	Sand	Sand	200	44.3	-105.133	44.654	0.71154	968	13	21.4	Pearson, 2002
NE2S	NA	Redstone Sand	Sand	Sand	140	0.5	-105.608	44.549	0.71271	1,660	740	5	Pearson, 2002
S1U	529688	BTP 4975 8-32	Wall	Upper Wyodak	1,795	45.6	-105.897	44.180	0.71479	624	1.2	8	Frost et al., 2002a
S2W	536103	SRU 23-22-4876	Big George	Wyodak Rider	1,450	53.5	-105.982	44.118	0.71496	-	-	17.7	Cambell, 2007
S3W	536109	SRU Iberlin 14-15-4876	Big George	Wyodak Rider	1,520	52.4	-105.988	44.129	0.71540	1,990	54.6	15.4	Cambell, 2007
S4W	541364	Schoonover Road CMB 21-15-4876	Big George	Wyodak Rider	1,688	51.7	-105.983	44.140	0.71402	1,308	2.34		Pearson, 2002
S5W	550056	Schoonover Road CMB 23-15-4876	Big George	Wyodak Rider	1,609	50.7	-105.984	44.133	0.71126	1,504	-	7.78	Cambell, 2007
S6W	1921071	Pilot State 16-32	Big George	Wyodak Rider	1,224	62.6	-105.118	44.136	0.71280	2,720	0.3	26	Frost et al., 2002a
S7W	1921141	Lantern CS State 1	Big George	Wyodak Rider	1,043	56.5	-105.051	44.002	0.71307	1,717	-		Pearson, 2002
S8W	1921469	Jones 11-1996	Big George	Wyodak Rider	1,561	57.4	-105.054	44.211	0.71386	1,418	17.8		Pearson, 2002
S9W	1922921	KU Illicit L&L 32-27-4777	Big George	Wyodak Rider	1,561	60.7	-105.097	44.019	0.71100	3,631	-	31.7	Cambell, 2007
S10W	1924064	Harriet L&L Fed 32-19-4877	Big George	Wyodak Rider	1,451	66.3	-105.159	44.122	0.71113	3,823	-	27.7	Cambell, 2007
S11W	1925501	SRU 12-30-4876	Big George	Wyodak Rider	1,205	56.9	-105.047	44.105	0.71288	2,699	0.2	21.8	Cambell, 2007
S12W	1925517	SRU 12-19-4876	Big George	Wyodak Rider	1,268	58.7	-105.048	44.121	0.71388	3,195	0.1	31	Cambell, 2007
S13W	1925557	SRU 12-25-4877	Big George	Wyodak Rider	1,179	58.9	-105.067	44.106	0.71460	3,795	-	29.6	Cambell, 2007
S14W	1925566	SRU 23-13-4877	Big George	Wyodak Rider	1,327	57.2	-105.063	44.132	0.71340	3,416	0.2	25.6	Cambell, 2007
S15W	1925568	SRU 21-13-4877	Big George	Wyodak Rider	1,539	57.2	-105.063	44.139	0.71348	3,270	0.1	24.8	Cambell, 2007
S16S	141663	Stramhan Federal 14 MG-1498 Sand	Sand	Sand	1,130	69.6	-105.217	44.215	0.71185	91.5	13.8		Pearson, 2002

Final Report: Produced Water Management and Beneficial Use

Sample Name	API Number	Well Name	Coal Name	Coal Zone	Depth (ft) zone (km)	Distance from east recharge (km)	Longitude	Latitude	87Sr/86Sr	TDS	SO4	SAR	Data Source
SH1U	3320292	Rice and sons 33C-2674	Carney	Upper Wyodak	646		-106.954	44.885	0.71164	954	0.11		Pearson, 2002
SH2U	3320317	Rice and sons 33M-2674	Monarch	Upper Wyodak	561		-106.954	44.884	0.71216	1,070	1.31		Pearson, 2002
SH3U	3320688	Pilch 11A-35-58-83	Anderson	Upper Wyodak	442		-106.835	44.958	0.70808	1,289	0.72		Pearson, 2002
SH4L	3320827	LPD 13M-3 57-83	Monarch	Lower Wyodak	660		-106.860	44.939	0.71121	1,284	0.04		Pearson, 2002
DS7C	2500321243	Consol 43EC-1990	Carney	Lower Wyodak	630		-106.872	45.029	0.71034	1199	-		Pearson, 2002
DS7C	2500321390	State/Consol 33C-3699	Carney	Lower Wyodak	705		-106.986	45.000	0.71000	1600	-		Pearson, 2002
DS6C	2500321390	Consol 33C-3699	Carney	Lower Wyodak	705		-106.896	45.000	0.70991	1536	-		Pearson, 2002
DS7C	2500321378	Consol 31C-3290	Carney	Lower Wyodak	650		-106.854	45.000	0.71060	1327	-		Pearson, 2002
DS9C	2500321512	Shell 44D-3399	Dietz	Upper Wyodak	318		-106.951	44.997	0.70937	1337	-		Pearson, 2002
DS9C	2500321400	Consol 43D-1990	Dietz	Upper Wyodak	321		-106.872	45.029	0.70903	1092	0.125		Pearson, 2002
DS10C	2500321313	State/Consol 33DI-3699	Dietz 1	Upper Wyodak	249		-106.896	45.000	0.70791	1899	0.23		Pearson, 2002
DS11C	2500321332	Consol 31DI-3290	Dietz 1	Upper Wyodak	297		-106.854	45.009	0.70850	1067	16.5		Pearson, 2002
DS12C	2500321299	Consol 33D2/3-3699	Dietz 2/3	Upper Wyodak	379		-106.896	45.000	0.70980	1074	0.15		Pearson, 2002
DS14C	2500321513	Shell 44M-3399	Monarch	Upper Wyodak	421		-106.951	44.997	0.71168	1,717	-		Pearson, 2002
DS16C	2500321396	Consol 14M-1990	Monarch	Upper Wyodak	354		-106.885	45.027	0.71051	932	-		Pearson, 2002
DS17C	2500321298	State/Consol 33M-3699	Monarch	Upper Wyodak	482		-106.896	45.000	0.71048	1250	-		Pearson, 2002
DS18C	2500321325	Consol 13M-2599	Monarch	Upper Wyodak	418		-106.906	45.015	0.71073	1219	0.03		Pearson, 2002
DS19C	2500321361	Consol 42M-3290	Monarch	Upper Wyodak	468		-106.852	45.005	0.71120	1216	0.074		Pearson, 2002

Results

Water quality results

Lee (1981) showed that deep ground waters in the Powder River Basin are chemically stable and of sodium-bicarbonate signature, but that shallow ground waters are chemically active and more variable in composition. Frost et al. (2002b) found that waters from shallow wells on the Jacobs Ranch Mine east of Wright, Wyoming completed in both coal and shale or sandstone aquifers are mainly sulfate- and calcium-dominated, although there is considerable variation.

The major ion chemistry of the water samples collected for this study both, deep sandstone wells and coal wells, are sodium-bicarbonate type (**Figure 4.8**). Although water from all coal zones is sodium-bicarbonate type and thus major ion compositions do not identify water from different coal zones, there are some spatial patterns in water quality.

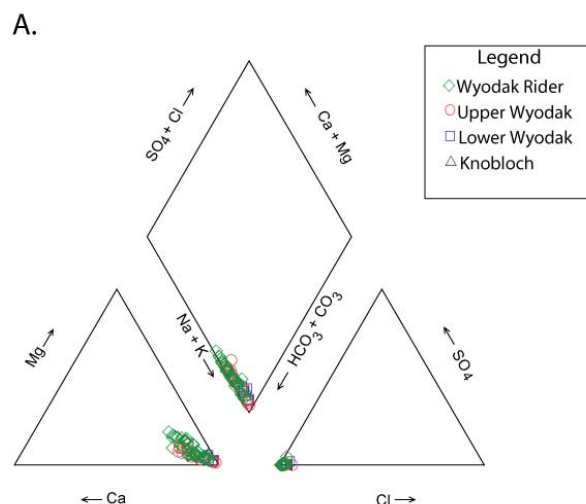


Figure 4.8: Trilinear diagram showing the sodium-bicarbonate character of all the wells analyzed in this study. Data from Campbell (2007).

Total dissolved solids (TDS) are lowest along the eastern margin of the Powder River Basin, typically under 1000 mg/L). They are highest along the Johnson/Campbell county line (exceeding 3000 mg/L in some wells) and intermediate in the area of Sheridan and Decker (**Figure 4.9**). SAR, sodium absorption ratio, defined as:

$$SAR\left(\frac{\sqrt{mmol}}{\sqrt{L}}\right) = \frac{[Na^+]}{\sqrt{[Ca^{2+} + Mg^{2+}]}}$$

also is highest along the Johnson/Campbell and Sheridan/Campbell county lines (**Figure 4.9**). Most water samples with SAR greater than 20 are found in this area of the basin.

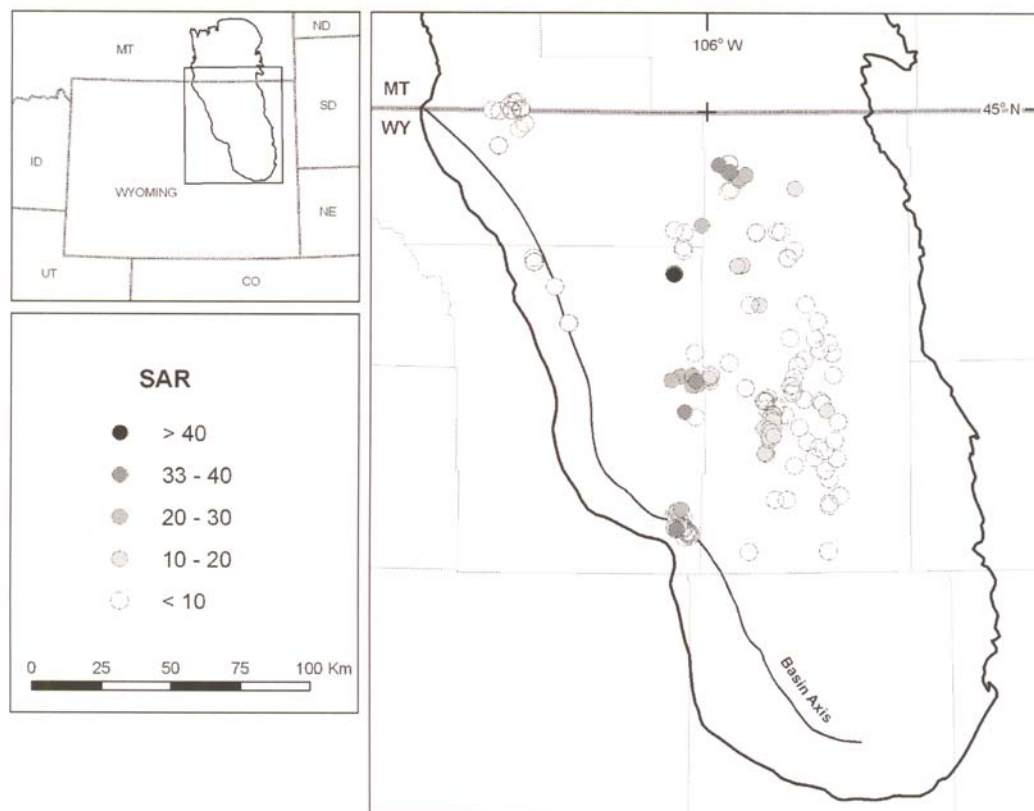


Figure 4.9: Geographic variations in sodium absorption ratio (SAR) for CBM produced water in the Powder River Basin.

Most of the samples in this study are located on the eastern side of the basin axis. The recharge area for these samples is along the eastern margin of the basin. A major recharge zone for coal aquifers is the clinker outcrops adjacent to the surface coal mines that extend from southeast of Wright to northeast of Gillette. Ground water recharged on the eastern side of the basin is driven westward by the topographic gradient towards the Powder River and the basin axis. The distance of the well from the eastern clinker outcrops is an approximation for relative ground water residence time, with wells closer to the clinker outcrop yielding water with shorter residence time than wells located farther west. Plotted as a function of distance from recharge, TDS of coal aquifer waters increases with increasing distance into the basin, and values of TDS higher than 2000 mg/L occur for samples collected more than 45 km from recharge (**Figure 4.10**). Some shallow wells in sandstone aquifers near the recharge area also have high TDS (**Figure 4.10**). Residence time appears to be more important than depth of coal seam: there is no strong correlation of TDS with well depth, although all CBM well waters with high TDS are from wells more than 1000 ft deep. SAR also increases with increasing distance from recharge zone (**Figure 4.11**), although there is considerable scatter.

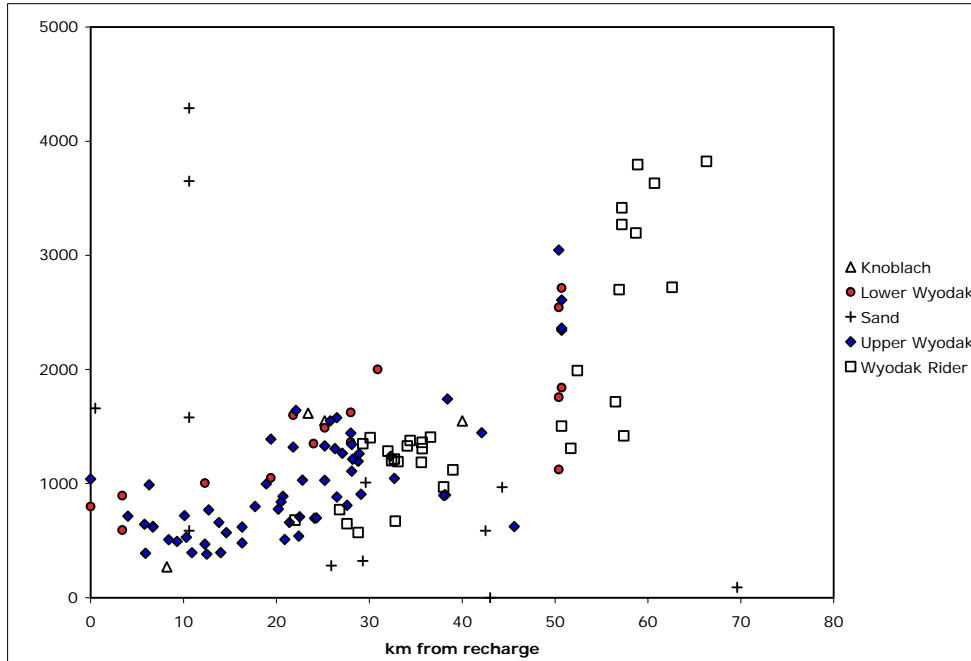


Figure 4.10: SAR plotted as a function of distance from the clinker outcrops along the eastern margin of the Powder River Basin for water samples recharged from the east.

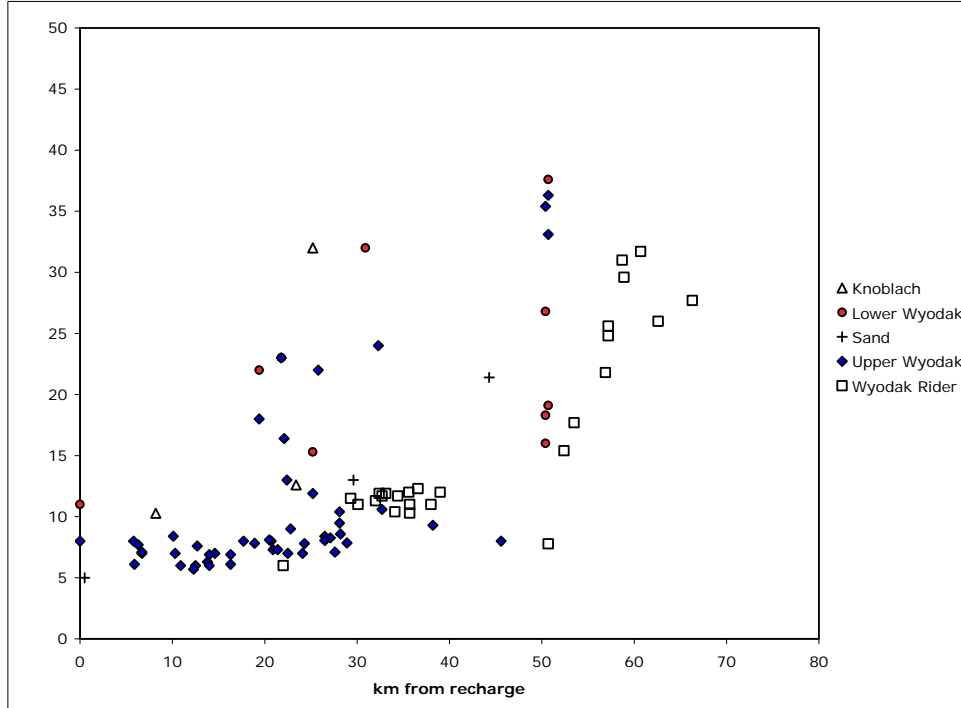


Figure 4.11: SAR plotted as a function of distance from the clinker outcrops along the eastern margin of the Powder River Basin for water samples recharged from the east.

Strontium isotope results

$^{87}\text{Sr}/^{86}\text{Sr}$ ratios for the ground waters in this study vary from less than 0.711 to more than 0.715 (the analytical uncertainty is ± 0.00002). The $^{87}\text{Sr}/^{86}\text{Sr}$ ratios are lowest in the Decker-Sheridan area along the Montana-Wyoming border, and highest along the Johnson/Campbell county line (Figure 4.12). Water from sandstone aquifers are generally among the lowest ratios, most between 0.7083 and 0.7127, although two samples have $^{87}\text{Sr}/^{86}\text{Sr}$ ratios > 0.713 .

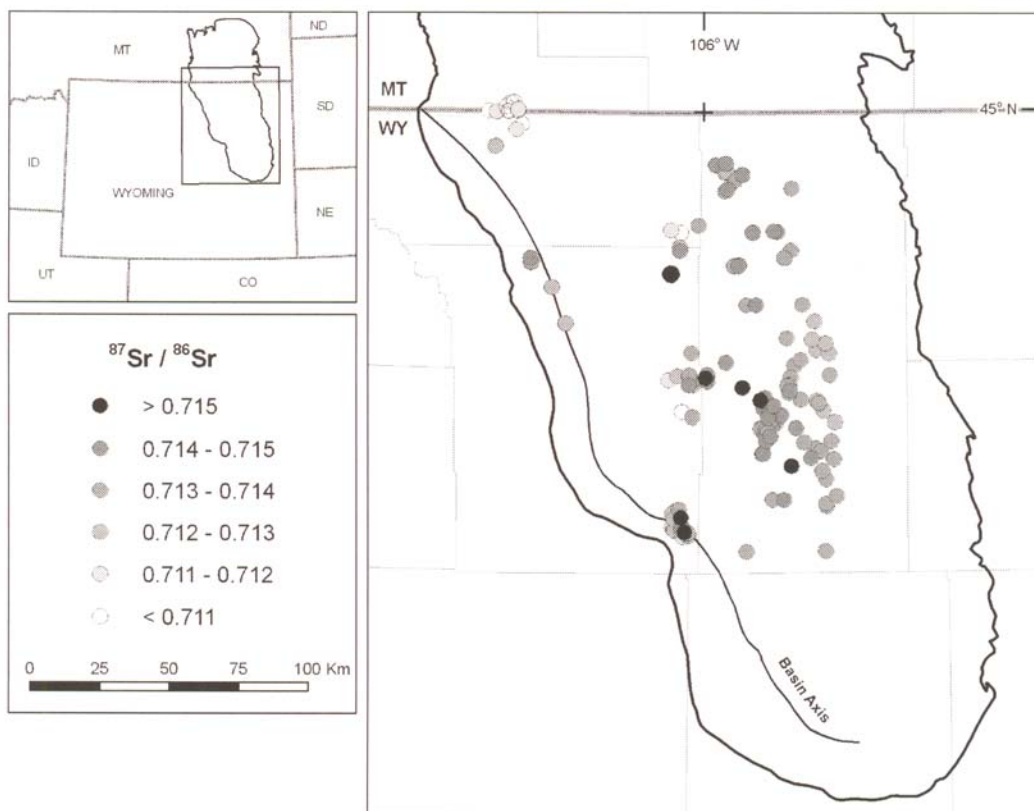


Figure 4.12: Variations in $^{87}\text{Sr}/^{86}\text{Sr}$ in CBM produced water as a function of geographic location. Note the highest ratios along the Johnson/Campbell county line and the low ratios in the Sheridan area.

Discussion

Trends in water quality and Sr isotopic composition in the Gillette-Schoonover area.

Because this portion of the basin was the first to be developed for the CBM resource, the preliminary studies of Frost et al. (2002a, 2002b) and Pearson (2002) were focused on wells located between Gillette and Wright (here referred to as the “Gillette area”). Most of these wells are completed in the Upper Wyodak coal zone. Our new analyses include a number of samples further westward into the basin, an area here referred to as the “Schoonover area.” Many of these wells are completed in the Wyodak Rider coal zone, in a thick seam informally called Big George. The TDS, SAR and ⁸⁷Sr/⁸⁶Sr ratios for waters from these wells are plotted as a function of distance from the recharge area along the eastern margin of the basin in **Figures 4.13, 4.14 and 4.15.**

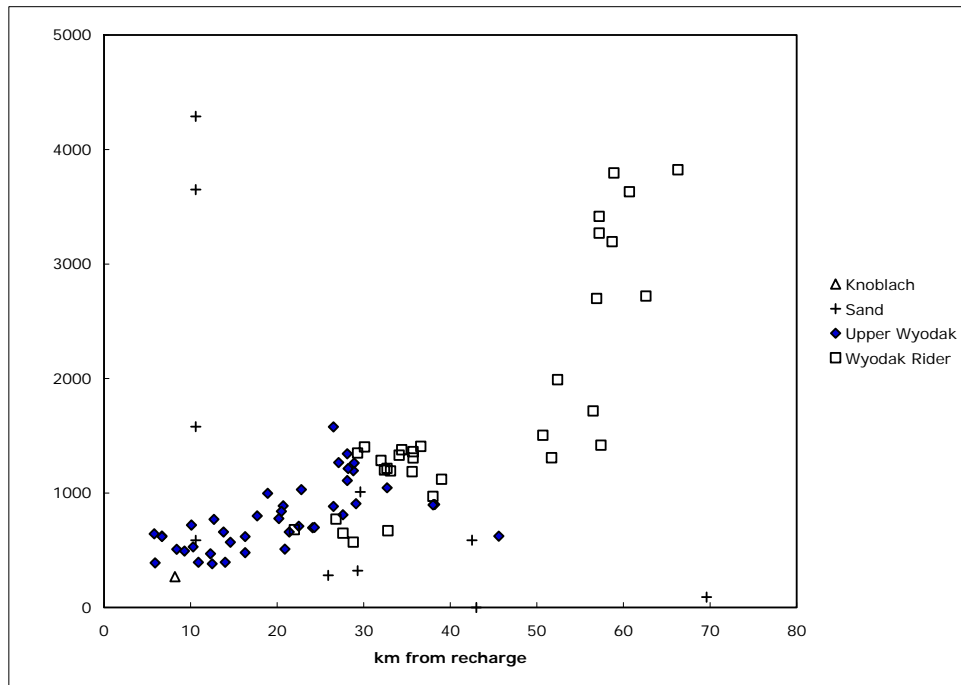


Figure 4.13: TDS plotted as a function of distance from the clinker outcrops along the eastern margin of the Powder River Basin for samples in the Gillette and Schoonover areas.

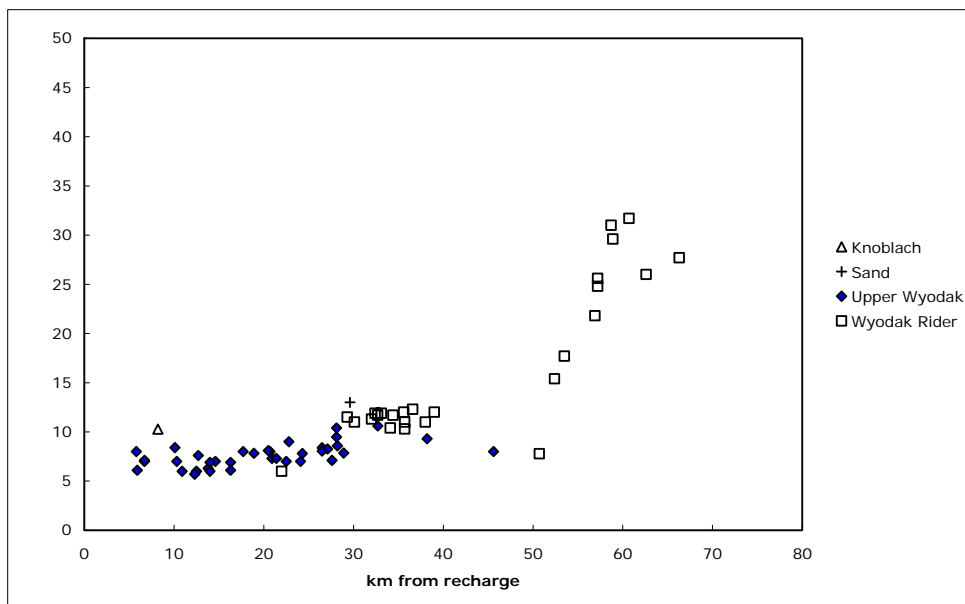


Figure 4.14: SAR plotted as a function of distance from the clinker outcrops along the eastern margin of the Powder River Basin for samples in the Gillette and Schoonover areas.

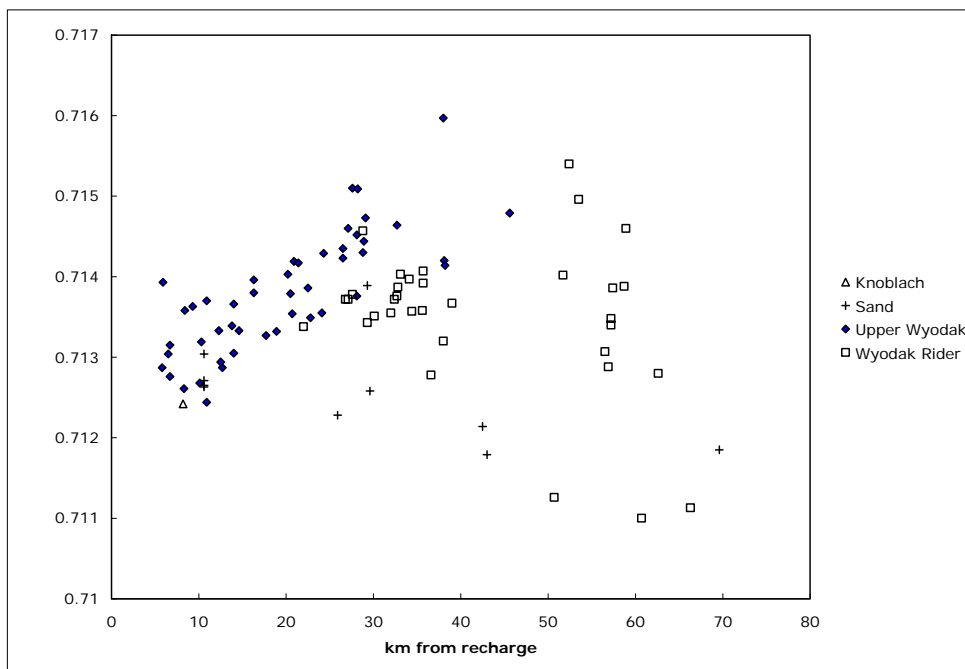


Figure 4.15: $^{87}\text{Sr}/^{86}\text{Sr}$ plotted as a function of distance from the clinker outcrops along the eastern margin of the Powder River Basin for samples in the Gillette and Schoonover areas.

Figures 4.13 and 4.14 show that water from the Upper Wyodak coal zone is low in SAR (<10) and TDS (<1000 mg/L), and that TDS increases slightly with increasing distance from the

recharge zone. Water from the Wyodak Rider coal zone extends the trend to higher TDS and SAR, particularly for samples more than 50 km from the recharge zone. The $^{87}\text{Sr}/^{86}\text{Sr}$ ratios of Upper Wyodak coal zone waters in the Gillette-Schoonover area show an increasing ratio with increasing distance from the recharge zone, as described by Frost et al. (2002a) (**Figure 4.19**). However, the Wyodak Rider coal zone waters fall below this trend, and extend to very low ratios. The sandstone aquifer waters in the Schoonover area are similarly low in $^{87}\text{Sr}/^{86}\text{Sr}$.

The trend in TDS results for CBM co-produced waters imply an increase in dissolved solids with increased water residence time. The correlation of $^{87}\text{Sr}/^{86}\text{Sr}$ ratios of the Upper Wyodak coal zone waters with distance into the basin from the recharge zone suggests that the $^{87}\text{Sr}/^{86}\text{Sr}$ ratio increases with increased water-rock interaction along flow path. The distinction between Upper Wyodak coal zone waters and water from sandstone aquifers, particularly for wells located more than 5 km into the basin, suggests that the Upper Wyodak aquifer system (which may include some intervening sand horizons like the one tapped by sample G71S at 29.3 km into the basin) is isolated from most sandstone aquifers.

In contrast, the range in TDS and $^{87}\text{Sr}/^{86}\text{Sr}$ ratios of the Wyodak Rider coal zone waters may indicate incomplete aquifer isolation and interaction of ground waters between coal and sandstone aquifers. This hypothesis is supported by a seismic survey conducted along the Johnson/Campbell county line at Burger Draw by Morozov (2002) that imaged the Big George coal and identified complex faulting with offsets of approximately 10 meters (30 feet) within the Big George coal and underlying strata. This faulting could cause hydraulic connections between coal and other aquifers.

We conclude that in the Gillette-Schoonover area, the Upper Wyodak coal zone appears to be isolated, and thus CBM development likely removes water only from these coals. On the other hand, the TDS, SAR and Sr isotopic characteristics of some of the waters from Wyodak Rider wells suggests that there may be leakage from adjacent aquifers when these wells are dewatered.

Comparison of Gillette-Schoonover area to the northeastern part of the Powder River Basin: Possible influence of faulting.

Figure 4.19 plots $^{87}\text{Sr}/^{86}\text{Sr}$ ratios as a function of distance from recharge for samples in the Gillette and Schoonover areas. **Figure 4.20** includes these samples plus samples located north of these wells in the northeastern part of the basin. Comparison of these figures shows that data from the northeastern wells increases scatter. Half of the northeast sample set plot above the Gillette trend and others plot below.

One distinction between the northeastern area and the Gillette-Schoonover areas is the presence of mapped faults in the northeast. These faults could act either as seals or conduits for water and gas flow. The group of samples lying above the Gillette trend are located in the eastern part of the Northeast area. These samples have comparatively low TDS (<1000 mg/L). The high $^{87}\text{Sr}/^{86}\text{Sr}$ ratios and low TDS suggest that these coals are well-isolated from sandstone aquifers and that if faults influence the hydrology of this area, they are acting as seals. The group of samples lying below the Gillette trend are located basin-ward of the high $^{87}\text{Sr}/^{86}\text{Sr}$ ratio group. These water samples also have higher TDS (1300-1800 mg/L). The combination of low $^{87}\text{Sr}/^{86}\text{Sr}$

ratios and high TDS suggests that in this area the coals are not completely isolated, possibly because the faults in this area are acting as conduits.

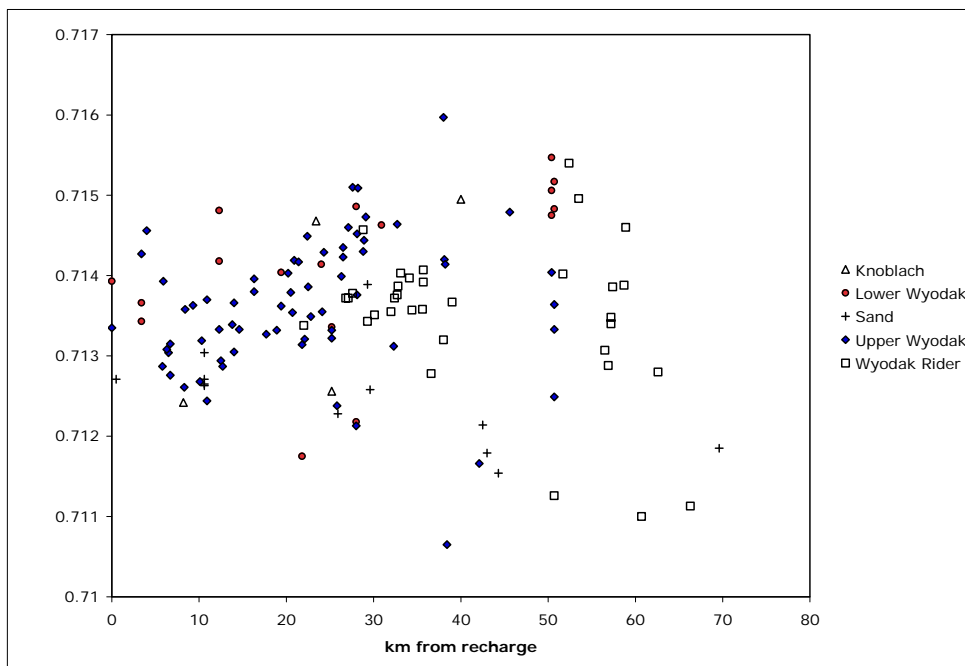


Figure 4.20: $^{87}\text{Sr}/^{86}\text{Sr}$ plotted as a function of distance from the clinker outcrops along the eastern margin of the Powder River Basin for samples in the Northeastern, Gillette and Schoonover areas. The scatter contributed by samples from the Northeastern area is indicated by comparing this figure with **Figure 4.19**.

Geographic and temporal variability due to depositional systems and sediment provenance.

Although the details are debated, most workers agree that the Paleocene and Eocene strata of the Powder River basin were deposited in a fluvial/lacustrine environment. Ayers and Kaiser (1984) envision a system of deltas supplying Lake Lebo. Each delta has a different source area, and therefore may be transporting clastic material with different $^{87}\text{Sr}/^{86}\text{Sr}$ ratios. Seeland (1992) suggests a north-flowing fluvial system fed by various uplifts around the basin. Some of the variations in $^{87}\text{Sr}/^{86}\text{Sr}$ ratio of water produced from coals in different parts of the Powder River basin may reflect these differences in sediment sources. For example, the samples from Decker-Sheridan area, which have the lowest $^{87}\text{Sr}/^{86}\text{Sr}$ ratios, may reflect input of sediment from the northern Bighorn Mountains, which expose Paleozoic and Mesozoic limestones.

Other variations in $^{87}\text{Sr}/^{86}\text{Sr}$ ratio may reflect temporal changes in depositional systems. For example, CBM is being developed in the Buffalo area from the Eocene Lake DeSmet and Felix coals. The Lake DeSmet coals have higher $^{87}\text{Sr}/^{86}\text{Sr}$ ratios than underlying Felix coals, which may reflect an increase in the amount of radiogenic (high $^{87}\text{Sr}/^{86}\text{Sr}$ ratio) Precambrian detritus being eroded from the Bighorn Mountains as these were uplifted in Eocene time (Whipkey et al.,

1991). We also note that the water and gas production from both of the Eocene coals appears to be significantly lower than that of the Paleocene coals in the area, however this conclusion is based on a limited number of samples and additional evaluation is warranted.

Correlation of Sr isotopic compositions to water enhancement and resulting fracture patterns.

Researchers involved in task 4 for this project have identified the orientation of hydraulic fracture propagation during well completion. We have obtained water samples and Sr isotopic compositions for 50 of the wells for which they have identified fracture pattern. Of these, 47 are vertically fractured, and 3 are horizontally fractured. The vertically fractured wells were subdivided into two groups: those wells that are high water producers (more than 6000 bbls/month) and those that are low water producers. There appears to be no general correlation between Sr isotopic composition and fracture pattern except in the southeastern corner of Johnson County, in a small, 10 km by 10 km area called “Bullwhacker” by Campbell (2007), where wells have been drilled into the Wyodak Rider coal zone. In this area, the vertically fractured, high water producing wells have $^{87}\text{Sr}/^{86}\text{Sr} = 0.71055\text{-}0.71271$; vertically fractured, low water producing wells have higher $^{87}\text{Sr}/^{86}\text{Sr} = 0.71200\text{-}0.71536$; and the one horizontally fractured well has the highest $^{87}\text{Sr}/^{86}\text{Sr} = 0.71806$ (Figure 4.21).

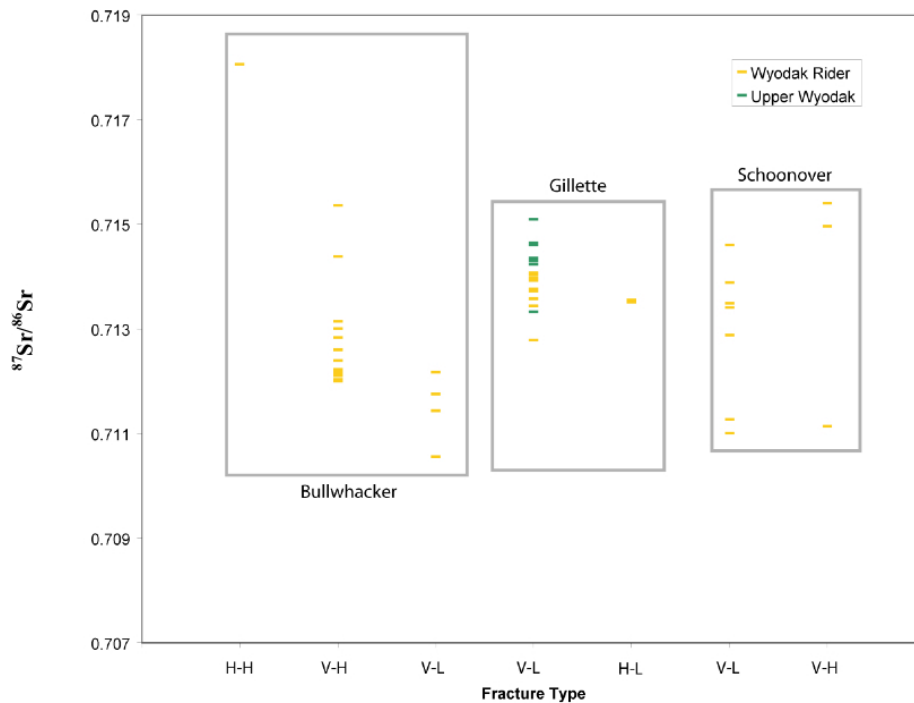


Figure 4.21: $^{87}\text{Sr}/^{86}\text{Sr}$ as a function of fracture type and region. V-L: vertical low, V-H: vertical high, H-H: horizontal high, H-L: horizontal low. The horizontal high is the most radiogenic $^{87}\text{Sr}/^{86}\text{Sr}$ value in the study and is distinct from all the other fracture types. Within Bullwhacker, vertical high and vertical low fracture samples have some overlap of values, however, the vertical low tend to be less radiogenic than the vertical high wells. Gillette and Schoonover both show overlap between fracture types.

No correlation between $^{87}\text{Sr}/^{86}\text{Sr}$ ratio and fracture pattern can be expected unless the fractures produce hydraulic connections that allow water to be introduced into the coal seam from another aquifer. If the fractures do not propagate into another aquifer because no sand horizons are within the thickness affected by fracturing, then no perturbation of Sr isotopic ratio is expected. Moreover, even if another aquifer is intersected by the induced fractures, this aquifer must contain water with a different $^{87}\text{Sr}/^{86}\text{Sr}$ ratio in order to affect the Sr isotopic ratio of the CBM produced water.

Conclusions: Subtask 3.2

The Sr isotopic ratios of groundwaters from coal in the Powder River Basin of Wyoming are influenced by a number of factors including the coal zone from which groundwaters are withdrawn, their residence time, the degree to which coal aquifers are confined, and geographic location. These factors and their effects on Sr isotopic ratios are summarized below.

1. The Upper Wyodak coal zone aquifer in the Gillette and Schoonover areas appears to be composed of a combined sand and coal aquifer unit. The groundwater of the Upper Wyodak coal zone in these areas also shows a trend of increasing distance from recharge resulting in more radiogenic groundwater due to the continued dissolution of radiogenic Sr-bearing components of the coal. The TDS value of these wells also increases with increasing distance from recharge due to water-rock interactions along the flow path.
2. The Wyodak Rider coal zone aquifers in the Gillette and Schoonover regions are only partially confined allowing interactions between sandstone and possibly other coal aquifers with the Wyodak Rider aquifer. This interaction results in a departure from the Upper Wyodak trend with the Wyodak Rider samples showing increased variability with increased distance from the recharge. Wells in the Schoonover area, where the $^{87}\text{Sr}/^{86}\text{Sr}$ and TDS variability is more pronounced also, on average, produce more water than wells from the Gillette Wyodak Rider and likewise may not be completely confined.
3. The $^{87}\text{Sr}/^{86}\text{Sr}$ ratios of the coal aquifer groundwater from the Northeast area appears to be influenced by faulting, with the faults acting as conduits to water flow, mixing water from different aquifers. There is significantly more variability in these samples than samples the same distance from the recharge located south of the Northeast area, in the Gillette area. Samples from the Northeast area that are below the Upper Wyodak Gillette and Schoonover trend of increasing radiogenic $^{87}\text{Sr}/^{86}\text{Sr}$ signature with increasing distance from recharge, produce more gas than samples lying above that trend. This has important implications for producers, who may wish to analyze the Sr isotope ratio of water samples from newly drilled wells in the Northeast area and use the results to help predict the future gas production from the well.
4. Depositional environment may play an important role in the spread of $^{87}\text{Sr}/^{86}\text{Sr}$ of groundwater throughout the basin. Models presented by Ayers (1986), Ayers and Kaiser (1984) and Seeland (1992) show variability in the source of sediments that compose the Fort Union and Wasatch Formations of the basin. These sources have high variability of $^{87}\text{Sr}/^{86}\text{Sr}$, which may be imparted to the groundwaters from each of these areas. The main trend is that areas in the western part of the basin, Buffalo and Sheridan, CBM produced waters tend to have lower $^{87}\text{Sr}/^{86}\text{Sr}$ than those in

the central and eastern margin of the basin, Northeast, Schoonover, and Gillette. Temporal changes in depositional environment may explain the higher Sr isotopic ratios of water withdrawn from the Lake DeSmet coal zone compared to the underlying Felix coal zone in the vicinity of Buffalo. We also note that the water and gas production from the Eocene coals appears to be significantly lower than that of the Paleocene coals, however this conclusion is based on a limited number of samples and additional evaluation is warranted.

5. Wells located along the basin axis in the Buffalo area show significantly less water and gas production than wells offset from the basin axis due to the increased hydrologic complexities along the basin axis, which may reduce connectivity within the aquifer, reducing gas production.

6. Evaluating the fracture direction and $^{87}\text{Sr}/^{86}\text{Sr}$ may be useful tools in evaluating wells with minimal gas production and high water production with sandstone located within 30 meters (100 feet) above or below the coal that may be in hydraulic communication with the producing coal. However, water from two aquifers with distinctive Sr isotope ratios need to mix in order for the direction of fracture propagation associated with the water enhancement process to be correlated with a Sr isotopic ratio of the produced water.

Subtask 3.3

Introduction

As described above, Sr isotope ratios have been used to fingerprint the CBM co-produced water (Frost and Brinck, 2005; Brinck and Frost, 2007). However, significant Sr contribution from local lithologies to CBM co-produced water and high costs of Sr isotope analysis may limit the applicability of this technique. For this reason, the objective of this subtask was to evaluate the possibility that stable isotopic ratios of oxygen, hydrogen, and/or carbon might provide lower cost environmental tracers of CBM co-produced water.

In order to predict the fate of this discharged water, the water budget of the local watershed must be understood. A generalized water budget can be expressed as:

$$\text{PPT} + \text{GW}_{\text{in}} + \text{SW}_{\text{in}} = \text{GW}_{\text{out}} + \text{SW}_{\text{out}} + \text{ET} \quad \text{equation 1}$$

PPT= precipitation

GW_{in} =groundwater in; GW_{out} =groundwater out

SW_{in} =surface water in; SW_{out} =groundwater out

ET=evapotranspiration.

In a generalized water budget, the water into a watershed equals water out when storage is zero. Of concern in CBM water disposal is how the water leaves the system, which requires constraining the variables on the right side of equation 1. Surface water (SW_{out}) can easily be measured using weirs and flow meters; however this still leaves two unknowns for the Beaver Creek equation, GW_{out} and ET. The goal of this research project is to constrain the evaporation rates in this part of the basin, which will leave one unknown (GW_{out}) to be estimated or calculated depending upon how well the other variables have been constrained.

In order to estimate the evaporation rate in this part of the Powder River Basin, the well-known behavior of light-element isotope fractionation in kinetic processes will be used. During evaporation in an open system, lighter isotopes of oxygen and hydrogen undergo Rayleigh distillation, which causes the remaining pool of water to be isotopically enriched in heavy isotopes. When graphed on a $\delta^{18}\text{O} - \delta^2\text{H}$ diagram, this results in the evaporative isotopic signature to be shifted off the global meteoric water line. Many variables play a role in the magnitude of this shift. The following equation is an estimate of evaporation rate given the hydrogen and oxygen isotopic values of the liquid and vapor:

$$\delta_E = \frac{\alpha_{v/l} \delta_l - h_N \delta_A + \varepsilon_{v/l} + \varepsilon_{diff}}{1 - h_N - \varepsilon_{diff}} \quad \text{equation 2}$$

δ_l = isotopic composition of lake water

h_N = relative humidity of atm over lake

δ_A = isotopic composition of atm over lake

$\alpha_{v/l}$ = isotope fractionation factor vapor to liquid

$\varepsilon_{v/l} = \alpha_{v/l} - 1$

ε_{diff} = kinetic fractionation

(formulated by Craig and Gordon, 1965).

Samples

Research was conducted at the Beaver Creek site in the Powder River Basin (**Figure 4.2**), approximately 50 miles southwest of Gillette, Wyoming. This watershed has been receiving CBM produced water for three and one half years at the time samples were collected. At this location the co-produced water is discharged into two holding ponds (upper and middle) that are allowed to flow overland, infiltrate and evaporate. Ten water samples were collected for this study from a variety of sources in the watershed. Four total well samples were collected from two wells at 5 and 10 meters (15 and 30 feet) deep at each of the upper and middle monitoring well sites within the Beaver Creek study area. The upper site represents the local groundwater and has no CBM water influence, while the middle site has a mixture of infiltrated CBM water and local groundwater as shown previously by strontium isotope data (Frost and Brinck, 2005). In addition to the well samples, one CBM well discharge point sample, and one holding pond sample were collected at each of the upper and middle pond locations. Two evaporation pans, one within the upper holding pond and one on land near the upper pond were also sampled. The samples were processed using mass spectrometry to determine the $\delta^{18}\text{O}$ and δD values.

Results

The data were normalized based on the University of Wyoming's stable isotope lab working standards of GLEES and HSW (**Table 4.5**). **Figure 4.22** represents these data on a $\delta^{18}\text{O} - \delta^2\text{H}$ diagram.

Table 4.5: Stable Oxygen and Hydrogen Data for the Beaver Creek Site

Sample	d 18O/16O	D/H
LOWER POND	-14.66	-122.52
UPPER POND	-10.04	-97.53
EVAP LAND	-9.16	-54.64
EVAP IN POND	-8.15	-50.76
UPPER BC-4	-16.59	-127.50
UPPER BC-2	-16.13	-126.26
MIDDLE BC-5	-17.87	-138.91
MIDDLE BC-7	-16.97	-134.97
UPPER CBM	-19.44	-151.10
LOWER CBM	-19.40	-147.82

Discussion

The CBM discharge, up-gradient wells, and evaporation pans are all interpreted to fall on the global meteoric water line (GMWL). A possible reason these data do not fall on the local meteoric water line (LMWL) include the fact that this local line represents Boulder, Colorado’s precipitation, so may not accurately represent Powder River Basin precipitation. Additionally, the CBM discharge water has been interpreted to be between 10,000 and 30,000 years old (Pearson, 2002), so it will not fall on a modern local meteoric water line for this region. The up-gradient wells fall near the meteoric water line because little evaporation occurs before infiltrating precipitation reaches the groundwater. The evaporation pans also fall near the meteoric line because the samples were collected shortly after a precipitation event and therefore only represent meteoric water.

The middle wells (labeled “mixed wells” in **Figure 4.22**) represent a mixture of evaporated pond water and local groundwater and are therefore slightly enriched compared to the meteoric water line. The upper pond is smaller in volume and shallower compared to the middle pond and has therefore experienced more evaporation. The triangle furthest removed from the meteoric water line represents this upper pond. These samples that have been evaporatively enriched fall below the GMWL.

A regression line was calculated for the evaporated water samples and was found to have a slope of 5.5. The slope of an evaporation line is directly related to the humidity. Based on equations from Clark and Fritz (1997), this represents an average humidity of 80%. This is not a realistic estimate for humidity in Wyoming’s arid Powder River Basin. This inaccuracy may be caused by the CBM inputs feeding the ponds that vary in rate and volume. Additionally, water leaves the ponds not only through evaporation, but transpiration, biota, overland flow, and infiltration. In the over three years of water production, the plant life has increased from negligible to significant, so transpiration can not be ignored. These variables limit the ability of equation 2 to predict evaporation rates. In addition to these variables that are not currently well constrained (such as biota, transpiration and surface water input) the other required variables in equation 2 such as the relative humidity, that isotopic composition of the atmosphere and the kinetic fractionation that is a function of wind speed and vector will also have to be estimated before this stable isotope method will prove useful in predicting evaporation rates.

Our data do show that the fractionation caused by evaporation of light-element isotopes can be used to identify watersheds that have been infiltrated by CBM holding ponds. The up-gradient wells fell very near the meteoric water line because the groundwater had not been enriched by evaporation, however the middle wells (the mixed wells) show a distinct shift off the meteoric water line. This shift is a clear indicator that the groundwater in this area has had additions of evaporatively enriched pond water. This indicator could be useful when infiltration rates are uncertain. It may be possible to estimate rates of infiltration of CBM waters to local watersheds by looking for the evaporation signal within watershed well water.

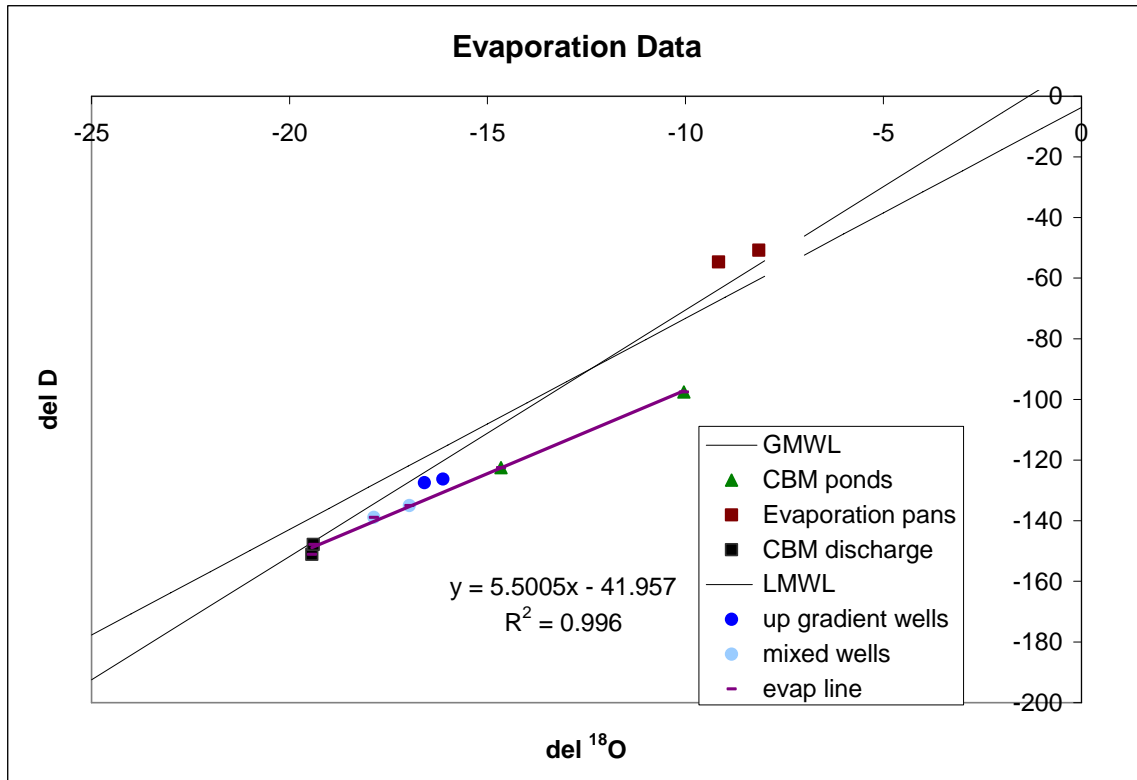


Figure 4.22: $\delta^{18}\text{O} - \delta^2\text{H}$ diagram of the Beaver Creek evaporation data. The purple line with slope 5.5 represents the evaporation line of the system comprised of the CBM discharge, holding ponds and middle monitoring wellfield “mixed” wells.

Measuring $\delta^{13}\text{C}$ (which is the $^{13}\text{C}/^{12}\text{C}$ ratio, expressed as per mil deviation from an international standard) of dissolved inorganic carbon (DIC) in ground water can provide another low cost diagnostic tool to trace water sources and to understand ground water interactions if there are large differences in $\delta^{13}\text{C}$ values among different carbon reservoirs in a particular region. The $\delta^{13}\text{C}$ of DIC is controlled by the isotopic composition of the carbon sources. The $\delta^{13}\text{C}$ of DIC in most surface and ground water varies from about -5‰ to -25‰ (Mook and Tan, 1999). Higher or more positive $\delta^{13}\text{C}_{\text{DIC}}$ (+10 to +30‰) can only be recorded in organic-rich systems where bacteria preferentially removes ^{12}C from the system during the process of microbial methanogenesis releasing isotopically light CH_4 , leaving the remaining dissolved inorganic carbon (DIC) in the formation waters highly enriched in ^{13}C (Simpkins and Parkin, 1993, Botz et

al., 1996; Taylor, 1997; Whiticar, 1999). Water co-produced with coalbed methane in the Powder River Basin has been shown to have positive δC values of up to +25‰ (Sharma and Frost, 2007).

A group of samples was analyzed from the Beaver Creek site. This includes samples from a standpipe that discharges co-produced waters from a number of CBM wells and from a retention pond into which this water is discharged, along with samples of the ambient shallow ground water from monitoring wells installed up gradient of this pond and a shallow monitoring well located within the ephemeral channel down gradient from the pond.

The ambient shallow ground water samples collected from the two up-gradient monitoring wells at Beaver Creek, BC-2 and BC-4, show low $d^{13}C_{DIC}$ values of -10.3‰ and -10.0‰, respectively (**Figure 4.23**). These are within the range of expected values for sub-surface waters in most natural systems. On the other hand water samples collected from the CBM discharge point (UP-CBM) and the corresponding CBM produced water retention pond (UPQ) yielded values of +19.8‰ and +17.8‰ respectively, within the range of $d^{13}C_{DIC}$ for the co-produced water samples discussed above. The water from the shallow ground water monitoring well below the retention pond at Beaver Creek (BC-7) shows a $d^{13}C_{DIC}$ value of +9.3‰, intermediate between the values of ambient ground water and CBM co-produced waters (**Figure 4.23**). Brinck and Frost (2007) used $^{87}Sr/^{86}Sr$ ratios and Sr concentrations of these same samples to calculate that a minimum of 70% of the water in monitoring well BC-7 originated from the CBM discharge. The intermediate $d^{13}C_{DIC}$ value of this water also suggests a mixed system containing both CBM water and ambient water. Although complicated by processes of carbonate dissolution and precipitation, the proportions of each end member suggested by the $d^{13}C_{DIC}$ values (approximately two-thirds CBM, one-third ambient ground water) is similar to the proportions calculated from Sr isotopic data.

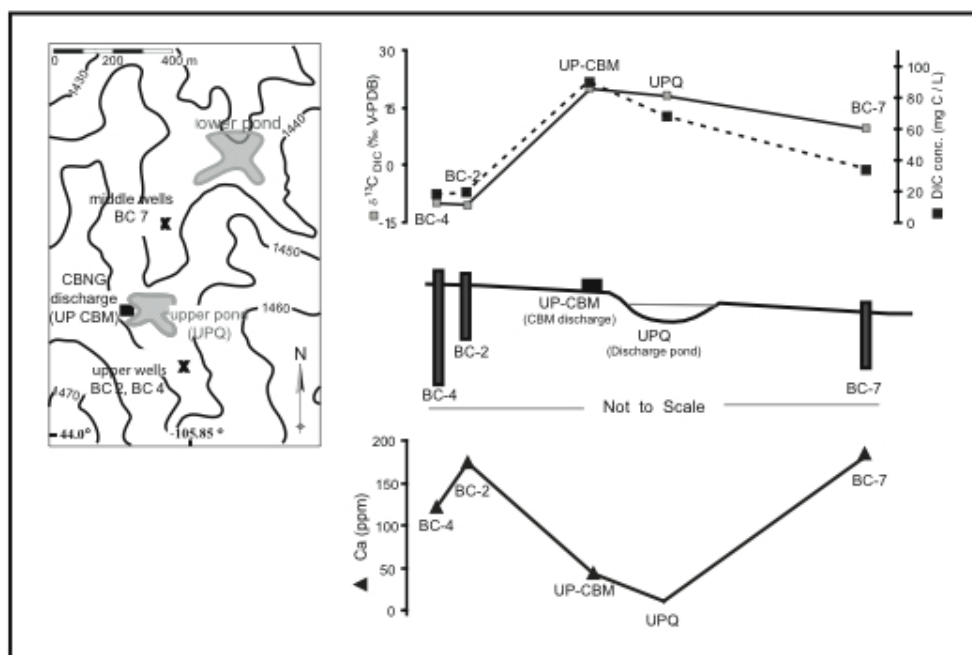


Figure 4.23: $\delta^{13}C_{DIC}$ and DIC concentration and Ca concentration trends in water samples collected from the Beaver Creek site. BC2 and BC 4 are groundwater monitoring wells upstream of the CBM discharge point UP-CBM. UPQ is the pond that holds the CBM co-produced water and BC-7 is a groundwater monitoring well installed downstream of the pond. The location of sampling sites is shown in the inset at the left upper corner.

Conclusions: Subtask 3.3

Our oxygen and hydrogen isotopic data show that the fractionation caused by evaporation of light-element isotopes can be used to identify watersheds that have been infiltrated by CBM holding ponds. This indicator could be useful when infiltration rates are uncertain. It may be possible to estimate rates of infiltration of CBM waters to local watersheds by looking for the $\delta^{18}O$ and δD signal of evaporation within shallow aquifer water.

Our initial carbon isotopic results demonstrate that $\delta^{13}C$ of dissolved inorganic carbon and DIC concentration in co-produced CBM water is distinct from shallow ground water and surface water in Powder River Basin. A monitoring well containing a mixture of ambient shallow ground water and infiltrating CBM co-produced water yielded an intermediate $\delta^{13}C_{DIC}$ that suggested proportions of each end member consistent with the fractions calculated from Sr isotopic mass balance.

RECOMMENDATIONS FOR FUTURE RESEARCH

For Subtask 1, to monitor the infiltration and dispersion of coal bed natural gas (CBNG)-produced water into the shallow subsurface, future research could include:

- Evaluation of degree to which soluble salts are mobilized in different soil types
- Weekly sampling of shallow monitoring wells during spring runoff to determine temporal pattern of salt mobilization

For Subtask 2, to determine locations where coal seams are isolated from adjacent aquifers and co-produced water will be limited to coal, we recommend:

- Resampling the same wells after a period of 1-2 years to determine if there is any temporal variation in Sr isotopic ratio that might indicate change in aquifer communication with over- or under-lying aquifers
- Modeling water/gas ratios for wells across the basin to determine if some geographic areas are characterized by greater water production than other areas (and perhaps are not economically favorable sites for gas production)

For Subtask 3, to evaluate what information may be provided by isotopic analyses of carbon, oxygen, and hydrogen in CBNG-co-produced waters.

- Additional sampling and measurement using carbon isotopes, as these appear to be the best fingerprint of CBNG co-produced water.
- Determine the amount of dissolved inorganic carbon in CBNG waters and determine if there is a correlation with Sr isotopes

REFERENCES

- Allison, J.D., and D.S. Brown, 1992.** MINTEQA2: a geochemical assessment model for environmental systems. Environmental Research Laboratory, Office of Research and Development. Athens, Georgia: USEPA.
- Ayres, W.B., Jr., and Kaiser, W.R., 1984.** Lacustrine-interdeltaic coal in the Fort Union Formation (Paleocene), Powder River Basin, Wyoming and Montana: in Rahmani, R.A., and Flores, R.M., eds., Sedimentology of coal and coal bearing sequences: International Association of Sedimentologists, Special Publication 7, p. 61-84.
- Botz, R., H.D. Polojski, M. Schmitt, and M. Thomm, 1996.** Carbon isotope fractionation during bacterial methanogenesis by CO₂ reduction. *Organic Geochemistry* 25, no.3: 255-262.
- Brinck, E.L., and C.D. Frost, 2007.** Detecting infiltration and impacts of introduced water using strontium isotopes. *Ground Water* 45, no.5: 554–568.
- Campbell, C.E., 2007.** Strontium isotopes as tracers of water co-produced with coalbed methane in the Powder River Basin, Wyoming. M.S. thesis, University of Wyoming, Laramie, 110 p.

- Clark, I.D. and Fritz, P., 1997.** Environmental Isotopes in Hydrogeology. New York: Lewis Publishers, 36-60.
- Craig, H., and Gordon, L., 1965.** Deuterium and oxygen-18 variations in the ocean and the marine atmosphere. In Symposium on marine geochemistry. Graduate School of Oceanography, University of Rhode Island, Occasional Publication 3, p. 277.
- Drever, J.I., 1997.** The geochemistry of natural waters, surface and groundwater environments, 3rd ed. Upper Saddle River, NJ: Prentice Hall.
- Drever, J.I. 2006.** Personal interview, November 13, Laramie, Wyoming.
- Drever, J.I., and C.L. Smith, 1978.** Cyclic wetting and drying of the soil zone as an influence on the chemistry of ground water in arid terrains. American Journal of Science 278, no. 10: 1448-1454.
- Essington, M.E. 2004.** Soil and water chemistry: an integrative approach. Boca Raton, Florida: CRC Press LLC.
- Faure, G., 1998.** Principles and applications of geochemistry. Upper Saddle River, NJ: Prentice Hall.
- Frost, C.D., B.N. Pearson, K.M. Ogle, E.L. Heffern, and R.M. Lyman, 2002a.** Sr isotopic tracing of aquifer interactions in an area of coal and methane production, Powder River Basin, Wyoming. Geology 30, no. 10: 923-926.
- Frost, C.D., J.E. Viergets, B.N. Pearson, E.L. Heffern, R.M. Lyman, and K.M. Ogle, 2002b.** Sr isotopic identification of coal and sandstone aquifers and monitoring of aquifer interactions in an area of active coal bed methane production, Powder River Basin, Wyoming. Wyoming Geological Association Fifty Second Field Conference: 107-121.
- Lee, R.W., 1981.** Geochemistry of water in the Fort Union Formation of the northern Powder River Basin, southeastern Montana: U.S. Geological Survey Water Supply Paper 2076, 17 p.
- Montana Bureau of Mines and Geology. Groundwater Information Center.**
<http://mbmgwic.mtech.edu/> (accessed September 2006).
- McBeth, I., K.J. Reddy, and Q.D. Skinner, 2003.** Chemistry of trace elements in coalbed methane product water. Water Research 37, no. 4: 884-890.
- Mook, W.G., and F.C.Tan, 1991.** Stable Carbon Isotopes in rivers and estuaries. In Biogeochemistry of Major World Rivers, ed. E.T. Degens, S. Kempe and J.E. Richey, 245-264. Chichester, UK : John Wiley and Sons.

- Morozov, I., 2002.** Institute of Energy Research/Anadarko Coal Bed Methane Project: Final report for contract 'Anadarko-IER 2001-02 (Geophysics)', April 5, 2002.
- NRCS, 2004.** Soil survey of Campbell County, Wyoming, southern part. Natural Resources Conservation Service.
- Patz, M.J., K.J. Reddy, and Q.D. Skinner, 2006.** Trace elements in coalbed methane produced water interacting with semi-arid ephemeral stream channels. *Water, Air, and Soil Pollution* 170: 55-67.
- Payne, A.A., 2004.** Surface water hydrology and shallow groundwater effects of coalbed methane development, upper Beaver Creek drainage, Powder River Basin, Wyoming. M.S. Thesis, Department of Geology and Geophysics, University of Wyoming.
- Payne, A.A., and D.M. Saffer, 2005.** Surface water hydrology and shallow groundwater effects of coalbed methane development, upper Beaver Creek drainage, Powder River Basin, Wyoming. In *Western Resources Project Final Report - Produced Groundwater Associated with Coalbed methane Production in the Powder River Basin*. Wyoming State Geological Survey Report of Investigations No. 55, ed. M.D. Zoback, 5-43. Laramie, Wyoming: WyGS.
- Pearson, B.N., 2002.** Sr Isotope ratio as a monitor of recharge and aquifer communication, Paleocene Fort Union Formation and Eocene Wasatch Formation, Powder River Basin, Wyoming and Montana. Thesis, University of Wyoming Department of Geology and Geophysics.
- Seeland, D., 1992,** Depositional systems of a synorogenic continental deposit--the Upper Paleocene and Lower Eocene Wasatch Formation of the Powder River Basin, Northeast, Wyoming, U.S. Geological Survey Bulletin 1917-H, 20 p.
- Shama, S., and Frost, C. D., 2007,** Tracing coalbed methane co-produced water using stable isotopes of carbon. *Ground Water*, in press.
- Simpkins, W.W. and T.B. Parkin, 1993.** Hydrogeology and redox geochemistry of CH₄ in a Late Wisconsin till and loess sequence in central Iowa. *Water Resources Research* 29, no.11: 3643-3657.
- Taylor, C. B., 1997.** On the isotopic composition of dissolved inorganic carbon in rivers and shallow groundwater: a diagrammatic approach to process identification and a more realistic model of the open system. *Radiocarbon* 39, no. 3: 251-269.
- Whiticar, M.J., 1999.** Carbon and hydrogen isotope systematics of bacterial formation and oxidation of methane. *Chemical Geology* 161, no.1: 291-314.

Whipkey, C.E., Cavaroc, V.V., and Flores, R.M., 1991. Uplift of the Bighorn Mountains, Wyoming and Montana- A sandstone provenance study, U.S. Geological Survey Bulletin 1917-D, 20 p.

Wheaton, J., and T.H. Brown, 2005. Predicting changes in groundwater quality associated with coalbed methane infiltration ponds in Western Resources Project Final Report - Produced Groundwater Associated with Coalbed methane Production in the Powder River Basin. In Western Resources Project Final Report - Produced Groundwater Associated with Coalbed methane Production in the Powder River Basin. Wyoming State Geological Survey Report of Investigations No. 55, ed. M.D. Zoback, 45-69. Laramie, Wyoming: WyGS. Wyoming State Water Plan. <http://www.waterplan.state.wy.us> (accessed December 2006).

Publications from Task 3:

Brinck, E. and Frost, C.D., 2007. Detecting infiltration and impacts of introduced water using strontium isotopes. *Ground Water*, v 45, p 554-569.

Brinck, E., 2006. Strontium isotope tracing of surface-groundwater interactions. EPA-STAR Fellowship Conference, Washington DC, September 2006. (No proceedings published)

Brinck, E.L., Drever, J.I., and Frost, C.D., Oct. 2007. The geochemical evolution of water co-produced with coalbed methane in the Powder River Basin, Wyoming. Submitted to *Environmental Geosciences*.

Brinck., E.L., 2007. Assessing environmental impacts of coalbed methane produced water using Sr isotopes. PhD thesis, University of Wyoming, Laramie.

Campbell, C. and Frost, C., 2007. Sr isotopic characterization of CBM co-produced water in the Powder River Basin, WY and MT. *Geological Society of America Abstracts with Programs* v. 39, abstract no. 125337.

Campbell, C., and Frost, C.D., 2006. Strontium isotopes as tracers of water co-produced with coalbed methane in the Powder River basin, Wyoming. *Geological Society of America Abstracts with Programs* v. 38, abstract no. 113434.

Campbell, C.E., Pearson, B.N., Frost, C.D., 2008. Strontium isotopes as indicators of aquifer communication in an area of coal bed natural gas production, Powder River Basin, Wyoming and Montana. *Rocky Mountain Geology* v. 43, no. 2, p. 149-175.

Campbell, Catherine E., 2007. Strontium isotopes as tracers of water co-produced with coalbed methane in the Powder River Basin, Wyoming. M.S. thesis, University of Wyoming, Laramie.

Catherine Campbell, April 2006. presentation on Subtask 2 for the University of Wyoming Graduate Student Symposium, Student Union, University of Wyoming, Laramie. (No proceedings published)

Frost, C.D., and Brinck, E., 2005. Strontium isotopic tracing of the effects of coalbed methane (CBM) development on shallow and deep groundwater systems in the Powder River Basin, Wyoming. Wyoming State Geological Survey Report of Investigations 55, p. 93-107.

**CHAPTER 5:
Regional Siting Concerns for Coalbed Methane Infiltration
Ponds in the Powder River Basin**

John Wheaton, Elizabeth Brinck Meredith,
Shawn Kuzara and Jay Hanson¹

EXECUTIVE SUMMARY

The goals of the research undertaken in Task 6 were: 1) to verify and improve methods used to evaluate proposed coalbed methane infiltration pond sites by evaluating changes in ground water conditions at specific sites; 2) to evaluate the mineral leonardite as a tool to sequester sodium and reduce salt loading associated with infiltration of coalbed methane production water; 3) evaluate multi-spectral satellite data as a tool to assess candidate infiltration pond sites with the intent of identifying sites that may not be appropriate for infiltration ponds due to mineral species of concern.

In order to produce coalbed methane (CBM) it is necessary to decrease the pressure in the coal seam, and to create a pressure gradient in the reservoir. This is typically achieved by pumping ground water out of the coal aquifer, which allows the methane to desorb from the coal surface and flow to the producing well. The production water must be disposed of economically to enhance gas development activities, yet in a manner that is sensitive to the semi-arid, agricultural area of southeastern Montana and northeastern Wyoming. During initial production from coalbed-methane wells, the water discharge rate is high. Infiltration ponds can accept high discharge rates. However, improper design and siting may lead to impacts such as unacceptable changes in shallow ground-water quality. Design considerations that may affect impacts from ponds include the materials which make up the sides and bottom of the impoundment, duration of use, size, number of ponds in an area, depth of excavation, mineralogy of the soil profile and in the shallow subsurface, aquifers which underlie the impoundment, distance to outcrop, and reclamation.

Infiltration ponds provide an economical means of managing CBM production water. Water infiltrating from these ponds may recharge shallow aquifers, potentially enhancing ground-water resources. However, as the infiltrating water moves through the previously unsaturated material, a series of geochemical reactions may occur that increase TDS and the concentration of other constituents. Predicting these changes is an important step in successfully designing and siting infiltration ponds.

Data from a 5-year study at the Coal Creek off-channel site show that about 64% of the total water discharged to the pond actually helped recharge shallow aquifers. However, reduced rates of infiltration with time at CBM ponds can be expected, especially at off-channel sites. Sodium in the CBM-production water appears to cause dispersion of the clays in the pond floor and walls, thus decreasing infiltration over a period of time. Even very small percentage clay can result in reduced infiltration rates. The vertical hydraulic conductivity at the Coal Creek

¹ Montana Bureau of Mines and Geology, Montana Tech of The University of Montana, 1300 North 27th Street, Billings, MT 59101. Correspondence: jwheaton@mtech.edu.

infiltration pond site was estimated to have decreased by one order of magnitude from approximately 0.1 to 0.01 feet/day, apparently in response to dispersion of clays.

Ground-water levels beneath and adjacent to ponds rise in direct response to infiltration and decrease as the pond bottoms seal or as the pond is allowed to dry when it no longer receives CBM water. Total dissolved solids (TDS) loads in the underlying and adjacent shallow aquifers increase, then decrease as available salts are flushed from the system. Both water levels and water quality have returned to near baseline conditions in monitoring wells around the perimeter of the pond. Directly beneath the pond TDS concentrations have remained high as the ground-water mound slowly dissipates. It is anticipated that the mobilized salts will eventually be sequestered as the decreased permeability of the pond floors reduces ground-water flow.

Ground and surface water quality and water level networks were maintained during this period of the project. Data collected (ground water and meteorological) have been entered in to GWIC, an internet based, publicly available database (<http://mbmaggwic.mtech.edu/>).

Drill cuttings and cores were collected through the Coal Creek pond floor both prior to it being filled with CBM water and again after it had dried out when CBM discharges ended. Data from these samples provide insight to the fate of the mobilized salts. Saturated paste extract (SPE) data indicate the salts originated from material between the pond floor down to a depth of 10 feet (ft), and migrated no further than 10 to 15 feet vertically to depths between 15 and 25 ft below the pond floor. Ground-water quality data from monitoring wells indicate the salts have moved horizontally about 200 ft beyond the pond perimeter.

The Beaver Creek study site consists of two on-channel infiltration ponds on a stream channel that was originally ephemeral and is now intermittent. Infiltration through the pond floors and along the stream channel recharged the alluvial aquifer creating a thicker profile of saturated soil. Salts within this newly saturated soil profile could then be dissolved and mobilized by the ground water.

Downstream from the upper pond, data from monitoring wells at the middle site show an initial increase in calcium, magnesium, sodium and sulfate concentrations which in time generally drop back to baseline or below. The increase is likely due to the dissolution of salts such as gypsum which were then flushed through the system. Increases in sodium and bicarbonate in the alluvial water likely reflects mixing with CBM water.

At the lower well site, downstream of both infiltration ponds, increases in calcium, magnesium, sodium and sulfate in the alluvial aquifer are due to dissolution of salts. The increase in sulfate concentrations (from 30 meq/L to 80 meq/L) and very little change in alkalinity and chloride concentrations suggest the majority of the salts dissolved are sulfate salts. The high concentration of bicarbonate in CBM produced water results in very low solubility of carbonate salts. The oxidation of pyritic materials may also contribute to the increased SO₄ levels.

Ground-water levels in alluvial monitoring wells dropped during 2007 due to a change in water management which decreased overland flow from the impoundments. This reduced water flow

should result in less water mounding below the stream channel, less salt mobilization, and eventually a return to baseline conditions.

Leonardite is a weathered form of coal that is used primarily to improve sodic soils. In laboratory tests, leonardite was tested as a possible treatment to reduce Na in produced water. The sodium adsorption ratio (SAR) was reduced in test samples; however this was due primarily to increases in Mg and Ca. The reduction in SAR was accompanied by an increase in TDS and a decrease in pH. Applications for using leonardite for reducing SAR of managed water appear to be limited.

Multispectral satellite data were evaluated to determine if specific mineral species in the soils could be identified and associated with salt loading in the ground water beneath the Coal Creek pond. Analysis of ASTER data indicate dominance of epsomite ($\text{MgSO}_4 \cdot 7\text{H}_2\text{O}$) in soils at the Coal Creek site which is consistent with water-quality changes measured beneath the pond. ASTER data may provide a useful tool to assess possible pond sites, but needs further evaluation. While this analysis did indicate a possible suite of specific mineral species, remote sensing data interpretations should be confirmed by soils analyses on the site.

Predictions of ground-water quality impacts and identification of possible problem sites is feasible using site-specific hydrogeologic investigations, SPE and remote sensing data. However, actual impact identification requires on-site monitoring through the life of the pond.

INTRODUCTION

In order to produce CBM it is necessary to decrease the pressure in the coal seam, and to create a pressure gradient in the reservoir. This is typically achieved by pumping ground water out of the coal aquifer, which allows the methane to desorb from the coal surface and flow to the producing well. This production water must be disposed of in an economic manner to enhance gas development activities, yet in a manner that is sensitive to the semi-arid, agricultural area of southeastern Montana and northeastern Wyoming. During initial production from coalbed-methane (CBM) wells, the water discharge rate is high. Infiltration ponds can accept high discharge rates. However, improper design and siting may lead to impacts such as unacceptable changes in shallow ground-water quality. Design considerations that may affect impacts from ponds include the materials which make up the sides and bottom of the impoundment, duration of use, size, number of ponds in an area, depth of excavation, mineralogy of the soil profile and in the shallow subsurface, aquifers which underlie the impoundment, distance to outcrop, and reclamation.

During the early stages of production, water is discharged at fairly high rates, often exceeding 20 gallons per minute (gpm). During later stages of production discharge rates are expected to decrease, possibly to 5 gpm or less. The productive life of individual wells is not yet known for the Powder River Basin, but estimates range from 5 to 20 years (U. S. Bureau of Land Management, 2003). Anecdotal evidence from producing fields indicates that 5 to 10 years may be a probable life expectancy for PRB wells. The potential number of wells, the average water production, and the life of the wells demonstrate that carefully designed and implemented water-management plans are crucial to successful development of coalbed methane.

Water produced with CBM is high in bicarbonate, is low or devoid of sulfate (reduced conditions), has low concentrations of calcium and magnesium, and has relatively high sodium concentrations (high sodium adsorption ratios or SAR) (Van Voast, 2003). In southeastern Montana where CBM is expected to be developed, coalbed water has higher salinity and higher SAR than in producing areas of the southern Powder River Basin in Wyoming.

Infiltration basins have been in use in Wyoming and Montana for several years. These basins have several advantages. They are an inexpensive means of disposing of production water and they may help recharge the shallow ground-water system. The basins also have several potential disadvantages. Flow directions and the ultimate destination of the infiltrating water are controlled by clay aquitards, discontinuous sandstone beds, and coal beds. The infiltrated water does not move into the original deep aquifers, but rather tends to move laterally as well as vertically, and in some situations may form sodic or saline seeps along hillsides or add sodic baseflow to streams. As the sodium-bicarbonate discharge water moves through the shallow weathered bedrock, a series of chemical reactions (primarily dissolution and oxidation) may increase the salt load in the water and detrimentally impact receiving waters.

The purpose of this study was to document short-term changes in the quality of shallow ground water in response to CBM infiltration ponds and to begin developing predictive tools. This report presents 5 years of data and interpretations of those data. Studies of two CBM infiltration ponds in Wyoming were undertaken during this study (**Figure 5.1**). A network of monitoring sites (**Appendix 5.A**) was established that included monitoring wells and surface-water sites. Data from these sites were collected and interpreted and include an estimated water budget for Coal Creek (**Appendix 5.B**), water quality data (**Appendix 5.C**) and water quality modeling listings (**Appendix 5.D**). Laboratory testing of the mineral species Leonardite was performed and data are listed in (**Appendix 5.E**). All data collected during this project are available to the public through the Montana Ground Water Information Center (GWIC) at: <http://mbmaggwic.mtech.edu/>.

ANTICIPATED WATER QUALITY CHANGES

The quality of ground water in the coal-bearing Fort Union Formation changes along the flow path producing well documented chemical signatures (Lee, 1981; Van Voast and Reiten, 1988). In recharge areas, calcium and magnesium carbonates are dissolved resulting in ground water that is dominated by the cations Ca and Mg, the HCO₃ anion, and having a moderate concentration of total dissolved solids (TDS). Dissolution of gypsum and other SO₄ containing minerals will add SO₄ to the water and dissolution of Na minerals will increase Na concentration. Slightly further along the flow path, oxidation of pyrite significantly increases both the SO₄ and TDS concentrations. Where ground water contacts sodic shales, Ca and Mg ions are exchanged for Na ions, further increasing TDS as the ionic valence requires desorption of two Na ions for each Ca or Mg ion. Under anaerobic conditions in deeper parts of the flow systems, SO₄ reducing bacteria cause precipitation of sulfide, which in turn causes Ca and Mg carbonate precipitation to maintain the cation/anion balance. The result of reactions in these deep anaerobic settings is ground water that is dominated by Na and HCO₃ ions, and has a moderate TDS concentration.

Water-quality and water-level data were collected in all wells, following standard protocol. Water levels were measured with electric tapes. Water quality samples were collected after purging the wells with a submersible pump. Purging was deemed complete after pumping the equivalent of 3 casing volumes and stable field parameters were obtained (specific conductance, pH, temperature and ORP).

During drilling on the pond floor at the Coal Creek site solid phase material (drill cuttings) were collected at specific depths for saturated paste extract analysis (SPE). Saturated paste extracts are used to evaluate soluble salts that are available for reaction with water within lithologic zones such as soils or overburden. The method was primarily developed for use in soils studies (U. S. Salinity Laboratory Staff, 1969). For this study, saturated pastes were prepared using the method described in Page (1982). A lithologic sample of 200 to 400 g of air dry material is saturated by adding distilled water until the saturated sample begins to flow but has no standing water. The sample is allowed to sit for 8 hours, and then the water is collected using a vacuum filter. The amount of water added is used to calculate the saturation water percentage. The water sample is analyzed using standard laboratory procedures. The results are reported in meq/L, and are used to describe the relative percentages of ions in the water.

Saturated-paste-extract data from lithologic material collected from overburden drill holes are used to predict the ratios of cation species in ground water in coal-mine-spoils aquifers. Dissolution reactions in the paste-extraction simulate those that occur in mine spoils and are also expected to occur during saturation beneath infiltration ponds. Saturated-paste-extract data, therefore, provide a simple model of changes in water quality. Concentrations of ions within spoils aquifers vary both locally and regionally, but typically increase rapidly as the spoils resaturate, then decrease as the ground-water flow system is established, and the available salts are flushed from the flow path.

It is important to note that rising water levels do not directly relate to the arrival of infiltrated water. Water-pressure increases can be transmitted ahead of the physical migration of water. Only in a water table aquifer does the rise in water level directly correspond with the arrival of infiltration water, and water-quality data are interpreted accordingly.

COAL CREEK STUDY SITE

Background

The primary study site for this research project was in the Coal Creek watershed near Ucross, Wyoming (**Figure 5.1**). At the Coal Creek site, monitoring wells and stations for obtaining surface-water data were installed prior to the discharge of CBM-production water and during construction of the infiltration pond (**Figure 5.2**). Monitoring site information is listed in **Appendix 5.A**. Additional discussions of the hydrogeology of this site are presented in this volume by both Frost and Saffer.

The Eocene Wasatch Formation is exposed at ground surface at the Coal Creek site. Underlying the infiltration pond are interbedded sandstone, clay and coal (**Figure 5.3**). Coalbed methane is produced from the Roland coal (Wasatch Fm) and to a lesser extent from the deeper Anderson

coal (Fort Union Fm). During July, 2003 CBM-production water began to be discharged to the infiltration pond used in this study and production continued through October, 2003.

The infiltration pond at Coal Creek is off-channel, constructed in a gently sloping uplands area, south of Coal Creek. Colluvial material was scraped away to expose weathered bedrock at the bottom of the pond. The bedrock material is a silty clay (46% clay, 43% silt, 11% sand).

Water Levels

The ground-water levels directly beneath the pond responded to CBM-production-water discharges to the pond in less than one month (wells 12ba7B and 12ba6B, **Plate 3**). Increased water levels were measured in all shallow wells (12ba9B, 12ba7B, 12ba6B, 12ba2B, 12ba1B, 12ba12B on **Plates 2 and 3**). Ground-water levels returned to near baseline levels during 2 to 3 years after CBM-water production ended, similar to the decreasing stage trend in the pond (**Figure 5.4**). Changes in ground-water levels were not seen in the deeper monitoring wells.

Water Budget

Infiltration rates from the Coal Creek pond were estimated using the following water budget equation:

$$\text{Inflow} = \text{Outflow} \pm \Delta \text{ Storage}$$

In this setting, the inflows to the pond were CBM-produced water and precipitation. Outflow was evaporation and infiltration, since there was no surface discharge. The change in storage represents the change in the volume of water in the pond.

Data for the water budget were obtained from several sources. CBM-water production records (July, 2003 through October, 2004) were obtained from the Wyoming Oil and Gas Commission website.

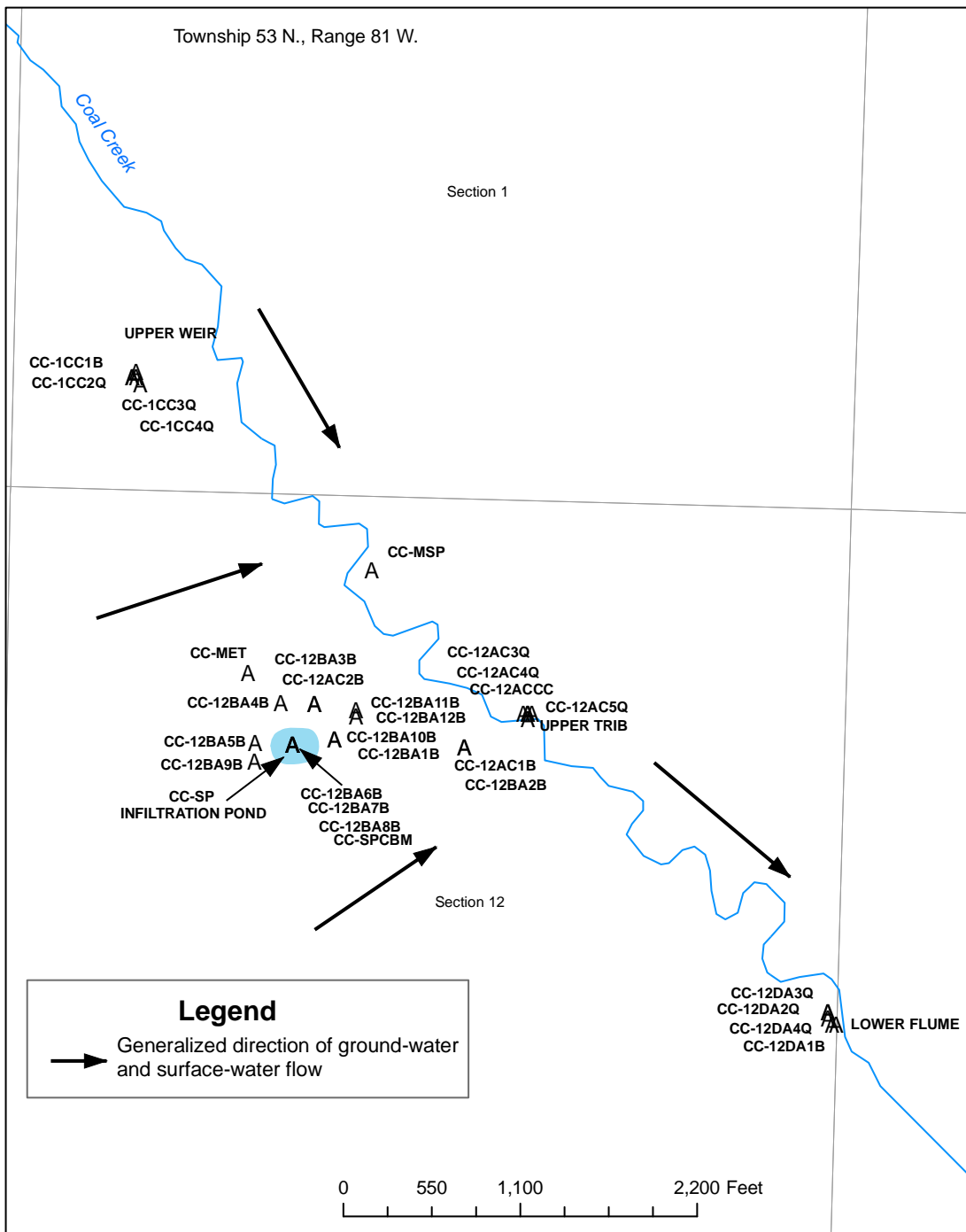


Figure 5.2: Location of sites in the Coal Creek Study area.

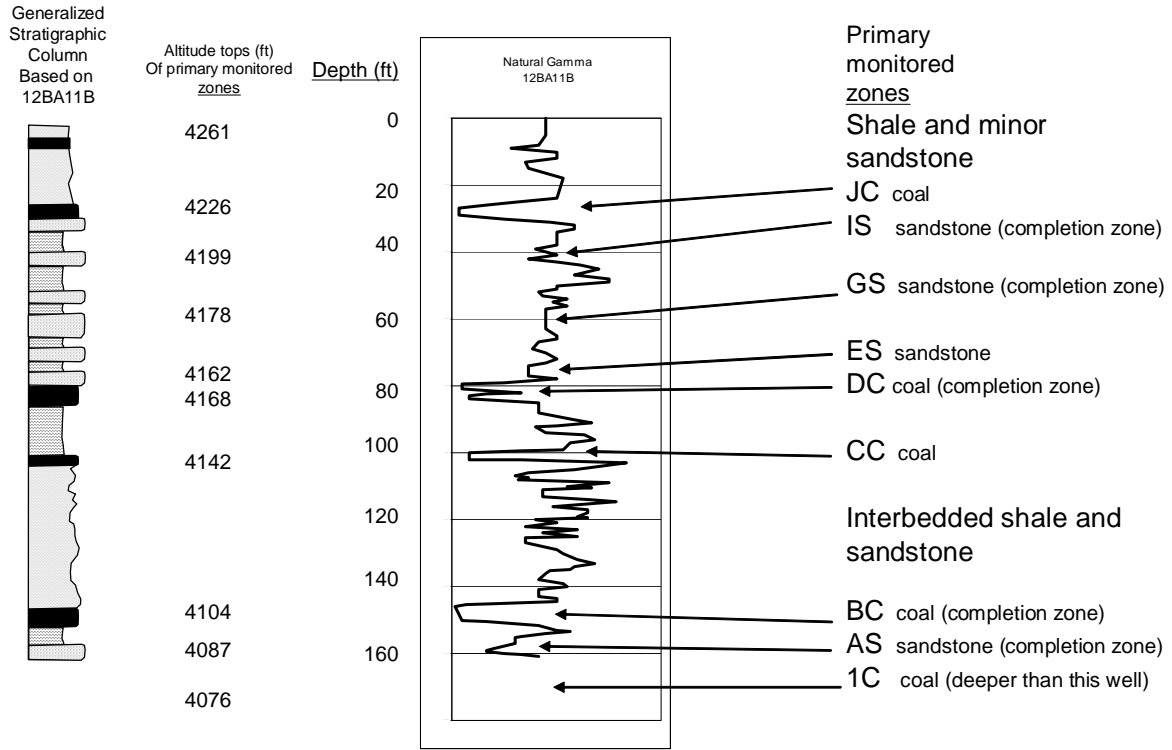


Figure 5.3: Generalized stratigraphic relationships at the Coal Creek infiltration pond site.

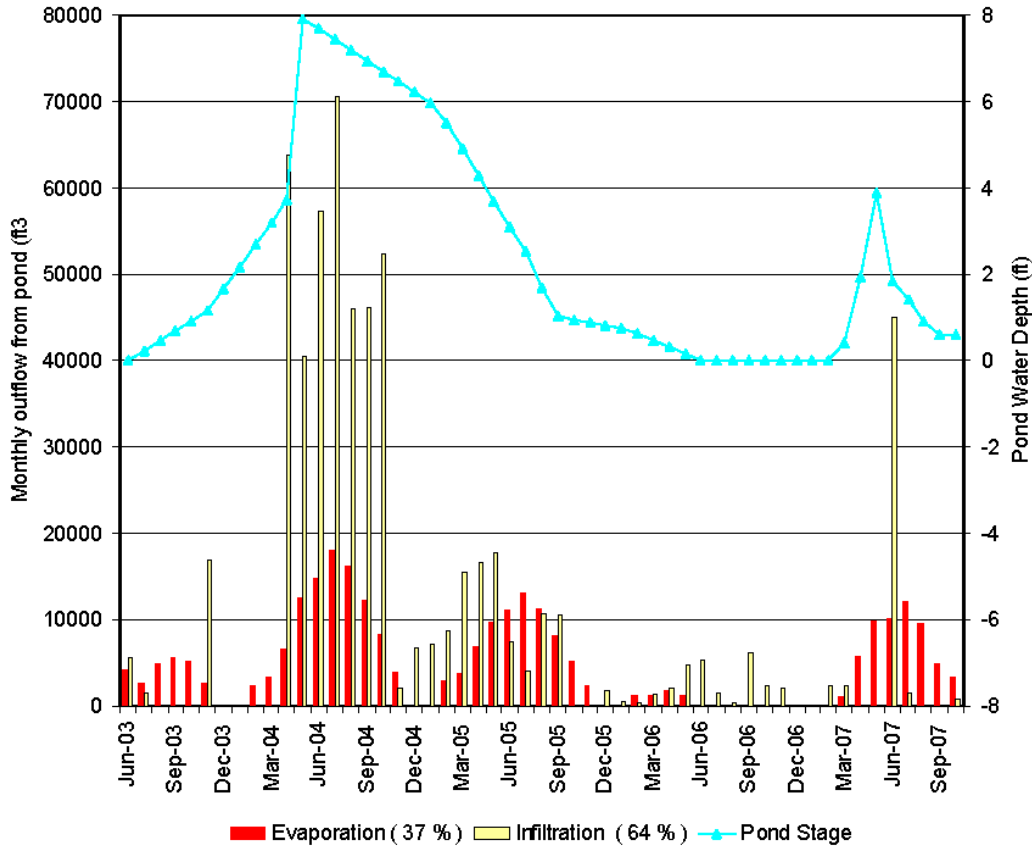


Figure 5.4. Estimated water budget for the Coal Creek infiltration pond.

Precipitation records were retrieved for the nearest weather station, located at Clearmont, Wyoming (<http://www.wrcc.dri.edu/cgi-bin/cliMAIN.pl?wy1816>). Pond stage was measured. A bathymetric survey of the pond provided the relationship of stage to volume and surface area. Evaporation was calculated from the pond surface area (adjusted for stage) and regional free-water evaporation rates. There was no surface discharge from this pond, therefore infiltration was calculated as the difference between inputs (CBM discharge and precipitation), change in storage in the pond, and evaporative loss from the pond. All data and calculations are listed in **Appendix 5.B** and the results summarized on **Figure 5.4**. The period of highest infiltration rate began after the material below the pond floor became saturated in April, 2004. Infiltration then decreased in November, 2004, apparently in response to dispersed clays plugging the flow paths. Evaporation eventually dried the pond completely during the summer of 2006. Interestingly, the large precipitation events that occurred during the spring and early summer, 2007, resulted in additional infiltration. This is interpreted to occur through the desiccation cracks that formed in the pond floor during 2006.

Using the water outflow calculations (**Figure 5.4**) and the pond-water levels and ground-water levels, the vertical hydraulic conductivity at the Coal Creek pond was estimated. The results, shown on **Figure 5.5**, indicate that the maximum vertical hydraulic conductivity was 0.1 ft/day and then it decreased to about 0.01 ft/day. The order of magnitude decrease likely is due to the

affect of sodium dispersion of clays. Significant reduction in infiltration rates with time can likely be considered the norm for ponds filled with high-SAR water.

Ground Water Model

A 4-layer steady-state conceptual model was constructed for the Coal Creek pond site using MODFLOW, a U. S. Geological Survey program. Commercial front-end software was utilized to aid data input and result output.

The model was based on data collected at the site and described here. The 4 layers were based on generalizations of drilling data under the pond (Pates 2 and 3). All layers in the model were assigned a vertical and horizontal hydraulic conductivity of 0.001ft/day. Isotropy was also assumed for all layers. These conductivity values were estimated from water budget calculations. A potentiometric surface was constructed from the monitoring wells, and the model grid was oriented with the direction of ground-water flow, northeast towards Coal Creek. A general head boundary of 1.5 ft³/day was assigned to provide a flux rate into and of the model. The steady-state model was calibrated with pre-pond-filling well water levels.

The model is an ongoing effort. The steady-state model will be used to create a transient model, with a polygon in layer 1 to simulate the pond dimensions. CBM water discharged into the pond will take place over one stress period divided by a series of time steps. The model will be used to evaluate potential surface seepage at aquifer outcrops for hypothetical relationships between distance to outcrop (vertical and horizontal) and different hydraulic conductivity values.

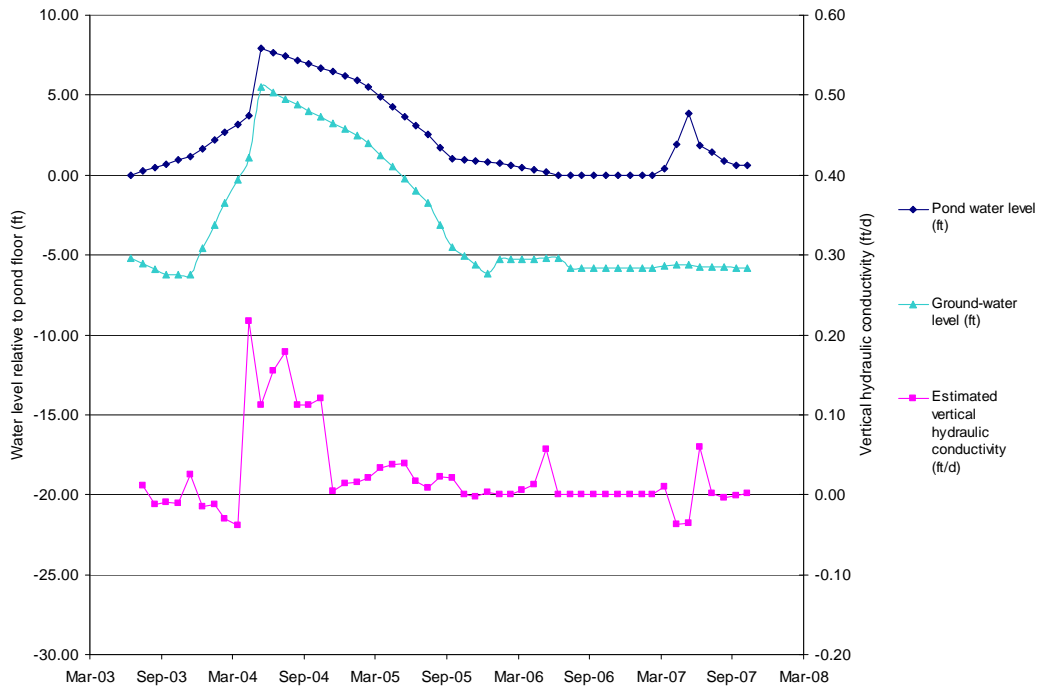


Figure 5.5: Estimated vertical hydraulic conductivity for the floor and immediate underlying layer beneath the Coal Creek infiltration pond.

Saturated Paste Extract Analyses

Solid phase material was collected while drilling the monitoring wells in the pond during June, 2003. This material represents unsaturated conditions beneath the pond before it was filled and water began seeping through this zone. Samples from specific depth intervals were evaluated using saturated paste extract (SPE) analyses and the results used to identify salt-rich zones beneath the pond and ions within those zones that would be expected to be mobilized by infiltrating water. These data were used to identify potential changes in ground-water quality that could be expected to occur. The laboratory data are presented as June, 2003 data points on **Figures 5.6 through 5.12**. The high values for Na, Mg, SO₄ and to a lesser extent Ca indicate likely increases of these ions in ground-water samples after the pond is filled.

After discharges to the pond ceased and the pond became dry, a second set of solid phase samples were collected to track the fate of the salts that were mobilized by the infiltration water. Data from the cores collected during November, 2006 are compared to earlier samples in **Figures 5.6 through 5.12**. Data from these cores provide insight to the fate of the mobilized salts. Saturated paste extract data indicate that most salts originated from the material between the pond floor and a depth of 10 feet and migrated down to a depth of 15 to 25 feet as shown by specific conductance (SC) data (**Figure 5.6**). This trend appears to be primarily due to Mg and Na movement (**Figures 5.9 and 5.10**).

Sodium adsorption ratio decreased directly beneath the pond floor but increased in the sand and clay zone at a depth of 15 to 25 ft below the pond primarily due to mobilization of sodium (**Figures 5.8 and 5.11**). Calcium does not appear to have been mobilized (**Figure 5.11**), but magnesium was removed from the shallow zone and moved to the zone at about 20 ft below the pond floor (**Figure 5.9**). Sulfate was also removed from the shallow zone (**Figure 5.12**).

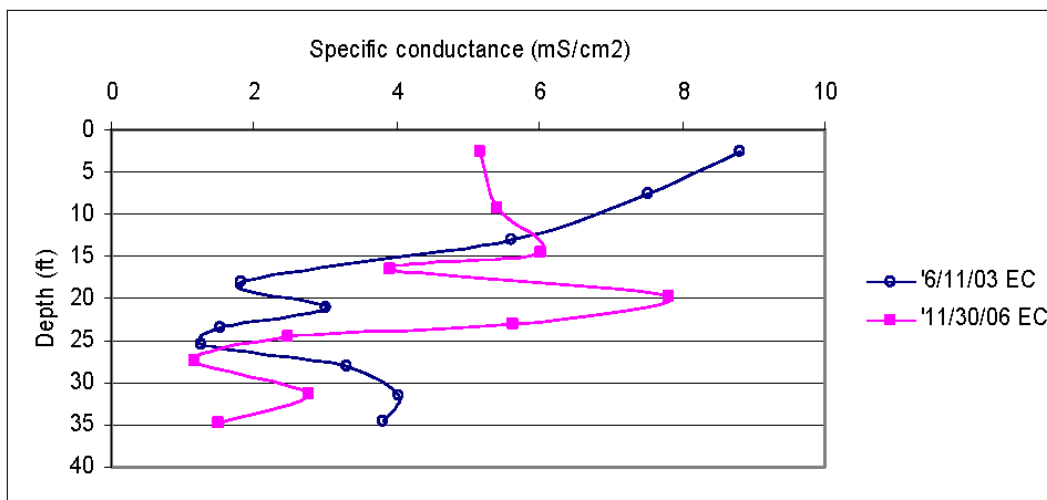


Figure 5.6: Specific conductance data for saturated paste extract analysis under the Coal Creek pond.

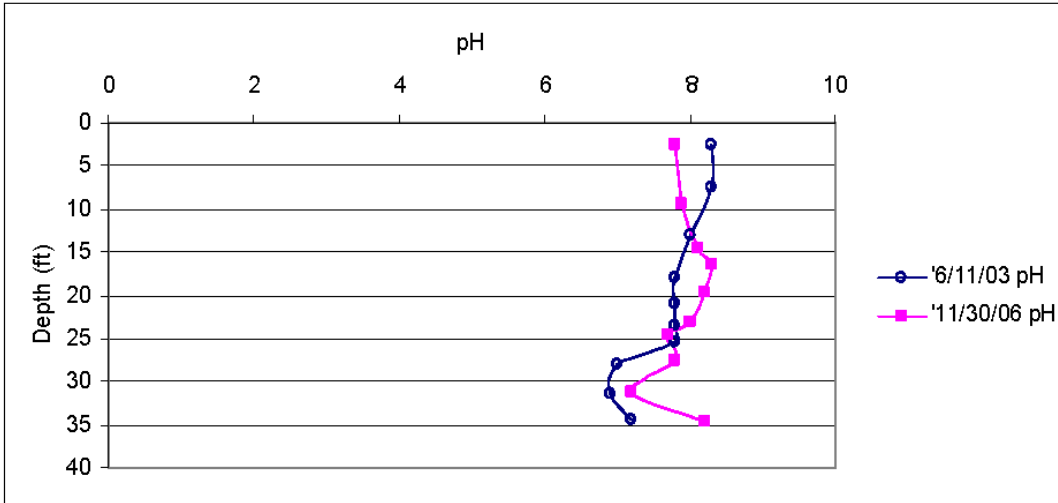


Figure 5.7: pH data for saturated paste extract analysis under the Coal Creek pond.

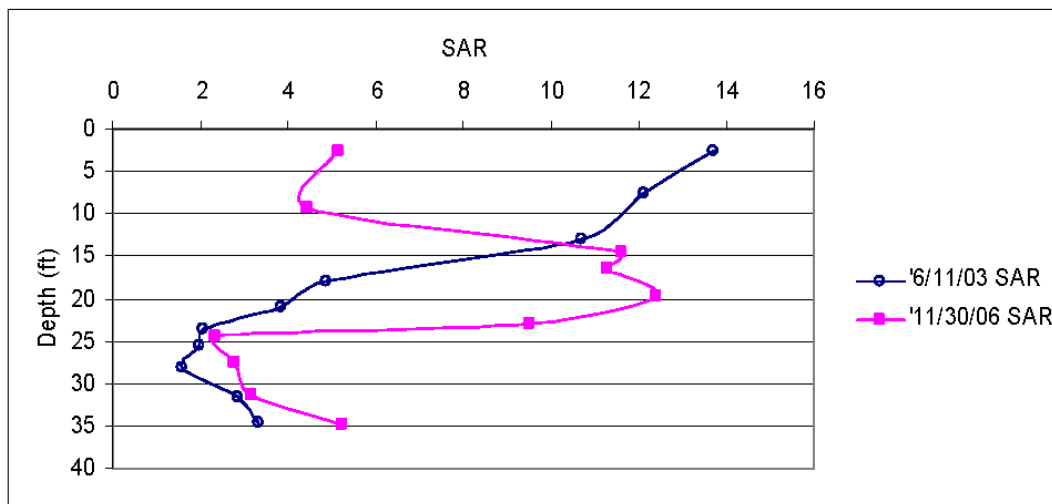


Figure 5.8: Sodium adsorption ratios (SAR) for saturated paste extract analysis under the Coal Creek pond.

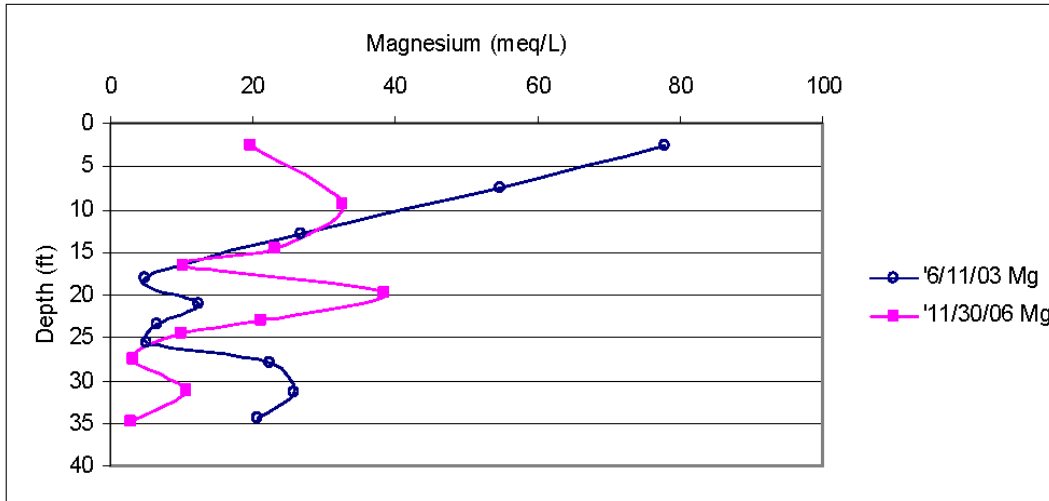


Figure 5.9: Magnesium concentrations from saturated paste extract analysis under the Coal Creek pond.

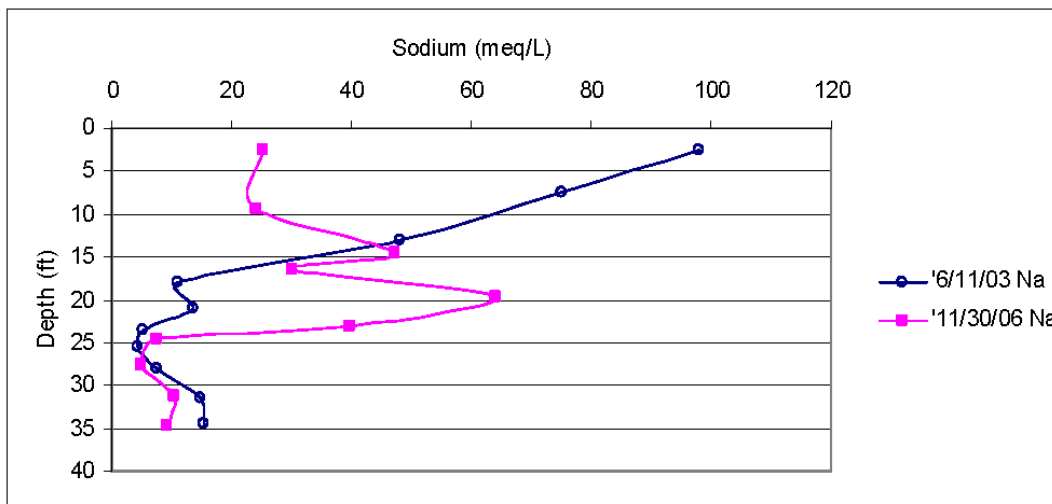


Figure 5.10: Sodium concentrations from saturated paste extract analysis under the Coal Creek pond.

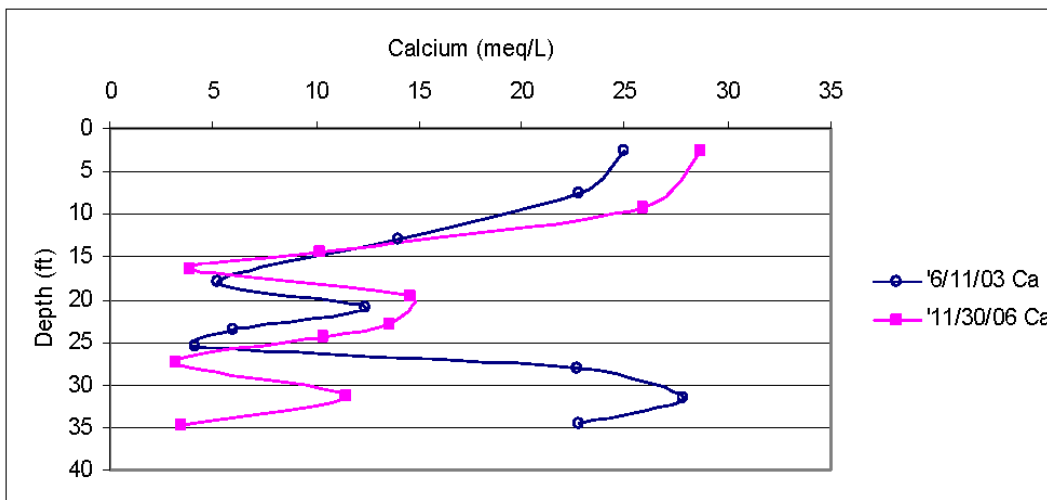


Figure 5.11: Calcium concentrations from saturated paste extract analysis under the Coal Creek pond.

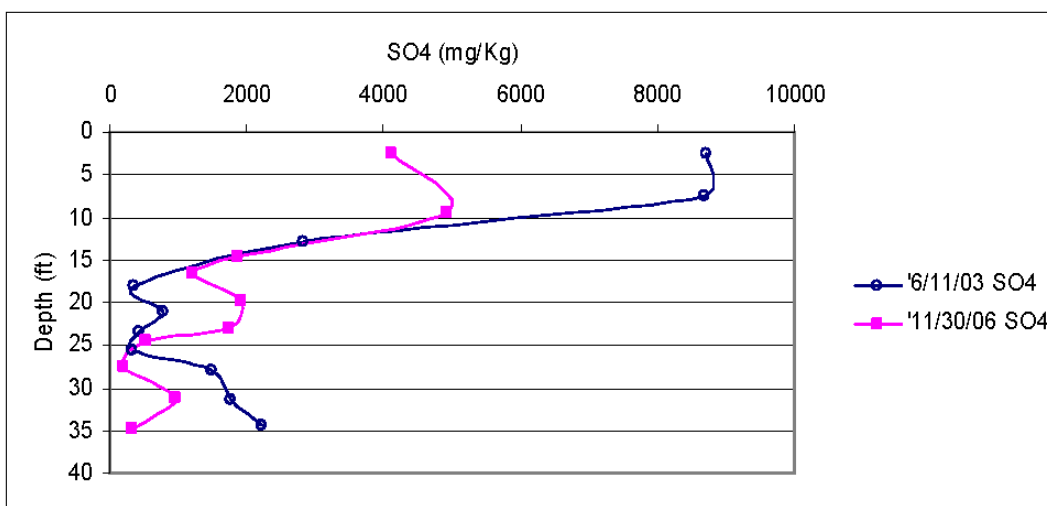


Figure 5.12: Sulfate concentrations from saturated paste extract analysis under the Coal Creek pond.

Water Quality

Results of laboratory analyses

Prior to discharge of CBM-produced water to the pond, shallow ground water at the Coal Creek site was generally dominated by near-equal concentrations of the cations Ca, Mg and Na with moderate levels of total dissolved solids (TDS) as reflected by SC. This is shown by early data from wells 12ba9B, 12ba7B, 12ba2B and 12ba1B (**Plates 2 and 3** and **Appendix 5.C**). Slightly deeper water in a thin coal was dominated by Na and HCO₃ ions and has a lower TDS concentration as shown in wells 12ba5B, 12ba3B and 12ba11B (**Plates 2 and 3** and **Appendix 5.C**). Apparently, even in this shallow system SO₄ may be removed from the system by means of sulfate-reducing bacteria which are common in Powder River Basin aquifers (Dockins and others, 1980). Sulfate-reducing bacteria in such a shallow flow system would be unusual, but if present may (with continued monitoring) afford an opportunity to observe the effects of this process on infiltrated CBM water.

Water quality in the pond is very similar to that measured at the CBM discharge point (**Appendix 5.C**). An exception to this is the sample collected from the pond in August, 2007 which is rain and snow melt, not CBM water.

Water-quality data from the sample collected from well 12ba7B during December, 2003 (1 month after the first discharge to the pond) show increases in concentrations of all cations and in SO₄ (**Plate 3** and **Appendix 5.C**). After the pond had been in use for one year, the TDS concentration at this well reached its maximum of 12,420 mg/L, dominated by ions of Na and SO₄. Coalbed-methane production water is dominated by anions of HCO₃, and depleted of SO₄. The SO₄ in the monitoring well is, therefore, a product of reactions along the flow path rather than ions in the CBM-production water. Also, the concentration of Na at well 12ba7B exceeds that in the CBM-produced water (97 meq/L versus 17 meq/L).

The highest TDS value measured was at well 12ba4B which reached 17,367 mg/L (**Appendix 5.C**). This well was dry prior to filling the pond, and became dry again early in 2006 as the pond stage was decreasing.

Northeast of the pond about 100 feet at well 12ba2B, TDS rose from 1,338 to 6,991 mg/L in response to rising water levels (**Appendix 5.C**). The TDS concentration decreased to 3,255 mg/L as water levels dropped. The increase in TDS closely followed the timing of the rising water level, however the decrease in TDS lagged about one year behind the dropping water levels (**Plate 3**).

No other wells showed distinct impacts from the arrival of CBM-produced water. One deeper well (12ba10B) shows significant water-quality changes but only minor water level change (**Plate 2**). This is interpreted to indicate either a well completion problem or outside influence.

The increases in TDS are likely associated with the dissolution of minerals present in the overburden material and are not directly associated with the constituents in CBM production water. In fact, similar TDS levels would be expected if a surface water source, or rain water, had

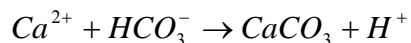
been pumped into the pond. Much of the increased concentrations of cations and anions in the water-table aquifer are associated with the dissolution of minerals and fossil salts present in the overburden materials.

Saturated paste extract data indicate the increase in Mg, Na and SO₄ that occurs directly beneath the pond, likely is occurring as the result of mineral dissolution in the uppermost 10 to 15 feet of material, and salts are being transported vertically downward by ground-water flow. Neither the concentrations nor the ratios of ions in the ground water are similar to that in the CBM-produced water. These data support the previous conclusion that the dissolution of soluble minerals, rather than infiltrating water quality, appears to control ultimate water quality in the receiving aquifer.

Water quality modeling

Water quality modeling of monitoring wells in and surrounding the Coal Creek pond was performed using Visual Minteq (Allison and Brown, 1992). The speciation and saturation indices for wells 12BA2B, 12BA7B and 12BA9B are presented in **Appendix 5.C**. Wells 7B and 2B show water level increases and changes in major ion chemistry associated with the introduction of CBM produced water to this system while the up-gradient well 9B shows only increased water level. Modeling was performed for two sample dates: March, 2005, which represents the period of high water level, and August, 2007, representing the period of water level recovery.

Modeling indicates that water samples from the three wells presented in **Appendix 5.C** are under-saturated with respect to sulfate salts such as gypsum and epsomite, which implies that if these species are present they can dissolve in this water. Spectral analysis of satellite imagery taken in the X-ray wavelength which reveals the presence of gypsum, epsomite and bloedite (an amorphous calcium-magnesium sulfate salt) down-gradient from the ponds, in addition to the increased sulfate concentration in wells 7B and 2B supports the theory that this water is encountering and dissolving these sulfate salts. Furthermore, modeling indicates that these water samples are over-saturated with respect to carbonates such as calcite, dolomite and, for wells 2 and 7, magnesite. The lower pH in the August 2007 wells increases the solubility of carbonates, which is one reason the saturation index has gone down for these minerals in the later sampling. The lower pH may be due to the precipitation of minerals such as calcite, the formation of which releases hydrogen ions:



Water sampled from wells 2B and 7B show prominent sulfate complexes in the Minteq model. These complexes are much less common in water from the up-gradient well 9B. This is due to the large amount of sulfate in aqueous form in wells 2B and 7B which is not present in well 9B. The dissolution of gypsum and epsomite, in addition to driving up sulfate concentrations also raise the magnesium and calcium concentrations, which in turn drives the precipitation of calcite, dolomite and magnesite. It is for this reason that major ion analysis does not show equal increases in cations (in meq/L) and sulfate.

It should be noted that the presence of magnesite as a mineral at equilibrium in this near surface environment is supported by research conducted by Kittrick and Peryea (1986) and Sadiq and

Lindsay (1976). However, other researchers have suggested that magnesite does not form under these conditions. As noted above, the modeling results of our data show that magnesite is likely controlling solution Mg levels. Thus at this time, this study will assume that magnesite is present and will form under the near surface environments.

Sodium may be entering the water in aquifers below the pond through several pathways. X-ray diffraction analysis suggests the presence of plagioclase feldspars in the soils in this area. Clark (1995) found feldspars, including plagioclase, were common in the Decker, Montana area. The dissolution of plagioclase, particularly the albite-rich variety would provide a source of sodium. Additionally, there is the possibility of cation exchange with the sodic shales which lie stratigraphically near the monitored aquifers. The dissolution of gypsum and epsomite provide calcium and magnesium ions which may then displace the sodium from the shale.

BEAVER CREEK STUDY SITE

This research site is at the head waters of Beaver Creek, located in the Powder River Basin south of Gillette, Wyoming (**Figure 5.1**). This site encompasses a stretch of a once ephemeral drainage which comprises part of a headwater tributary of Beaver Creek which is a tributary of the Powder River. Within this stretch of drainage, two on-channel CBM produced water impoundments were constructed by erecting dams across the channel or enhancing existing stock ponds. On-channel ponds are, in general, maintained at a predetermined depth and excess water discharges and flows overland through the stream channel. The addition of CBM produced water to this drainage has turned this drainage from ephemeral to intermittent. This introduced water infiltrates to the ground water both through the floor of the ponds and through infiltration along the stream channel.

In order to monitor potential changes to the ground water due to the infiltration of the CBM produced water, three sets of nested monitoring wells were installed: up-gradient from both ponds (upper well site), between the two impoundments (middle well site), and below both impoundments (lower well site) (**Figure 5.13**). Within each set of nested monitoring wells, individual wells were completed in the alluvium and in the shallow weathered bedrock directly underlying the alluvium. Details of the well completions are listed in **Appendix 5.A**. The alluvium consists of fine sand, silt, and gravel which overlies the weathered sandstone of the Eocene Wasatch Formation. The Wasatch Formation is exposed in areas within the study site where it is not covered by the alluvial deposits. Physical hydrology and isotope geochemical analyses of this research site are presented in this volume by Damian Saffer and Carol Frost, respectively.

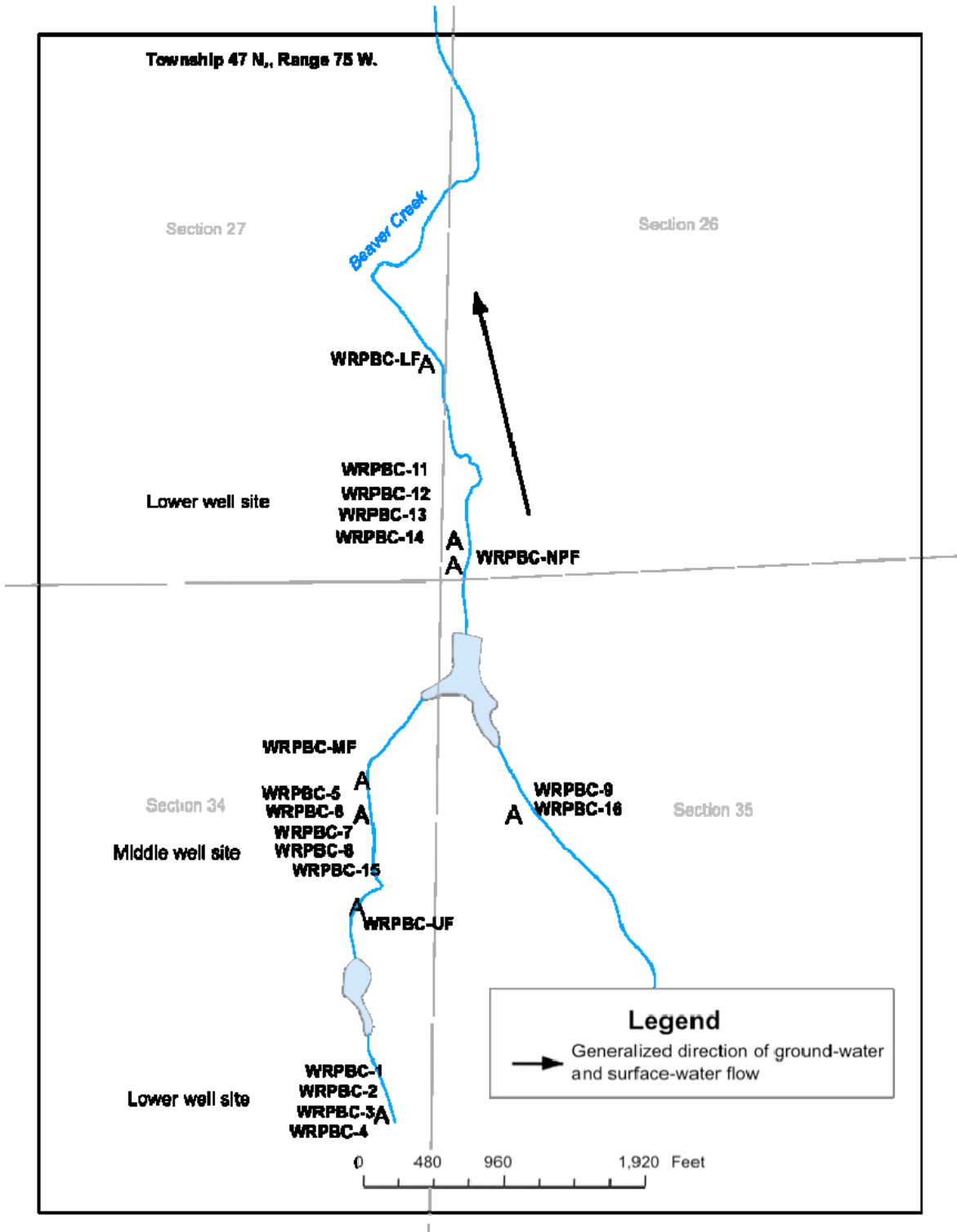


Figure 5.13: Location of sites in the Beaver Creek study area.

In this part of the Powder River Basin, coalbed methane production is generally from the Paleocene Fort Union Formation, Big George Coal. Coalbed methane production and resultant produced water discharge to these two infiltration ponds began in November, 2002. Water sampling from the installed monitoring wells began shortly thereafter in January, 2003. As part of this study water samples were collected and analyzed for major ions and trace elements twice in 2003 and once in 2007. However, concurrent studies performed on this study site have published geochemical data from samples collected in August of 2003, 2004, 2005 and February 2005 (Brinck and Frost, 2007). Geochemical data for this site have been compiled in **Appendix 5.C**. Graphs showing the concentrations of major ions are presented on **Plate 4**. On this plate, the monitoring locations and generalized geology are shown in cross section to provide perspective of the locations of water quality samples. A water budget was calculated and presented by Payne (2004).

RESULTS

Water samples collected from the upper well site, which is considered to be outside the influence of CBM infiltration and therefore representative of baseline conditions, indicate the ground-water quality is dominated by ions of Ca, SO₄ and HCO₃ (**Plate 4**). In contrast, the water produced during coalbed-methane production is dominated by ions of Na and HCO₃, with TDS concentrations ranging from 1,266 mg/L to 1,445 mg/L (**Appendix 5.C**). The alluvial water table and the shallow bedrock water level rose in response to infiltration from the ponds and stream in the middle and lower well sites. The CBM produced water, therefore, has the potential to impact the water quality in these areas. Major ion concentration, SC, SAR and water level changes with time and distance downstream for two wells from each set of monitoring wells are presented on **Plate 4**. Wells BC-2, BC-6/7 and BC-14 are completed in the alluvial material while wells BC-4, BC-5 and BC-11 are completed in the underlying Wasatch formation.

Upper Well Site

The upper well site showed very little variation in water chemistry and water level from year to year. Due to the location of these wells up-gradient from the two CBM impoundments they would not be expected to be influenced by infiltration of CBM produced water. Both wells BC-1 and BC-2 are completed at 18 ft and all but the last water sample displayed on BC-2/1 figures on **Plate 4** were collected from well BC-2. The last sample collected in November, 2007 shows an increased concentration of SO₄. However, the November, 2007 sample was collected from well BC-1 due to damage that had occurred at well BC-2 since the last sample was collected. Data from this sample may not be comparable to data for other samples from the upper well site. This conclusion is supported by the lack of a similar trend in well BC-4 which is also in the upper set of monitoring wells.

Middle Well Site

Wells BC-5, BC-6 and BC-7 are at the middle well site. Wells BC-6 and BC-7 are completed in depths 25.8 ft and 25 ft respectively and are therefore included on the same figures (**Plate 4**). All wells at the middle well site show an initial increase in sulfate concentrations over the baseline conditions measured at the upper well site. These concentrations quickly drop back to baseline

concentrations or below, however well BC-5 shows a subsequent increase in sulfate concentration in November, 2007. The concentrations of calcium, magnesium and sodium in well BC-5 show a similar trend to that of sulfate. This is most-likely due to the dissolution of sulfate salts initially, which were then flushed through the system. The very low concentration of sulfate in CBM produced water precludes the interpretation that the observed changes in water chemistry in the middle wells could result strictly from mixing of CBM produced water and local water.

The reduction in SC with time in the middle wells also suggests minerals such as gypsum, dolomite and magnesite are being depleted and that a large percentage of the resulting dissolved constituents are being leached from the system. The upper impoundment is a former stock pond, the presence of which may have enhanced local recharge - flushing salts from the drainage system. The subsequent increase in major ion concentrations in BC-5 may be due to the infiltrating water interacting with additional soil due to mounding below the pond and stream bed. Well BC-6/7 shows a slight increase in bicarbonate and sodium concentrations which peak in the summer of 2004. These increases may be due to local ground water mixing with the sodium-bicarbonate-rich CBM produced water. This trend is not seen in BC-5, presumably because it is deeper (38 ft) than wells BC-6/7. The influence of CBM produced water at that depth is seen, however, by the mobilization of sulfate salts. This same extent of mobilization may not be seen in the shallower wells because the shallow alluvium was more frequently flushed of these salts during spring runoff prior to the introduction of CBM production.

Lower Well Site

A significant amount of salt was mobilized in water monitored at the lower well site as evidenced by the increases in calcium, magnesium, sodium and sulfate in well BC-14. This same increase in ion concentrations was not seen in well BC-11 due to the greater depth and further distance from the stream channel than well BC-14. The significant increase in sulfate concentrations of over 50 meq/L and very little change in alkalinity and chloride concentrations suggest the majority of the salts dissolved are sulfate salts. The oxidation of pyritic materials may also contribute to the increased SO_4 levels as evidenced by the increase in iron concentration. The high concentration of bicarbonate in CBM produced water results in very low solubility of carbonate salts and there is, in general, very little chloride and chloride salt in this part of the Powder River Basin. The slight upward trend in the bicarbonate concentration that can be seen in the water monitored by well BC-14 might originate with the CBM produced water or may be due to the slow dissolution of carbonate salts.

PROJECTED TRENDS

Alluvial ground-water levels began dropping in early 2007 due to a change in water management which limited overland flow from the impoundments. As a result of the decreased water mounding below the stream channel there should be less dissolution and mobilization of salts. Natural ground-water flow should eventually move the dissolved salts through the system. Continued monitoring would be expected to show a slow return to baseline conditions. Additionally, due to the flushing of salts caused by the introduction of CBM produced water,

natural runoff events in the future may show lower spikes in salt concentration in surface flow than prior to CBM development.

LEONARDITE TESTS

A laboratory experiment was conducted to determine if leonardite could potentially be used to sequester sodium from CBM-production water. Leonardite, a highly weathered lignite which can contain as much as 85% humic acids, was tested for its ability to remove sodium and lower the SAR of CBM production water. Water collected from an active CBM producing well in the Powder River Basin south of Gillette, Wyoming was run through columns containing either washed quartz silica sand (labeled “Control” on **Figures 5.14 and 5.15**) or leonardite (**Figures 5.16 and 5.17**). Water fractions were collected after 2, 15, 21, and 87 pore volumes and analyzed for major ions and trace elements (**Appendix 5.E**). **Figures 5.14 and 5.16** present the changes in specific conductance and pH of the treated water compared to the total volume of water passed through the column. **Figures 5.15 and 5.17** present the specific conductance and SAR change with volume treated.

Water, collected from CBM wells, was exposed to uniformly sized, granular leonardite in flow-through columns. Water was pumped into the columns from the bottom to allow complete saturation. The water was left in contact with the leonardite for 48 hours, then displaced by the next pore volume of water. During the seventh replication, piping became apparent in the column, and thereafter only a limited portion of the leonardite was exposed to each successive batch of water.

Treatment of CBM co-produced water with leonardite resulted in lower SAR and higher TDS (as represented by SC) compared to the control samples (**Figures 5.15 and 5.17**). This lower SAR was due primarily to initial increases in magnesium and calcium rather than the removal of sodium in leonardite treated samples. Sodium concentration was higher in the sample collected from the leonardite treatment than the control after 2 pore volumes, however the sodium concentration in the treated sample did decrease from the initial higher concentrations to concentrations lower than the control samples after 21 pore volumes (**Appendix 5.E**). The divalent cations magnesium and calcium behaved differently from sodium in that, after initial concentration increases in the leonardite-treated samples, the concentrations then fell to similar values as those found in the control samples. The sodium concentration, however, was initially higher after 2 pore volumes in the leonardite treated samples then fell after 21 pore volumes to concentrations slightly less than the control sodium concentrations.

Concentrations of sulfate increased substantially in the leonardite treated samples as compared to the control samples, whereas bicarbonate concentrations decreased (**Appendix 5.E**). After 87 pore volumes the concentration of sulfate in leonardite treated samples was similar to control samples. Bicarbonate concentrations remained lower in leonardite treated samples throughout the duration of the experiment (87 pore volumes) but the difference between the treated and control samples decreased with total pore volume. Iron concentrations increased in the leonardite treated water sample as compared to the control sample. Geochemical modeling suggests that the higher concentrations of iron found in the leonardite samples are not in steady state equilibrium and will precipitate as sulfides and hydroxides.

Divalent species such as magnesium, calcium and sulfate all increased in concentration when CBM co-produced water was treated with leonardite, whereas the monovalent species sodium and bicarbonate, in general, decreased. These concentration changes may be due to reverse ion exchange where the monovalent species are displacing the divalent species adsorbed onto the leonardite.

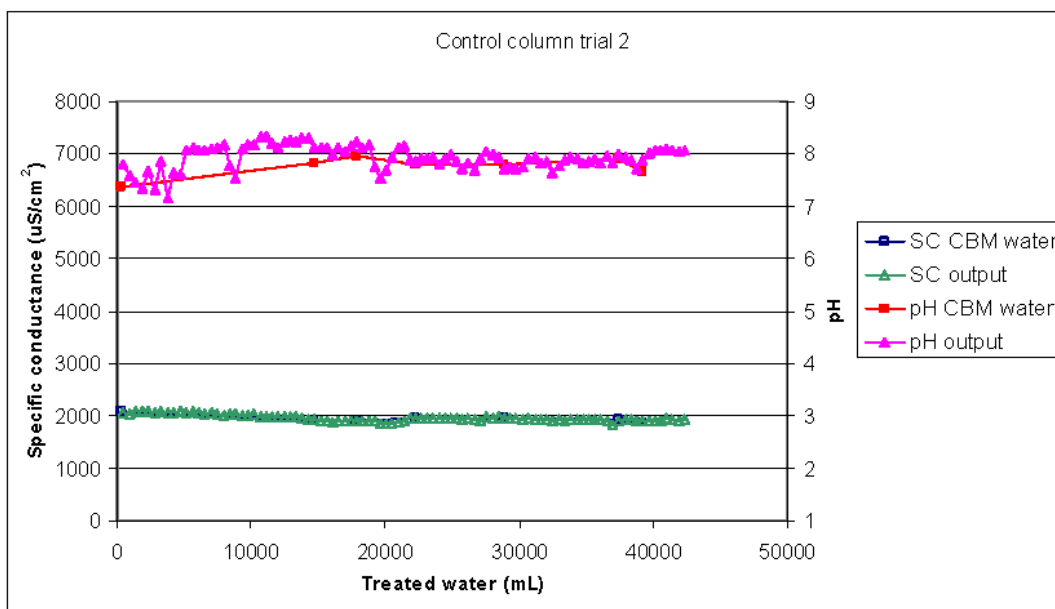


Figure 5.14: Specific conductance and pH data from control column in leonardite treatment trial.

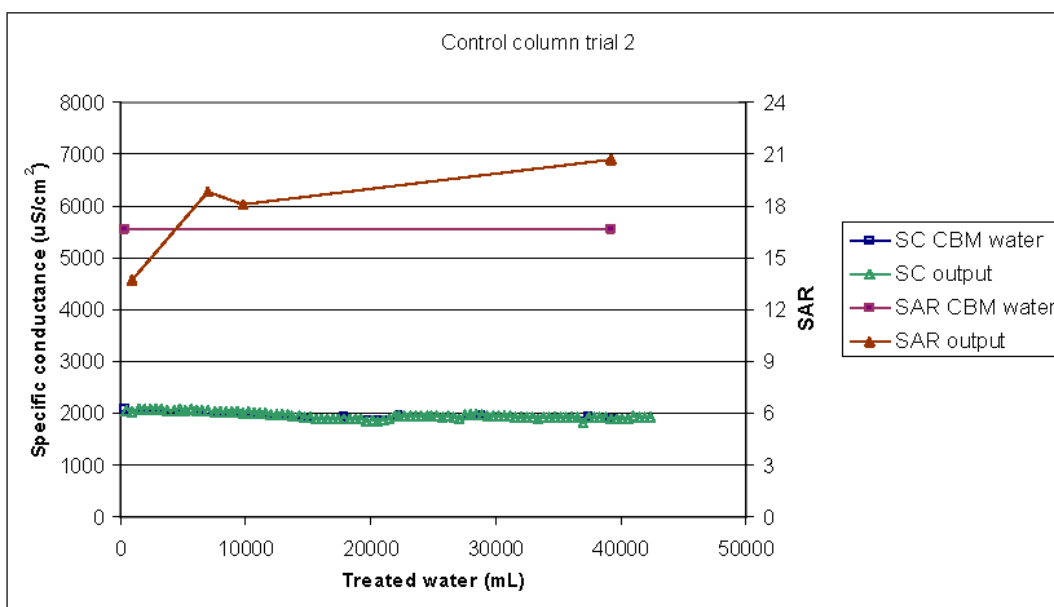


Figure 5.15: Specific conductance and SAR data from control column in leonardite treatment trial.

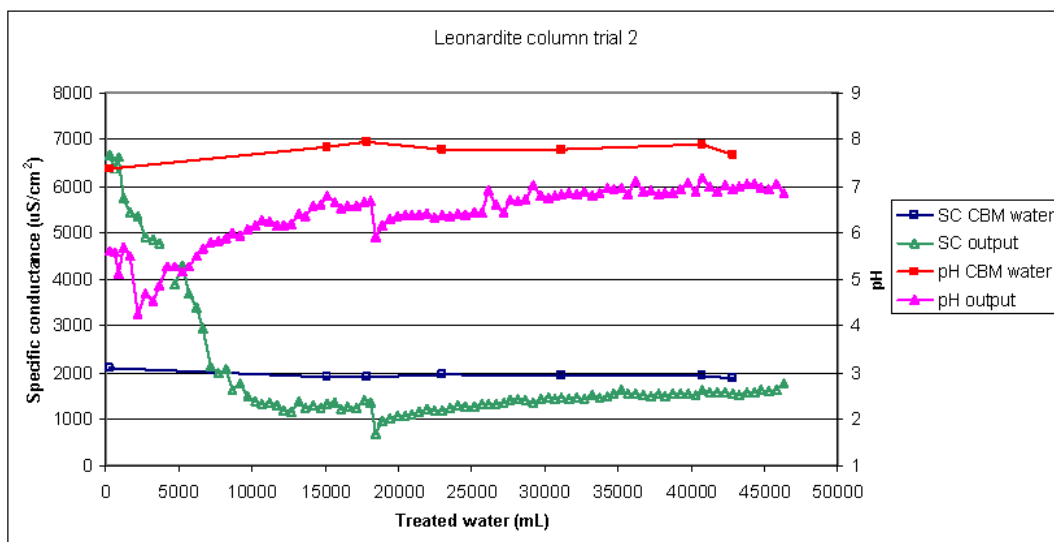


Figure 5.16: Specific conductance and pH data from leonardite column in leonardite treatment trial.

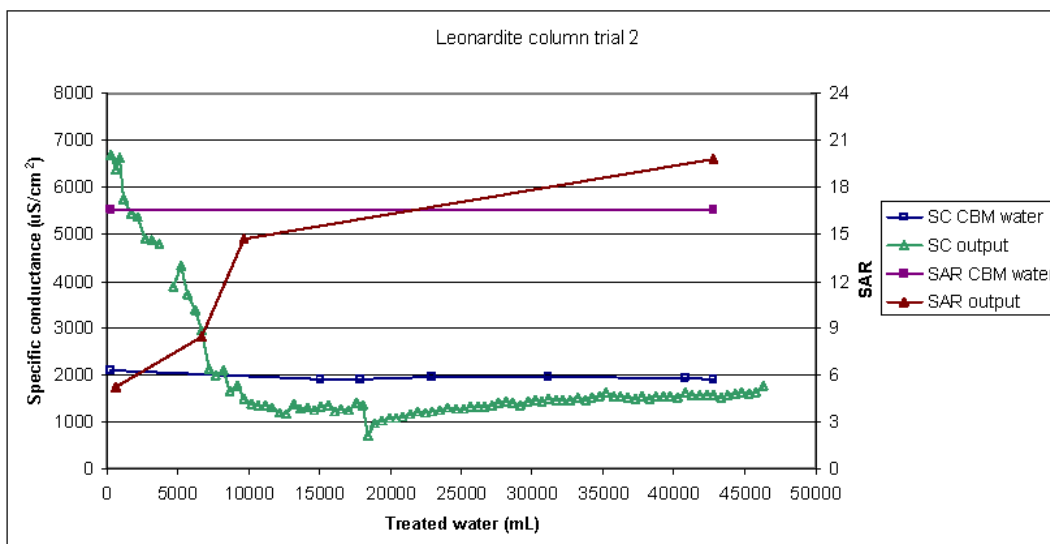


Figure 5.17: Specific conductance and SAR data from leonardite column in leonardite treatment trial.

Geochemical modeling indicates the majority of aqueous species are in their non-complex, ionic form. After 2 pore volumes, almost 70% of the alkalinity is in the form of bicarbonate with 25% comprised of carbonic acid. Over 44% of the calcium is in the form of $\text{CaSO}_4(\text{aq})$ and nearly 40% of the magnesium is in the form of $\text{MgSO}_4(\text{aq})$. After 21 pore volumes, approximately half of the alkalinity is in the form of carbonic acid and slightly under half in the form of bicarbonate. Approximately 20% of the calcium is in the form of $\text{CaSO}_4(\text{aq})$ and just over 16% of the magnesium is in the form $\text{MgSO}_4(\text{aq})$. After 87 pore volumes over 10% of calcium is in the form of CaHCO_3^+ and 5% of sulfate species occurs as NaSO_4^- .

Trace element analyses indicate increased concentrations of aluminum, boron, copper, lithium, strontium, titanium and zinc in water treated with leonardite as compared to the control samples. Like the trend of calcium, magnesium and sulfate, concentrations of boron, copper, and lithium return to levels close to those of the control samples by the 87th pore volume. While the concentrations of aluminum, titanium and zinc do decrease with increasing pore volume, they do not, however, return to the concentrations associated with the control water samples. Strontium, in contrast, increases in concentration initially in the leonardite treated samples and then decreases to the point that by the 87th pore volume the concentration is well below the concentrations associated with the control samples. The concentration of barium is the only trace element which initially decreases in the leonardite treated water samples as compared to the control samples. This is most likely due to the fact that the low sulfate concentration in the CBM co-produced water allows the barium to remain in solution. However, the sulfate concentration in leonardite treated water samples increases substantially which will then drive the precipitation of barite (BaSO_4) and subsequently result in lower dissolved barium concentrations.

As a treatment method to lower SAR, leonardite works for approximately the first 20 pore volumes of water passed through the material. The reduction in SAR is primarily through increasing magnesium and calcium, rather than the removal of sodium. Additional benefits of

using leonardite as a treatment for CBM produced water include the reduction of the bicarbonate concentration of the treated water. A lower bicarbonate concentration will allow the SAR to remain lowered because calcium carbonate is less likely to precipitate. Additionally, the lower pH of water treated with leonardite will facilitate the dissolution of locally occurring calcite on soils with which the treated water interacts. However, by not removing sodium and increasing the overall salinity of the water the resulting water chemistry may not be ideal for land application.

REMOTE SENSING EVALUATION

As discussed in this report, changes occur in ground-water quality as CBM-produced water infiltrates beneath ponds. Local geochemical conditions control these changes; at some sites only small changes may occur whereas at other sites the changes may be greater and unacceptable. Remote sensing was briefly evaluated during this project to identify if it could be used as a tool to efficiently identify evaporite minerals that could contribute to possible problem sites.

An ASTER image of the Coal Creek study area was taken in Aug 7, 2001. Data from three wavelength bands of the image were acquired and processed (georectified, resized and calibrated). The three bands were: Band 1 – 0.5560 micrometers; Band 2 – 0.6610 micrometers; and Band 3N – 0.8070 micrometers. The bands were analyzed using Spectral Image Mapper. The results were then compared to USGS spectral signatures for calcite, epsomite ($\text{MgSO}_4 \cdot 7\text{H}_2\text{O}$), gypsum, kaolinite, montmorillonite, and halite (a control species). Each pixel in the image was assigned the mineral value for the best match. The values were then plotted on a map of the Coal Creek study area (**Figure 5.18**). The mineral species were selected based on published analyses in the Powder River Basin.

This analysis suggests that epsomite may be the most predominant evaporate mineral species in the soils near the Coal Creek pond. Epsomite is highly soluble and provides a potential source for Mg and SO_4 , which are major contributors to the increased TDS noted in infiltrated water. Large areas of the image on **Figure 5.18** did not indicate a predominant mineral species, which may be a matter of the bands chosen for analysis or the mineral species (spectral signatures) used, or it may indicate that the pixels represent areas with multiple mineral species and no dominant signal. These preliminary results indicate that multispectral data may be a useful tool for site evaluations and that further research in this application is warranted.

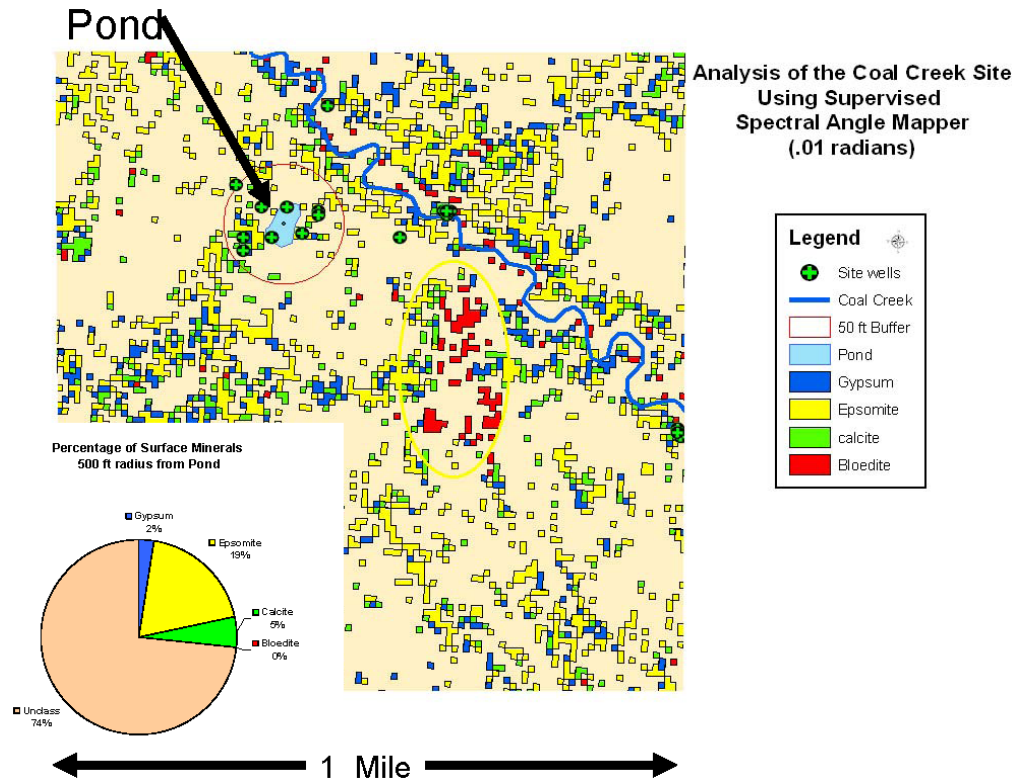


Figure 5.18: Remote sensing based potential mineral associations for Coal Creek study area.

CONCLUSIONS

Infiltration ponds provide an economical means of managing CBM production water. Water infiltrating from these ponds may recharge shallow aquifers, potentially enhancing ground-water resources. However, as the infiltrating water moves through the previously unsaturated material, a series of reactions occurs that may temporarily increase TDS and other constituents. Predicting these changes is an important step in successfully designing and siting infiltration ponds.

Data from a 5-year study at the Coal Creek site show that about 64% of the total water discharged to pond actually helped recharge shallow aquifers. However, reduced rates of infiltration with time at CBM ponds can be expected, especially at off-channel sites. The vertical hydraulic conductivity at the Coal Creek infiltration pond site was estimated to have decreased by one order of magnitude from approximately 0.1 to 0.01 feet/day.

Data and interpretations from the Coal Creek pond indicate changes in water quality that will occur as CBM-production water infiltrates into the shallow aquifers. Significant increases in TDS, Mg, Na and SO₄ occurred. The maximum increase in SO₄ reached nearly 14 times the baseline concentrations and the maximum TDS increase reached over 8 times the baseline concentration at well 12ba7B located in the pond. The increase in salt loading noted beneath ponds is temporary as it decreases with time due to flushing of salts along the flow path and dilution as infiltrated water mixes with native ground water. Ground-water quality data from

monitoring wells indicate there are elevated concentrations of salts as far, horizontally, as about 200 feet beyond the pond perimeter.

Drill cuttings and cores were collected through the pond floor at the Coal Creek infiltration pond both prior to it being filled with CBM water and again after it had dried out when CBM discharges ended. Saturated paste extract data from the cores indicate the salts migrated vertically to a depth of 20 to 25 ft below the pond floor.

At off-channel ponds, the quality of the infiltrating water has little effect on the ultimate water quality within the monitored time frames of this study. Mineralogy controls the reactions and resultant concentrations, which so far exceed any CBM-production-water ionic concentrations. For this reason, the Na concentration in the CBM water is less of a concern than is the mobilization of pre-existing salts which have accumulated in the unsaturated zone over thousands of years. In on-channel sites where natural ground-water recharge and flow have flushed the salts from the alluvial aquifer, water quality may be diluted by CBM discharge.

In shallow ground water near two on-channel ponds on a tributary to Beaver Creek both increases and decreases in TDS have occurred. Increases of SO_4 and TDS are nearly double the baseline concentrations. Where decreasing concentrations occurred, concentrations of SO_4 and TDS have dropped by as much as 80% and 40%, respectively. These responses indicate the presence of available salts along the ground-water flow paths, or the lack of salts due to historical flushing during recharge events.

Leonardite may have applications for reducing SAR of managed water. The reduction in SAR was, however, due primarily to increases in Mg and Ca. The reduction in SAR was accompanied by an increase in TDS and a decrease in pH.

Analysis of ASTER data indicate epsomite may be the dominant soluble mineral in soils at the Coal Creek site which is consistent with water-quality changes measured beneath the pond. ASTER data may provide a useful tool to assess possible pond sites, but needs further evaluation.

RECOMMENDATIONS FOR FUTURE RESEARCH

Coal mine spoils studies have shown the value of long-term studies, and similar continued research is vital to successfully evaluating CBM ponds. The Coal Creek site chosen for this research is well established with monitoring wells and stream gauging stations. The research now underway should be maintained until recovery of water quality in underlying aquifers is documented.

Continued work should include the use of coal-mine spoils data and publications on mine-spoils aquifers as a basis for understanding the influences of CBM production on surface and ground water issues. Water quality in mine-spoils aquifers reflects saturation of geologic material that has not previously been saturated. Dissolution of salts and eventual flushing of those salts are processes that parallel the processes near CBM infiltration ponds.

A decision matrix could be developed that uses infiltration rates, SPE data, and ground-water data to determine the suitability of specific locations for siting CBM infiltration ponds. Regulators should work together with researchers to develop such a decision matrix.

ACKNOWLEDGEMENTS

Several landowners have allowed access to property for the purpose of this research. The cooperation and support of Tom Davis (Gillette, WY), Apache Foundation and the State of Wyoming (Ucross, WY) is greatly appreciated. Anadarko E&P Co. is also thanked for access to one of their project areas.

REFERENCES

- Allison, J.D., and D.S. Brown. 1992.** MINTEQA2: a geochemical assessment model for environmental systems. Environmental Research Laboratory, Office of Research and Development. Athens, Georgia: USEPA.
- Brinck, E.L., Frost, C.D., 2007.** Detecting infiltration and impacts of introduced water using strontium isotopes. *Ground Water* 45, 554-568.
- Clark, D.W., 1995.** Geochemical processes in ground water resulting from surface mining of coal at the Big Sky and West Decker Mine Areas, Southeastern Montana: U.S. Geological Survey Water Resources Investigation Report 95-4097, 80 pages.
- Dockins, W. S., Olson, G. J., McFeters, G. A., Turbak, S. C., and Lee, R. W., 1980.** Sulfate reduction in ground water of southeastern Montana: U. S. Geological Survey Water-Resources Investigation 80-9, 132 pgs.
- Frost, C. D.** this volume, Strontium isotopic tracing of the effects of coal bed natural gas (CBNG) development on shallow and deep groundwater systems in the Powder River Basin, Wyoming.
- Harrington, A. H., 1984.** Compilation of overburden saturated paste analyses from the Fort Union Formation coal region: Montana Bureau of Mines and Geology Open File Report 141, 301 pgs.
- Kittrick, J. A., and F. J. Peryea, 1986.** Determination of the Gibbs free energy of formation of magnesite by solubility methods, *Soil Sci. Soc. Am. J.* 50:243-247.
- Lee, R. W., 1981.** Geochemistry of water in the Fort Union Formation of the northern Powder River Basin, southeastern Montana: U. S. Geological Survey Water Supply Paper 2076, 17 p.
- Page, A. L. (Editor), 1982.** Methods of Soil Analysis part 2 Chemical and Microbiological Procedures: American Society of Agronomy, Inc., Soil Science Society of America, Inc., Madison, WI.

- Payne, A., 2004.** Surface water hydrology and shallow groundwater effects of coalbed methane development, upper Beaver Creek drainage, Powder River Basin, Wyoming, M.S., Department of Geology and Geophysics, University of Wyoming, 116 p.
- Sadiq, M, and W. L. Lindsay, 1979.** Selection of standard free energies of formation for use in soil chemistry, Colorado State Univ. Exp. Sta. Tech. Bull. 134.
- U. S. Bureau of Land Management, 2003.** Montana Final statewide oil and gas environmental impact statement and proposed amendment of the Powder River and Billings resource management plans: U. S. Bureau of Land Management, BLM/MT/PL-03/005, 2 vol.
- U. S. Salinity Laboratory Staff, 1969.** Diagnosis and improvement of saline and alkali soils: U. S. Dept. of Agric. Handbook 60, 160 p.
- Van Voast, W., 2003.** Geochemical signature of formation waters associated with coalbed methane: American Association of Petroleum Geologists Bulletin, V 87, No. 4, pgs 667-676.
- Van Voast, W. A., and Reiten, Jon C., 1988.** Hydrogeologic responses: Twenty years of surface coal mining in southeastern Montana: Montana Bureau of Mines and Geology Memoir 62, 30 p.

APPENDIX 5.A: Monitoring Site Information
(page 1)

Site Name	CWIC ID	Type	Latitude	Longitude	Altitude	Township	Ranise	Section	Tract	County	Site Name	Well Depth (ft. below ground surface)	Aquifer	Informal Unit	Lithology	Static Water Level	Static Water Level Date	Yield	Date Completed
BC-11	207118	Nwell	44.0133	-105.8490	4700.00	47N	75W	35	BBBC	CAMPBELL	BC-11	38.0	15.0	Wasatch	Coal & siltstone	6.65	9/7/2007	0.0	12/14/2002
BC-12	207119	Nwell	44.0132	-105.8490	4700.00	47N	75W	35	BBBC	CAMPBELL	BC-12	15.0	Aluminum		6.84	9/7/2007	0.0	12/14/2002	
BC-13	207120	Nwell	44.0132	-105.8490	4700.00	47N	75W	35	BBBC	CAMPBELL	BC-13	15.0	Aluminum		6.53	9/7/2007	0.0	12/14/2002	
BC-14	207121	Nwell	44.0132	-105.8490	4700.00	47N	75W	35	BBBC	CAMPBELL	BC-14	15.0	Aluminum		6.74	9/7/2007	0.0	12/13/2002	
BC-15	207122	Nwell	44.0092	-105.8514	4720.00	47N	75W	34	ADAC	CAMPBELL	BC-15	38.0	Wasatch	Sandstone	13.01	9/7/2007	1.2	12/13/2002	
BC-6	207123	Nwell	44.0092	-105.8514	4720.00	47N	75W	34	ADAC	CAMPBELL	BC-6	25.0	Aluminum	Sand	11.61	9/7/2007	1.0	12/13/2002	
BC-7	207125	Nwell	44.0092	-105.8514	4720.00	47N	75W	34	ADAC	CAMPBELL	BC-7	23.5	Aluminum	Sand	11.48	9/7/2007	1.0	12/13/2002	
BC-8	207127	Nwell	44.0092	-105.8474	4725.00	47N	75W	35	BCAC	CAMPBELL	BC-8	12.0	Aluminum	Sand	Dry	9/7/2007	0.0	12/15/2002	
BC-9	207128	Nwell	44.0092	-105.8474	4725.00	47N	75W	35	BCAC	CAMPBELL	BC-9	28.0	Wasatch	Sandstone & siltstone	22.82	9/7/2007	0.0	12/15/2002	
BC-1	207129	Nwell	44.0026	-105.8508	4755.00	47N	75W	34	DAAC	CAMPBELL	BC-1	11.39	Aluminum	Siltstone	11.39	9/7/2007	0.7	12/15/2002	
BC-2	207130	Nwell	44.0026	-105.8508	4755.00	47N	75W	34	DAAC	CAMPBELL	BC-2	18.0	Aluminum	Siltstone	12.68	9/7/2007	0.5	12/14/2002	
BC-3	207131	Nwell	44.0026	-105.8508	4755.00	47N	75W	34	DAAC	CAMPBELL	BC-3	18.0	Aluminum	Siltstone	12.11	9/7/2007	0.0	12/14/2002	
BC-4	207132	Nwell	44.0026	-105.8508	4755.00	47N	75W	34	DAAC	CAMPBELL	BC-4	31.5	Wasatch	Sandstone & siltstone	10.66	9/7/2007	0.5	7/10/2003	
BC-LF	208571	Stream	44.0128	-105.8484	4700.00	47N	75W	35	BBBC	CAMPBELL	BC-LF				Dry	9/7/2007		7/10/2003	
BC-NPF	208572	Stream	44.0133	-105.8490	4710.00	47N	75W	34	AAEA	CAMPBELL	BC-NPF				FL Union	9/7/2007		7/10/2003	
BC-UP CBM	209043	CBM well	44.0133	-105.8490	4710.00	47N	75W	34	BBBC	CAMPBELL	BC-UP CBM				Coal	9/7/2007			
BC-LP CBM	209044	Pond	44.0133	-105.8490	4710.00	47N	75W	34	BBBC	CAMPBELL	BC-LP CBM				Coal	9/7/2007			
BC-LP P	209045	Pond overflow	44.0133	-105.8490	4700.00	47N	75W	35	BBBC	CAMPBELL	BC-LP P				Coal	9/7/2007			
BC-MS	209046	Stream	44.0092	-105.8514	4720.00	47N	75W	34	ADAC	CAMPBELL	BC-MS				Coal	9/7/2007			
BC-UP CBM	209047	CBM well	44.0092	-105.8514	4720.00	47N	75W	34	ADAC	CAMPBELL	BC-UP CBM				Coal	9/7/2007			
BC-UP G	209048	Pond overflow	44.0026	-105.8508	4730.00	47N	75W	34	ADAC	CAMPBELL	BC-UP G				Coal	9/7/2007			
BC-UP P	209049	Pond overflow	44.0026	-105.8508	4740.00	47N	75W	34	ADAC	CAMPBELL	BC-UP P				Coal	9/7/2007			
BC-UP	209050	Stream	44.0026	-105.8508	4725.00	47N	75W	34	ADAC	CAMPBELL	BC-UP				Coal	9/7/2007			
CC-UTW	202185	Stream	44.5622	-106.5569	4161.47	53N	81W	1	CBBA	SHERIDAN	CC-UTW					0.01	9/27/2007		9/23/2003
CC-LF	202186	Stream	44.5771	-106.5494	4108.64	53N	80W	7	CBBC	SHERIDAN	CC-LF					Dry	9/27/2007		8/7/2002
CC-UW	202187	Stream	44.5980	-106.5654	4172.75	53N	81W	1	CCAC	SHERIDAN	CC-UW					0.13	9/27/2007		8/10/2002
CC-12DA1B	207105	Nwell	44.5771	-106.5495	4119.00	53N	81W	12	DAAA	SHERIDAN	CC-12DA1B	36.0	Wasatch	Sandstone	13.09	9/27/2007	0.2	10/9/2002	
CC-12DA2Q	207106	Nwell	44.5773	-106.5496	4116.26	53N	81W	12	DAAA	SHERIDAN	CC-12DA2Q	17.0	Aluminum	Sand	8.71	9/27/2007	1.0	11/6/2002	
CC-12DA3Q	207107	Nwell	44.5773	-106.5496	4116.86	53N	81W	12	DAAA	SHERIDAN	CC-12DA3Q	18.0	Aluminum	Sand	9.33	9/27/2007	1.0	11/6/2002	
CC-12DA4Q	207108	Nwell	44.5772	-106.5496	4115.22	53N	81W	12	DAAA	SHERIDAN	CC-12DA4Q	20.0	Aluminum	Sand	9.36	9/27/2007	3.0	11/6/2002	
CC-12C1B	207109	Nwell	44.5879	-106.5655	4177.27	53N	81W	1	CCAC	SHERIDAN	CC-12C1B	27.0	Wasatch	Sandstone	4.26	9/27/2007	2.0	10/9/2002	
CC-12C2Q	207110	Nwell	44.5879	-106.5655	4176.54	53N	81W	1	CCAC	SHERIDAN	CC-12C2Q	17.0	Aluminum	Sand	3.14	9/27/2007	2.0	11/7/2002	
CC-12C3Q	207111	Nwell	44.5879	-106.5654	4175.83	53N	81W	1	CCAC	SHERIDAN	CC-12C3Q	19.0	Aluminum	Sand	3.49	9/27/2007	1.0	11/6/2002	
CC-12C4Q	207112	Nwell	44.5878	-106.5663	4174.72	53N	81W	1	CCAC	SHERIDAN	CC-12C4Q	19.5	Aluminum	Sand	3.37	9/27/2007	1.0	11/6/2002	
CC-12AC1B	207113	Nwell	44.5817	-106.5594	4169.73	53N	81W	12	ACBD	SHERIDAN	CC-12AC1B	57.0	Wasatch	Coal	34.19	9/27/2007	0.3	10/10/2002	
CC-12AC2B	207114	Nwell	44.5817	-106.5594	4169.83	53N	81W	12	ACBD	SHERIDAN	CC-12AC2B	36.0	Wasatch	Coal	21.47	9/27/2007	1.0	10/10/2002	
CC-12AC3Q	207115	Nwell	44.5823	-106.5570	4137.61	53N	81W	12	ACAD	SHERIDAN	CC-12AC3Q	14.0	Aluminum	Sand	5.23	9/27/2007	1.5	11/7/2002	
CC-12AC4Q	207116	Nwell	44.5823	-106.5569	4137.59	53N	81W	12	ACAD	SHERIDAN	CC-12AC4Q	23.0	Aluminum	Sand	5.13	9/27/2007	1.5	11/7/2002	
CC-12AC5Q	207117	Nwell	44.5823	-106.5568	4137.46	53N	81W	12	ACAD	SHERIDAN	CC-12AC5Q	17.0	Aluminum	Sand	5.51	9/27/2007	1.0	11/6/2002	
CC-12BA1B	208365	Nwell	44.5818	-106.5615	4247.68	53N	81W	12	CCCC	SHERIDAN	CC-12BA1B	42.3	Wasatch	Sandstone	34.18	9/27/2007	0.3	6/10/2003	
CC-12BA2B	208366	Nwell	44.5824	-106.5620	4241.42	53N	81W	12	CCCC	SHERIDAN	CC-12BA2B	35.6	Wasatch	Sandstone	29.75	9/27/2007	0.8	6/9/2003	
CC-12BA3B	208367	Nwell	44.5824	-106.5620	4241.43	53N	81W	12	CCCC	SHERIDAN	CC-12BA3B	137.0	Wasatch	Sandstone	97.34	9/27/2007	0.8	6/10/2003	
CC-12BA4B	208368	Nwell	44.5824	-106.5628	4235.58	53N	81W	12	CCAA	SHERIDAN	CC-12BA4B	21.7	Wasatch	Siltstone	Dry	9/27/2007	0.4	6/10/2003	
CC-12BA5B	208369	Nwell	44.5817	-106.5634	4267.89	53N	81W	12	CCBD	SHERIDAN	CC-12BA5B	155.6	Wasatch	Sandstone	120.69	9/27/2007	1.0	6/20/2003	
CC-12BA6B	208370	Nwell	44.5817	-106.5625	4238.57	53N	81W	12	CCDD	SHERIDAN	CC-12BA6B	35.0	Wasatch	Sandstone	13.78	9/27/2007	0.5	6/11/2003	
CC-12BA7B	208371	Nwell	44.5817	-106.5625	4238.59	53N	81W	12	CCDD	SHERIDAN	CC-12BA7B	23.5	Wasatch	Sandstone	13.15	9/27/2007	0.5	6/11/2003	
CC-12BA8B	208372	Nwell	44.5814	-106.5634	4238.88	53N	81W	12	CCDD	SHERIDAN	CC-12BA8B	5.8	Wasatch	Silty clay	5.83	9/27/2007	0.3	6/11/2003	
CC-12BA9B	208374	Nwell	44.5814	-106.5634	4268.22	53N	81W	12	CCBB	SHERIDAN	CC-12BA9B	58.4	Wasatch	Sandstone	43.81	9/27/2007	0.6	6/11/2003	
CC-12BA10B	208375	Nwell	44.5818	-106.5615	4247.82	53N	81W	12	CCCC	SHERIDAN	CC-12BA10B	103.64	9/27/2007	1.0	6/12/2003				
CC-12BA11B	208375	Nwell	44.5823	-106.5610	4261.75	53N	81W	12	CCAB	SHERIDAN	CC-12BA11B	118.33	9/27/2007	1.0	6/12/2003				

APPENDIX 5.B: Water Budget for the Coal Creek CBM Infiltration Pond near Ucross, Wyoming.
(page 1)

INFLOW (monthly totals)					STORAGE (monthly totals)				
Date	CBM-produced water discharge (ft3)	Precipitation (inches)	Precipitation (ft3)	Total inflow (ft3)	Date	Pond Stage (ft above floor)	Pond area (ft2)	Pond volume (ft3)	Change in storage (ft3)
June-03	0	2.79	9817	9817	June-03	0.00	0	0	0
July-03	5171	0.31	1037	6208	July-03	0.23	4117	2059	2059
August-03	3549	0.00	0	3549	August-03	0.46	8234	4117	2058
September-03	0	1.11	3335	3335	September-03	0.69	12351	6176	2059
October-03	0	0.12	340	340	October-03	0.92	16468	8234	2058
November-03	19316	0.64	1781	21097	November-03	1.15	18132	9724	1490
December-03	943	0.76	2139	3082	December-03	1.66	18920	22202	12478
January-04	3745	0.59	1680	5425	January-04	2.17	19709	34679	12477
February-04	0	0.75	2161	2161	February-04	2.68	20497	47157	12478
March-04	0	0.21	612	612	March-04	3.19	21286	59635	12478
April-04	82063	0.36	1061	83124	April-04	3.71	22090	72357	12722
May-04	149246	1.94	6241	155487	May-04	7.90	28567	174869	102512
June-04	64466	0.75	2403	66869	June-04	7.68	28232	169565	-5304
July-04	73657	2.84	9053	82710	July-04	7.44	27860	163671	-5894
August-04	55274	0.26	824	56098	August-04	7.19	27475	157580	-6091
September-04	50102	0.68	2146	52248	September-04	6.94	27090	151490	-6090
October-04	52197	0.75	2355	54552	October-04	6.70	26705	145399	-6091
November-04	0	0.03	94	94	November-04	6.45	26333	139505	-5894
December-04	0	0.18	559	559	December-04	6.21	25948	133414	-6091
January-05	0	0.35	1083	1083	January-05	5.96	25563	127324	-6090
February-05	0	0.26	797	797	February-05	5.51	24872	116396	-10928
March-05	0	1.36	4112	4112	March-05	4.89	23917	101277	-15119
April-05	0	2.95	8805	8805	April-05	4.29	22993	86647	-14630
May-05	0	4.19	12340	12340	May-05	3.68	22037	71528	-15119
June-05	0	1.34	3895	3895	June-05	3.08	21113	56898	-14630
July-05	0	1.20	3445	3445	July-05	2.52	20250	43242	-13656
August-05	0	0.63	1775	1775	August-05	1.70	18978	23117	-20125
September-05	0	0.70	1942	1942	September-05	1.02	17931	6543	-16574
October-05	0	2.49	7010	7010	October-05	0.94	16880	8440	1897
November-05	0	0.25	717	717	November-05	0.87	15627	7813	-627
December-05	0	0.38	1108	1108	December-05	0.81	14499	7250	-563
January-06	0	0.00	0	0	January-06	0.76	13604	6802	-448
February-06	0	0.07	214	214	February-06	0.61	10919	5460	-1342
March-06	0	0.44	1397	1397	March-06	0.46	8234	4117	-1343
April-06	0	0.73	2400	2400	April-06	0.31	5549	2775	-1342
May-06	0	1.34	4555	4555	May-06	0.16	2864	1432	-1343
June-06	0	1.10	3871	3871	June-06	0.00	0	0	-1432
July-06	0	0.43	1513	1513	July-06	0.00	0	0	0
August-06	0	0.07	246	246	August-06	0.00	0	0	0
September-06	0	1.74	6123	6123	September-06	0.00	0	0	0
October-06	0	0.68	2392	2392	October-06	0.00	0	0	0
November-06	0	0.58	2041	2041	November-06	0.00	0	0	0
December-06	0	0	0	0	December-06	0.00	0	0	0
January-07	0	0	0	0	January-07	0.00	0	0	0
February-07	0	0.68	2392	2392	February-07	0.00	0	0	0
March-07	0	2.16	6956	6956	March-07	0.40	7160	3580	3580
April-07	0	1.04	2946	2946	April-07	1.93	19338	28807	25227
May-07	0	5.57	16470	16470	May-07	3.86	22322	76027	47220
June-07	0	2.10	5937	5937	June-07	1.85	19214	26850	-49177
July-07	0	0.92	2575	2575	July-07	1.40	18518	15840	-11010
August-07	0	0.00	0	0	August-07	0.90	16110	8055	-7785
September-07	0	0.62	1904	1904	September-07	0.60	10740	5370	-2685
October-07	0	1.32	4054	4054	October-07	0.60	10740	5370	0
TOTALS	559729	52.76	162648	722377					5370

APPENDIX 5.C-1: Water Quality for the Coal Creek Sites
(page 1)

Gwic Id	Site Name	Site Type	Aquifer	Depth (ft)	Sample Date	Water Temperature	Lab	Lab pH	Lab SC	Calcium (mg/l)	Magnesium (mg/l)	Sodium (mg/l)	Potassium (mg/l)
207110	CC-1CC2Q	WELL	110ALVM	17	7/1/2003 15:00	10	MBMG	7.56	1818	123.0	129.0	159.0	5.9
207110	CC-1CC2Q	WELL	110ALVM	17	7/27/2005 15:10	9.8	MBMG	7.68	2150	161.0	161.0	173.0	7.3
207110	CC-1CC2Q	WELL	110ALVM	17	1/25/2006 13:45	9.8	MBMG	7.52	2160	157.0	164.0	168.0	7.0
207110	CC-1CC2Q	WELL	110ALVM	17	6/22/2006 9:25	10.9	MBMG	7.36	2070	153.0	161.0	183.0	7.0
207110	CC-1CC2Q	WELL	110ALVM	17	8/6/2007 13:04	10	MBMG	7.48	1965	142.0	150.0	158.0	7.0
207109	CC-1CC1B	WELL	124WSTC	27	9/16/2003 16:30	9.8	MBMG	7.69	1603	94.1	67.2	203.0	5.6
207109	CC-1CC1B	WELL	124WSTC	27	6/22/2006 9:00	9.8	MBMG	7.12	1737	92.0	65.0	232.0	6.4
202187	CC-UW	STREAM			4/4/2003 12:15	12.1	MBMG	7.84	1560	130.0	105.0	89.4	12.3
202187	CC-UW	STREAM			7/1/2003 12:00	18.2	MBMG	7.83	1152	93.8	74.0	73.9	8.6
202185	CC-UTW	STREAM			4/4/2003 13:00	11.1	MBMG	8.18	1555	99.4	99.7	113.0	10.2
209364	CC-SPCBM	WELL	125TGRV		12/4/2003 19:00	3.8	MBMG	8.03	1647	11.7	5.7	393.0	3.3
209363	CC-SP	POND			12/4/2003 12:15	0.8	MBMG	8.46	1590	11.4	5.8	382.0	3.2
209363	CC-SP	POND			6/3/2004 12:00	12.2	MBMG	8.97	1482	7.4	7.4	391.0	3.0
209363	CC-SP	POND			3/2/2005 11:45	7.47	MBMG	8.91	1813	7.7	8.6	464.0	3.2
209363	CC-SP	POND			7/28/2005 8:20	18.6	MBMG	9.74	1545	4.7	7.9	416.0	2.5
209363	CC-SP	POND			8/1/2007		MBMG	8.84	6880	5.7	4.8	139.0	2.7
208365	CC-12BA1B	WELL	124WSTC	42.3	6/27/2003 11:30	13.2	MBMG	7.64	3150	238.0	154.0	410.0	9.6
208365	CC-12BA1B	WELL	124WSTC	42.3	6/3/2004 17:00	17.8	MBMG	7.75	3320	220.0	157.0	381.0	9.4
208365	CC-12BA1B	WELL	124WSTC	42.3	3/2/2005 15:30	9.93	MBMG	7.05	3260	243.0	177.0	384.0	9.3
208365	CC-12BA1B	WELL	124WSTC	42.3	7/28/2005 13:30	13.8	MBMG	7.8	2970	259.0	186.0	400.0	9.6
208365	CC-12BA1B	WELL	124WSTC	42.3	1/24/2006 12:00	9.8	MBMG	7.42	3190	255.0	182.0	393.0	9.1
208365	CC-12BA1B	WELL	124WSTC	42.3	6/21/2006 11:15	11.9	MBMG	6.45	3110	247.0	171.0	398.0	9.3
208365	CC-12BA1B	WELL	124WSTC	42.3	1/9/2007 8:30	6.3	MBMG	6.99	3080	212.0	148.0	360.0	9.0
208365	CC-12BA1B	WELL	124WSTC	42.3	8/7/2007 8:05		MBMG	6.33	3130	209.0	150.0	379.0	9.2
208366	CC-12BA2B	WELL	124WSTC	35.6	6/27/2003 12:40	14.9	MBMB	7.52	1936	104.0	58.0	275.0	5.9
208366	CC-12BA2B	WELL	124WSTC	35.6	6/3/2004 19:15	19.4	MBMG	7.81	3710	259.0	258.0	390.0	9.6
208366	CC-12BA2B	WELL	124WSTC	35.6	3/2/2005 17:30	11.16	MBMG	7.52	6510	418.0	614.0	835.0	7.8
208366	CC-12BA2B	WELL	124WSTC	35.6	7/29/2005 8:25	10.1	MBMG	7.59	6420	412.0	572.0	977.0	6.7
208366	CC-12BA2B	WELL	124WSTC	35.6	1/24/2006 16:15	9.8	MBMG	7.69	6620	437.0	550.0	912.0	8.3
208366	CC-12BA2B	WELL	124WSTC	35.6	6/21/2006 16:00	12	MBMG	7.76	6160	515.0	530.0	725.0	9.9
208366	CC-12BA2B	WELL	124WSTC	35.6	1/9/2007 13:00	11	MBMG	7.42	4010	258.0	273.0	486.0	7.8
208366	CC-12BA2B	WELL	124WSTC	35.6	8/7/2007 10:16	11	MBMG	6.77	4420	279.0	283.0	558.0	10.5
208366	CC-12BA2B	WELL	124WSTC	35.6	1/3/2008 12:00	9.4	MBMG	7.16	3840	243.0	235.0	492.0	9.2
208367	CC-12BA3B	WELL	124WSTC	137	6/20/2003 15:54	13.1	MBMG	8.26	1059	6.9	3.6	267.0	2.2
208367	CC-12BA3B	WELL	124WSTC	137	7/29/2005 8:32	11.6	MBMG	8.29	1118	6.6	3.8	293.0	2.3
208367	CC-12BA3B	WELL	124WSTC	137	1/24/2006 15:30	12.4	MBMG	8.28	1086	6.0	3.5	250.0	2.1
208367	CC-12BA3B	WELL	124WSTC	137	6/21/2006 15:25	14.8	MBMG	7.64	1815	6.2	3.6	289.0	2.1
208367	CC-12BA3B	WELL	124WSTC	137	1/10/2007 13:00	12	MBMG	7.72	1094	6.0	3.6	279.0	2.1
208367	CC-12BA3B	WELL	124WSTC	137	8/7/2007 10:17	15.4	MBMG	7.18	1250	6.1	3.7	283.0	2.2
208368	CC-12BA4B	WELL	124WSTC	21.7	3/3/2005 10:00	9.8	MBMG	7.6	12810	408.0	1582.0	2381.0	8.9
208368	CC-12BA4B	WELL	124WSTC	21.7	7/29/2005 8:05	10.1	MBMG	7.95	12550	382.0	1612.0	2573.0	8.1
208368	CC-12BA4B	WELL	124WSTC	21.7	1/25/2006 8:50	9.3	MBMG	7.77	11530	375.0	1386.0	2294.0	<2.50

APPENDIX 5.C-1: Water Quality for the Coal Creek Sites
(page 2)

Gwic Id	Site Name	Site Type	Aquifer	Depth (ft)	Sample Date	Water Temperature	Lab	Lab pH	Lab SC	Calcium (mg/l)	Magnesium (mg/l)	Sodium (mg/l)	Potassium (mg/l)
208369	CC-12BA5B	WELL	124WSTC	155.6	6/20/2003 16:45	15.5	MBMG	7.95	1181	11.2	5.8	282.0	2.5
208369	CC-12BA5B	WELL	124WSTC	155.6	6/21/2006 18:00	11.2	MBMG	7.61	1187	7.2	4.0	291.0	2.2
208370	CC-12BA6B	WELL	124WSTC	35	6/20/2003 9:36	13.2	MBMG	7.45	1865	136.0	84.2	230.0	7.6
208370	CC-12BA6B	WELL	124WSTC	35	12/4/2003 16:00	8.8	MBMG	7.34	1906	130.0	80.8	221.0	7.4
208370	CC-12BA6B	WELL	124WSTC	35	6/3/2004 15:20	9.1	MBMG	7.59	2150	122.0	80.6	242.0	7.1
208370	CC-12BA6B	WELL	124WSTC	35	3/2/2005 10:10	9.16	MBMG	7.37	1881	101.0	66.4	260.0	6.6
208370	CC-12BA6B	WELL	124WSTC	35	7/28/2005 10:30	11.8	MBMG	7.47	1971	132.0	80.9	268.0	7.5
208370	CC-12BA6B	WELL	124WSTC	35	1/25/2006 11:10	8.9	MBMG	7.55	1984	134.0	81.8	258.0	7.6
208370	CC-12BA6B	WELL	124WSTC	35	6/20/2006 13:30	11.3	MBMG	7.08	1941	133.0	85.3	272.0	7.7
208370	CC-12BA6B	WELL	124WSTC	35	1/8/2007 16:06	8.2	MBMG	6.75	1955	130.0	84.8	268.0	7.8
208370	CC-12BA6B	WELL	124WSTC	35	8/8/2007 9:30	11.4	MBMG	6.52	2170	128.0	83.6	254.0	7.2
208370	CC-12BA6B	WELL	124WSTC	35	1/2/2008		MBMG	7.21	1984	128.0	83.7	254.0	7.7
208370	CC-12BA7B	WELL	124WSTC	23.5	6/20/2003 12:00	13.2	MBMG	7.95	1902	155.0	102.0	203.0	7.0
208371	CC-12BA7B	WELL	124WSTC	23.5	12/4/2003	9.9	MBMG	7.62	6350	444.0	520.0	898.0	9.5
208371	CC-12BA7B	WELL	124WSTC	23.5	6/3/2004 13:00	8.6	MBMG	7.89	10590	361.0	849.0	2236.0	8.4
208371	CC-12BA7B	WELL	124WSTC	23.5	3/2/2005 11:00	9.3	MBMG	7.51	9390	382.0	668.0	1904.0	9.0
208371	CC-12BA7B	WELL	124WSTC	23.5	7/28/2005 9:30	12	MBMG	7.81	9190	342.0	692.0	1985.0	10.6
208371	CC-12BA7B	WELL	124WSTC	23.5	1/25/2006 11:40	9.2	MBMG	7.65	8980	312.0	687.0	1880.0	9.0
208371	CC-12BA7B	WELL	124WSTC	23.5	6/20/2006 13:30	13	MBMG	7.92	9320	347.0	740.0	2025.0	9.5
208371	CC-12BA7B	WELL	124WSTC	23.5	1/8/2007 16:05	6.6	MBMG	7.38	9790	313.0	750.0	2081.0	9.7
208371	CC-12BA7B	WELL	124WSTC	23.5	8/8/2007 9:30	12.1	MBMG	7.04	8190	231.0	573.0	1544.0	6.3
208371	CC-12BA7B	WELL	124WSTC	23.5	1/3/2008 11:00	9.1	MBMG	7.49	9450	290.0	691.0	1772.0	7.8
208372	CC-12BA8B	WELL	124WSTC	5.8	6/3/2004 13:10	10.7	MBMG	8.24	3000	72.0	71.2	665.0	4.0
208372	CC-12BA8B	WELL	124WSTC	5.8	3/2/2005 10:25	6.9	MBMG	7.65	5480	341.0	305.0	970.0	5.9
208372	CC-12BA8B	WELL	124WSTC	5.8	7/28/2005 8:20	16.4	MBMG	8.47	5680	418.0	390.0	936.0	7.1
208373	CC-12BA9B	WELL	124WSTC	58.4	6/27/2003 13:30	12.2	MBMG	7.36	2090	198.0	133.0	184.0	6.9
208373	CC-12BA9B	WELL	124WSTC	58.4	6/4/2004 12:00	17.5	MBMG	7.63	2190	192.0	128.0	181.0	7.0
208373	CC-12BA9B	WELL	124WSTC	58.4	3/3/2005 13:33	12.1	MBMG	7.29	2160	182.0	120.0	181.0	7.1
208373	CC-12BA9B	WELL	124WSTC	58.4	7/29/2005 11:15	10.9	MBMG	7.44	2090	198.0	126.0	204.0	7.5
208373	CC-12BA9B	WELL	124WSTC	58.4	1/25/2006 9:25	9.2	MBMG	7.59	2120	195.0	120.0	184.0	6.9
208373	CC-12BA9B	WELL	124WSTC	58.4	6/22/2006 17:50	11.2	MBMG	6.83	1978	192.0	124.0	195.0	7.2
208373	CC-12BA9B	WELL	124WSTC	58.4	1/9/2007 14:20		MBMG	7.06	2150	183.0	119.0	197.0	7.1
208373	CC-12BA9B	WELL	124WSTC	58.4	8/7/2007		MBMG	6.39	2150	182.0	119.0	184.0	7.2
208374	CC-12BA10B	WELL	124WSTC	143.2	6/20/2003 14:30	14.5	MBMG	8.01	2270	46.1	28.7	467.0	5.3
208374	CC-12BA10B	WELL	124WSTC	143.2	3/3/2005 11:30	13.1	MBMG	7.37	5050	333.0	216.0	782.0	10.4
208374	CC-12BA10B	WELL	124WSTC	143.2	7/28/2005 14:24	13.7	MBMG	7.61	4550	351.0	244.0	701.0	9.3
208374	CC-12BA10B	WELL	124WSTC	143.2	1/24/2006 10:40	13.6	MBMG	7.32	5210	414.0	365.0	691.0	10.9
208374	CC-12BA10B	WELL	124WSTC	143.2	6/21/2006 11:53	17.1	MBMG	7.01	4850	326.0	274.0	702.0	9.6
208374	CC-12BA10B	WELL	124WSTC	143.2	1/10/2007 12:10	10.9	MBMG	7.55	3730	120.0	79.7	819.0	7.2
208374	CC-12BA10B	WELL	124WSTC	143.2	8/7/2007		MBMG	6.5	5010	304.0	262.0	727.0	10.4
208375	CC-12BA11B	WELL	124WSTC	158.2	6/27/2003 9:30	12.6	MBMG	7.92	1063	6.9	4.0	260.0	2.2
208375	CC-12BA11B	WELL	124WSTC	158.2	7/28/2005 12:30	10.9	MBMG	8.27	1045	6.5	3.8	287.0	2.5
208375	CC-12BA11B	WELL	124WSTC	158.2	1/24/2006 14:20	13.1	MBMG	8	1304	5.8	3.4	298.0	2.0
208375	CC-12BA11B	WELL	124WSTC	158.2	6/21/2006		MBMG	7.22	1171	6.4	3.6	279.0	2.2

APPENDIX 5.C-1: Water Quality for the Coal Creek Sites
(page 3)

Gwic Id	Site Name	Site Type	Aquifer	Depth (ft)	Sample Date	Water Temperature	Lab	Lab pH	Lab SC	Calcium (mg/l)	Magnesium (mg/l)	Sodium (mg/l)	Potassium (mg/l)
208375	CC-12BA11B	WELL	124WSTC	158.2	1/10/2007 8:22		MBMG	7.75	1080	6.0	3.5	264.0	2.1
208375	CC-12BA11B	WELL	124WSTC	158.2	8/7/2007 9:20		MBMG	7.74	1135	5.9	3.5	259.0	2.1
208376	CC-12BA12B	WELL	124WSTC	63.9	6/27/2003 8:30	13.8	MBMG	7.37	2770	163.0	88.3	469.0	8.0
208376	CC-12BA12B	WELL	124WSTC	63.9	3/2/2005 14:15	11	MBMG	7.01	3010	180.0	98.6	448.0	8.6
208376	CC-12BA12B	WELL	124WSTC	63.9	7/28/2005 16:00	35	MBMG	7.31	2890	191.0	97.3	495.0	8.7
208376	CC-12BA12B	WELL	124WSTC	63.9	1/24/2006 12:55	10.4	MBMG	7.36	2900	180.0	102.0	442.0	8.1
208376	CC-12BA12B	WELL	124WSTC	63.9	6/21/2006 14:15	12.2	MBMG	7.15	2790	187.0	102.0	465.0	8.2
208376	CC-12BA12B	WELL	124WSTC	63.9	1/9/2007 11:30	9.4	MBMG	7.01	2800	190.0	103.0	445.0	8.5
208376	CC-12BA12B	WELL	124WSTC	63.9	8/7/2007 9:20	11.2	MBMG	6.81	2920	185.0	111.0	449.0	9.1
211060	CC-MSP	SPRING		2.75	6/4/2004 13:35	9.8	MBMG	7.81	2890	212.0	215.0	247.0	4.7
211060	CC-MSP	SPRING		2.75	3/3/2005 8:45	8	MBMG	7.38	2730	197.0	194.0	235.0	4.4
211060	CC-MSP	SPRING		2.75	7/27/2005 16:15	13.4	MBMG	7.7	2480	193.0	189.0	239.0	4.6
211060	CC-MSP	SPRING		2.75	1/25/2006 14:50	9.1	MBMG	7.59	2520	185.0	184.0	232.0	4.0
211060	CC-MSP	SPRING		2.75	6/22/2006 10:55	17.1	MBMG	7.23	2320	178.0	177.0	231.0	4.6
211060	CC-MSP	SPRING		2.75	1/9/2007 15:32	1.4	MBMG	7.4	2470	180.0	191.0	228.0	4.2
211060	CC-MSP	SPRING		2.75	8/6/2007 14:37	12.1	MBMG	7.14	2440	178.0	171.0	215.0	4.2
211060	CC-MSP	SPRING		2.75	1/3/2008 12:00		MBMG	7.4	2640	192.0	188.0	219.0	4.3
207115	CC-12AC3Q	WELL	110ALVM	14	7/1/2003 18:20	10.8	MBMG	7.59	2770	189.0	196.0	266.0	9.5
207115	CC-12AC3Q	WELL	110ALVM	14	1/26/2006 12:00	7.4	MBMG	7.54	3340	245.0	245.0	357.0	11.2
207115	CC-12AC3Q	WELL	110ALVM	14	6/22/2006 16:00		MBMG	7.58	3760	267.0	272.0	478.0	12.9
207115	CC-12AC3Q	WELL	110ALVM	14	1/10/2007 8:15	7.3	MBMG	7.53	3340	244.0	232.0	406.0	11.6
207115	CC-12AC3Q	WELL	110ALVM	14	8/6/2007 15:47	13.5	MBMG	7.16	3480	236.0	245.0	351.0	10.9
207113	CC-12AC1B	WELL	124WSTC	57	7/2/2003 10:00	13.9	MBMG	7.89	1902	22.2	13.5	389.0	3.3
207114	CC-12AC2B	WELL	124WSTC	36	7/2/2003 13:15	11.8	MBMG	7.48	2310	202.0	118.0	224.0	4.0
207113	CC-12AC1B	WELL	124WSTC	57	1/26/2006 11:08	9.4	MBMG	7.93	1710	21.5	12.3	416.0	3.4
207114	CC-12AC2B	WELL	124WSTC	36	6/20/2006 18:00	10.6	MBMG	7.12	1642	160.0	89.2	179.0	3.5
207114	CC-12AC2B	WELL	124WSTC	36	1/10/2007 9:06	7.1	MBMG	7.18	1612	156.0	86.2	156.0	3.2
207113	CC-12AC1B	WELL	124WSTC	57	1/10/2007 9:10		MBMG	7.68	1797	22.0	12.9	441.0	3.5
207113	CC-12AC1B	WELL	124WSTC	57	8/6/2007		MBMG	7.5	2020	21.0	12.6	435.0	3.3
207114	CC-12AC2B	WELL	124WSTC	36	8/6/2007 15:22	9.9	MBMG	6.97	1545	182.0	73.0	99.5	2.6
209338	CC-12ACCC	STREAM			7/1/2003 18:30	25.4	MBMG	7.96	2350	151.0	170.0	221.0	8.4
202186	CC-LF	STREAM			4/4/2003 14:15	8.2	MBMG	7.88	1778	122.0	117.0	146.0	11.1
207106	CC-12DA2Q	WELL	110ALVM	17	7/2/2003 15:15	9.5	MBMG	7.48	2670	215.0	184.0	261.0	8.2
207106	CC-12DA2Q	WELL	110ALVM	17	7/27/2005 17:30	9.6	MBMG	7.8	2830	229.0	184.0	300.0	9.3
207106	CC-12DA2Q	WELL	110ALVM	17	1/25/2006 16:40	9.4	MBMG	7.56	2810	253.0	187.0	292.0	10.0
207106	CC-12DA2Q	WELL	110ALVM	17	6/22/2006 13:00	13.5	MBMG	7.64	3020	245.0	193.0	328.0	9.9
207105	CC-12DA1B	WELL	124WSTC	36	7/2/2003 17:30	11.3	MBMG	7.37	4240	276.0	211.0	665.0	11.6
207105	CC-12DA1B	WELL	124WSTC	36	6/22/2006 15:15	11.4	MBMG	7.08	4400	270.0	197.0	683.0	11.9

APPENDIX 5.C-1: Water Quality for the Coal Creek Sites
(page 4)

Gwic Id	Iron (mg/l)	Manganese (mg/l)	Silica (mg/l)	Bicarbonate (mg/l)	Carbonate (mg/l)	Sulfate (mg/l)	Chloride (mg/l)	Nitrate (mg/l)	Flouride (mg/l)	Orthophosphate (mg/l)	Silver (ug/l)	Aluminum (ug/l)	Arsenic (ug/l)
207110	0.022	0.051	17.7	586.8	0.0	644.0	5.6	0.99 P	1.840		<5	<30	<5
207110	<0.005	0.094	22.0	614.1	0.0	903.0	<10.0	1.14 P	<1.0	<1.0	<5	<30	<5
207110	<0.005	0.070	18.7	645.8	0.0	916.0	<10	1.30 P	<1.0	<1.0	<5	<30	<5
207110	<0.005	0.091	21.2	715.8	0.0	699.0	4.7	<1.0 P	0.412	<0.05	<5	<30	<5
207110	<0.005	<0.001	21.0	619.8	0.0	831.0	5.0	1.10 P	0.701	<0.50	<1.0	<1.0	2.1
207109	0.748	0.217	8.3	567.3	0.0	464.0	<5.0	<0.5 P	1.560		<5	<30	<5
207109	0.879	0.228	10.2	509.4	0.0	463.0	3.0	<0.5 P	0.313	<0.05	<1	<10	<1
202187	0.331	0.303	8.4	542.9	0.0	530.5	<5.00	1.23 P	<0.50	<0.50	<5	<150	<5
202187	0.048	0.048	11.6	475.8	0.0	293.0	<5.0	<0.5 P	<0.5	<0.5	<1	<30	1.4
202185	0.106	0.042	8.1	416.6	0.0	609.9	6.5	1.92 P	<0.50	<0.50	<5	<150	5.9
209364	1.600	0.046	9.8	1128.9	0.0	<2.5	13.9	<0.5 P	0.089	0.056	<1	47.2	2.0
209363	0.503	0.041	9.2	1121.2	12.0	<2.5	14.0	<0.5 P	0.084	<0.05	<5	<30	<5
209363	0.114	0.003	8.1	899.4	48.5	22.0	16.4	<0.5 P	<0.05	<0.05	<1	140.0	1.4
209363	0.027	0.001	5.6	1106.5	88.8	13.7	19.2	<0.5 P	<0.05	<0.05	<5	<30	<5
209363	0.008	<0.001	0.6	575.2	166.2	31.2	16.3	<0.5 P	<0.05	<0.05	<1	28.5	3.4
209363	<0.05	<0.01	2.1	274.5	40.8	50.2	1.5	<0.05 P	0.934	<0.05	<10.0	<10.0	3.5
208365	0.084	0.448	11.0	673.4	0.0	1425.0	10.7	<0.5 P	<0.05	<2.50	<5	<150	<5
208365	0.127	0.544	10.2	780.8	0.0	1363.0	7.5	<2.5 P	<0.5	<0.5	<5	<150	<5
208365	0.104	0.871	8.6	804.0	0.0	1456.0	7.3	3.95 P	<0.5	<0.5	<5	<50	<5
208365	0.071	0.939	8.9	614.9	0.0	1561.0	<10.0	<2.5 P	1.190	<1.0	<10	<100	<10
208365	0.185	0.963	7.8	653.9	0.0	1656.0	<2.5	<2.5 P	<2.5	<2.5	<5	<50	<5
208365	0.100	0.898	9.5	624.6	0.0	1490.0	<12.5	<1.0 P	<1.25	<1.25	<5	<50	<5
208365	0.018	0.665	9.4	735.7	0.0	1253.0	<20	<0.5 P	<2.0	<2.0	<5	<30	<5
208365	0.084	0.625	9.3	751.5	0.0	1338.0	7.0	<1.25 P	<0.63	<0.63	<5.0	<5.0	<1.0
208366	0.183	0.565	12.8	635.6	0.0	558.0	8.0	<0.5 P	1.570		<5	65.5	<5
208366	2.010	0.119	26.9	496.5	0.0	2080.0	11.3	8.76 P	<0.5	<0.5	<10	2629.0	<10
208366	0.095	<0.010	10.3	413.6	0.0	4745.0	<50.0	34.8 P	<5.0	<5.0	<10	<100	<10
208366	0.077	<0.010	11.8	478.2	0.0	4737.0	<50.0	21.8 P	<5.0	<5.0	<10	<100	<10
208366	<0.05	<0.010	11.1	575.8	0.0	4781.0	<50	16.9 P	<5.0	<5.0	<10	<100	<10
208366	<0.05	<0.01	11.6	518.5	0.0	4221.0	35.9	25.6 P	<2.50	<2.50	<10	<100	<10
208366	<0.05	0.026	10.9	651.5	0.0	2237.0	<25.0	9.15 P	<2.5	<2.5	<10	<300	<10
208366	<0.05	0.371	10.8	713.7	0.0	2127.0	<25.0	<2.50 P	2.810	<2.50	<10.0	<10.0	<2.0
208366	<0.025	0.235	10.8	685.6	0.0	1907.0	15.5	1.88 P	0.280	<0.25	<5.0	<5.0	<1.0
208367	0.013	0.010	6.8	674.7	0.0	22.6	5.1	<0.5 P	0.668	0.115	<5	<30	<5
208367	<0.005	0.027	7.4	733.2	0.0	38.8	4.8	<0.5 P	0.248	0.124	<1	<10	<1
208367	0.010	0.022	6.6	639.7	0.0	23.4	5.5	<0.5 P	<0.05	0.111	<1	<10	<1
208367	0.009	0.027	7.5	678.5	0.0	35.8	5.5	<0.5 P	0.858	<0.05	<1	<10	<1
208367	0.011	0.038	7.7	680.4	0.0	25.6	5.7	<0.5 P	0.862	0.125	<1	<30	<1
208367	0.025	0.047	7.4	652.3	0.0	39.0	5.3	<0.05 P	0.876	0.051	<1.0	<1.0	0.3
208368	<0.50	<0.010	9.2	714.3	0.0	12015.0	30.4	7.50 P	<2.5	<2.5	<50	<300	<50
208368	<0.05	<0.01	8.2	730.8	0.0	12409.0	<12.5	<12.5 P	<12.5	<12.5	<20	<200	<20
208368	<0.25	<0.05	8.1	646.6	0.0	10750.0	<12.5	<12.5 P	<12.5	<12.5	<50	<500	<50

APPENDIX 5.C-1: Water Quality for the Coal Creek Sites
(page 5)

Gwic Id	Iron (mg/l)	Manganese (mg/l)	Silica (mg/l)	Bicarbonate (mg/l)	Carbonate (mg/l)	Sulfate (mg/l)	Chloride (mg/l)	Nitrate (mg/l)	Flouride (mg/l)	Orthophosphate (mg/l)	Silver (ug/l)	Aluminum (ug/l)	Arsenic (ug/l)
208369	0.040	0.022	7.3	734.9	0.0	90.5	3.1	<0.5 P	0.469	0.076	<5	<30	<5
208369	0.014	0.036	7.3	675.4	0.0	74.3	3.5	<0.5 P	0.778	<0.05	<1	<10	<1
208370	1.480	0.116	10.1	734.4	0.0	594.5	<5.0	<0.5 P	<0.50	<0.5	<5	33.4	<5
208370	0.021	0.057	10.1	613.7	0.0	605.0	<5.0	0.717 P	<0.5	<0.5	<5	<300	<5
208370	1.430	0.107	10.1	698.7	0.0	536.0	<5.0	<0.5 P	<0.5	<0.5	<1	<30	<1
208370	0.402	0.105	9.4	782.6	0.0	495.0	<5.0	<0.5	<0.5	<0.5	<5	<30	<5
208370	1.370	0.128	10.7	675.9	0.0	648.0	<10.0	<1.0 P	<1.0	<1.0	<5	<30	<5
208370	1.200	0.206	9.3	649.0	0.0	646.0	<10.0	<1.0	<1.0	<1.0	<5	<30	<5
208370	1.350	0.178	10.4	644.2	0.0	660.0	3.3	<0.5 P	<0.25	<0.25	<10	<100	<10
208370	1.520	0.172	10.6	714.3	0.0	637.0	<10.0	<0.5 P	<1.0	<1.0	<1	<30	<1
208370	1.440	0.144	10.1	711.3	0.0	636.0	<5.0	<0.50 P	<0.50	<0.50	<1.0	<1.0	0.8
208370	1.750	0.117	10.7	638.5	0.0	652.0	4.2	<0.25 P	0.063	<0.05	<1.0	<1.0	0.6
208371	0.045	0.127	11.2	664.9	0.0	626.8	<5.0	0.54	<0.50	<0.50	<5	<30	<5
208371	0.273	0.069	12.0	634.4	0.0	4575.0	16.5	7.40 P	<1.0	<1.0	<10	<300	<10
208371	0.091	0.059	8.3	642.9	0.0	8604.0	26.7	1.23 P	<2.5	<2.5	<10	327.0	<10
208371	0.161	0.152	8.8	750.9	0.0	7314.0	<25.0	<5.0 P	<2.5	<2.5	<50	<300	<50
208371	<0.005	0.289	9.8	677.1	0.0	7216.0	<50.0	<5.0 P	<5.0	<5.0	<1	<10	5.3
208371	<0.050	0.312	8.1	688.1	0.0	7185.0	<125	<12.5 P	<12.5	<12.5	<10	<100	<10
208371	<0.05	0.371	9.1	706.4	0.0	7761.0	<25.0	<5.0 P	<2.50	<2.50	<10	<100	<10
208371	<0.05	0.279	9.5	679.5	0.0	7065.0	<125	5.34 P	<12.5	<12.5	<10	308.0	<10
208371	<0.100	0.019	8.5	661.2	0.0	5620.0	<25.0	9.02 P	3.870	<2.5	<10.0	<20.0	3.0
208371	<0.100	0.046	8.7	649.0	0.0	6729.0	25.2	11.4 P	2.640	<1.25	<20.0	<20.0	<4.0
208372	0.028	0.042	6.1	808.9	0.0	1164.0	14.1	<0.5 P	<0.5	<0.5	<5	<150	<5
208372	0.108	0.063	6.8	659.4	0.0	3673.0	12.2	<2.5 P	<1.0	<1.0	<10	<100	<10
208372	0.083	0.104	10.4	474.6	51.6	3897.0	14.2	<5.0 P	<5.0	<0.5	<10	<100	<10
208373	0.040	0.242	10.7	778.4	0.0	752.0	5.7	<0.5 P	2.090	<1.0	<5	<30	<5
208373	0.931	0.411	12.3	682.4	0.0	824.0	<10.0	<0.5 P	<1.0	<1.0	<5	62.5	<5
208373	0.658	0.533	11.7	736.3	0.0	788.0	<10	1.85 P	<1.0	<1.0	<5	<30	<5
208373	1.760	0.326	12.8	666.9	0.0	801.0	<10.0	<1.0 P	<1.0	<1.0	<1	<10	<1
208373	0.934	0.481	10.6	694.2	0.0	781.0	<10	<1.0	<1.0	<1.0	<5	<30	<5
208373	1.770	0.318	12.6	616.7	0.0	772.0	5.1	<0.5 P	<0.50	<0.50	<5	<30	<5
208373	1.360	0.356	12.4	656.4	0.0	743.0	<5.0	<1.0 P	<0.5	<0.5	<1	<30	<1
208373	0.931	0.322	12.1	572.2	0.0	774.0	<5.0	<0.50 P	0.564	<0.50	<1.0	<1.0	0.5
208374	0.029	0.071	8.9	718.6	0.0	652.4	<5.0	<0.5 P	<0.50	<0.50	<5	37.0	<5
208374	1.990	0.867	10.5	716.8	0.0	2772.0	14.6	4.43 P	<1.0	<1.0	<10	<100	<10
208374	2.410	0.727	12.3	832.0	0.0	2611.0	<25.0	<2.5 P	<2.5	<2.5	<10	<100	<10
208374	3.370	0.691	10.4	805.2	0.0	3207.0	<50.0	<5.0 P	<5.0	<5.0	<10	<300	<10
208374	3.350	0.723	11.5	658.8	0.0	2730.0	<25.0	<2.5 P	<2.50	<2.50	<10	<100	<10
208374	1.220	0.494	9.5	657.6	0.0	1676.0	12.4	<1.0 P	<1.0	<1.0	<5	<30	<5
208374	3.740	0.755	11.4	633.2	0.0	2746.0	17.9	<5.0 P	2.660	<2.50	<10.0	<10.0	<2.0
208375	0.011	0.012	6.6	685.2	0.0	9.8	5.5	<0.5 P	<0.05	<0.05	<1	<30	<1
208375	<0.005	0.023	7.7	732.7	0.0	5.9	5.3	<0.5 P	0.197	0.149	<1	<10	1.6
208375	0.011	0.015	6.3	703.1	0.0	143.0	5.4	<0.5 P	0.911	<0.5	<1	<10	1.1
208375	0.011	0.020	7.6	751.1	0.0	3.9	5.9	<0.5 P	0.745	<0.05	<1	<10	<1

APPENDIX 5.C-1: Water Quality for the Coal Creek Sites
(page 6)

Gwic Id	Iron (mg/l)	Manganese (mg/l)	Silica (mg/l)	Bicarbonate (mg/l)	Carbonate (mg/l)	Sulfate (mg/l)	Chloride (mg/l)	Nitrate (mg/l)	Flouride (mg/l)	Orthophosphate (mg/l)	Silver (ug/l)	Aluminum (ug/l)	Arsenic (ug/l)
208375	0.018	0.019	7.4	709.1	0.0	3.7	6.0	<0.5 P	0.755	0.145	<1	<30	<1
208375	0.008	0.022	7.3	702.3	0.0	4.3	5.8	0.070 P	0.835	<0.05	<1.0	<1.0	0.2
208376	0.092	0.417	12.4	961.4	0.0	843.0	10.0	<0.5 P	2.690	<5	<5	<150	<5
208376	0.091	0.607	9.8	1015.0	0.0	941.0	<10	<1.0 P	<1.0	<1.0	<5	<50	<5
208376	0.074	0.680	10.7	954.0	0.0	1050.0	<10.0	<2.5 P	<1.0	<1.0	<5	<50	<5
208376	2.870	0.310	9.2	889.4	0.0	1047.0	<10	<1.0 P	<1.0	<1.0	<5	<50	<5
208376	3.000	0.347	10.8	857.6	0.0	1000.0	5.3	<1.0 P	<0.50	<0.50	<5	<50	<5
208376	1.010	0.403	10.6	984.5	0.0	1085.0	<10	<0.5 P	<1.0	<1.0	<1	<30	<1
208376	1.190	0.420	12.0	872.3	0.0	1018.0	6.8	<0.50 P	0.692	<0.50	<1.0	<1.0	0.4
211060	0.296	0.202	20.3	671.0	0.0	1352.0	<10.0	<1.0 P	<1.0	<1.0	<5	<150	<5
211060	0.531	0.139	19.0	666.7	0.0	1227.0	<5.0	<2.5	<0.5	<0.5	<5	<50	<5
211060	0.702	0.199	22.1	634.4	0.0	1185.0	<10.0	<1.0 P	1.260	<1.0	<5	<50	<5
211060	0.317	0.123	18.1	627.8	0.0	1198.0	<25	<2.5 P	<2.5	<2.5	<5	<50	<5
211060	0.100	0.143	22.3	674.3	0.0	1100.0	5.4	<1.0 P	<0.50	<0.50	<5	<30	<5
211060	<0.005	0.025	16.2	585.6	0.0	1123.0	6.5	<1.0 P	<0.5	<0.5	<1	<30	1.6
211060	0.152	0.172	21.2	612.4	0.0	1096.0	6.9	<0.10 P	1.040	<0.63	<1.0	<1.0	1.2
211060	<0.025	0.104	20.9	535.6	0.0	1190.0	6.7	<0.50 P	<0.50	<0.50	<5.0	<5.0	<1.0
207115	0.095	<0.005	12.0	612.4	0.0	1261.0	7.4	<0.5 P	2.640		<5	<150	<5
207115	<0.005	0.453	9.7	607.6	0.0	1913.0	<25	<2.5 P	<2.5	<2.5	<5	<30	<5
207115	<0.025	0.213	12.4	671.0	0.0	2144.0	<12.5	<2.5 P	<1.25	<1.25	<5	<50	<5
207115	<0.005	0.219	10.7	678.3	0.0	1775.0	10.9	<1.0 P	<1.0	<1.0	<1	<30	<1
207115	<0.025	<0.005	13.3	656.4	0.0	1853.0	<12.5	<1.25 P	1.270	<1.25	<5.0	<5.0	<1.0
207113	0.012	0.147	6.8	623.5	0.0	503.0	5.2	<0.5 P	2.020		<5	<30	<5
207114	0.037	0.073	9.6	598.5	0.0	814.0	5.5	<0.5 P	2.230		<5	<30	<5
207113	0.016	0.078	6.4	616.7	0.0	489.0	<5.0	<0.5 P	0.645	<0.5	<5	<30	<5
207114	<0.005	0.038	11.8	616.7	0.0	549.0	3.9	<0.5 P	0.401	<0.05	<10	<10	<1
207114	0.034	0.048	11.5	597.0	0.0	526.0	<5.0	<0.5 P	<0.5	<0.5	<1	<30	<1
207113	0.052	0.042	7.4	635.6	0.0	507.0	<5.0	<0.5 P	<0.5	<0.5	<1	<30	<1
207113	0.027	0.046	7.2	591.7	0.0	494.0	4.5	0.415 P	1.140	<0.25	<1.0	<1.0	0.3
207114	0.042	0.048	13.1	664.9	0.0	383.0	3.6	<0.25 P	0.382	<0.05	<1.0	<1.0	0.5
209338	0.037	0.007	14.6	751.5	0.0	839.0	<5.0	<0.5 P	2.450		<5	<30	<5
202186	0.106	0.081	8.3	492.9	0.0	751.5	6.4	3.04 P	<0.50	<0.50	<5	<150	<5
207106	0.062	0.111	14.2	697.5	0.0	1281.0	8.4	<0.5 P	2.600		<5	<30	<5
207106	0.264	0.100	16.6	523.4	0.0	1422.0	<10.0	<2.5 P	1.180	<1.0	<5	<50	<5
207106	2.780	0.405	16.6	655.1	0.0	1494.0	<25	<2.5 P	<2.5	<2.5	<5	<30	7.5
207106	2.550	0.376	17.3	689.3	0.0	1510.0	<12.5	<2.5 P	<1.25	<1.25	<5	<50	<5
207105	0.807	1.050	9.2	772.3	0.0	2251.0	7.8	<0.5 P	3.790		<10	<300	<10
207105	0.911	0.829	9.4	640.5	0.0	2346.0	<25.0	<2.5 P	<2.50	<2.50	<5	<50	<5

APPENDIX 5.C-1: Water Quality for the Coal Creek Sites
(page 7)

Gwic Id	Boron (ug/l)	Barium (ug/l)	Beryllium (ug/l)	Bromide (ug/l)	Cadmium (ug/l)	Cobalt (ug/l)	Chromium (ug/l)	Copper (ug/l)	Mercury (ug/l)	Lithium (ug/l)	Molybdenum (ug/l)	Nickel (ug/l)	Lead (ug/l)	Antimony (ug/l)
207110	268.0	23.1	<2	<500	<1	<2	<10	<5		81	<10	<2	<10	<10
207110	248.0	24.2	<2	<1000	<1	<2	<10	<5		91.2	<10	<2	<10	<10
207110	193.0	23.7	<2	<1000	<1	<2	<10	<5		87.3	<10	3.04	<10	<0
207110	266.0	26.4	<2	<50	<1	<2	<10	<5		86.3	<50	2.07	<10	<10
207110	210.0	18.9	<0.1	<500	<0.1	0.230	<0.1	1.98		87.7	2.32	2.05	<0.2	<0.1
207109	137.0	29.6	<2	<500	<1	<2	<10	<5		72.4	<5	<2	<10	<10
207109	118.0	23.6	<2	<50	<1	<2	3.62	<2		78.6	<10	<2	<2	<2
202187	<150	93.8	<2	<500	<2	<10	<10	<10		57.6	<10	<50	<10	<10
202187	175.0	38.8	<2	<500	<1	<2	<2	<2		51.1	<10	3.52	<2	<2
202185	<150	40.5	<2	<500	<2	<10	<10	<10		56.1	<10	13.6	<10	<10
209364	122.0	256.0	<2	104	<1	<2	3.94	10.1		43.1	<10	<2	<2	<2
209363	<5	201.0	<2	131	<1	<2	<10	<5		42.9	<10	<2	<10	<10
209363	132.0	61.6	<2	155	<1	<2	3.17	3.95		37.2	<10	<2	<2	<2
209363	<150	67.8	<2	<50	<1	<2	<10	<5		45.6	<10	<2	<10	<10
209363	126.0	29.9	<2	145	<1	<2	3.88	5.1		34.4	<10	<2	<2	<2
209363	113.0	24.5	<1.0	<50	<1.0	<1.0	<1.0	5.36		19.4	<10.0	3.94	<2.0	<1.0
208365	163.0	119.0	<10	<50	<5	<10	<10	<10		130	<50	10.6	<10	<10
208365	188.0	41.7	<10	<500	<5	<10	<10	<10		128	<50	17.2	<10	<10
208365	223.0	31.8	<10	<500	<5	<10	<10	<10		132	<10	<10	<10	<10
208365	<300	33.2	<20	<1000	<10	<20	<20	<20		133	<100	<20	<20	<20
208365	187.0	31.8	<10	<2500	<5	<10	<10	<10		126	<50	<10	<10	<10
208365	182.0	30.8	<10	<1250	<5	<10	<10	<10		131	<50	<10	<10	<10
208365	202.0	26.5	<10	<2000	<5	<10	<10	<10		123	<10	<50	<10	<10
208365	188.0	25.0	<0.5	<630	<0.5	0.734	<0.5	2.75		131	<5.0	3.73	<1.0	<0.5
208366	173.0	173.0	<2	<500	<1	<2	<10	<5		88.4	<10	5.75	<10	<10
208366	<300	128.0	<20	<500	<10	<20	<20	<20		148	<100	30.1	<20	<20
208366	519.0	<20	<20	<5000	<10	<20	<20	<20		139	<100	<20	<20	<20
208366	450.0	<20	<20	<5000	<10	<20	<20	<20		140	<100	<20	<20	<20
208366	401.0	<20	<20	<5000	<10	<20	<20	<20		178	<100	<20	<20	<20
208366	<300	<20	<20	<2500	<10	<20	<20	<20		178	<100	<20	<20	<20
208366	<300	<20	<20	<2500	<10	<20	<20	<20		134	<100	<20	<20	<20
208366	326.0	16.8	<1.0	<2500	<1.0	<1.0	12.9	<2.0		151	<10.0	4.43	<2.0	<1.0
208366	323.0	21.8	<0.5	<500	<0.5	0.662	<0.5	1.05		142	<5.0	6.57	<1.0	<0.5
208367	71.1	110.0	<2	<50	<1	<2	<10	<5		25.4	<50	<2	<10	<10
208367	65.9	71.0	<2	128	<1	<2	9.04	<2		25.6	<10	<2	<2	<2
208367	61.2	83.9	<2	<50	<1	<2	4.11	2.77		24.9	<10	<2	<2	<2
208367	66.6	86.0	<2	<50	<1	<2	5.77	<2		24.5	<10	<2	<2	<2
208367	60.4	76.8	<2	<50	<1	<2	2.33	<2		24.7	<10	2.5	<2	<2
208367	61.4	97.7	<0.1	<50	<0.1	<0.1	<1.0	<0.2		27	1.03	1.67	<0.2	<0.1
208368	1185.0	<20	<20	<2500	<10	<20	<100	<50		426	<100	<20	<100	<40
208368	1005.0	<40	<20	<12500	<20	<40	<40	<40		418	<100	<20	50.8	<40
208368	<1500	<100	<100	<12500	<50	<100	<100	<100		360	<500	<100	<100	<100

APPENDIX 5.C-1: Water Quality for the Coal Creek Sites
(page 8)

Gwic Id	Boron (ug/l)	Barium (ug/l)	Beryllium (ug/l)	Bromide (ug/l)	Cadmium (ug/l)	Cobalt (ug/l)	Chromium (ug/l)	Copper (ug/l)	Mercury (ug/l)	Lithium (ug/l)	Molybdenum (ug/l)	Nickel (ug/l)	Lead (ug/l)	Antimony (ug/l)
208369	76.8	79.5	<2	<50	<1	<2	<10	<5	28.8	<10	<10	3.81	<10	<10
208369	69.8	107.1	<2	<50	<1	<2	8.57	<2	26.8	<2	<10	<2	<2	<2
208370	213.0	25.3	<2	<500	<1	<2	<10	<5	102	<10	<10	<2	<10	<10
208370	235.0	16.1	<2	<500	<1	<2	<10	<10	101	<10	<10	<2	<10	<10
208370	218.0	33.9	<2	<500	<1	<2	3.32	5	94.5	<10	<10	5.27	<2	<2
208370	208.0	44.8	<2	<500	<1	<2	<10	<5	90.8	<10	<10	<2	<10	<10
208370	227.0	29.1	<2	<1000	<1	<2	<10	<5	102	<10	<10	<2	<10	<10
208370	179.0	28.7	<2	<1000	<1	<2	<10	<5	99.4	<10	<10	<2	<10	<10
208370	<300	30.3	<2	<250	<10	<20	<20	<20	104	<100	<100	<20	<20	<20
208370	243.0	24.1	<2	<1000	<1	<2	3.1	<2	103	<10	<10	2.14	<2	<2
208370	203.0	19.5	<0.1	<500	<0.1	0.358	<0.1	0.604	100	<10	<10	1.36	<0.2	<0.1
208370	192.0	18.8	<0.1	<100	<0.1	0.302	<0.1	0.31	107	<10	<10	1.04	<0.2	<0.1
208371	225.0	124.0	<2	<500	<5	<2	<10	<5	97.3	<50	<50	<2	<10	<10
208371	321.0	38.5	<20	<1000	<10	<20	<20	<20	161	<100	<100	<20	<20	<20
208371	461.0	44.6	<20	<2500	<10	<20	<20	<20	178	<100	<100	20.2	<20	<20
208371	510.0	33.8	<20	<2500	<10	<20	<100	<50	182	<100	<100	<20	<100	<100
208371	383.0	20.3	<2	<5000	<1	<2	<2	17.9	190	<10	<10	3.31	<2	<2
208371	472.0	22.0	<20	<12500	<10	<20	<20	21.6	179	<100	<100	<20	<20	<20
208371	506.0	<20	<20	<2500	<10	<20	<20	<20	174	<100	<100	<20	<20	<20
208371	598.0	<20	<20	<12500	<10	<20	<20	<20	173	<100	<100	<20	<20	<20
208371	636.0	15.0	<1.0	<2500	<10	<1.0	<1.0	3.75	160	<10.0	<10.0	2.29	<2.0	<1.0
208371	124.0	<4.0	<2.0	<2500	<2.0	<2.0	<2.0	<4.0	154	<20	<20	<2.0	<4.0	<1.0
208372	241.0	186.0	<10	<500	<5	<10	<10	<10	53.5	<50	<50	<10	<10	<10
208372	337.0	36.4	<20	<1000	<10	<20	<20	<20	90.3	<100	<100	<20	<20	<20
208372	863.0	29.5	<20	<500	<10	<20	<20	<20	109	<100	<100	<20	<20	<20
208373	294.0	124.0	<2	<500	<1	<10	<10	<5	109	<10	<10	12.8	<10	<10
208373	307.0	50.9	<10	<1000	<1	<10	<10	<10	107	<10	<10	12.4	<10	<10
208373	270.0	55.0	<2	<1000	<1	<2	<10	<5	110	<10	<10	20.3	<10	<10
208373	261.0	34.1	<2	<1000	<1	<2	2.16	<2	113	<10	<10	2.69	2.62	<2
208373	233.0	46.6	<2	<1000	<1	<2	<10	<5	105	<10	<10	4.67	<10	<10
208373	261.0	33.6	<10	<500	<5	<10	10.3	<10	107	<10	<10	2.46	<10	<10
208373	293.0	38.0	<2	<500	<1	<2	2.71	<2	108	<10	<10	3.91	<2	<2
208373	257.0	30.6	<0.1	<500	<0.1	1.010	<0.1	1.09	111	<10	<10	2.77	<0.2	<0.1
208374	102.0	84.0	<2	<500	<1	<2	<10	<5	72.9	<10	<10	<2	<10	<10
208374	<300	86.6	<20	<1000	<10	<20	<20	<20	168	<100	<100	<20	<20	<20
208374	<300	52.6	<20	<2500	<10	<20	<20	<20	131	<100	<100	<20	<20	<20
208374	<300	45.2	<20	<5000	<10	<20	<20	<20	140	<100	<100	<20	<20	<20
208374	<300	48.4	<20	<2500	<10	<20	<20	<20	123	<100	<100	<20	73.9	<20
208374	102.0	36.1	<10	<1000	<5	<10	<10	<10	102	<50	<50	<10	<10	<10
208374	195.0	36.4	<1.0	<2500	<1.0	1.080	<1.0	<2.0	138	<10.0	<10.0	7.54	<2.0	<1.0
208375	68.6	77.2	<2	<50	<1	<2	<2	<2	26.6	<10	<10	<2	<2	<2
208375	64.8	80.9	<2	374	<1	<2	8.66	<2	26.4	<10	<10	<2	<2	<2
208375	59.8	96.4	<2	<500	<1	<2	5.94	2.98	24.4	<10	<10	2.06	<2	<2
208375	70.0	96.8	<2	<500	<1	<2	8.37	<2	25.4	<10	<10	<2	<2	<2

APPENDIX 5.C-1: Water Quality for the Coal Creek Sites
(page 9)

Gwic Id	Boron (ug/l)	Barium (ug/l)	Beryllium (ug/l)	Bromide (ug/l)	Cadmium (ug/l)	Cobalt (ug/l)	Chromium (ug/l)	Copper (ug/l)	Mercury (ug/l)	Lithium (ug/l)	Molybdenum (ug/l)	Nickel (ug/l)	Lead (ug/l)	Antimony (ug/l)
208375	70.6	93.4	<2	<50	<1	<2	2.6	<2		25.2	<10	<2	<2	<2
208375	62.1	102.0	<0.1	<50	<0.1	<0.1	<0.1	<0.2		26.3	<1.0	1.55	<0.2	<0.1
208376	<150	110.0	<10	<500	<5	<10	<10	<10		117	<10	<10	<10	<10
208376	<150	30.6	<10	<1000	<5	<10	<10	<10		122	<50	<10	<10	<10
208376	<150	31.2	<10	<1000	<5	<10	<10	<10		124	<10	<10	<10	<10
208376	<150	17.8	<10	<1000	<5	<10	<10	<10		121	<50	<10	<10	<10
208376	<150	19.6	<10	<500	<5	<10	12.9	<10		123	<10	10.8	<10	<10
208376	142.0	23.3	<2	<1000	<1	<2	4.74	<2		117	<10	4.57	<2	<2
208376	99.5	19.7	<0.1	<500	<0.1	1.300	<0.1	0.423		135	<1.0	2.53	<0.2	<0.1
211060	444.0	48.9	<10	<1000	<5	<10	<10	<10		84.7	<50	13.7	<10	<10
211060	382.0	13.9	<10	<2500	<5	<10	<10	<10		82.9	<50	<10	<10	<10
211060	380.0	16.3	<10	<1000	<5	<10	<10	<10		86.4	<10	<10	<10	<10
211060	347.0	12.6	<10	<2500	<5	<10	<10	<10		80.3	<50	<10	<10	<10
211060	432.0	16.8	<2	<500	<1	<2	<10	<5		84.2	<10	2.08	<10	<10
211060	324.0	13.5	<2	<500	<1	<2	3.03	<2		82	<10	4.45	<2	<2
211060	294.0	13.4	<0.1	<630	<0.1	0.554	<0.1	0.53		81.6	3.9	2.8	<0.2	<0.1
211060	336.0	15.4	<0.5	<1000	<0.5	0.554	<0.5	<1.0		82.9	<5.0	3.94	<1.0	<0.5
207115	288.0	25.8	<10	<500	<5	<10	<10	<10		98.3	<50	<10	<10	<10
207115	229.0	33.6	<2	<2500	<1	<2	<10	<5		105	<10	5.01	<10	<10
207115	246.0	40.3	<10	<1250	<5	<10	<10	<10		115	<50	<10	<10	<10
207115	269.0	41.2	<2	<1000	<1	<2	2.13	<2		109	<10	8.88	<2	<2
207115	321.0	26.9	<0.5	<1250	<0.5	<0.5	<0.5	1.81		113	<5.0	3.32	<1.0	<0.5
207113	80.4	26.8	<2	<500	<1	<2	<10	<5		45.5	<10	<2	<10	<10
207114	124.0	93.9	<2	<500	<1	<2	<10	<5		77.2	<10	<2	<10	<10
207113	<150	13.5	<2	<500	<1	<2	<10	<5		41.7	<10	<2	<10	<10
207114	96.6	65.5	<2	<50	<1	<2	3.35	<2		64.5	<10	<2	<2	<2
207114	110.0	75.1	<2	<50	<1	<2	2.51	<2		57.4	<10	2.16	<2	<2
207113	74.3	13.0	<2	<500	<1	<2	2.35	<2		42.5	<10	<2	<2	<2
207113	63.2	11.4	<0.1	<250	<0.1	0.109	<0.1	<0.2		41.6	<1.0	0.551	<0.2	<0.1
207114	67.1	112.0	<0.1	<50	<0.1	0.436	4.36	0.855		45.8	<1.0	1.44	<0.2	<0.1
209338	333.0	3.8	<2	<500	<1	<2	<10	<5		93.9	<10	3.1	<10	<10
202186	<150	33.6	<2	<500	<2	<10	<10	<10		60.3	<50	<10	<10	<10
207106	237.0	34.0	<2	<500	<1	<10	<10	<10		83.2	<10	<10	<10	<10
207106	227.0	26.6	<10	<1000	<5	<10	<10	<10		85.5	<50	<10	<10	<10
207106	215.0	35.5	<2	<2500	<1	<2	<10	<5		83.8	<10	4.52	<10	<10
207106	213.0	35.0	<10	<2500	<5	<10	<10	<10		83	<50	<10	<10	<10
207105	<300	21.8	<20	<500	<10	<20	<20	<20		154	<100	<20	<20	<20
207105	<150	17.9	<10	<2500	<5	<10	<10	<10		147	<50	14.4	<10	<10

APPENDIX 5.C-1: Water Quality for the Coal Creek Sites
(page 10)

Gwic Id	Selenium (ug/l)	Tin (ug/l)	Strontium (ug/l)	Titanium (ug/l)	Thallium (ug/l)	Uranium (ug/l)	Vanadium (ug/l)	Zinc (ug/l)	Zirconium (ug/l)	Procedure	Total Dissolved Solids (mg/L)	SAR
207110	11.9		1844	<1	<25	10.1	<10	2.06	<2	DISSOLVED	1377	2.4
207110	16.4		2256	<1	<25	12.3	<10	6.23	<2	DISSOLVED	1732	2.3
207110	21.3		2085	<1	<25	12.1	<10	<2	<2	DISSOLVED	1751	2.2
207110	26.4		2132	<1	<25	12.5	<25	<10	<2	DISSOLVED	1584	2.5
207110	38.3		2008	1.77	<0.1	12.3	0.575	4.18	<0.1	DISSOLVED	1622	2.2
207109	<5		1308	<1	<25	<2.5	<10	3.97	<2	DISSOLVED	1125	3.9
207109	<1		1357	<1	<5	0.695	<5	<2	<2	DISSOLVED	1125	4.5
202187	<5		1340	1.07	<25	13.9	<25	<10	<2	DISSOLVED	1145	1.4
202187	<1		997	<1	<5	5.67	<5	<2	<2	DISSOLVED	790	1.4
202185	6.41		1370	<1	<25	16	<25	<10	<2	DISSOLVED	1153	1.9
209364	6.32		343	<1	<5	<1	<5	<2	<2	DISSOLVED	995	23.6
209363	<5		325	<1	<25	<3	<10	2.87	<2	DISSOLVED	990	23.0
209363	2.26		182	3.58	<5	3.37	<5	<2	<2	DISSOLVED	947	24.3
209363	<5		217	<1	<25	<3	<10	<2	<2	DISSOLVED	1155	27.3
209363	3.07		113	<1	<5	5.65	5.38	<2	<2	DISSOLVED	929	27.2
209363	<5.0		103	<10.0	<1.0	5.11	5.21	<2.0	<1.0	DISSOLVED	383	10.4
208365	<5		3532	<5	<25	16.3	<25	19	<10	DISSOLVED	2594	5.1
208365	<5		4344	<5	<25	4.99	<25	11.2	<10	DISSOLVED	2538	4.8
208365	<5		4316	<10	<25	6.01	<25	<10	<10	DISSOLVED	2686	4.6
208365	<10		4500	<10	<50	5.86	<50	<20	<20	DISSOLVED	2734	4.6
208365	<5		4223	<5	<25	5.52	<25	11.8	<10	DISSOLVED	2830	4.6
208365	<5		4328	<5	<25	5.38	<25	<10	<10	DISSOLVED	2638	4.8
208365	<5		3784	1.8	<25	3	<25	17.4	<2	DISSOLVED	2358	4.6
208365	<2.5		4163	<5.0	<0.5	2.81	<0.5	21.7	<0.5	DISSOLVED	2476	4.9
208366	<5		1319	4.24	<25	10.2	<10	7.55	<2	DISSOLVED	1338	5.4
208366	28.5		5020	57.8	<50	58.1	<50	21.3	<20	DISSOLVED	3289	4.1
208366	174		7136	<10	<50	59.3	<50	31	<20	DISSOLVED	6842	6.1
208366	159		6803	<10	<50	71	<50	<20	<20	DISSOLVED	6959	7.3
208366	142		7636	<10	<50	67.4	<10	<20	<20	DISSOLVED	6991	6.9
208366	134.2		10411	<10	<50	46.1	<50	<20	<20	DISSOLVED	6314	5.4
208366	33		5163	<10	<50	32.8	<50	42.7	<20	DISSOLVED	3598	5.0
208366	<5.0		5633	<10.0	<1.0	30.5	<1.0	6.17	<1.0	DISSOLVED	3629	5.6
208366	3.08	<0.5	4673	29.5	<0.5	26.2	<0.5	3.3	<0.5	DISSOLVED	3255	5.4
208367	<5		159	<1	<25	<3	<10	<2	<2	DISSOLVED	647	20.5
208367	2.23		156	<1	<5	0.544	<5	<2	<2	DISSOLVED	718	22.5
208367	1.32		148	<1	<5	<0.5	<5	<2	<2	DISSOLVED	612	20.0
208367	<1		153	<1	<5	<1	<5	<2	<2	DISSOLVED	684	22.9
208367	<1		146	<1	<5	<1	<5	<2	<2	DISSOLVED	665	22.3
208367	<0.5		160	<1.0	<0.1	0.169	<0.1	<0.2	<0.1	DISSOLVED	669	22.3
208368	278		13379	<10	362	111	<100	<20	<20	DISSOLVED	16801	11.9
208368	300		13144	<10	<100	139	<100	<20	<20	DISSOLVED	17367	12.9
208368	197		12016	<50	<250	112	<250	<100	<100	DISSOLVED	15144	12.2

APPENDIX 5.C-1: Water Quality for the Coal Creek Sites
(page 11)

Gwic Id	Selenium (ug/l)	Tin (ug/l)	Strontium (ug/l)	Titanium (ug/l)	Thallium (ug/l)	Uranium (ug/l)	Vanadium (ug/l)	Zinc (ug/l)	Zirconium (ug/l)	Procedure	Total Dissolved Solids (mg/L)	SAR
208369	<5		216	<1	<25	<3	<10	11.3	<2	DISSOLVED	765	17.0
208369	<1		183	<1	<5	<1	<5	<2	<2	DISSOLVED	723	21.6
208370	<5		2800	<1	<25	<3	<10	11.7	<2	DISSOLVED	1428	3.8
208370	<5		4970	<1	<25	<3	<10	<2	4.13	DISSOLVED	1361	3.8
208370	<1		2425	<1	<5	15.6	<5	6.03	<2	DISSOLVED	1346	4.2
208370	<5		1971	1.14	<25	<3	<10	3.81	<2	DISSOLVED	1326	4.9
208370	<5		2542	<1	<25	<2.5	<10	2.04	<2	DISSOLVED	1484	4.5
208370	<5		2406	<1	<25	<2.5	<10	<2	<2	DISSOLVED	1460	4.3
208370	<10		2760	<10	<50	<5	<50	<20	<20	DISSOLVED	1493	4.5
208370	<1		2510	1.45	<5	<1	<5	4.09	<2	DISSOLVED	1494	4.5
208370	<0.5		2625	1.47	<0.1	0.202	<0.1	4.68	<0.1	DISSOLVED	1473	4.3
208370	<0.5	<0.1	2537	7.76	<0.1	0.074	<0.1	1.92	<0.1	DISSOLVED	1459	4.3
208371	<5		2675	<1	<25	2.54	<10	27.1	<2	DISSOLVED	1436	3.1
208371	198		8707	<10	<50	32.9	<50	<20	<20	DISSOLVED	6797	6.9
208371	224		9097	<10	<50	75.6	<50	<20	<20	DISSOLVED	12420	14.7
208371	58.6		8441	<10	<250	55.8	<100	<20	<20	DISSOLVED	10665	13.6
208371	102		7136	<1	<5	67.3	<5	11.5	<2	DISSOLVED	10597	14.2
208371	52		7930	<10	<50	61.4	<50	<20	<20	DISSOLVED	10428	13.6
208371	73.1	8270	<10	<50	71.9	<50	<20	<20	<20	DISSOLVED	11248	14.1
208371	77.4		7583	<10	<50	59.6	<50	<20	<20	DISSOLVED	10571	14.6
208371	51.2		6091	<10.0	<1.0	48.1	<1.0	18.8	<1.0	DISSOLVED	8319	12.4
208371	12.1	<2.0	7345	22	<2.0	9.65	<2.0	<4.0	<2.0	DISSOLVED	9853	12.9
208372	8.77		1167	<5	<25	46	<25	<10	<10	DISSOLVED	2396	13.3
208372	<10		4564	<10	<50	108	<50	<20	<20	DISSOLVED	5643	9.2
208372	<10		5406	<10	<50	128	<50	<20	<20	DISSOLVED	5964	7.9
208373	<5		3189	<1	<25	2.9	<10	428	<2	DISSOLVED	1680	2.5
208373	<5		3117	6.41	<25	21.8	<25	<10	<2	DISSOLVED	1685	2.5
208373	<1		2899	1.72	<25	<3	<10	11.6	<2	DISSOLVED	1656	2.6
208373	<1		3313	<1	<5	<0.5	<5	4.26	<2	DISSOLVED	1683	2.8
208373	<5		2789	<1	<25	<2.5	<10	2.37	<2	DISSOLVED	1643	2.6
208373	<5		3059	1.63	<25	<3	<10	<10	<2	DISSOLVED	1617	2.7
208373	<1		2834	1.97	<5	<1	<5	13.7	<2	DISSOLVED	1589	2.8
208373	<0.5		3013	2.4	<0.1	0.272	<0.1	13.3	0.176	DISSOLVED	1565	2.6
208374	<5		912	<1	<25	<3	<10	<2	<2	DISSOLVED	1563	13.3
208374	<10		6924	<10	<50	<5	<50	<20	<20	DISSOLVED	4501	8.2
208374	<10		6872	<10	<50	<5.0	<50	<20	<20	DISSOLVED	4348	7.0
208374	<10		7980	<10	<50	<5.0	<50	<20	<20	DISSOLVED	5106	6.0
208374	<10		5980	<10	<50	<5	<50	28.3	<20	DISSOLVED	4387	6.9
208374	<5		2264	<1	<25	<3	<25	<10	<2	DISSOLVED	3051	14.2
208374	<5.0		5012	<10.0	<1.0	<0.50	<1.0	51.4	<1.0	DISSOLVED	4403	7.4
208375	<1		166	1.04	<5	<0.5	<5	<2	<2	DISSOLVED	632	19.5
208375	4.94		156	<1	<5	<0.5	<5	<2	<2	DISSOLVED	680	22.1
208375	1.56		143	<1	<5	<0.5	<5	<2	<2	DISSOLVED	811	24.3
208375	<1		158	<1	<5	<1	<5	<2	<2	DISSOLVED	679	21.9

APPENDIX 5.C-1: Water Quality for the Coal Creek Sites
(page 12)

Gwic Id	Selenium (ug/l)	Tin (ug/l)	Strontium (ug/l)	Titanium (ug/l)	Thallium (ug/l)	Uranium (ug/l)	Vanadium (ug/l)	Zinc (ug/l)	Zirconium (ug/l)	Procedure	Total Dissolved Solids (mg/L)	SAR
208375	<1		153	<1	<5	<1	<5	<2	<2	DISSOLVED	643	21.2
208375	<0.5		154	<1.0	<0.1	0.119	<0.1	<0.2	<0.1	DISSOLVED	634	20.9
208376	<5		2290	<5	<25	8.28	<25	34.7	<10	DISSOLVED	2072	7.4
208376	6.47		2882	<5	<25	<3	<25	11.4	<10	DISSOLVED	2189	6.7
208376	5.39		2915	<5	<25	<2.5	<25	<10	<10	DISSOLVED	2326	7.3
208376	<5		2902	<5	<25	<2.5	<25	<10	<10	DISSOLVED	2232	6.5
208376	<5		3061	<5	<25	<3	<25	<10	<10	DISSOLVED	2207	6.8
208376	<1		2788	1.85	<5	<1	<5	3.75	<2	DISSOLVED	2331	6.5
208376	<0.5		3303	2.42	<0.1	0.247	<0.1	3.4	0.158	DISSOLVED	2226	6.4
211060	<5		2416	<5	<25	26.8	<25	<10	<10	DISSOLVED	2384	2.9
211060	<5		2376	<5	<25	20.7	<25	<10	<10	DISSOLVED	2208	2.8
211060	<5		2324	<5	<25	18.7	<25	<19	<10	DISSOLVED	2150	2.9
211060	<5		2176	<5	<2	18.8	<25	<10	<10	DISSOLVED	2133	2.9
211060	<5		2129	<1	<25	19.4	<10	<2	<2	DISSOLVED	2053	2.9
211060	14.7		2028	1.44	<5	47.3	<5	<2	<2	DISSOLVED	2039	2.8
211060	0.671		2095	2.19	<0.1	.22	0.458	1.12	0.166	DISSOLVED	1997	2.8
211060	<2.5	<0.5	2421	17.7	<0.5	18.2	<0.5	1.21	<0.5	DISSOLVED	2087	2.7
207115	<5		2533	<5	<25	19.8	<25	<10	<10	DISSOLVED	2248	3.2
207115	<5		2938	<1	<25	23.9	<10	5.48	<2	DISSOLVED	3083	3.9
207115	<5		3804	<5	<25	28.4	<25	<10	<10	DISSOLVED	3521	4.9
207115	<1		3229	2.04	<5	29.8	<5	2.43	<2	DISSOLVED	3028	4.5
207115	<2.5		3365	<5.0	<0.5	21	<0.5	7.78	<0.5	DISSOLVED	3037	3.8
207113	<10	<5		501	<1	<3	<10	2.78	<2	DISSOLVED	1252	16.1
207114	<5		2649	<1	<25	<2.5	<10	3.93	<2	DISSOLVED	1677	3.1
207113	<5		477	<1	<25	<2.5	<10	<2	<2	DISSOLVED	1253	17.7
207114	<1		1934	<1	<5	5.05	<5	<2	<2	DISSOLVED	1302	2.8
207114	<1		1771	1.82	<5	7.44	<5	<2	<2	DISSOLVED	1235	2.5
207113	<1		527	<1	<5	<1	<5	<2	<2	DISSOLVED	1307	18.5
207113	<0.5		541	<1.0	<0.1	0.188	<0.1	1.97	0.1	DISSOLVED	1270	18.5
207114	<0.5		1637	2.44	<0.1	14.5	<0.1	3.72	<0.1	DISSOLVED	1086	1.6
209338	<5		2273	<1	<25	4.86	<10	<2	<2	DISSOLVED	1779	2.9
202186	<5		1470	1.22	<25	11.6	<25	<10	<2	DISSOLVED	1406	2.3
207106	<5		2221	<1	<25	14.7	<25	<10	<2	DISSOLVED	2320	3.2
207106	<5		2608	<5	<25	16.6	<25	<10	<10	DISSOLVED	2423	3.6
207106	<5		2560	<1	<25	15.3	<10	<2	<2	DISSOLVED	2581	3.4
207106	<5		2922	<5	<25	17.2	<25	<10	<10	DISSOLVED	2648	3.8
207105	<10		5248	<10	<50	<5	<50	<20	<20	DISSOLVED	3822	7.3
207105	<5		5565	<10	<25	<3	<25	<10	<10	DISSOLVED	3840	7.7

APPENDIX 5.C-2: Water Quality for the Beaver Creek Sites
(page 1)

Gwic Id	Site Name	Site Type	Aquifer	Depth (ft)	Sample Date	Water Temperature	Lab	Lab pH	Lab SC	Calcium (mg/l)	Magnesium (mg/l)	Sodium (mg/l)
207130 BC-2	WELL UPSTREAM	110ALVM	18	01/20/03	10.1	MBMG	7.50	1127	124.0	45.5	59.4	
207130 BC-2	WELL UPSTREAM	110ALVM	18	08/06/03		UWYO	7.29		132.5	41.9	74.9	
207130 BC-2	WELL UPSTREAM	110ALVM	18	12/17/03	6.1	MBMG	7.52	1216	134.0	50.6	63.1	
207130 BC-2	WELL UPSTREAM	110ALVM	18	08/21/04		UWYO	7.35		142.6	44.1	77.2	
207130 BC-2	WELL UPSTREAM	110ALVM	18	02/05/05		UWYO	6.89		125.2	46.7	69.9	
207130 BC-2	WELL UPSTREAM	110ALVM	18	08/09/05		UWYO	7.50		120.8	38.5	57.6	
207129 BC-1	WELL UPSTREAM	110ALVM	18	10/10/07	12.4	MBMG	7.75	1920	235.0	79.7	152.0	
207132 BC-4	WELL UPSTREAM	124WSTC	31.5	01/20/03	11.1	MBMG	7.39	1477	162.0	46.4	112.0	
207132 BC-4	WELL UPSTREAM	124WSTC	31.5	08/06/03		UWYO	6.79		173.2	41.8	121.7	
207132 BC-4	WELL UPSTREAM	124WSTC	31.5	12/17/03	11.1	MBMG	7.52	1631	173.0	48.5	115.0	
207132 BC-4	WELL UPSTREAM	124WSTC	31.5	08/21/04		UWYO	7.20		180.5	42.7	123.3	
207132 BC-4	WELL UPSTREAM	124WSTC	31.5	02/05/05		UWYO	6.85		173.5	49.3	127.8	
207132 BC-4	WELL UPSTREAM	124WSTC	31.5	08/09/05		UWYO	7.00		173.4	40.9	116.1	
207132 BC-4	WELL UPSTREAM	124WSTC	31.5	10/09/07	12.3	MBMG	7.03	1580	200.0	56.1	129.0	
209047 BC-UPCBM	COALBED METHANE WELL	125TGRV		01/10/03	19.5	MBMG	7.91	2100	46.7	21.2	532.0	
209047 BC-UPCBM	COALBED METHANE WELL	125TGRV		08/06/03		UWYO	7.20		43.9	18.4	483.3	
209047 BC-UPCBM	COALBED METHANE WELL	125TGRV		12/17/03	20.3	MBMG	7.56	2050	46.0	20.5	436.0	
209047 BC-UPCBM	COALBED METHANE WELL	125TGRV		08/21/04		UWYO	7.41		47.4	18.7	502.2	
209047 BC-UPCBM	COALBED METHANE WELL	125TGRV		02/05/05		UWYO	7.28		48.9	22.2	528.0	
209047 BC-UPCBM	COALBED METHANE WELL	125TGRV		08/09/05		UWYO	6.90		44.4	19.5	484.9	
209050 BC-UPP	POND			08/06/03		UWYO	8.63		17.1	16.9	486.1	
209050 BC-UPP	POND			12/19/03	6.1	MBMG	8.56	2130	22.5	21.9	473.0	
209050 BC-UPP	POND			02/05/05		UWYO	7.98		17.8	20.1	483.0	
209050 BC-UPP	POND			08/09/05		UWYO	8.70		10.4	19.9	629.2	
209050 BC-UPP	POND			10/10/07	12.4	MBMG	9.35	2520	7.3	15.3	676.0	
209049 BC-UPQ	POND OVERFLOW			01/09/03	3.5	MBMG	8.47	2040	24.0	21.0	481.0	
209049 BC-UPQ	POND OVERFLOW			12/17/03	2.7	MBMG	8.65	2160	22.4	22.3	463.0	
209051 BC-UF	STREAM			12/19/03	0	MBMG	8.35	2250	43.2	31.1	475.0	
207124 BC-6	WELL MIDDLE	110ALVM	25.8	01/20/03	11.2	MBMG	7.64	1664	207.0	60.0	107.0	
207125 BC-7	WELL MIDDLE	110ALVM	25	08/06/03		UWYO	7.49		193.8	38.6	136.7	
207124 BC-6	WELL MIDDLE	110ALVM	25.8	12/17/03	4.9	MBMG	7.22	1312	212.0	49.2	49.8	
207125 BC-7	WELL MIDDLE	110ALVM	25	08/21/04		UWYO	7.20		175.6	34.7	304.2	
207125 BC-7	WELL MIDDLE	110ALVM	25	02/05/05		UWYO	6.51		171.0	38.4	155.0	
207125 BC-7	WELL MIDDLE	110ALVM	25	08/09/05		UWYO	6.90		181.8	34.6	169.9	
207124 BC-6	WELL MIDDLE	110ALVM	25.8	10/11/07	12.1	MBMG	7.23	1360	172.0	46.5	75.3	
207123 BC-5	WELL MIDDLE	124WSTC	38	01/10/03	10.7	MBMG	7.74	2780	385.0	106.0	195.0	
207123 BC-5	WELL MIDDLE	124WSTC	38	12/17/03	9.4	MBMG	7.67	1298	146.0	42.0	93.0	
207123 BC-5	WELL MIDDLE	124WSTC	38	08/21/04		UWYO	7.33		151.9	38.2	88.8	

APPENDIX 5.C-2: Water Quality for the Beaver Creek Sites
(page 2)

Gwic Id	Site Name	Site Type	Aquifer	Depth (ft)	Sample Date	Water Temperature	Lab	Lab pH	Lab SC	Calcium (mg/l)	Magnesium (mg/l)	Sodium (mg/l)
207123 BC-5		WELL MIDDLE	124WSTC	38	02/05/05		UWYO	6.69		172.6	49.3	97.2
207123 BC-5		WELL MIDDLE	124WSTC	38	08/09/05		UWYO	6.90		147.7	36.6	92.3
207123 BC-5		WELL MIDDLE	124WSTC	38	10/11/07	11.1	MBMG	7.27	1760	232.0	64.1	126.0
209046 BC-MF		STREAM			01/20/03		MBMG			6.9	4.5	105.0
209046 BC-MF		STREAM			08/06/03		UWYO	9.20		17.1	17.1	502.6
209046 BC-MF		STREAM			12/19/03	0	MBMG	8.45	2700	39.0	35.9	567.0
209046 BC-MF		STREAM			02/05/05		UWYO	7.42		181.7	70.7	441.8
209042 BC-LPCBM		COALBED METHANE WELL	125TGRV		01/09/03	19.9	MBMG	7.79	2050	46.1	19.4	464.0
209042 BC-LPCBM		COALBED METHANE WELL	125TGRV		08/06/03		UWYO	7.65		49.0	18.4	459.6
209042 BC-LPCBM		COALBED METHANE WELL	125TGRV		12/18/03	21.1	MBMG	7.75	1940	43.0	22.2	459.0
209042 BC-LPCBM		COALBED METHANE WELL	125TGRV		08/21/04		UWYO	7.26		54.1	18.3	481.6
209042 BC-LPCBM		COALBED METHANE WELL	125TGRV		02/05/05		UWYO	7.23		47.3	20.3	479.9
209042 BC-LPCBM		COALBED METHANE WELL	125TGRV		08/09/05		UWYO	7.30		50.7	17.1	458.0
209043 BC-LPP		POND			08/06/03		UWYO	8.97		19.4	18.1	488.6
209043 BC-LPP		POND			12/18/03	2.2	MBMG	8.54	1966	25.5	22.2	471.0
209043 BC-LPP		POND			02/05/05		UWYO	8.65		24.4	20.3	478.5
209043 BC-LPP		POND			08/09/05		UWYO	8.40		15.5	20.2	548.8
209043 BC-LPP		POND			10/11/07	12.2	MBMG	8.59	2140	11.2	21.1	496.0
209044 BC-LPQ		POND OVERFLOW			01/09/03	4.4	MBMG	8.27	1857	25.8	18.1	461.0
208572 BC-NPF		STREAM			12/18/03	1.8	MBMG	8.05	1936	64.4	30.6	394.0
207121 BC-14		WELL DOWNSTREAM	110ALVM	15	01/20/03		MBMG	7.58	2610	364.0	142.0	127.0
207121 BC-14		WELL DOWNSTREAM	110ALVM	15	01/21/03		UWYO	7.05		322.1	144.1	136.1
207121 BC-14		WELL DOWNSTREAM	110ALVM	15	04/09/03		UWYO	7.40		336.6	138.9	131.1
207121 BC-14		WELL DOWNSTREAM	110ALVM	15	08/06/03		UWYO	6.83		495.7	173.9	150.0
207121 BC-14		WELL DOWNSTREAM	110ALVM	15	10/05/03		UWYO	7.73		542.7	261.0	326.4
207121 BC-14		WELL DOWNSTREAM	110ALVM	15	12/18/03	9.5	MBMG	8.19	4110	490.0	307.0	328.0
207121 BC-14		WELL DOWNSTREAM	110ALVM	15	02/13/04		UWYO	7.23		481.5	351.6	462.2
207121 BC-14		WELL DOWNSTREAM	110ALVM	15	05/15/04		UWYO	7.64		473.7	397.0	556.5
207121 BC-14		WELL DOWNSTREAM	110ALVM	15	08/21/04		UWYO	7.50		458.6	461.9	713.6
207121 BC-14		WELL DOWNSTREAM	110ALVM	15	09/18/04		UWYO	7.96		425.9	424.5	666.4
207121 BC-14		WELL DOWNSTREAM	110ALVM	15	02/05/05		UWYO	6.64		447.4	398.0	483.1
207121 BC-14		WELL DOWNSTREAM	110ALVM	15	05/07/05		UWYO	8.66		446.6	376.3	524.4
207121 BC-14		WELL DOWNSTREAM	110ALVM	15	08/09/05		UWYO	7.30		449.9	371.5	528.0
207121 BC-14		WELL DOWNSTREAM	110ALVM	15	11/04/05		UWYO	7.70		451.1	348.0	361.8
207121 BC-14		WELL DOWNSTREAM	110ALVM	15	10/11/07		MBMG	7.20	3920	493.0	296.0	286.0
207118 BC-11		WELL DOWNSTREAM	124WSTC	38	01/20/03	10.3	MBMG	7.57	1976	224.0	72.1	152.0
207118 BC-11		WELL DOWNSTREAM	124WSTC	38	08/06/03		UWYO	6.93		250.4	73.1	156.6

APPENDIX 5.C-2: Water Quality for the Beaver Creek Sites
(page 3)

Gwic Id	Site Name	Site Type	Aquifer	Depth (ft)	Sample Date	Water Temperature	Lab	Lab pH	Lab SC	Calcium (mg/l)	Magnesium (mg/l)	Sodium (mg/l)
207118	BC-11	WELL DOWNSTREAM	124WSTC	38	12/18/03	9.5	MBMG	7.35	1917	228.0	78.8	148.0
207118	BC-11	WELL DOWNSTREAM	124WSTC	38	08/21/04		UWYO	7.37		239.5	69.4	157.8
207118	BC-11	WELL DOWNSTREAM	124WSTC	38	02/05/05		UWYO	6.50		229.0	77.4	154.6
207118	BC-11	WELL DOWNSTREAM	124WSTC	38	08/09/05		UWYO	7.30		237.8	70.5	154.8
207118	BC-11	WELL DOWNSTREAM	124WSTC	38	10/11/07	11.4	MBMG	7.31	1897	240.0	77.2	150.0
208571	BC-LF	STREAM			08/06/03		UWYO	8.52		25.0	20.5	447.6
208571	BC-LF	STREAM			12/19/03	0	MBMG	8.06	2200	79.0	39.3	426.0
208571	BC-LF	STREAM			08/21/04		UWYO	8.76		15.8	22.9	496.6
208571	BC-LF	STREAM			02/05/05		UWYO	7.31		75.6	32.6	415.3
208571	BC-LF	STREAM			08/09/05		UWYO	8.30		15.2	21.9	490.7

APPENDIX 5.C-2: Water Quality for the Beaver Creek Sites
(page 4)

Gwic Id	Potassium (mg/l)	Iron (mg/l)	Manganese (mg/l)	Silica (mg/l)	Bicarbonate (mg/l)	Carbonate (mg/l)	Sulfate (mg/l)	Chloride (mg/l)	Nitrate (mg/l)	Flouride (mg/l)	Orthophosphate (mg/l)	Silver (ug/l)	Aluminum (ug/l)
207130	1.3	0.0	0.2	8.0	418.7	0.0	321.1	<5.0	0.5 P	<0.5	<0.5	<5	<30
207130	1.7	4.3	0.2	5.0	507.0	0.0	321.8	4.08					443.5
207130	1.6	0.7	0.2	10.0	393.5	0.0	374.0	<5.0	<0.5 P	<0.5	<0.5	<5	398.0
207130	1.8	4.7	0.2	5.4	371.0		359.4	3.20					462.5
207130	1.5	0.6	0.1	4.2	486.0		323.6	2.90					71.3
207130	1.9	2.1	0.2	3.9	530.0		298.6	4.37					83.5
207129	3.6	0.0	0.3	10.9	420.9	0.0	897.0	4.07	0.115 P	0.501	<0.10	<0.5	<2.0
207132	4.2	2.5	0.4	11.7	387.9	0.0	576.8	<10	1.0 P	<1.0	<1.0	<5	<30
207132	4.3	12.2	0.4	5.9	388.0		519.2	3.49					18.5
207132	4.1	2.7	0.4	11.9	434.3	0.0	597.0	<5.0	<0.5 P	<0.5	<0.5	<5	<30
207132	4.4	13.1	0.4	5.8	397.0		551.7	2.90					33.8
207132	4.2	2.2	0.4	5.8	471.0		586.0	2.86					19.5
207132	4.5	10.9	0.4	5.1	509.0		591.6	3.68					46.0
207132	4.4	1.7	0.5	11.6	382.3	0.0	662.0	2.88	<0.10 P	0.292	<0.10	<0.5	<2.0
209047	8.3	3.9	0.1	9.1	1540.5	0.0	<2.5	6.00	2.9 P	<0.05	<0.05	<5	<30
209047	8.0	3.3	0.0	4.7	2081.0		<0.2	8.12					4.5
209047	8.1	0.6	0.0	9.5	1531.9	0.0	<2.5	5.79	0.723 P	0.223	<0.05	<5	<30
209047	8.5	3.2	0.0	5.2	2106.0		0.2	8.59					15.5
209047	8.6	0.5	0.0	5.8	1893.0		12.8	6.99					9.1
209047	8.0	2.3	0.0	4.8	2126.0		1.1	13.79					6.1
209050	8.6	0.7	0.0	2.7	2095.0		6.0	8.70					130.8
209050	8.3	0.0	0.0	7.7	1244.4	39.6	7.8	7.16	1.47 P	0.211	<0.05	<5	<30
209050	8.6	0.2	0.0	3.2	1681.0		5.9	7.13					144.8
209050	10.5	1.1	0.0	1.2	2670.0		4.6	12.81					311.6
209050	9.0	0.0	<0.001	2.9	1232.2	241.6	4.5	11.80	<0.5 P	0.094	<0.05	<2.5	<10.0
209049	8.5	0.0	0.0	8.8	1384.7	36.0	5.4	6.50	1.2 P	0.370	<0.05	<5	<30
209049	8.1	0.0	0.0	7.4	1403.0	36.0	7.7	6.90	<0.5 P	0.199	<0.05	<5	<30
209051	8.3	0.1	0.0	8.0	1489.6	14.4	106.0	7.61	<0.5 P	0.192	<0.05	<5	<30
207124	2.9	0.0	0.0	9.9	300.1	0.0	806.8	<10	2.2 P	<1.0	<1.0	<5	<30
207125	3.8	4.2	0.0	6.7	800.0		63.5	7.93					178.7
207124	3.0	0.0	0.0	11.9	620.2	0.0	320.0	6.40	0.944 P	<0.5	<0.5	<5	<30
207125	3.1	3.7	0.0	6.5	1069.0		183.8	10.21					129.8
207125	2.9	0.7	0.0	6.5	1044.0		128.2	7.40					65.8
207125	3.0	3.2	0.0	6.0	827.0		178.9	8.47					91.7
207124	2.7	<0.005	<0.001	13.9	669.7	0.0	151.0	7.36	0.292 P	0.296	<0.10	<0.5	<2.0
207123	5.4	3.3	0.5	9.0	388.0	0.0	1602.4	<30.0	1.6 P	<3.0	<3.0	<5	<150
207123	3.6	1.1	0.2	9.7	491.1	0.0	379.0	8.77	<0.5 P	<0.05	<0.05	<5	43.0
207123	2.8	6.4	0.1	5.0	481.0		265.8	7.04					74.7

APPENDIX 5.C-2: Water Quality for the Beaver Creek Sites
(page 5)

Gwic Id	Potassium (mg/l)	Iron (mg/l)	Manganese (mg/l)	Silica (mg/l)	Bicarbonate (mg/l)	Carbonate (mg/l)	Sulfate (mg/l)	Chloride (mg/l)	Nitrate (mg/l)	Flouride (mg/l)	Orthophosphate (mg/l)	Silver (ug/l)	Aluminum (ug/l)
207123	3.0	1.7	0.2	4.9	479.0		487.9	8.50					136.2
207123	2.8	4.7	0.1	4.1	463.0		397.8	11.27					41.1
207123	3.5	1.5	0.2	9.9	485.2	0.0	723.0	6.66	<0.10 P	0.187	<0.10	<0.5	<2.0
209046	2.0	0.1	0.0	2.4								<1	49.0
209046	9.4	0.8	0.0	2.6	2145.0		7.5	9.24					130.5
209046	11.0	0.1	0.0	10.0	1523.8	34.8	114.0	10.60	3.98 P	<0.5	<0.5	<5	<30
209046	6.1	0.9	0.2	3.3	1225.0		726.5	10.58					27.7
209042	8.1	8.3	0.1	9.4	1427.4	0.0	<2.5	6.20	1.1 P	<0.05	<0.05	<5	<30
209042	8.2	4.9	0.0	4.7	1982.0		0.1	7.99					22.9
209042	8.3	0.7	0.0	9.8	1497.0	0.0	<2.5	5.84	<0.5 P	0.231	<0.05	<5	<30
209042	8.3	2.8	0.1	4.8	1994.0		0.5	8.25					34.8
209042	8.3	0.5	0.0	4.8	1784.0		1.8	6.30					10.2
209042	8.0	4.0	0.1	4.7	2000.0		0.5	8.95					14.3
209043	9.2	0.7	0.0	4.1	2079.0		4.7	9.01					126.3
209043	8.4	0.1	0.0	3.4	1282.2	50.4	5.1	6.56	<0.5 P	0.197	<0.05	<5	<30
209043	8.1	0.1	<0.029	0.9	1866.0		6.1	6.34					14.4
209043	10.7	0.0	0.0	4.6	2279.0		1.9	11.80					44.4
209043	10.6	0.0	<0.001	4.5	1324.1	36.8	6.6	19.10	<0.10 P	1.060	<0.10	<2.5	<10.0
209044	8.2	0.2	0.0	9.0	1454.2	0.0	<2.5	6.20	0.7 P	0.320	<0.05	<5	<30
208572	6.6	0.2	0.1	4.2	1957.9	0.0	69.7	6.98	<0.5	0.134	<0.05	<5	<30
207121	1.4	0.1	0.1	9.2	445.8	0.0	1514.9	<25	<1.0 P	<2.5	<2.5	<5	<30
207121	1.3	1.7	0.0	4.8	284.0		1411.6	4.40					0.2
207121	1.2	1.7	<0.029	4.4	331.0		1343.3	4.78					10.7
207121	1.6	2.0	0.1	5.1	511.0		1839.5	6.02					35.2
207121	2.4	2.2	0.0	4.9	504.0		2711.6	5.82					76.3
207121	1.5	0.1	<0.01	7.8	416.0	0.0	2848.0	5.15	<0.5 P	<0.5	<0.5	<10	<300
207121	1.8	2.4	0.0	3.9	474.0		3088.2	5.26					42.6
207121	1.5	2.2	0.0	3.7	492.0		3494.7	6.56					38.1
207121	1.7	2.3	0.0	4.1	549.0		3878.9	7.93					18.5
207121	5.5	2.2	0.0	4.3	547.0		3575.4	10.53					21.7
207121	0.9	2.3	0.0	4.0	620.0		3193.8	6.75					33.8
207121	0.9	7.4	0.0	3.4	708.0		3125.3	8.66					5.6
207121	1.0	8.9	0.1	4.3	813.0		3162.6	9.77					104.1
207121	0.9	8.4	0.1	4.9	900.0		2735.9	9.94					172.8
207121	0.7	<0.05	0.2	11.6	757.6	0.0	2447.0	<25.0	<2.5 P	<2.5	<2.5	<2.5	<10.0
207118	3.7	2.3	0.4	9.8	400.2	0.0	906.9	<10	4.6 P	<1.0	<1.0	<5	<30
207118	3.5	14.1	0.2	6.5	319.0		851.7	4.85					667.2

APPENDIX 5.C-2: Water Quality for the Beaver Creek Sites
(page 6)

Gwic Id	Potassium (mg/l)	Iron (mg/l)	Manganese (mg/l)	Silica (mg/l)	Bicarbonate (mg/l)	Carbonate (mg/l)	Sulfate (mg/l)	Chloride (mg/l)	Nitrate (mg/l)	Flouride (mg/l)	Orthophosphate (mg/l)	Silver (ug/l)	Aluminum (ug/l)
207118	3.3	2.2	0.3	9.9	381.9	0.0	868.0	<5.0	<0.5 P	<0.5	<0.5	<5	<30
207118	3.1	10.5	0.2	4.9	380.0		843.6	4.63					23.0
207118	3.2	2.0	0.2	5.1	502.0		877.1	4.53					54.1
207118	4.3	11.6	0.2	5.7	453.0		831.5	6.22					529.7
207118	3.4	2.2	0.3	10.1	405.9	0.0	884.0	4.53	<0.10 P	0.356	<0.10	<0.5	<2.0
208571	8.4	0.6	0.0	3.3	1900.0		22.4	8.52					42.1
208571	7.1	0.1	0.0	3.0	1313.9	0.0	181.0	7.43	<0.5 P	0.118	<0.05	<5	<30
208571	7.8	0.4	0.0	1.4	1984.0		50.2	9.37					13.5
208571	5.7	0.4	0.1	2.2	1393.0		166.7	6.67					8.7
208571	8.3	-0.3	0.0	2.7	2003.0		80.5	9.38					13.7

APPENDIX 5.C-2: Water Quality for the Beaver Creek Sites
(page 7)

Gwic Id	Arsenic (ug/l)	Boron (ug/l)	Barium (ug/l)	Beryllium (ug/l)	Bromide (ug/l)	Cadmium (ug/l)	Cobalt (ug/l)	Chromium (ug/l)	Copper (ug/l)	Lithium (ug/l)	Molybdenum (ug/l)	Nickel (ug/l)	Lead (ug/l)	Antimony (ug/l)
207130	<5	<150	19.0	<2	<500	<1	<2	<10	<10	37.3	<10	<10	<10	<10
207130		27.2	32.7											
207130	<5	<150	25.5	<2	<500	<1	<2	<10	<5	39.3	<10	3.01	<10	<10
207130		33.6	27.0											
207130		36.0	48.8											
207130		36.1	28.3											
207129	0.829	27.0	17.3	<0.1	<200	<0.1	0.883	<0.1	0.93	65.7	1.7	4.45	<0.2	<0.1
207132	<5	<150	16.2	<2	<1000	<1	<2	<10	<10	43.4	<10	<10	<10	<10
207132		23.9	14.3											
207132	<5	<30	13.4	<2	<500	<1	<2	<10	<5	43.6	<10	<2	<10	<10
207132		28.8	35.6											
207132		34.2	31.9											
207132		39.7	22.4											
207132	1.280	21.7	14.5	<0.1	<200	<0.1	0.82	<0.1	1.49	46.3	1.11	4.01	<0.2	<0.1
209047	<5	<150	1050.0	<2	<50	<1	<2	<10	<10	55.1	<10	<10	<10	<10
209047		90.0	929.6											
209047	<5	89.2	1076.0	<2	<50	<1	<2	<10	<5	52.8	<10	<2	<10	<10
209047		98.6	907.7											
209047		112.6	950.6											
209047		116.9	871.0											
209050	<5	88.0	288.9	<2	<50	<1	<2	<10	<5	56.8	<10	<2	<10	<10
209050		95.8	458.0											
209050		108.4	456.5											
209050		140.2	268.1											
209050	20.300	136.0	158.0	<0.5	<100	<0.5	0.559	<0.5	5.21	47.3	5.21	3.7	12	0.93
209049	<5	<150	465.0	<2	60	<1	<2	<10	<10	55.3	<10	<10	<10	<10
209049	<5	92.1	449.0	<2	62	<1	<2	<10	<5	55.5	<10	<2	<10	<10
209051	<5	92.5	356.0	<2	62	<1	<2	<10	<5	59.9	<10	<2	<10	<10
207124	<5	<150	45.2	<2	<1000	<1	<2	<10	<10	11.4	<10	<10	<10	<10
207125	<5	70.3	80.9											
207124	<5	<150	42.9	<10	<500	<1	<2	<10	<5	14	<10	4.12	<10	<10
207125		90.4	76.9											
207125		51.9	80.6											
207125		48.2	73.5											
207124	0.711	13.7	41.2	<0.1	<200	<0.1	0.281	<0.1	1.3	14.5	<10	1.94	1.91	<0.1
207123	<5	<150	27.9	<2	<1000	<1	<2	<10	<10	32	<10	<10	<10	<10
207123	<5	<150	27.4	<2	<50	<1	<2	<10	<5	17.2	<10	<2	<10	<10
207123		24.6	35.1											

APPENDIX 5.C-2: Water Quality for the Beaver Creek Sites
(page 8)

Gwic Id	Arsenic (ug/l)	Boron (ug/l)	Barium (ug/l)	Beryllium (ug/l)	Bromide (ug/l)	Cadmium (ug/l)	Cobalt (ug/l)	Chromium (ug/l)	Copper (ug/l)	Lithium (ug/l)	Molybdenum (ug/l)	Nickel (ug/l)	Lead (ug/l)	Antimony (ug/l)
207123	25.9	23.3	42.7											
207123	25.9	23.3	28.3											
207123	0.667	18.0	40.7	<0.1	<200	<0.1	0.389	<0.1	0.536	25	<1.0	2.61	<0.2	<0.1
209046	<1	<30	59.3	<2		<1	<2	<2	<2	12.1	<10	<2	<2	<2
209046	89.1	89.1	153.6											
209046	<5	<150	381.0	<2	<500	<1	<2	<10	<5	71.4	<10	<2	<10	<10
209046	78.5	78.5	180.0											
209042	<5	<150	1140.0	<2	<50	<1	<2	<10	<10	59.8	<10	<10	<10	<10
209042	87.4	87.4	969.5											
209042	<5	97.2	1066.0	<2	75	<1	<2	<10	<5	56.3	<10	<2	<10	<10
209042	92.7	92.7	937.6											
209042	100.7	100.7	982.7											
209042	83.7	83.7	876.3											
209043	92.6	92.6	376.8											
209043	<5	90.3	607.0	<10	57	<1	<2	<10	<5	53.7	<10	<2	<10	<10
209043	95.5	95.5	687.7											
209043	103.3	103.3	507.2											
209043	3.560	104.0	669.0	<0.5	<200	<0.5	<0.5	<0.5	2.11	54.1	<5.0	1.8	2.25	<0.5
209044	<5	<150	441.0	<2	<50	<1	<2	<10	<10	50.4	<10	<10	<10	<10
208572	<5	<150	416.0	<2	83	<1	<2	<10	<5	47.3	<10	<2	<10	<10
207121	<5	<150	28.6	<2	<2500	<1	<2	<10	<10	42.1	<10	11.3	<10	<10
207121	49.6	49.6	17.7											
207121	40.5	40.5	28.9											
207121	67.2	67.2	30.5											
207121	107.1	107.1	24.6											
207121	<10	<300	<20	<20	<500	<10	<20	<20	<20	51.4	<100	<20	<20	<20
207121	95.9	95.9	55.2											
207121	96.8	96.8	23.3											
207121	144.1	144.1	36.8											
207121	142.5	142.5	42.8											
207121	106.4	106.4	30.1											
207121	115.2	115.2	15.3											
207121	150.7	150.7	25.0											
207121	153.6	153.6	26.9											
207121	<1.0	120.0	10.4	<0.5	<2500	<0.5	0.985	<0.5	2.76	79.6	<5.0	9.07	<1.0	<0.5
207118	<5	<150	11.5	<2	<1000	<1	<2	<10	<10	31.9	<10	<10	<10	<10
207118	28.1	28.1	15.4											

APPENDIX 5.C-2: Water Quality for the Beaver Creek Sites
(page 9)

Gwifc Id	Arsenic (ug/l)	Boron (ug/l)	Barium (ug/l)	Beryllium (ug/l)	Bromide (ug/l)	Cadmium (ug/l)	Cobalt (ug/l)	Chromium (ug/l)	Copper (ug/l)	Lithium (ug/l)	Molybdenum (ug/l)	Nickel (ug/l)	Lead (ug/l)	Antimony (ug/l)
207118	<5	<30	10.7	<2	<500	<1	<2	<10	<5	31	<10	<2	<10	<10
207118		28.8	12.5											
207118		32.2	33.2											
207118		34.6	44.7											
207118	0.571	20.8	9.9	<0.1	<200	<0.1	0.383	<0.1	0.554	30.7	<1.0	2.21	<0.2	<0.1
208571		88.5	256.9											
208571	<5	89.0	396.0	<2	77	<1	<2	<10	<5	52.2	<10	2.06	<10	<10
208571		93.7	99.8											
208571		84.6	411.4											
208571		93.8	141.5											

APPENDIX 5.C-2: Water Quality for the Beaver Creek Sites
(page 10)

Gwic Id	Selenium (ug/l)	Strontium (ug/l)	Titanium (ug/l)	Thallium (ug/l)	Uranium (ug/l)	Vanadium (ug/l)	Zinc (ug/l)	Zirconium (ug/l)	Total Dissolved Solids (mg/L)	SAR
207130	<5	1670.0	1.77	<25	23.90	<25	<10	<10	767	1.2
207130		1150.6			22.62				791	1.5
207130	<5	1759.0	11.00	<25	25.90	<10	8.94	<2	830	1.2
207130		1240.0			22.63				788	1.4
207130		1155.4							771	1.4
207130		1053.0			20.32				742	1.2
207129	1.27	3147.0	2.88	<0.1	45.30	0.199	1.7	0.218	1593	2.2
207132	<5	2140.0	1.57	<25	<2.5	<25	<10	<10	1109	2.0
207132	<5	1463.4			1.12				1039	2.2
207132	<5	2280.0	<1	<25	<3	<10	6.47	<	1168	2.0
207132		1524.2			1.04				1085	2.1
207132		1572.2							1142	2.2
207132		1461.9			1.04				1152	2.1
207132	<0.5	2786.0	2.44	<0.1	0.86	<0.1	22.7	0.1	1259	2.1
209047	<5	1520.0	<1	<25	<2.5	<25	38.3	<10	1387	16.2
209047		1038.6			-0.01				1411	15.5
209047	<5	1465.0	<1	<25	<3	<10	<2	<2	1283	13.4
209047		1037.1			0.19				1445	15.6
209047		1115.2							1399	15.7
209047		980.8			0.05				1438	15.3
209050		559.9			0.45				1394	20.0
209050	<5	1058.0	<1	<25	<3	<10	<2	<2	1202	17.0
209050		785.1							1225	18.6
209050		668.3			0.81				1769	26.4
209050	<2.5	627.0	<1.0	<0.5	2.65	9.04	<1.0	2.76	1575	32.7
209049	<5	1100.0	<1	<25	<2.5	<25	<10	<10	1274	17.3
209049	<5	1057.0	<1	<25	<3	<10	<2	2.61	1266	16.6
209051	<5	1250.0	<1	<25	<3	<10	<2	2.04	1428	13.5
207124	<5	1730.0	1.61	<25	30.90	<25	<10	<10	1343	1.7
207125		942.4			15.30				779	2.3
207124	7.41	982.0	<1	<25	30.40	<10	177	<2	959	0.8
207125		872.1			28.46				1162	5.5
207125		947.9							932	2.8
207125		887.6			22.55				920	3.0
207124	3.22	1346.0	2.59	<0.1	29.50	<0.1	6.85	0.127	800	1.3
207123	<5	3270.0	<1	<25	5.04	<25	<10	<10	2501	2.3
207123	<5	1335.0	4.05	<25	10.80	<10	2.33	<2	926	1.7
207123		911.3			9.24				760	1.7

APPENDIX 5.C-2: Water Quality for the Beaver Creek Sites
(page 11)

Gwic Id	Selenium (ug/l)	Strontium (ug/l)	Titanium (ug/l)	Thallium (ug/l)	Uranium (ug/l)	Vanadium (ug/l)	Zinc (ug/l)	Zirconium (ug/l)	Total Dissolved Solids (mg/L)	SAR
207123		1147.4							1019	1.7
207123		881.6			9.78				885	1.8
207123	<0.5	2133.0	2.75	<0.1	10.10	<0.1	5.73	<0.1	1398	1.9
209046	<1	417.0	1.60	<5	<0.5	<5	2.07	<2	122	7.6
209046		486.5			0.92				1434	20.6
209046	<5	1294.0	<1	<25	<3	<10	2.63	2.2	1573	15.8
209046		1771.7			0.06				1937	7.0
209042	<5	1470.0	<1	<25	<2.5	<25	<10	<10	1266	14.5
209042		1011.3			-0.05				1346	14.2
209042	<5	1593.0	<1	<25	<3	<10	5.71	<2	1288	14.2
209042		1089.4			0.06				1385	14.4
209042		1053.1							1283	14.7
209042		1047.1			-0.05				1361	14.2
209043		631.2			0.39				1395	19.2
209043	<5	1136.0	<1	<25	<3	<10	<2	2.21	1225	16.5
209043		895.3							1218	17.3
209043		778.7			0.02				1535	21.6
209043	<2.5	1336.0	<1.0	<0.5	0.47	1.51	1.05	0.741	1260	20.1
209044	<5	999.0	<1	<25	<2.5	<25	<10	<10	1245	17.0
208572	<5	1267.0	<1	<25	5.67	<10	<2	<2	1246	10.1
207121	<5	4760.0	1.37	<25	65.50	<25	<10	<10	2383	1.4
207121		3593.3							2133	1.6
207121		3572.3							2096	1.5
207121		5277.9							2880	1.5
207121		6347.4							4061	2.9
207121	<10	9413.0	<10	<50	178.00	<50	<20	<20	4202	2.9
207121		6448.7							4599	3.9
207121		7068.3							5135	4.6
207121		7375.9							5751	5.6
207121		6925.1							5336	5.5
207121		7004.0							4787	4.0
207121		7270.0			269.21				4779	4.4
207121		7350.2			276.49				4865	4.5
207121		6769.1			263.54				4285	3.1
207121	<2.5	9454.0	<10.0	<0.5	242.00	<0.5	21	0.605	3917	2.5
207118	<5	2360.0	1.53	<25	2.88	<25	<10	<10	1570	2.3
207118		1702.2			6.65				1490	2.2

APPENDIX 5.C-2: Water Quality for the Beaver Creek Sites
(page 12)

Gwic Id	Selenium (ug/l)	Strontium (ug/l)	Titanium (ug/l)	Thallium (ug/l)	Uranium (ug/l)	Vanadium (ug/l)	Zinc (ug/l)	Zirconium (ug/l)	Total Dissolved Solids (mg/L)	SAR
207118	<5	2410.0	<1	<25	3.76	<10	<2	<2	1529	2.2
207118		1628.0			5.41				1487	2.3
207118		1710.8							1556	2.3
207118		1635.5			7.85				1505	2.3
207118	0.699	2667.0	2.70	<0.1	5.15	<0.1	4.08	<0.1	1574	2.2
208571		578.9			1.99				1305	16.1
208571	<5	1524.0	<1	<25	6.57	<10	<2	2.59	1391	9.8
208571		386.6			3.49				1407	18.7
208571		972.8							1268	10.1
208571		384.7			4.90				1438	18.9

APPENDIX 5.D: Coal Creek Water Quality Modeling
(page 1)

		Species Distribution for 3 Coal Creek Wells						
Component	Species	% of total component concentration						
		Well 12BA9B			Well 12BA7B		Well 12BA2B	
		March-05	August-07	August-07*	March-05	August-07	March-05	August-07
	pH	7.29	6.39	6.93	7.51	7.04	7.52	6.77
SO4-2	SO4-2	73.09	72.44	72.453	67.97	69.86	65.43	69.27
	MgSO4 (aq)	12.11	12.32	12.315	16.65	17.40	20.60	15.97
	CaSO4 (aq)	13.16	13.56	13.545	6.46	4.80	9.66	11.07
	NaSO4-	1.54	1.57	1.572	8.89	7.92	4.27	3.63
	KSO4-	0.05	0.05	0.046	0.03	0.02	0.03	0.05
	FeSO4 (aq)	0.04	0.05	0.052				
	MnSO4 (aq)	0.02	0.01	0.013				
CO3-2	CO3-2	0.14	0.01	0.053	0.32	0.10	0.30	0.04
	HCO3-	87.48	55.28	78.998	87.28	81.49	86.92	73.32
	H2CO3* (aq)	8.40	42.31	17.438	4.35	12.24	4.40	22.01
	MgCO3 (aq)	0.10	1.06	0.041	0.35	0.11	0.43	0.04
	MgHCO3+	1.66	1.15	1.517	4.01	3.58	4.57	2.38
	CaHCO3+	1.78	0.01	1.646	1.53	0.97	2.11	1.62
	CaCO3 (aq)	0.18	0.15	0.072	0.22	0.05	0.32	0.05
	NaCO3-				0.14	0.04	0.07	0.54
	NaHCO3 (aq)	0.24		0.219	1.78	1.42	0.85	
	Mg2CO3+2				0.03		0.03	
	MnCO3 (aq)	0.01						
Ca+2	Ca+2	70.59	71.77	71.678	46.06	49.14	52.60	61.21
	CaSO4 (aq)	23.78	24.05	24.034	51.60	48.68	45.76	35.20
	CaHCO3+	5.13	4.13	4.109	2.05	2.08	1.42	3.49
	CaCO3 (aq)	0.51	0.05	0.179	0.29	0.10	0.21	0.10
Mg+2	Mg+2	75.20	76.17	76.113	51.83	54.88	58.30	66.51
	MgSO4 (aq)	20.12	20.28	20.272	46.12	43.18	40.29	30.38
	MgCO3 (aq)	0.27	0.03	0.095	0.16	0.06	0.12	0.05
	MgHCO3+	4.40	3.53	3.514	1.86	1.87	1.27	3.05
	Mg2CO3+2				0.02		0.02	
Na+1	Na+1	97.99	98.11	98.103	91.53	92.83	94.02	96.35
	NaSO4-	1.61	1.58	1.582	8.18	6.90	5.81	3.31
	NaCO3-	0.02	0.31		0.02	0.26	0.01	0.33
	NaHCO3 (aq)	0.39		0.31	0.27		0.16	
K+1	K+1	97.93	97.97	97.965	89.68	91.26	92.63	95.76
	KSO4-	2.07	2.04	2.035	10.32	8.74	7.37	4.24
Fe+2	Fe+2	69.57	70.59	70.522	44.45	47.50	50.90	59.75
	FeOH+	0.32	0.04	0.144	0.24	0.09	0.31	0.07
	FeSO4 (aq)	25.11	25.35	25.338	53.36	50.42	47.44	36.81
	FeHCO3+	5.00	4.01	3.997	1.95	1.99	1.36	3.37
Mn+2	Mn+2	62.76	72.88	70.154	46.95	52.69	54.32	63.12
	MnOH+	0.02	18.96		0.02	40.52	0.02	28.17
	MnSO4 (aq)	16.41	6.57	18.26	40.83	3.49	36.68	5.64
	MnHCO3+	7.14	1.59	6.301	3.27	3.30	2.30	3.07
	MnCO3 (aq)	13.66		5.276	8.93		6.68	
H4SiO4	H4SiO4	99.49	99.79	99.684	97.84	98.58	98.42	99.45
	H3SiO4-	0.34	0.04	0.147	0.64	0.21	0.63	0.11
	H4SiO4SO4-2	0.17	0.17	0.169	1.53	1.20	0.95	0.45

*indicates model used pH measured in the field.

APPENDIX 5.D: Coal Creek Water Quality Modeling

(page 2)

Saturation Indices for 3 Coal Creek Wells

Mineral	Saturation Index						
	Well 12BA9B			Well 12BA7B		Well 12BA2B	
	March-05	August-07	August-07*	March-05	August-07	March-05	August-07
TDS (mg/L)	1656	1565	1565	10665	8319	6842	3629
Anhydrite	-0.96	-0.96	-0.959	-0.29	-0.54	-0.31	-0.60
Aragonite	0.48	-0.51	0.028	0.58	-0.10	0.48	-0.04
Artinite	-5.54	-8.34	-6.717	-4.18	-5.67	-4.28	-6.68
Brucite	-5.25	-7.05	-5.968	-4.43	-5.39	-4.35	-6.06
CaCO ₃ xH ₂ O	-0.71	-1.70	-1.163	-0.62	-1.29	-0.71	-1.23
Calcite	0.63	-0.37	0.172	0.72	0.04	0.62	0.10
Chalcedony	-0.36	-0.35	-0.348	-0.48	-0.49	-0.41	-0.40
Chrysotile	-4.49	-9.84	-6.598	-2.25	-5.15	-1.88	-6.97
Cristobalite	-0.56	-0.55	-0.548	-0.68	-0.69	-0.61	-0.60
Dolomite (disordered)	0.90	-1.09	-0.017	1.53	0.33	1.25	0.05
Dolomite (ordered)	1.45	-0.54	0.533	2.08	0.88	1.80	0.60
Epsomite	-3.13	-3.13	-3.133	-2.01	-2.11	-2.11	-2.58
Fe(OH) ₂ (am)	-4.30	-5.94	-4.858	-4.87	-16.21	-4.97	-16.56
Fe(OH) ₂ (c)	-3.70	-5.34	-4.258	-4.27	-15.61	-4.37	-15.96
Greenalite	-1.07	-5.95	-2.711	-2.99	-37.07	-3.18	-37.92
Gypsum	-0.71	-0.71	-0.709	-0.04	-0.29	-0.06	-0.35
Huntite	-1.25	-5.24	-3.087	0.46	-1.80	-0.18	-2.76
Hydromagnesite	-10.54	-16.33	-13.098	-7.56	-10.63	-8.20	-12.66
Lime	-20.92	-22.71	-21.625	-20.54	-21.65	-20.38	-21.92
Magnesite	-0.33	-1.33	-0.789	0.21	-0.32	0.03	-0.66
Melanterite	-5.71	-5.55	-5.552	-5.98	-16.46	-6.26	-16.61
Mg(OH) ₂ (active)	-6.95	-8.74	-7.662	-6.12	-7.08	-6.05	-7.76
MgCO ₃ :5H ₂ O	-3.25	-4.25	-3.709	-2.71	-3.24	-2.89	-3.58
Mirabilite	-5.79	-5.78	-5.778	-3.17	-3.41	-4.00	-4.55
MnCO ₃ (am)	-0.07	-1.23	-0.706	-0.79	-2.13	-11.36	-0.88
MnSO ₄	-10.63	-10.78	-10.8	-10.76	-11.67	-21.26	-10.55
Natron	-8.12	-9.11	-8.57	-6.08	-6.75	-6.99	-7.76
Nesquehonite	-3.12	-4.12	-3.579	-2.58	-3.11	-2.76	-3.45
Periclase	-9.74	-11.53	-10.452	-8.91	-9.87	-8.84	-10.55
Portlandite	-10.92	-12.71	-11.63	-10.54	-11.65	-10.38	-11.92
Pyrochroite	-6.13	-8.08	-7.019	-6.56	-8.33	-16.88	-7.41
Quartz	0.09	0.10	0.102	-0.03	-0.04	0.04	0.06
Rhodochrosite	0.43	-0.73	-0.206	-0.29	-1.63	-10.86	-0.38
Sepiolite	-3.81	-7.35	-5.189	-2.50	-4.47	-2.15	-5.52
Sepiolite (A)	-6.83	-10.37	-8.209	-5.52	-7.49	-5.17	-8.54
Siderite	0.15	-0.70	-0.16	-0.70	-11.62	-1.07	-11.64
SiO ₂ (am,gel)	-1.20	-1.19	-1.188	-1.32	-1.33	-1.25	-1.24
SiO ₂ (am,ppt)	-1.17	-1.16	-1.158	-1.29	-1.30	-1.22	-1.21
Thenardite	-7.22	-7.21	-7.214	-4.60	-4.84	-5.43	-5.98
Thermonatrite	-10.07	-11.06	-10.518	-8.03	-8.70	-8.94	-9.71
Vaterite	0.06	-0.93	-0.394	0.15	-0.52	0.06	-0.46

Grey shaded areas indicate over-saturation.

*indicates model used pH measured in the field.

APPENDIX 5.D: Coal Creek Water Quality Modeling
(page 3)

Mineral Stoichiometry

Mineral	Stoichiometry				
Anhydrite	1 Ca+2	1 SO4-2			
Aragonite	1 Ca+2	1 CO3-2			
Artinite	-2 H+1	2 Mg+2	1 CO3-2		5 H2O
Brucite	1 Mg+2	2 H2O	-2 H+1		
CaCO3xH2O	1 Ca+2	1 CO3-2	1 H2O		
Calcite	1 Ca+2	1 CO3-2			
Chalcedony	1 H4SiO4	-2 H2O			
Chrysotile	3 Mg+2	2 H4SiO4	1 H2O		-6 H+1
Cristobalite	1 H4SiO4	-2 H2O			
Dolomite (disordered)	1 Ca+2	1 Mg+2	2 CO3-2		
Dolomite (ordered)	1 Ca+2	1 Mg+2	2 CO3-2		
Epsomite	1 Mg+2	1 SO4-2	7 H2O		
Fe(OH)2 (am)	1 Fe+2	2 H2O	-2 H+1		
Fe(OH)2 (c)	1 Fe+2	-2 H+1	2 H2O		
Greenalite	-6 H+1	3 Fe+2	2 H4SiO4		1 H2O
Gypsum	1 Ca+2	1 SO4-2	2 H2O		
Huntite	3 Mg+2	1 Ca+2	4 CO3-2		
Hydromagnesite	5 Mg+2	4 CO3-2	-2 H+1		6 H2O
Lime	-2 H+1	1 Ca+2	1 H2O		
Magnesite	1 Mg+2	1 CO3-2			
Melanterite	1 Fe+2	1 SO4-2	7 H2O		
Mg(OH)2 (active)	1 Mg+2	2 H2O	-2 H+1		
MgCO3.5H2O	1 Mg+2	1 CO3-2	5 H2O		
Mirabilite	2 Na+1	1 SO4-2	10 H2O		
MnCO3 (am)	1 Mn+2	1 CO3-2			
MnSO4	1 Mn+2	1 SO4-2			
Natron	2 Na+1	1 CO3-2	10 H2O		
Nesquehonite	1 Mg+2	1 CO3-2	3 H2O		
Periclase	-2 H+1	1 Mg+2	1 H2O		
Portlandite	1 Ca+2	2 H2O	-2 H+1		
Pyrochroite	1 Mn+2	2 H2O	-2 H+1		
Quartz	1 H4SiO4	-2 H2O			
Rhodochrosite	1 Mn+2	1 CO3-2			
Sepiolite	2 Mg+2	3 H4SiO4	-4 H+1		-0.5 H2O
Sepiolite (A)	-0.5 H2O	2 Mg+2	3 H4SiO4		-4 H+1
Siderite	1 Fe+2	1 CO3-2			
SiO2 (am,gel)	1 H4SiO4	-2 H2O			
SiO2 (am,ppt)	1 H4SiO4	-2 H2O			
Thenardite	2 Na+1	1 SO4-2			
Thermonatrite	2 Na+1	1 CO3-2	1 H2O		
Vaterite	1 Ca+2	1 CO3-2			

APPENDIX 5.E: Column Leach Trials
(page 1)

Repetition	Tube	Material	Mass of material (g)	Pore Volume number	Cumulative treated water (mL)	Comments	Sample Date	Lab	Lab pH	Lab SC	TDS (mg/L)
1		Source water				CBM water	4/17/06 0:00	MBMG	8.13	2290	1336
1	1	Control	2405.8	1	633	Washed silica sand	4/17/06 0:00	MBMG	7.75	2100	1373
1	1			2	1283		4/19/06 0:00	MBMG	8.03	2170	1394
1	1			5	3272		4/25/06 0:00	MBMG	8.28	2240	1475
1	1			10	6686		5/5/06 0:00	MBMG	8.23	2100	1331
1	1			14	9300		5/15/06 0:00	MBMG	8.25	2260	1307
1	1			27	17816		6/10/06 0:00	MBMG	8.2	2060	1310
1	2	Coal	1171.8	1	316	sub-bituminous	4/17/06 0:00	MBMG	7.49	2360	1853
1	2			2	1164	from Powder River Basin	4/19/06 0:00	MBMG	6.62	964	572
1	2			5	3220	near Decker, MT	4/25/06 0:00	MBMG	6.93	1230	764
1	2			10	6527		5/5/06 0:00	MBMG	7.02	1614	989
1	2			15	9840		5/17/06 0:00	MBMG	7.19	1733	934
1	2			27	17911		6/10/06 0:00	MBMG	7.5	1931	1216
1	3	Leonardite	1131.2	1	792	from North Dakota	4/21/06 0:00	MBMG	4.44	5120	5699
1	3			2	1450		4/23/06 0:00	MBMG	4.25	4570	4913
1	3			5	3392		4/29/06 0:00	MBMG	5.52	4220	4176
1	3			10	6593		5/9/06 0:00	MBMG	5.19	3030	3060
1	3			14	9095		5/19/06 0:00	MBMG	4.11	2980	2845
1	3			25	15188		6/10/06 0:00	MBMG	5.04	687	437
1	4	Clay and fine silt		1	384	Drill cuttings from	4/17/06 0:00	MBMG	8.54	2270	1342
1	4			2	869	beneath Coal Ck pond	4/19/06 0:00	MBMG	8.55	2320	1301
						Tube plugged, abandoned					
1	5	Sand and silt	2352.2	1	522	Drill cuttings from	4/17/06 0:00	MBMG	8.13	2650	1656
1	5			2	1077	beneath Coal Ck pond	4/19/06 0:00	MBMG	8.01	2250	1413
						Tube plugged, abandoned					
2	0	Source water				CBM water	7/27/07 13:00	MBMG	7.75	2060	1316
2	1	Control	1603.7	2	940	Washed silica sand	7/14/07 9:00	MBMG	7.78	2030	1150
2	1			15	7016		7/27/07 9:15	MBMG	8.11	2060	1240

APPENDIX 5.E: Column Leach Trials
(page 2)

Repetition	Tube	Material	Mass of material [g]	Pore Volume number	Cumulative treated water [mL]	Comments	Sample Date	Lab	Lab pH	Lab SC	TDS (mg/L)
2	1			21	9752		8/2/07 9:00	MBMG	7.9	2010	1186
2	1			87	39187		10/7/07 9:00	MBMG	8.25	1891	1291
2	2	Leonardite	717.6	2	600	from North Dakota	7/14/07 9:00	MBMG	6.65	6350	6180
2	2			15	6682		7/27/07 9:15	MBMG	6.17	2960	2087
2	2			21	9674		8/2/07 9:00	MBMG	6.21	1495	956
2	2			87	42796		10/7/07 9:00	MBMG	7.54	1557	989

Material sizes used for column leach trials

	screen size	mm	inch	column fill material
maximum size	16	1.168		column fill material
minimum size	35	0.495	0.0469	sand, coal, leonardite
			0.0197	
maximum size	65	0.227		0.00905 clay
minimum size	200	0.074		0.0029
maximum size	35	0.495		0.0197 sand
minimum size	65	0.227		0.00905

APPENDIX 5.E: Column Leach Trials
(page 3)

Repetition	Tube	Material	SAR	Ca (mg/l)	Mg (mg/l)	Na (mg/l)	K (mg/l)	Fe (mg/l)	Mn (mg/l)	SiO2 (mg/l)	HCO3 (mg/l)	CO3 (mg/l)	SO4 (mg/l)	Cl (mg/l)	NO3 (mg/l)	F (mg/l)	OPO4 (mg/l)	Ag (ug/l)	Al (ug/l)	As (ug/l)	
1		Source water	54.3	5.72	2.42	614	4.77	<0.005	0.005	9.74	1355.8	0	<2.5	32.3	<0.05	<0.05	<0.05			<30	
1	1	Control	20.0	36	11.7	539	7.83	<0.005	0.028	18.1	1472.5	0	<2.5	35.2	<0.05	<0.05	<0.05			<30	
1	1		38.3	11.3	4.44	600	4.72	<0.005	0.006	15.6	1471.3	0	<2.5	33.9	0.09	<0.05	<0.05			<30	
1	1		59.1	4.61	2.16	613	4.32	<0.005	<0.001	11.5	1638.5	0	<2.5	32.9	<0.05	<0.05	<0.05			<30	
1	1		61.7	4.3	2.13	626	4.98	0.018	<0.001	12.3	1324.1	0	<2.5	29.9	<0.05	<0.05	<0.05			39.3	
1	1		59.9	4.09	2.2	604	4.67	<0.005	<0.001	12.1	1321.3	0	<2.5	29.4	<0.05	<0.05	<0.05			34.2	
1	1		58.5	4.11	2.38	602	4.72	0.007	<0.001	11	1334.7	0	<2.5	29.3	<0.05	<0.05	<0.05			37.5	
1	2	Coal	2.6	193	139	192	13.6	<0.005	0.187	34.8	357.5	0	1056	42.6	1.08	<1.0	<1.0			<30	
1	2		5.0	37.3	28.4	166	7.15	0.229	0.038	15.1	415.2	0	78.1	34.2	<0.05	<0.05	<0.05			92.4	
1	2		13.0	16.7	12.9	290	5.05	0.015	0.018	10.4	790.6	0	5.37	33.4	<0.05	0.382	<0.05			61.1	
1	2		27.0	8.37	6.05	420	3.43	0.014	<0.001	11.1	1036.2	0	<2.5	29.6	<0.05	<0.05	<0.05			<30	
1	2		38.5	5.08	3.65	466	2.8	<0.005	0.002	11.2	844.2	0	<2.5	29.7	<0.05	<0.05	<0.05			<30	
1	2		57.4	2.9	2.06	523	3.16	<0.005	<0.001	10.5	1311.5	0	<2.5	29.2	<0.05	<0.05	<0.05			<30	
1	3	Leonardite	1.5	527	629	210	10.5	0.463	4.68	44.4	0	0	4232	<50.0	26.9	<5.0	<5.0			2996	
1	3		1.3	471	551	180	9.56	0.406	4.06	13.5	0	0	3671	<50.0	<5.0	<5.0	<5.0			2900	
1	3		2.3	427	351	270	8.02	0.401	3.16	11.6	76.9	0	3030	26.5	<0.50	<0.50	<0.50			2027	
1	3		2.9	449	157	281	1.94	0.894	2.07	11.8	50.02	0	2124	<25.0	<2.5	<2.5	<2.5			1454	
1	3		2.6	498	90.4	244	0.89	0.628	1.78	11.7	0	0	1990	<25.0	<2.5	<2.5	<2.5			1208	
1	3		5.7	76.1	3.49	186	0.64	7.86	0.256	11	73.7	0	75.1	25.9	<0.5	1.38	<0.5			10693	
1	4	Clay and fine silt	50.2	5.31	2.94	581	6.4	0.167	0.003	10.1	1327.4	36	8	37.6	0.716	0.087	0.059			58.2	
1	4		51.4	4.79	3.05	585	6.49	0.211	0.022	10.2	1237.1	40.8	5.55	36	0.151	0.087	0.063			43.5	
1	5	Sand and silt	26.4	29.9	12.1	678	12.8	0.622	0.037	18.8	1357.9	0	180	50.1	4.4	0.306	<0.10			380	
1	5		27.1	20.3	8.56	578	11.5	0.252	0.031	16.6	1487.2	0	16.1	29.3	0.058	0.154	<0.05			155	
2	0	Source water	16.6	30.9	19.7	480	7.72	<0.005	<0.001	10.4	1545.7	0	<2.5	4.16	1.886 P	0.111	<0.05	<5.0			<1.0
2	1	Control	13.7	35.5	19.7	409	8.84	0.008	0.219	16.4	1296.4	0	<2.5	19.6	<0.05	1.25	<0.05	<5.0			5.3
2	1		18.8	23	19.6	507	8.95	0.007	0.021	10.5	1349.3	0	<2.5	4.83	<0.05	0.178	<0.05	<5.0			<1.0

APPENDIX 5.E: Column Leach Trials
(page 4)

Repetition	Tube	Material	SAR	Ca (mg/l)	Mg (mg/l)	Na (mg/l)	K (mg/l)	Fe (mg/l)	Mn (mg/l)	SiO2 (mg/l)	HCO3 (mg/l)	CO3 (mg/l)	SO4 (mg/l)	Cl (mg/l)	NO3 (mg/l)	F (mg/l)	OPO4 (mg/l)	Ag (ug/l)	Al (ug/l)	As (ug/l)
2	1		18.1	20.1	20.5	482	8.81	0.006	0.017	11.9	1288.3	0	<2.5	5.02	1.9	0.212	<0.05	<2.5	<10.0	<1.0
2	1		20.7	19.4	18.8	534	8.95	<0.005	0.004	13.3	1378	0	6.79	7.73	1.63	1.01	<0.10	<0.5	5.8	0.394
2	2	Leonardite	5.2	370	623	702	13.4	0.54	3.89	19.5	258.6	0	4231	18.3	31.3	<1.25	<1.25	<10.0	3736	7.06
2	2		8.4	130	86.5	503	10.4	0.633	0.399	11.2	184.8	0	1248	<50.0	<5.0	<5.0	<5.0	<10.0	1193	3.23
2	2		14.7	21.1	13.1	349	6.39	0.957	0.081	10.9	368.4	0	360	6.42	1.93	0.944	<0.25	<2.5	1716	2.8
2	2		21.3	14.9	10.3	437	6.78	1.01	0.035	12.6	1023.6	0	<50.0	<10.0	<1.0	1.07	<1.0	<0.5	889	1.9

APPENDIX 5.E: Column Leach Trials
(page 5)

Repetition	Tube	Material	B (ug/l)	Ba (ug/l)	Be (ug/l)	Br (ug/l)	Cd (ug/l)	Co (ug/l)	Cr (ug/l)	Cu (ug/l)	Li (ug/l)	Mo (ug/l)	Ni (ug/l)	Pb (ug/l)	Sb (ug/l)	Se (ug/l)	Sr (ug/l)	Ti (ug/l)	Ti (ug/l)	U (ug/l)	V (ug/l)	
1		Source water				222					115						259					
1	1	Control				262					96.1						388					
1	1					246					111						152					
1	1					212					110						78.5					
1	1		118	66.7	<2	<500	<1	<2	<10	20.6	114	<10	<2	<10	<10	<15	86.1	<1	22.1		<10	
1	1		116	66.9	<2	<500	<1	<2	<10	20.2	110	<10	<2	<10	<10	<15	116	<1	38.6		<10	
1	1		113	139	<2	<500	<1	<2	<10	16.5	112	<10	2.37	<10	<10	<15	225	<1	36		<10	
1	2	Coal				<1000					442						4517					
1	2					337					199						938					
1	2					277					97.7						447					
1	2		455	27.3	<2	<500	<1	<2	<10	<5	82.9	<10	<2	<10	<10	<15	244	<1	31.2		<10	
1	2		292	18.3	<2	<500	<1	<2	<10	<5	88.8	<10	<2	<10	<10	<15	158	<1	27.8		<10	
1	2		174	13.7	<2	<500	<1	<2	<10	<5	95.7	<10	<2	<10	<10	<15	95.4	<1	29.2		<10	
1	3	Leonardite				<5000					211						11149					
1	3					<5000					137						9778					
1	3					<500					76.5						8073					
1	3		935	16.1	<2	<2500	<1	<2	<10	19.1	60.9	<10	3.14	<10	<10	<15	5462	28.2	25.1		<10	
1	3		742	22.2	<2	<2500	<1	<2	<10	9.6	64	<10	3.1	<10	<10	<15	5411	22.6	<20		<10	
1	3		546	172	<4	<500	<2	<4	<20	59.1	45.2	<20	7.33	<20	<20	<30	836	2.09	<40		<20	
1	4	Clay and fine silt				247					103						171					
1	4					255					105						128					
1	5	Sand and silt				276					53.3						405					
1	5					255					47.2						301					
2	0	Source water	86.3	954	<0.5	<50	<0.5	<0.5	<0.5	1.25	54.1	<5.0	2.2	<1.0	<0.5	<2.5	1438	<1.0	<0.5	<0.25	<0.5	
2	1	Control	110	632	<0.5	<50	<0.5	0.917	<0.5	39.7	56	<5.0	2.46	4.24	<0.5	<2.5	1226	<1.0	<0.5	3.02	0.846	
2	1		102	782	<0.5	<50	<0.5	<0.5	<0.5	32.6	55.2	<5.0	1.85	1.54	<0.5	<2.5	1270	<1.0	<0.5	<0.25	<0.5	

APPENDIX 5.E: Column Leach Trials
(page 6)

Repetition	Tube	Material	B (ug/l)	Ba (ug/l)	Be (ug/l)	Br (ug/l)	Cd (ug/l)	Co (ug/l)	Cr (ug/l)	Cu (ug/l)	Li (ug/l)	Mo (ug/l)	Ni (ug/l)	Pb (ug/l)	Sb (ug/l)	Se (ug/l)	Sr (ug/l)	Ti (ug/l)	Tl (ug/l)	U (ug/l)	V (ug/l)
2	1		99.3	704	<0.5	<50	<0.5	<0.5	<0.5	35.4	58.7	<5.0	2.29	<1.0	<0.5	<2.5	1344	<1.0	<0.5	<0.25	<0.5
2	1		81.2	776	<0.1	<200	0.262	<0.1	<0.1	37.7	62.1	<1.0	7.01	0.869	<0.1	0.54	1232	<0.2	27.6	0.057	<0.1
2	2	Leonardite	24942	311	<1.0	<1250	<2.0	2.81	<1.0	219	357	<10.0	8.29	9.25	1.16	14.1	7586	111	<1.0	<0.50	2.69
2	2		2698	197	<1.0	<5000	<1.0	<1.0	<1.0	55.9	86.4	<10.0	2.12	2.07	<1.0	<5.0	2039	53.6	<1.0	<0.50	1.86
2	2		1313	58.3	<0.5	<250	<0.5	0.71	<0.5	62.4	50.3	5.34	3.02	1.62	<0.5	<2.5	429	66.1	<0.5	<0.25	2.95
2	2		216	212	<0.1	<1000	0.675	0.419	0.154	52.4	48.6	3.62	5.08	2.75	0.125	1	507	65.1	53.4	0.225	2.37

APPENDIX 5.E: Column Leach Trials
(page 7)

Repetition	Tube	Material	Zn (ug/l)	Zr (ug/l)
1		Source water		
1	1	Control		
1	1			
1	1			
1	1		3.83	<2
1	1		<2	<2
1	1		5.75	<2
1	2	Coal		
1	2			
1	2			
1	2		<2	<2
1	2		<2	<2
1	2		<2	<2
1	3	Leonardite		
1	3			
1	3			
1	3		49.8	9.36
1	3		37.4	8.44
1	3		52.4	19.9
1	4	Clay and fine silt		
1	4			
1	5	Sand and silt		
1	5			
2	0	Source water	3.02	<0.5
2	1	Control	27.9	10.4
2	1		17.4	2

APPENDIX 5.E: Column Leach Trials
(page 8)

Repetition	Tube	Material	Zn (ug/l)	Zr (ug/l)
2	1		18.1	1.1
2	1		24.8	0.581
2	2	Leonardite	2210	12.8
2	2		62.6	6.45
2	2		45.2	8.19
2	2		125	2.47

Plate 5.1: Geologic Cross-sections of the Coal Creek Site

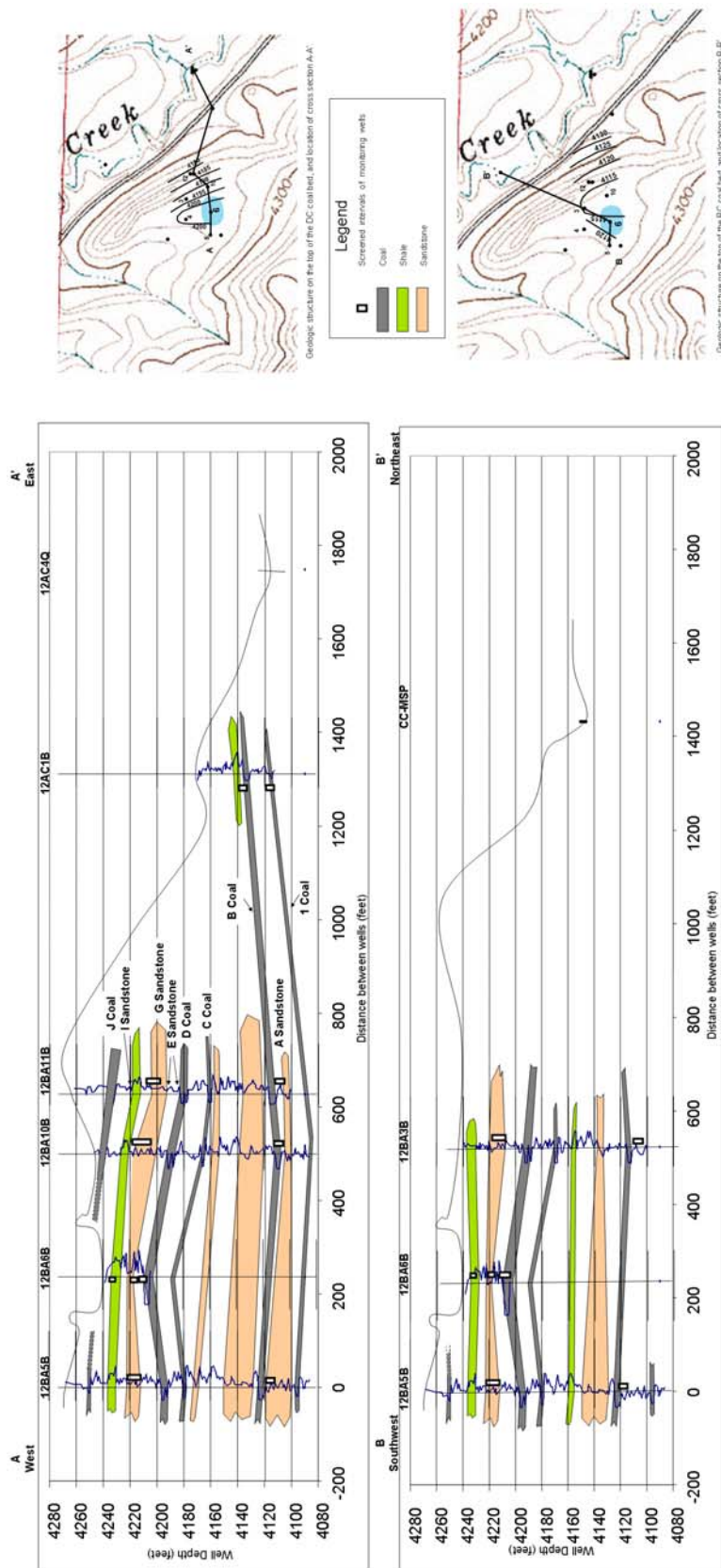


Plate 5.2: Specific Conductivity, Water Depth, SAR and Major Ion Chemistry Changes with Time And Distance Down-Gradient at the Coal Creek Research Site.

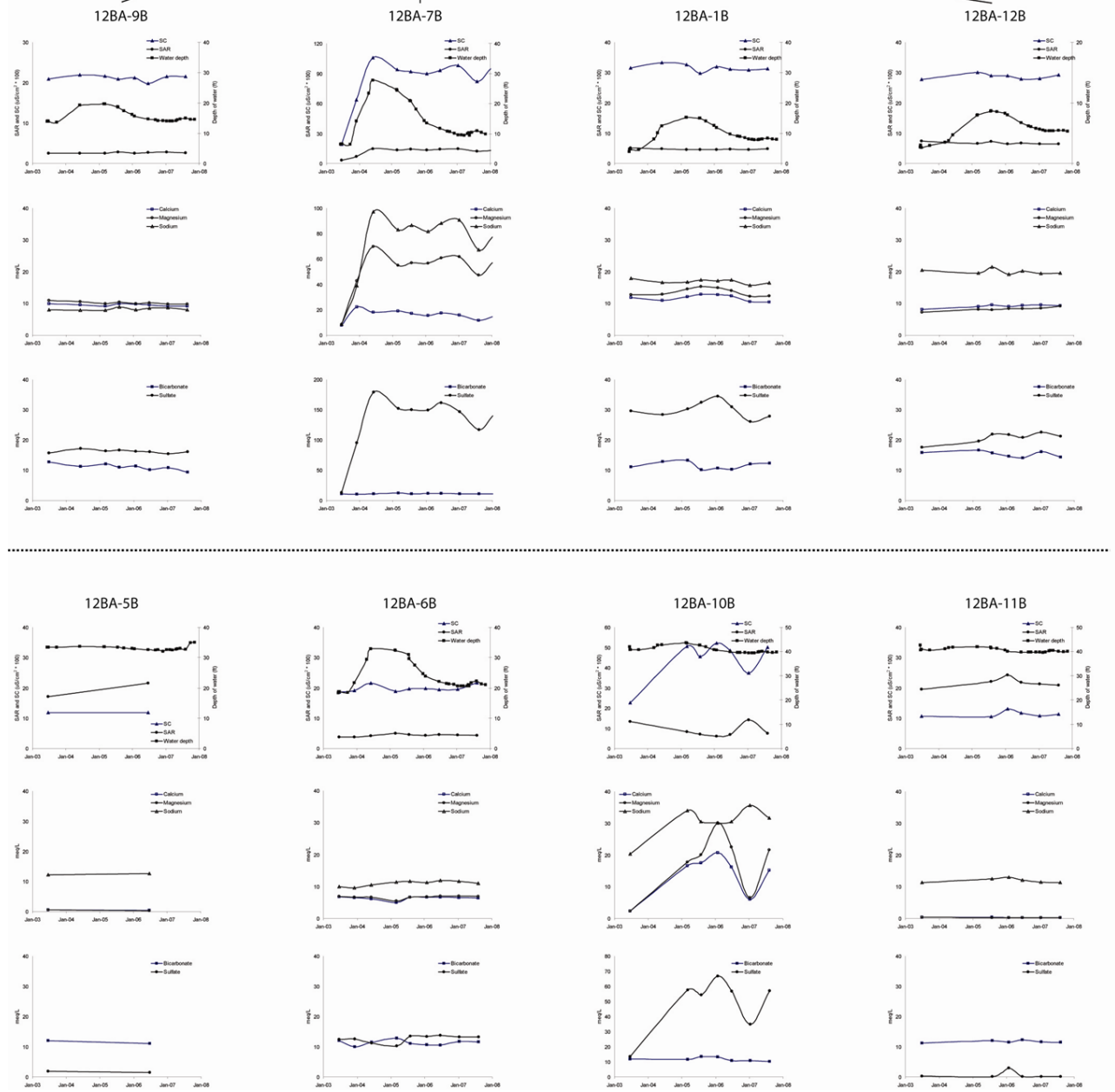
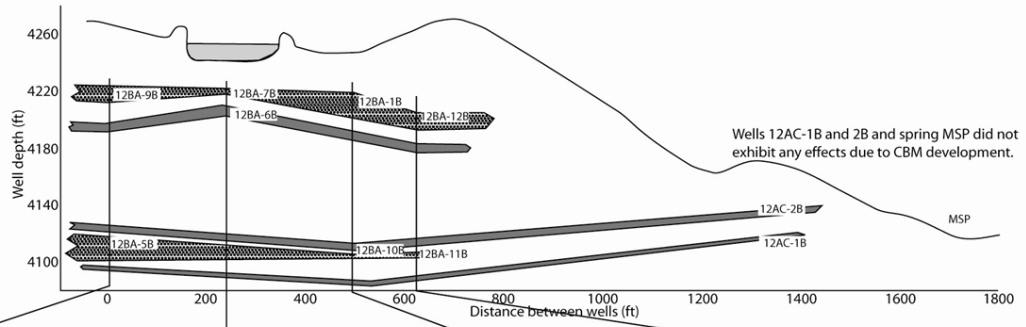


Plate 5.3: Specific Conductivity, Water Depth, SAR and Major Ion Chemistry Changes with Time And Distance Down-Gradient at the Coal Creek Research Site.

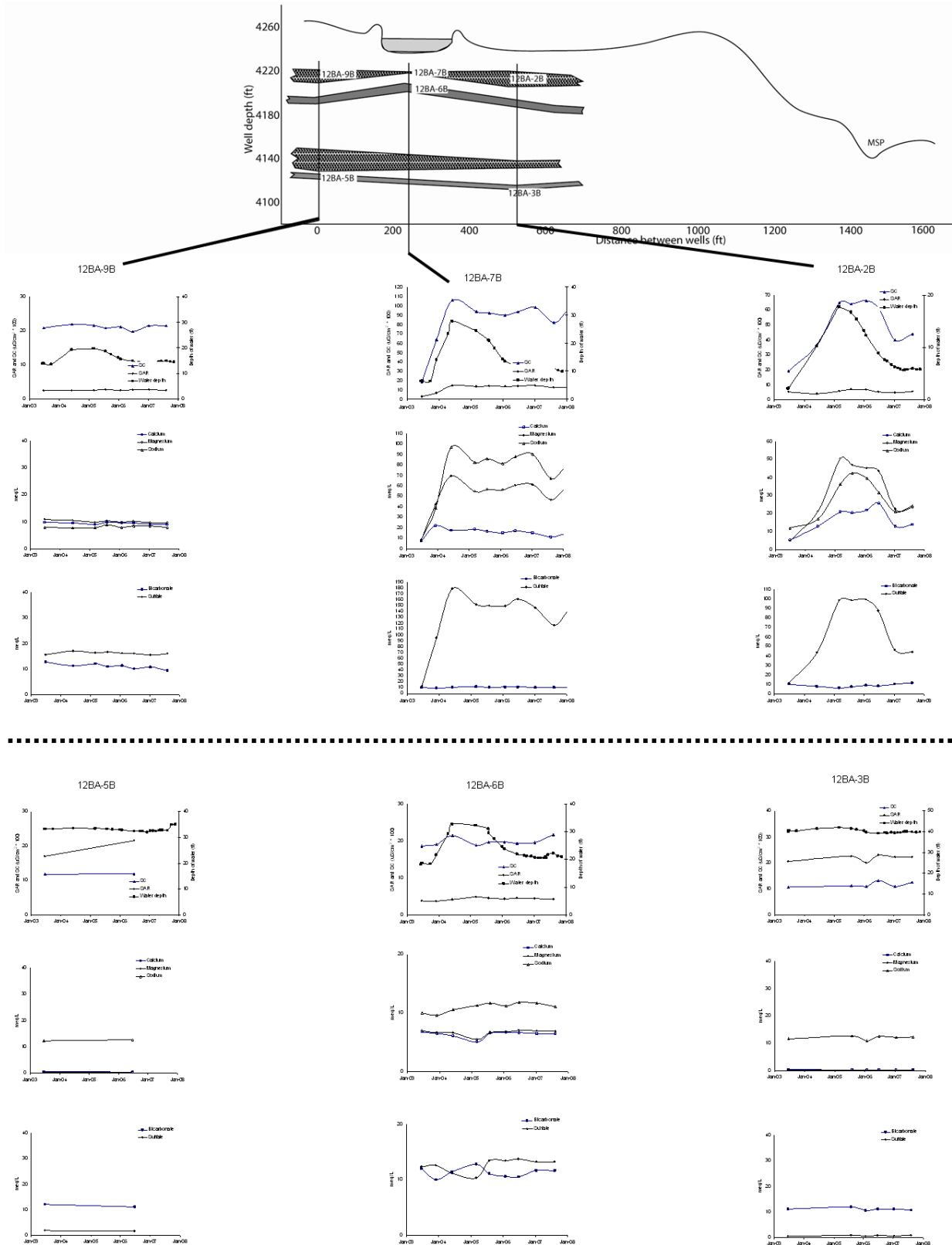
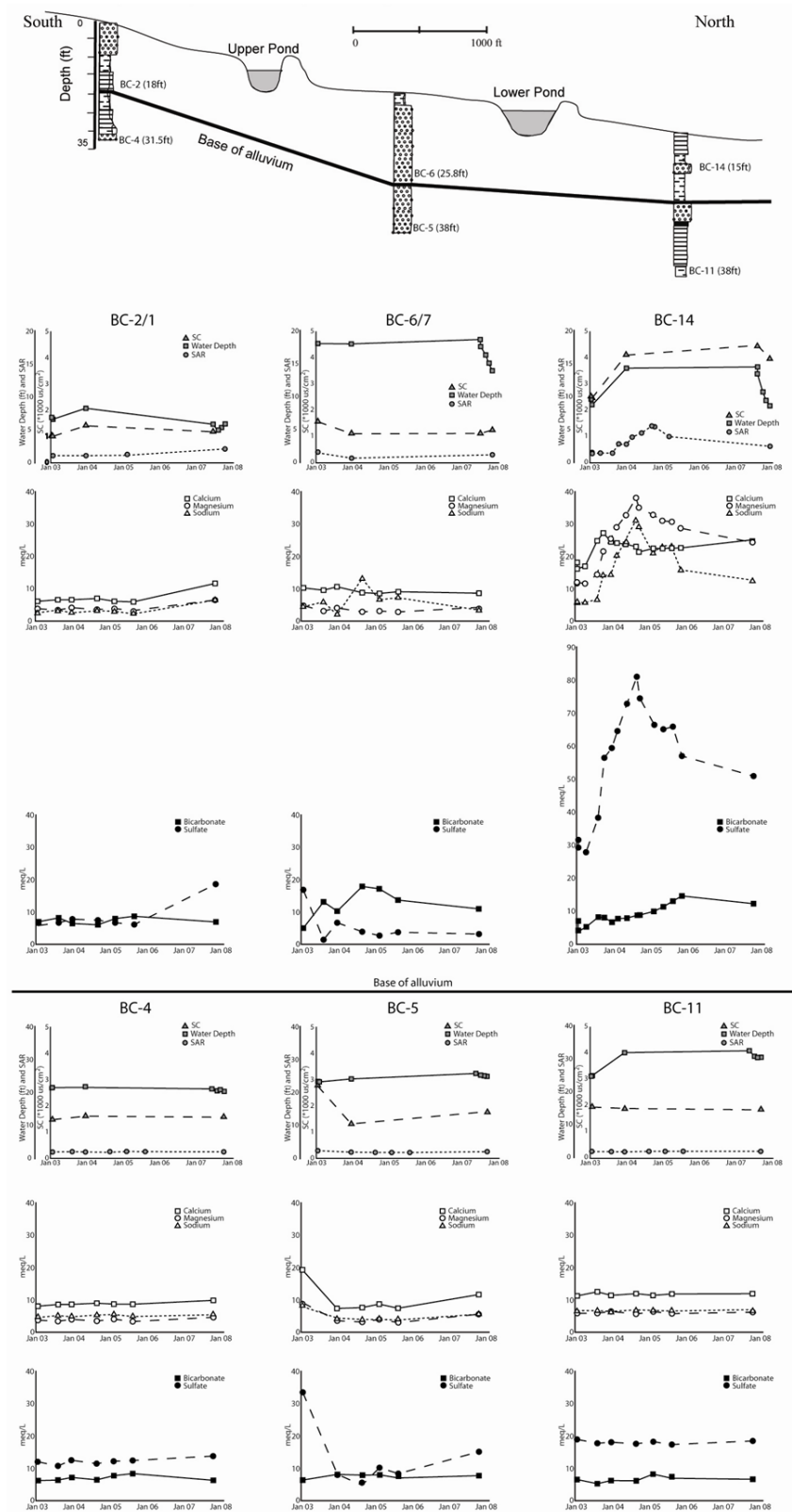


Plate 5.4: Specific Conductivity, Water Depth, SAR and Major Ion Changes with Time And Distance Downstream at the Beaver Creek Research Site.



CHAPTER 6: Controls on the Fate of CBM Co-Produced Waters and Impacts to Shallow Aquifer Levels

Demian Saffer and Kurt McCoy¹

EXECUTIVE SUMMARY

The overall project objective for Task #7 is to use a detailed case study to characterize the fate and transport of CBM co-produced waters. Specific project activities focus on evaluating and quantifying the factors controlling the exchange of CBM discharge to shallow groundwater through field data collection, calibration of infiltration and flow models, and transfer of models to the watershed scale.

Specific Tasks

- SubTask 1: Evaluate and quantify controls on fate of discharged waters. Generate both time-averaged and time series of water budgets.
- SubTask 2: Formulate models of surface runoff using field observations, and extend them to investigate at the watershed scale.
- SubTask 3: Evaluate proxies for predicting the fate of CBM waters, including rainfall-runoff analyses and infiltration tests.

INTRODUCTION

Overview of Project and Results

Activities on Task #7, “Controls on the fate of CBM Co-produced waters and impacts to shallow aquifer groundwater quality,” were focused on four fronts: (1) maintaining and downloading data from remote hydrologic field data collection stations, (2) developing water budgets for in-channel impoundments and analyzing temporal trends in the water budgets, (3) using the field data to project watershed scale surface water flows for a range of development scenarios, and (4) evaluating the utility of proxies for infiltration as a tool to predict the fate and transport of CBM discharge *a priori*. In the course of the project, we have recorded data from weirs, shallow aquifer/alluvial monitoring wells, and rain gauges at the Beaver Creek Site. The full dataset extends from July 2003 through the end of 2006. The water budget datasets are limited to non-winter months from 2003-2005. Well hydrograph data are available for the full 3-year period.

Analysis of well water level data indicate a continuing trend of groundwater mounding beneath the stream channel. The rate of mounding has decreased over time. Two well nests at different distances downstream of in-channel discharge sites exhibited water level increases (referenced to a control site) of 2.6 ft and 3.3 ft from July 2003-2004, and rises of 0.9 ft and ~1.2 ft from July 2004-2005. From fall 2005 through October 2006, the relative water levels increased by ~0.8 ft.

¹ Department of Geosciences, The Pennsylvania State University, 310 Deike Building, University Park, PA 16802. Correspondence: dsaffer@geosc.psu.edu.

Water budget analysis shows that conveyance losses in the channel and ponds themselves account for ~50% of the discharged water, with the remainder of discharged water flowing down-channel out of the study area as artificial surface runoff - though this varies substantially through time. Based on infiltration rates deduced from water budget analyses, we project that runoff leaving the study site will fully infiltrate within 2 miles of stream length. The full-time series of water budgets shows that water losses in ponds has decreased systematically over the study period. In contrast, conveyance losses in stream channels have increased and seasonal variation has increased as vegetation cover and transpiration have increased.

The temporal trends in the water budget are a key finding, because they indicate (1) significantly increased peak transpiration losses in the channels over time resulting from vegetation growth, and (2) decreased infiltration rates in the ponds, most likely caused by disruption of clays and/or silting.

Watershed routing models show that for the entire Beaver Creek watershed, surface water loading at the confluence with the Powder River is most sensitive to soil type. Discharge on a per-pond basis has a secondary effect. Incorporation of temporal variability in conveyance losses into surface water routing models illustrates that projected loading to the Powder River from the Beaver Creek watershed should exhibit strong seasonality. Flows during the late fall through early spring will be significantly larger than those during the summer. The long term trend toward increased transpiration does not affect projected winter flow, but decreases the summer flow with each year since initial development. In evaluating impacts of co-produced waters on surface water flows and water budgets, it is critical to consider the range of expected flows rather than a single average value. More realistic and complex models, which include spatial heterogeneity in soils, are necessary to fully understand and estimate flows in future development scenarios.

Analysis of rainfall-runoff response in the study area indicates that the watershed behaves predictably to storm events. Forward models of the rainfall-runoff response are consistent with observations only if (a) there is little dependence on antecedent moisture, and (b) the soils have a high infiltration capacity. This is broadly consistent with field observations, and suggests that similar analyses of gauged watersheds prior to development may be a useful tool for estimating or predicting spatially averaged conveyance losses. Direct measurements of infiltration are consistent with the basic trend of higher infiltration rates in channel reaches than within the ponds, but the magnitude of the directly measured rates is far higher (~10 times larger) than those inferred from the water budget analysis. This suggests that direct infiltration tests are of only limited use for predicting impacts in undeveloped watersheds.

EXPERIMENTAL METHODS

SubTask 1: Evaluate and Quantify Controls on Fate of Discharged Waters. Generate Both Time-Averaged and Time Series of Water Budgets.

The purpose of the field instrumentation at the Beaver Creek site was to establish a water budget and determine the fate of the CBM co-produced water, with emphasis on quantifying conveyance losses. Within the scope of this study, conveyance loss is categorized as evapo-transpiration and/or infiltration. Four v-notch weirs were installed at locations between and downstream of the two in-channel CBM infiltration ponds, in order to separate the study area into four distinct “blocks”, including two blocks with ponds, and two containing only stream channel reaches (**Figure 6.1**). This allowed analysis of water budgets for each separate block. A floating evaporation pan was installed in the upper pond, and a ground evaporation pan was installed next to the upper pond. A rain gauge was placed in the approximate center of the study site. Monitoring wells were installed at four locations to determine the response of the shallow aquifer.

Monitoring wells were installed at three locations; up-gradient of the two CBM ponds, between the two ponds, and downstream of the lower pond. Barometrically compensated water level loggers (Global Water WL-15 Loggers, range 0-15 feet) were installed in one well at each of the three main well sites: BC-3 at the upper Site, BC-6 at the middle Site, and BC-12 at the lower Site. These loggers provide a submersible pressure transducer which measures water depth. These loggers gathered hourly data until the final year of the study period, in which the loggers failed and periodic manual readings were conducted. Manual water level measurements were also gathered at the remaining non-instrumented wells during each field visit, and as a periodic check on data the data logger records.

The monitoring wells at the upper site serve as a control on the regional water level in the shallow aquifer. Because the wells are higher topographically and up-gradient of regional groundwater flow (generally parallel to surface stream flow to the north), the water levels in these wells are assumed to act independently of the CBM co-produced water which begins infiltrating in the upper pond. The wells at the middle and lower sites serve to gauge the shallow aquifer response to this introduction of CBM water at two proximal locations within the site. It is assumed that any change in the upper wells represents a change in the regional water table. Removing the water level changes at the upper well location from the water level change in the middle and lower wells allows quantification of aquifer response (e.g., groundwater mounding) due to infiltrating CBM water.

Assuming steady state, the surface water budget is described by:

$$(CBM\ water + Precipitation + Runoff_{in}) - (Runoff_{out} + Evaporation + Transpiration + Infiltration) = 0$$

Barring a major storm event, $Runoff_{in}$ is equal to zero, and no non-CBM water drains into the system. Recorded rainfall events at the study site tend to be of short duration, and weir surface

flow peaks related to stormflow dissipate relatively quickly. Because rainfall quickly moves out of the system, these time intervals are not included in the water budget analysis.

Evaporation and runoff within each block were calculated following Payne & Saffer (2005). Evaporation losses were determined by the product of the adjusted measured monthly average evaporation rate and the measured area of surface water bodies (channel + pond area) within each block in the study area (**Figure 6.1**). Total conveyance losses were determined by differencing the flow in to each block, including both surface runoff measured at the upstream weir and any CBM discharge within the block (Blocks I and III only), and flow out of the block measured at the downstream weir (Payne & Saffer, 2005; Payne, 2004). Conveyance losses were converted into equivalent rates per unit area by dividing by the measured surface water body area of each block. Daily average values of CBM input to the ponds (Blocks I and III) were obtained from the producing company until late 2005, after which water production was sporadic and the producer changed.

The sum of (transpiration + infiltration) is determined from total conveyance loss, less the evaporation loss. Based on the seasonality of conveyance losses, the components of transpiration and infiltration can be separated by assuming that (1) transpiration decreases to zero from late fall through early spring, and (2) infiltration losses are uniform over the year.

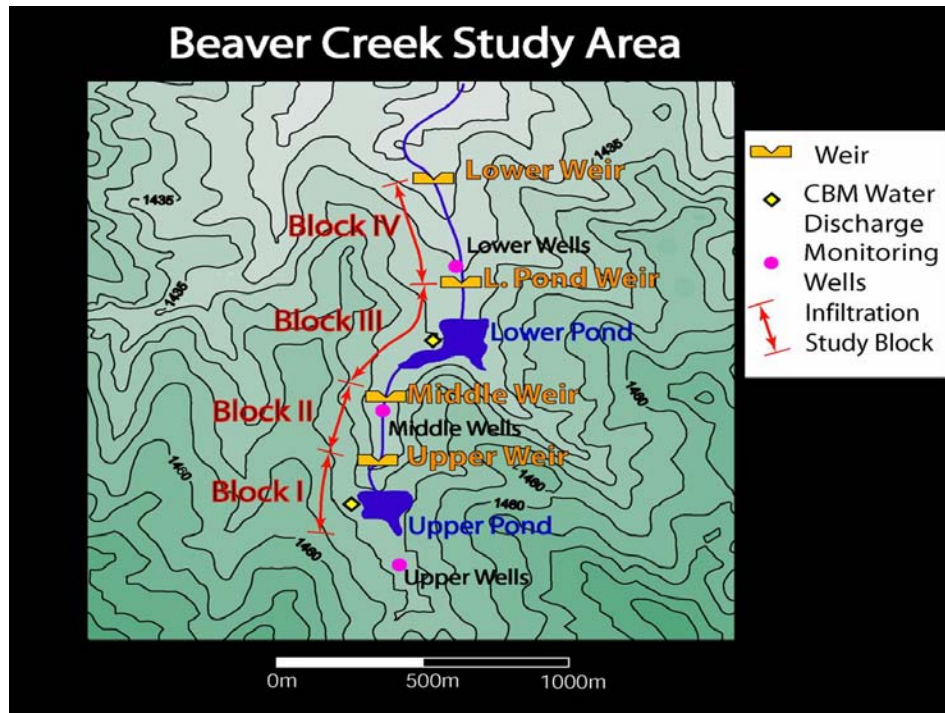


Figure 6.1: Location map of the Beaver Creek Study site showing all field instrumentation and indicating the division of the study area into four separate blocks.

Subtask 2: Formulate and Calibrate Models of Groundwater Flow and Surface Runoff at the Local (Km) Scale Using Field Observations.

Based on good agreement between variably saturated groundwater flow models and field observations of in-channel infiltrative losses (Payne and Saffer, 2005; Payne, 2004), a set of simple surface water routing models were developed for the Beaver Creek watershed as part of Task #7. The goals of these models were twofold. First, the models were used to investigate the sensitivity of simulated surface flow to a variety of forcing factors, including soil type (infiltration capacity) and magnitude of discharge on a per pond basis. Second, the effects of temporal trends in conveyance loss and water production were evaluated.

Surface water runoff is calculated by dividing the main channel of Beaver Creek into a series of stream reaches between (a) discharge ponds, or (b) confluence with tributary streams. Within each reach, discharge decreases with linear stream channel distance based on observed/calculated conveyance losses from SubTask #1. At each pond or tributary, discharge increases. In the case of ponds, it is increased by the CBM water discharged to the pond, less the conveyance loss from the pond itself. For tributaries, discharge is calculated in the same manner as described above for the main channel of Beaver Creek, and any discharge in the channel at its confluence with Beaver Creek is added to that in the main channel.

In these models, the following observations/assumptions are incorporated:

- Infiltration and temporal changes in channel conveyance loss follow the observations from the Beaver Creek study site throughout the watershed.
- Mean monthly evaporation losses follow those measured in floating pan apparatus.
- Pond infiltration losses decrease linearly over time by 0.15 inches/day per year, in accordance with observations from the two ponds at the study site.
- Two scenarios for water discharge to ponds in the watershed are considered: one in which it remains constant through time at or near initial levels, and one in which it decreases over time following the trend expected for individual wells (DeBruin et al., 2001).
- In all simulations, for simplicity, only the discharge permit locations as of 2004 in the Beaver Creek watershed are used (i.e. a static development scenario is assumed) (**Figure 6.2**).

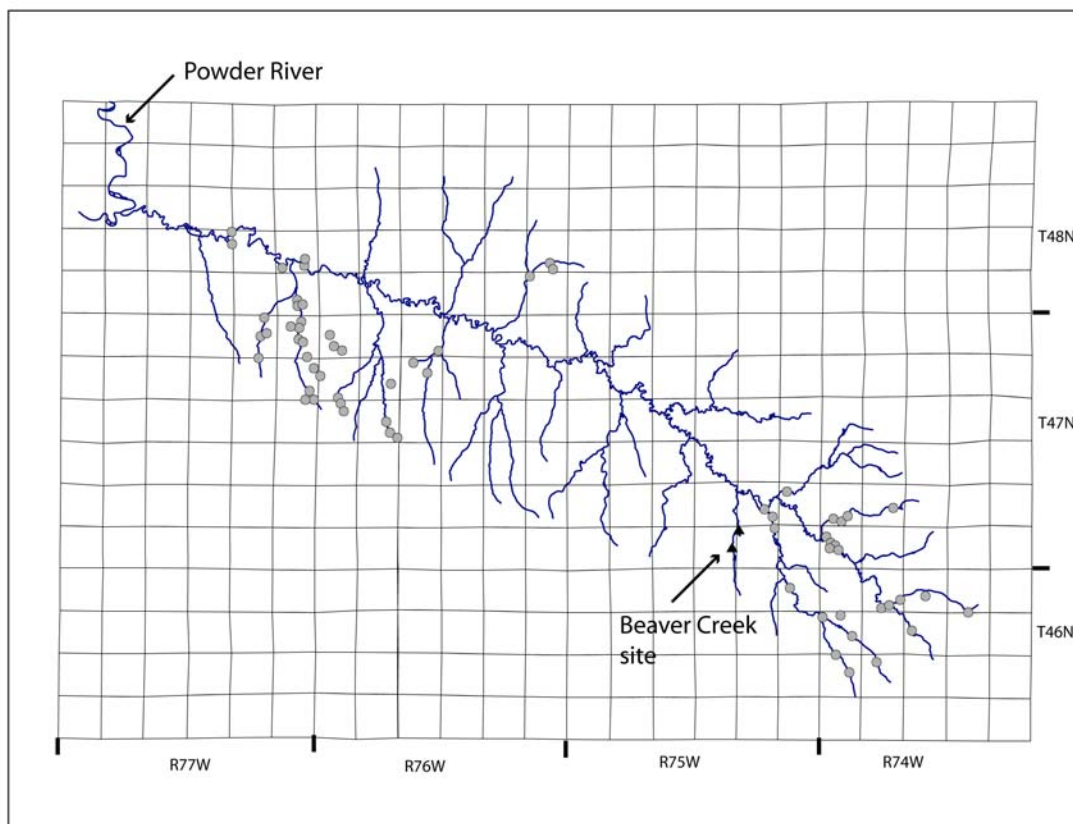


Figure 6.2: Map showing CBM discharge permits in the Beaver Creek watershed as of fall, 2004. The in-channel discharge points (ponds) in this configuration were used for surface water routing models. Results are reported as projected discharge: (a) versus distance along the main channel of Beaver Creek, and (b) at the confluence of Beaver Creek with the Powder River.

Subtask 3: Evaluate Proxies for Predicting the Fate of CBM Waters, including Rainfall-Runoff Analyses and Infiltration Tests.

Infiltration tests

A series of infiltration tests were completed in June 2007 at various locations in the stream channel and upland areas of the Beaver Creek watershed. During this series of fieldwork we obtained data for 10 long-term (12 hr) and 20 short-term tests (2-4 hr) conducted with a double-ring soil infiltrometer. Fieldwork (21 tests) focused on a 2-km section of stream channel both upstream and downstream of two infiltration ponds (**Figure 6.3**). The remaining tests were conducted in the adjacent hillslope areas (4 tests), terrace deposits (3 tests), and exposed pond sediments (2 tests). The intent of the individual site selection was to provide (1) adequate spatial coverage of the main channel and adjacent tributary channel in the area of interest, and (2) a dataset for the evaluation of soil properties in various areas of a watershed receiving CBM discharge.

For each site location GPS coordinates, vegetative characteristics, channel morphology and hydrologic conditions were recorded. Dense vegetation at most sites required cropping prior to placing infiltrometers into the soil. The inner ring of the infiltrometer was inserted to a depth of ~10 cm, filled with water, and the rates of infiltration were recorded on intervals of 15 to 60 minutes. At four sites upstream of the Lower Pond, infiltrometers were inserted into 45 cm deep holes excavated using post-hole diggers. At these four sites, soil moisture, color, texture, and root depth were noted.

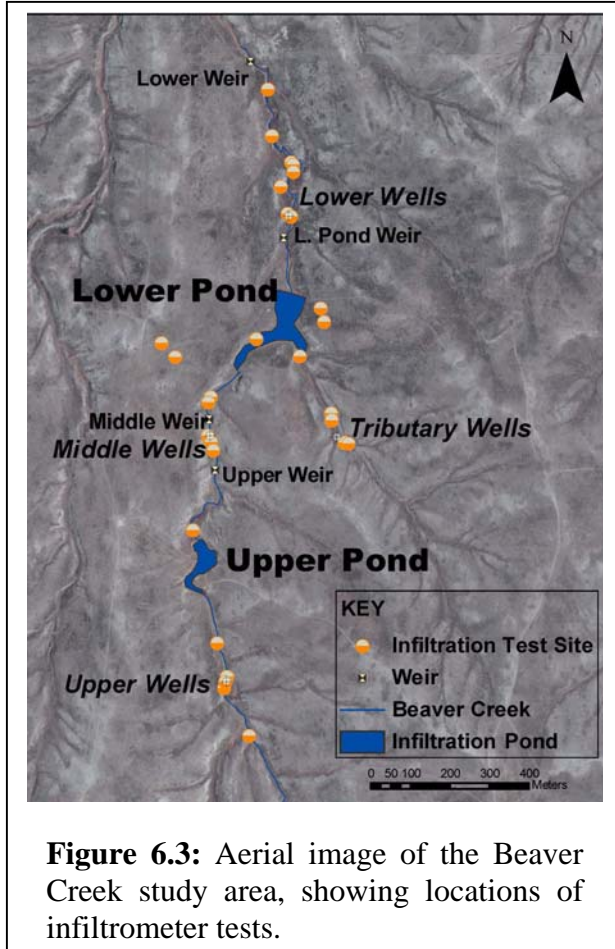


Figure 6.3: Aerial image of the Beaver Creek study area, showing locations of infiltrometer tests.

Data were analyzed using the Philip (1957) two-term model which describes infiltration in unsaturated media. The two-term model is represented by:

$$I = St^{1/2} + At$$

and

$$i = \frac{1}{2}St^{-1/2} + A, (2)$$

where I is cumulative infiltration (L), i is infiltration rate (L/t), S is sorptivity (L/t^{1/2}), t is time, and A (L/t) is a constant that depends on soil properties and is related to the hydraulic conductivity of the media. When t is small, the medium's ability to absorb or desorb water by capillary uptake, S dominates (Williams et al., 1998). When t is large, horizontal infiltration due to gravity increases in importance. By using infiltration data from the field, S and A were defined for all 30 tests using best-fit regression techniques (Tindall et al, 1999).

Values of A were then compared to conveyance losses and calculated infiltration

rates from the water budget analysis (SubTask #1), to evaluate to utility of infiltration tests as a reliable proxy for assessment or prediction of conveyance losses in undeveloped watersheds.

Rainfall runoff models

By determining the effective precipitation (the portion of the precipitation in the watershed that becomes stream discharge), spatially averaged infiltration properties of a watershed can be estimated. Normally, this approach is applied as a forward model to predict runoff from storms of particular intensity and/or duration; here it is used to evaluate the utility of rainfall-runoff systematics as a proxy for infiltration behavior.

In general, the fate of precipitation (W) falling in a watershed can be described by:

$$W_{eff} = W - (E-T + DS_c + DD + Dq),$$

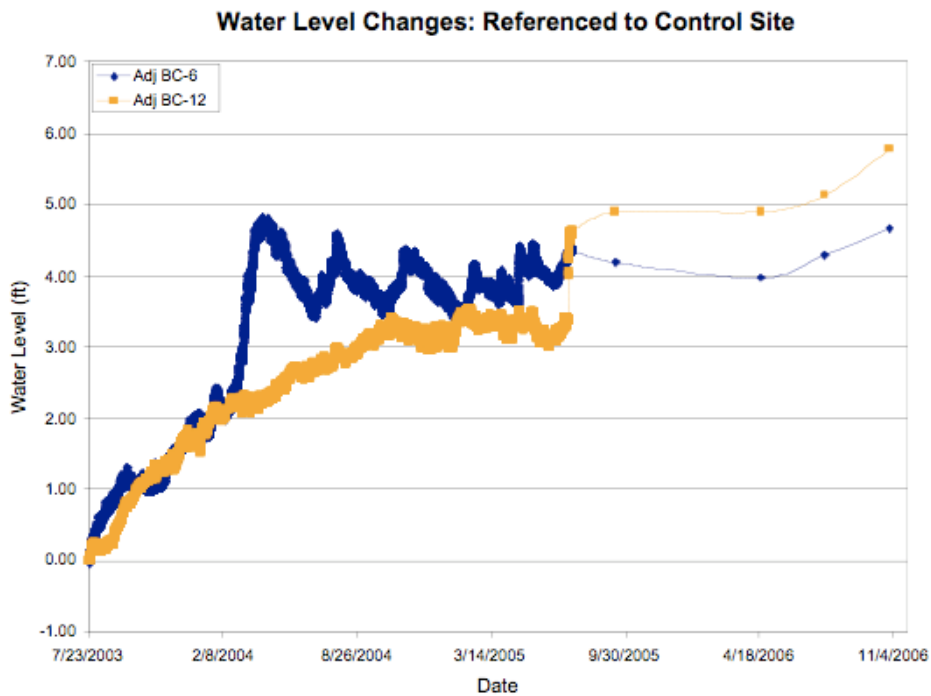
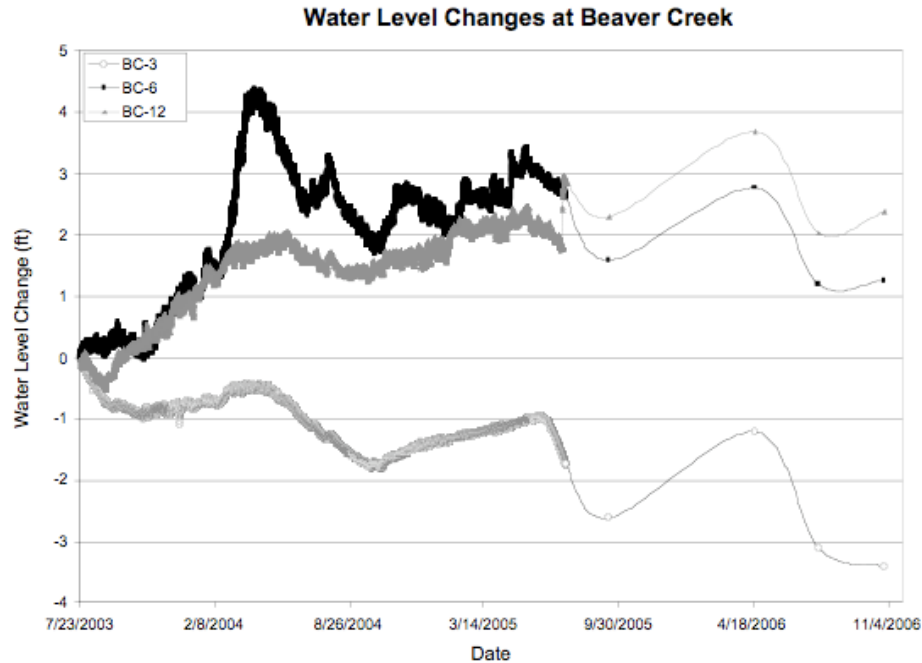
where $E-T$ is evapotranspiration, DS_c is the change in storage in a vegetation canopy), DD is the change in depression storage, and Dq is change in soil water content associated with infiltration. All except Dq are all inconsequential for the small Beaver Creek watershed; $E-T$ is typically small during rainfall events because relative humidity is high ($RH = \sim 100\%$), and D and S_c are negligible at the Beaver Creek site. Therefore, W_{eff} , or the ratio W_{eff}/W , depends primarily on the spatially averaged infiltration properties of the soil in the watershed. For areas characterized by soils with high infiltration capacity, W_{eff}/W is expected to be small, and vice-versa (USCS, 1964).

Total event streamflow can be determined by integration of the hydrograph over time after separation of baseflow. At Beaver Creek, baseflow is constant and approximately equal to the CBM input, and so is easily separated from the hydrograph. The effective precipitation (W_{eff}) is determined for each event by: $W_{eff} = Q_{int}/A_D$, where A_D is the drainage basin area. The drainage basin area is different for each weir, and is calculated from USGS digital elevation data.

RESULTS AND DISCUSSIONS

SubTask 1: Evaluate and Quantify Controls on Fate of Discharged Waters. Generate Both Time-Averaged and Time Series of Water Budgets.

Water levels at Beaver Creek monitoring wells indicate the infiltration of co-produced waters from the stream channel and ponds, and associated groundwater mounding beneath the stream channel. Water levels at all three nested monitoring sites (pink circles in **Figure 6.1**) vary over time due to both seasonal recharge and variations in precipitation and snowmelt from year to year (see BC 3 record in **Figure 6.4a**). After differencing the “control” hydrograph from those for the wells within the area influenced by CBM discharge (BC-6 at the middle site; BC-12 at the lower site), the contribution of groundwater mounding due to infiltration of co-produced waters can be isolated (**Figure 6.4b**). The results indicate continued water level increases when compared with the control site (**Figure 6.4b**). Notably, the rate of water level increase has decreased over time. This is expected, due to (1) spreading of the groundwater mound as the lateral head gradients increase over time, and (2) decreased and intermittent flows out of the two ponds due to declining water production.



Figures 6.4a and 6.4b: a) (Top). Well hydrographs for monitoring wells within well nests at the southern (BC-3), middle (BC-6), and northern (BC-12) positions shown on **Figure 6.1**. All hydrographs are referenced to zero at the start of data logging on July 23, 2003, to show changes in water level since project inception. b) (Bottom). Hydrographs for BC-6 and BC-12, with the assumed regional water level changes removed (as recorded in the control well BC-3).

Water budget calculations document systematic decreases in conveyance losses over time for the pond-dominated blocks (Blocks I and III) (**Figure 6.5a**). When evaporation losses are taken into account, a consistent trend of decreasing infiltration + transpiration losses is apparent (**Figure 6.5b**). Because the ponds have little or no vegetation, transpiration losses are assumed to be negligible, and the total conveyance losses less evaporation provides a close approximation of infiltration losses (**Figure 6.5b**). This trend of decreasing infiltration loss over time in both pond blocks is attributed to the effects of salts on clay permeability, and settling of fine particles in the ponds.

For the stream channels, the water budget calculation shows that (1) peak conveyance losses have *increased* over the study period due to growth of vegetation cover and the accompanying increase in transpiration losses, and (2) the magnitude of seasonal variability in conveyance loss is substantial and has increased as vegetation density has increased from year to year (**Figures 6.6a-b**). The channel conveyance losses can be fit by a sinusoidally varying transpiration component that increases in amplitude linearly with time, combined with a constant infiltration component. Overall, the water budget results imply that vegetation changes (growth, expansion, and changes in dominant species in the stream channel) that occur in response to increased water availability from produced water discharge will slowly change the local water budget and cause a decline in the volume of surface discharge that reaches the Powder River during summer months. During winter months, the vegetation is dormant and has a minimal effect, and the volume of water reaching the Powder River should depend primarily on infiltration.

Based on the data shown in **Figures 6.6a-b**, the conveyance losses can be separated into a “baseline” infiltration component of 1.5-2 in/d, which remains constant throughout the study period, and transpiration losses that increase from 2.2 in/d in Block IV and 0.5 in/d in Block II in year 1, to 4.3 in/d and 3.3 in/d in year 2, respectively, to 6.8 in/d in year 3 (Block IV only). This increase is coincident with the qualitative observation of significant increase in peak vegetation cover over time (**Figure 6.7**). Evaporation losses are negligible in comparison, ranging from 0.04 inches/day in the winter, to 0.25 inches/day in July-August.

Comparison of the two stream reaches in the study area illustrate additional complexities related to stream channel morphology that must be considered. Specifically, in Block II (the upper stream reach), which runs in a broad, shallow channel, the temporal evolution of conveyance losses is different than in the well-confined lower channel of Block IV (**Figures 6.6a-b**). In general, the same monotonic increase in transpiration with time is evident in both reaches, but the signal is superimposed on significant variations in channel width in Block II associated with increased discharge. As a result, in this channel reach, conveyance losses are largest during spring runoff, when transpiration and infiltration act as sinks over a large channel area. At these times, transpiration is moderately increased, and channel width is extremely large due to runoff and snow melt. In summer, conveyance losses are moderate, due to offsetting factors of increased transpiration (which tends to increase conveyance loss), and decreased channel area.

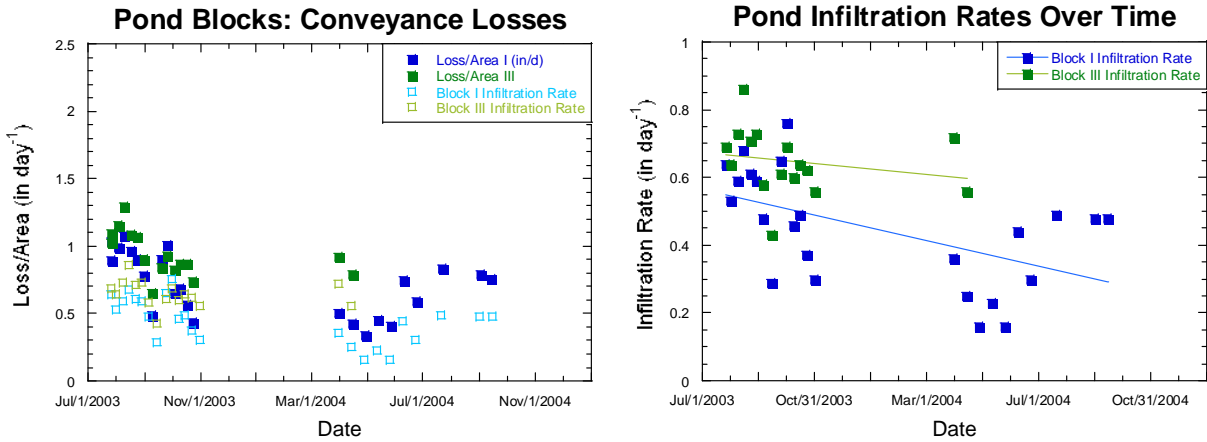


Figure 6.5a and 6.5b: a) (left): Total conveyance loss in pond blocks determined for two-week intervals. (Blocks I and III), normalized by area. B) (right): Infiltration loss in Blocks I and III.

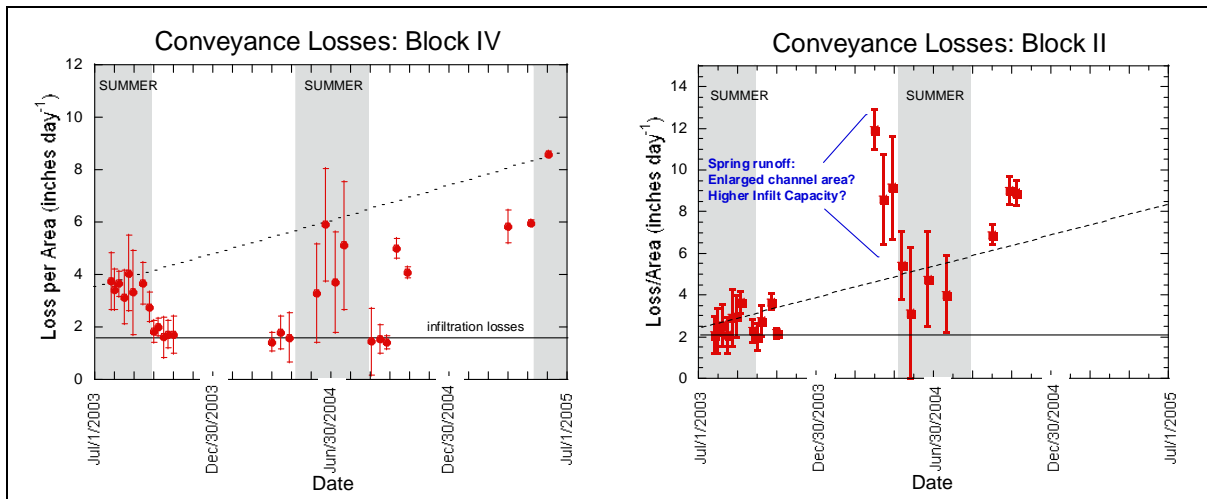


Figure 6.6: a) (left) Time series of conveyance losses in stream channel for well-confined channel reach in Block IV. B) (right) Conveyance losses for the broad, shallow channel reach in Block II. Conveyance losses during the cold months reflect only infiltration (solid line). Increased peak losses during the summer are not explained by evaporation, and are interpreted to reflect increasing transpiration losses. This trend is shown by the dashed line. Note that highest conveyance losses in the broad channel of Block II occur in spring and fall.



Figure 6.7: Top Left: Photo of stream channel North of Lower Pond (in Block IV) in July, 2003. Top Right: Photo of stream channel (taken near the shrubs on the left bank of the channel in the photo to left) in July, 2005. Bottom Left: Photo of stream channel North of Upper Pond (in Block II) in July, 2003. Bottom Right. Stream channel in April, 2006 (photo taken upstream of wells and of photo at left; wells can be seen in the distance).

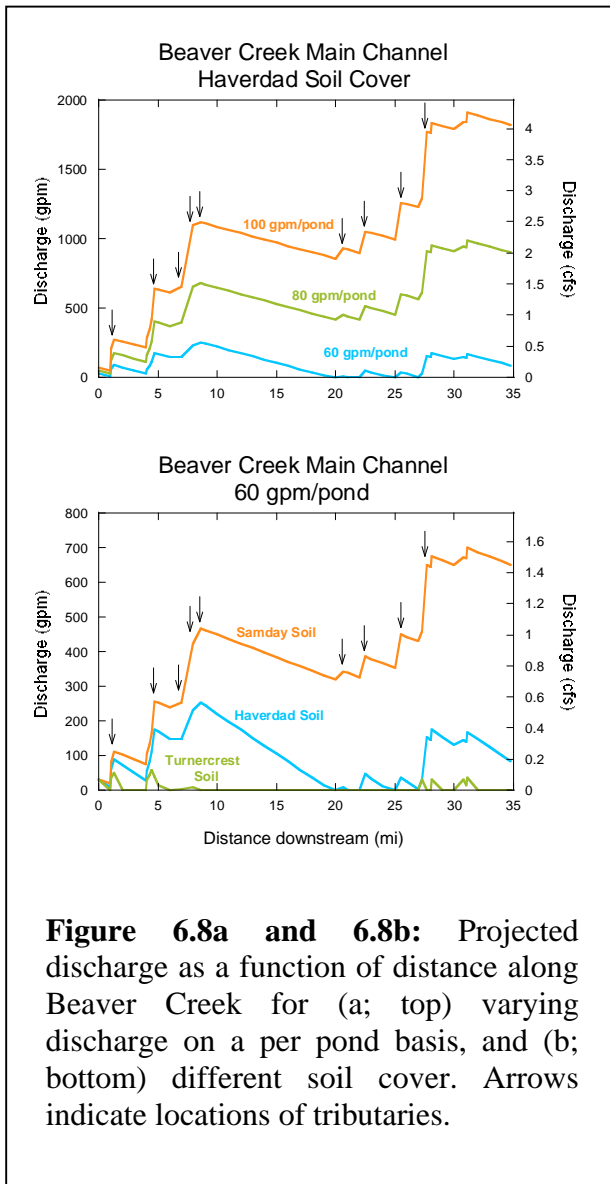
Subtask 2: Formulate and Calibrate Models of Groundwater Flow and Surface Runoff at the Local (Km) Scale Using Field Observations.

Watershed routing model results indicate that surface flows are sensitive to both the magnitude of discharge on a per pond basis (**Figure 6.8a**) and the soil infiltration capacity (**Figure 6.8b**). For the sensitivity analysis, surface water flows were projected for several scenarios:

- To evaluate sensitivity to discharges on a per pond basis, a uniform soil cover was assumed for the entire watershed, and the discharge per pond was varied from (60 gpm to 100 gpm). These projections used the infiltration rates of 2.3 in/day simulated by Payne (2004) for the Haverdad soil, a soil type mapped throughout the Powder River Basin, and characterized by an intermediate infiltration rate (Munn & Arneson, 1999; Payne, 2004)
- To evaluate sensitivity to soil cover, three mapped soils within the Powder River Basin were considered. For these projections, the discharge per pond was fixed at 60 gpm. The three soil types were chosen to reflect the full range of infiltration rates for mapped soils in the basin as simulated using a variably saturated groundwater flow model Payne (2004): the Samday soil, characterized by a low

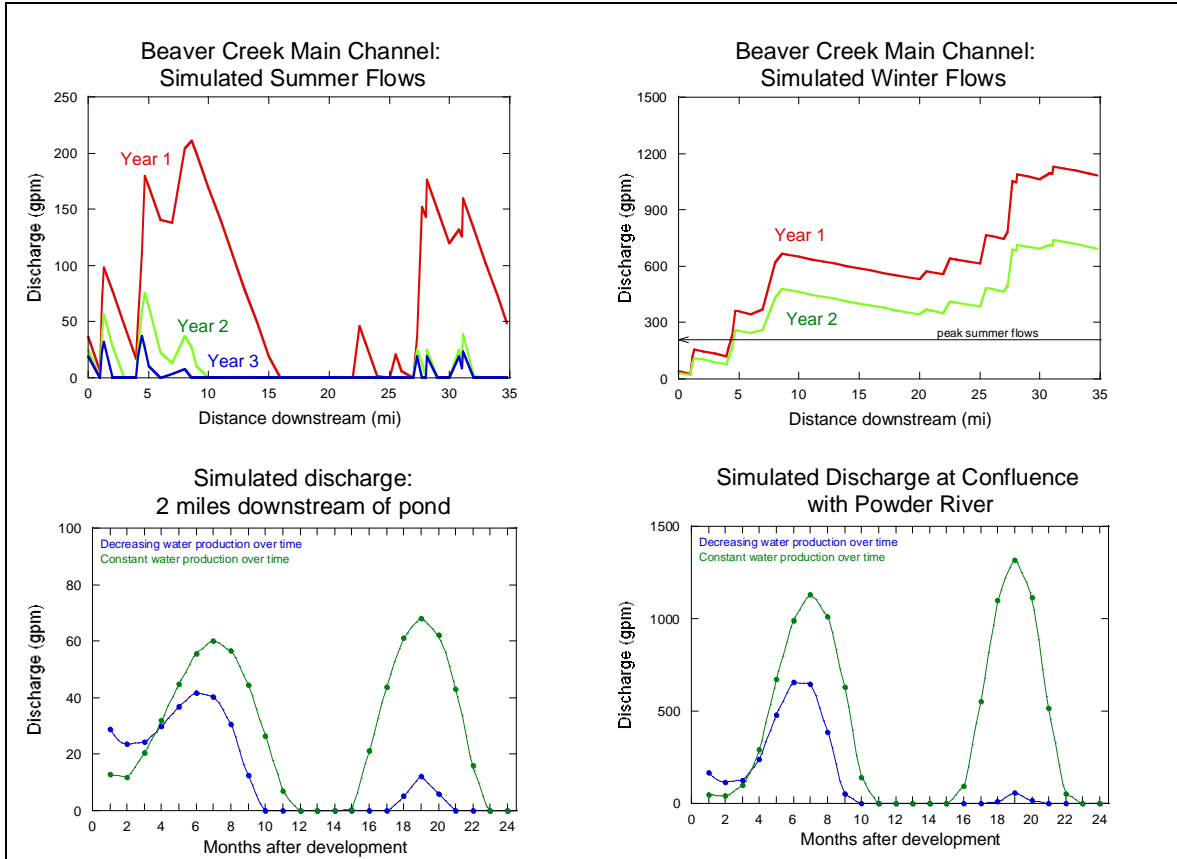
infiltration capacity (1.2 in/day); the Haverdad soil (described above); and the Turnercrest soil, characterized by a high infiltration capacity (8.4 in/day).

Results show that surface discharge at the confluence of Beaver Creek and the Powder River (referred to herein as “surface water loading” of the Powder River) increases substantially as per pond discharge increases. For discharge of 60, 80, and 100 gpm per pond, projected surface water loading is 90 gpm (0.2 cfs), 900 gpm (2 cfs), and 1800 gpm (4 cfs), respectively (**Figure 6.8a**). As soil infiltration capacity decreases, surface water loading also increases markedly. For the Turnercrest, Haverdad, and Samday soils (and a fixed per pond discharge of 60 gpm), surface water loading is 0 gpm, 90 gpm, and 650 gpm, respectively (**Figure 6.8b**).



When temporal trends in both water discharge and conveyance losses from SubTask #1 are incorporated into the surface water discharge projections, increasing transpiration losses coupled with dropping production dominate summer flow. These effects result in strong decreases in summer surface water loading to the Powder River over time, as well as extended lengths of dry stream channel (**Figure 6.9a**). Winter flows are less variable between simulation years, because conveyance losses are less variable and reflect only the decreasing infiltration capacity of ponds. In general, simulated winter surface water loading is considerably larger than for summer, and there should be no significant lengths of dry channel (neglecting the possibility of freezing) (**Figure 6.9b**). Decreased production over time outweighs the effects of decreasing pond conveyance losses, and results in an overall decrease in simulated winter flow between years 1 and 2.

For a scenario with constant water production (and constant discharge to ponds), peak winter flow increases each year due to the decrease in pond infiltration (**Figures 6.9c-d**). Summer flows decrease each year, and the length of time over which the channel is dry increases, due to the increase in transpiration losses. For the case of declining water production over time, both the simulated summer and winter flows are reduced (**Figures 6.9c-d**).



Figures 6.9a through 6.9d: a) (top left): Simulated July discharge in the main channel of Beaver Creek from headwaters (distance = 0 miles) to its confluence with the Powder River (distance = 35 miles), for a scenario with decreasing water production through time. b) (top right) Simulated December discharge. Line shows the magnitude of the peak summer flow in year 1 for comparison. Discontinuities in flow reflect the confluence of tributaries with the main channel. c) (bottom left) and d) (bottom right): Simulated discharge through time after initial development: 2 miles downstream of a simulated “generic” pond (c), and at the confluence of Beaver Creek with the Powder River (d).

Subtask 3: Evaluate Proxies for Predicting the Fate of CBM Waters, including Rainfall-Runoff Analyses and Infiltration Tests.

Rainfall runoff models

Results of rainfall-runoff models show that for the study area, W_{eff} increases with W , but the ratio W_{eff} / W is generally very small, ranging from 0.002 to 0.2 (**Figure 6.10**). In general, this is broadly consistent with high infiltration rates, which limit runoff. To more precisely evaluate the implications of the rainfall-runoff data as a predictor of infiltration properties, runoff was modeled using the SCS method (U.S. Soil Conservation Service, 1964). In this method, W_{eff} is related to W through a set of empirical parameters that describe general soil infiltration behavior and antecedent moisture conditions. The results show that in order to fit the data, there must be

little dependence on antecedent moisture, and SCS soil types with moderate to high infiltration capacity (0.15-0.30 in/hr) are necessary (**Figures 6.10a-b**).

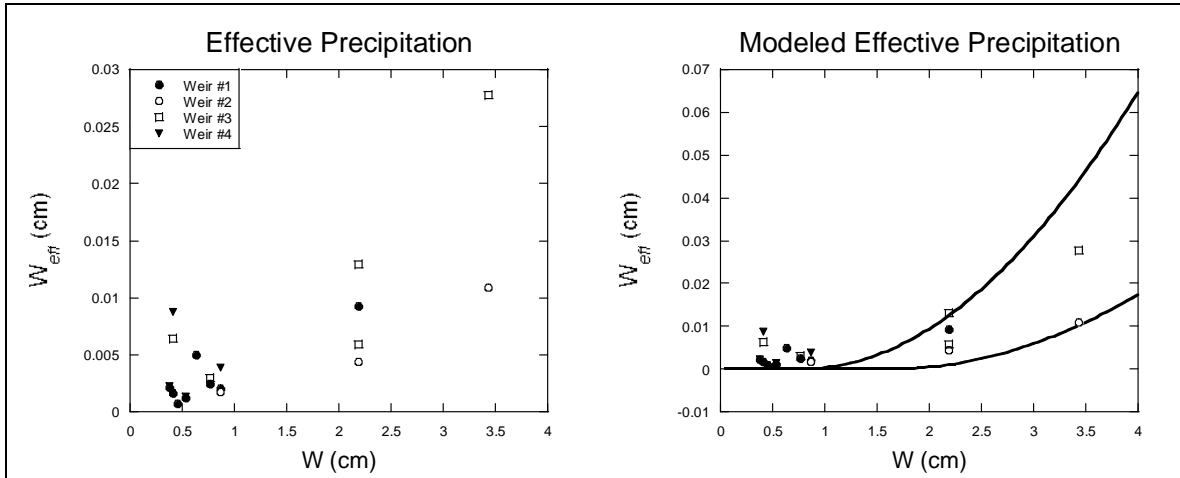


Figure 6.10a and 6.10b: Plots of W_{eff} vs. W . a) (left): W_{eff} determined as described in text, W measured directly by tipping bucket rain gauge at Weir #2, for all precipitation events from July, 2003 through Oct., 2005. b) (right): Data plotted with modeled W_{eff} based on SCS method. Upper curve corresponds to a curve number (CN) of 8, lower curve is for CN = 6.

These model results are consistent with the observation of high infiltration capacity in the Beaver Creek watershed (c.f. **Figure 6.6**), and with data indicating that runoff does not increase with antecedent rainfall (**Figure 6.11**). Broadly, the systematic and consistent results suggest that the use of rainfall-runoff models holds promise as a tool for predicting watershed response to CBM discharge. However, considerably more detailed work is needed in order to use such data sets as a quantitative predictor of infiltration.

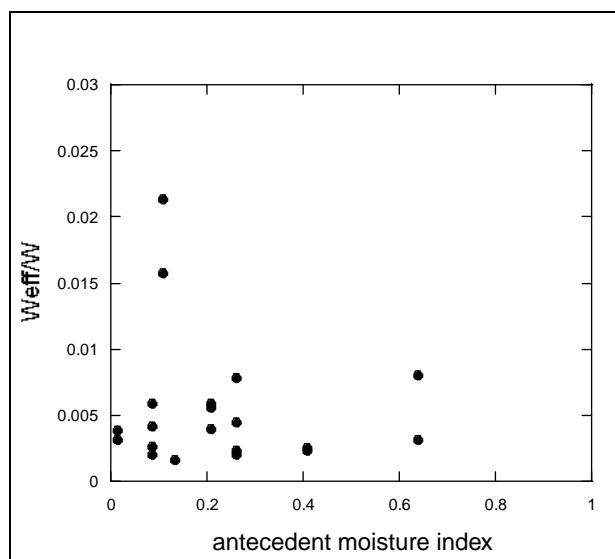


Figure 6.11: W_{eff} vs. antecedent rainfall, indicating little dependence of W_{eff} (and therefore of infiltration losses).

Infiltration tests

Downstream of the Lower Pond the stream channel becomes incised and steep banks rise as much as 3 meters above the channel bottom. Cores showed the soils in the incised section to be near saturation prior to testing and the depth to water to range from 13 to 26 cm below land surface. Results from infiltration tests characterize this area by low S (3.65 mm/hr^{1/2}) and high A (41.8 mm/hr) values that likely represent the dominance of gravity driven infiltration in nearly saturated soils (**Figure 6.12a; Table 6.1**). The morphology of the incised section is in contrast with wider channels at the base of gentle slopes upstream of the Lower Pond. In this section, the main channel is 10 to 15 meters in width and soils were initially unsaturated to depths exceeding 45 cm. S and A values in this section of stream were 25.4 mm/hr^{1/2} and 32.6 mm/hr¹ upstream of the Upper Pond and 5.02 mm/hr^{1/2} and 28.6 mm/hr downstream of the Upper Pond, respectively. The results of tests outside of the channel on adjacent hill slopes and terrace deposits showed higher values of S and A than those noted within the channel (**Table 6.1**).

Four test holes dug to 45-cm depth were used to assess the variability of infiltration with depth in the main stream channel and the influence of vegetation on test results. Soil structure at this depth was thought unaffected by transpiration or fracturing of the soil due to vegetation; root depths at these sites ranged from 21 to 26 cm. The results in figure 7 indicate that 3 of the tests on the 45-cm deep holes resulted in S values of 0.15 mm/hr^{1/2} and A values of 5.06 mm/hr¹, amongst the lowest in the entire dataset. The fourth test resulted in S of 65.4 mm/hr^{1/2} and A of 125 mm/hr¹ which were comparable to results from the adjacent terrace and hillslope deposits. This anomaly occurred in an area characterized by drier soils than at the other 3 sites, and it may be the result of sediment reworking near the base of a breached dam. These results, excepting of this anomalous test data, suggest that infiltration through the subsurface clearly diminishes at or below the depth of the root zone.

The effects of transpiration were noted in 4 of the 12-hr tests which were conducted in heavily vegetated areas; 2 tests in the tributary channel, 1 test in the main channel, and 1 test on terrace deposits at the site of the lower wells. In these four cases, cumulative rates of infiltration initially decreased as expected during the first early morning hour of testing (**Figure 6.12b**). At the onset of prime sunlight hours, infiltration rates at these sites began to increase and continued to rise until evening hours. Three of these 4 cases are in areas presumably unaffected by CBM discharge; however, their results show that transpiration by in-stream vegetation may constitute a significant component of the overall water budget.

Overall, the values of A, which are thought to reflect infiltration rates under saturated conditions (closely approximating saturated hydraulic conductivity), are considerably higher than the infiltration rates – as well as the total conveyance losses per area – determined by water budget analysis. The directly measured infiltration capacity for the pond is 2.7 in/day; for the main channel, values range from 21 – 57 in/day. These are approximately on order of magnitude larger than the infiltration rates inferred from the water budgets or 0.2-0.6 in/day for the ponds, and of ~2 in/day for the stream channel.

Table 6.1: Infiltrometer testing results by category from Beaver Creek, northeastern Wyoming. Key: #, number of tests; S, sorptivity ($\text{mm}^2 \cdot \text{hr}^{-1/2}$); A, soil conductivity parameter ($\text{mm}^2 \cdot \text{hr}^{-1}$).

Category	<12-hr test			12-hr test		
	#	S	A	#	S	A
<i>Channel Location</i>						
pond	2	0.54	2.86	-	-	-
main channel	10	2.15	46.2	7	1.29	26.4
tributary channel	2	3.28	56.9	2	5.32	201
outside channel	5	30.6	103	1	32.1	105
<i>Channel Morphology</i>						
channel w/steep banks	4	2.86	75.6	4	1.58	38.5
channel w/gently sloping banks						
upstream of Upper Pond	4	15.3	54.2	2	22.8	36.4
downstream of Upper Pond	6	5.64	38.2	2	5.02	28.6
hillslope	4	31.0	103	-	-	-
terrace	2	35.7	109	1	32.1	105
<i>Depth</i>						
Surface	16	1.58	66.2	10	0.23	73.4
45-cm depth	4	0.85	23.1	-	-	-

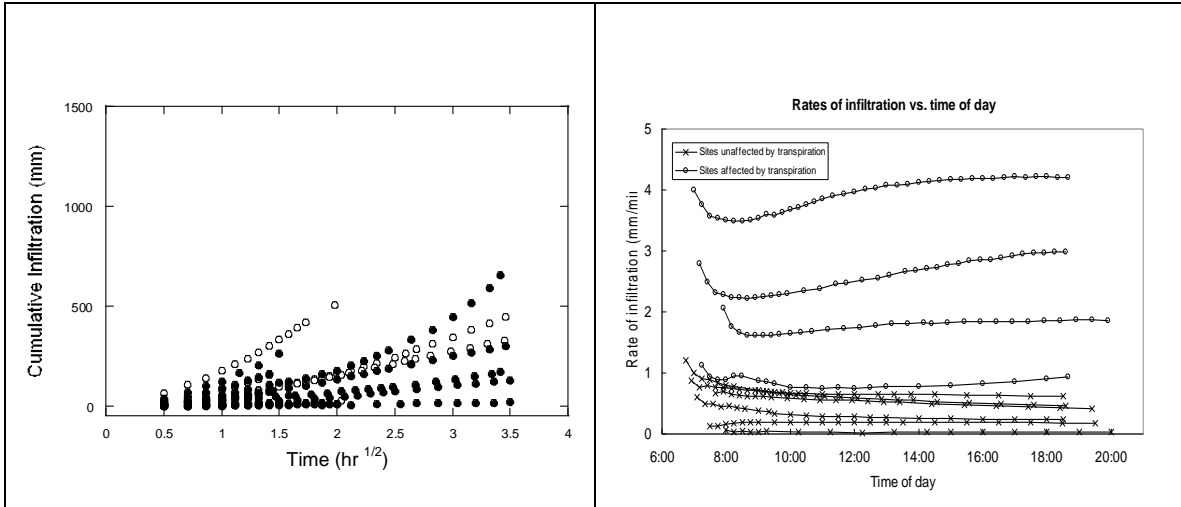


Figure 6.12a and 6.12b: a) (left): Results for full suite of infiltration tests conducted in the main channel of Beaver Creek. Open symbols are for tests upstream of the CBM discharge (above the “Upper Pond”). Closed symbols are downstream of CBM discharge points. b) (right): Infiltration rate (from infiltration tests) as a function of time of day.

CONCLUSIONS

1. Use of reference wells is a useful approach to isolate the effects of CBM discharge-related groundwater mounding. Results from this study document ~5-6 feet of mounding over a 3 ½ year period.
2. Conveyance losses in the Beaver Creek watershed are generally moderate to high (2–8 in/day in channels, and 0.2 – 1.0 in/day in ponds).
3. Temporal variation in conveyance losses is a key factor that must be considered when projecting the fate and transport of CBM co-produced waters. Specifically, peak conveyance losses in the channels themselves are expected to increase over time, as vegetation density increases and streambed ecology responds to increased water availability – both leading to increased transpiration. This also results in a significant seasonality to conveyance losses, which should result in considerably smaller surface water flows in the peak growing season (late spring through early fall).
4. Surface water flows are sensitive to both soil type and discharge on a per pond basis.
5. Rainfall-runoff analyses and infiltration tests are broadly consistent with observations of conveyance loss, in that they produce similar trends. However, these approaches are not immediately useful as quantitative proxies for infiltration or conveyance loss. Variably saturated groundwater flow models, coupled with detailed information about soil texture, remain the best quantitative predictor of infiltration losses (Payne ,2004).

REFERENCES

- De Bruin, R.H., Lyman, R.M., Jones, R.W., and Cook, L., 2001.** Coalbed methane in Wyoming: Wyoming State Geological Survey Information Pamphlet 7 (revised), 19 pp.
- Munn, L. C., and Arneson, C. S., 1999.** Draft 1:100,000-Scale Digital Soils Map of Campbell County: University of Wyoming Agricultural Experiment Station.
- Payne, 2004.** Surface water hydrology and shallow groundwater effects of coalbed methane development, upper Beaver Creek drainage, Powder River Basin, WY, MSc Thesis, University of Wyoming, 131 pp.
- Payne, A., and Saffer, D.M., 2005.** Surface water hydrology and shallow groundwater effects of coalbed methane development, upper Beaver drainage, Powder River Basin, WY, in Zoback, M.D. (Ed.), Wyoming State Geological Survey, Report of Investigations, v. 55.
- Philip, J.R., 1957.** The Theory of Infiltration: 1. The Infiltration Equation and Solution, Soil Science, vol. 83:345-357.
- Tindall, J.A., Kunkel, J.R., and Anderson, D.E., 1999.** Unsaturated Zone Hydrology for Scientists and Engineers: Prentice Hall, New Jersey, p. 624.
- U.S. Soil Conservation Service, 1964.** Hydrology. Section 4. SCS National Engineering Handbook. U.S. Soil Conservation Service.
- Williams, J.R., Ouyang, Y., and Chen, J-S., 1998.** Estimation of infiltration rate in the vadose zone: application of selected mathematical models Vol. II, U.S. EPA report 600/R-97/128b, 117 p.

TOPIC AREA: BENEFICIAL USE

CHAPTER 7: Agricultural Application of Untreated CBM Waters

Terry Brown¹

EXECUTIVE SUMMARY

Use of saline waters with a high SAR (sodium adsorption ratio) for irrigation of agricultural lands can lead to decreased productivity caused by a phenomenon known as soil dispersion (loss of soil structure) that results in decreased soil permeability. This research was conducted to examine the effect of untreated CBM co-produced waters on the physical and chemical nature of Powder River Basin soils and ways to mitigate associated soil damage. To accomplish this goal, four different studies were undertaken; 1) an irrigation site (WJ Research Site) was established to study the physical and chemical changes to soil when using untreated CBM water for irrigation, both with and without the use of soil amendments intended to prevent soil damage, 2) a USDA soil salinity model (FAO-SWS) was calibrated for use in the Powder River Basin and used to predict the effects of using untreated CBM water and soil amendments for a 10 year period, 3) soil fertility studies were performed to assess the impact of untreated CBM water and soil amendments on crop productivity and 4) a study was conducted to examine the efficacy of using applications of gypsum to reclaim soils impacted by untreated CBM water.

Task one was the WJ Research Site. This is a unique study in that it is the first time the effects of applying untreated Powder River Basin CBM water to soil have been systematically studied on a field-scale basis. The field site was first instrumented with probes and data loggers to measure soil moisture, solution salt content, and temperature during the irrigation season. Additionally, a lysimeter (Gee Drain Gauge) was placed below an intact, vegetated soil monolith to measure water infiltration rate. Soil samples were collected and analyzed so that baseline soil chemistry and hydraulic properties could be evaluated preceding the installation of two center-pivot irrigation systems. Various amounts of gypsum and sulfur, known to alleviate soil damage from sodic water containing carbonate, were applied to test plots and then CBM water was applied by the center-pivots for an abbreviated first season followed by a full second irrigation season. Soil samples were collected and analyzed following both irrigation seasons. Visual evaluation of the test plots following the first irrigation season indicated that the amendments were successful in maintaining soil permeability while untreated plots suffered reduced permeability as evidenced by ponding and crusting of soil. The conditions of the soil at the end of the second irrigation period were noticeably deteriorated compared to the previous year. The soil surfaces for all treatments were dispersed. The primary reason for the dispersion can be attributed to the fact that the amendments were depleted during the second irrigation season due to dissolution, indicating that more amendments need to be applied for continued soil protection.

For the second task, an irrigation model was completed using baseline conditions to simulate projected soil conditions over a 10-year period. The data collected from the research plot was compared to the results of the model to determine whether additional calibration was needed for

¹ Poudre Valley Environmental Sciences, Inc., 2835 Schooners Court, Loveland, CO 80538. Correspondence: tbrown1400@comcast.net.

Wyoming and Montana climatic conditions. After 2 seasons of irrigation, the data collected at the field irrigation site appear to support the initial model calibration.

For task three, soil fertility evaluations were conducted to determine the impact of soil amendments and CBM produced water on the production of alfalfa. The work was accomplished at two center-pivot sites located north of Sheridan, Wyoming and in a greenhouse study conducted at Colorado State University. Adverse impacts to soil fertility were attributed to phosphorous deficiency and low soil pH. The phosphorous deficiency is likely due to the addition of gypsum (added to decrease soil SAR), causing the precipitation of calcium phosphate minerals (e.g., hydroxyapatite). This finding shows that fertilizer applications will be required at some irrigation sites. The low soil pH was caused by the application of sulfur as an amendment to remove carbonate from the CBM water (oxidation of elemental sulfur produces sulfuric acid, the acidic conditions promote off-gassing of carbonate as CO₂). Ag-lime can be added to increase the soil pH and buffering capacity. The results illustrate the need to closely manage the application of amendments based on soil conditions throughout the irrigation period.

And finally, for task four, reclamation of sodic soil sites impacted by CBM produced water was accomplished by applying two tons of gypsum per acre at the surface without incorporation. One year after amendment application, soil evaluations showed a decrease in the average SAR value. The decline in SAR values at the site translated into a less dispersed soil. The reclamation was achieved with no supplemental irrigation (natural climatic conditions). Data show that gypsum re-established soil conditions that support productive plant growth under the climatic conditions existing in northern Wyoming.

INTRODUCTION

Irrigation with untreated Powder River Basin (PRB) CBM co-produced water can lead to the loss of soil structure, a process known as dispersion. Soil dispersion results in a compacted soil that has little permeability so that water runs off the surface rather than infiltrating, decreasing crop production. Soil dispersion is caused when divalent cations, primarily calcium and magnesium that normally form ionic bridges between clay particles are displaced by mono-valent cations such as sodium causing the bridge to be destroyed. A ratio known as the sodium adsorption ratio (SAR) that characterizes the amount of sodium in a water relative to the amount of magnesium and calcium is commonly used to predict when soil dispersion will occur. Typically, water with a SAR of less than 4 is considered to be safe for irrigation purposes, PRB water has a SAR much higher than 4.

CBM water can cause soil dispersion in two ways. First, CBM water is typically high in sodium and low in divalent cations, leading to the displacement of divalent cations in the soil structure with sodium ions. Secondly, PRB CBM water also has a high carbonate concentration. The high carbonate concentration leads to scavenging of calcium and magnesium ions from the soil through the precipitation of CaCO₃ and MgCO₃ minerals, lowering the soil water SAR. Two strategies can be used to combat these effects. The mineral gypsum (CaSO₄) can be added to the soil. Gypsum is highly soluble and increases the Ca²⁺ concentration in soil water. The other strategy commonly used is to add elemental sulfur as a soil amendment. Microbially catalyzed

oxidation of elemental sulfur produces sulfuric acid, the acidic conditions promote off-gassing of the carbonate ions in the CBM water as CO₂.

SUBTASK 1: APPLICATION OF UNTREATED POWDER RIVER BASIN CBM WATER TO SOIL

Subtask 1.1: Collect Baseline Soil Chemistry, Soil Hydraulic Properties and Produced Water Chemistry at the WJ Irrigation Site

Initial site evaluation

The WJ (initials of land owners) irrigation site that was used to evaluate the use of amendments intended to prevent degradation of soil structure was characterized. Soils were characterized using thirteen backhoe pits. Soil samples were collected by horizon and were analyzed. The location of the soil pits are shown in **Figures 7.1 and 7.2**. The soil morphological properties were evaluated according to USDA National Soil Survey Center Standards. A single soil series covers the site with the most variability associated with differences in texture class (**Figure 7.3**).

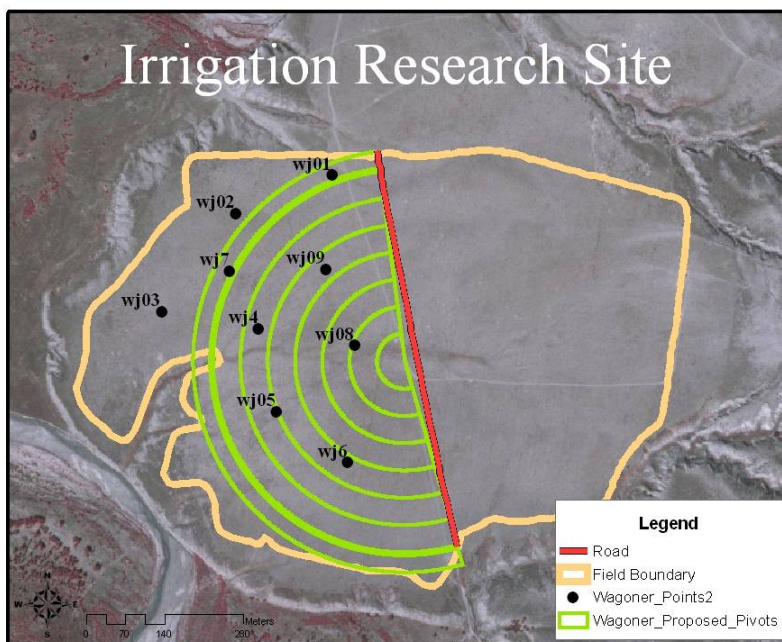


Figure 7.1: Field test site showing the location of the half-pivot irrigation system (green lines) and locations of soil evaluation pits (black points).

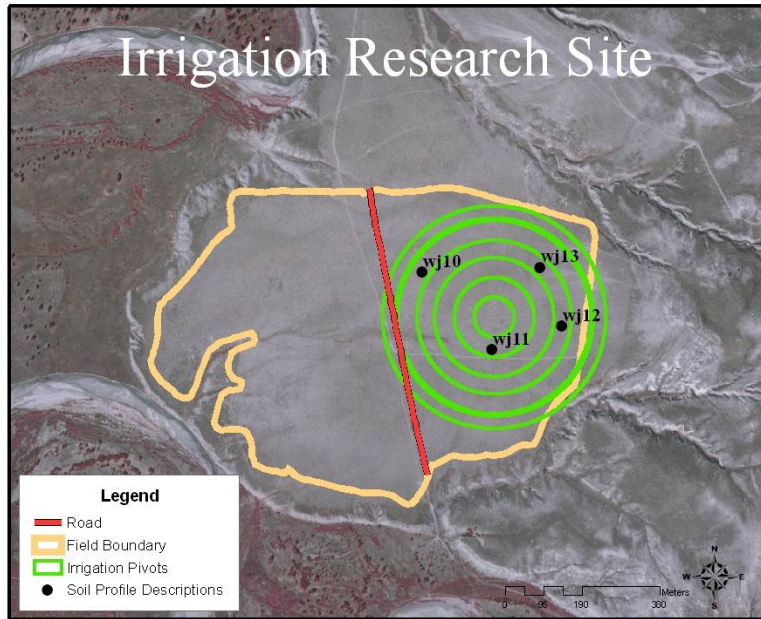


Figure 7.2: Field test site showing the location of the full-pivot irrigation system (green lines) and locations of soil evaluation pits (black points).



Figure 7.3: Typical soil profile associated with the WJ research site.

Experimental design and baseline development

The experimental design was developed with the cooperation of the Statistics Department at Colorado State University. Eight plots were established at randomly located sites in the two pivot areas. Each plot consisted of seven treatments. The treatment subplots were 5m (W) by 5m (L). The treatment subplots were oriented side by side in an area that was 10 meters (W) by 15 m (L) with one 5m by 5m plot placed adjacent to one of the subplots at the end of the plot. The diagram shown in **Figure 7.4** shows the orientation of the subplots. Baseline soil chemistry conditions were determined by collecting 1 sample from each subplot located in each plot, resulting in a treatment replication of 8.

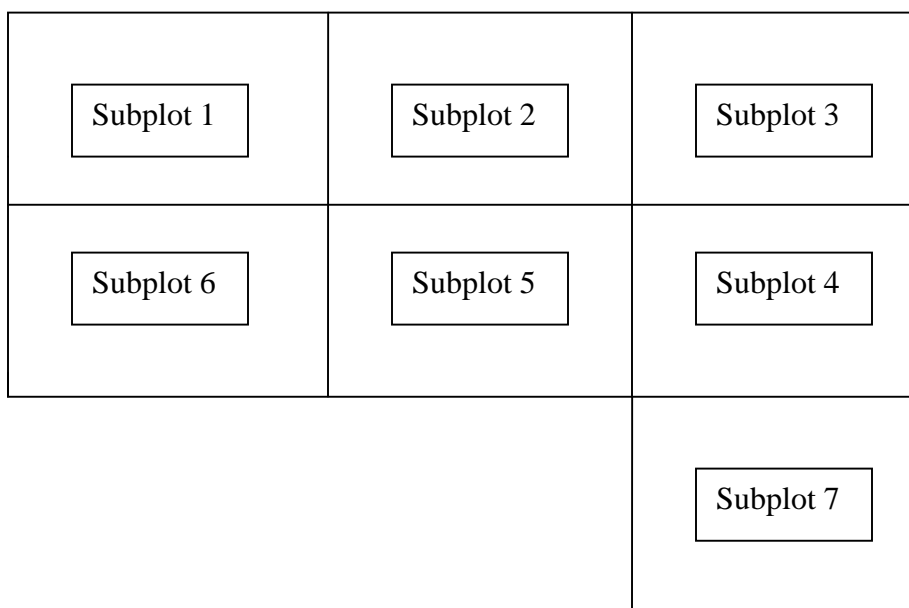


Figure 7.4: Plot diagram showing the 7 subplots, each subplot is associated with a different treatment.

Samples were collected in a similar location in each subplot. The parameters analyzed were pH, electrical conductivity (EC), sodium adsorption ratio (SAR), percent saturation, bicarbonate, Cl^- , SO_4^{-2} , Ca^{+2} , Mg^{+2} , Na^+ , particle size analysis, texture, cation exchange capacity (CEC), and exchangeable sodium percentage (ESP). The data associated with the baseline sampling is presented in **Appendix 7.2; Table 1.1.1**.

Subtask 1.2: Installation and Operation of Lysimeter and Temperature, Soil Water and EC Probes

A Gee Drain Gauge Lysimeter was placed in the soil below the root zone of an intact soil monolith (**Figure 7.5**) to characterize the drainage water resulting from the irrigation treatment. The drain gauge is constructed to measure the amount of water migrating through the root zone and also allows collection of water samples for chemical analysis. The lysimeter was located

near Subplot 5 adjacent to one of the treatment plots. An adjacent site was also instrumented with ECH₂O probes measuring soil water, soil solution salinity and temperature at one-foot depth intervals to a total depth of 6 feet (**Figure 7.6**). One additional site located adjacent to Plot 1 was instrumented with ECH₂O probes to a depth of 5 feet measuring soil water, EC and temperature. The ECH₂O probes and the drain gauge generate continuous data that is integrated over 1 hour intervals and collected with an Em50 data logging system (**Figure 7.7**). The data loggers were placed underground utilizing control boxes often used for yard sprinkler system installations.



Figure 7.5: Excavation of the soil monolith to be placed on the drainage gauge lysimeters.

The system worked well collecting soil water content, soil EC and soil temperature data. Water did not penetrate to the depth of the lysimeter collection system in 2006 and therefore data was not collected. Water is expected to reach such depths during the next full season of irrigation allowing collection of water samples and providing a measure of water quality migrating to lower depths in the profile.



Figure 7.6: Installation of the ECH₂O soil probes measuring soil water content, soil EC and soil temperature.



Figure 7.7: Em50 Decagon data logger with underground connections to soil probes measuring soil water content, soil EC and soil temperature.

Data has been downloaded from the data logging systems established at three locations. The rain gauge was short lived at the site as cattle completely demolished the apparatus early in the fall of 2006. The data collected from the drain gauge constructed in the lower level of the root zone has not collected water in the two-year monitoring period. Data collected from the soil probes measuring temperature, soil water content and salt successfully collected data over the 14-month period with few problems.

Subtask 1.3: Treatment Application and Irrigation at the WJ Irrigation Study Site

Application of amendments

Each subplot (except for the control) was treated with an amendment prior to irrigation. The treatments used were as follows: Treatment 1 = no treatment (control); 2 = Gypsum ($\text{CaSO}_{4(s)}$) – level 1 (4 tons per acre); 3 = Gypsum – level 2 (6 tons per acre); 4 = Gypsum level 1 and Sulfur level 1 (1.6 tons per acre); 5 = Gypsum level 2 and Sulfur level 1; 6 = Gypsum level 1 and Sulfur level 2 (0.8 tons per acre); and 7 = Gypsum level 2 and Sulfur level 2. The various quantities of amendments were applied to each subplot by hand, carefully weighing and placing the material evenly across each site (**Figure 7.8**).



Figure 7.8: Application of amendment treatments to subplots.

Installation of two pivot irrigation systems

Two pivot irrigation systems were constructed at the research site during the summer of 2006 (**Figure 7.9**). The system is expected to be operational for a minimum of ten years.



Figure 7.9: Pivot irrigation system operating at the WJ research site.



Figure 7.10: Pivot irrigation system at the WJ research site.

Subtask 1.4. Monitoring Results

The operation of the pivot irrigation systems was initiated in August 2006 and ran into October 2006. A significant amount of time was spent for start up and shakedown procedures. The amount of water applied was about 9.5 inches. During the 2007 irrigation system, approximately 24 inches of water was applied to the study sites.

Baseline samples were collected prior to the initial irrigation and after the first and second years. The site was sampled by collecting a single sample from each of the seven subplots located at the eight plots. The samples were sent to Energy Laboratories in Helena Montana for analysis. Data associated with the first irrigation season are presented in **Appendix 7.3; Table 1.4.1**. Samples were also collected following the second year of irrigation in November 2007. These data are presented in **Appendix 7.4; Table 1.4.2**.

Results

Several relationships are shown to demonstrate some of the differences found from the use of CBM water for irrigation. The change in EC with respect to treatment is presented in **Figure 7.11** for the 0 to 0.5 foot depth increment. Although the data show EC levels increased for each treatment, all samples are not considered to be saline ($EC > 4$ dS/m). However, a definite trend toward salty soil conditions is occurring. The salt levels will not reach toxic levels as an

appropriate leaching fraction will be implemented once the irrigation program reaches full capacity and appropriate amounts of water are applied.

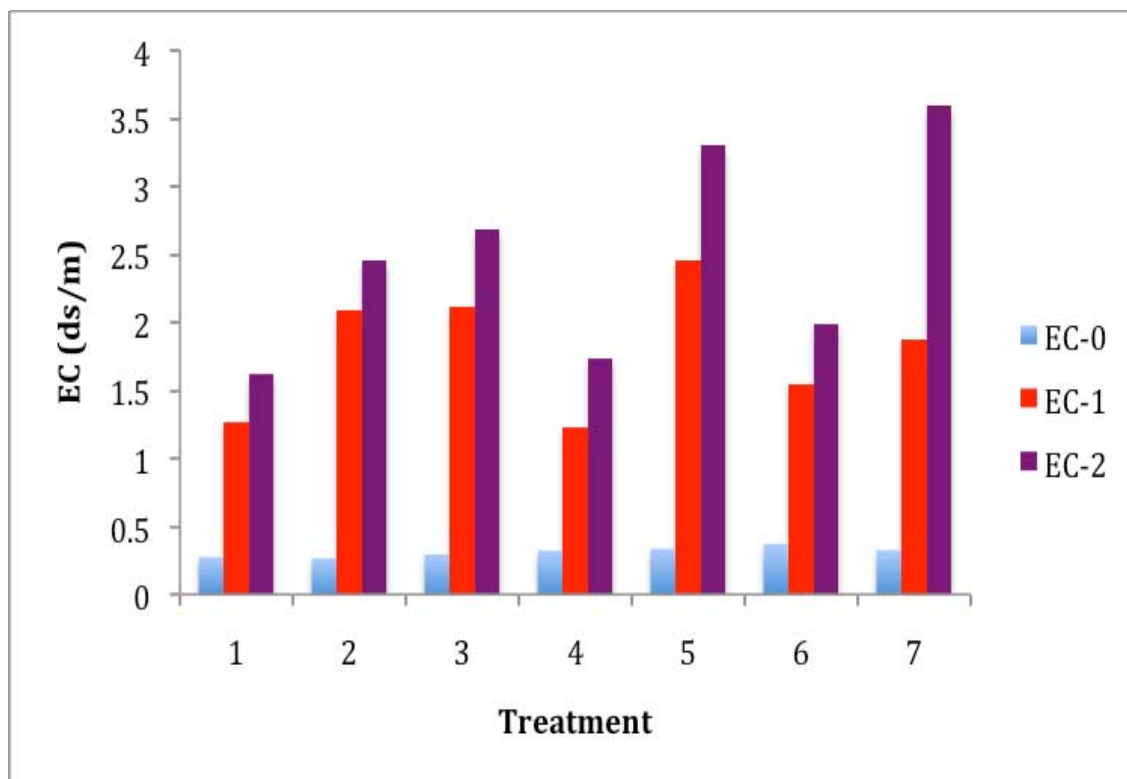


Figure 7.11: Change in EC over project period. EC-0 are the baseline value, EC-1 values were measured after the first irrigation season and EC-2 values were measured after the second irrigation season.

The change in SAR values by treatment for the surface soil (top 0.5 feet of soil) is presented in **Figure 7.12**. Significant changes in SAR values have occurred as a result of irrigation. While treatment 1, which is the control subplot (no amendments) is characterized by the highest SAR value at the end of first year, treatments 2 and 5 are very similar and the rest are still high. The poor results in year one are suspected to be due to insufficient acid generation through sulfur oxidation as evidenced by the pH data (see below) to prevent the loss of soluble calcium by the precipitation of calcite (calcium carbonate). **Figure 7.13** shows that all subplots reacted with similar pH shifts to the addition of CBM co-produced water. For the first irrigation season the sulfur was applied several days prior to the initiation of irrigation operations and probably did not have ample time to oxidize and form acid. By the end of the second irrigation season, all of the amendments had dissolved allowing all of the treated subplots to react adversely to the CBM water.

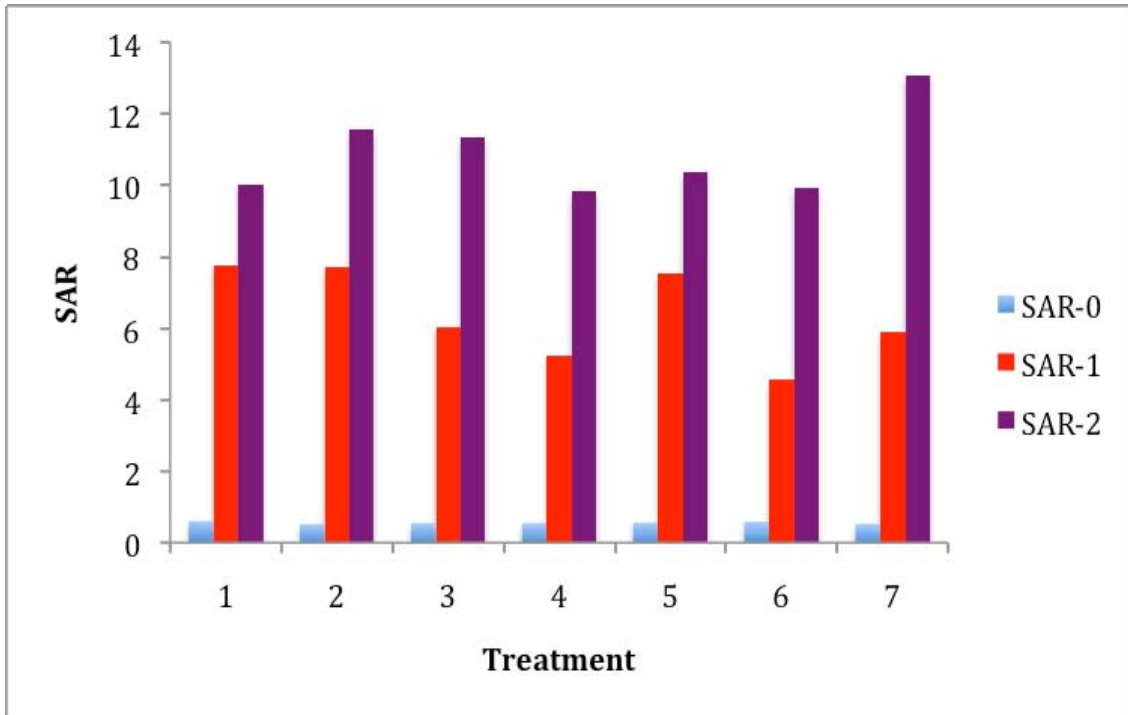


Figure 7.12: Change in SAR over project period. SAR-0 are the baseline values, SAR-1 values were measured after the first irrigation season and SAR-2 values were measured after the second irrigation season.

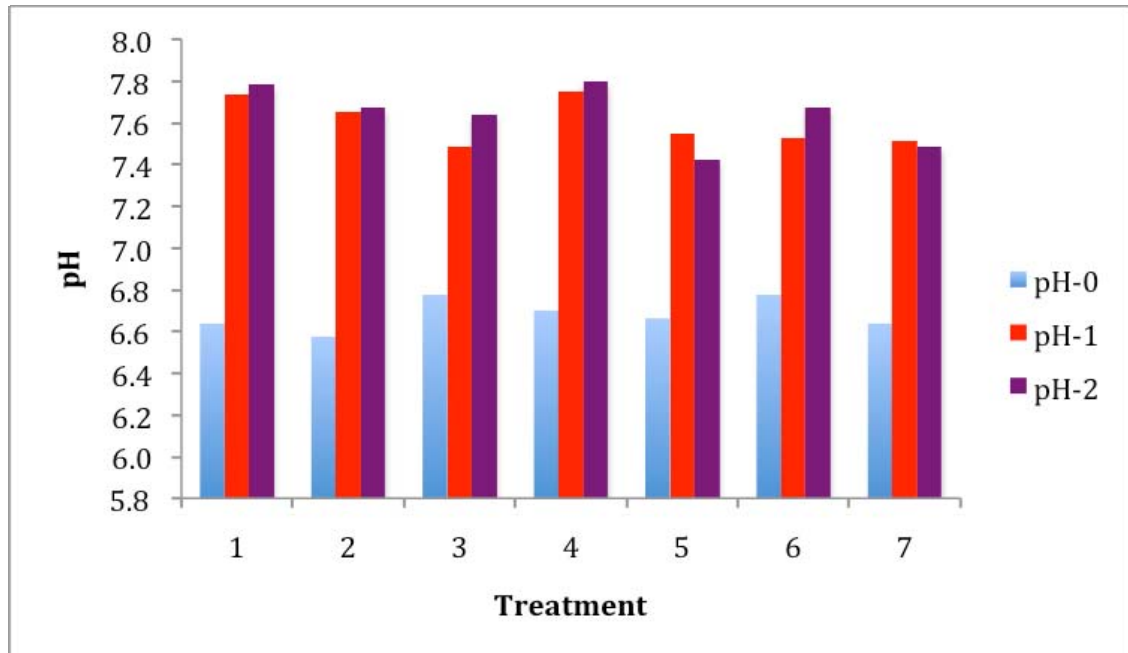


Figure 7.13: Change in soil pH over project period. pH-0 are the baseline values, pH-1 values were measured after the first irrigation season and pH-2 values were measured after the second irrigation period.

Although the soil chemistry data suggests that soil damage could be occurring, significant visual differences were found between the untreated subplots and the treated subplots at the end of the first irrigation season. **Figure 7.14** shows the untreated soil with the classical characteristics of a sodic soil condition. The surface is crusted, soil pores plugged and water is ponding on the surface as is shown in the dark, wet areas. The treated soil in **Figure 7.15** displays a great contrast as the surface is not dispersed and soil aggregation is maintained, allowing good water infiltration. It is apparent that the current sampling program did not show the differences demonstrated by the comparison between photos of the treated and untreated plots. This may be due to special heterogeneity that was not captured by the single core from each subplot or that six inches is too long of an depth interval.



Figure 7.14: Untreated soil irrigated with CBM co-produced water characterized with high SAR values.



Figure 7.15: Soil amended with gypsum and sulfur irrigated with CBM co-produced water characterized with high SAR values.

At the termination of the project following the second year of irrigation, the site was again sampled. The data associated with this sampling effort are shown in **Appendix 7.4**. The conditions of the soil at the end of the second irrigation period were noticeably deteriorated compared to the previous year (**Figure 7.16**). The soil surfaces for all treatments were dispersed. The primary reason for the dispersion can be attributed to the fact that the amendments were depleted during the irrigation season due to dissolution (amendments were not applied to the test plots during the second irrigation season). As a result, the highly sodic water and the impact of water droplets at the surface resulted in soil dispersion.



Figure 7.16: Previously treated soil with noticeably deteriorated conditions compared to the previous year.

In general, the SAR and EC values of the surface soils were found to be much higher compared to samples collected at the end of the first irrigation season. However, the samples also showed a large amount of variability as was found in the previous data set. In fact, due to the high variability in data, no significant differences were noted between treatments (**Appendix 7.5**). The same differences for depth changes were noted as shown for Year 1 data. Significant differences in SAR were found by depth. Again, the apparent differences noted in the visual condition of soils at the surface may have been discernable if samples were collected using smaller depth intervals at the surface.

Conclusions: Subtask 1

Visual conditions at the site demonstrate that amendments provide protection to the soil when irrigated with sodic water. However, the sampling method, either due to the specific depth intervals used or spatial heterogeneity of the soils or amendment application, resulted in a data set that did not represent actual soil conditions at the surface after the first year. Additional sampling using smaller depth intervals at the surface is required to characterize the actual conditions existing at the site. The results also indicate that amendments need to be closely monitored and reapplied as necessary.

SUBTASK 2: MODELING – IRRIGATION MODELING

Soil Water Salinity Model: Pre-irrigation Conditions

The USDA Soil Salinity Laboratory has shown the FAO-SWS (Food and Agricultural Organization of the United Nations - soil water salinity) model to be an effective tool for irrigation management using CBM co-produced water on irrigated lands in California. Poudre Valley Environmental Sciences, Inc has completed an initial calibration of the model to predict the effect of irrigation with CBM co-produced water on rangeland in the Powder River Basin. The work conducted at the WJ research plot will be used to continue this calibration effort. The model considers water flow, carbon dioxide production and transport, transport and chemistry of major dissolved ion species including cation exchange and mineral dissolution and precipitation, and plant water extraction with consideration of water and salt stress. The model was used to simulate the long-term effects of using CBM co-produced water to irrigate the WJ irrigation site when the soil is amended with gypsum. The simulation was made for a period of 10 years starting on July 1, which was the estimated start date at that time.

The primary consideration of the model simulation was to determine how irrigation with CBM co-produced water is expected to impact the major soil chemical parameters when the soil is amended with gypsum. Therefore, soil chemical characteristics such as EC, SAR, and solution concentrations of calcium, magnesium, sodium and sulfate were modeled over the 10-year simulation period. In addition, an estimate of the relative crop yield over the simulation period was determined in the context of the saline and sodic conditions existing in the soil.

The primary concerns with using CBM co-produced water to irrigate crops and rangeland plant communities are associated with the influence that such water has on the salinity and sodicity characteristics of the irrigated soils. The expected salinity and SAR characteristics of soils located at the WJ research irrigation site over the 10-year simulation period are presented in **Figures 7.17 and 7.18**, respectively. The SAR values projected in time and by depth resemble the shape of the EC simulation. However, a seasonal trend does appear to exist. The peak SAR level following one year of irrigation is 12 at a depth below the root zone of about 0.7 m. The trend is downward and continues in that direction throughout the life of the irrigation project.

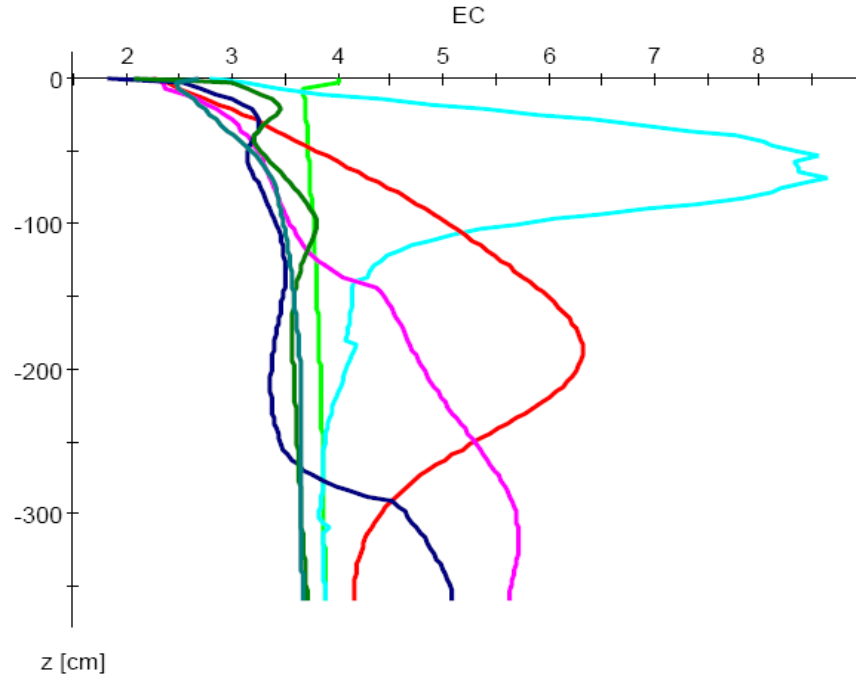


Figure 7.17: Simulation showing the EC by soil depth over the 10-year simulation period. (green – 0; turquoise –1 year; red – 3 years; pink – 5 years; blue – 7 years; dark green – 8.8 years; blue green – 9.3 years).

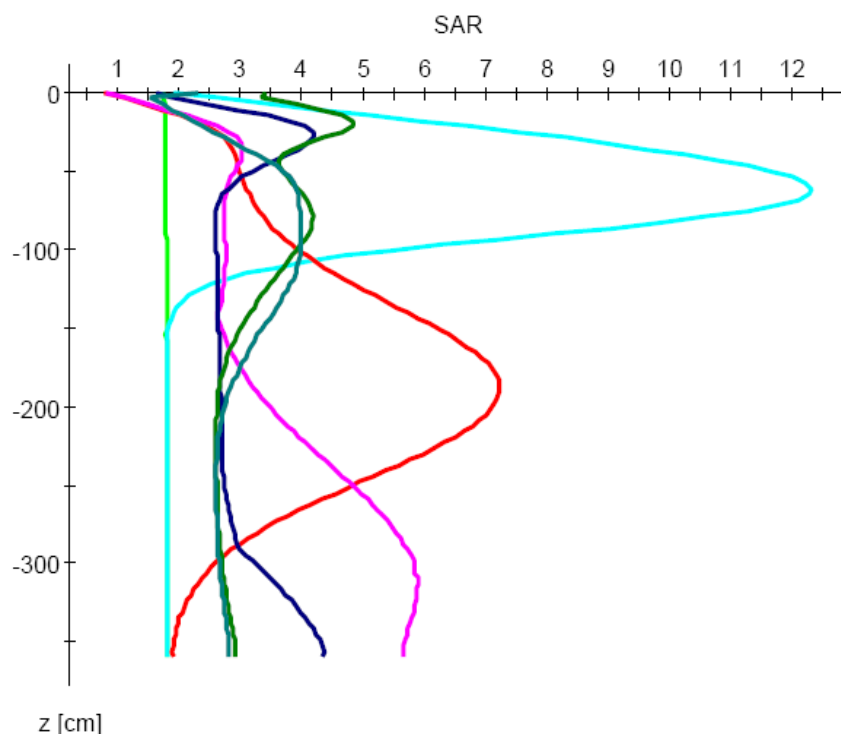


Figure 7.18: Simulation showing the SAR by soil depth over the 10-year simulation period (green – 0; turquoise –1 year; red – 3 years; pink – 5 years; blue – 7 years; dark green – 8.8 years; blue green – 9.3 years).

The data shown in **Figure 7.17** provide an estimate of the salt accumulation expected at the site under the projected irrigation application rates and the average precipitation levels. In general, the simulation shows that during the initial stages of irrigation, salt levels are tending to migrate to lower depths below the root zone. It is important to note that a maximum salt concentration of about 4 dS/m is reached in the profile below the root zone during much of the irrigation period. The salt levels in the profile are shown to decrease below the baseline conditions during much of the 10-year irrigation period. The data show a continuous downward movement and the rate of downward migration does not appear to be seasonal. The general downward migration is associated with the corresponding movement of elements such as sodium (**Figure 7.18**), calcium (**Figure 7.19**), magnesium (**Figure 7.20**) and sulfate (**Figure 7.21**). The primary elements responsible for EC changes with depth appear to be sodium, magnesium, and sulfate. Calcium levels tend to be rather constant to a depth of about 0.8 m due to equilibrium chemistry followed by a general leaching profile below with time.

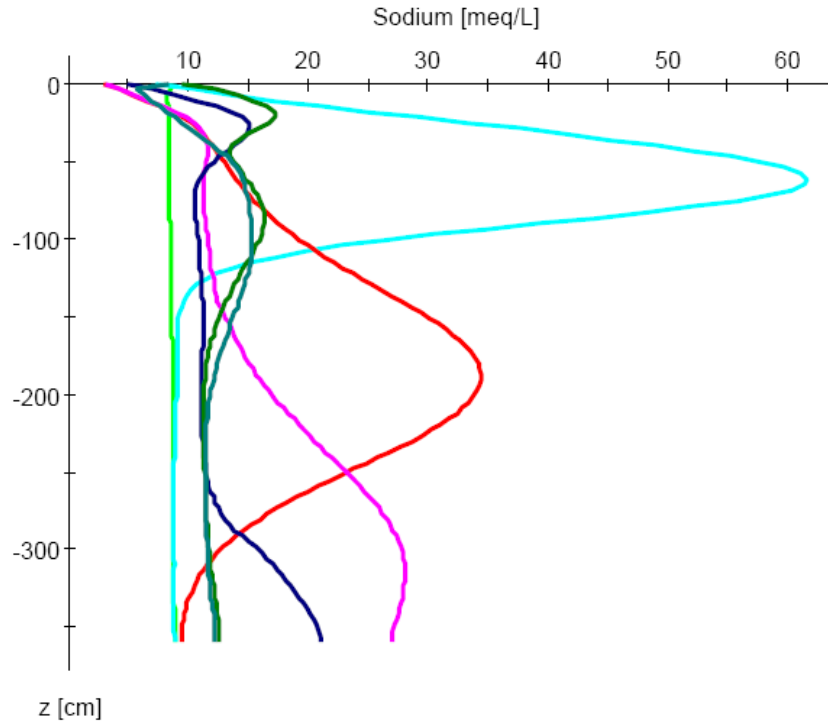


Figure 7.18: Simulation showing the solution sodium levels by soil depth over the 10-year simulation period. (green – 0; turquoise – 1 year; red – 3 years; pink – 5 years; blue – 7 years; dark green – 8.8 years; blue green – 9.3 years).

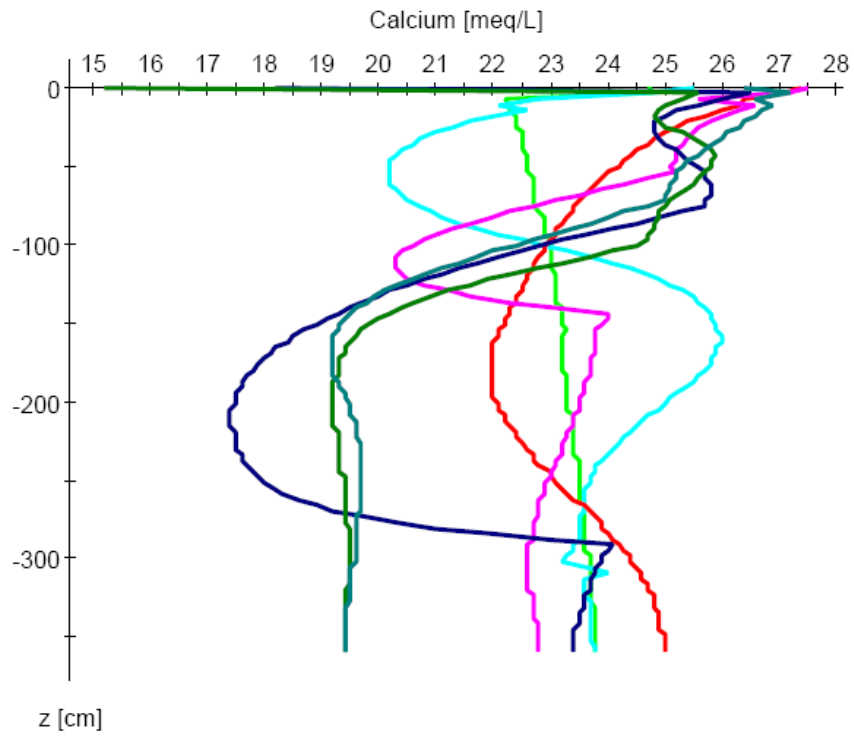


Figure 7.19: Simulation showing the solution calcium levels by soil depth over the 10-year simulation period. (green – 0; turquoise – 1 year; red – 3 years; pink – 5 years; blue – 7 years; dark green – 8.8 years; blue green – 9.3 years).

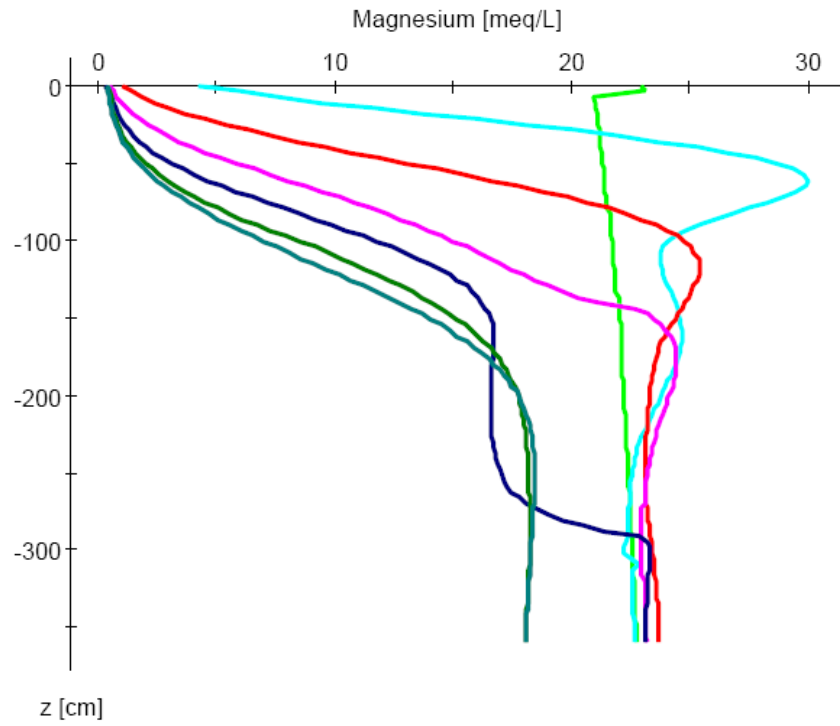


Figure 7.20: Simulation showing the solution magnesium levels by soil depth over the 10-year simulation period. (green – 0; turquoise –1 year; red – 3 years; pink – 5 years; blue – 7 years; dark green – 8.8 years; blue green – 9.3 years).

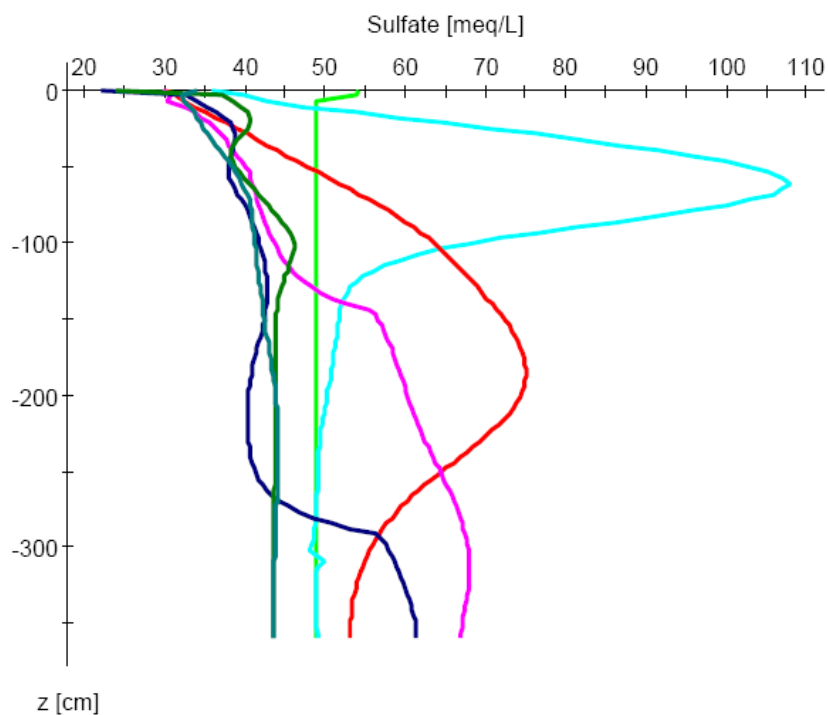


Figure 7.21: Simulation showing the solution sulfate levels by soil depth over the 10-year simulation period. (green – 0; turquoise – 1 year; red – 3 years; pink – 5 years; blue – 7 years; dark green – 8.8 years; blue green – 9.3 years).

The SAR values will change with respect to changes in sodium (**Figure 7.18**), calcium (**Figure 7.19**) and magnesium (**Figure 7.20**). The movement of sodium and magnesium closely resembles the simulation results found for SAR. These results reflect the relatively constant level of calcium in the upper portion of the profile and the declining levels of magnesium and sodium through the profile with time.

At the termination of the 10-year simulation, EC values peak below the root zone at about 8.5 dS/M. Levels at the surface will remain at about 4 dS/M during the 10-year period. In general, the simulation shows that CBM co-produced water should increase soil pH near the surface by several tenths of a unit (**Figure 7.22**). In addition, the simulation indicates that the pH will not increase at depth.

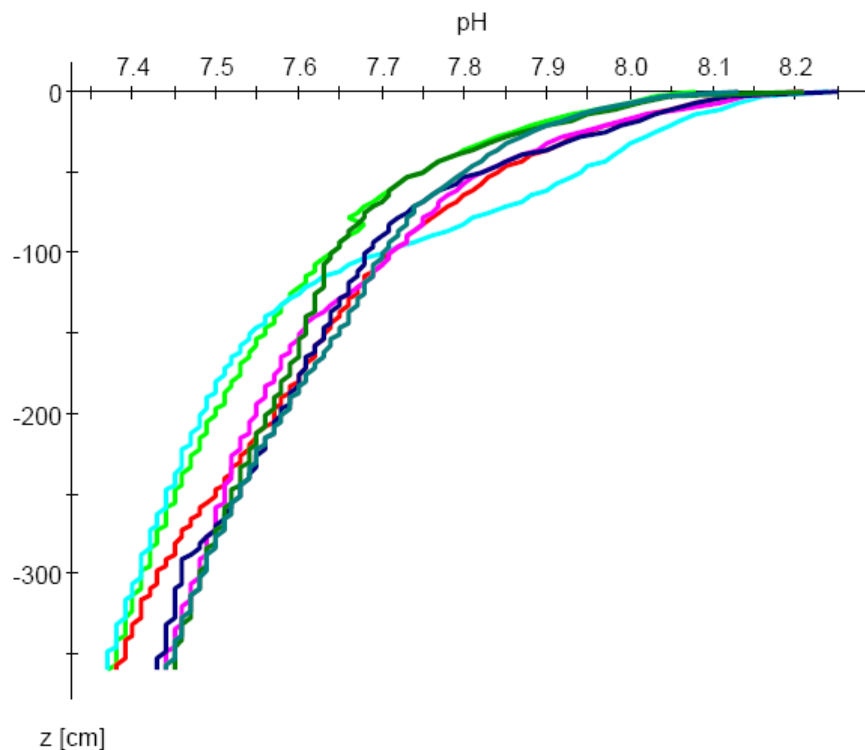


Figure 7.22: Simulation showing the pH by soil depth over the 10-year simulation period. (green – 0; turquoise –1 year; red – 3 years; pink – 5 years; blue – 7 years; dark green – 8.8 years; blue green – 9.3 years).

The FAO-SWS model provides an evaluation of how the soil conditions might affect plant growth. The impact is based on relative productivity due to water and salt stress. The simulation assumes that soil fertility and agriculture management are at optimum conditions for crop production. The relative yield simulation is provided in **Figure 7.23**. The simulation indicates that the potential crop production is expected to decrease to about 93% under the conditions resulting from 10-years of irrigation with CBM co-produced water under the proposed management strategy.

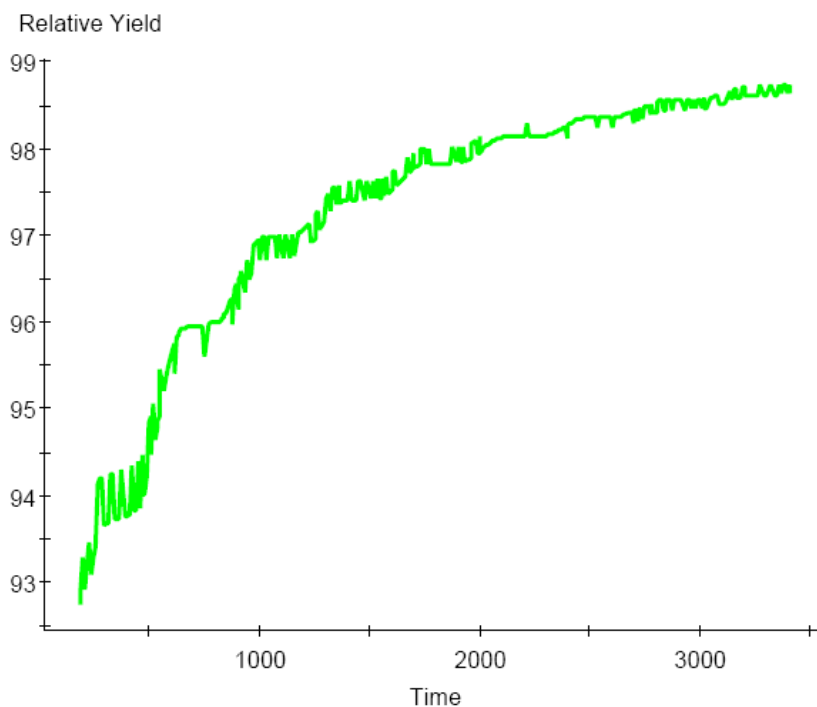


Figure 7.23: Simulation showing the relative crop yield over the 10-year simulation period. (the time variable is in days).

The FAO-SWS simulation for the Jenkins project demonstrates that using CBM co-produced water for irrigation purposes should not cause significant impacts to the soil and surrounding environment. Salts should concentrate below the root zone and the resulting sodium accumulations will move deeper in the soil profile below the root zone. The only stipulation to this outcome is that the irrigation project must be closely managed, which includes a detailed monitoring and maintenance program. Issues that appear must be dealt with using appropriate techniques. The irrigation program may require changes dependent on the results of the monitoring program.

Soil Water Salinity Model: Post-irrigation Conditions

The research plan indicated that following the second year of irrigation, the resulting soil chemistry would be compared to the baseline model to determine whether the initial adjustment to the model provided the necessary modifications to allow use in the Powder River Basin. The model would be modified to enhance the prediction capability.

The data collected following the initial irrigation can be used to evaluate the baseline model. However, data collected following Year 2 of irrigation cannot be considered a valid comparison. During the second year of irrigation, the amendments applied to the soil surface were completely dissolved allowing the sodic water to significantly impact the soil surface causing dispersion. Since the baseline model was developed on continuous availability of gypsum, the results of the

model and the actual field data are not comparable. Continuation of the project will include the development of a model based on the actual site conditions.

The average values of SAR and EC for the 0 to 6 inch depth interval after the initial irrigation period are 6.4 and 1.8 dS/m, respectively. The estimated values taken from the model for SAR and EC are about 6.0 and 3.0 dS/m, respectively. These values are comparable even though the estimated amount of irrigation water actually applied to the site was less than the amount used in the model and the depth interval for the sample was too large. Future data collected at the site is expected to provide validation.

Results

The average values of SAR and EC for the 0 to 6 inch depth interval after the initial irrigation period are 6.4 and 1.8 dS/m, respectively. The estimated values taken from the model for SAR and EC are about 6.0 and 3.0 dS/m, respectively. These values are comparable even though the estimated amount of irrigation water actually applied to the site was less than the amount used in the model and the depth interval for the sample was too large. Future data collected at the site is expected to provide validation.

SUBTASK 3: SOIL FERTILITY EVALUATIONS

Three plant fertility studies were conducted to evaluate the impact of CBM co-produced water and soil amendments on the production of alfalfa. Two of the studies examined fertility problems at two pivot irrigation field sites located north of Sheridan, Wyoming on private property. These sites have been irrigated for 4 years with CBM co-produced water with SAR values of 30+. The third study was conducted in a greenhouse located at Colorado State University.

The fertility problems at the field sites were associated with the application of excess water and sulfur amendments to the soil. The results of the field studies will be used to better manage such irrigation projects to prevent fertility losses. The greenhouse study evaluated the use of soil amendments and CBM produced water on the growth of alfalfa.

Plant Nutritional Issues Related to Elemental Toxicity

The alfalfa at both pivot areas was characterized by an apparent toxicity, which was thought to be associated with either salts or some type of elemental toxicity or deficiency (**Figure 7.24**).



Figure 7.24: General view of the alfalfa at an impacted area showing the range of impact from dead to healthy green vegetation.

The alfalfa stands at both sites were characterized by uneven growth with some areas looking very good while other parts of the field were stunted (**Figure 7.25**). In addition, a significant portion of the plants were yellow and many of the leaves were dead. Impacted plants also had very limited rhizobium nodule formation in the roots, which may explain some of the yellowing of leaves resulting from nitrogen deficiency. This finding was somewhat puzzling since at many sites adjacent plants showed no sign of toxicity either in the leaves or the roots. The first inclination was that salts had accumulated at various locations in the field causing reduced growth and in some areas death of the plants. However, the symptoms also resembled those that might be associated with elemental toxicity such as manganese and sulfur deficiency. An interesting finding was that many of the dead alfalfa plants were located in circular patterns matching the pattern of the pivot. After some thought, it was theorized that such patterns might result from excess water application or from amendment application. Areas of excess water due to the direction of water spray may result in problems resulting from water logging conditions. In addition, the amendments were applied in a circular pattern and may have been overlapped, which may have resulted in large amounts of sulfur placed on the soil at various locations in the pivot areas resulting in a toxic impact due to the excess formation of sulfuric acid.



Figure 7.25: Side by side comparison of un-impacted alfalfa to an adjacent impacted (dead) stand of alfalfa.

The general condition of the soils was very good. An accumulation of excess salts near or at the surface was not apparent. In addition, the structure of the soil looked good at each sampling location without any indication that soil sodicity was impacting the availability of water or nutrients to the plants.

As indicated previously, soil samples were collected from locations selected from impacted and non-impacted sites located at each pivot area (North and South Pivots). Impacted sites were associated with alfalfa characterized with severe yellowing or leaf necrosis, while un-impacted sites did not show any apparent toxicity. Samples were collected from two depths from 0 to 6 inches and from 6 to 12 inches at each sampling location. A number of samples were collected from impacted sites and non-impacted sites that were located within 10 feet of each other. Samples collected from the following sites represent this comparison: SP-2 and SP-3, SP-4 and SP-5, SP-6 and SP-7, NP-1 and NP-2, and NP-3 and NP-4.

The soil samples were submitted to InterMountain Laboratories and analyzed for pH, SAR, EC and available plant nutrients. The vegetation samples were submitted to the Soils and Plant Tissue Analysis Laboratory at Colorado State University and were evaluated for macro and micro-nutrients. In addition, the plant tissue was submitted to the diagnostic laboratory at Colorado State University for disease evaluation.

The results of the soil analysis for samples collected at the South and North Pivot areas are provided in **Table 7.1**. The soil is currently experiencing limited impact related to saline and/or sodic conditions as the electrical conductivity (EC) and sodium adsorption ratio (SAR) values are lower than existed during previous samplings. The large amount of natural precipitation and the 6 inches or so of irrigation applied to the pivot areas prior to sampling have reduced the amount of salts in the root zone. Salt management is going very well.

High levels of plant available iron and manganese were found in the soils collected from sites where alfalfa and grass show toxic impacts compared to the levels associated with non-impacted sites. Other elements analyzed did not appear to be toxic or to be out of balance causing problems with plant growth. It is theorized that as the soil becomes saturated with water, it tends to become deficient in oxygen (O₂), which causes reduced conditions in the soil resulting in the reduction of some elements. Both iron and manganese are elements that are reduced under oxygen deficient conditions and tend to become soluble. In addition, as soils become more acidic (lower pH) elements such as iron, manganese and aluminum become more soluble. With the addition of sulfur to the soil acid is formed. In the vicinity of the acid formation, iron, manganese and aluminum become soluble. As the acidity reacts with the calcite, the acid is neutralized and the aluminum should precipitate from solution. However, iron and manganese will tend to stay in solution due to the reducing conditions of the soil. Therefore, these elements are anticipated be more available for plant uptake and potentially causing toxicity. Once the soil becomes less saturated with water and oxygen becomes more plentiful, the solution levels of iron and manganese should decrease. However, high manganese levels could be maintained in solution much longer compared to iron since rather high pH levels are required to cause manganese precipitation from solution.

Several of the samples are characterized with acidic pH values. Sample SP-1 (0 to 6 inches) has a pH of 4.7. This pH level could also cause the solubility of such elements as manganese and aluminum, which can cause toxicity to plants. Sample NP-1 also is becoming acidic as it has a pH of 5.6. The development of lower pH soils at the RC25 pivots is associated with the oxidation of sulfur at the surface forming sulfuric acid. The sulfur is applied to remove bicarbonate from the CBM co-produced water, which will help prevent sodification of the soils irrigated with the produced water. The acid is also reacting with the calcite originating in the soil removing it from the system. The calcite present in the soil provides a buffering mechanism that tends to hold the pH of the soil in the 7 to 8 range. If too much sulfur is added to the system, much of the pH buffering capacity is removed and the addition of more acid causes the soil pH to change with little addition of acid. A primary concern is that the addition of sulfur may be removing much of the soil buffering capacity in portions of the North and South Pivot areas. This issue will be addressed in the next section.

The data associated with plant analysis are presented in **Table 7.2**. A review of these data show that the levels of iron and manganese found in the plant tissue appear to be the only constituents that show a consistent difference between impacted and non-impacted vegetation. This information provides evidence that high levels of manganese and iron either individually or in combination, have resulted in the negative impact on plant growth. This is an interesting observation since examples of iron and manganese toxicity found in the literature usually are associated with higher levels than found in this study.

The pivot sites were evaluated again in August 2005 (**Figure 7.26**). The condition of the alfalfa fields at both the North and South Pivot sites improved substantially since the visit conducted during June 2006. Both fields appear to be more productive and should yield considerable more hay compared to the first cutting. The soil system became less saturated and more oxidized, decreasing the soluble iron and manganese available for plant uptake. Soil and vegetation samples were not collected during this visit.



Figure 7.26: Alfalfa at the North Pivot during August 2005, showing improvement from the previous toxic impact.

Table 7.1: Analysis of Soil Samples Collected on June 23, 2005

Sample #	Depth (Inches)	Impacted Yes(Y) or No(N)	pH	EC mS/cm	Calcium (Ca) meq/L	Magnesium (Mg) meq/L	Sodium (Na) meq/L	SAR	Iron (Fe) (AB-DTPA) ppm	Manganese (Mn) (AB-DTPA) ppm
SP-1	0-6	Y	4.7	3.03	17.2	4.72	13.8	4.2	100	63
SP-1A	6-12	Y	7.5	2.83	6.33	2.16	23	11.2	11.5	14.8
SP-2	0-6	N	7.1	2.29	13.3	1.64	14.4	5.3	5.04	22.4
SP-2A	6-12	N	7.4	2.3	17.4	4.76	9.15	2.8	3.34	2.7
SP-3	0-6	Y	7.4	3.96	15.9	3.76	29.4	9.4	48.2	105
SP-3A	6-12	Y	8.2	1.99	3.1	1.23	18.3	12.4	5.72	29.2
SP-4	0-6	Y	7.4	4.33	16.3	4.43	34.1	10.6	75.6	86.6
SP-4A	6-12	Y	7.9	4.55	14.9	9.06	33.2	9.6	9.38	44.2
SP-5	0-6	N	7.3	2.87	17.4	3.49	15.5	4.8	5.62	9.42
SP-5A	6-12	N	7.5	2.58	9.17	3.7	17.8	7.0	13	31.8
SP-6	0-6	Y	7.1	2.32	16.6	2.2	10.3	3.4	3.44	3.86
SP-6A	6-12	Y	7.5	2.17	13.7	3.25	10.4	3.6	2.58	2.15
SP-7	0-6	N	7.4	1.4	5.67	0.81	8.22	4.6	3	3.8
SP-7A	6-12	N	7.5	1.23	2.86	0.93	8.65	6.3	1.78	2.82
NP-1	0-6	Y	5.8	2.69	22.7	5.44	10.8	2.9	42	28.4
NP-1A	6-12	Y	7.6	3.17	18.5	7.73	17	4.7	2.68	2.5
NP-2	0-6	N	7.5	2.53	16.6	5.15	11	3.3	3.04	2.52
NP-2A	6-12	N	7.9	2.26	5.13	6.04	13.2	5.6	2.1	1.08
NP-3	0-6	Y	7.1	2.81	14.9	4.76	12.7	4.0	18.7	29.2
NP-3A	6-12	Y	7.4	3.19	14.6	6.47	15.9	4.9	7.5	13.5
NP-4	0-6	N	7.4	2.76	17.3	4.49	12	3.6	13.2	22.2
NP-4A	6-12	N	7.4	2.33	10.6	5.58	10.5	3.7	4.6	9.9

SP = south pivot; NP = north pivot

Table 7.2: Plant analysis of samples collected on June 23, 2005.

Sample #	Plant	Impacted	N	P	K	Ca	Mg	Fe	Mn	B	Zn	Cu
		Y or N	%	%	%	%	%	mg/kg	mg/kg	mg/kg	mg/kg	mg/kg
SP-1	alfalfa	Y	1.99	0.10	1.32	0.91	0.18	224	185	3.5	17.6	3.3
SP-2	alfalfa	Y	0.69	0.10	0.80	0.69	0.15	230	57	4.1	15.2	2.6
SP-3	alfalfa	N	3.01	0.23	2.03	0.90	0.29	67.5	48.5	1.3	24.8	3.5
SP-4	alfalfa	N	3.71	0.16	1.95	1.13	0.22	77.2	34	3.4	28.8	5.4
SP-5	grass	Y	2.01	0.11	1.85	0.44	0.12	149	127	1.8	31.2	6.0
SP-6	alfalfa	Y	2.37	0.15	1.77	1.10	0.25	91.4	186	3.4	25.6	5.2
NP-1	alfalfa	Y	3.49	0.20	1.80	1.13	0.36	129	259	3.9	38.4	7.2
NP-2	alfalfa	N	3.55	0.21	2.05	0.95	0.37	52.7	24.2	2.2	20	4.7
NP-3	alfalfa	Y	3.44	0.17	2.28	1.00	0.33	136	157	5.3	24.0	5.8
NP-4	alfalfa	N	3.62	0.21	1.90	1.03	0.33	77.9	51.1	4.5	26.4	5.9

Conclusions of this study

1. Excess water causing reducing conditions in the soil is an important factor causing the alfalfa toxicity by increasing the availability of potentially toxic elements such as iron and manganese.
2. Excess acidity caused by the oxidation of sulfur to sulfuric acid contributed to the toxicity by making iron and manganese more available for plant uptake.
3. The reduction in the amount of water that was applied to the field as natural precipitation and irrigation resulting in less “water logging”, which allowed the soils to become more oxidized causing iron and manganese to become less available for plant uptake.
4. Care must be taken in the spring of the year to apply the amount of water required in excess of the natural precipitation by the crop to satisfy the evapotranspiration demand. Excess water can result in conditions that impact plant growth.
5. The application of sulfur to the irrigated soils to remove bicarbonate from the CBM co-produced water is resulting in decreasing soil pH values. The acid is reacting with the calcite naturally present in the soils gradually removing it from the soil. The levels of sulfur added to the soil must be carefully evaluated. In addition, alternative treatment for bicarbonate such as the treatment of CBM co-produced water directly with sulfuric acid should be evaluated.
6. Soils with reduced or eliminated pH buffer capacity may require treatment with calcite, lime or other materials.

Plant Nutritional Issues Relating to Soil Buffer Capacity Losses

A major concern that was anticipated resulting from the decline in pH over much of the pivot areas was associated with the maintenance of the pH buffer capacity of the soil or the lime content (calcite) of the soils. The generating of acidity resulting from sulfur oxidation would react with calcite removing it from the soil allowing the pH levels to decline. The current situation and the potential long-term impacts of calcite dissolution were evaluated.

Soil samples were collected from 10 random sampling locations selected from each pivot area (North and South Pivots). Samples were collected from two depth intervals, 0 to 6 inches and

from 6 to 12 inches at each sampling location. The soil samples were submitted to Energy Laboratories and analyzed for pH, SAR, EC, and lime (calcite content percentage). The results of the soil analysis for samples collected at the South and North Pivot areas are provided in **Tables 7.3 and 7.4**, respectively.

Within the impacted areas, the data show that some soil samples are characterized by low pH, which appears to be caused by the oxidation of elemental sulfur and the resulting elimination of the natural lime (calcite) present in PRB soils. Generally, samples collected from the bare areas were characterized with low pH values. Such sites are located where excess S had been placed mostly in areas of application overlap by an inexperienced operator. As a result, oxidation of the excess S resulted in higher levels of sulfuric acid causing a decline in pH. Samples collected from the North Pivot Area tended to have lower pH levels as compared to the South Pivot Area.

The lime (calcite) percentages in the South Pivot Area are characterized with 5 of the 20 samples containing levels below 2%. However, it is obvious that the trend is toward reduced lime (calcite) content with the resulting reduction in soil pH with continued oxidation of elemental sulfur that appears to be present in the soils.

The lime (calcite or neutralization potential) percentages in the North and South Pivot Areas tend to follow pH levels consistently. As lime percentages decrease to about 1%, pH levels tend to decline below neutrality. For example, the only soil sample that has a pH value below 7 is Sample SP-1-7, 0 to 6 inches with a pH of 5.4, had a lime percentage of 1%. The samples collected from the North Pivot with pH values below 7 ranged from 0.2 % lime with a pH of 3.5 to 1.1 % with a pH of 6.7. These data show that as the lime content (neutralization potential) approaches 1%, the soil buffer capacity for pH is approaching a critical level where additional acid formation will cause significant decreases in soil pH.

The final analysis indicates that the soils in the South Pivot area have pH values greater than 7 except for one sample. However, five samples have lime percentages of near 1%, which may indicate that pH values may decrease at those sites in the near future. Lime levels will tend to increase in the future due to the precipitation of calcium carbonate due to the high levels of bicarbonate in the CBM co-produced water if sulfur is not applied during the next field season.

The samples collected from the North Site indicated that 10 samples out of a total of 20 samples were characterized with pH values below 7. These data seem to demonstrate an overall reduction in pH compared to the Spring 2006 sampling, which showed that 6 samples were characterized with pH values less than 7. As noted previously, acid continues to be generated due to oxidation of sulfur. However, the formation of lime due to precipitation of calcium carbonate should increase the pH buffer capacity and the pH levels, if sulfur (potential acidity) is not used as an amendment at the site.

Conclusions of this study

The addition of elemental sulfur to the irrigated soils is resulting in decreasing soil pH values. The acid is also reacting with the lime (calcite) naturally present in the soils gradually removing it from the soil. The soils are becoming acidic. The North Pivot Area is at a critical point and will

require an application of ag-lime (calcite) to increase the neutralization potential of the soils to negate the acidity resulting from the oxidation of the excess sulfur that has been added to the soil.

As the lime content (neutralization potential) approaches 1%, the soil buffer capacity for pH is approaching a critical level where additional acid formation will cause significant decreases in soil pH.

Table 7.3: Analysis of Soil Samples Collected at the South Pivot October 2006.

Sample #	Depth	pH	EC	Calcium (Ca)	Magnesium (Mg)	Sodium (Na)	SAR	Lime (calcite)	Iron (Fe) (AB-DTPA)	Manganese (Mn) (AB-DTPA)
	(Inches)		mS/cm	meq/L	meq/L	meq/L		%	ppm	ppm
SP-1	0 - 6	7.2	3.42	26.6	4.67	22.5	5.7	2.6	22.8	1.81
SP-1	6 -12	7.8	3.63	17.0	2.90	28.7	9.1	7.1	3.29	0.56
SP-2	0 - 6	7.8	3.22	18.5	2.32	23.0	7.1	3.6	0.68	0.76
SP-2	6 -12	7.8	4.06	21.9	4.60	28.6	7.9	11.4	0.61	0.36
SP-3	0 - 6	7.9	2.14	3.39	0.62	19.8	14	1.3	3.42	1.80
SP-3	6 -12	8.1	2.27	2.96	1.20	20.8	14	5.4	2.36	0.56
SP-4	0 - 6	7.7	3.21	15.6	0.92	21.6	7.5	5.7	1.71	1.09
SP-4	6 -120	8.1	1.77	3.46	0.55	14.3	10	15.5	1.11	0.55
SP-5	0 - 6	7.7	3.56	14.3	1.69	28.4	10	4.7	1.88	1.59
SP-5	6 -12	8.0	3.62	15.3	3.20	26.1	8.6	6.2	1.14	0.86
SP-6	0 - 6	7.6	3.65	22.9	3.06	28.0	7.8	5.7	1.98	1.90
SP-6	6 -12	8.0	2.28	5.59	1.61	18.9	9.9	5.3	3.85	1.21
SP-7	0 - 6	5.4	3.74	28.1	10.1	19.3	4.4	1.0	423	59.5
SP-7	6 -12	7.6	4.41	25.9	7.76	29.0	7.1	7.6	5.33	0.66
SP-8	0 - 6	7.8	1.91	2.87	0.59	19.8	15	2.2	12.6	13.1
SP-8	6 - 12	8.2	1.17	1.05	0.37	10.4	12	1.2	3.76	3.61
SP-9	0 - 6	7.5	4.42	20.8	4.49	37.4	10	1.1	1.32	1.71
SP-9	6 - 12	7.8	4.40	18.2	8.10	37.5	10	1.1	1.15	0.64
SP-10	0 - 6	7.0	4.27	30.0	9.76	24.7	5.6	3.3	39.4	2.66
SP-10	6 - 12	7.8	3.20	18.7	4.76	22.2	6.5	8.4	1.	0.47

Table 7.4: Analysis of Soil Samples Collected at the North Pivot October 2006.

Sample #	Depth	pH	EC	Calcium (Ca)	Magnesium (Mg)	Sodium (Na)	SAR	Lime (calcite)	Iron (Fe) (AB-DTPA)	Manganese (Mn) (AB-DTPA)
	(Inches)		mS/cm	meq/L	meq/L	meq/L		%	ppm	ppm
NP-1	0 - 6	4.4	3.45	32.0	6.86	12.8	2.9	0.6	166	37.3
NP-1	6 -12	5.6	4.60	21.8	17.2	34.9	7.9	1.0	25.9	8.90
NP-2	0 - 6	7.6	3.50	5.55	1.60	32.9	17	2.4	11.5	4.90
NP-2	6 -12	7.9	4.15	11.4	3.80	38.3	14	2.5	4.72	1.66
NP-3	0 - 6	3.5	4.69	22.1	14.4	36.1	8.4	0.2	451	60.8
NP-3	6 -12	6.1	4.12	27.8	9.65	26.7	6.2	1.1	14.4	6.60
NP-4	0 - 6	5.1	3.24	26.1	7.23	16.6	4.0	0.7	76.7	27.2
NP-4	6 -12	7.7	4.16	23.2	5.86	28.7	7.5	5.4	2.07	0.83
NP-5	0 - 6	5.3	4.34	18.5	10.4	33.5	8.8	0.9	41.5	20.2
NP-5	6 -12	7.6	4.20	11.7	10.2	39.4	12	1.7	4.71	0.94
NP-6	0 - 6	6.7	3.20	20.9	4.13	18.5	5.2	1.4	13.3	6.64
NP-6	6 -12	7.2	3.10	17.1	6.40	19.7	5.8	1.2	3.47	0.95
NP-7	0 - 6	3.8	3.75	26.4	9.20	17.8	4.2	0.4	282	55.1
NP-7	6 -12	7.0	4.18	25.2	12.5	27.7	6.4	1.5	6.55	2.85
NP-8	0 - 6	7.9	1.39	1.95	0.54	13.5	12	1.5	8.35	1.43
NP-8	6 -12	8.3	1.51	1.99	0.70	13.5	12	1.5	5.29	0.83
NP-9	0 - 6	7.5	2.68	11.0	2.90	21.0	8.0	1.6	3.43	1.89
NP-9	6 - 12	7.7	4.45	20.7	8.46	32.4	8.5	3.3	1.03	1.07
NP-10	0 - 6	5.4	3.09	24.6	3.75	16.1	4.3	0.6	27.5	13.2
NP-10	6 - 12	6.7	3.38	26.1	7.47	18.6	4.5	1.1	6.75	2.69

Greenhouse Study: Alfalfa Production Using CBM Co-Produced Water and Soil Amendments.

A greenhouse study was conducted to develop an understanding of how CBM co-produced water and soil amendments including gypsum and sulfur would impact the productivity of alfalfa (**Figure 7.27**). Twelve treatments were implemented that included the addition of gypsum, ag-lime and sulfur at various levels to soils collected at the Young’s Creek irrigation site (**Table 7.5**). The amendments were applied to the soils and the amended soils were irrigated with CBM produced water collected from the water source used at the Young’s Creek site.



Figure 7.27: Setup of greenhouse fertility study.

Table 7.5: Experimental treatments for the greenhouse fertility study.

Treatment Number Used	Treatment
1	Control – No treatment
2	Gypsum Only (4 tons/acre)
3	Ag Lime – 1 (1 ton/acre)
4	Gypsum and Ag Lime-1
5	P2O5 (50 pounds/acre)
6	Gypsum + P2O5
7	Ag Lime-1 + P2O5
8	Gypsum + Ag Lime-1 + P2O5
9	Ag Lime-2 (2 tons/acre)
10	Gypsum + Ag Lime-2
11	Ag Lime-2 + P2O5
12	Ag Lime-2 + Gypsum + P2O5

The results of the greenhouse study are presented in **Table 7.6**. In general, the data provide an indication that various treatments differ from one-another. However, the standard deviation of the data resulted in few significant differences. Treatment 1 is the baseline condition, which provides plant production without the application of amendments. The only significant

differences found in the data collected from the North Pivot soils were associated with treatment numbers 4 and 11. The application of gypsum and ag-lime (treatment 4) resulted in a significantly higher plant production. In addition, the application of ag-lime at the higher application rate in combination with phosphorous also increased the production above the baseline levels. The amendments to soils collected from the South Pivot area did not increase production levels above baseline conditions for any treatment during the first cutting, while treatments 5 and 12 resulted in significant increased plant production for the second cutting.

Conclusions of this study

1. The application of gypsum and ag-lime to the North Pivot soil material significantly increased plant production. The ag-lime neutralized the acidity resulting from the oxidation of sulfur and the gypsum prevented soil structure problems due to the sodic water used to irrigate the site.
2. The North Pivot material also reacted to ag-lime at the highest application rate in combination with added phosphorus. Again, the ag-lime neutralized the acidity and the addition of phosphorus enhanced soil fertility. The addition of phosphorus is often required as soils become acidic due to phosphorus fixation or complexation with elements such as Al and Fe.
3. The South Pivot material did not react to any treatments for the first cutting.
4. The addition of phosphorus alone significantly increased the plant production in the South Pivot soil material for the second cutting.
5. The South Pivot soil material also significantly increased plant production for the second cutting when treated with phosphorus, gypsum and high levels of ag-lime.

Table 7.6: Plant production for the first cutting (10 seeds planted in each pot) July 14, 2006.

North Pivot First Cutting				South Pivot First Cutting			
Pot #	Treatment	Dry Weight (g)	Avg/Trt	Pot #	Treatment	Dry Weight (g)	Avg/Trt
16	1	0.4977		30	1	1.1	
18	1	0.3		38	1	0.9	
27	1	0.4		12	1	0.8	
4	1	0.4	0.3994	1	1	1.2	1.0000
13	2	0.5		9	2	1	
3	2	0.4		24	2	1.2	
29	2	0.6		4	2	1.4	
47	2	0.5	0.5000	36	2	0.7	1.0750
6	3	0.5		17	3	0.9	
7	3	0.5		42	3	1.5	
3	3	0.6		16	3	1.2	
37	3	0.4	0.5000	25	3	1	1.1500
12	4	0.8		46	4	1.1	
28	4	0.8		8	4	0.9	
42	4	0.5		41	4	1.3	
30	4	0.7	0.7000	7	4	1.3	1.1500
44	5	0.4		45	5	1.2	
33	5	0.4		15	5	1.2	

Final Report: Produced Water Management and Beneficial Use

20	5	0.5		26	5	1.6	
31	5	0.4	0.4250	2	5	0.8	1.2000
14	6	0.1		10	6	1.1	
5	6	0.3		19	6	0.9	
39	6	0.2		27	6	1.4	
36	6	0.6	0.3000	22	6	1.2	1.1500
17	7	0.4754		31	7	0.8	
2	7	0.5		29	7	1.5	
8	7	0.5		49	7	1.2	
32	7	0.6	0.5189	48	7	1.2	1.1750
19	8	0.5154		44	8	1.1	
45	8	0.5		21	8	1.2	
38	8	0.5		3	8	1.2	
40	8	0.9	0.6039	6	8	1	1.1250
15	9	0.5		20	9	1	
22	9	0.7		28	9	1	
11	9	0.4		11	9	1.3	
46	9	0.8	0.6000	23	9	1.4	1.1750
35	10	0.3		43	10	0.9	
11	10	0.5		34	10	0.8	
48	10	0.6		35	10	1.2	
41	10	0.6	0.5000	33	10	1.2	1.0250
34	11	0.9		14	11	1.3	
23	11	0.7		18	11	1.2	
1	11	0.9		32	11	1	
24	11	0.7	0.8000	5	11	1.2	1.1750
21	12	0.9		13	12	2.5	
43	12	0.3		47	12	1.4	
10	12	0.5		37	12	1.1	
25	12	0.8	0.6250	39	12	1.2	1.5500

North Pivot Second Cutting

South Pivot Second Cutting

Pot #	Treatment	Dry Weight (g)	Avg/Trt	Pot #	Treatment	Dry Weight (g)	Avg/Trt
16	1	0.4977		30	1	0.9	
18	1	0.3		38	1	1	
27	1	0.4		12	1	0.3	
4	1	0.4	0.275	1	1	1.1	0.8250
13	2	0.5		9	2	1	
3	2	0.4		36	2	0.9	
29	2	0.6		24	2	1	
47	2	0.5	0.325	4	2	1.3	1.0500
6	3	0.5		16	3	1.4	
7	3	0.5		42	3	1.1	
3	3	0.6		25	3	0.6	
37	3	0.4	0.4	16	3	1	1.0250
12	4	0.8		7	4	1.3	
28	4	0.8		8	4	1.2	
42	4	0.5		46	4	1.2	
30	4	0.7	0.5500	41	4	1	1.1750

44	5	0.4		45	5	1.4	
33	5	0.4		2	5	1.1	
20	5	0.5		26	5	1.3	
31	5	0.4	0.2500	15	5	1.2	1.2500
14	6	0.1		22	6	1.1	
5	6	0.3		19	6	0.8	
39	6	0.2		10	6	1.1	
36	6	0.6	0.1250	27	6	1.1	1.0250
17	7	0.4754		48	7	1.4	
2	7	0.5		40	7	1.3	
8	7	0.5		29	7	1.1	
32	7	0.6	0.4500	31	7	0.8	1.1500
19	8	0.5154		21	8	1.1	
45	8	0.5		6	8	1	
38	8	0.5		3	8	1.1	
40	8	0.9	0.5000	44	8	1.2	1.1000
15	9	0.5		28	9	0.8	
22	9	0.7		23	9	1.3	
0.4	9	11		11	9	1.1	
46	9	0.8	0.4750	20	9	1.1	1.0750
35	10	0.3		34	10	1.1	
11	10	0.5		35	10	1.2	
48	10	0.6		43	10	1.4	
41	10	0.6	0.3750	33	10	1.1	1.2000
34	11	0.9		5	11	1.2	
23	11	0.7		32	11	1.1	
1	11	0.9		14	11	1.1	
24	11	0.7	0.5750	18	11	1.2	1.1500
21	12	0.9		37	12	1	
43	12	0.3		39	12	1.3	
10	12	0.5		47	12	1.2	
25	12	0.8	0.6000	13	12	1.5	1.2500

SUBTASK 4: USE OF AMENDMENTS TO RECLAIM SITES IMPACTED BY CBM CO-PRODUCED WATER

A sodic soil site (**Figure 7.28**) impacted by CBM produced water was reclaimed during 2005. Baseline samples collected prior to reclamation are presented in **Table 7.7**. Samples were also collected from the site during Fall 2006 to show the status of the reclamation process (**Table 7.8**). The primary purpose for the addition of gypsum to the site is to reduce the SAR values of the surface materials to eliminate the dispersion that resulted from the previous application of CBM produced water containing elevated levels of sodium.

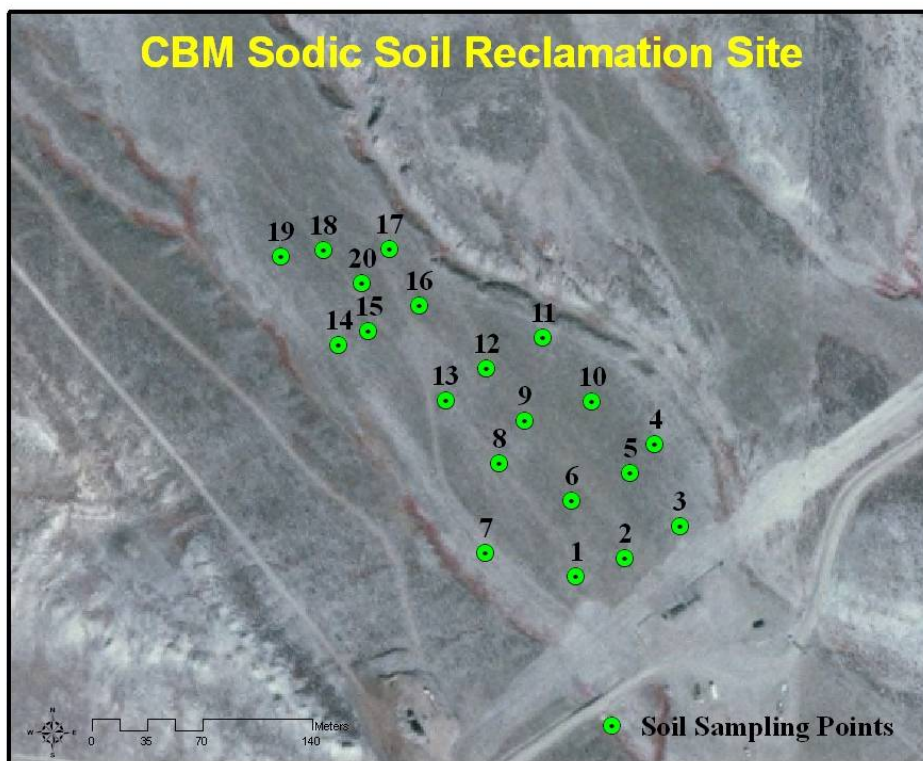


Figure 4.1: Sodic field impacted with CBM co-produced water that was reclaimed using an application of gypsum.

The site chosen for the reclamation evaluation was located at the Dave Perry Ranch located east of Sheridan Wyoming had been used for disposal of CBM produced water via irrigation. The surface of the soil was dispersed as a result of the sodic nature of the irrigation water and due to the impact of the water drops on the surface.

Reclamation of the site was accomplished by applying two tons of gypsum per acre at the surface without incorporation. One year after amendment application, soil evaluations showed a decrease in an average SAR value from 9.1 with a range of 13 to 5 to an average SAR value of 6.5 with a range of 9.6 to 2.8. The decline in SAR values at the site translated into a less dispersed soil at the surface and no change at depth. The EC levels associated with the surface soil did not change as expected due to the addition of gypsum.

Conclusions of This Study

1. Reclamation was successful with the application of two tons of gypsum per acre.
2. After only one year, SAR values were lower with the application of gypsum and no irrigation. Such results are expected to take significant periods of time under natural climatic conditions.

RECOMMENDATIONS FOR FUTURE RESEARCH

Management of Coal-Bed Natural Gas Produced Water

The use of produced water for irrigation has been shown to be successful. However, the long-term impact of amendment application to soils is unknown. Long-term research activities are required to assess this impact.

The application of CBNG produced water to soils via surface and sub-surface irrigation practices results in the addition of large quantities of salts to the soil. Irrigation modeling is currently used to estimate the movement of salts in the profiles. Such modeling has been calibrated for surface application but has not been demonstrated for sub-surface drip irrigation systems. Additional calibration work is needed.

Table 7.7: Baseline Soils Evaluation.

Table 4.1. Baseline soils evaluation Dave Perry reclamation site (2005).

Sample ID	Depth in	pH su	EC mmhos/cm	Percent		SAR	Ca meq/L	Mg meq/L	Na meq/L	Sand %	Silt %	Clay %	Texture
				Sat %	Sat %								
DP-RC-1	0-6	7.8	0.92	49	8.1	0.98	0.9	7.86	25	38	37	cl	
	6-12	7.2	0.87	57	2.8	2.25	2.66	4.32	18	38	44	cl	
	12-18	8.1	1.69	60	2.3	3.22	7.57	5.3	20	41	39	sicl	
DP-RC-2	0-6	9.2	0.87	48	8.4	1.43	0.65	8.62	27	42	31	cl	
	6-12	8.6	0.52	42	5.8	0.81	0.55	4.78	23	45	32	cl	
	12-18	8.4	0.58	50	4	1.09	1.2	4.32	19	39	42	c	
DP-RC-3	0-6	7.4	0.51	48	5	0.72	0.55	3.97	22	41	37	cl	
	6-12	7.8	0.44	70	2.2	1.71	1.14	2.59	16	43	41	sic	
	12-18	8.4	0.34	59	1.3	1.36	1.12	1.49	20	42	38	sicl	
DP-RC-4	0-6	8.8	0.96	47	8.3	2.04	0.76	9.87	33	36	31	cl	
	6-12	8.7	0.52	37	6	0.92	0.35	4.79	18	52	30	sicl	
	12-18	8.3	0.38	46	3.7	0.82	0.57	3.11	22	40	38	cl	
DP-RC-5	0-6	8.3	0.46	45	6.2	0.73	0.33	4.51	31	38	31	cl	
	6-12	8	0.96	51	2.1	3.51	2.45	3.63	21	45	34	cl	
	12-18	8	2.7	57	2.1	7.99	11.8	6.72	18	46	36	sicl	
DP-RC-6	0-6	8.2	0.69	43	8.3	0.9	0.53	7.04	29	40	31	cl	
	6-12	8	0.49	48	5.6	0.64	0.58	4.34	19	43	38	sicl	
	12-18	8.3	0.4	54	3.2	0.84	0.8	2.87	19	42	39	sicl	
DP-RC-7	0-6	7.9	2.5	56	13	2.22	2.31	19	19	40	41	c	
	6-12	7.9	1.25	54	2.6	2.81	3.64	4.72	18	43	39	sicl	
	12-18	8.5	0.79	53	1.7	1.44	4.2	2.92	24	41	35	cl	
DP-RC-8	0-6	8	0.87	45	9.6	0.82	0.73	8.45	21	43	36	cl	

Final Report: Produced Water Management and Beneficial Use

	6-12	7.9	0.91	53	3.4	1.99	2.92	5.29	19	42	39	sicl
	12-18	8.1	2.68	56	2.2	4.46	18.1	7.51	20	44	36	sicl
DP-RC-9	0-6	8.4	0.82	44	9.2	1	0.62	8.32	24	43	33	cl
	6-12	8.1	0.67	52	3.2	1.73	1.62	4.2	19	44	37	sicl
	12-18	8.2	1.1	56	1.4	2.51	5.04	2.82	15	47	38	sicl
DP-RC-10	0-6	8.6	0.99	44	9.9	1.34	0.48	9.43	36	35	29	cl
	6-12	8.5	0.73	35	6.1	1.26	0.59	5.85	39	33	28	cl
	12-18	8.3	0.38	38	1.8	1.26	1.06	1.93	35	35	30	cl
DP-RC-11	0-6	8.8	0.82	42	9.2	1.04	0.38	7.72	39	34	27	cl
	6-12	8.3	1.46	42	8.3	1.93	1.07	10.2	37	33	30	cl
	12-18	8.2	1.15	45	3.3	2.24	2.81	5.21	31	35	34	cl
DP-RC-12	0-6	7.8	1.91	47	13	1.94	1.3	16.8	18	44	38	sicl
	6-12	7.9	0.88	55	2.9	2.5	2.52	4.62	15	46	39	sicl
	12-18	7.8	3.47	49	2.4	8.45	20.2	8.88	29	36	35	cl
DP-RC-13	0-6	8.4	1.12	58	9.8	1.05	0.87	9.61	22	41	37	cl
	6-12	7.6	0.88	53	4.5	1.45	2	5.87	16	43	41	sic
	12-18	8.3	2.55	58	4.5	3.21	11.3	12.1	17	42	41	sic
DP-RC-14	0-6	8.1	0.72	48	6.9	1.29	0.6	6.73	19	45	36	sicl
	6-12	8	0.77	57	2.1	2.88	2.38	3.45	17	41	42	sic
	12-18	8.2	0.94	58	1.2	2.59	4.85	2.23	12	44	44	sic
DP-RC-15	0-6	8.1	1.35	53	9.8	1.77	1.21	11.9	18	45	37	sicl
	6-12	8.2	1.36	55	3.1	2.68	4.09	5.78	14	47	39	sicl
	12-18	8.3	2.25	52	2.5	2.98	13.6	7.27	20	43	37	sicl
DP-RC-16	0-6	7.7	1.21	47	10	1.57	1.15	11.7	17	46	37	sicl
	6-12	7.4	0.66	53	2.8	2	1.93	4	15	45	40	sic
	12-18	8	1.51	58	1.9	4.5	6.68	4.59	12	47	41	sic
DP-RC-17	0-6	8.1	1.3	43	11	1.88	1.01	12.6	24	45	31	cl
	6-12	7.8	0.62	50	4.6	1.3	0.93	4.85	17	47	36	sicl

	12-18	8.2	0.41	54	1.8	1.62	1.48	2.2	12	49	39	sicl
DP-RC-18	0-6	8.2	1.18	49	9.4	1.56	0.84	10.4	20	45	35	sicl
	6-12	8.1	1.37	52	4.8	2.46	2.81	7.87	20	46	34	sicl
	12-18	8.4	0.79	50	3.4	1.27	2.91	4.98	23	45	32	cl
DP-RC-19	0-6	8.1	1.67	55	9.3	2.03	1.04	11.6	21	44	35	cl
	6-12	8.2	0.76	53	2.5	2.34	2.13	3.75	18	46	36	sicl
	12-18	8.3	0.88	57	1.4	1.79	4.86	2.62	17	42	41	sic
DP-RC-20	0-6	8.1	0.91	50	7.2	1.63	0.68	7.72	20	45	35	sicl
	6-12	8.4	1.47	60	3.8	2.59	4.86	7.33	14	50	36	sicl
	12-18	8.4	0.67	57	2.8	1.6	2.45	4.05	14	48	38	sicl

Table 7.8: Post-reclamation Sample Analysis Collected from the Dave Perry Reclamation Site.

Table 4.2. Post-reclamation sample analyses collected from the Dave Perry reclamation site.

Sample ID	Depth	pH	EC mmhos/cm	Percent		Ca meq/L	Mg meq/L	Na meq/L
				SAR	Sat %			
DP-6-1	0to 6	7.5	0.92	51	6.8	1.24	1.25	7.63
	6 to 12	7.5	1.06	54	3.3	2.26	3.01	5.32
	12 to 18	8	2.36	52	2.8	4.33	14.8	8.6
	18 to 24	8.2	5.3	55	3.4	5.99	38.5	16.1
DP-6-2	0to 6	7.7	0.73	51	5.7	0.97	0.61	5.05
	6 to 12	7.9	0.61	51	3	2.12	1.86	4.29
	12 to 18	8.1	1.01	47	2.2	2.1	6.15	4.37
	18 to 24	8.2	2.56	57	2.8	4.04	19.5	9.72
DP-6-3	0to 6	7.7	1.15	55	8.3	1.52	1.53	10.2
	6 to 12	7.5	0.76	50	4.5	1.44	1.81	5.74
DP-6-4	0to 6	7.6	4.36	54	9.6	15.2	9.1	33.4
	6 to 12	7.2	1.22	55	2.7	5.25	4.27	5.93
	12 to 18	7.7	3.13	52	3	9.64	16.9	11
	18 to 24	7.9	6.41	55	4.2	11.4	37	20.6
DP-6-5	0to 6	7.6	2.28	52	7.9	7.39	3.32	18.3
	6 to 12	7.8	0.64	56	2.5	1.9	1.44	3.27
	12 to 18	8	1.1	57	2.4	2.82	4.07	4.41
	18 to 24	8	2.95	56	3.2	5.46	13	9.86
DP-6-6	0to 6	7.9	0.71	52	7.2	1.19	0.43	6.48
	6 to 12	8.2	0.71	52	4.7	1.53	1.11	5.4
	12 to 18	8.4	2.99	54	2.6	5.53	20.2	9.52
	18 to 24	8.6	7.53	53	3.1	11.2	53.8	17.6
DP-6-7	0to 6	7.3	1.03	53	9.6	1.31	0.84	9.97
	6 to 12	7.4	0.54	48	4	1.28	0.77	4.02
	12 to 18	7.9	1.51	51	3.4	3.07	5.04	6.83
	18 to 24	8.1	2.35	51	5.3	1.88	15	15.5
DP-6-8	0to 6	7.6	0.42	46	4.4	0.62	0.63	3.45
	6 to 12	7.8	0.66	53	3	1.62	1.75	3.85
	12 to 18	7.8	1.5	52	2.4	3.79	8.58	6.04
	18 to 24	7.9	5.2	53	3	7.41	33.1	13.5
DP-6-9	0to 6	7.6	0.73	52	2.9	2.66	1.52	4.15
	6 to 12	7.8	1.05	54	1.6	4.11	5	3.43
	12 to 18	7.8	4.34	56	3	9.87	25	12.4
	18 to 24	7.9	6.96	57	2.8	14.4	44.4	14.9
DP-6-10	0to 6	7.6	0.6	46	2.8	2.25	0.88	3.49
	6 to 12	7.8	0.83	49	3.4	2.61	1.58	4.92
	12 to 18	7.9	0.56	52	1.2	1.81	2.43	1.67
	18 to 24	7.9	1.45	50	2	3.09	7.56	4.54

APPENDIX 7.1: Results of Pre-irrigation Soil Sample Analysis from the WJ Irrigation Site

ENERGY LABORATORIES, INC. • P.O. Box 5688 • 3161 East Lyndale Ave. • Helena, MT 59604
 877-472-0711 • 406-442-0711 • 406-442-0712 fax • helena@energylab.com



LABORATORY ANALYTICAL REPORT

Client: Poudre Valley Environmental Sciences
Project: Managed Irrigation Research
Workorder: H06050051

Report Date: 05/09/06
Date Received: 04/17/06

Sample ID	Client Sample ID	Analysis		pH-SatPst	COND	Percent Sat	SAR	HCO3 SatPst	Cl	Ca-SatPst	Mg-SatPst	Na-SatPst	SO4-SatPst	Cl-SatPst	
		Units	Results												
		Up	Low												
H06050051-001	WJ-08 0-7"	0	7	7.1	0.48	42.5	1.3	4.40	14	2.27	1.25	1.77	0.90	0.38	
H06050051-002	WJ-08 7-13"	7	13	7.5	0.52	47.8	0.72	3.00	45	2.85	1.51	1.06	1.03	1.26	
H06050051-003	WJ-08 13-20"	13	20	7.8	0.57	53.1	0.73	2.40	82	2.75	1.99	1.13	0.88	2.32	
H06050051-004	WJ-08 20-30"	20	30	8.2	0.42	54.0	1.4	3.80	14	2.10	1.59	1.97	0.91	0.40	
H06050051-005	WJ-08 30-42"	30	42	8.3	0.56	49.8	3.1	3.60	13	1.42	1.57	3.84	1.88	0.35	
H06050051-006	WJ-08 42-60"	42	60	8.3	0.56	52.1	4.0	4.00	19	1.12	1.32	4.39	1.99	0.54	
H06050051-007	WJ1 0-6"	0	6	7.1	0.48	52.6	0.64	2.40	62	2.15	1.68	0.88	0.50	1.76	
H06050051-008	WJ1 6-11"	6	11	7.6	0.98	58.6	0.69	2.60	219	4.77	3.62	1.42	0.63	6.18	
H06050051-009	WJ1 11-15"	11	15	8.0	0.57	54.8	1.7	3.80	61	2.10	1.97	2.46	0.59	1.72	
H06050051-010	WJ1 15-27"	15	27	8.5	0.80	53.3	5.7	4.99	53	1.19	1.64	6.78	1.70	1.50	
H06050051-011	WJ1 27-39"	27	39	8.8	1.60	47.0	9.6	4.99	108	1.11	2.44	12.8	7.90	3.04	
H06050051-012	WJ1 39-52"	39	52	8.2	7.58	44.1	7.7	4.00	348	22.5	38.9	42.6	100	9.75	
H06050051-013	WJ2 0-7"	0	7	7.7	0.72	49.7	0.28	4.40	50	6.59	1.69	0.53	2.51	1.42	
H06050051-014	WJ2 7-11"	7	11	7.9	0.52	53.2	0.48	3.20	42	4.09	1.56	0.80	1.40	1.18	
H06050051-015	WJ2 11-24"	11	24	7.8	2.50	45.0	0.28	2.80	68	26.4	11.7	1.11	36.9	1.92	
H06050051-016	WJ2 24-48"	24	48	7.8	4.15	41.6	1.7	2.00	179	26.1	24.0	8.30	56.0	5.04	
H06050051-017	WJ2 48-60"	48	60	8.2	8.16	44.9	4.9	1.60	300	21.9	67.8	32.9	122	8.48	

APPENDIX 7.1: Results of Pre-irrigation Soil Sample Analysis from the WJ Irrigation Site

ENERGY LABORATORIES, INC. • P.O. Box 5688 • 3161 East Lyndale Ave. • Helena, MT 59604
 877-472-0711 • 406-442-0711 • 406-442-0712 fax • helena@energylab.com



LABORATORY ANALYTICAL REPORT

Client: Poudre Valley Environmental Sciences **Report Date:** 05/09/06
Project: Managed Irrigation Research **Date Received:** 04/17/06
Workorder: H06050051

Sample ID	Client Sample ID	Units		Sand	Silt	Clay	Texture	CEC	Lime	Na-Ext	Exch Na	ESP
		Up	Low									
		Results	Results									
H06050051-001	WJ-08 0-7"	0	7	35	44	21	L	20.5	1.0	0.50	0.4	2.0
H06050051-002	WJ-08 7-13"	7	13	31	39	30	CL	27.2	1.3	0.37	0.3	1.2
H06050051-003	WJ-08 13-20"	13	20	24	39	37	CL	31.3	2.2	0.47	0.4	1.3
H06050051-004	WJ-08 20-30"	20	30	21	40	39	CL	31.4	7.4	0.68	0.6	1.8
H06050051-005	WJ-08 30-42"	30	42	28	40	32	CL	26.0	6.8	1.08	0.9	3.4
H06050051-006	WJ-08 42-60"	42	60	20	47	33	SiCL	28.5	6.4	1.32	1.1	3.8
H06050051-007	WJ1 0-6"	0	6	26	39	35	CL	31.1	1.2	0.47	0.4	1.4
H06050051-008	WJ1 6-11"	6	11	20	41	39	SiCL	35.8	4.4	0.51	0.4	1.2
H06050051-009	WJ1 11-15"	11	15	17	45	38	SiCL	30.2	10.9	0.77	0.6	2.1
H06050051-010	WJ1 15-27"	15	27	25	41	34	CL	26.0	9.6	2.00	1.6	6.3
H06050051-011	WJ1 27-39"	27	39	34	39	27	CL	21.1	5.1	2.84	2.2	11
H06050051-012	WJ1 39-52"	39	52	39	33	28	CL	21.7	4.3	3.74	1.9	8.6
H06050051-013	WJ2 0-7"	0	7	34	38	28	CL	28.5	7.7	0.46	0.4	1.5
H06050051-014	WJ2 7-11"	7	11	32	35	33	CL	29.5	15.5	0.44	0.4	1.4
H06050051-015	WJ2 11-24"	11	24	39	32	29	CL	24.7	20.4	0.42	0.4	1.5
H06050051-016	WJ2 24-48"	24	48	48	39	13	L	18.1	10	1.11	0.8	4.2
H06050051-017	WJ2 48-60"	48	60	36	51	13	SiL	21.4	4.4	2.67	1.2	5.6

APPENDIX 7.2: Baseline – Soil Chemistry Data for the Research Plots

Table 1.1.1 Baseline – Soil chemistry data for the research plots.

WJ Sites	Treatment	Depth	pH	EC	Sat %	SAR	Ca	Mg	Na	Sand	Silt	Clay	Texture	CEC	Ext. Na	Exch Na	ESP
WJ1-1	2	0-6	6.4	0.21	33.1	0.37	0.88	0.62	0.32	33	41	26	l	23.1	0.32	0.3	1.3
	2	6-12	6.9	0.14	38.8	0.41	0.61	0.45	0.30	24	40	36	cl	30.3	0.34	0.3	1.1
	2	12-18	7.5	0.24	47.1	1.10	0.78	0.60	0.88	24	29	47	cl	39.0	0.42	0.4	1.0
WJ1-2	2	18-24	7.9	0.39	42.1	0.71	1.67	1.43	0.89	34	29	37	cl	30.8	0.44	0.4	1.3
	5	0-6	6.7	0.25	45.3	0.59	1.20	0.59	0.56	32	44	24	l	22.9	0.30	0.3	1.2
	5	6-12	6.9	0.42	43.0	0.58	2.23	1.25	0.76	32	39	29	cl	27.1	0.32	0.3	1.1
WJ1-3	5	12-18	7.5	0.35	55.0	0.61	1.90	1.16	0.75	25	32	43	cl	36.3	0.44	0.4	1.1
	5	18-24	8.1	0.41	47.6	0.81	1.84	1.39	1.03	29	37	34	cl	27.4	0.47	0.4	1.5
	1	0-6	6.6	0.27	44.4	0.91	0.34	0.58	0.22	33	42	25	l	24.4	0.34	0.3	1.3
WJ1-4	1	6-12	6.7	0.21	47.1	0.60	1.16	0.63	0.57	34	33	33	cl	28.9	0.32	0.3	1.0
	1	12-18	7.2	0.22	51.1	0.72	0.99	0.60	0.64	28	33	39	cl	31.2	0.45	0.4	1.3
	1	18-24	7.9	0.32	50.1	0.66	1.94	1.29	0.84	24	37	39	cl	33.6	0.50	0.5	1.4
WJ1-5	7	0-6	6.5	0.23	44.7	0.63	1.06	0.68	0.59	32	43	25	l	24.6	0.34	0.3	1.3
	7	6-12	7.0	0.28	56.4	0.60	1.37	0.91	0.64	30	31	39	cl	34.4	0.38	0.3	1.0
	7	12-18	7.6	0.30	50.0	0.72	1.66	1.17	0.86	29	32	39	cl	35.1	0.50	0.5	1.3
WJ1-6	6	18-24	8.2	0.33	47.4	0.97	1.54	1.22	1.14	37	31	32	cl	26.8	0.48	0.4	1.6
	6	0-6	7.1	0.26	42.5	0.65	1.46	0.82	0.69	28	46	26	l	25.4	0.30	0.3	1.1
	6	6-12	7.5	0.25	47.5	0.48	1.44	0.78	0.51	30	39	31	cl	28.0	0.38	0.4	1.3
WJ1-7	6	12-18	8.0	0.20	44.7	0.65	1.07	0.77	0.62	35	33	32	cl	28.4	0.30	0.3	1.0
	6	18-24	6.7	0.29	48.1	0.65	1.79	1.14	0.79	31	34	35	cl	30.8	0.37	0.3	1.1
	3	0-6	7.2	0.21	44.8	0.49	1.19	0.72	0.48	35	40	25	l	24.5	0.34	0.3	1.3
WJ2-1	3	6-12	7.7	0.29	53.9	0.53	1.54	1.04	0.60	30	29	41	c	36.7	0.40	0.4	1.0
	3	12-18	8.2	0.32	52.8	0.59	1.78	1.32	0.74	30	31	39	cl	36.9	0.51	0.5	1.3
	3	18-24	8.1	0.30	49.3	0.88	1.41	1.27	1.02	32	33	35	cl	31.7	0.50	0.4	1.4
WJ2-1	4	0-6	7.0	0.38	46.8	0.36	2.74	1.19	0.50	33	40	27	cl	29.2	0.39	0.4	1.3
	4	6-12	7.7	0.32	43.6	0.54	2.26	0.95	0.68	29	43	28	cl	26.0	0.34	0.3	1.2
	4	12-18	8.1	0.35	48.9	1.10	1.83	1.19	1.37	35	33	32	cl	31.6	0.66	0.6	1.9
WJ2-1	4	18-24	7.9	0.28	53.4	0.83	1.55	0.83	0.91	26	35	39	cl	37.3	0.46	0.4	1.1
	3	0-6	7.0	0.29	46.4	0.72	1.30	1.30	0.82	30	39	31	cl	29.0	0.47	0.4	1.5

APPENDIX 7.2: Baseline – Soil Chemistry Data for the Research Plots

	3	6-12	7.3	0.29	51.7	0.96	1.05	1.08	0.99	27	34	39	cl	35.1	0.50	0.4	1.3
	3	12-18	8.0	0.38	49.2	1.30	1.32	1.62	1.61	29	37	34	cl	30.3	1.43	1.4	4.5
	3	18-24	8.6	0.49	49.1	3.40	1.07	1.29	3.70	32	35	33	cl	27.4	1.32	1.1	4.2
WJ2-2	2	0-6	6.6	0.18	45.9	0.75	0.74	0.61	0.62	28	39	33	cl	28.5	0.41	0.4	1.3
	2	6-12	7.4	0.26	52.2	0.80	1.09	1.01	0.82	24	36	40	c	35.5	0.52	0.5	1.4
	2	12-18	8.2	0.33	50.0	1.50	1.39	1.20	1.70	27	36	37	cl	30.1	0.75	0.7	2.2
	2	18-24	8.4	0.43	47.2	3.50	0.90	0.98	3.35	27	38	35	cl	27.2	1.23	1.1	3.9
WJ2-3	4	0-6	6.9	0.27	46.6	0.86	1.02	1.09	0.88	31	38	31	cl	28.3	0.41	0.4	1.3
	4	6-12	7.3	0.28	53.8	1.50	0.77	0.96	1.36	28	31	41	c	37.8	0.76	0.8	2.0
	4	12-18	8.2	0.44	49.7	2.50	1.15	1.30	2.80	27	35	38	cl	32.4	0.99	0.8	2.6
	4	18-24	8.6	0.64	45.4	4.80	0.82	1.15	4.73	28	37	35	cl	27.1	1.58	1.4	5.1
WJ2-4	5	0-6	6.6	0.25	49.0	0.47	1.09	1.16	0.50	30	39	31	cl	27.9	0.49	0.5	1.7
	5	6-12	7.3	0.48	56.6	0.84	2.25	2.57	1.30	25	32	43	c	35.5	0.58	0.5	1.4
	5	12-18	8.0	0.38	51.0	1.50	1.47	1.64	1.83	23	37	40	c	28.2	0.86	0.8	2.7
	5	18-24	8.6	0.54	46.8	4.00	0.88	1.43	4.32	25	41	34	cl	26.6	1.32	1.1	4.2
WJ2-5	7	0-6	6.4	0.25	48.6	0.59	1.11	1.05	0.61	30	35	35	cl	29.8	0.40	0.4	1.2
	7	6-12	7.1	0.24	53.5	1.10	0.90	0.89	1.02	27	33	40	c	37.0	0.66	0.6	1.6
	7	12-18	8.2	0.41	52.7	1.80	1.84	1.54	2.27	27	36	37	cl	31.1	0.91	0.8	2.5
	7	18-24	8.7	0.46	50.6	3.70	1.09	0.93	3.72	23	41	36	cl	27.2	1.51	1.3	4.9
WJ2-6	6	0-6	6.9	0.25	46.2	1.30	0.77	0.84	1.14	24	39	37	cl	32.7	0.57	0.5	1.6
	6	6-12	7.7	0.44	53.4	2.00	1.31	1.56	2.40	19	38	43	c	36.9	1.07	0.9	2.5
	6	12-18	8.5	0.48	48.3	3.10	1.26	1.12	3.41	25	39	36	cl	28.7	1.49	1.3	4.6
	6	18-24	8.6	0.90	51.2	6.80	0.99	1.42	7.41	23	42	35	cl	25.7	2.45	2.1	8.1
WJ2-7	1	0-6	6.8	0.28	43.6	0.53	1.34	1.19	0.60	31	43	26	l	24.1	0.36	0.3	1.4
	1	6-12	7.3	0.29	55.4	0.60	1.55	1.38	0.73	22	37	41	c	36.9	0.51	0.5	1.3
	1	12-18	8.0	0.33	52.2	1.10	1.51	1.36	1.27	22	41	37	cl	29.9	0.60	0.5	1.8
	1	18-24	8.3	0.42	51.8	3.00	1.24	1.13	3.21	21	43	36	cl	28.5	1.29	1.1	3.9
WJ3-1	1	0-6	6.7	0.26	44.7	0.81	0.90	0.94	0.78	21	37	42	c	35.2	0.53	0.5	1.4
	1	6-12	7.4	0.46	52.0	0.91	1.75	1.83	1.22	24	31	45	c	35.5	0.51	0.4	1.3
	1	12-18	8.1	0.44	48.7	1.30	1.33	1.58	1.57	14	40	46	c	35.2	0.76	0.7	2.1
	1	18-24	8.4	0.39	47.7	2.50	0.91	0.89	2.40	21	41	38	cl	28.0	1.06	1.0	3.4
WJ3-2	2	0-6	6.7	0.20	41.6	0.96	0.74	0.73	0.82	27	38	35	cl	32.1	0.45	0.4	1.3
	2	6-12	7.4	0.41	54.3	1.00	1.48	1.35	1.21	17	39	44	c	40.1	0.51	0.4	1.1
	2	12-18	8.1	0.38	50.1	1.10	1.47	1.54	1.37	16	41	43	sic	38.5	0.63	0.6	1.5

APPENDIX 7.2: Baseline – Soil Chemistry Data for the Research Plots

WJ3-3	2	18-24	8.4	0.43	46.8	2.30	0.92	1.21	2.40	28	34	38	cl	36.4	1.00	0.9	2.4
	4	0-6	7.0	0.40	45.4	0.51	1.74	1.58	0.66	23	38	39	cl	38.6	0.44	0.4	1.1
	4	6-12	7.5	0.43	52.2	0.71	1.71	1.62	0.92	19	38	43	c	43.1	0.57	0.5	1.2
	4	12-18	8.1	0.36	53.3	1.10	2.02	1.43	1.39	17	41	42	sic	40.0	0.79	0.7	1.8
	4	18-24	8.4	0.52	52.1	3.00	1.06	1.14	3.16	13	42	45	sic	39.7	1.33	1.2	2.9
WJ3-4	6	0-6	7.0	0.48	46.8	0.63	2.03	1.96	0.89	21	38	41	c	40.6	0.52	0.5	1.2
	6	6-12	7.5	0.41	53.8	0.98	1.44	1.52	1.19	17	38	45	c	43.9	0.75	0.7	1.6
	6	12-18	8.2	0.39	56.1	1.60	1.19	1.12	1.69	11	44	45	sic	40.0	0.91	0.8	2.1
	6	18-24	8.4	0.46	53.5	2.80	0.89	1.00	2.77	11	46	43	sic	37.1	1.35	1.2	3.2
WJ3-5	3	0-6	6.8	0.35	43.1	0.71	1.36	1.29	0.82	27	40	33	cl	40.8	0.49	0.4	1.1
	3	6-12	7.4	0.45	54.9	0.84	1.86	1.91	1.16	18	39	43	c	39.0	0.61	0.6	1.4
	3	12-18	8.2	0.37	53.6	1.40	1.22	1.17	1.49	12	44	44	sic	33.6	0.79	0.7	2.1
	3	18-24	8.4	0.47	51.4	2.20	1.63	1.27	2.62	14	43	43	sic	34.7	1.29	1.2	3.3
WJ3-6	7	0-6	6.9	0.56	48.1	0.51	2.74	2.68	0.84	23	37	40	c	39.5	0.50	0.5	1.2
	7	6-12	7.4	0.51	48.8	0.75	2.25	2.30	1.13	17	39	44	c	37.0	0.56	0.5	1.4
	7	12-18	8.1	0.42	48.3	1.30	1.34	1.49	1.53	20	39	41	c	32.1	0.68	0.6	1.9
	7	18-24	8.4	0.41	47.6	2.60	0.74	1.00	2.38	21	41	38	cl	30.6	1.06	1.0	3.1
WJ3-7	5	0-6	6.8	0.27	46.6	0.90	0.89	0.78	0.82	22	41	37	cl	34.4	0.47	0.4	1.3
	5	6-12	7.7	0.46	51.7	0.75	1.94	1.88	1.03	15	44	41	sicl	36.9	0.53	0.5	1.3
	5	12-18	8.2	0.37	51.4	1.20	1.18	1.28	1.33	14	45	41	sicl	36.4	0.75	0.7	1.9
	5	18-24	8.4	0.46	51.1	2.60	0.97	1.10	2.63	22	38	40	c	34.3	1.22	1.1	3.2
WJ4-1	4	0-6	6.8	0.38	48.2	0.77	1.56	1.20	0.90	17	45	38	sicl	36.0	0.53	0.5	1.4
	4	6-12	7.5	0.51	47.3	0.44	2.61	2.06	0.67	15	48	37	sicl	35.6	0.45	0.4	1.2
	4	12-18	8.0	0.50	47.2	0.61	2.32	2.29	0.93	18	46	36	sicl	34.8	0.50	0.5	1.3
	4	18-24	8.3	0.33	46.8	1.30	1.05	1.26	1.42	23	46	31	cl	28.4	0.74	0.7	2.4
WJ4-2	5	0-6	6.6	0.40	47.4	0.63	1.95	1.42	0.82	18	47	35	sicl	34.6	0.50	0.5	1.3
	5	6-12	7.6	0.54	47.5	0.49	3.13	2.25	0.80	19	46	35	sicl	34.5	0.57	0.5	1.5
	5	12-18	8.1	0.35	45.8	0.53	1.78	1.69	0.70	23	43	34	cl	31.6	0.47	0.4	1.4
	5	18-24	8.2	0.43	47.0	0.88	1.57	2.10	1.19	19	49	32	sicl	30.4	0.66	0.6	2.0
WJ4-3	2	0-6	7.1	0.39	47.3	0.40	2.18	1.58	0.55	18	46	36	sicl	33.8	0.39	0.4	1.1
	2	6-12	7.7	0.38	48.2	0.35	2.26	1.60	0.49	13	48	39	sicl	35.5	0.47	0.4	1.3
	2	12-18	8.1	0.30	48.3	0.47	1.66	1.39	0.58	16	44	40	sic	34.0	0.44	0.4	1.2
	2	18-24	8.2	0.37	49.5	0.86	1.34	1.90	1.09	11	51	38	sicl	31.7	0.54	0.5	1.5
WJ4-4	6	0-6	6.6	0.50	49.4	0.49	2.70	2.05	0.75	20	43	37	sicl	34.4	0.45	0.4	1.2

APPENDIX 7.2: Baseline – Soil Chemistry Data for the Research Plots

	6	6-12	7.6	0.44	48.6	0.48	2.47	1.91	0.71	17	45	38	sicl	41.1	0.40	0.4	0.9
	6	12-18	8.0	0.36	49.9	0.74	1.61	1.58	0.94	13	45	42	sic	42.1	0.61	0.6	1.3
	6	18-24	8.3	0.48	47.7	1.60	1.25	1.85	1.93	16	48	36	sicl	31.5	0.83	0.7	2.3
WJ4-5	7	0-6	6.7	0.29	49.8	0.43	1.37	1.08	0.48	16	47	37	sicl	34.8	0.40	0.4	1.1
	7	6-12	7.5	0.40	48.0	0.56	2.07	1.58	0.76	18	45	37	sicl	35.0	0.43	0.4	1.1
	7	12-18	8.1	0.35	52.6	0.73	1.63	1.48	0.91	11	48	41	sic	34.5	0.50	0.4	1.3
	7	18-24	8.3	0.45	53.9	1.50	1.31	1.74	1.89	19	43	38	sicl	32.9	0.77	0.7	2.0
WJ4-6	3	0-6	6.7	0.29	47.2	0.62	1.23	0.87	0.64	16	48	36	sicl	35.9	0.32	0.3	0.8
	3	6-12	7.7	0.34	48.2	0.47	1.94	1.36	0.60	19	45	36	sicl	35.3	0.45	0.4	1.2
	3	12-18	8.1	0.32	47.7	0.77	1.42	1.25	0.89	13	49	38	sicl	32.4	0.56	0.5	1.6
	3	18-24	8.3	0.30	45.8	1.30	0.93	1.12	1.31	21	46	33	cl	26.8	0.69	0.6	2.4
WJ4-7	1	0-6	6.7	0.26	44.9	0.51	1.32	0.86	0.53	19	45	36	sicl	33.8	0.40	0.4	1.1
	1	6-12	7.5	0.41	45.5	0.48	2.37	1.69	0.68	22	45	33	cl	31.8	0.41	0.4	1.2
	1	12-18	8.1	0.30	49.7	0.93	1.40	1.30	1.08	14	46	40	sic	35.2	0.58	0.5	1.5
	1	18-24	8.3	0.33	47.1	1.50	1.21	1.33	1.67	14	50	36	sicl	32.4	0.78	0.7	2.2
WJ5-1	6	0-6	6.2	0.33	37.1	0.47	1.56	0.99	0.53	32	38	30	cl	28.3	0.47	0.4	1.6
	6	6-12	7.0	0.47	35.8	0.29	2.74	1.81	0.43	26	43	31	cl	32.1	0.38	0.4	1.1
	6	12-18	7.8	0.41	32.3	0.36	2.15	1.61	0.49	22	46	32	cl	29.7	0.43	0.4	1.4
	6	18-24	8.1	0.32	41.2	0.63	1.37	1.39	0.74	19	46	35	sicl	31.8	0.56	0.5	1.7
WJ5-2	1	0-6	6.5	0.21	37.3	0.58	0.92	0.61	0.51	41	36	23	l	22.7	0.43	0.4	1.8
	1	6-12	7.4	0.32	35.4	0.68	1.54	1.06	0.77	27	42	31	cl	31.8	0.53	0.5	1.6
	1	12-18	8.1	0.30	38.2	1.10	1.25	0.85	1.14	21	49	30	cl	26.3	0.65	0.6	2.3
	1	18-24	8.3	0.43	47.1	2.00	1.10	1.06	2.08	13	51	36	sicl	30.5	1.11	1.0	3.3
WJ5-3	5	0-6	6.8	0.45	30.1	0.55	2.28	1.49	0.76	37	37	26	l	23.1	0.42	0.4	1.7
	5	6-12	7.2	0.34	36.4	0.71	1.50	1.07	0.80	26	40	34	cl	30.5	0.53	0.5	1.6
	5	12-18	8.0	0.33	37.7	1.20	1.32	0.95	1.30	26	44	30	cl	25.9	0.68	0.6	2.4
	5	18-24	8.2	0.55	41.5	2.70	1.22	1.33	3.00	13	50	37	sicl	30.1	1.12	1.0	3.3
WJ5-4	2	0-6	6.6	0.24	36.5	0.54	0.94	0.64	0.48	33	39	28	cl	22.5	0.44	0.4	1.9
	2	6-12	7.5	0.35	41.0	0.48	1.88	1.22	0.60	25	43	32	cl	29.7	0.46	0.4	1.5
	2	12-18	8.0	0.34	35.2	0.85	1.47	1.15	0.97	29	41	30	cl	25.1	0.53	0.5	2.0
	2	18-24	8.2	0.43	41.2	1.80	1.12	1.25	1.98	12	50	38	sicl	30.3	0.96	0.9	2.9
WJ5-5	4	0-6	6.5	0.23	38.2	0.54	1.08	0.66	0.50	40	36	24	l	21.2	0.37	0.4	1.7
	4	6-12	7.1	0.23	39.0	0.55	0.98	0.67	0.50	33	36	31	cl	28.0	0.46	0.4	1.6
	4	12-18	8.0	0.31	43.4	0.62	1.56	1.03	0.71	23	47	30	cl	27.7	0.44	0.4	1.5

APPENDIX 7.2: Baseline – Soil Chemistry Data for the Research Plots

WJ5-6	4	18-24	8.2	0.36	41.8	1.30	1.23	1.21	1.42	15	49	36	sid	28.9	0.78	0.7	2.5
	7	0-6	6.4	0.24	34.5	0.63	1.01	0.70	0.58	38	34	28	cl	25.7	0.44	0.4	1.6
	7	6-12	7.4	0.39	35.7	0.50	2.01	1.43	0.66	32	36	32	cl	29.7	0.43	0.4	1.4
	7	12-18	8.0	0.34	28.7	0.83	1.47	1.27	0.97	28	42	30	cl	25.3	0.59	0.6	2.2
	7	18-24	8.2	0.38	30.2	1.80	1.09	1.14	1.95	21	47	32	cl	28.5	0.89	0.8	2.9
WJ5-7	3	0-6	6.6	0.33	31.8	0.46	1.77	1.14	0.56	39	39	22	l	19.5	0.52	0.5	2.6
	3	6-12	7.0	0.34	32.7	0.58	1.62	1.11	0.68	17	47	36	sid	33.6	0.60	0.6	1.7
	3	12-18	7.8	0.37	29.6	0.68	1.75	1.34	0.84	25	46	29	cl	28.1	0.66	0.6	2.3
	3	18-24	8.2	0.34	33.6	1.40	1.13	1.01	1.49	18	46	36	sid	29.1	0.78	0.7	2.5
WJ6-1	4	0-6	6.5	0.28	36.2	0.44	1.43	0.92	0.48	27	37	36	cl	31.0	0.45	0.4	1.4
	4	6-12	7.6	0.39	36.9	0.32	2.28	1.43	0.44	20	46	34	sid	33.2	0.42	0.4	1.2
	4	12-18	8.1	0.30	33.0	0.46	1.51	1.23	0.54	25	43	32	cl	28.6	0.55	0.5	1.9
	4	18-24	8.1	0.33	32.6	0.93	1.02	1.16	0.97	27	45	28	cl	23.6	0.52	0.5	2.1
WJ6-2	2	0-6	6.2	0.30	31.3	0.42	1.57	1.06	0.48	31	39	30	cl	29.9	0.37	0.4	1.2
	2	6-12	7.3	0.43	29.0	0.33	2.45	1.51	0.47	25	42	33	cl	28.1	0.44	0.4	1.5
	2	12-18	8.0	0.31	36.7	0.50	1.49	1.12	0.57	23	45	32	cl	27.2	0.59	0.6	2.1
	2	18-24	8.1	0.35	33.7	0.82	1.11	1.24	0.89	32	37	31	cl	26.2	0.53	0.5	1.9
WJ6-3	3	0-6	6.9	0.30	39.0	0.42	1.72	0.97	0.49	33	37	30	cl	27.7	0.41	0.4	1.4
	3	6-12	7.5	0.31	37.8	0.49	1.69	0.97	0.56	31	40	29	cl	26.3	0.48	0.5	1.7
	3	12-18	8.1	0.27	39.1	0.62	1.42	1.03	0.69	17	49	34	sid	29.6	0.45	0.4	1.4
	3	18-24	8.2	0.31	39.3	0.94	1.17	1.16	1.01	32	35	33	cl	25.7	0.56	0.5	2.0
WJ6-4	7	0-6	7.4	0.37	42.5	0.33	2.47	1.02	0.43	36	34	30	cl	26.7	0.41	0.4	1.5
	7	6-12	7.9	0.34	41.8	0.52	2.01	1.09	0.65	30	38	32	cl	26.3	0.44	0.4	1.6
	7	12-18	8.1	0.27	38.6	0.63	1.23	1.03	0.67	28	40	32	cl	26.3	0.48	0.4	1.7
	7	18-24	8.1	0.35	39.9	1.00	1.08	1.36	1.10	30	38	32	cl	24.6	0.54	0.5	2.0
WJ6-5	1	0-6	6.6	0.23	39.7	0.67	0.99	0.60	0.60	30	40	30	cl	27.7	0.37	0.4	1.3
	1	6-12	7.6	0.34	42.9	0.59	1.99	1.13	0.74	34	36	30	cl	27.6	0.40	0.4	1.3
	1	12-18	8.0	0.34	43.2	0.75	1.56	1.17	0.88	25	42	33	cl	27.0	0.47	0.4	1.6
	1	18-24	8.1	0.35	41.7	1.10	1.13	1.34	1.18	35	35	30	cl	25.8	0.51	0.5	1.8
WJ6-6	6	0-6	6.9	0.43	42.7	0.47	2.42	1.44	0.65	30	37	33	cl	27.2	0.34	0.3	1.1
	6	6-12	7.9	0.30	41.5	0.71	1.62	0.95	0.81	33	37	30	cl	25.8	0.43	0.4	1.6
	6	12-18	8.1	0.30	39.6	1.00	1.06	0.99	1.06	31	40	29	cl	24.6	0.44	0.4	1.6
	6	18-24	8.2	0.37	40.7	1.70	0.93	1.17	1.73	28	40	32	cl	25.2	0.75	0.7	2.7
WJ6-7	5	0-6	6.8	0.26	40.9	0.43	1.36	0.76	0.44	35	39	26	l	25.9	0.29	0.3	1.0

APPENDIX 7.2: Baseline – Soil Chemistry Data for the Research Plots

WJ7-1	5	6-12	7.7	0.38	43.6	0.39	2.39	1.16	0.52	34	34	32	cl	28.3	0.32	0.3	1.1
	5	12-18	8.0	0.30	41.5	0.60	1.41	1.07	0.67	33	36	31	cl	24.5	0.32	0.3	1.2
	5	18-24	8.2	0.31	42.3	0.88	1.08	1.19	0.94	37	37	33	cl	26.7	0.43	0.4	1.5
	3	0-6	6.5	0.26	38.1	0.51	1.30	0.73	0.51	40	26	34	cl	29.8	0.38	0.4	1.2
	3	6-12	7.2	0.47	35.7	0.40	2.89	1.65	0.61	49	23	28	scl	25.5	0.37	0.4	1.4
	3	12-18	7.9	0.35	37.4	0.60	1.73	1.11	0.72	46	25	29	scl	23.8	0.41	0.4	1.6
	3	18-24	8.0	0.35	39.0	1.20	1.33	1.16	1.30	38	32	30	cl	25.2	0.52	0.5	1.9
WJ7-2	4	0-6	6.5	0.37	39.3	0.64	1.99	0.99	0.78	44	25	31	cl	28.7	0.32	0.3	1.0
	4	6-12	7.5	0.51	35.8	0.42	3.39	1.48	0.65	57	19	24	scl	21.3	0.36	0.3	1.6
	4	12-18	7.8	0.46	35.5	0.42	2.67	1.49	0.60	51	25	24	scl	19.9	0.39	0.4	1.9
	4	18-24	7.9	0.45	36.5	0.61	2.02	1.75	0.84	47	26	27	scl	21.5	0.40	0.4	1.7
WJ7-3	6	0-6	6.4	0.35	41.1	0.48	1.77	1.03	0.57	42	25	33	cl	29.0	0.33	0.3	1.1
	6	6-12	7.2	0.35	38.6	0.35	3.81	1.92	0.60	50	22	28	scl	25.6	0.35	0.3	1.3
	6	12-18	7.8	0.47	46.3	0.39	2.73	1.86	0.59	44	24	32	cl	29.6	0.34	0.3	1.0
	6	18-24	8.0	0.40	41.5	0.45	1.78	1.82	0.60	48	24	28	scl	23.0	0.35	0.3	1.4
WJ7-4	5	0-6	6.6	0.38	46.7	0.47	2.09	1.12	0.60	44	23	33	cl	31.2	0.32	0.3	0.9
	5	6-12	7.1	0.52	47.2	0.26	3.81	1.93	0.44	47	22	31	scl	29.5	0.35	0.3	1.1
	5	12-18	7.7	0.47	41.1	0.32	3.23	1.83	0.51	47	25	28	scl	24.9	0.41	0.4	1.6
	5	18-24	7.9	0.40	39.8	0.42	2.11	1.78	0.59	56	20	24	scl	21.8	0.39	0.4	1.7
WJ7-5	1	0-6	6.5	0.39	46.6	0.42	2.41	1.36	0.58	42	25	33	cl	31.8	0.32	0.3	0.9
	1	6-12	7.2	0.58	47.9	0.36	4.15	2.14	0.64	45	24	31	cl	30.7	0.39	0.4	1.2
	1	12-18	7.8	0.36	43.2	0.42	2.25	1.41	0.57	52	22	26	scl	23.4	0.37	0.4	1.5
	1	18-24	7.9	0.45	41.3	0.73	2.07	1.87	1.02	48	26	26	scl	21.9	0.48	0.4	2.0
WJ7-6	2	0-6	6.4	0.31	49.0	0.43	1.85	1.12	0.53	44	23	33	cl	30.7	0.43	0.4	1.3
	2	6-12	7.2	0.47	44.9	0.31	3.44	2.02	0.52	48	22	30	scl	28.5	0.34	0.3	1.1
	2	12-18	7.8	0.39	42.0	0.38	2.45	1.68	0.54	49	23	28	scl	25.9	0.37	0.4	1.4
	2	18-24	8.0	0.38	41.9	0.68	1.81	1.73	0.91	44	30	26	l	24.8	0.28	0.2	1.0
WJ7-7	7	0-6	6.2	0.42	43.2	0.65	2.21	1.20	0.85	47	30	23	l	25.9	0.45	0.4	1.6
	7	6-12	6.8	0.37	46.5	0.40	2.31	1.46	0.55	49	21	30	scl	33.0	0.38	0.4	1.1
	7	12-18	7.6	0.47	42.0	0.47	3.14	1.81	0.74	52	22	26	scl	24.9	0.34	0.3	1.2
	7	18-24	7.9	0.38	42.0	0.37	2.25	1.65	0.52	44	32	24	l	23.4	0.40	0.4	1.6
WJ8-1	1	0-6	6.7	0.30	45.0	0.42	1.81	1.12	0.51	40	32	28	cl	31.1	0.34	0.3	1.0
	1	6-12	7.6	0.37	43.9	0.26	2.82	1.68	0.39	40	33	27	cl	28.4	0.37	0.4	1.2
	1	12-18	7.9	0.38	45.9	0.45	2.04	1.78	0.62	33	32	35	cl	25.8	0.41	0.4	1.5

APPENDIX 7.2: Baseline – Soil Chemistry Data for the Research Plots

WJ8-2	1	18-24	8.0	0.43	42.1	1.10	1.72	2.25	1.49	36	40	24		24.4	0.50	0.4	1.8
	7	0-6	6.6	0.25	45.8	0.45	1.37	0.86	0.47	36	34	30	cl	32.2	0.31	0.3	0.9
	7	6-12	7.6	0.42	44.8	0.41	2.74	1.64	0.61	42	32	26		26.1	0.37	0.3	1.3
	7	12-18	7.9	0.37	44.4	0.40	2.14	1.81	0.56	41	34	25		25.0	0.36	0.3	1.4
WJ8-3	7	18-24	8.1	0.38	42.8	0.65	1.67	1.77	0.85	44	32	24		22.8	0.41	0.4	1.6
	4	0-6	6.4	0.27	42.9	0.31	1.61	1.09	0.36	39	36	25		29.4	0.34	0.3	1.1
	4	6-12	7.3	0.57	48.7	0.26	4.07	2.60	0.48	38	37	25		33.4	0.33	0.3	0.9
	4	12-18	8.0	0.34	46.4	0.39	1.83	1.49	0.50	42	32	26		25.7	0.37	0.4	1.4
WJ8-4	4	18-24	8.0	0.38	40.8	0.68	1.46	1.76	0.86	44	32	24		24.0	0.41	0.4	1.5
	2	0-6	6.6	0.29	45.5	0.29	1.62	1.10	0.34	45	31	24		30.0	0.26	0.2	0.8
	2	6-12	7.6	0.44	48.0	0.24	2.84	1.83	0.36	37	34	29	cl	31.1	0.39	0.4	1.2
	2	12-18	7.9	0.40	44.8	0.40	2.08	1.96	0.57	36	35	29	cl	27.3	0.40	0.4	1.4
WJ8-5	2	18-24	8.0	0.40	42.5	0.66	1.58	2.10	0.90	44	32	24		25.4	0.38	0.3	1.3
	3	0-6	6.5	0.33	43.7	0.48	1.91	1.21	0.60	36	38	26		30.3	0.32	0.3	1.0
	3	6-12	7.6	0.46	49.5	0.32	3.07	1.79	0.50	36	36	28	cl	29.8	0.35	0.3	1.1
	3	12-18	8.0	0.40	51.0	0.32	2.43	1.82	0.47	39	32	29	cl	28.1	0.29	0.3	1.0
WJ8-6	3	18-24	8.0	0.37	45.3	0.43	2.08	2.14	0.63	45	32	23		23.6	0.33	0.3	1.3
	5	0-6	6.4	0.43	46.8	0.46	2.71	1.78	0.69	36	37	27	cl	32.2	0.31	0.3	0.9
	5	6-12	7.5	0.42	45.9	0.32	2.89	1.77	0.49	36	39	25		29.2	0.32	0.3	1.0
	5	12-18	8.0	0.40	50.3	0.34	1.99	1.68	0.46	30	39	31	cl	30.9	0.43	0.4	1.3
WJ8-7	5	18-24	8.1	0.34	45.4	0.61	1.46	1.92	0.79	36	39	25		24.3	0.41	0.4	1.5
	6	0-6	7.1	0.37	49.1	0.19	2.78	1.26	0.27	36	43	21		25.8	0.25	0.2	0.9
	6	6-12	7.6	0.38	45.5	0.31	3.04	1.47	0.47	42	35	23		25.9	0.34	0.3	1.2
	6	12-18	7.9	0.35	58.4	0.43	2.27	1.55	0.60	36	36	28	cl	28.5	0.36	0.3	1.1
	6	18-24	8.0	0.37	52.4	0.61	1.71	1.76	0.81	32	30	28	cl	30.1	0.35	0.3	1.0

APPENDIX 7.3: Soil Chemistry Data Collected from Treated Subplots Located at the Eight Research Plots after One Season of Irrigation.

Table 1.4.1. Soil chemistry data collected from treated subplots located at the eight (8) research plots after one (1) season of irrigation.

Sample ID	Plot	Treatment	Depth	pH	EC	% Sat	SAR	Ca	Mg	Na	Sand	Silt	Clay	Texture	CEC	Na-Ext	Exch Na
WJ-1-1	1	1	0-6	7.4	3.9	43	9.1	8.49	3.69	22.6	35	41	24	L	25.4	3.80	2.8
WJ-1-1	1	1	6-12	7.0	1.9	54	1.9	8.80	5.79	5.16	25	35	40	C	38.1	1.39	1.1
WJ-1-1	1	1	12-18	7.4	2.1	56	0.49	14.0	11.1	1.74	28	33	39	CL	37.2	0.579	0.48
WJ-1-1	1	1	18-24	7.7	1.5	50	0.62	7.51	7.73	1.72	35	30	35	CL	31.7	0.611	0.52
WJ-1-2	1	2	0-6	7.4	5.2	46	9.5	16.0	6.89	32.1	34	42	24	L	26.8	3.87	2.4
WJ-1-2	1	2	6-12	7.1	1.8	52	2.1	7.61	4.37	5.16	31	42	27	CL	29.9	1.39	1.1
WJ-1-2	1	2	12-18	7.2	2.3	56	0.89	15.1	10.8	3.22	24	35	41	C	43.9	0.788	0.61
WJ-1-2	1	2	18-24	7.6	2.1	50	0.50	12.1	10.4	1.66	33	32	35	CL	34.4	0.628	0.55
WJ-1-3	1	3	0-6	7.9	2.4	47	15	2.37	1.10	19.7	33	43	24	L	27.1	3.92	3.0
WJ-1-3	1	3	6-12	7.2	0.72	47	2.4	2.49	1.26	3.36	32	36	32	CL	32.7	1.03	0.87
WJ-1-3	1	3	12-18	7.1	0.76	48	0.49	4.05	2.38	0.88	39	32	29	CL	29.4	0.473	0.43
WJ-1-3	1	3	18-24	7.5	1.0	51	0.48	6.55	4.46	1.12	23	38	39	CL	38.4	0.504	0.44
WJ-1-4	1	4	0-6	7.3	3.3	40	7.4	8.15	3.80	18.1	33	42	25	L	26.3	2.85	2.1
WJ-1-4	1	4	6-12	6.9	1.8	57	1.1	10.4	7.28	3.35	31	30	39	CL	42.8	0.938	0.75
WJ-1-4	1	4	12-18	7.4	1.2	54	0.76	6.35	5.20	1.83	27	34	39	CL	39.8	0.55	0.45
WJ-1-4	1	4	18-24	7.8	0.60	50	1.2	2.11	1.97	1.73	29	35	36	CL	34.4	0.841	0.75
WJ-1-5	1	5	0-6	7.7	0.58	44	5.5	1.33	0.77	5.59	30	44	26	L	28.1	3.96	3.7
WJ-1-5	1	5	6-12	7.3	0.82	49	2.7	2.66	1.28	3.78	27	42	31	CL	32.7	1.14	0.95
WJ-1-5	1	5	12-18	7.1	0.69	56	0.47	4.36	2.52	0.88	33	36	31	CL	31.7	0.528	0.48
WJ-1-5	1	5	18-24	7.5	1.1	50	0.37	7.03	4.79	0.89	33	35	32	CL	31.9	0.498	0.46
WJ-1-6	1	6	0-6	7.6	3.0	47	10	5.76	2.42	21.1	34	41	25	L	25.5	4.22	3.2
WJ-1-6	1	6	6-12	7.4	1.2	49	3.0	3.84	2.25	5.16	34	34	32	CL	32.5	1.79	1.5
WJ-1-6	1	6	12-18	7.4	1.7	54	0.33	10.4	7.85	1.00	29	34	37	CL	39.3	0.587	0.54
WJ-1-6	1	6	18-24	7.7	1.2	50	0.55	5.64	5.56	1.30	34	32	34	CL	32.2	0.539	0.47
WJ-1-7	1	7	0-6	7.7	0.89	44	4.2	2.22	0.77	5.16	31	40	29	CL	30.9	1.71	1.5
WJ-1-7	1	7	6-12	7.6	0.60	47	0.59	3.54	1.35	0.92	32	40	28	CL	28.8	0.594	0.55
WJ-1-7	1	7	12-18	7.7	0.67	53	0.63	3.73	1.92	1.06	28	31	41	C	44.9	0.616	0.56
WJ-1-7	1	7	18-24	7.8	0.55	51	1.1	2.53	1.79	1.60	32	32	36	CL	37.1	0.734	0.65
WJ-2-1	2	1	0-6	7.9	0.54	50	8.0	0.75	0.67	6.8	27	37	36	CL	44.1	2.34	2.0

APPENDIX 7.3: Soil Chemistry Data Collected from Treated Subplots Located at the Eight Research Plots after One Season of Irrigation.

WJ-2-1	2	1	6-12	7.3	0.30	54	1.2	1.21	1.10	1.3	24	37	39	CL	44.8	0.776	0.71
WJ-2-1	2	1	12-18	7.7	0.35	50	0.86	1.67	1.75	1.12	29	34	37	CL	36.0	0.652	0.59
WJ-2-1	2	1	18-24	8.0	0.40	48	1.9	1.15	1.65	2.23	28	39	33	CL	33.3	0.978	0.87
WJ-2-2	2	2	0-6	7.7	1.7	55	8.4	3.27	2.12	13.9	33	34	33	CL	36.6	4.88	4.1
WJ-2-2	2	2	6-12	7.9	0.51	57	5.1	0.71	0.54	4.01	27	37	36	CL	42.0	3.04	2.8
WJ-2-2	2	2	12-18	8.0	0.69	53	3.3	1.77	1.76	4.35	31	35	34	CL	32.7	1.75	1.5
WJ-2-2	2	2	18-24	8.0	0.70	52	2.1	1.69	3.10	3.28	25	42	33	CL	34.3	1.22	1.0
WJ-2-3	2	3	0-6	7.8	0.93	49	8.7	1.03	0.73	8.18	34	36	30	CL	32.1	4.26	6.2
WJ-2-3	2	3	6-12	7.7	0.70	56	3.9	1.33	1.38	4.54	22	36	42	C	42.6	2.01	1.8
WJ-2-3	2	3	12-18	7.7	0.71	53	1.6	2.39	3.36	2.68	27	37	36	CL	36.6	1.07	0.93
WJ-2-3	2	3	18-24	8.0	0.75	52	2.8	1.61	3.05	4.26	32	36	32	CL	33.5	1.52	1.3
WJ-2-4	2	4	0-6	7.7	1.6	57	10	2.03	1.43	13.4	28	40	32	CL	34.8	4.90	4.1
WJ-2-4	2	4	6-12	7.7	0.53	54	3.5	1.09	1.02	3.58	25	35	40	C	41.2	2.23	2.0
WJ-2-4	2	4	12-18	7.8	0.65	51	1.1	2.56	2.89	1.88	28	39	33	CL	38.4	0.847	0.75
WJ-2-4	2	4	18-24	7.9	0.86	69	1.6	2.17	4.85	2.91	27	40	33	CL	33.4	0.915	0.71
WJ-2-5	2	5	0-6	7.6	0.65	53	5.9	0.95	0.58	5.14	31	39	30	CL	39.1	4.61	4.3
WJ-2-5	2	5	6-12	7.5	0.82	44	3.8	1.79	1.65	5.05	25	38	37	CL	40.3	1.89	1.7
WJ-2-5	2	5	12-18	7.7	0.73	54	1.1	3.11	3.48	1.95	27	41	32	CL	34.3	0.711	2.9
WJ-2-5	2	5	18-24	7.9	0.85	33	1.5	2.40	4.57	2.85	22	44	34	CL	30.8	1.02	0.93
WJ-2-6	2	6	0-6	7.9	0.41	51	6.1	0.34	0.32	3.52	27	41	32	CL	37.7	5.61	5.4
WJ-2-6	2	6	6-12	8.0	0.17	56	2.8	0.23	0.26	1.36	25	37	38	CL	41.3	2.93	2.8
WJ-2-6	2	6	12-18	8.1	0.54	54	3.3	1.29	1.24	3.75	23	40	37	CL	33.6	1.89	1.7
WJ-2-6	2	6	18-24	8.2	0.57	53	2.6	1.25	2.18	3.47	25	42	33	CL	30.3	1.35	1.1
WJ-2-7	2	7	0-6	7.7	0.87	52	5.5	1.66	0.88	6.17	26	42	32	CL	33.9	4.60	4.3
WJ-2-7	2	7	6-12	7.8	0.16	59	2.2	0.25	0.46	1.28	19	39	42	C	42.4	3.94	3.9
WJ-2-7	2	7	12-18	7.9	0.62	58	2.5	1.94	1.88	3.50	18	43	39	SiCL	40.0	1.58	1.4
WJ-2-7	2	7	18-24	8.0	0.73	53	0.97	2.58	4.48	1.83	22	44	34	CL	31.5	0.767	0.67
WJ-3-1	3	1	0-6	8.1	0.29	50	3.9	0.39	0.68	2.86	28	37	35	CL	38.5	5.07	4.9
WJ-3-1	3	1	6-12	7.9	0.81	57	5.1	1.58	1.65	6.43	20	37	43	C	44.0	1.91	1.6
WJ-3-1	3	1	12-18	7.9	0.52	57	1.4	1.84	2.25	1.96	18	40	42	C	37.3	1.10	0.99
WJ-3-1	3	1	18-24	8.0	0.52	55	1.6	1.58	2.16	2.24	16	40	44	C	37.2	1.04	0.92
WJ-3-2	3	2	0-6	7.8	2.4	52	13	2.88	2.38	20.6	27	37	36	CL	37.7	4.93	3.9
WJ-3-2	3	2	6-12	7.5	0.93	57	2.8	2.42	2.55	4.43	18	38	44	C	42.4	1.67	1.4
WJ-3-2	3	2	12-18	7.7	1.0	57	0.77	4.40	5.16	1.69	14	43	43	SiC	40.4	0.730	0.63

APPENDIX 7.3: Soil Chemistry Data Collected from Treated Subplots Located at the Eight Research Plots after One Season of Irrigation.

WJ-3-2	3	2	18-24	7.8	1.1	59	0.93	3.73	6.78	2.13	18	40	42	C	37.6	0.827	0.70
WJ-3-3	3	3	0-6	7.7	2.2	54	10	2.84	2.14	15.7	24	38	38	CL	37.3	4.90	4.0
WJ-3-3	3	3	6-12	7.7	0.85	58	3.6	1.79	1.66	4.71	20	37	43	C	44.4	1.96	1.7
WJ-3-3	3	3	12-18	7.7	1.0	59	0.95	4.03	4.67	1.99	15	43	42	SiC	42.8	0.854	0.73
WJ-3-3	3	3	18-24	7.9	1.2	58	1.7	3.57	6.59	3.75	12	46	42	SiC	37.7	1.20	0.98
WJ-3-4	3	4	0-6	7.0	4.5	55	5.2	15.9	11.0	18.9	22	38	40	C	38.0	3.98	2.9
WJ-3-4	3	4	6-12	7.0	1.3	55	2.1	4.97	5.49	4.70	19	39	42	C	43.4	1.39	1.1
WJ-3-4	3	4	12-18	7.6	1.5	56	1.6	5.86	7.94	4.25	12	43	45	SiC	41.0	1.24	1.0
WJ-3-4	3	4	18-24	7.9	1.6	59	1.7	4.43	9.61	4.43	14	44	42	SiC	36.9	1.24	0.98
WJ-3-5	3	5	0-6	7.5	0.21	53	2.2	0.25	0.25	1.09	23	38	39	CL	42.1	4.05	4.0
WJ-3-5	3	5	6-12	7.2	2.0	55	0.70	10.7	12.0	2.36	16	42	42	SiC	42.3	0.923	0.79
WJ-3-5	3	5	12-18	7.8	1.1	57	1.2	3.48	5.33	2.46	11	43	46	SiC	39.9	1.16	1.0
WJ-3-5	3	5	18-24	8.0	0.78	55	2.9	1.36	2.76	4.13	14	42	44	SiC	38.3	1.63	1.4
WJ-3-6	3	6	0-6	7.6	1.4	58	6.8	1.75	1.53	8.65	22	36	42	C	41.8	4.40	3.9
WJ-3-6	3	6	6-12	7.2	1.3	54	0.68	6.49	6.48	1.74	19	39	42	C	43.6	0.697	0.61
WJ-3-6	3	6	12-18	7.7	1.6	53	0.59	8.07	10.5	1.80	21	37	42	C	36.1	0.625	0.52
WJ-3-6	3	6	18-24	7.8	0.79	50	1.3	2.13	4.25	2.36	20	42	38	SiCL	32.9	1.06	0.94
WJ-3-7	3	7	0-6	7.6	0.83	57	5.0	1.49	1.07	5.69	22	40	38	CL	40.4	4.73	4.4
WJ-3-7	3	7	6-12	7.6	0.60	54	2.7	1.56	1.32	3.21	16	44	40	SiC	39.7	1.96	1.8
WJ-3-7	3	7	12-18	7.7	0.71	52	1.1	2.55	3.08	1.89	14	46	40	SiC	34.6	1.00	0.90
WJ-3-7	3	7	18-24	7.9	0.86	56	0.61	3.38	6.62	1.36	13	46	41	SiC	34.8	0.662	0.58
WJ-4-1	4	1	0-6	7.2	3.7	57	5.8	19.0	10.4	22.2	18	46	36	SiCL	39.5	4.39	3.1
WJ-4-1	4	1	6-12	7.3	1.1	53	1.5	4.62	3.30	2.99	16	46	38	SiCL	41.6	1.22	1.1
WJ-4-1	4	1	12-18	7.6	1.7	53	0.31	8.92	8.61	0.92	14	48	38	SiCL	36.4	0.675	0.62
WJ-4-1	4	1	18-24	7.8	1.8	50	0.57	5.58	8.46	1.51	22	44	34	CL	31.9	1.09	1.0
WJ-4-2	4	2	0-6	7.4	2.7	59	5.2	9.13	5.11	13.8	23	31	46	C	41.0	4.49	3.7
WJ-4-2	4	2	6-12	7.6	0.85	52	2.8	3.27	2.41	4.67	22	40	38	CL	39.3	1.73	1.5
WJ-4-2	4	2	12-18	7.7	0.85	55	0.32	3.88	5.30	0.69	24	39	37	CL	37.7	0.482	0.44
WJ-4-2	4	2	18-24	7.8	1.0	53	0.41	4.43	7.64	1.00	18	47	35	SiCL	35.1	0.523	0.47
WJ-4-3	4	3	0-6	8.1	0.14	59	1.6	0.88	0.76	1.44	20	43	37	SiCL	41.9	2.65	2.6
WJ-4-3	4	3	6-12	7.8	0.37	54	1.9	1.63	1.03	2.20	16	45	39	SiCL	40.8	0.703	0.58
WJ-4-3	4	3	12-18	7.9	0.34	55	0.40	1.67	1.45	0.50	12	47	41	SiC	42.3	0.552	0.52
WJ-4-3	4	3	18-24	7.8	2.8	53	0.65	1.71	2.22	0.91	14	49	37	SiCL	34.7	0.604	0.55
WJ-4-4	4	4	0-6	6.8	2.1	55	3.9	4.65	7.67	9.62	20	43	37	SiCL	41.8	2.77	2.2

APPENDIX 7.3: Soil Chemistry Data Collected from Treated Subplots Located at the Eight Research Plots after One Season of Irrigation.

WJ-5-5	5	5	18-24	8.0	0.42	49	1.2	1.77	1.86	1.67	18	47	35	SiCL	36.7	0.792	0.71
WJ-5-6	5	6	0-6	7.7	0.47	40	4.6	0.70	0.44	3.47	42	33	25	L	27.3	3.28	3.1
WJ-5-6	5	6	6-12	7.2	0.89	47	0.62	4.55	3.22	1.23	34	34	32	CL	35.5	0.591	0.53
WJ-5-6	5	6	12-18	7.7	1.0	45	0.52	5.63	5.85	1.24	26	44	30	CL	33.4	0.537	0.48
WJ-5-6	5	6	18-24	7.9	0.86	50	1.8	2.78	3.93	3.31	19	46	35	SiCL	35.4	1.06	0.89
WJ-5-7	5	7	0-6	7.1	2.9	38	6.9	11.5	4.89	19.7	23	57	20	SIL	23.3	3.27	2.5
WJ-5-7	5	7	6-12	7.0	1.2	51	2.9	5.30	3.56	6.19	21	42	37	CL	40.5	1.61	1.3
WJ-5-7	5	7	12-18	7.6	1.7	46	6.8	3.54	1.97	11.2	26	43	31	CL	35.0	0.66	0.14
WJ-5-7	5	7	18-24	7.8	1.8	49	0.74	7.51	9.06	2.12	19	44	37	SiCL	35.1	0.728	0.63
WJ-6-1	6	1	0-6	7.5	0.97	51	0.38	4.08	5.43	0.83	29	36	35	CL	38.9	4.32	4.3
WJ-6-1	6	1	6-12	7.4	1.1	48	2.7	4.68	3.08	5.30	29	39	32	CL	37.3	1.34	1.1
WJ-6-1	6	1	12-18	7.8	0.83	47	0.52	4.96	4.57	1.14	29	40	31	CL	32.3	0.485	0.43
WJ-6-1	6	1	18-24	7.9	0.97	45	0.34	4.60	5.52	0.77	31	39	30	CL	31.1	0.452	0.42
WJ-6-2	6	2	0-6	8.0	0.34	45	5.5	0.79	0.50	4.4	31	37	32	CL	36.7	4.69	4.5
WJ-6-2	6	2	6-12	7.9	0.47	48	3.2	1.30	0.69	3.16	28	41	31	CL	36.0	1.49	1.3
WJ-6-2	6	2	12-18	7.8	0.38	49	0.53	2.16	1.88	0.76	26	43	31	CL	35.2	0.462	0.42
WJ-6-2	6	2	18-24	8.0	0.42	45	1.2	1.70	2.12	1.59	35	36	29	CL	27.6	0.597	0.53
WJ-6-3	6	3	0-6	7.4	2.3	53	0.23	12.9	11.0	0.81	32	36	32	CL	35.1	3.45	3.4
WJ-6-3	6	3	6-12	7.5	1.3	51	0.75	8.97	5.52	2.03	32	38	30	CL	31.5	0.642	0.54
WJ-6-3	6	3	12-18	7.7	1.9	51	0.23	13.5	11.7	0.81	21	47	32	CL	34.4	0.357	0.32
WJ-6-3	6	3	18-24	7.8	1.4	45	0.44	7.95	10.2	1.32	38	31	31	CL	30.1	0.475	0.42
WJ-6-4	6	4	0-6	7.9	1.9	51	3.2	7.59	3.47	7.55	41	31	28	CL	30.7	4.09	3.7
WJ-6-4	6	4	6-12	7.8	1.1	53	3.4	4.73	2.42	6.36	28	41	31	CL	34.0	1.56	1.2
WJ-6-4	6	4	12-18	7.8	1.0	49	0.51	6.11	5.34	1.23	29	42	29	CL	31.7	0.470	0.41
WJ-6-4	6	4	18-24	7.8	1.3	46	0.56	6.20	9.18	1.54	34	35	31	CL	31.9	0.563	0.49
WJ-6-5	6	5	0-6	8.0	1.1	50	12	1.37	0.57	11.8	35	34	31	CL	31.7	4.81	4.2
WJ-6-5	6	5	6-12	7.8	0.70	50	2.2	3.19	1.70	3.38	32	37	31	CL	33.7	1.16	0.99
WJ-6-5	6	5	12-18	7.8	0.66	46	0.42	3.85	3.44	0.81	29	43	28	CL	28.0	0.428	0.39
WJ-6-5	6	5	18-24	7.9	0.68	47	0.63	2.99	4.08	1.18	37	34	29	CL	27.9	0.503	0.44
WJ-6-6	6	6	0-6	7.2	3.4	57	0.75	16.2	17.1	3.06	32	38	30	CL	35.6	3.59	3.4
WJ-6-6	6	6	6-12	7.6	1.3	53	1.6	7.01	4.81	3.97	31	40	29	CL	32.0	0.978	0.77
WJ-6-6	6	6	12-18	7.7	1.2	54	0.49	3.94	6.30	1.12	28	44	28	CL	31.8	0.513	0.45
WJ-6-6	6	6	18-24	7.8	0.98	48	0.47	4.17	6.24	1.07	32	39	29	CL	30.4	0.573	0.52
WJ-6-7	6	7	0-6	7.4	3.0	53	6.3	7.95	3.39	15.0	37	34	29	CL	34.6	4.31	3.5

APPENDIX 7.3: Soil Chemistry Data Collected from Treated Subplots Located at the Eight Research Plots after One Season of Irrigation.

WJ-6-7	6	7	6-12	7.5	1.0	49	3.6	3.61	1.87	5.95	36	36	28	CL	31.5	1.78	1.5
WJ-6-7	6	7	12-18	7.7	0.94	49	0.66	5.58	4.89	1.51	28	43	29	CL	29.7	0.559	0.49
WJ-6-7	6	7	18-24	7.8	1.2	52	0.35	5.16	7.69	0.88	26	42	32	CL	32.1	0.469	0.42
WJ-7-1	7	1	0-6	7.2	3.8	54	6.4	20.2	8.10	24.1	46	24	30	SCL	30.9	3.42	2.1
WJ-7-1	7	1	6-12	7.4	1.2	48	3.0	5.98	2.86	6.20	51	21	28	SCL	30.9	1.59	1.3
WJ-7-1	7	1	12-18	7.6	1.3	47	0.70	9.59	5.25	1.92	49	25	26	SCL	28.0	0.561	0.47
WJ-7-1	7	1	18-24	7.7	1.3	47	0.35	8.60	7.40	0.99	48	26	26	SCL	27.8	0.437	0.39
WJ-7-2	7	2	0-6	7.9	0.080	47	2.1	0.11	0.09	0.67	46	25	29	SCL	34.8	4.44	4.4
WJ-7-2	7	2	6-12	7.8	0.45	44	0.46	3.13	1.55	0.70	46	27	27	SCL	30.2	1.58	1.6
WJ-7-2	7	2	12-18	7.6	0.54	41	0.47	3.78	1.68	0.77	54	22	24	SCL	25.2	0.374	0.34
WJ-7-2	7	2	18-24	7.6	0.54	42	0.35	3.31	2.45	0.59	52	24	24	SCL	23.8	0.337	0.32
WJ-7-3	7	3	0-6	7.9	0.16	43	3.6	0.24	0.10	1.50	47	25	28	SCL	31.2	3.56	3.5
WJ-7-3	7	3	6-12	7.6	0.40	40	1.9	1.63	0.76	2.03	54	22	24	SCL	27.7	0.835	0.75
WJ-7-3	7	3	12-18	7.6	0.34	46	0.62	2.27	1.27	0.82	46	28	26	L	29.6	0.467	0.43
WJ-7-3	7	3	18-24	7.7	0.51	44	0.77	2.07	2.52	1.17	45	28	27	CL	25.4	0.548	0.50
WJ-7-4	7	4	0-6	7.7	0.62	46	6.8	0.80	0.41	5.26	44	28	28	CL	31.9	4.80	4.6
WJ-7-4	7	4	6-12	7.5	0.88	44	3.6	3.20	1.54	5.48	53	20	27	SCL	28.8	1.53	1.3
WJ-7-4	7	4	12-18	7.5	0.83	42	0.56	5.66	3.09	1.18	61	18	21	SCL	22.7	0.491	0.44
WJ-7-4	7	4	18-24	7.6	0.95	42	0.23	6.59	4.95	0.55	50	25	25	SCL	23.0	0.383	0.36
WJ-7-5	7	5	0-6	7.7	0.52	44	5.4	0.79	0.43	4.19	44	27	29	CL	29.6	4.35	4.2
WJ-7-5	7	5	6-12	7.7	0.49	42	4.5	1.05	0.48	3.92	54	19	27	SCL	27.9	1.99	1.8
WJ-7-5	7	5	12-18	7.6	0.66	37	0.92	3.78	2.12	1.58	58	20	22	SCL	21.4	0.507	0.45
WJ-7-5	7	5	18-24	7.7	0.78	43	0.36	4.29	3.98	0.74	47	27	26	SCL	24.0	0.449	0.42
WJ-7-6	7	6	0-6	7.3	1.5	49	2.2	5.64	2.93	4.47	46	24	30	SCL	31.3	3.17	3.0
WJ-7-6	7	6	6-12	7.2	0.82	49	1.6	4.29	2.38	2.91	46	22	32	SCL	34.3	1.06	0.92
WJ-7-6	7	6	12-18	7.5	0.98	45	0.40	7.06	4.45	0.95	52	23	25	SCL	24.7	0.472	0.43
WJ-7-6	7	6	18-24	7.6	1.0	48	0.32	6.10	6.06	0.79	40	32	28	CL	28.1	0.332	0.29
WJ-7-7	7	7	0-6	7.1	3.0	43	6.7	14.3	5.48	21.0	46	29	25	L	26.9	3.98	3.1
WJ-7-7	7	7	6-12	6.9	1.1	45	2.0	5.45	2.81	4.06	53	21	26	SCL	27.4	1.28	1.1
WJ-7-7	7	7	12-18	7.4	1.3	42	0.28	10.3	6.21	0.80	52	23	25	SCL	27.1	0.354	0.32
WJ-7-7	7	7	18-24	7.6	1.2	41	0.31	8.02	6.74	0.83	50	22	28	SCL	25.7	0.344	0.31
WJ-8-1	8	1	0-6	7.6	1.8	54	7.3	4.73	2.30	13.8	38	38	24	L	30.2	3.51	2.8
WJ-8-1	8	1	6-12	7.6	0.92	46	0.76	6.22	3.52	1.68	37	35	28	CL	29.3	0.658	0.58
WJ-8-1	8	1	12-18	7.6	1.4	47	0.21	8.81	7.72	0.61	43	32	25	L	26.0	0.380	0.35

APPENDIX 7.3: Soil Chemistry Data Collected from Treated Subplots Located at the Eight Research Plots after One Season of Irrigation.

WJ-8-1	8	1	18-24	7.7	1.2	44	0.37	6.05	8.52	0.99	39	37	24	L	24.3	0.445	0.41
WJ-8-2	8	2	0-6	7.6	1.5	48	7.3	3.36	1.82	11.8	39	33	28	CL	31.0	4.60	4.0
WJ-8-2	8	2	6-12	7.6	0.99	46	2.8	3.87	2.03	4.79	40	32	28	CL	28.7	1.39	1.2
WJ-8-2	8	2	12-18	7.7	0.83	52	0.38	5.91	4.75	0.88	32	35	33	CL	32.6	0.470	0.42
WJ-8-2	8	2	18-24	7.8	0.74	50	0.40	4.19	4.53	0.84	40	31	29	CL	26.1	0.474	0.43
WJ-8-3	8	3	0-6	8.0	0.96	50	8.7	1.31	0.65	8.64	37	33	30	CL	31.3	5.46	5.0
WJ-8-3	8	3	6-12	8.0	0.62	49	5.0	1.53	0.70	5.25	39	32	29	CL	31.6	2.43	2.2
WJ-8-3	8	3	12-18	7.8	0.61	46	1.6	2.68	2.06	2.51	35	36	29	CL	27.6	0.907	0.79
WJ-8-3	8	3	18-24	7.9	0.68	46	0.58	3.07	3.85	1.08	43	31	26	L	22.9	0.464	0.41
WJ-8-4	8	4	0-6	7.4	2.2	52	6.8	7.76	4.29	16.8	38	34	28	CL	30.5	3.44	4.9
WJ-8-4	8	4	6-12	7.4	0.83	46	1.1	4.85	2.84	2.12	40	34	26	L	29.0	0.684	0.58
WJ-8-4	8	4	12-18	7.7	0.89	46	0.26	5.66	4.60	0.59	38	32	30	CL	28.1	0.378	0.35
WJ-8-4	8	4	18-24	7.8	0.67	45	0.38	3.18	3.96	0.71	40	34	26	L	23.7	0.444	0.41
WJ-8-5	8	5	0-6	7.8	1.0	50	8.8	1.70	0.81	9.90	34	37	29	CL	33.7	4.28	3.8
WJ-8-5	8	5	6-12	7.9	0.79	49	4.6	2.01	0.98	5.62	34	36	30	CL	32.9	2.06	1.7
WJ-8-5	8	5	12-18	7.8	0.68	47	1.3	2.77	2.18	2.07	34	35	31	CL	28.7	0.740	0.64
WJ-8-5	8	5	18-24	7.9	0.57	47	0.43	2.60	3.33	0.74	42	32	26	L	24.5	0.526	0.50
WJ-8-6	8	6	0-6	7.7	0.92	47	8.0	1.44	0.69	8.25	35	35	30	CL	32.7	3.88	3.5
WJ-8-6	8	6	6-12	7.6	0.71	48	2.4	2.86	1.62	3.64	34	38	28	CL	30.1	1.30	1.1
WJ-8-6	8	6	12-18	7.7	0.72	48	0.59	3.95	3.38	1.13	32	38	30	CL	29.5	0.546	3.0
WJ-8-6	8	6	18-24	7.8	0.90	40	0.37	4.57	6.04	0.85	44	33	23	L	22.7	0.449	0.42
WJ-8-7	8	7	0-6	8.2	0.47	49	10	0.55	0.12	5.8	35	37	28	CL	33.1	5.82	5.5

APPENDIX 7.4: Soil Chemistry Data Collected from Treated Subplots Located at the Eight Research Plots after Two Seasons of Irrigation.

Table 1.4.2 Soil chemistry data collected from treated subplots located at the 8 research plots after 2 seasons of irrigation.

Sample #	Treatment	Depth inch	pH-SatPst su	EC mmhos/cm	Percent Sat %	SAR	Ca-SatPst meq/L	Mg-SatPst meq/L	Na-SatPst meq/L
WJ1-1	1	0-6	7.4	5.68	44.7	19	9.26	5.14	51.7
	1	6-12	7.3	2.08	49.8	5.2	5.18	3.52	10.9
	1	12-18	7.3	1.46	51.1	1.0	7.16	5.50	2.57
	1	18-24	7.6	1.15	46.2	0.48	5.38	5.76	1.14

APPENDIX 7.4: Soil Chemistry Data Collected from Treated Subplots Located at the Eight Research Plots after Two Seasons of Irrigation.

WJ1-2	2	0-6	8.1	1.32	42.1	10	0.86	1.01	10.1
	2	6-12	7.6	1.36	39.5	5.6	3.11	1.63	8.68
	2	12-18	7.3	1.17	51.8	0.98	6.22	3.77	2.18
	2	18-24	7.6	1.45	50.6	0.40	8.42	6.16	1.09
WJ1-3	3	0-6	7.8	2.05	48.3	19	1.66	0.96	22.1
	3	6-12	7.7	1.19	45.1	8.6	1.57	1.04	9.80
	3	12-18	7.2	1.00	46.5	2.0	4.13	2.31	3.50
	3	18-24	7.3	1.19	40.6	0.48	7.46	4.65	1.19
WJ1-4	4	0-6	7.5	3.77	47.0	14	6.86	2.90	31.6
	4	6-12	7.4	2.25	52.0	4.4	7.70	5.11	11.0
	4	12-18	7.3	1.45	51.7	0.84	8.16	6.36	2.25
	4	18-24	7.6	1.25	45.8	0.79	6.11	6.25	1.97
WJ1-5	5	0-6	6.9	4.43	48.0	12	11.9	5.50	36.6
	5	6-12	7.2	1.51	45.9	5.3	3.44	1.90	8.62
	5	12-18	7.1	1.24	49.1	1.4	6.52	4.11	1.04
	5	18-24	7.5	1.39	49.3	0.39	8.00	5.56	1.02
WJ1-6	6	0-6	7.6	3.40	48.2	13	6.84	2.32	27.2
	6	6-12	7.4	3.10	55.0	6.4	9.65	6.20	17.9
	6	12-18	7.6	1.86	51.3	2.7	7.50	5.86	6.99
	6	18-24	7.7	1.57	49.2	0.86	7.18	7.47	2.34
WJ1-7	7	0-6	8.2	0.80	46.5	9.7	0.80	0.43	7.63
	7	6-12	7.7	0.64	46.8	1.5	2.56	1.24	2.10
	7	12-18	7.7	0.45	48.2	1.0	1.82	1.12	1.21
	7	18-24	7.8	0.75	46.6	1.3	2.89	2.44	2.14
WJ2-1	1	0-6	8.0	3.10	44.6	20	2.88	1.99	31.9
	1	6-12	7.3	0.61	47.5	2.7	1.69	1.12	3.24
	1	12-18	7.3	0.66	50.4	0.67	3.41	2.40	1.14
	1	18-24	7.7	0.51	49.7	0.62	2.07	1.90	0.88

APPENDIX 7.4: Soil Chemistry Data Collected from Treated Subplots Located at the Eight Research Plots after Two Seasons of Irrigation.

WJ2-2	2	0-6	7.9	0.68	50.7	9.0	0.62	0.47	6.66
	2	6-12	7.6	0.49	53.0	3.4	0.95	0.85	3.22
	2	12-18	7.9	0.42	47.6	1.7	1.16	1.20	1.88
	2	18-24	7.9	0.52	48.6	1.6	1.33	1.92	2.01
WJ2-3	3	0-6	7.8	1.71	55.7	15	1.65	0.97	16.9
	3	6-12	7.7	1.34	56.0	7.6	1.55	1.47	9.40
	3	12-18	7.9	1.18	51.4	4.4	2.20	2.53	6.73
	3	18-24	7.9	1.11	53.2	2.1	2.19	5.01	3.90
WJ2-4	4	0-6	7.6	3.73	53.0	14	5.57	5.33	31.9
	4	6-12	7.7	1.69	54.3	6.1	2.87	3.43	10.8
	4	12-18	7.7	1.74	49.4	3.0	5.02	7.19	7.44
	4	18-24	8.0	1.78	49.7	3.0	3.17	8.43	7.28
WJ2-5	5	0-6	7.6	4.34	54.5	10	13.6	7.42	32.6
	5	6-12	7.6	1.91	55.4	7.1	3.03	3.15	12.4
	5	12-18	7.8	1.54	54.4	4.4	3.27	3.75	8.33
	5	18-24	7.8	1.64	49.5	2.4	4.28	8.58	6.21
WJ2-6	6	0-6	7.9	2.40	54.8	15	2.84	2.37	24.6
	6	6-12	7.8	1.10	52.9	4.8	2.18	2.12	7.11
	6	12-18	7.6	0.97	52.0	1.4	3.39	4.10	2.81
	6	18-24	7.8	1.11	52.1	0.92	3.34	6.60	2.06
WJ2-7	7	0-6	7.4	4.13	61.9	11	8.48	7.16	32.0
	7	6-12	7.6	2.31	57.4	7.3	3.86	4.35	14.7
	7	12-18	7.8	1.88	51.8	4.9	3.59	5.49	10.4
	7	18-24	8.1	1.36	52.7	3.1	1.83	5.09	5.78
WJ3-1	1	0-6	8.0	1.07	56.1	10	0.92	0.86	9.80
	1	6-12	7.7	1.36	56.4	3.1	3.52	4.06	6.09
	1	12-18	7.9	1.37	53.2	1.3	3.50	7.01	3.04
	1	18-24	8.1	1.68	51.9	3.5	2.16	6.71	7.44

APPENDIX 7.4: Soil Chemistry Data Collected from Treated Subplots Located at the Eight Research Plots after Two Seasons of Irrigation.

WJ3-2	2	0-6	8.1	0.54	62.0	9.0	0.29	0.39	5.24
	2	6-12	8.0	1.17	55.4	7.0	1.31	1.43	8.18
	2	12-18	7.9	0.62	52.7	2.9	1.09	1.68	3.41
	2	18-24	8.1	0.52	53.4	3.4	0.67	1.28	3.32
WJ3-3	3	0-6	7.9	2.08	57.4	14	1.91	1.76	18.9
	3	6-12	7.6	1.11	54.9	4.7	1.96	1.98	6.63
	3	12-18	7.6	1.53	51.7	0.94	6.63	7.94	2.55
	3	18-24	7.8	1.83	55.6	0.83	6.16	11.6	2.48
WJ3-4	4	0-6	7.6	2.63	60.9	11	3.31	2.99	19.9
	4	6-12	7.3	2.11	53.3	3.9	6.61	7.12	10.2
	4	12-18	7.6	1.44	53.3	1.4	5.17	7.31	3.39
	4	18-24	7.9	1.12	48.4	1.6	2.73	5.74	3.34
WJ3-5	5	0-6	7.6	3.76	62.5	12	6.26	5.35	29.7
	5	6-12	7.1	2.05	54.6	3.2	6.95	6.74	8.38
	5	12-18	7.6	1.60	51.7	0.83	6.83	8.17	2.26
	5	18-24	7.8	1.48	56.5	1.0	5.40	8.21	2.73
WJ3-6	6	0-6	8.1	1.76	54.5	15	1.36	1.61	17.7
	6	6-12	7.8	1.21	56.4	5.9	1.79	1.85	7.96
	6	12-18	7.8	1.30	51.8	2.5	3.28	4.67	4.95
	6	18-24	8.0	1.40	54.9	1.5	2.93	7.59	3.50
WJ3-7	7	0-6	6.7	5.02	60.2	9.6	14.4	11.9	35.0
	7	6-12	7.3	1.96	51.9	3.3	6.24	6.23	8.34
	7	12-18	7.6	1.91	50.9	0.93	8.18	10.6	2.85
	7	18-24	7.9	2.20	56.0	1.3	5.94	12.4	3.87
WJ4-1	1	0-6	7.7	3.05	63.5	11	5.19	3.58	23.6
	1	6-12	7.5	1.83	55.0	5.9	3.34	3.12	10.6
	1	12-18	7.8	1.28	50.0	3.4	3.31	3.89	6.42
	1	18-24	7.9	1.25	52.7	1.5	3.25	6.20	3.35

APPENDIX 7.4: Soil Chemistry Data Collected from Treated Subplots Located at the Eight Research Plots after Two Seasons of Irrigation.

WJ4-2	2	0-6	7.1	3.19	64.0	11	5.76	3.22	22.9
	2	6-12	7.5	2.44	56.9	5.6	5.85	4.24	12.5
	2	12-18	7.5	2.57	54.7	1.5	11.7	11.4	5.05
	2	18-24	7.6	2.32	49.8	0.63	9.83	14.7	2.19
WJ4-3	3	0-6	7.8	0.87	61.2	6.8	0.88	0.75	6.12
	3	6-12	7.9	1.32	51.4	7.6	1.76	1.08	9.07
	3	12-18	7.9	1.00	50.1	3.8	2.36	2.01	5.64
	3	18-24	7.8	1.18	54.2	1.2	3.60	5.44	2.64
WJ4-4	4	0-6	7.8	1.54	59.7	13	1.05	0.82	13.0
	4	6-12	7.8	0.80	52.4	3.7	1.78	1.26	4.61
	4	12-18	7.9	0.47	55.2	1.3	1.63	1.42	1.62
	4	18-24	8.0	0.41	53.3	1.0	1.34	1.49	1.21
WJ4-5	5	0-6	7.5	2.92	59.6	13	3.99	2.51	24.1
	5	6-12	7.6	2.55	53.7	3.8	10.3	7.50	11.4
	5	12-18	7.6	1.86	54.2	0.91	9.61	10.1	2.85
	5	18-24	7.7	1.88	52.0	0.63	6.99	11.5	1.92
WJ4-6	6	0-6	7.9	1.40	57.5	12	1.10	0.86	11.7
	6	6-12	7.5	1.46	53.7	2.0	5.76	4.51	4.65
	6	12-18	7.7	1.78	58.2	0.39	8.85	11.1	1.22
	6	18-24	7.8	1.37	50.0	0.79	4.45	8.39	2.00
WJ4-7	7	0-6	7.7	2.95	64.2	15	3.18	2.06	24.0
	7	6-12	7.9	1.94	56.0	7.1	3.52	2.54	12.3
	7	12-18	7.8	1.48	54.6	2.7	4.39	4.54	5.72
	7	18-24	7.8	1.13	48.5	1.0	3.59	5.83	2.27
WJ5-1	1	0-6	7.6	2.56	62.2	12	3.76	2.36	21.3
	1	6-12	7.7	1.60	54.2	5.5	3.90	2.71	10.0
	1	12-18	7.7	1.52	56.1	2.1	6.07	6.40	5.24
	1	18-24	7.8	1.66	55.0	0.72	5.57	9.78	1.99

APPENDIX 7.4: Soil Chemistry Data Collected from Treated Subplots Located at the Eight Research Plots after Two Seasons of Irrigation.

WJ5-2	2	0-6	8.0	1.31	49.1	9.2	1.21	0.95	9.60
	2	6-12	7.7	1.62	50.0	5.3	4.04	2.39	9.52
	2	12-18	7.7	1.55	46.4	1.2	7.97	6.39	3.10
	2	18-24	7.7	1.15	46.5	0.93	4.59	5.23	2.05
WJ5-3	3	0-6	7.2	5.63	46.9	14	14.4	8.61	46.7
	3	6-12	7.4	3.13	49.7	5.3	11.0	6.83	15.9
	3	12-18	7.7	2.24	48.6	1.6	11.9	11.2	5.25
	3	18-24	7.8	1.77	51.2	0.72	7.41	10.4	2.16
WJ5-4	4	0-6	7.5	2.77	45.8	16	2.68	1.75	23.4
	4	6-12	7.4	1.04	49.7	3.7	2.79	2.03	5.71
	4	12-18	7.6	1.36	46.3	0.73	7.24	7.17	1.95
	4	18-24	7.8	1.22	52.0	1.4	4.10	6.34	3.22
WJ5-5	5	0-6	8.0	0.13	46.9	2.0	0.19	0.28	0.95
	5	6-12	7.8	0.40	43.6	0.95	1.74	1.52	1.21
	5	12-18	7.7	0.65	40.7	5.5	1.03	0.73	5.12
	5	18-24	7.9	0.40	50.3	1.4	1.31	1.17	1.61
WJ5-6	6	0-6	7.5	5.26	47.9	20	6.84	3.60	46.1
	6	6-12	7.8	1.67	46.1	7.8	2.31	1.59	11.0
	6	12-18	7.8	2.05	46.6	3.7	6.68	6.08	9.30
	6	18-24	7.7	1.95	52.6	1.6	7.07	9.68	4.69
WJ5-7	7	0-6	7.8	0.41	40.0	3.9	0.42	0.41	2.52
	7	6-12	7.5	1.09	47.9	3.9	2.92	2.13	6.16
	7	12-18	7.7	1.34	49.8	1.5	4.42	4.99	3.16
	7	18-24	7.8	1.38	51.6	1.3	3.90	6.39	3.05
WJ6-1	1	0-6	7.4	4.71	58.7	13	11.5	5.80	37.2
	1	6-12	7.6	4.01	48.1	7.4	13.1	8.08	24.1
	1	12-18	7.6	2.58	50.0	1.8	10.5	11.9	6.03
	1	18-24	7.7	2.25	49.0	0.73	8.72	14.8	2.51
WJ6-2	2	0-6	7.6	4.19	49.6	12	10.0	5.02	32.3

APPENDIX 7.4: Soil Chemistry Data Collected from Treated Subplots Located at the Eight Research Plots after Two Seasons of Irrigation.

	2	6-12	7.6	3.08	47.3	6.3	9.51	5.67	17.4
	2	12-18	7.6	2.01	46.4	1.3	10.6	9.25	4.14
	2	18-24	7.7	1.65	53.8	0.45	7.11	9.65	1.31
WJ6-3	3	0-6	7.5	4.43	47.2	14	8.23	5.60	37.1
	3	6-12	7.1	1.97	45.3	2.0	9.18	6.25	5.57
	3	12-18	7.7	0.82	46.0	1.4	2.69	2.44	2.27
	3	18-24	7.9	0.60	50.2	1.6	1.59	1.85	2.05
WJ6-4	4	0-6	7.4	4.71	58.7	13	11.5	5.80	37.2
	4	6-12	7.6	4.01	48.1	7.4	13.1	8.08	24.1
	4	12-18	7.6	2.58	50.0	1.8	10.5	11.9	6.03
	4	18-24	7.7	2.25	49.0	0.73	8.72	14.8	2.51
WJ6-5	5	0-6	7.8	0.33	59.7	3.4	0.37	0.39	2.10
	5	6-12	7.8	0.80	55.0	3.9	1.66	1.14	4.65
	5	12-18	7.8	0.53	46.3	0.80	1.84	1.84	1.09
	5	18-24	7.9	0.44	47.4	0.93	1.25	1.83	1.15
WJ6-6	6	0-6	7.5	1.06	55.8	8.7	0.97	0.57	7.60
	6	6-12	7.8	2.86	50.7	8.6	6.17	3.31	18.7
	6	12-18	7.8	1.66	48.6	3.9	4.12	3.30	7.55
	6	18-24	7.7	1.39	42.2	1.0	5.07	6.69	2.55
WJ6-7	7	0-6	7.4	3.80	53.6	11	6.80	3.47	25.8
	7	6-12	7.8	2.74	60.6	4.8	7.76	4.98	12.1
	7	12-18	7.7	1.80	46.3	1.2	6.37	7.40	3.22
	7	18-24	7.8	1.51	48.6	0.61	4.77	8.53	1.57
WJ7-1	1	0-6	7.7	0.38	51.5	4.7	0.28	0.29	2.49
	1	6-12	7.9	1.20	53.4	6.0	1.95	1.13	7.42
	1	12-18	7.8	0.79	49.1	1.3	2.56	2.49	2.12
	1	18-24	7.8	0.65	45.5	0.55	2.21	2.97	0.89
WJ7-2	2	0-6	7.5	0.49	50.6	5.5	0.38	0.35	3.30

APPENDIX 7.4: Soil Chemistry Data Collected from Treated Subplots Located at the Eight Research Plots after Two Seasons of Irrigation.

	2	6-12	7.8	1.43	51.3	6.7	2.46	1.51	9.46
	2	12-18	7.7	1.71	48.9	2.7	5.86	5.65	6.49
	2	18-24	7.7	2.00	47.4	0.79	8.05	12.0	2.51
WJ7-3	3	0-6	7.8	0.50	53.7	5.2	0.49	0.37	3.44
	3	6-12	7.7	1.84	46.7	6.8	3.46	2.23	11.4
	3	12-18	7.7	1.67	46.2	2.6	4.84	5.64	6.00
	3	18-24	7.8	1.35	47.3	1.0	3.80	6.68	2.41
WJ7-4	4	0-6	7.9	0.20	52.4	2.2	0.13	0.32	1.06
	4	6-12	8.0	0.32	43.0	3.6	0.52	0.46	2.49
	4	12-18	8.0	0.76	48.2	5.6	1.14	0.70	5.38
	4	18-24	8.0	0.59	44.0	1.7	1.58	1.71	2.20
WJ7-5	5	0-6	7.5	0.82	49.4	7.7	0.74	0.40	5.80
	5	6-12	7.7	2.38	40.9	8.4	4.95	1.95	15.6
	5	12-18	7.9	1.47	36.1	4.4	4.08	2.29	7.76
	5	18-24	7.9	1.00	44.3	1.9	3.52	3.18	3.43
WJ7-6	6	0-6	7.1	2.77	52.1	8.6	6.14	3.09	18.5
	6	6-12	7.7	2.03	42.8	6.5	4.39	2.50	12.1
	6	12-18	7.8	1.81	41.6	3.2	5.92	4.46	7.30
	6	18-24	7.8	1.74	41.5	1.7	6.42	7.88	4.56
WJ7-7	7	0-6	7.6	1.30	50.1	8.5	1.44	0.87	9.13
	7	6-12	7.8	1.05	45.5	3.9	2.65	1.58	5.66
	7	12-18	7.6	1.07	46.9	0.78	5.24	4.31	1.71
	7	18-24	7.8	0.91	49.7	0.52	3.61	4.82	1.06
WJ8-1	1	0-6	8.1	0.33	53.0	5.0	0.20	0.25	2.39
	1	6-12	7.8	1.16	39.5	7.9	1.45	0.75	8.27
	1	12-18	7.7	0.96	40.6	1.7	3.85	2.62	3.00
	1	18-24	7.8	0.78	41.1	0.50	3.33	3.46	0.92
WJ8-2	2	0-6	6.7	4.68	54.2	11	13.6	6.75	34.3

APPENDIX 7.5: ANOVA Evaluations for Data Collected from the WJ Amendment Plots after One and Two Years of Irrigation.

ANOVA evaluation for differences in SAR by depth associated with soils collected from the WJ Amendment Plots – Year 1

Analysis of Variance for SAR

Source	DF	SS	MS	F	P
Depth	3	1118.32	372.77	95.12	0.000
Error	220	862.21	3.92		
Total	223	1980.53			

Individual 95% CIs For Mean
Based on Pooled StDev

Level	N	Mean	StDev	CI
0-6	56	6.394	3.382	(--*--)
12-18	56	0.973	1.068	(--*--)
18-24	56	0.875	0.663	(--*--)
6-12	56	2.593	1.631	(--*--)

Pooled StDev = 1.980

ANOVA evaluation for Treatment vs SAR associated with soils collected from the WJ Amendment Plots – Year 1

Analysis of Variance for SAR

Source	DF	SS	MS	F	P
Treatment	6	42.1	7.0	0.59	0.740
Error	49	587.0	12.0		
Total	55	629.1			

Individual 95% CIs For Mean
Based on Pooled StDev

Level	N	Mean	StDev	CI
1	8	5.285	3.130	(-----*-----)
2	8	7.613	3.364	(-----*-----)
3	8	7.166	4.948	(-----*-----)
4	8	7.288	3.777	(-----*-----)
5	8	5.888	3.280	(-----*-----)
6	8	5.544	2.999	(-----*-----)
7	8	5.975	2.060	(-----*-----)

Pooled StDev = 3.461

APPENDIX 7.5: ANOVA Evaluations for Data Collected from the WJ Amendment Plots after One and Two Years of Irrigation.

ANOVA evaluation for differences in SAR by depth associated with soils collected from the WJ Amendment Plots – Year 2

Analysis of Variance for SAR

Source	DF	SS	MS	F	P
Depth	3	2944.86	981.62	165.11	0.000
Error	220	1307.96	5.95		
Total	223	4252.81			

Individual 95% CIs For Mean
Based on Pooled StDev

Level	N	Mean	StDev	CI Lower	CI Upper
0-6	56	10.484	4.247	2.000	18.968
12-18	56	2.184	1.336	0.512	3.856
18-24	56	1.183	0.753	0.683	1.683
6-12	56	5.396	1.842	2.712	8.080

Pooled StDev = 2.438

ANOVA evaluation for Treatment vs SAR associated with soils collected from the WJ Amendment Plots – Year 2

Analysis of Variance for SAR

Source	DF	SS	MS	F	P
Treatmen	6	103.7	17.3	0.95	0.467
Error	49	888.2	18.1		
Total	55	991.9			

Individual 95% CIs For Mean
Based on Pooled StDev

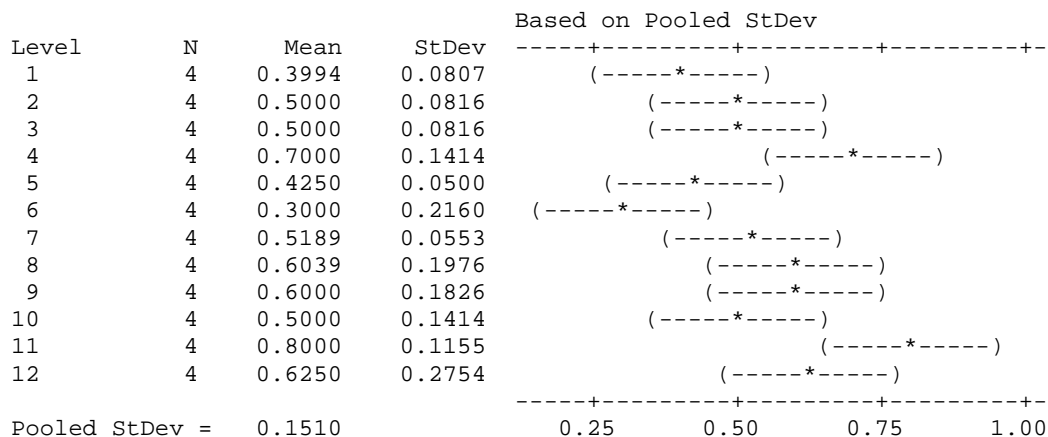
Level	N	Mean	StDev	CI Lower	CI Upper
1	8	10.550	4.722	1.106	19.994
2	8	10.238	4.082	1.974	18.502
3	8	12.663	3.604	5.455	19.871
4	8	9.138	4.552	0.034	18.242
5	8	12.213	5.181	1.851	20.571
6	8	8.788	4.744	0.200	17.376
7	8	9.800	2.206	7.388	12.212

Pooled StDev = 4.258

APPENDIX 7.6: Greenhouse Study - ANOVA Evaluations for Plant Production Data Collected from the North and South Pivot Area Fertility Plots

ANOVA evaluation for plant production associated with soils collected from the North Pivot – First Cutting

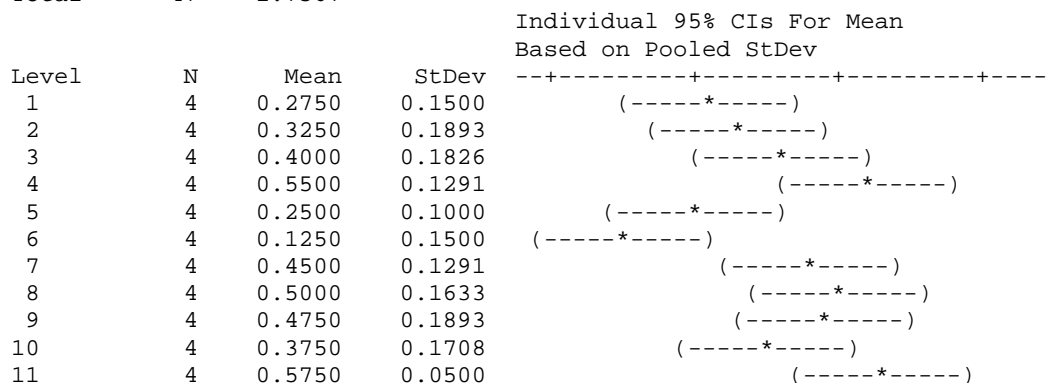
Individual 95% CIs For Mean



ANOVA evaluation for plant production associated with soils collected from the North Pivot – Second Cutting

Analysis of Variance for Weight

Source	DF	SS	MS	F	P
Treatmen	11	0.9217	0.0838	3.70	0.001
Error	36	0.8150	0.0226		
Total	47	1.7367			



APPENDIX 7.6: Greenhouse Study - ANOVA Evaluations for Plant Production Data Collected from the North and South Pivot Area Fertility Plots

ANOVA evaluation for plant production associated with soils collected from the South Pivot – First Cutting

Analysis of Variance for Weight

Source	DF	SS	MS	F	P
Treatmen	11	0.8269	0.0752	0.92	0.534
Error	36	2.9500	0.0819		
Total	47	3.7769			

Individual 95% CIs For Mean
Based on Pooled StDev

Level	N	Mean	StDev
1	4	1.0000	0.1826
2	4	1.0750	0.2986
3	4	1.1579	0.2549
4	4	1.1500	0.1915
5	4	1.2000	0.3266
6	4	1.1500	0.2082
7	4	1.1750	0.2872
8	4	1.1250	0.0957
9	4	1.1750	0.2062
10	4	1.0250	0.2062
11	4	1.1750	0.1258
12	4	1.5500	0.6455

Pooled StDev = 0.2863

ANOVA evaluation for plant production associated with soils collected from the South Pivot – Second Cutting

Analysis of Variance for Weight

Source	DF	SS	MS	F	P
Treatmen	11	0.6206	0.0564	1.33	0.249
Error	36	1.5275	0.0424		
Total	47	2.1481			

Individual 95% CIs For Mean
Based on Pooled StDev

Level	N	Mean	StDev
1	4	0.8250	0.3594
2	4	1.0500	0.1732
3	4	1.0250	0.3304
4	4	1.1750	0.1258
5	4	1.2500	0.1291
6	4	1.0250	0.1500
7	4	1.1500	0.2646
8	4	1.1000	0.0816
9	4	1.0750	0.2062
10	4	1.2000	0.1414
11	4	1.1500	0.0577
12	4	1.2500	0.2082

Pooled StDev = 0.2060

TOPIC AREA: DISPOSAL BY INJECTION

**CHAPTER 8:
Sub-Hydrostatic Pore Pressure in Aquifers of the Powder River Basin, Wyoming, and
Implications for Disposal of Coalbed Methane Water Through Injection**

Mark D. Zoback and Hannah E. Ross¹

EXECUTIVE SUMMARY

Coalbed methane (CBM) production in the Powder River Basin (PRB), Wyoming, is associated with the production of large volumes of CBM water. In some places, CBM water from the PRB has high saline and sodium contents, making it unsuitable for agricultural use and potentially environmentally damaging if discharged at the surface. One option for the disposal of CBM water is injection into aquifers, but for injection to be feasible the porosity and permeability of the sands needs to be high, the pore pressure would ideally be sub-hydrostatic, and the aquifer cannot be in hydraulic communication with coalbeds or aquifers used for irrigation.

In order to determine if pore pressures in the aquifers are low enough to allow for significant CBM water injection and to determine whether the coals and sands are in hydraulic communication with each other we have determined pore pressures in 250 wells that monitor water levels in coalbeds and adjacent sands within the PRB. All 250 wells have pore pressures below hydrostatic pressure, suggesting that injection of CBM water should be feasible from that perspective. However, by analyzing pore pressure changes with time for both the coals and their overlying/underlying sands, we find after 8 to 13 years of water level monitoring that ~60% of the sands less than 200 ft from producing coals appear to be in hydraulic communication with the coalbeds. In contrast, sands further than 200 ft from producing coalbeds show no changes in pore pressure over the 8 to 13 year time period. Therefore, we recommend that injection of CBM water should be carried out in sands further than at least 200 ft from adjacent coalbeds to be sure that the disposed water does not migrate into producing coalbeds over time.

In addition, we ran fluid flow simulations to determine the rates at which CBM water can be injected into shallow (~300 ft) and deep (~1000 ft) aquifers. We find that for the shallow sand model we can inject water at a rate of ~160 bbl/day, whereas for the deeper sand, whose pore pressures are lower than the shallow sand, the rate is ~435 bbl/day. Both these rates are higher than the average water production rate from CBM wells in the PRB, which is ~100 bbl/day. This implies that for deep aquifer injection sites, it would take only one injection well to dispose of the water production from approximately four CBM wells.

GOALS AND OBJECTIVES

The goals of this research are to investigate options for the disposal of CBM waters. One option for the disposal of CBM water is injection into deep aquifers, not suitable for irrigation or domestic use. However, for injection to be feasible, the porosity and permeability of the sands needs to be high, the pore pressure would ideally be subhydrostatic, and the aquifer cannot be in

¹ Department of Geophysics, Mitchell Building Room 347, Stanford University, Stanford, CA 94305-2215. Correspondence: zoback@stanford.edu.

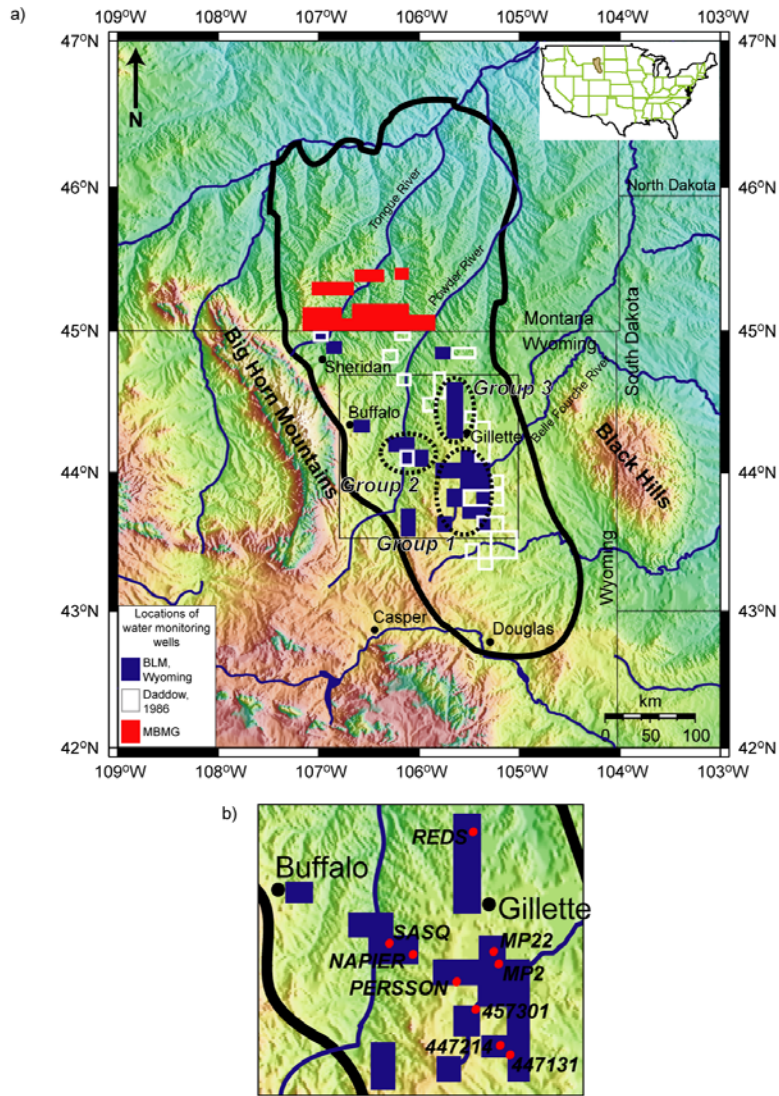
hydraulic communication with coalbeds or other aquifers that are used for irrigation or domestic use. In addition, to determine if pore pressures in potential disposal aquifers are low enough to allow for significant CBM water injection (and to determine whether the coals and sands are in communication with each other), pore pressure data in about 250 wells that monitor water levels in coalbeds and adjacent sands within the PRB was collected. The objectives are 1) to identify the sands and coalbeds with sub-hydrostatic pore pressures and are not in hydraulic communication with either producing coalbeds or useful aquifers and 2) to carry-out fluid flow simulations to estimate that the water injection rate into both shallow and deep sands to assess the number of CBM well needed to dispose of CBM produced waters in the PRB.

INTRODUCTION

Coalbed methane (CBM) production in the Powder River Basin (PRB) began in the early 1980s and by 1989 there were 22 CBM wells (De Bruin et al., 2004; Wyoming Oil and Gas Conservation Commission (WOGCC), 2007). Following this limited early success, production expanded rapidly and today there are ~17,000 wells (WOGCC, 2007), with another 34,000 expected to be drilled over the next 5 to 10 years (Environmental News Network, 2001) (**Figure 8.1a**). CBM gas from the PRB accounts for ~17% of the total gas produced in Wyoming (WOGCC, 2007). However, CBM production in the PRB is associated with the production of large volumes of CBM water. In 2006 ~590 million barrels (bbl) of CBM water were produced, at an average rate of ~100 bbl/well/day (WOGCC, 2006). Even though the water quality is generally sufficient for drinking water and livestock use, its saline and sodium contents are too high for agricultural use in many places (Wheaton and Donato, 2004; Bartos and Ogle, 2002; The Ruckelshaus Institute of Environment and Natural Resources, 2005). CBM in the PRB is produced through de-watering of the coalbeds (pumping water out of the coalbeds), which reduces the reservoir pressure and causes methane (CH₄) to desorb and flow to the production wells. Because the volumes of CBM water being produced are very large, there is far too much for immediate human and livestock consumption, so most of it is discharged into evaporation/infiltration ponds or streams (Advanced Resources International, 2002; The Ruckelshaus Institute of Environment and Natural Resources, 2005). However, the high saline and sodium contents mean that when the CBM water comes into contact with soil, the ions precipitate out of solution and lower the permeability of the soil, thus reducing the productivity of the soil (Wheaton and Donato, 2004). This in turn can cause soil erosion and ultimately damage to wildlife habitats.

One option for the disposal of CBM water is injection into aquifers, but for injection to be feasible both the porosity and permeability of the aquifer need to be high (for capacity and injectivity), the pore pressure needs to be low (for capacity and injectivity) and the aquifer cannot be in hydraulic communication with coalbeds or other aquifers (for containment). High porosity and permeability and low pore pressures in the aquifer result in a large capacity for water and increased injectivity. In addition, the water quality of the CBM water should be comparable to that of the aquifer water, so that the CBM water does not degrade the aquifer (Chapter 4, section 5 of the Rules and Statutes set out by the WOGCC, 2007). In order to determine if pore pressures in the aquifers are low enough to allow for significant CBM water injection and whether the coals and sands are in hydraulic communication with each other, we have determined pore pressures as a function of time in ~250 wells that monitor water levels in

coalbeds and adjacent sands within the PRB. In this study we assumed that an aquifer with sufficient pore pressure below hydrostatic would have storage capacity and ran fluid flow simulations to determine the feasibility of injecting CBM water into those aquifers.



Figures 8.1a and 8.1b: a) Location map of the Powder River Basin, WY and MT, and of the water monitoring wells used in this study (modified from Colmenares and Zoback, 2007). The orange dots correspond to CBM wells. The red squares correspond to the township and range location of water monitoring wells maintained by the Montana Bureau of Mines and Geology (MBMG) and Montana Tech of the University of Montana. Blue squares correspond to the township and range location of water monitoring wells maintained by the Wyoming Bureau of Land Management (BLM). White squares correspond to the township and range location of historic water monitoring wells from Daddow (1986). Dotted ovals surrounding the water monitoring wells correspond to groups 1, 2 and 3 mentioned in the text. b) Location map of individual water monitoring wells mentioned in the text. The black box in **Figure 8.1a** outlines the area encompassed by this map.

POWDER RIVER BASIN HYDROGEOLOGY

A number of studies have been carried out on the hydrogeology of the PRB and many of these are summarized in Lindner-Lunsford and Wilson (1992). More recent studies have focused on water drawdown from CBM production (Wheaton and Metesh, 2002; Bartos and Ogle, 2002; Applied Hydrology Associates and Greystone Environmental Consultants, 2002), water quality (Bartos and Ogle, 2002; The Ruckelshaus Institute of Environment and Natural Resources, 2005) and groundwater systems in the basin (Bartos and Ogle, 2002; Applied Hydrology Associates and Greystone Environmental Consultants, 2002). Bartos and Ogle (2002) used 23 water-level monitoring wells in the Wyoming part of the PRB to look at the hydraulic potential for vertical water flow and the ground water quality at each of these well sites. They found that there was a strong drive for vertical water flow in all but one well site. In addition, they used water chemistry to distinguish isolated ground water systems present in the PRB. The water chemistry revealed the potential for two different aquifer systems in the PRB, a shallow system dominated by a mixed cation composition, with either sulfate or bicarbonate as the dominant anion, and a deeper system composed of sodium-bicarbonate-type waters. They proposed that either there are two ground water systems within the PRB, one shallow and the other deeper (with no vertical flow between them), or that there is one system, where water migrates downward from shallow levels and its composition is changed through chemical interactions and mixing to become sodium-bicarbonate rich.

Applied Hydrology Associates and Greystone Environmental Consultants (2002) also used water level monitoring data in the Wyoming part of the PRB to look at the effect of CBM production on sand and coal aquifers in the basin. They were interested in the volume of recoverable groundwater from these aquifers and what the rate of recharge to the aquifers would be, based on various water management strategies. They proposed that water production from CBM production could induce water “leakage” into the coalbeds from overlying and underlying sand units that occur within 100 ft of the coal, but that leakage would be minimized because most of the coals are isolated from these sand units by fine grained silts/shales that vary in thickness from 11 to 363 ft. To test this they analyzed hydraulic heads in two sets of paired Bureau of Land Management (BLM) monitoring wells (where one well in the pair is perforated in coal and the other in overlying sandstone) and observed a water level decline over time of ~250 ft in the coals and a ~20 ft decline in the overlying sands. The coals and sands are ~40 ft apart, so they concluded that the water from the sand had migrated into the underlying coal, but that the confining unit between the sand and coal limited their hydraulic communication. We have carried out a similar study, but have used changes in pore pressure with time to infer hydraulic communication between the sands and underlying/overlying coals.

POWDER RIVER BASIN GEOLOGY

Coals in the Tongue River Member of the Paleocene Fort Union Formation are the targets for CBM production in the PRB. **Figure 8.2** is a cross-section through the central part of the basin, from W-E. The Fort Union Formation is overlain by the Eocene Wasatch Formation, which is exposed at the surface over much of the Wyoming part of the basin (Bartos and Ogle, 2002). Both the Fort Union and Wasatch Formations were deposited in fluvial, lacustrine and swamp environments. The Wasatch Formation is composed of lenticular, discontinuous, fine to medium

grained sandstones that are interbedded with siltstones, shales and coals (Applied Hydrology Associates and Greystone Environmental Consultants, 2002; Bartos and Ogle, 2002). The formation varies in thickness from 0 ft at outcrop to ~3000 ft in the central part of the basin (Applied Hydrology Associates and Greystone Environmental Consultants, 2002).

The Fort Union Formation is also composed of interbedded sandstones, siltstones, shales and coals. The Wyodak-Anderson coal zone, part of the Tongue River Member, is the coal zone of interest for CBM production. The coal zone ranges in thickness from less than an inch to 200 ft, and the coals merge and split into as many as 11 beds (Flores and Bader, 1999; Flores, 2004). The coal zone is considered an aquifer and represents the most continuous hydrologic unit in the lower Tertiary part of the PRB (Bartos and Ogle, 2002). The Tongue River Member comprises the upper part of the Fort Union Formation, and the Wyodak-Anderson coal zone is separated from overlying sands in the Wasatch Formation by low permeability siltstones and shales which act as a confining unit (Applied Hydrology Associates and Greystone Environmental Consultants, 2002; Bartos and Ogle, 2002). Applied Hydrology Associates and Greystone Environmental Consultants (2002) report that the permeability of the confining unit ranges from 0.009 mD to 2 mD in the horizontal directions and 0.002 mD to 0.02 mD in the vertical direction. It is thought that this confining unit ranges in thickness from 11 to 363 ft, but averages ~30 ft across the basin (Applied Hydrology Associates and Greystone Environmental Consultants, 2002).

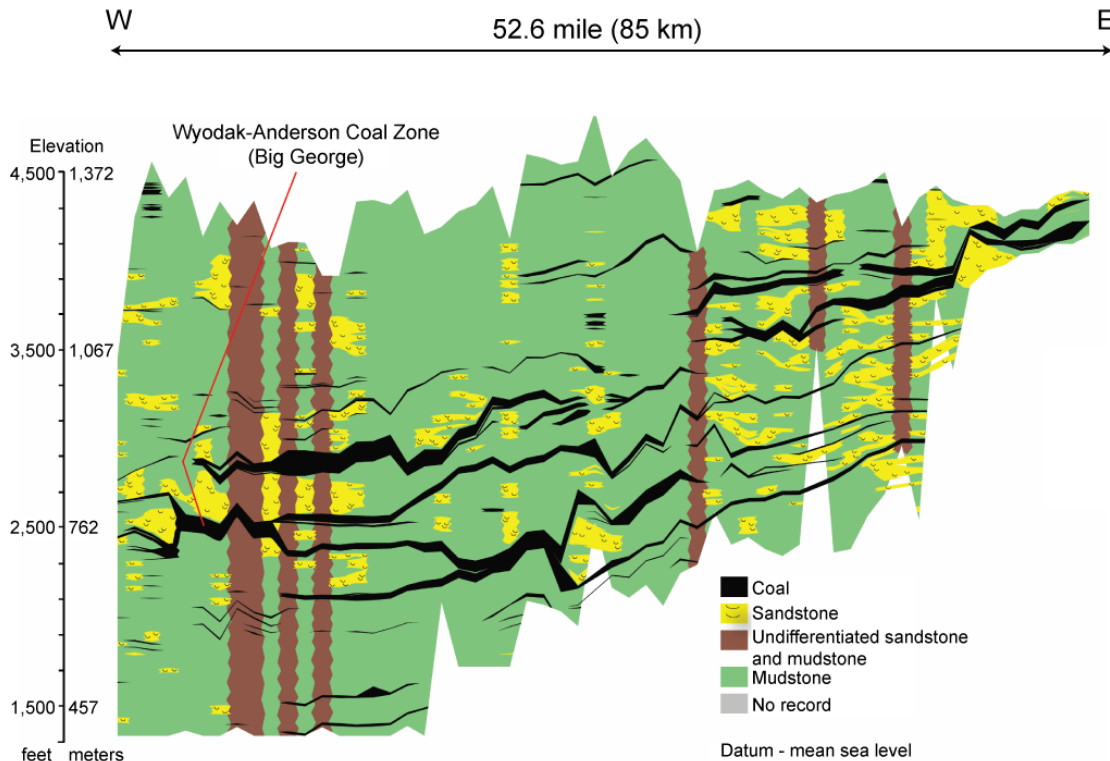


Figure 8.2: Cross section of the upper part of the Fort Union Formation, across the central part of the PRB, from W to E (modified from Flores, 2004).

WATER LEVEL DATA

We obtained water level data from active and historic water monitoring wells across the PRB that monitor water levels in both sand and coalbed units of the Wasatch and Fort Union Formations respectively. In the Montana part of the basin, 219 water monitoring wells are currently operated by the Montana Bureau of Mines (MBMG) and Geology and Montana Tech of the University of Montana; and in the Wyoming part of the basin the Wyoming BLM operates 134 water monitoring wells. We also obtained water level data from 62 historic water monitoring wells in Wyoming, which were in operation before CBM production began in the PRB (Daddow, 1986).

The water monitoring databases contain information on the location, ground elevation, well completion, depth, geologic unit and water level for the wells. However, information for some of the monitoring wells is incomplete, so for the Montana part of the basin we used 144 wells in our analysis, and for the Wyoming part of the basin we used 69 wells from the BLM database and 40 of the historic wells. The locations of all the monitoring wells used in this study are shown in **Figure 8.1**.

Records for the Montana water monitoring wells go as far back as 1974 and monitoring has been continuous from 1974 to the present. In contrast, the BLM monitoring began much later, in 1993, after CBM production had begun in the basin. Hence, the historic wells (Daddow, 1986) were used to establish water levels before CBM production in the Wyoming part of the basin.

Both the Montana and BLM monitoring databases contain paired wells/well clusters, which are a series of wells located close to one another, where each well is completed at successively shallower depths. Paired wells can be used to determine the potential for vertical fluid flow and whether overlying units are in hydraulic communication with underlying units. In the Wyoming part of the PRB there are 23 well pairs, while in Montana there are 11.

CALCULATING PORE PRESSURE

We used water level data from monitoring wells to calculate pore pressures for coals and sands in the PRB. The pore pressure (P_p) (fluid pressure) at a position P in the monitoring well is found as follows:

$$P_p = \psi g \rho, \quad (1)$$

where ψ is the height of the water column above P (**Figure 8.3**), ρ is the water density and g is gravity (Freeze and Cherry, 1979).

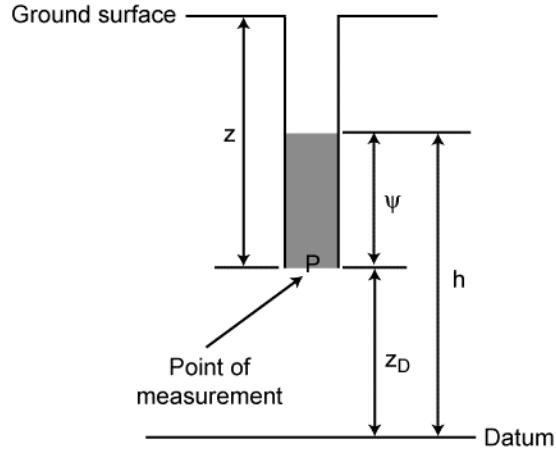


Figure 8.3: Hydraulic head, h , height of the water column above P , ψ , and elevation head, z_D , for a piezometer (modified from Freeze and Cherry, 1979). The datum, where $z_D = 0$, is usually defined to be sea level.

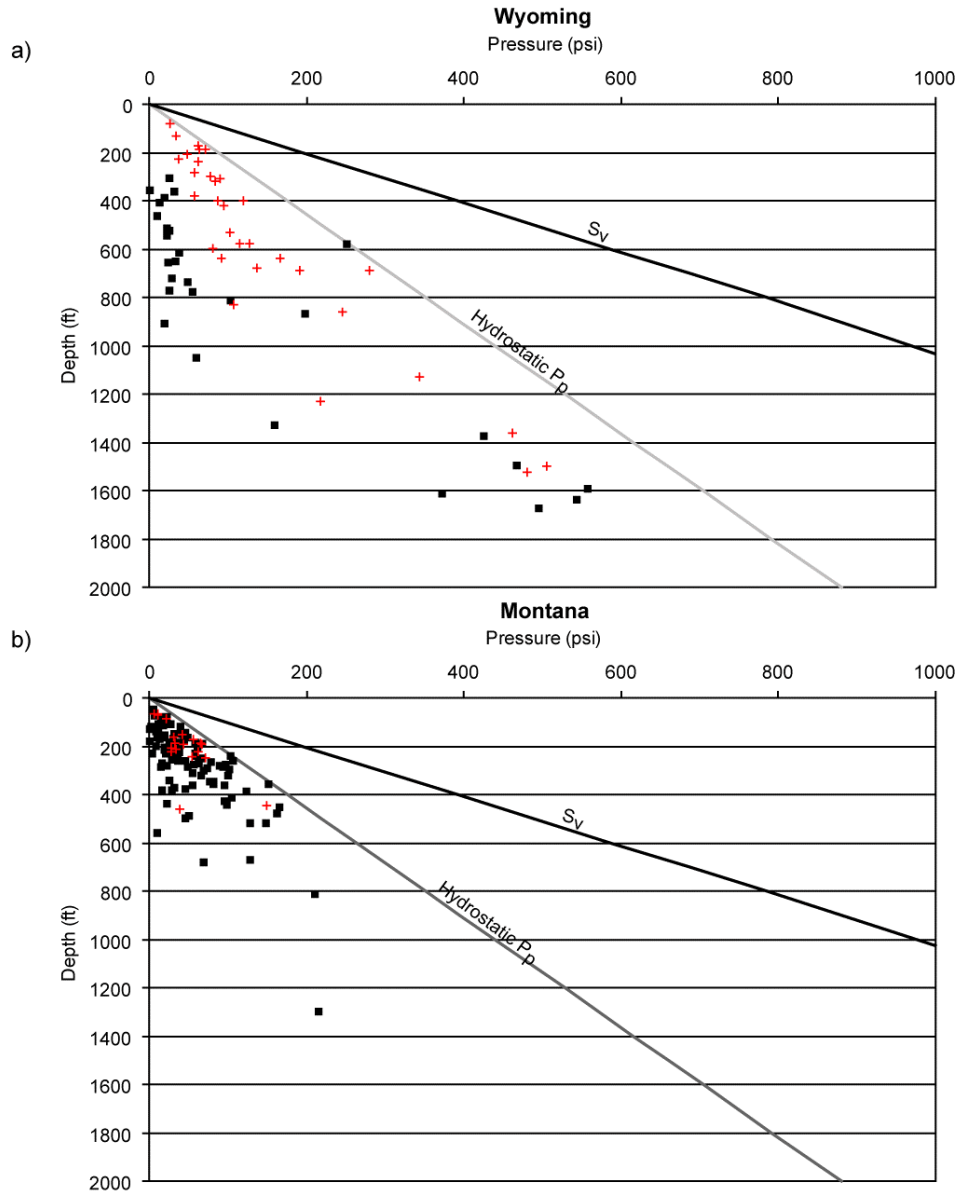
Additional pressure gradients that we will be referring to in the following sections are the hydrostatic and overburden pressure gradients. Hydrostatic pressure is the pressure exerted by a column of water from the ground surface to point P . The gradient is taken as ~ 0.44 psi/ft. To calculate the overburden pressure, S_v , rock densities are integrated from the surface to the depth of interest, z , where

$$S_v = \int \rho(z)gz \cong \bar{\rho}gz, \quad (2)$$

and $\rho(z)$ is the density as a function of depth, g is the gravitational acceleration and $\bar{\rho}$ is the mean overburden density. Because density logs are not available for any of the monitoring wells analyzed we used a mean overburden density of 2.3 g/cc, which is a reasonable average for the lithological units above the coal in the PRB (interbedded shales and sands).

PORE PRESSURE ANALYSIS: PRESENT DAY SAND AND COAL PORE PRESSURE MAGNITUDES IN THE POWDER RIVER BASIN

We calculated present day (2005) pore pressures for sands and coals in both the Montana and Wyoming parts of the PRB and found that they are sub-hydrostatic everywhere that data is available (**Figure 8.4**). **Figure 8.4** shows that the pore pressure magnitudes for both coals and sands in Montana and Wyoming plot below the hydrostatic pore pressure line, indicating that pore pressures are sub-hydrostatic. Pore pressures for the coalbeds are much lower than for overlying sands because of CBM production, which has reduced pore pressures in the coalbeds through water extraction.

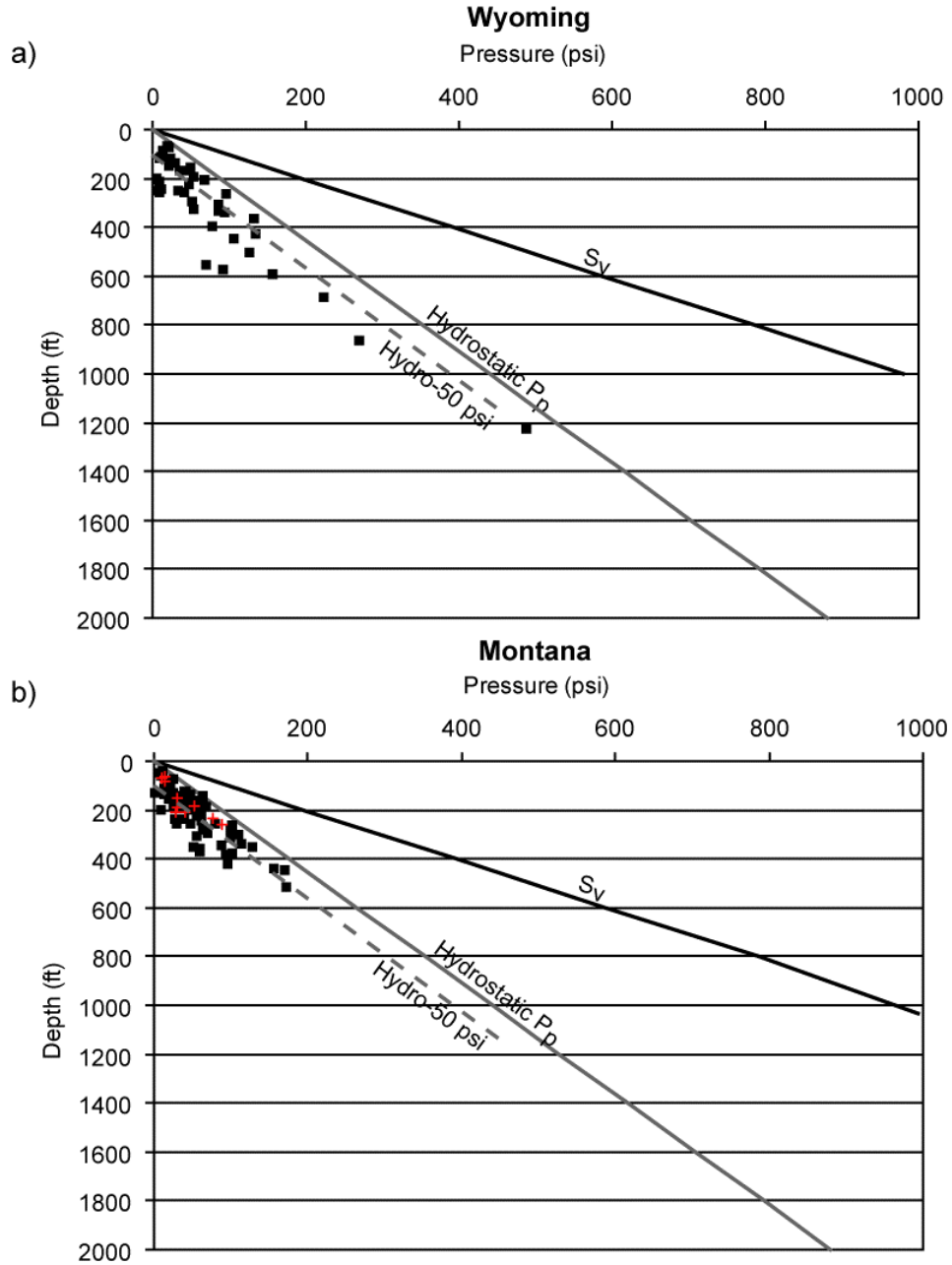


Figures 8.4a and 8.4b: Present day pore pressure in a) Wyoming and b) Montana. S_v corresponds to the overburden pressure and the black line is the overburden pressure gradient. The grey line corresponds to the hydrostatic pore pressure gradient (~0.44 psi/ft). Black squares correspond to pore pressures in coal and red crosses to pore pressures in sand.

GROUNDWATER SYSTEM BEFORE CBM PRODUCTION IN THE POWDER RIVER BASIN

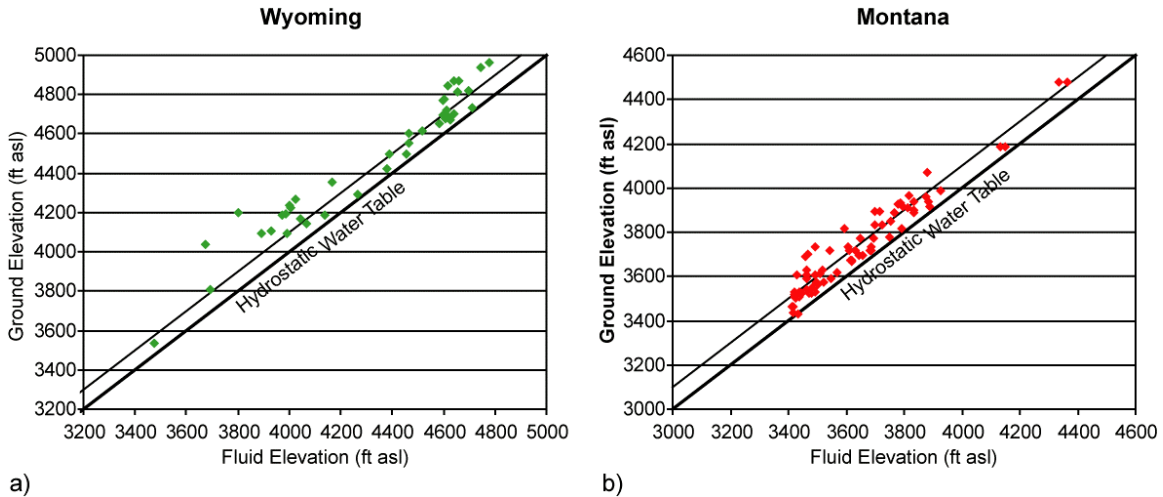
Taking water level data from 1972 to 1984 from both the Montana and Wyoming parts (Daddow, 1986) of the PRB, we calculated sand and coal pore pressure magnitudes across the basin before CBM production began in the basin. We find that pore pressures in both the sands and coals plot

below hydrostatic where we have historic data (**Figure 8.5**), indicating that pore pressures were sub-hydrostatic before CBM production in the basin.



Figures 8.5a and 8.5b: Pore pressure in a) Wyoming and b) Montana before CBM production (1972-1984) in the PRB. S_v corresponds to the overburden pressure and the black line is the overburden pressure gradient. The grey line corresponds to the hydrostatic pore pressure gradient (~ 0.44 psi/ft). The dashed grey lines correspond to the coal and sand pore pressure gradient, where hydro-50 psi means that the gradient is 50 psi less than hydrostatic pressure. Black squares correspond to pore pressures in coal and red crosses to pore pressures in sand.

By plotting the fluid elevation measured in each well versus ground level elevation (both in feet above sea level), we observe a linear trend between these two parameters, but the linear trend lies ~100 ft above the hydrostatic water level line (**Figure 8.6**). This suggests that the water level in sands and coals before CBM production in the basin followed topography, but was ~100 ft below the ground surface (**Figure 8.7**).



Figures 8.6a and 8.6b: Ground elevation versus fluid elevation in feet above sea level for a) Wyoming and b) Montana.

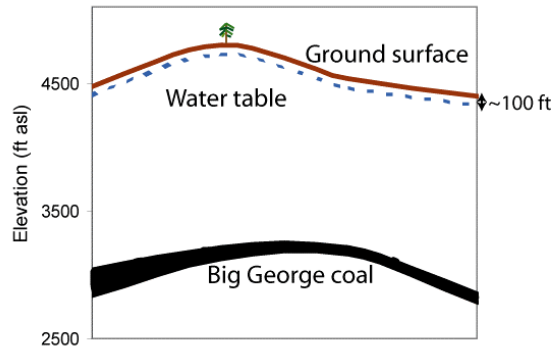


Figure 8.7: Schematic cross section showing the water table in the PRB before CBM production, where it followed topography but was ~100 ft below the ground surface.

INITIAL PORE PRESSURE MAGNITUDES FROM THE BLM DATABASE

Before analyzing initial pore pressures from the BLM data, we filtered the data by removing all wells whose first water level measurements appear to have been affected by prior CBM production. Wells were removed if we observed changes in pore pressure with time immediately after monitoring began. After filtering out CBM production effects we observe in **Figure 8.8** that the shallower coals and sands have slightly higher pore pressures than the deeper coals and

sands. The shallower coals and sands have pore pressures ~50 psi less than hydrostatic, whereas the deeper coals and sands have pore pressures ~150 psi less than hydrostatic. The observed difference in pore pressures between coals and sands at different depths could be because the deeper coals and sands are part of a confined aquifer, rather than being connected to the water table (Applied Hydrology Associates and Greystone Environmental Consultants, 2002; Bartos and Ogle, 2002).

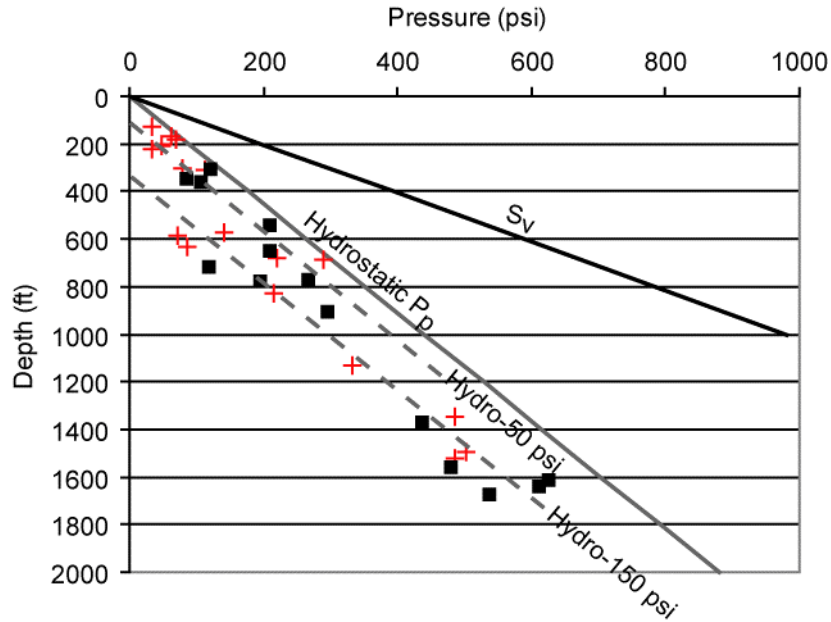


Figure 8.8: Pore pressures for sands and coals monitored by the BLM after removing those wells in the database whose initial water levels appear to have been affected by CBM production. Note that the pore pressures for the deeper coals and sands are much lower than hydrostatic compared to the shallower sands and coals. S_v corresponds to the overburden pressure and the black line is the overburden pressure gradient. The grey line corresponds to the hydrostatic pore pressure gradient (~0.44 psi/ft). The dashed grey lines correspond to the coal and sand pore pressure gradients, where hydro-50 psi means that the gradient is 50 psi less than hydrostatic pressure and hydro-150 psi means that the gradient is 150 psi less than hydrostatic pressure. Black squares correspond to pore pressures in coal and red crosses to pore pressures in sand.

HYDRAULIC COMMUNICATION BETWEEN SANDS AND COALBEDS IN THE POWDER RIVER BASIN

Wyoming

Because water levels have been continuously monitored over time in almost all of the BLM water level monitoring wells in the PRB, we were able to calculate pore pressure changes with time for the monitored sand aquifers. Using paired wells, we find that after 8 to 13 years of water

level monitoring that ~60% of sands less than ~200 ft from underlying/overlying coalbeds show the greatest change in pore pressure with time (**Figure 8.9**).

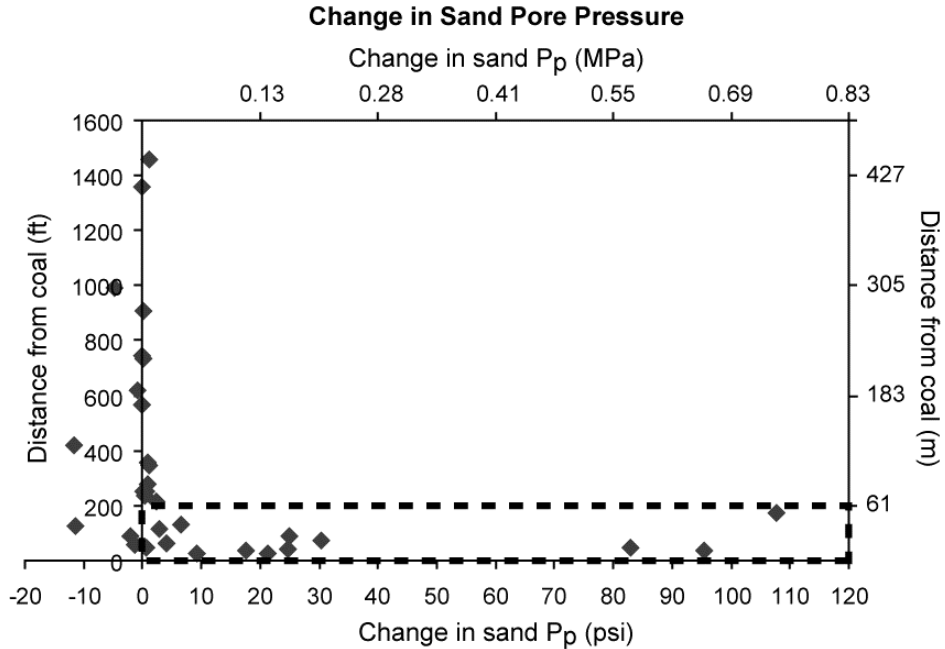


Figure 8.9: Separation between sand and coal pairs (in feet) versus change in pore pressure (P_p) with time for monitored sands in Wyoming. Black box highlights the sands with the greatest change in pore pressure, which are all within 200 ft of a producing coalbed. A positive change in pore pressure corresponds to a decrease in pore pressure with time.

To determine if the large changes in pore pressure for the overlying/underlying sands are due to hydraulic communication with the coalbeds, we looked at pore pressure changes with time for each coalbed and its overlying/underlying paired sand. We grouped the BLM data into three groups based on CBM production areas (**Figure 8.1a**). For each well in each group we determined the pore pressure with respect to a datum, using the deepest coalbed in each area as the datum. We plotted pore pressure against time for all paired wells, investigating the possibility that overlying/underlying sands had similar pore pressure depletion histories to their underlying/overlying coalbeds.

We found that 10 out of 16 monitored sands within ~200 ft of their paired coalbed had similar pore pressure trends as their paired coal, implying that the sands are in hydraulic communication with the coalbeds. Using **Figure 8.10** as an example, we see that pore pressures for the coals decrease with time and the pore pressure curves for the overlying sands follow similar pore pressure paths as the underlying coal. In some cases (7 out of the 10 pairs with similar pore pressure trends) pore pressures in the sands do not start to decline until several years after pore pressures in the coals start to decline (e.g. well MP2, well 447131 (**Figure 8.1b** for well locations)). We also found that several (6 pairs) of the sands within ~200 ft of an underlying coal show no change in pore pressure with time even though pore pressures in the underlying coals have decreased significantly (**Figure 8.11**, the NAPIER well, and **Figure 8.12**, the REDS well

(Figure 8.1b well for locations)). It appears that most of the coal and sand pairs that show similar pore pressure depletion trends are located in group 1, south of Gillette, where CBM production and coal mining first began in the Wyoming part of the PRB (Figure 8.1a) (Ayers, 2002; Hower et al., 2003).

Water monitoring in the Wyoming part of the basin started approximately 13 years ago, so our observations are based on a limited data set. However, at present, the water monitoring data show that ~60% of the sands within ~200 ft of a producing coalbed are in hydraulic communication with that coalbed. Therefore, sand aquifers closer than ~200 ft to a coalbed should not be used as water disposal sites as there is a strong possibility that the disposed water will migrate from the aquifer into the producing coalbeds. In contrast, sand aquifers further than 200 ft from producing coalbeds show no change in pore pressure after 8 to 13 years of water level monitoring and could be potential sites for CBM water disposal. Additional investigations will need to be carried out to make sure that sand aquifers further than ~200 ft from a coalbed are not in hydraulic communication with the coalbed and will not communicate with the coalbed at a future date.

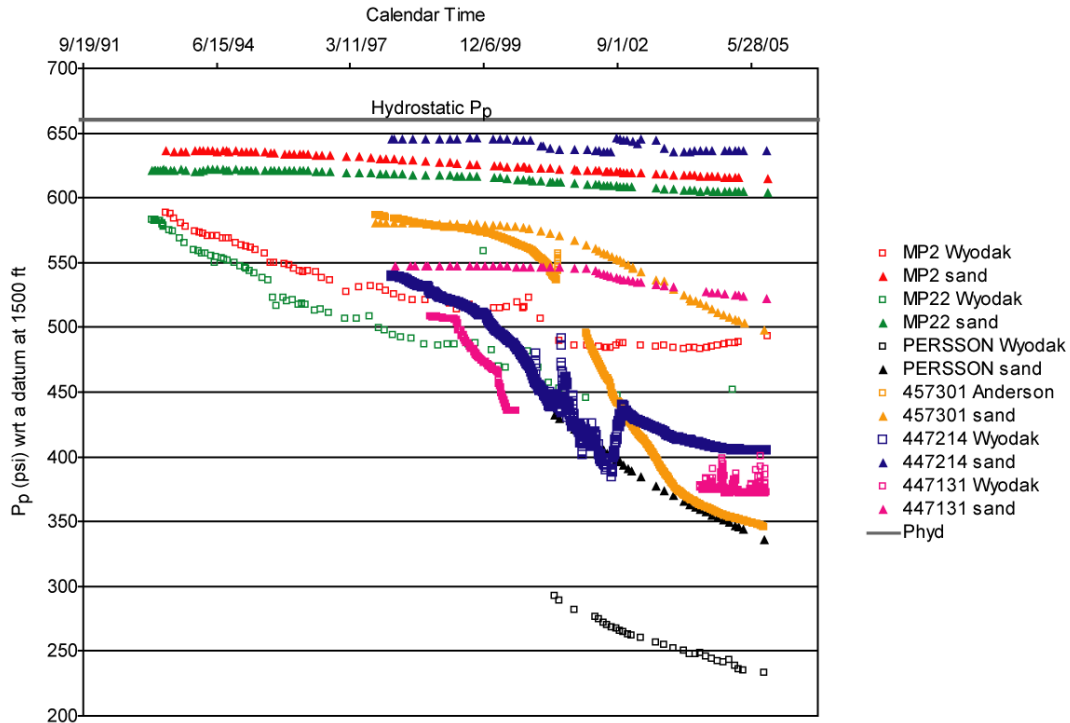


Figure 8.10: Pore pressure changes with time for water monitoring wells with sand and coal pairs less than 200 ft from one another in group 1. The names in capital letters in the key are the names given for the water monitoring wells and their locations are marked on Figure 8.1b. Wyodak stands for the Wyodak coal and Anderson, the Anderson coal.

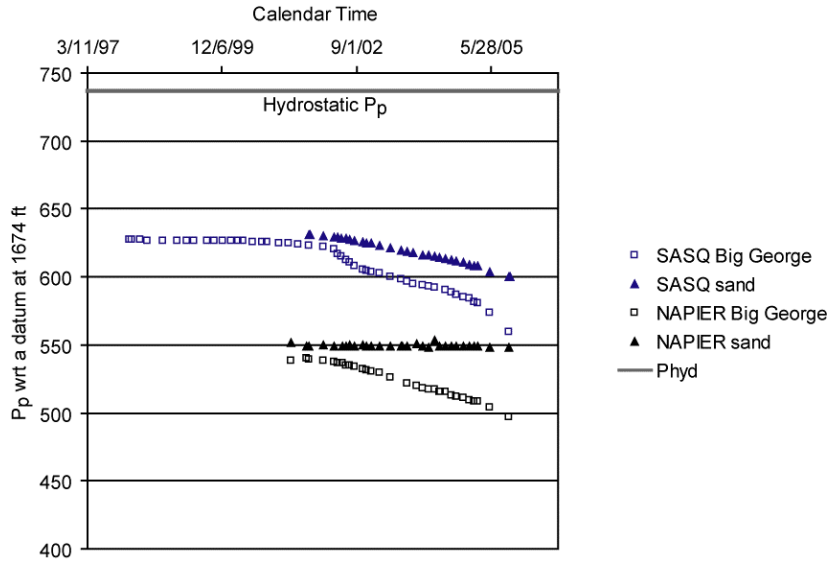


Figure 8.11: Pore pressure changes with time for water monitoring wells with sand and coal pairs less than 200 ft from one another in group 2. The names in capital letters in the key are the names given for the water monitoring wells and their locations are marked on **Figure 8.1b**. Big George stands for the Big George coal.

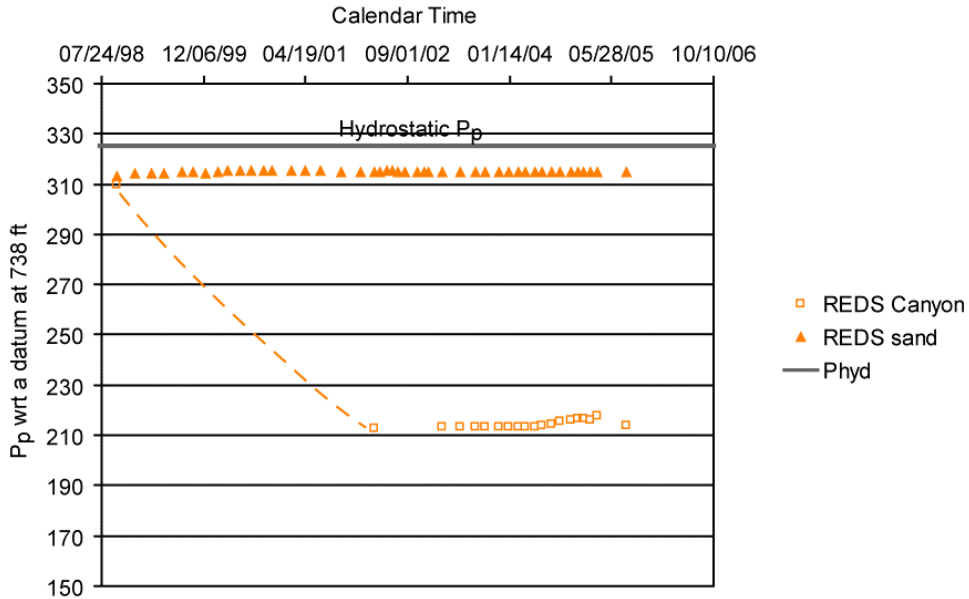


Figure 8.12: Pore pressure changes with time for water monitoring wells with sand and coal pairs less than 200 ft from one another in group 3. The name in capital letters in the key is the name given to the water monitoring well and its location is marked on **Figure 8.1b**. Canyon stands for the Canyon coal.

We also investigated the potential for vertical flow between paired sand and coalbed wells to help support our observation that some sands and coals are in hydraulic communication with each other. The potential for vertical flow is determined by using the water head elevation for each well in the well pairs (Bartos and Ogle, 2002). If the shallower unit has a higher head than the underlying unit, the potential for vertical flow is downward. We find that the vertical flow potential is in the downward direction in all but one of the well pairs. In addition, one of the monitoring wells monitors water levels in sand that is below its paired coalbed and we find that the potential for vertical flow is upward from the sand to the overlying coalbed. The direction for vertical flow is consistent with the large decrease in pore pressure observed over time for the underlying sand, implying that CBM production is removing water from the underlying sand aquifer.

Montana

CBM production in Montana is on a much smaller scale than in the Wyoming part of the PRB. In 1990 there were 3 drilling permits issued in Montana and as of the end of 2006 there have been only ~1500 issued (MBOGC, 2007). Because of the limited CBM activities in the Montana part of the basin we have observed much smaller ground water drawdown than in the Wyoming part of the basin. Hence, when analyzing pore pressure changes with time for the 11 paired wells in Montana, only 5 of the 11 coals had significant decreases in pore pressure with time (between 50 and 90 psi). From our limited dataset it appears that at present overlying sand aquifers are not being drained through CBM production. The greatest pore pressure decrease observed in overlying sands is ~5 psi (Figure 8.13), compared with over 100 psi in the Wyoming part of the basin. Even if we analyze pore pressure changes with time for overlying sands not part of well pairs, the greatest decrease in pore pressure is only 2 psi.

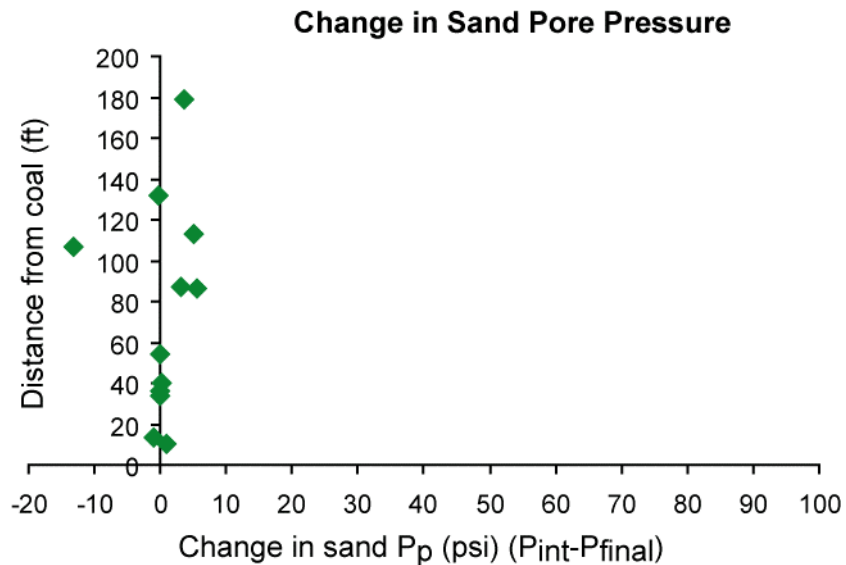


Figure 8.13: Separation between sand and coal pairs (in feet) versus change in pore pressure (P_p) with time for sand and coal pairs in Montana. P_{int} stands for initial pressure and P_{final} stands for final pressure. A positive change in pore pressure corresponds to a decrease in pore pressure with time.

IMPLICATIONS FOR INJECTION OF CBM WATER INTO SAND AQUIFERS

Modeling CBM Water Injection into Sand Aquifers

From our pore pressure analysis it appears that most sand and coal units in the PRB have sub-hydrostatic pore pressures, which means that injection of CBM water into sand aquifers should be feasible, as there should be no initial pressure resistance to injection. However, based on 8 to 13 years of water monitoring data, we believe it is important that potential sand aquifers for disposal sites are further than ~200 ft from producing coalbeds and are vertically confined so that water does not migrate into adjacent coals.

With this in mind, we have constructed two 3D stochastic reservoir models of conceptualized sand units in the PRB (using geostatistics to populate our models with sand permeability and porosity data) and have run fluid flow simulations to determine the rate at which CBM water can be injected into the aquifers. The first model is of a shallow sand unit with depth to the top ranging from 166-316 ft, and the second model is of a deeper sand body, with depth to the top ranging from 1034-1184 ft. We modeled water injection into both shallow and deep sands because our pore pressure analysis showed that deeper sands and coals have lower initial pore pressures than the shallower sands and coals (**Figure 8.8**), suggesting that we should be able to inject a larger volume of CBM water into the deeper sands. In order to be able to compare our results between the two sand units we kept the thickness the same for both, ~40 ft (average thickness of sands being monitored by the BLM monitoring wells), and populated the models with permeability and porosity values using the same property distributions and variograms.

Each 3D model grid contains 16830 grid cells, 55 in the x direction, 51 in the y direction and 6 in the z direction. Each grid cell is 67ft by 67 ft by 7 ft and the total area of the model is ~160 acres (**Figure 8.14**).

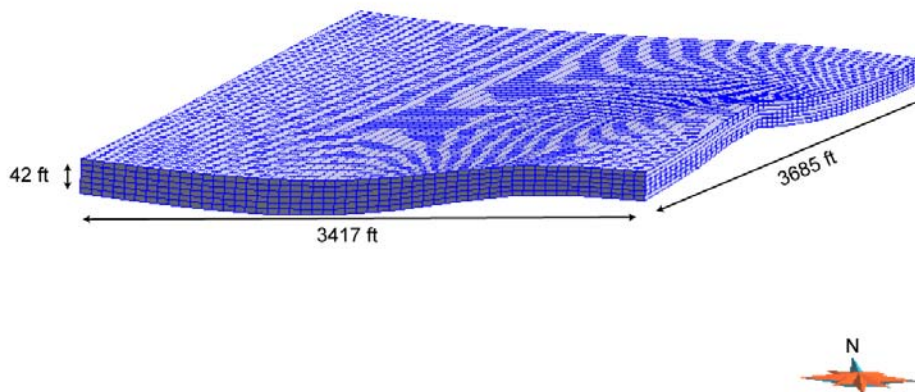


Figure 8.14: Simulation grid for general 3D sand model.

We obtained permeability and porosity distributions from Applied Hydrology Associates and Greystone Environmental Consultants (2002), who reported hydraulic conductivity values for sand units and determined porosity values from their modeling of recharge into the Wasatch and Fort Union formations. We calculated permeability from hydraulic conductivity using the following equation,

$$K = \frac{k\rho g}{\mu}, \tag{3}$$

where k is permeability in Darcies, K is hydraulic conductivity in ft/s, ρ is the fluid density, μ is the dynamic viscosity of the fluid and g is gravity.

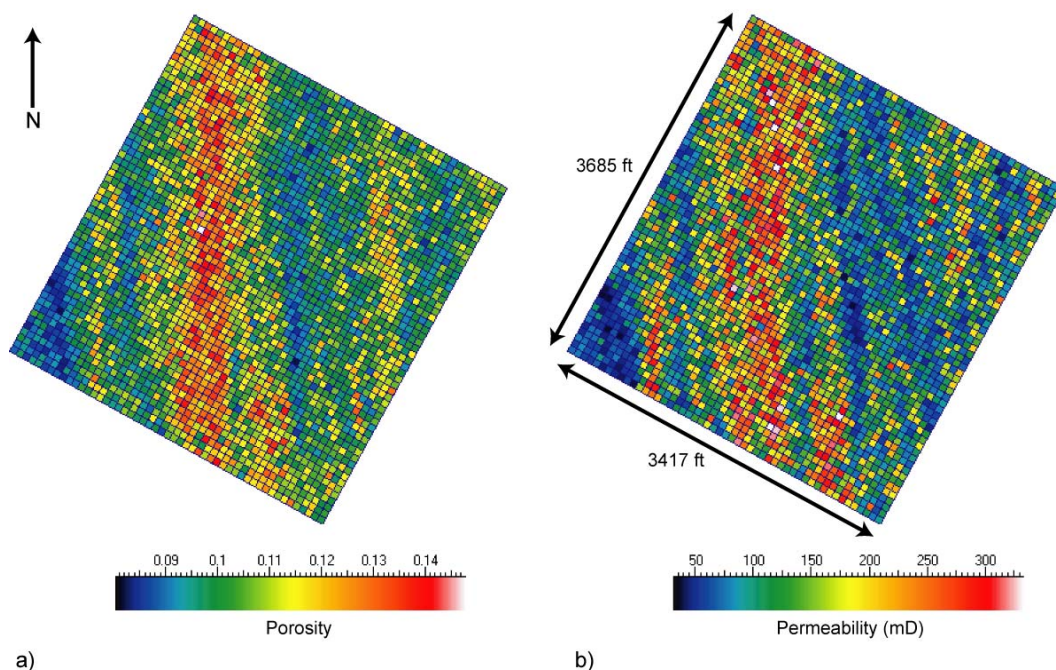
Applied Hydrology Associates and Greystone Environmental Consultants (2002) report measured hydraulic conductivity values representative of fine to medium grained sand, which is the sand grain-size given by Flores (2004) for sandstone reservoirs in the Wasatch and Fort Union Formations. Applied Hydrology Associates and Greystone Environmental Consultants (2002) give an average hydraulic conductivity of 2E-6 ft/s (70 mD) for the sands, with an upper limit of 1E-5 ft/s (350 mD), and in their model they use a porosity of 10% for the sand units.

In our geostatistical modeling we used triangular property distributions to represent the range in permeability and porosity values reported by Applied Hydrology Associates and Greystone Environmental Consultants (2002) for sandstone reservoirs in the Wasatch and Fort Union Formations. **Table 8.1** shows the maximum, minimum and mode values of our distributions.

Table 8.1: Triangular distribution parameters for sand permeability and porosity.

Property	Minimum and Maximum Value	Mode
Permeability	30-350 mD	70 mD
Porosity	0.08-0.15	0.1

To populate our 3D stochastic models we used simple Kriging and sequential Gaussian simulation (SGS) to generate 20 equally probable permeability and porosity realizations (Deutsch, 2002). To incorporate the spatial variability of the permeability and porosity distributions into the SGS algorithm we used a spherical semivariogram (Deutsch, 2002). However, because we have no hard data, our choice of semivariogram is highly subjective. Since the sands are fine to medium grained, contain ~30% clay particles and are moderately sorted (Flores, 2004), we used a correlation coefficient of 0.7 between the porosity and permeability. Also, the sands were deposited by meandering rivers (Flores,2004), so we created a semivariogram that captured the channelized nature of the sands and which also reduced the permeability correlation in the vertical direction to mimic both bedding and the lower vertical hydraulic conductivities found in the sands (Applied Hydrology Associates and Greystone Environmental Consultants, 2002). Our spherical semivariogram model had a nugget of 0.2 and a range in the north direction of 16,400 ft, in the east direction of 1640 ft and in the vertical direction of 1.6 ft. **Figure 8.15** shows one realization of our sand model with its associated permeability and porosity distributions.



Figures 8.15a and 8.15b: a) Porosity and b) permeability distributions for one realization of our general sand model.

We used the Computer Modeling Group’s Generalized Equation-of-State Model Compositional Reservoir Simulator (GEM) and the fluid flow simulations were carried out by injecting water through an injection well located in the middle of the simulation grid (the well is perforated for the entire thickness of the sand). We used a higher reservoir pressure gradient for the shallower sand (60 psi less than hydrostatic) than for the deeper sand (150 psi less than hydrostatic) (**Figure 8.8**), but all other parameters required by the simulator were set the same. The sands were modeled as semi-infinite in the horizontal direction, with constant-pressure boundaries, but confined vertically.

We injected water until the injection well bottom hole pressure (BHP) reached hydrostatic pressure, which means that the reservoir pressure of the aquifer is close to hydrostatic. At this point, rather than the water flowing under gravity into the aquifer when reservoir pressures are below hydrostatic, the operators would need to pump the water down the injection well at a higher pressure than hydrostatic for it to flow into the aquifer and away from the well (need a pressure gradient). Water could be injected into the sand aquifer until the reservoir pressure reaches the fracture pressure of the aquifer, but we do not know the fracture pressure of the sands in the Wasatch and Fort Union formations so the hydrostatic BHP is a good cutoff, since injection costs would increase with the need to start pumping.

Our simulations show that for the shallower sand, water can be injected at a rate of ~160 bbl/day for ~4000 days before the BHP reaches hydrostatic (**Figure 8.16, 8.17a**). In contrast, for the deeper sand, water can be injected at a rate of ~435 bbl/day for ~4000 days (**Figure 8.16, 8.17b**). At present the average water production rate per CBM well in the PRB is ~100 bbl/day (WOGCC, 2007) and the average lifetime of a CBM well is ~7 to 15 years (2555 to 5500 days)

(Ayers, 2002; De Bruin et al., 2004). Therefore, if operators were to inject CBM water into shallow sands they will be able to dispose of the water production from one and a half CBM wells every 160 acres using one disposal well (assuming the sand properties throughout the basin are similar to those in our model). If injection takes place in deeper sands, operators will be able to dispose of the water production from four CBM wells every 160 acres using one disposal well.

In **Figure 8.16** we have marked the water injection rate achievable in our two different sand models and have also plotted the average water production in bbl/day for CBM wells analyzed by Colmenares and Zoback (2007) and Ross (2007). Colmenares and Zoback (2007) looked at over 500 water-enhancement tests that are used by CBM operators in the PRB to connect the natural coal fracture network to their CBM wells. The procedure involves pumping water down the CBM wells at a rate of ~60 bpm for ~15 min. Through their analysis, Colmenares and Zoback (2007) showed that water-enhancement actually hydraulically fractures the coal and in some areas the fractures grow horizontally (because the least principal stress is equal to the overburden stress) and in other areas they propagate vertically (because the least principle stress is equal to the minimum horizontal stress). Interestingly, they found a correlation between fracture orientation and water and gas production from CBM wells. Wells with horizontal hydraulic fractures typically produce small volumes of both gas and water, whereas some wells with vertical hydraulic fractures produce manageable volumes of water, but are actually good gas producers. However, ~30% of wells with vertical hydraulic fractures produce excessive volumes of water and little to no gas. Colmenares and Zoback (2007) define excessive water production as ~230 bbl/day and higher. From **Figure 8.16** we see that deeper sand aquifers will need to be used as water disposal sites for CBM wells with excessive water production. The shallower sands do not have the capacity to store water from excessive water producing wells over the lifetime of the CBM well.

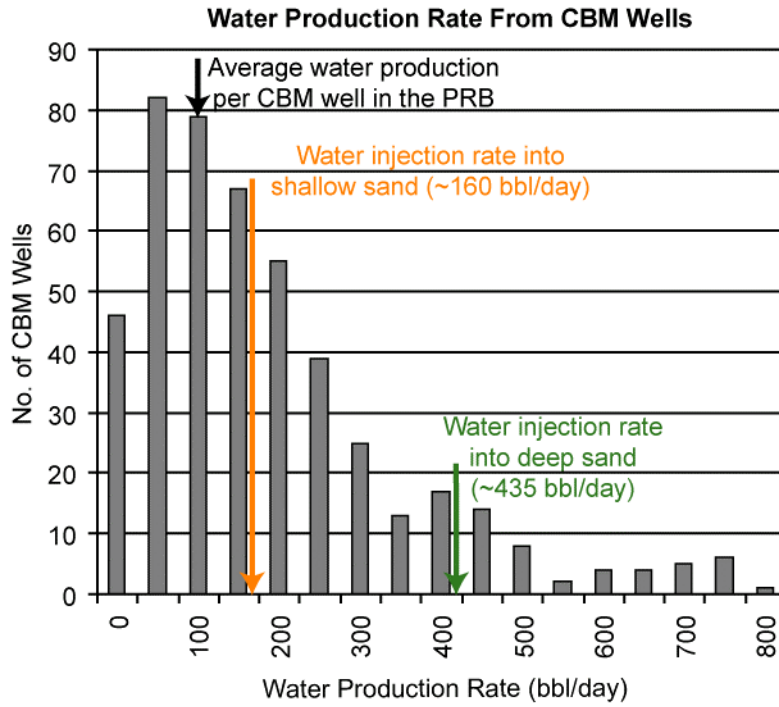


Figure 8.16: Water production rate per well for CBM wells analyzed by Colmenares and Zoback (2007) and Ross (2007) compared with the injection rates obtained from fluid flow simulations for our shallow (orange) and deep (green) sand models. Average CBM water production for the PRB is from the WOGCC (2007).

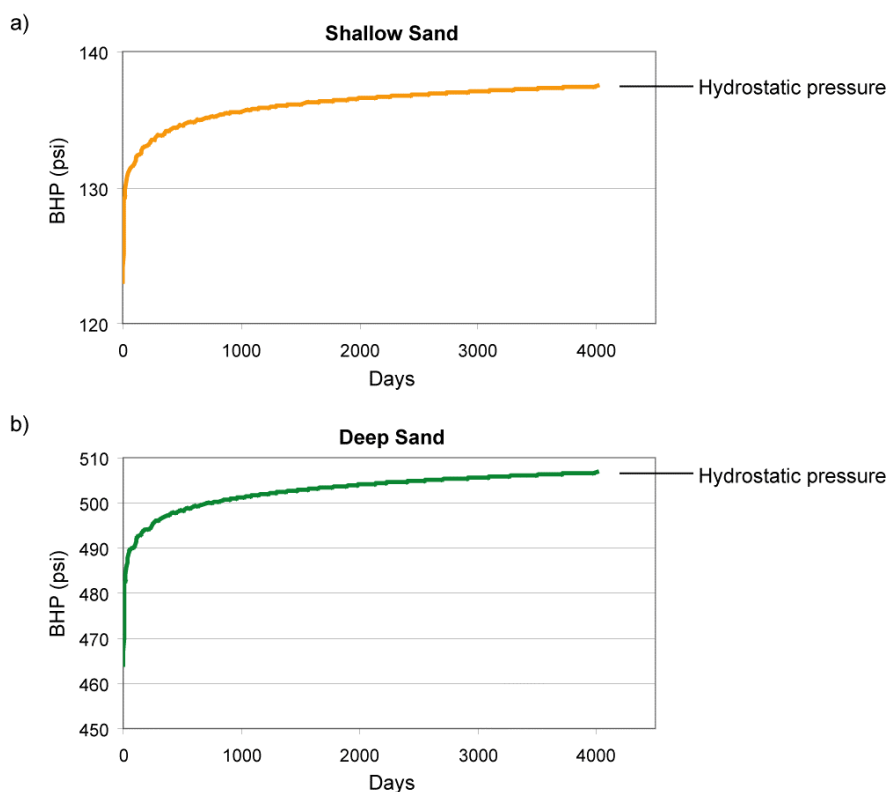
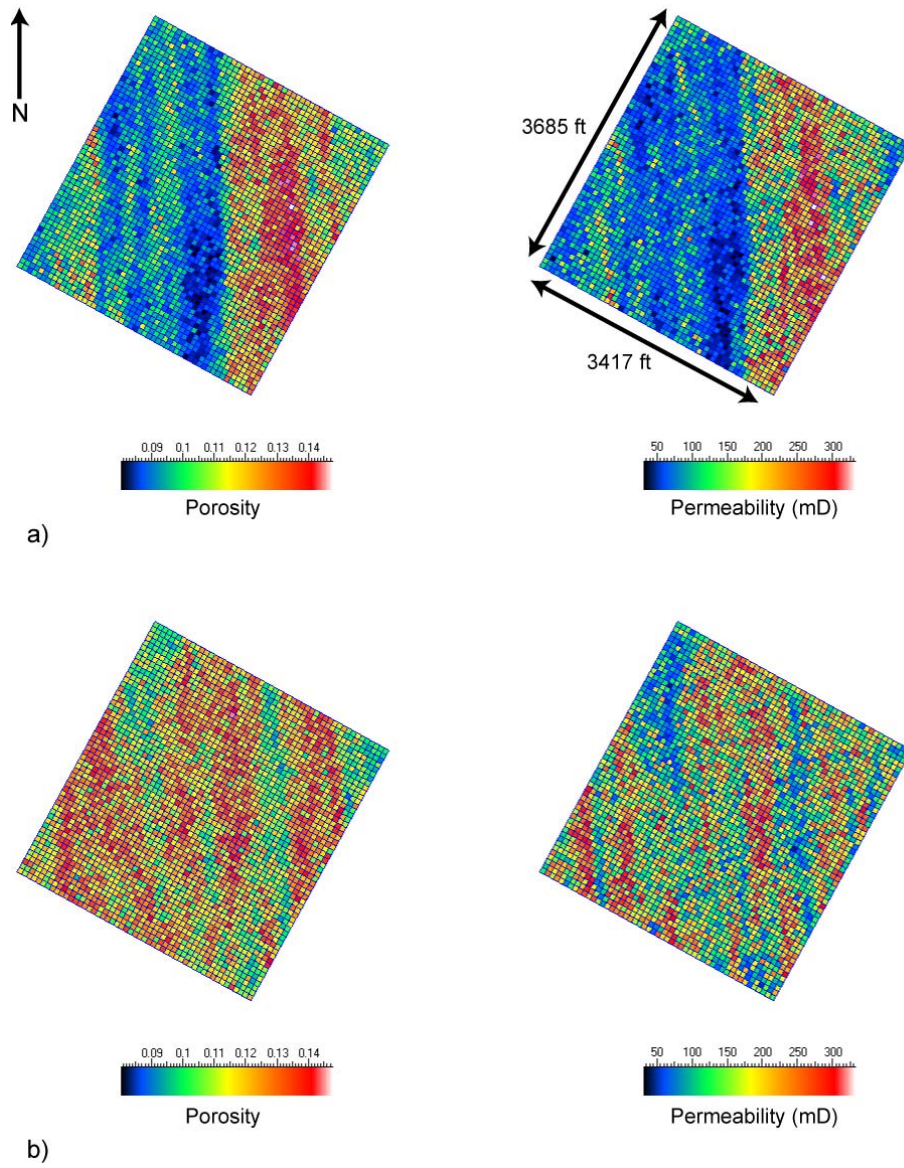
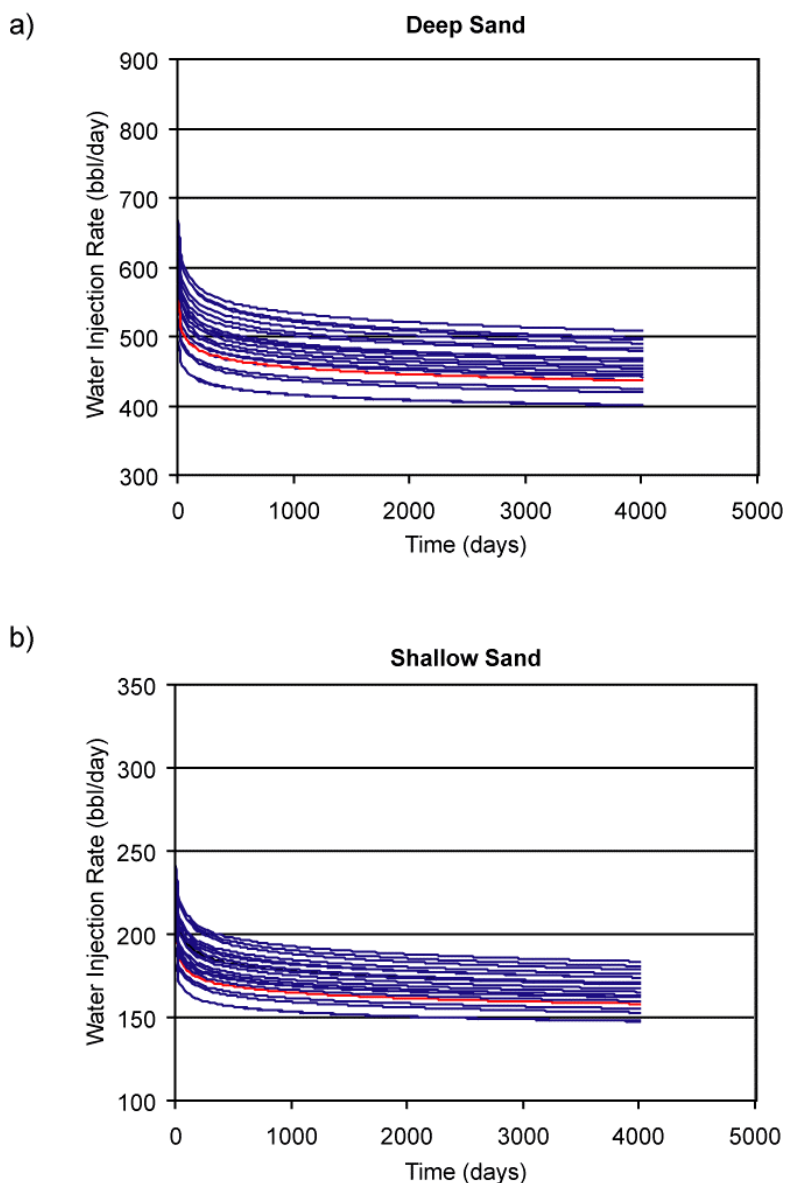


Figure 8.17: Bottom hole injection pressure (BHP) for the a) shallow (orange) and b) deep (green) sand models.

As mentioned earlier, we generated 20 sand porosity and permeability realizations to capture the uncertainty in our knowledge of the sand geology in the PRB. In **Figure 8.18** we show two examples of the 20 permeability and porosity realizations generated for our injection modeling. The results from our realization runs are shown in **Figure 8.19**. The range in water injection rate due to uncertainty in the permeability and porosity distributions for the deep sand model is ~400 to ~510 bbl/day and the range in injection rate for the shallow sand model is ~150 to ~190 bbl/day. The red lines correspond to the base case results reported above.



Figures 8.18a and 8.18b: a) Porosity and permeability distribution for realization 17. b) Porosity and permeability distribution for realization 3.



Figures 8.19a and 8.19b: a) Water injection rate (bbl/day) results from 20 realization runs for the deep sand model. b) Water injection rate (bbl/day) results from 20 realization runs for the shallow sand model. The red lines correspond to the base case results for both models.

We have also run a sensitivity analysis on sand permeability, assuming that in general the sands have permeabilities closer to the reported average of ~70 mD and rarely have permeabilities as high as 350 mD (Applied Hydrology Associates and Greystone Environmental Consultants, 2002). We effectively modeled the sand as if it were only fine grained. **Table 8.2** outlines the permeability distribution used for our fine grained sensitivity analysis and **Figure 8.20** shows the

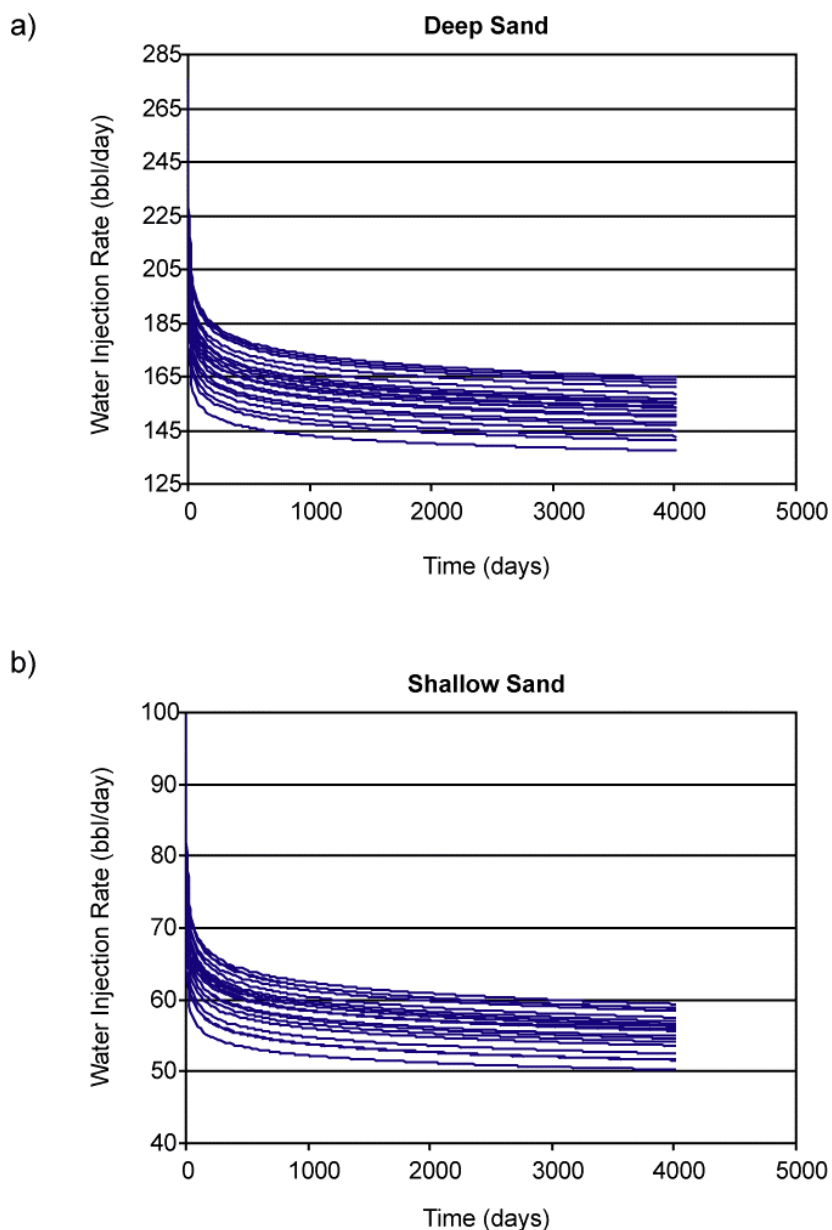
water injection rates that could be obtained if water is injected into both a shallow and deep fine grained sand body in the PRB.

Table 8.2: Triangular distribution parameters for fine grained sand permeability and porosity.

Property	Minimum and Maximum Value	Mode
Permeability	10-70 mD	65 mD
Porosity	0.08-0.15	0.1

Our simulations show that for a shallow fine grained sand aquifer the water injection rate could range from ~55 to ~60 bbl/day, whereas for a deeper fine grained sand body the injection rate could range from ~150 to ~170 bbl/day (**Figure 8.20**).

The water injection rates estimated from our fine grained sand sensitivity analysis are significantly lower than for a sand model that includes slightly coarser grained sands found in the PRB. We show that a deep fine grained sand aquifer would only be able to hold water produced from one average CBM well, compared with four for the deep sand model with coarser grains. This implies that operators need to find the coarser grained sand bodies within the PRB for CBM water disposal to minimize disposal costs.



Figures 8.20a and 8.20b: a) Water injection rate (bbl/day) results from 20 realization runs for the deep fine grained sand model. b) Water injection rate (bbl/day) results from 20 realization runs for the shallow fine grained sand model.

Characteristics of the Confining Unit between Coalbeds and Aquifers in the PRB

Aquifers designated for CBM water disposal not only need to have low pore pressures and adequate permeability and porosity, which we modeled in the previous section, but aquifer water has to be of similar quality to CBM water and the sands should not be in hydraulic communication with producing coalbeds. In terms of hydraulic communication, we have found that at present, ~60% of sands within ~200 ft of producing coals are probably in hydraulic communication with the coalbeds and should not be sites for CBM water disposal. However,

coalbeds in the Upper Fort Union Formation are typically overlain by a confining unit and are rarely in direct contact with a sand body (J. Wheaton, personal communication, 2007; Applied Hydrology Associates and Greystone Environmental Consultants, 2002; Bartos and Ogle, 2002). So why do we observe hydraulic communication after 8 to 13 years of water level monitoring between coals and sands that are within ~200 ft of each other?

It is possible that sands that show delays in pore pressure reduction, compared with when pore pressure decline in the coalbeds started, are separated from the coal by a thicker confining unit than in areas where we see declines in sand pore pressures almost immediately after pressures in the coal start to decline (**Figures 8.10, 8.1b**). Areas where pore pressures in both the coals and sands start decreasing at similar times may be where sand bodies immediately overlie the coalbeds or the confining unit is very thin (**Figures 8.10, 8.11, 8.1b**). Gamma ray logs for the monitoring wells are not available, but through analysis of gamma ray logs from CBM wells located in the same sections as the monitoring wells we see no correlation between the geologic units above the coals and timing or magnitude of pore pressure changes in the overlying monitored sands (**Figure 8.21**). In two sections, 1-45-73 (monitoring well 457301, **Figures 8.10, 8.1b**), where the pore pressure in the overlying sand has started to decrease at the same time as in the underlying coalbed, and 32-47-73 (monitoring well PERSSON, **Figures 8.10, 8.1b**), where the sand pore pressure change is large, the coals are overlain by ~4 ft and ~36 ft of shale respectively (**Figure 8.21**). In contrast, in sections where there is a delay between the start in decline of the coal pore pressure and the start in decline of the sand pore pressure, the shale units overlying the coals are only ~10 ft thick (monitoring wells MP2 and MP22, **Figures 8.21, 8.10, 8.1b**).

It seems that hydraulic communication may be more of a function of the properties of the shale and the rate at which the CBM well is pumping water, rather than just thickness alone. A “leaky” confining unit will allow water to flow from the sand, through the confining unit, and into the coalbed. In addition, a “leaky” confining unit will contain water itself and some of the initial water entering the coal may be from the confining unit. Sands that have delays in pore pressure decline could be separated from the coalbeds by confining units with very low permeability, limiting the migration of water to the coalbed.

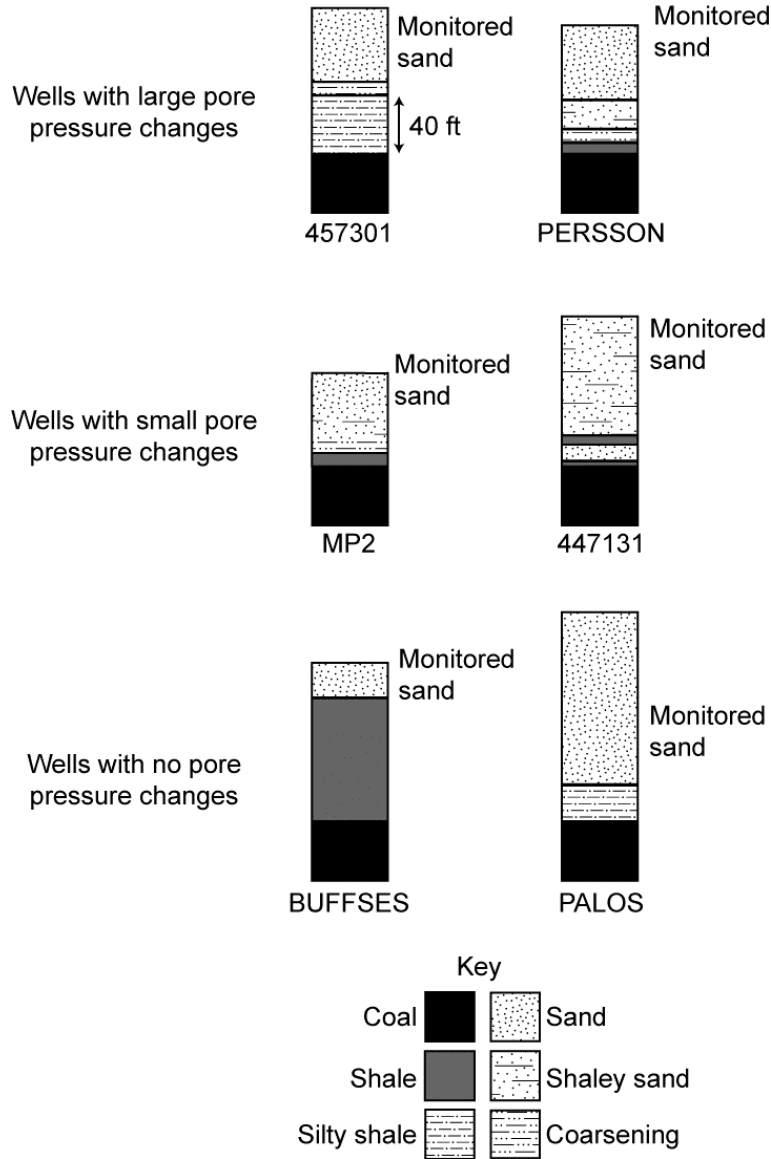


Figure 8.21: Examples of the lithology found directly above coalbeds in the PRB. These examples are from water monitoring wells 457301, PERSSON, MP2, 447131, BUFFSES and PALOS (the well locations are marked on **Figure 8.1b**). The lithology comes from gamma logs from CBM wells in the same sections as the monitoring wells. Large pore pressure changes are on the order of ~100 psi, whereas small pore pressure changes are ~20 psi.

CONCLUSIONS

Through the analysis of water level data from water monitoring wells located in both Montana and Wyoming, we have determined that sands and coals in the PRB have sub-hydrostatic pore pressures. In addition, pore pressure changes with time reveal that at present ~60% of sands less

than 200 ft from underlying/overlying coals appear to be in hydraulic communication with the coalbeds. In contrast, sand aquifers further than 200 ft from producing coalbeds show no change in pore pressure after 8 to 13 years of water level monitoring. These findings have important implications for the disposal of CBM water through injection into sand aquifers. The occurrence of sub-hydrostatic pore pressures means that the sands have the capacity to store water, but to insure that the disposed water does not reach producing coalbeds in the future; we recommend that sands closer than ~200 ft to producing coals should not be used as disposal sites because they may be in hydraulic communication with the coalbeds.

Furthermore, we ran fluid flow simulations to determine the rates at which CBM water could be injected into shallow (~300 ft) and deep (~1000 ft) aquifers. We found that for the shallow sand model an injection water rate of ~160 bbl/day could be achieved, whereas for the deeper sand, whose pore pressures are lower than the shallow sand, the rate was ~435 bbl/day. Both these rates are higher than the average water production rate from CBM wells in the PRB, which is ~100 bbl/day. This implies that for deep aquifer injection sites, only one injection well would be required to dispose of the water produced from four CBM wells, reducing the cost of CBM water disposal.

RECOMMENDATIONS FOR FUTURE RESEARCH

Improved modeling needs to be done that takes into account the exact geometry (thickness and lateral extent) and flow properties of candidate aquifers to determine the volumetric capacity of the respective units as well as the rates and pressures at which injection can be carried out.

REFERENCES

- Advanced Resources International, Inc., 2002.** Powder River Basin coalbed methane development and produced water management: DOE/NETL-2003/1184.
- Applied Hydrology Associates, Inc. and Greystone Environmental Consultants, Inc., 2002.** Groundwater modeling of impacts associated with mining coal bed methane development in the Powder River Basin: Technical Report Powder River Basin Oil and Gas Environmental Impact Statement, U.S. Bureau of Land Management, Buffalo Field Office, <http://www.blm.gov/wy/st/en/info/NEPA/bfodocs/prb_eis/prb-feis.html>.
- Ayers, W., 2002.** Coalbed gas systems, resources, and production and a review of contrasting cases from the San Juan and Powder River basins: AAPG Bulletin, 86, 1853-1890.
- Bartos, T. T., and K. M. Ogle, 2002.** Water quality and environmental isotopic analyses of ground-water samples collected from the Wasatch and Fort Union Formations in areas of coalbed methane development — implications to recharge and ground-water flow, Eastern Powder River Basin, Wyoming: U.S. Geological Survey Water-Resources Investigations Report 02-4045.

- Colmenares, L. B., 2004.** Rock strength under true triaxial loading, seismotectonics of Northern South America and geomechanics and Coal Bed Methane Production in the Powder River Basin: unpublished PhD Thesis, Stanford University, Stanford, California.
- Colmenares, L. B., and M. D. Zoback, 2007.** Hydraulic Fracturing and Wellbore Completion of Coalbed Methane (CBM) Wells in the Powder River Basin, Wyoming: Implications for Water and Gas Production: AAPG Bulletin, 91, 51-67.
- Daddow, P. B., 1986.** Potentiometric-surface map of the Wyodak-Anderson coal bed, Powder River structural basin, Wyoming, 1973-84: U.S. Geological Survey Water-Resources Investigations Report 85-4305, 1 sheet, Scale 1:250,000.
- De Bruin, R. H., R. M. Lyman, R. W. Jones, and L. W. Cook, 2004.** Coalbed Methane in Wyoming: State of Wyoming Geological Survey Information Pamphlet 7, Laramie, Wyoming.
- Deutsch, C. V., 2002.** Geostatistical reservoir modeling: Oxford University Press.
- Environmental News Network, 2001.** Coalbed methane boom in Wyoming's Powder River Basin: <<http://www.enn.com/archive.html?id=25012&cat=archives>>, accessed April 2007.
- Flores, R. M., 2004.** Coalbed methane in the Powder River Basin, Wyoming and Montana: An assessment of the Tertiary-Upper Cretaceous coalbed methane total petroleum system: U.S. Geological Survey Digital Data Series, DDS-69-C, chapter 2.
- Flores, R. M., and L. R. Bader, 1999.** Fort Union coal in the Powder River Basin, Wyoming and Montana: A synthesis: U.S. Geological Survey Professional Paper, 1625-A, PS8-PS29.
- Freeze, R. A., and J. A. Cherry, 1979.** Groundwater: Prentice-Hall.
- GEM, 2004.** GEM 2004.10 User's Guide: Computer Modelling Group Ltd., Calgary, Alberta, Canada.
- GEM, 2005.** GEM 2005.15 User's Guide: Computer Modelling Group Ltd., Calgary, Alberta, Canada.
- Hower, T. L., J. E. Jones, D. M. Goldstein, and W. Harbridge, 2003.** Development of the Wyodak coalbed methane resource in the Powder River Basin: SPE 84428, presented at the SPE Annual Technical Conference and Exhibition, Denver, Colorado, October 5-8.
- Hubbert, M. K., and D. G. Willis, 1957.** Mechanics of hydraulic fracturing: Petroleum Transactions of the American Institute of Mining Metallurgical and Petroleum Engineers, 210, 153-163.

Montana Board of Oil and Gas Conservation (MBOGC), 2007.

<<http://bogc.dnrc.state.mt.us/>>, accessed March 2007.

Ross, H. E., 2007. Carbon dioxide sequestration and enhanced coalbed methane recovery in unmineable coalbeds of the Powder River Basin, Wyoming: unpublished PhD Thesis, Stanford University, Stanford, California.

The Ruckelshaus Institute of Environment and Natural Resources, 2005. Water production from coalbed methane development in Wyoming: A summary of quantity, quality and management options: Final report prepared for the Office of the Governor, State of Wyoming, <<http://www.uwyo.edu/enr/ienr/cbm.asp>>, accessed February 2007.

Wheaton, J., and J. Metesh, 2002. Potential Ground-Water Drawdown and Recovery from Coalbed Methane Development in the Powder River Basin, Montana: Project Completion Report to the U.S. Bureau of Land Management, Montana Bureau of Mines and Geology Open File Report 458, <<http://www.mt.blm.gov/mcfo/cbm/eis/CBM3DGWReport.pdf>>, accessed March 2007.

Wheaton, J., and T. Donato, 2004. Coalbed-methane basics: Powder River Basin, Montana: Montana Bureau of Mines and Geology Information Pamphlet 5, <www.mbm.mtech.edu/pdf/ip_5.pdf>, accessed March 2007.

Wyoming Oil and Gas Conservation Commission (WOGCC), 2004-2007.

<<http://wogcc.state.wy.us/>>, accessed between 2004 and 2007.

Zoback, M. D., C. A. Barton, M. Brudy, D. A. Castillo, T. Finkbeiner, B. Grollmund, D. B. Moos, P. Peska, C. D. Ward and D. J. Wiprut, 2003. Determination of stress orientation and magnitude in deep wells: International Journal of Rock Mechanics and Mining Sciences, 40, 1049–1076.

Zoback, M. D., 2007. Reservoir geomechanics: Cambridge University Press.

CHAPTER 9: Coalbed Methane Produced Water Disposal by Injection

David A. Lopez¹
Leo A. Heath²

EXECUTIVE SUMMARY

Coal-bed methane (CBM) development in the Paleocene Fort Union Formation in the Powder River Basin is currently one of the most active gas plays in the United States.

Gas in coal beds is trapped by hydrodynamic pressure. Therefore gas production requires reduction in water pressure in order to release the gas held in the coal. The pressure reduction is achieved by the pumping of relatively large volumes of water from coal bed reservoirs.

CBM produced-water in Montana is of sufficiently good quality for domestic and livestock uses. But, it has high sodium adsorption ratio (SAR) values, making it unusable for irrigation for most of the soils in the area ($SAR = [Na / (Ca + Mg)]^{1/2}$). Consequently, disposal options must preserve beneficial use while not degrading surface waters that are used for irrigation.

Most of the CBM development is in coal beds in the Tongue River Member of the Fort Union Formation. The Fort Union Formation is divisible into three members: the Tullock, Lebo, and Tongue River, in ascending order.

The focus of this research was to identify specific potential injection targets. A complicating factor for disposal by injection is that potential shallow injection zones are water saturated. In addition, injectivity in these zones is not as great as well known deep injection zones, such as limestone beds in the Mississippian Madison Group. Channel sandstones are probably the best targets for injection because they have more favorable porosity and permeability and because injecting into coal beds may have conflicts with future CBM development. Six channel sandstone units were identified in the Tongue River Member, informally named 'A' through 'F' in ascending order. Clearly evident from isopach maps is that the channels are widely distributed and potential injection targets will not be available in every location where an injection well is desired. In other words, injection may not be technically feasible in all locations at any cost.

Because the uncertainty inherent in the mapping of channels, the design of an injection well was based on an existing well with excellent channel sandstone development instead of at a location based solely on channel isopach mapping. The well chosen is the International Nuclear Corporation, State MT Minerals #1, in Sec 28, T9S, R44E, Big Horn County, Montana, which encountered well-developed channel sandstones in the 'A', 'C', and 'D' intervals and has good resistivity and sonic logs.

¹ Montana Bureau of Mines and Geology, Montana Tech of The University of Montana, 1300 West Park Street, Butte, MT 59701. Correspondence: dlopez@mtech.edu.

² Department of Petroleum Engineering, PET 210, Montana Tech of The University of Montana, 1300 West Park Street, Butte, MT 59701. Correspondence: lheath@mtech.edu.

Coalbed methane well production in the Powder River Basin typically starts with significant water rates, in excess of 200 B/D, and low gas rates. Over time water rates decrease to smaller volumes, and gas rates increase to their maximum values. This requires the handling of variable water volumes, and supports the central gathering of water from multiple wells for combined disposal or treatment.

Data from four active water disposal wells completed in Wasatch and Ft. Union sand aquifers in the northern Powder River Basin show reasonable injection rates (200 – 4500 B/D) depending on formation sand thicknesses completed, and well pressures that do not exceed an estimated fracture gradient of 0.70 psi/ft. Disposal well histories over a period of 2 to 16 months indicate no change or increase in well pressures for injected volumes of 36,000 to 600,000 BW. These data correspond to an average effective formation permeability of 31.5 md, which does not require stimulation treatment to achieve reasonable injection rates. This experience confirms data and calculations from our analysis of the International Nuclear Corporation well.

Well completion designs for new drilled injection wells of approximately 2000 ft depth would reasonably assume injection down production casing. The casing would be cemented fully to surface and perforated with at least 4 holes per foot in target sands totaling 100 ft to 300 ft of net pay thickness.

The analysis here indicates that significant, but limited, volumes of water could be injected into zones identified in the Tongue River Member of the Ft. Union Formation. Because of the difficulties in locating well-developed channel sandstones and because the target zones are already at least partly water saturated, a combination of water disposal methods, including surface discharge, infiltration ponds, direct agricultural and domestic use, treatment, and injection, will probably yield the most feasible disposal plans and a balance between environmental and economic constraints.

In the Powder River Basin the quality of water associated with CBM development is sufficient for domestic and livestock use but, it has high SAR values making it unsuitable for irrigation. Therefore, disposal methods should preserve beneficial use and cannot include the discharge of large volumes of water into streams that are used for irrigation. Because of these restraints, water disposed by injection must be in zones shallow enough to be economically recovered. The main goal of this project was to identify potential zones for disposal in the Tongue River Member of the Fort Union Formation (above the Lebo Shale Member). Of particular interest are thick porous and permeable channel sandstone units. In addition, deeper coal beds in the Tongue River Member may also be targets for injection if they are not being developed for CBM. This study was not intended to find injection targets capable of handling the disposal of all the produced water, but to use injection in conjunction with other approved methods to develop an economically and environmentally feasible disposal system.

Mapping and correlation of channel sandstones in the Tongue River Member have defined stacked north- and northeast-trending paleo-river systems. Some of the channel sandstones are more than 100 feet thick and have porosities as high as 30%. These sandstone bodies should prove to be excellent zones for injection of CBM produced-water.

Engineering injectivity evaluation concludes that re-injection of significant volumes of water into channel sandstone is possible. Reasonable injection rates (200 – 4500 B/D) depending on formation sand thicknesses completed, and well pressures that do not exceed an estimated fracture gradient of 0.70 psi/ft can be expected. Available porosity and permeability data indicate that stimulation treatment will not be required to achieve reasonable injection rates.

INTRODUCTION

Goals

The main goal of the project was to test the feasibility of disposal of produced water in shallow zones to preserve beneficial use.

Objectives

1. Identify potential zones for disposal in the Tongue River Member of the Fort Union Formation (above the Lebo Shale Member). Of particular interest are thick porous and permeable channel sandstone units. Focus will be in the immediate area of CBM developments with high SAR produced water. In addition, deeper coal beds in the Tongue River Member may also be targets for injection if they are not being developed for CBM.
2. Identify areas where permeability may be naturally enhanced in regional fracture systems.
3. By petrophysical analysis determine the potential for zones identified to accept large volumes of injected water. Develop a well design for shallow injection wells.

Project Location

The project area is the Powder River Basin of southeastern Montana, encompassing parts of Yellowstone, Bighorn, Rosebud, Treasure, Powder River, and Custer Counties (**Figure 9.1**).

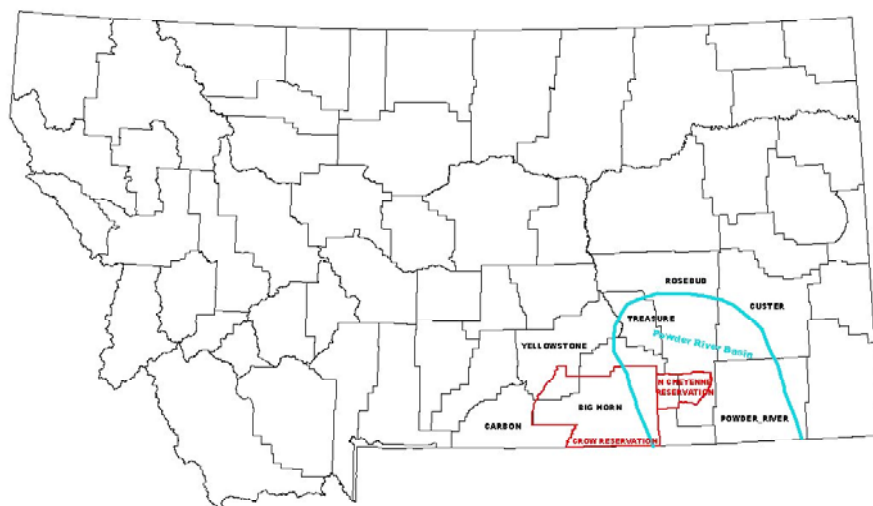


Figure 9.1: Index map showing project area, Powder River Basin of southeastern Montana.

Background

Coal-bed methane (CBM) development in the Powder River Basin is currently one of the most active gas plays in the United States. In 2002 monthly production reached about 26 BCF in the Wyoming portion of the basin. Coal bed gas reserves for the Wyoming portion of the basin are approximately 25 trillion cubic feet (TCF).

Although coal beds in the Powder River Basin extend well into Montana, the only CBM development in Montana to date is a single field, the CX Ranch, near the Wyoming border operated by Fidelity Exploration.

Gas in coal beds is trapped by hydrodynamic pressure. Therefore gas production requires reduction in water pressure in order to release the gas held in the coal. The pressure reduction is achieved by the pumping of relatively large volumes of water from coal bed reservoirs. Production of CBM by this method is reviewed more fully by Wheaton and Donato (2004).

Water Issues

Total Dissolved solids (TDS) values for CBM produced-water in Montana range from 900 to 2500 ppm. Dissolved solids are mainly Na and HCO₃. Water is, therefore, of sufficient quality for domestic and livestock uses. But, it has high sodium adsorption ratio (SAR) values, making it unusable for irrigation for most of the soils in the area ($SAR = [Na / (Ca + Mg)]^{1/2}$). Consequently, disposal options must preserve beneficial use while not degrading surface waters that are used for irrigation.

GEOLOGY OF THE MONTANA PORTION OF THE POWDER RIVER BASIN

Structural Geology

The Powder River Basin is a Laramide asymmetrical structural basin with the axis near the western margin. The Montana portion of the basin is bounded on the west by the Bighorn Mountains, on the east by the Black Hills uplift, and on the north by the Miles City Arch (**Figure 9.2**).

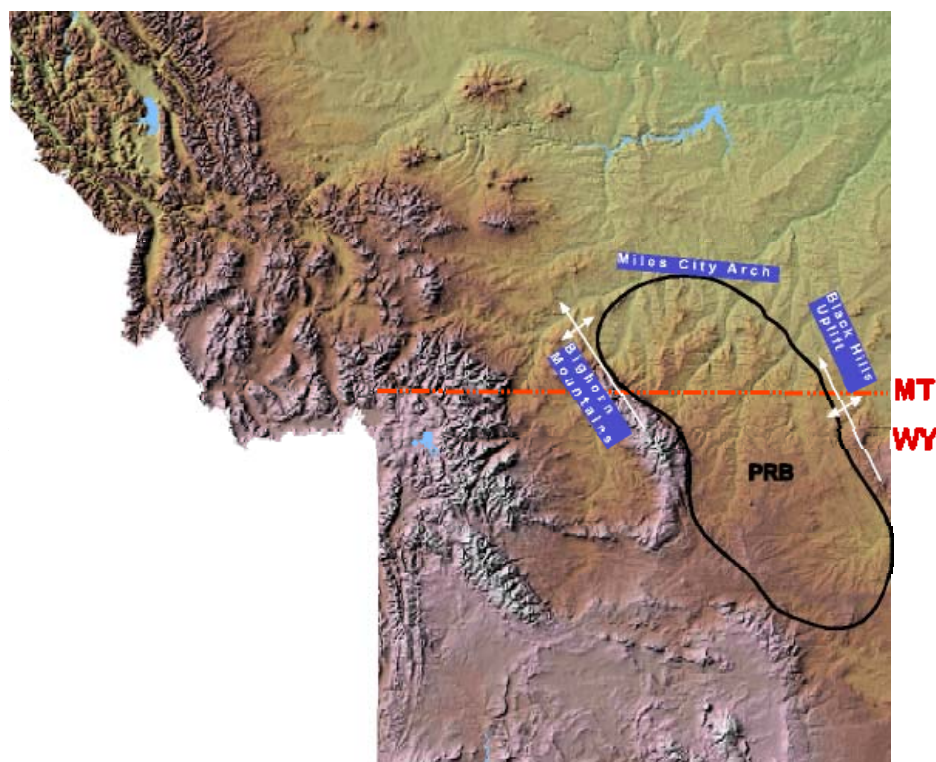


Figure 9.2: Structural Index map showing the location of the Powder River Basin and regional tectonic elements in southeastern Montana.

A structural contour map on the top of the Lebo Shale Member of the Fort Union Formation for the region illustrates that the structural axis of the Powder River Basin trends north-northeastward from the lowest point at the Wyoming border in Ranges 40 and 41 East (Lopez, 2005). The Basin is not a simple smooth syncline but has isolated structural closures and anticlinal ridges (Lopez, 2005) that are probably controlled by Laramide basement faults. These structures may have formed traps where natural gas from coal beds may have migrated into sandstone reservoirs.

A system of northeast-trending, en echelon, normal faults is present in Townships 1 and 2 South and Ranges 38-40 East. These faults are thought to be an extension of the Lake Basin Fault Zone of central Montana. Another system of northeast-trending, en echelon, normal faults is present at the south edge of the region, controlling the Ash Creek oil field and passing through the CX

Ranch CBM field. This fault system is probably the surface expression of a strike-slip basement fault zone that is the eastward extension of the Nye-Bowler Fault Zone.

Lineaments that may represent fracture systems are for the most part in two sets: one is parallel and sub-parallel to the faults mapped in the area; the other set is approximately orthogonal to this set.

Stratigraphy

The project area is underlain, in most part, by rocks of the Paleocene Fort Union Formation. Locally in the southern part of the area the overlying Wasatch Formation is present. The Fort Union Formation is divisible into three members: the Tullock, Lebo, and Tongue River (**Figure 9.3**). The Tullock Member is 130 to 1000 feet thick in the area, thickening to the south, toward the center of the basin. This member consists of interbedded mudstone and argillaceous sandstone and minor amounts of coal.

The Lebo Member is about 100 to 500 feet thick and is for the most part made up of mudstone and lesser amounts of sandstone and impure coal beds.

The Tongue River Member is about 500 to over 2000 feet thick, thickening to the south into the center of the basin. It is composed of inter-bedded mudstone, argillaceous sandstone, and coal. There are also several thick clean channel sandstone units within this member. Coal beds in the Tongue River Member in Montana are numerous and extensive and can reach as much as 80 feet in thickness (**Figure 9.3**). The coal deposits will not be described in detail, as they are not the focus of this report.

Depositional Settings of the Ft. Union Formation

During the Paleocene, the Fort Union Formation was deposited in continental environments dominated by fluvial systems, their associated floodplains, lakes, swamps, and wetlands; these fluvial systems were graded to, and flowed eastward and northeastward toward the Cannonball Sea in what is now North Dakota and South Dakota (Brown, 1958; Robinson, 1972; McDonald, 1972; Flores and Ethridge 1985; Cherven and Jacob, 1985; USGS Fort Union Coal Assessment Team, 1999). In the Powder River Basin region of Montana and Wyoming, deposition was partly controlled and affected by continued Laramide uplift of mountain ranges (USGS Fort Union Coal Assessment Team, 1999).

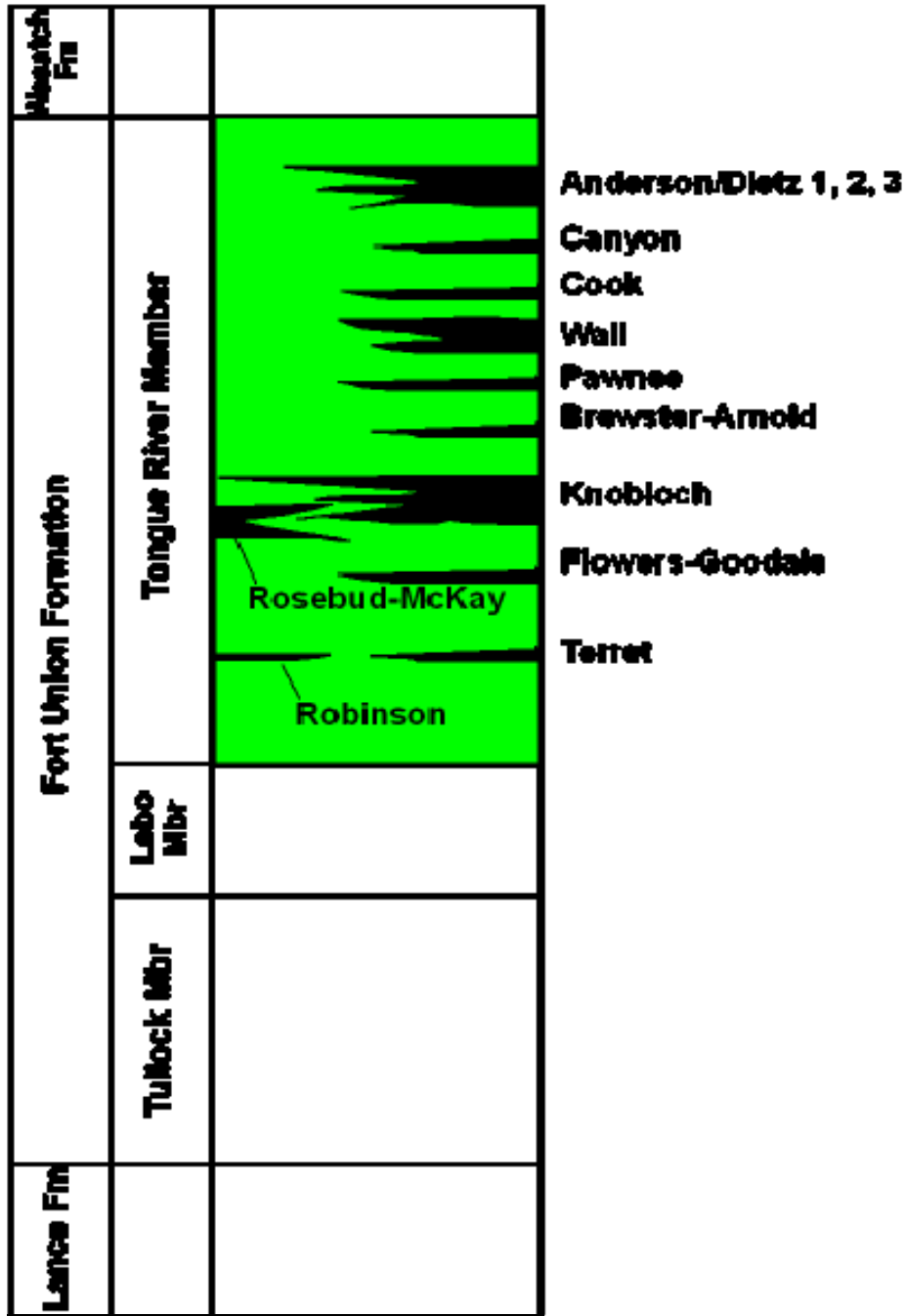


Figure 9.3: Generalized stratigraphic column Fort Union Formation in the Montana portion of the Powder River Basin, showing coal beds generally present. Not all coal beds are included and thicknesses are not to scale.

GEOLOGIC ASSESSMENT OF INJECTION TARGETS

Because CBM produced-water quality is sufficient for domestic and livestock uses, it should be injected in a zone that will preserve economic beneficial use. Therefore, potential zones for injection must be relatively shallow. Potential zones for injection include coal beds not being

developed for CBM and porous and permeable sandstone in the Fort Union Formation; other formations are too deep to preserve economically feasible beneficial use.

The focus of this research was to identify specific potential injection targets. A complicating factor for disposal by injection is that potential shallow injection zones are water saturated. In addition, injectivity in these zones is not as great as well known deep injection zones, such as limestone beds in the Madison Group. Therefore, a combination of water disposal methods, including surface discharge, infiltration ponds, direct agricultural and domestic use, treatment, and injection, will probably yield the most feasible disposal plans and a balance between environmental and economic constraints.

Water chemistry in injection target zones must be similar to that of the CBM produced water in order to prevent precipitation that could inhibit injection and to avoid ground water quality degradation. Based on available data and knowledge of the ground water flow systems in the Powder River Basin, it is assumed that because the ground water flow paths are similar, water quality in channel sandstones will be similar to that in nearby coal beds. Chemical and biochemical processes transform calcium-magnesium ground water near recharge areas to sodium-bicarbonate water in areas of CBM accumulations (Van Voast, 2003; Wheaton and Donato, 2004). Nance Petroleum Corporation, who operates several injection wells just south of the Montana-Wyoming border, has sampled ground water from Tongue River Member sandstones and found that the water is chemically similar to CBM produced water and is not of better quality so that degradation restrictions do not apply (Personal Communication, 2006; Dwayne Zimmerman; Nance Petroleum Corp).

As mentioned above the main potential targets for injection are coal beds and thick porous channel sandstone units. We have chosen to focus on channel sandstones because they have more favorable porosity and permeability for injection and because injecting into coal beds may have conflicts with future CBM development. Six channel sandstone units were identified in the Tongue River Member of the Ft. Union Formation. **Figure 9.4** illustrates the stratigraphic position of the sandstone units relative to the regional coal stratigraphy.

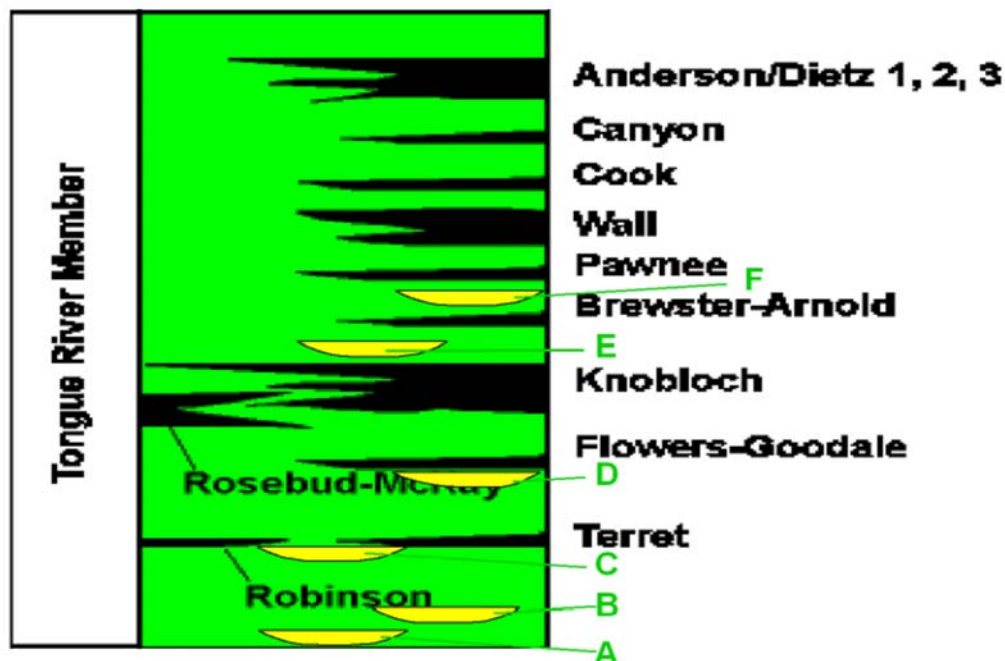


Figure 9.4: Approximate stratigraphic position of channel sandstones relative to major coal beds in the Tongue River Member of the Ft. Union Formation.

There are inherent difficulties and uncertainties with attempting regional mapping of channel sandstones in the Ft Union Formation due to data quality and availability. Because injected water must remain in the subsurface for a relatively long period of time, shallow zones are not feasible because they are likely to crop out and injected water would most likely produce springs. Therefore, abundant shallow drilling to evaluate strippable coal deposits is not useful and deeper oil and gas exploration drilling data must be relied upon.

Significant uncertainty in mapping of the channel sandstone units results because of available data for three reasons: 1) commonly, oil and gas well logs begin below surface casing, at depths of approximately 500 to 1000 feet; 2) oil and gas exploration well density is low (in many townships only a few wells have been drilled); and 3) correlating coal stratigraphy on logs from older wells is difficult and very uncertain because only e-logs are available.

In the project area, six channel sandstone units were mapped that form a stacked sequence of paleo-channels. The channel sandstones are informally named ‘A’-‘F’, from bottom to top; ‘A’ being the basal sandstone in the Tongue River Member. The thicknesses of some of the channel sandstone units are 100 feet or more. The typical log signature of a channel sandstone is shown in **Figure 9.5**. Channel sandstone isopach maps define the drainage patterns of these stacked channels. The coincidence of the traces of the channels reflect similar paleo-geography through time and suggests that there may have been paleo-structural control on their locations.

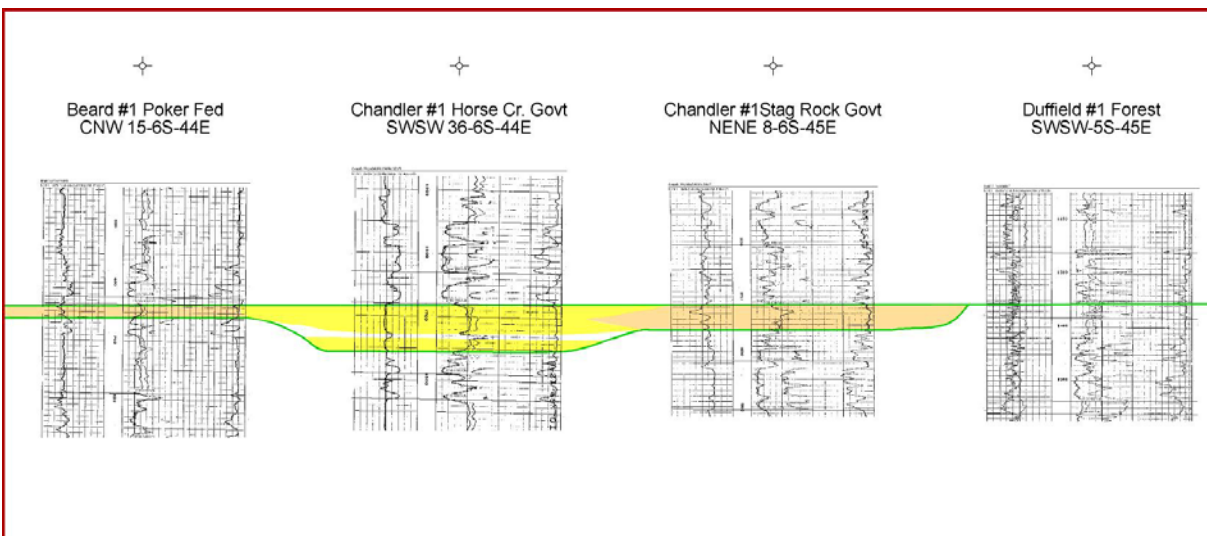


Figure 9.5: Typical log signature of Tongue River Member Channel Sandstone. “D” Sandstone shown in this example.

Clearly evident from isopach maps is that the channels are widely distributed and potential injection targets will not be available in every location where an injection well is desired. In other words, injection may not be technically feasible at all locations at any cost. For example, at the CX Ranch field, a channel sandstone unit could not be located and mapped in the subsurface using available oil and gas exploration well data. Transport of water over long distances will make injection uneconomical in most instances.

Density-Neutron and sonic log data indicate that porosity in the channel sandstones is as great as 30% and lab measurements of porosity from plugs of outcrop samples of the ‘D’ sandstone were 27% and 33% (Wo et al., 2004). Permeability measurements from those same outcrop samples were 286 and 1062 millidarcies (Wo et al., 2004). Fracturing will increase the permeability of these units and enhance their use for water injection. ASTER satellite imagery was used to predict the presence of fractures. A fracture map interpreted from imagery lineaments shows areas where the fracturing may be present and would potentially enhance the permeability of channel sandstone units.

Because of the uncertainty inherent in the mapping of channels as discussed above, the design of an injection well was based on an existing well with excellent channel sandstone development instead of at a location based solely on channel isopach maps. The intent is that an injection well could be developed successfully by twinning such a well. The well chosen is the International Nuclear Corporation, State MT Minerals #1, in Sec 28, T9S, R44E, Big Horn County, Montana. This well encountered well-developed channel sandstones in the ‘A’, ‘C’, and ‘D’ intervals and has good resistivity and sonic logs. Logs from this well illustrating the signature of two sandstone units are shown in **Figure 9.6**. Faults and lineaments mapped in the area suggest that fracturing may enhance the permeability of the sandstones in the vicinity of this well.

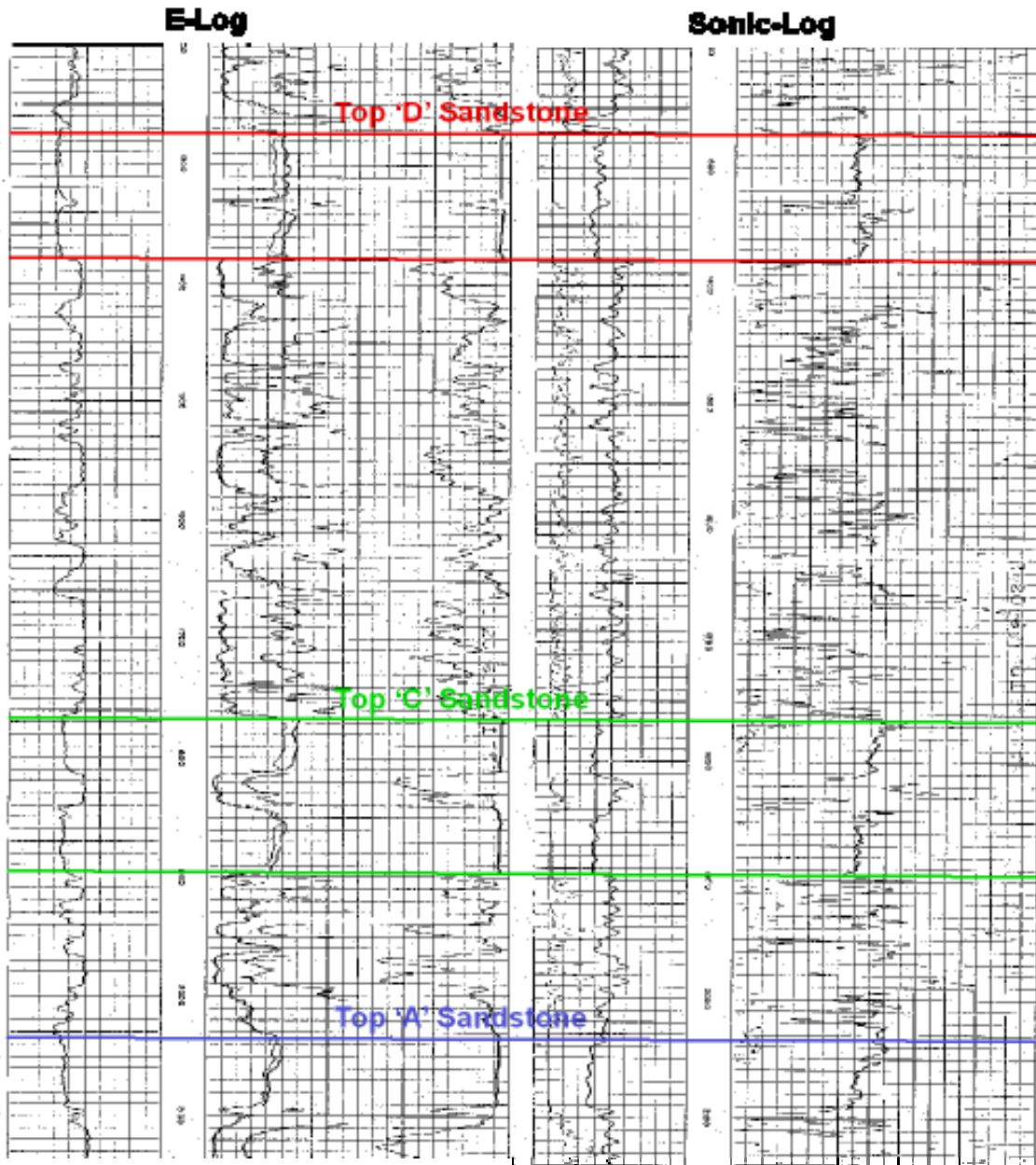


Figure 9.6: E-log and Sonic logs from the International Nuclear Corporation, State MT Minerals #1 well. Top and bottom of the 'D' and 'C' sandstone intervals are also indicated.

ENGINEERING DISCUSSION AND INJECTION DESIGN

Down-hole Water-Gas Separation

The production of natural gas from coalbed reservoirs requires the removal of water from the coal system (cleats and fractures) so as to reduce the system pressure and allow the gas to desorb from the coal. Initial CBM well production may be totally water until enough pressure reduction is gained to initiate gas flow. Usually the gas production continues to increase with time as water production decreases with time. Powder River basin CBM wells generally produce average initial water rates of 200 – 400 B/D per well, decreasing to small rates over a period of a few months to two years (US DOI and State of MT, 2002).

The continually decreasing rate of water production in typical CBM gas wells does not support the method of down-hole water-gas separation and re-injection in the same wellbore. The re-injection process will require some degree of pump-in pressure and therefore the installation of some type of mechanical pumping system. The pumping system must be sized to re-inject the initial water volumes, but at some point the pump will become over-sized. Inefficient use of over-sized pumps will lead to pump failures, or expensive changes to smaller pump sizes, both of which are economically unfeasible.

The down-hole water-gas separation systems currently available in the industry are relatively expensive (\$120,000-\$300,000), and still face several technical challenges (Ogunsina and Wiggins, 2005). For the given CBM water disposal volumes it is generally more cost effective to use individual well pumps to lift the decreasing water volumes from each well, and then re-inject a combined larger volume gathered from multiple wells into a dedicated water disposal well. Current operators are successfully utilizing the method of re-injecting combined CBM produced water streams into aquifers below the coal reservoirs in the Ft. Union sands of the Powder River basin (Dwayne Zimmerman; Nance Petroleum Corp; Personal Communication, 2006).

Water Injection Expected Performance

Rate and pressure performance

Injectivity of water disposal wells, that is the rate and pressure performance, is determined by a number of subsurface reservoir conditions. The pertinent conditions are: permeability, reservoir pressure, reservoir size (area, thickness, & porosity), fluid viscosity, wellbore skin damage, and wellbore pressure losses. These conditions are related to injection rate in the expression of Darcy's law for fluid flow in porous media.

Darcy’s law for steady-state, radial flow can be expressed as follows (Tiab and Donaldson, 2004):

$$q = \frac{0.00708kh(P_e - P_w)}{\mu \ln(r_e / r_w)}$$

- Where: q = flow rate, bbls/day
 k = permeability, md
 h = net pay thickness, ft
 P_e = reservoir boundary pressure, psia
 P_w = wellbore injection pressure, psia
 μ = fluid viscosity, cp (assume water = 1.0 cp)
 r_e = injection boundary radius, ft
 r_w = wellbore radius, ft

This equation form assumes:
 No gas dissolved in the water.
 No inherent skin damage or skin improvement.
 Reservoir flow rate at radial boundary equals well flow rate.

To determine the range of injection rates and pressures to be expected for given reservoirs, actual data from the subject reservoirs should be examined, and if necessary reasonable assumptions made for the parameters.

Expected Reservoir Conditions

A Montana producer currently operates several water injection wells in Sheridan County, Wyoming for disposal of CBM produced water. These wells are completed in various Ft. Union and Wasatch sands, identical to the potential disposal zones “A” through “F” identified the geologic assessment. Information from four disposal wells is given in the table below, and effective reservoir permeabilities are calculated (Dwayne Zimmerman; Nance Petroleum Corp; Personal Communication, 2006). Assumptions made in these calculations are the same as those described in later sections.

An average of the effective permeabilities from these wells is 31.5 md, which is the assumed value used in estimating area well injectivity.

	(1)	(2)	(3)	(4)
	Sec 29 T58N-R79W	Sec 14 T57N-R76W	Sec 21 T58N-R79W	Sec 21 T57N-76W
Compl. date	7/8/05	5/22/06	5/22/06	3/15/05
Cum Inj, bbls	63,520	36,168	201,326	610,890
q, B/D	200	600	1000	4500
h, ft	30	81	64	196
P _e -P _w , psia	194	550	530	975
k _{eff} , md	43	17	37	29

The identification of potential disposal zones in the project study area is characterized by a type well with available open-hole Induction Electric and Sonic porosity logs. The type well is the

International Nuclear Corporation, State MT Minerals #1 (**Figure 9.6**). Several potential disposal sands are evaluated from the type logs, and are assumed to be representative of the Ft. Union sands mapped for this project. A table of general log analysis by zone is shown below:

Zone	Depths	Net Thickness	Δt	$\phi_{s,s}$	GR	SP	R_{ILD}	V_{sh}	ϕ_{sc}
A	2034-94'	60'	96	.265	72	-20	20	.275	.192
C1	1745-1813'	48'	93	.245	80	-13	25	.36	.157
C2	1840-98'	58'	98	.280	80	-15	22	.36	.179
D1	1258-1328;	70'	100	.290	80	-16	22	.36	.186
D2	1335-80'	45'	97	.275	75	-17	23	.30	.193

Log analysis assumptions used:

Matrix sonic velocity = 19,500 ft/sec (sandstone)

Fluid sonic velocity = 5,300 ft/sec (fresh water mud)

Shale sonic travel time = 110 μ sec/ft

Sonic compaction correction factor = 1.15

Dual Water Model shaly sand analysis method

V_{sh} determined from GR readings

From this type log analysis, the total available net sand thickness is 281 ft. The weighted average sonic porosity, corrected for shaliness, is 18.2%. The total combined vertical porosity-foot volume is 51.14 ϕ -ft. Depending on the number of sands completed in a wellbore, the range of expected thickness is assumed to be from 100 ft. to 300 ft. throughout the study area.

Potential injection zones in the Ft. Union are reported to be slightly under-pressured at a gradient of 0.36 psi/ft (Dwayne Zimmerman; Nance Petroleum Corp; Personal Communication, 2006). This is a reservoir pressure of 720 psia at 2000 ft, and is assumed to be the average native reservoir pressure throughout the study area. Considering the wellbore hydrostatic pressure of water to be that of fresh water, a filled wellbore would exert a bottomhole pressure of 863 psia. Without additional wellhead pressure the static pressure differential (ΔP) in an injection well would be 143 psia. The application of wellhead pump pressure would directly increase the ΔP magnitude.

The reservoir area affected by injection is arbitrarily assumed to be one mile in diameter surrounding an injection well. This is a reasonable limit considering that the Ft. Union sands extend for long distances with little expected change in rock properties. For calculation purposes, the injected area radius is therefore determined to be $r_e = 2640$ ft. Also, a typical injection wellbore radius is assumed to be $r_w = 0.5$ ft.

Rate and Pressure Performance Correlations

Substituting the assumed values for viscosity, injection radius and wellbore radius into the Darcy formula gives the following expression:

$$q = 0.0008(kh)(\Delta P)$$

With this formula the injection rate can be estimated based on a given reservoir thickness and desired wellhead pressure, using the expected $k_{eff} = 31.5$ md. **Figure 9.7** is a plot of injection rate versus pay thickness for wellhead pressures of 100 psia, 350 psia, and 800 psia. Also plotted are the four points of current actual injection performance from the previously referenced Sheridan County, Wyoming wells.

These estimates assume negligible pressure losses in the wellbore and perforations. The actual well data are from wells injecting down 7” diameter casing and with four perforation shots per foot of net sand pay. For tubing injection or very high rates, additional frictional pressure losses must be accounted for.

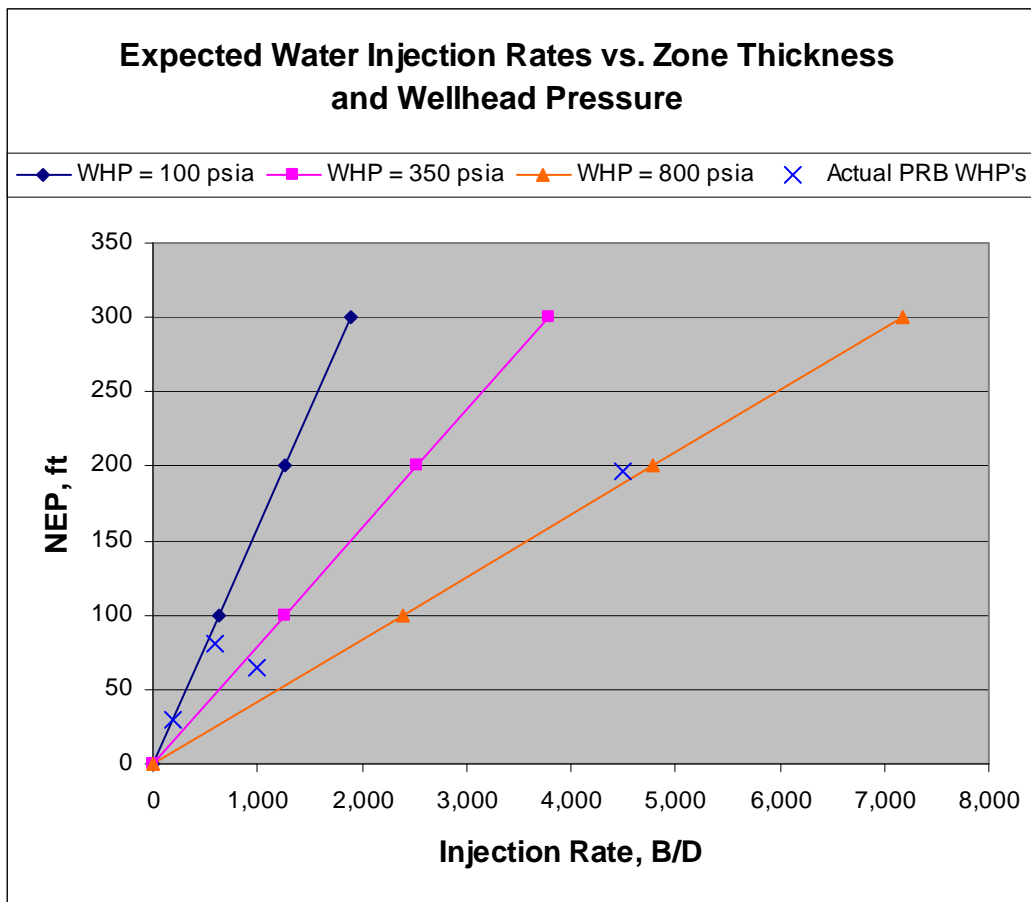


Figure 9.7: Expected Water Injection Rates vs. Zone Thickness and Wellhead Pressure

General conclusions can be drawn from this correlation as follows:

Expected Injectivity of Water Into Ft. Union Disposal Zones in PRB	
Wellhead Pressure = 100 psia	6.3 B/D per foot of NEP
Wellhead Pressure = 350 psia	12.6 B/D per foot of NEP
Wellhead Pressure = 800 psia	23.9 B/D per foot of NEP

Water Volume Expected Performance

The expected volume of water that is capable of being disposed into the Ft. Union sands is not adequately known. The four referenced disposal wells have been active since early 2005 for periods from 2 to 16 months, and have injected water volumes from 36,000 bbls to over 600,000 bbls. The wellhead rates and pressures are reported to have not changed appreciably since injection began, indicating that formation water is moving outward from the wellbores. (Dwayne Zimmerman; Nance Petroleum Corp; Personal Communication, 2006). The Ft. Union sands are water saturated and injection of more water displaces the native water away from the injection point. Eventually the displacement wave will reach a structural or stratigraphic barrier, or the radial distance will become great enough to cause an appreciable pressure drop due to the long tortuous flow path. Water is relatively incompressible and when the system becomes full, the pressure will increase significantly with added injection. A pressure limit is reached when the bottom-hole injection pressure reaches the fracture gradient. The Ft. Union fracture gradient is estimated to be about 0.70 psi/ft. This would equate to a wellhead pressure of about 1,250 psia at a depth of 2000 ft. A fluid-filled volume limit will eventually be reached in all such disposal wells, but current actual results show water is steadily moving away from the injection points.

INJECTION SYSTEM DESIGN

Wellbore Design

The design assumption is that all available Ft. Union sand intervals will be completed in a disposal wellbore, to a total depth of 2000 ft. If new casing is installed and properly cemented to surface, the casing can be used as the injection conduit directly to the disposal zones. The use of 4 ½" nominal casing size will accommodate a flow rate of over 10,000 B/D within an accepted friction limit of 40 psi/1000' of pressure loss. Larger casing, such as 5 ½" or 7" diameters, will have capacity for even higher injection rates and lower friction pressures. If existing wellbores are used for disposal it may be advisable to protect the casing from undue pressure or corrosion, and install tubing and a packer for water injection. Both designs will be considered with examples.

For a new well example, 7"OD, 23#/ft, K-55, STC oil well casing is a common pipe to run for large flow capacity and adequate strength factors. The casing should be cemented completely from TD to surface, typically inside a 8 ¾" drilled hole, and centralized across the disposal zones from 2000' to 1500'. The 7" casing would be installed inside a section of surface casing, such as 9 5/8"OD, 36#/ft, K-55, STC oil well casing set below the surface gravels and aquifers at approximately 350' depth and also cemented back to the surface. **Appendix 9.A** contains a

schematic of a typical 7” casing wellbore design. **Appendix 9.B** includes typical cementing designs for the 9 5/8” surface casing and the 7” casing installations. A cement bond log should be run inside the 7” casing to verify the cement integrity for isolating the various disposal zones. Completion of the well would be performed with wireline conveyed jet perforations, at 4 shots per foot density, and 90° shot phasing. A large entrance hole diameter should be used, greater than 0.4”, with medium shot penetration distance, greater than 12” API test length. Well stimulation should not be required unless skin damage was developed during drilling and cementing. A water pump-in rate test will verify the injectivity, and if necessary breakdown of the perforations could be performed with ball sealers or diverting material. Water disposal could take place directly into the casing with gauges to monitor pressure and flow rate. Regulatory UIC injection permits will require periodic pressure integrity tests of the 7” casing every five years, at which times a retrievable bridge plug could be run on wireline to easily perform the test.

For an existing well with old casing, or a need to protect the casing from injected fluid, tubing can be run with a packer set above the desired injection zones. Common oil well tubing sizes are 2 3/8” OD, 2 7/8” OD, and 3 1/2” OD, with designs based on the casing size and desired injection rates. The friction pressure loss from water flow down tubing should not exceed 40 psi/1000’. Maximum flow rates at this criteria limit are as follows (Brown and Coberly, 1960):

Tubing Size	Maximum Flow Rate
2 3/8”OD, 4.7#/ft, J-55, EUE	2,300 B/D
2 7/8”OD, 6.5#/ft, J-55, EUE	3,900 B/D
3 1/2”OD, 9.3#/ft, J-55, EUE	6,500 B/D

At the shallow depth of 2000 ft a tension set packer is advisable (Baker “AD-1” or “J-Lok” types). The injection pressures below the packer will help to insure a positive seat, and tubing stretch changes due to pressure differentials or injecting of cold water will act to increase the tension on the packer. UIC integrity tests can be performed easily by pressuring the tubing-casing annulus.

Injection Water Handling Design

The primary concerns for handling CBM water for re-injection are to remove all fine solid particles and prevent the entry of oxygen into the water. Fine solids can be carried from the coalbeds and producing wellbores in the water stream. These solids can cause injection pump wear and plugging of the down-hole disposal perforations. Solids removal is usually effective with ample settling time in a quiet tank (**Figure 9.8**) (Rose et al., 2001). In cases where adequate settling time is not practical the use of cartridge or bag type filters may be considered (**Figure 9.10**) (Rose et al., 2001).

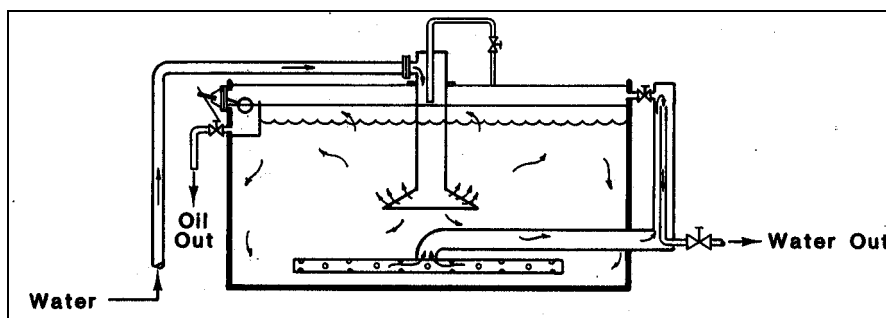


Figure 9.8: Skimmer and Sedimentation Tank

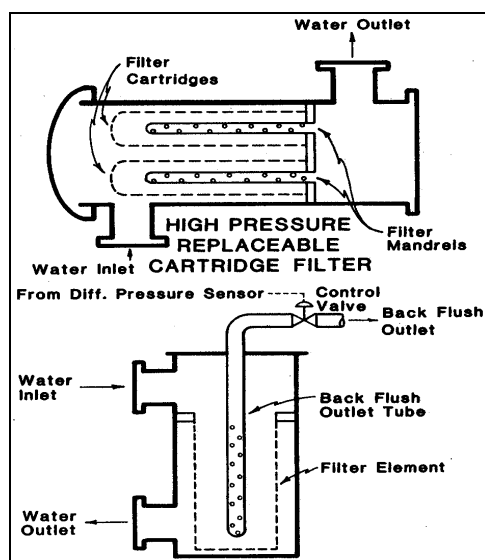


Figure 9.9: Cartridge Type Filters

The entry of air (oxygen) into the disposal water can have serious effects from oxygen-iron corrosion (rusting and rust particles) and increased bacterial action. The preferred treatment is to prevent oxygen entry by keeping the entire water system at a positive pressure to atmosphere. This requires monitoring to prevent system leaks, not allowing open production well casings, and providing positive gas blankets on all water tanks. A typical gas blanket design is shown in **Figure 9.10** (Rose et al., 2001).

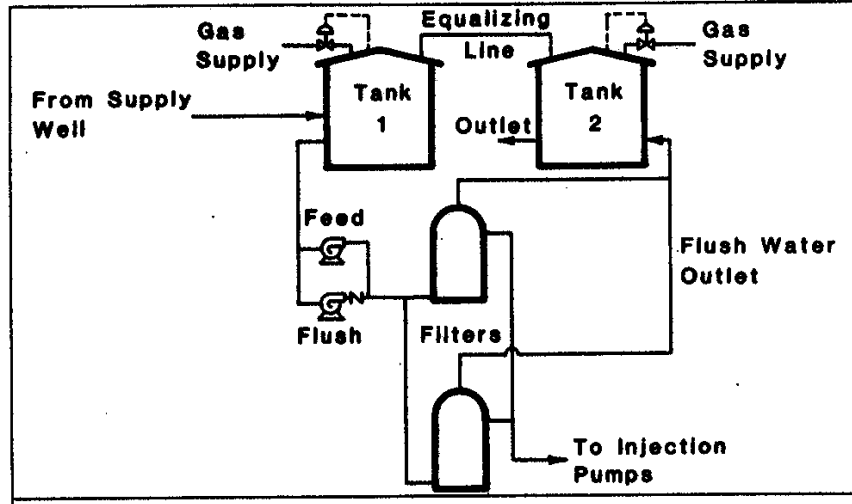


Figure 9.10: Gas Blanket Design Example

Injection Pump Design

Various types and sizes of pumps are used for injection systems, depending on the required rates and pressures, the available power sources, initial purchase and maintenance costs, and the familiarity of field personnel with pump operations. For higher pressure systems a positive displacement type pump, such as a plunger pump, is a common choice. For lower pressure systems a centrifugal type pump is often used. A currently popular type pump for use in the lower pressure ranges, such as expected in CBM water disposal, is an Electric Submersible Pump (ESP), installed either horizontally or vertically. ESP's are also frequently used to lift water from CBM wells and are already operated and maintained in the adjacent field areas.

All pumps, both PD and centrifugal, require an adequate fluid pressure at the suction inlet, to prevent cavitation and mechanical damage. Pump manufacturers will provide information for the minimum required suction pressure, known as Net Positive Suction Head (NPSH). The required NPSH is a function of piping diameter and length, fluid properties, pump type, and water level height above the pump suction (Figure 9.11) (Rose et al., 2001).

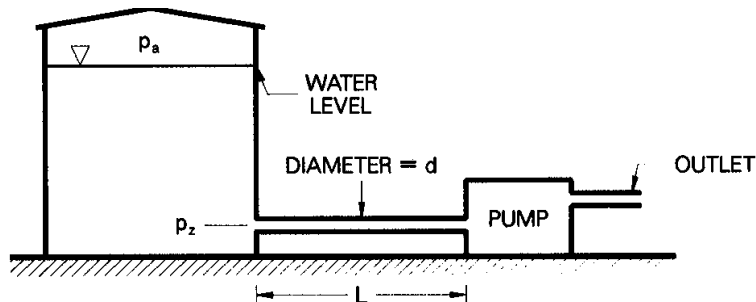


Figure 9.11: Typical Water Pumping System

SUMMARY AND CONCLUSIONS

Coal-bed methane (CBM) development in the Paleocene Fort Union Formation in the Powder River Basin is currently one of the most active gas plays in the United States.

Gas in coal beds is trapped by hydrodynamic pressure. Therefore gas production requires reduction in water pressure in order to release the gas held in the coal. The pressure reduction is achieved by the pumping of relatively large volumes of water from coal bed reservoirs.

CBM produced-water in Montana is of sufficiently good quality for domestic and livestock uses. But, it has high sodium adsorption ratio (SAR) values, making it unusable for irrigation for most of the soils in the area ($SAR = [Na/(Ca+Mg)]^{1/2}$). Consequently, disposal options must preserve beneficial use while not degrading surface waters that are used for irrigation.

Most of the CBM development is in coal beds in the Tongue River Member of the Fort Union Formation. The Fort Union Formation is divisible into three members: the Tullock, Lebo, and Tongue River, in ascending order.

The focus of this research was to identify specific potential injection targets. A complicating factor for disposal by injection is that potential shallow injection zones are water saturated. In addition, injectivity in these zones is not as great as well known deep injection zones, such as limestone beds in the Madison Group. Therefore, a combination of water disposal methods, including surface discharge, infiltration ponds, direct agricultural and domestic use, treatment, and injection, will probably yield the most feasible disposal plans and a balance between environmental and economic constraints. Channel sandstones are probably the best targets for injection because they have more favorable porosity and permeability and because injecting into coal beds may result in conflicts with future CBM development. Six channel sandstone units were identified in the Tongue River Member of the Ft. Union Formation, informally named 'A' through 'F' in ascending order. The paleo-drainage pattern for each of these six channel systems are very similar, which may be due to similar paleogeography through time, but also suggests that there was paleo-structural control on the channel systems. Clearly evident from isopach maps is that the channels are widely distributed and potential injection targets will not be available in every location where an injection well is desired. In other words, injection is not technically feasible in all locations at any cost.

Because the uncertainty inherent in the mapping of channels, the design of an injection well was based on an existing well with excellent channel sandstone development instead of at a location based solely on channel isopach mapping. The well chosen is the International Nuclear Corporation, State MT Minerals #1, in Sec 28, T9S, R44E, Big Horn County, Montana, which encountered well-developed channel sandstones in the 'A', 'C', and 'D' intervals and has good resistivity and sonic logs.

Coalbed methane well production in the Powder River Basin typically starts with significant water rates, in excess of 200 B/D, and low gas rates. Over a period of two years the water rates decrease to small volumes, and gas rates increase to their maximum values as water is removed from the coal system allowing gas to desorb in the decreasing pressure environment. This typical

well performance requires the handling of variable water volumes, and supports the central gathering of water from multiple wells for combined disposal or treatment.

Considering subsurface re-injection of the produced water as the disposal method, formations are present at depths below the coalbeds for re-injection of significant volumes of water. Data from four studied active water disposal wells completed in Wasatch and Ft. Union sand aquifers show reasonable injection rates (200 – 4500 B/D) depending on formation sand thicknesses completed, and well pressures that do not exceed an estimated fracture gradient of 0.70 psi/ft. Disposal well histories over a period of 2 – 16 months indicate no change or increase in well pressures for injected volumes of 36,000 – 600,000 BW. These data correspond to an average effective formation permeability of 31.5 md, which does not require stimulation treatment to achieve reasonable injection rates.

Well completion designs for new drilled injection wells of +/-2000 ft depth would reasonably assume injection down production casing. The casing would be cemented fully to surface and perforated with at least 4 holes per foot in water sands totaling from 100 ft to 300 ft in net pay thickness. Existing recompleted disposal wells would consider installation of tubing and packers to protect the casing, but rate friction losses would decrease the well injection capacity. Surface treating of the collected produced water would consist of oxygen (air) elimination, and removal of fines and solids through gravity tank settling or filtering prior to pressurizing for well disposal.

RECOMMENDATIONS FOR FUTURE RESEARCH

The obvious next step is to conduct a pilot study with industry cooperation. In a geologically favorable area construct an injection well using the results and conclusions for this study to enhance injection capabilities.

REFERENCES

- Brown, F. B., and Coberly, C. J., 1960.** Friction losses in vertical tubing as related to hydraulic pumps: Society of Petroleum Engineers Paper 1555-G, Annual Meeting Proceedings.
- Brown, R. W., 1958.** Fort Union Formation in the Powder River Basin, Wyoming: Wyoming Geological Association 13th Annual Field Conference Guidebook, p. 111-113.
- Cherven, V. B., and Jacob, A. F., 1985.** Evolution of Paleogene depositional systems, Williston Basin, in response to global sea level changes: in Flores, R. M., and Kaplan, S. S. (eds.), Cenozoic Paleogeography of west-central United States: Rocky Mountain Section of SEPM Symposium volume 3, p. 127-170.
- Flores, R. M., and Ethridge, F. G., 1985.** Evolution of intermontane fluvial systems of Tertiary Powder River Basin, Montana and Wyoming: *in* Flores, R. M., and Kaplan, S. S. (eds.), Cenozoic Paleogeography of west-central United States: Rocky Mountain Section of SEPM Symposium volume 3, p. 107-126.

- McDonald, R. E., 1972.** Eocene and Paleocene rocks of the southern and central Basins, *in* Rocky Mountain Association of Geologists, 1972, Geologic Atlas of the Rocky Mountain Region, p. 243-256.
- Ogunsina, O. O., and Wiggins, M. L., 2005.** Review of Down-hole Separation Technology: SPE Technical Paper No. 94276.
- Robinson, Peter, 1972.** Tertiary History, in Rocky Mountain Association of Geologists, 1972, Geologic Atlas of the Rocky Mountain Region, p. 233-242.
- Rose, S. C., Buckwalter, J. F., and Woodhall, R. J., 2001.** The Design Engineering Aspects of Water flooding: Society of Petroleum Engineers, Monograph 11, p. 11-23.
- Tiab, D., and Donaldson, E. C., 2004. Radial Flow Systems, Petrophysics: Reservoir Rock Properties, Gulf Publishing Company, p. 434-447.**
- U.S. Dept. of the Interior and State of Montana, 2002.** Final Statewide Oil and Gas Environmental Impact Statement and Proposed Amendment of the Powder River and Billings Resource Management Plans:
- U.S.G.S. Fort Union Coal Assessment Team, 1999.** 1999 Resource Assessment of selected Tertiary coal beds and zones in the northern Rocky Mountains and Great Plains region: U.S.G.S. Professional Paper 1625-D, compact discs 1 & 2.
- Van Voast, W. A., 2003.** Geochemical signature of formation waters associated with coalbed methane: American Association of Petroleum Geologists Bulletin, vol. 87, no. 4, p. 667-676.
- Vuke, S. M., Heffern, E. L., Bergantino, R. N., and Colton, R. B., 2001.** Geologic map of the Lame Deer 30' X 60' Quadrangle, eastern Montana: Montana Bureau of Mines and Geology Open-File Report MBMG-428, scale 1:100,000.
- Vuke, S. M., Heffern, E. L., Bergantino, R. N., and Colton, R. B., 2001.** Geologic map of the Powderville 30' X 60' Quadrangle, eastern Montana: Montana Bureau of Mines and Geology Open-File Report MBMG-429, scale 1:100,000.
- Vuke, S. M., Heffern, E. L., Bergantino, R. N., and Colton, R. B., 2001.** Geologic map of the Birney 30' X 60' Quadrangle, eastern Montana: Montana Bureau of Mines and Geology Open-File Report MBMG-431, scale 1:100,000.
- Vuke, S. M., Heffern, E. L., Bergantino, R. N., and Colton, R. B., 2001.** Geologic map of the Broadus 30' X 60' Quadrangle, eastern Montana: Montana Bureau of Mines and Geology Open-File Report MBMG-432, scale 1:100,000.
- Wheaton, John, and Donato, Teresa, 2004.** Coalbed-methane basics: Powder River Basin, Montana: Montana Bureau of Mines and Geology, Information Pamphlet 5, 20 p.

Wo, Shaochang, Lopez, D. A., and Whiteman, Jason, Sr., 2004. Northern Cheyenne Reservation coal bed natural resource assessment and analysis of produced water disposal options: Idaho National Engineering and Environmental Laboratory final report for DOE Contract DE-AC07-99ID13727, 46p.

Appendix 9.A



Appendix 9.B – Technical Discussion

CEMENTING BEST PRACTICES

SOURCE: Halliburton Energy Services, Evansville, WY, July 2006.

1. Cement quality and weight: You must choose a cement slurry that is designed to solve the problems specific to each casing string.
2. Waiting time: You must hold the cement slurry in place and under pressure until it reaches its' initial set without disturbing it. A cement slurry is a time-dependent liquid and must be allowed to undergo a hydration reaction to produce a competent cement sheath. A fresh cement slurry can be worked (thickening or pump time) as long as it is in a plastic state and before going through it's' transition phase. If the cement slurry is not allowed to transition without being disturbed, it may be subjected to changes in density, dilution, settling, water separation, and gas cutting that may lead to a lack of zonal isolation and possible bridging in the annulus.
3. Pipe movement: Pipe movement may be one of the single most influential factors in mud removal. Reciprocation and/or rotation mechanically breaks up gelled mud and changes the flow patterns in the annulus to improve displacement efficiency.
4. Mud properties (for cementing):
 - a. Rheology:
 - i. Plastic Viscosity (PV) < 15 centipoise (cp)
 - ii. Yield Point (YP) < 10 lb/100 ft²
 - iii. These properties should be reviewed with the Mud Engineer, Drilling Engineer, and Company Representative(s) to ensure no hole problems are created.
 - b. Gel Strength:
 - i. The 10-second/10-minute gel strength values should be such that the 10-second and 10-minute readings are close together or flat (i.e., 5/6).
 - ii. The 30-minute reading should be less than 20 lb/100 ft².
 - iii. Sufficient shear stress may not be achieved on a primary cement job to remove mud left in the hole if the mud were to develop more than 25 lb/100 ft² of gel strength.
 - c. Fluid Loss:
 - i. Decreasing the filtrate loss into a permeable zone enhances the creation of a thin, competent filter cake.
 - ii. A thin, competent filter cake created by a low fluid loss mud system is desirable over a thick, partially gelled filter cake.
 - iii. A mud system created with a low fluid loss will be more easily displaced. The fluid loss value should be < 15 cc's (ideal would be 5 cc's).
5. Circulation: Prior to cementing circulate full hole volume twice, or until well conditioned mud is being returned to the surface. There should be no cutting in the mud returns. An annular velocity of 260 feet per minute is optimum (SPE/IADC 18617), if possible.
6. Flow rate: Turbulent flow is the most desirable flow regime for mud removal. If turbulence cannot be achieved pump at as high a flow rate that can practically and safely be used to

create the maximum flow energy. The highest mud removal is achieved when the maximum flow energy is obtained.

7. Pipe Centralization: Cement will take the path of least resistance; therefore, proper centralization is important to help prevent the casing from contacting the borehole wall. A minimum standoff of 70% should be targeted for optimum displacement efficiency.
8. Rat hole: A weighted viscous pill placed in the rat hole prior to cementing will minimize the risk of higher density cement mixing with lower density mud when the well is static.
9. Top and Bottom plugs: A top and bottom plug are recommended to be run on all primary casing jobs. The bottom plug should be run after the spacer and ahead of the first cement slurry.
10. Spacers and flushes: Spacers and/or flushes should be used to prevent contamination between the cement slurry and the drilling fluid. They are also used to clean the wellbore and aid with bonding. To determine the volume, either a minimum of 10 minutes contact time or 1000 ft. of annular fill, whichever is greater, is recommended.

Calculations 9 5/8" Surface Casing Cement

Spacer:

Total Spacer	= 112.29 ft ³
	= 20.00 bbl

Cement : (350.00 ft fill)

350.00 ft * 0.3132 ft ³ /ft * 100 %	= 219.23 ft ³
Primary Cement	= 219.23 ft ³
	= 39.05 bbl

Shoe Joint Volume: (40.00 ft fill)

40.00 ft * 0.4419 ft ³ /f	= 17.68 ft ³
	= 3.15 bbl
Tail plus shoe joint	= 236.91 ft ³
	= 42.19 bbl
Total Tail	= 132 sks

Total Pipe Capacity:

350.00 ft * 0.4419 ft ³ /ft	= 154.66 ft ³
	= 27.55 bbl

Displacement Volume to Shoe Joint:

Capacity of Pipe - Shoe Joint	= 27.55 bbl - 3.15 bbl
	= 24.40 bbl

Job Recommendation 9 5/8" Surface Casing Cement

Fluid Instructions

Fluid 1: Water Based Spacer

Water Spacer		Fluid Density:	8.34 lbm/gal
42 gal/bbl	Fresh Water (Base Fluid)	Fluid Volume:	20 bbl

Fluid 2: Rockies LT

Rockies LT		Fluid Weight	13.50 lbm/gal
0.125 lbm/sk Poly-E-Flake (Additive Material)		Slurry Yield:	1.80 ft ³ /sk
0.25 lbm/sk Kwik Seal (Additive Material)		Total Mixing Fluid:	9.33 Gal/sk
		Top of Fluid:	0 ft
		Calculated Fill:	350 ft
		Volume:	42.19 bbl
		Calculated Sacks:	131.61 sks
		Proposed Sacks:	140 sks

Fluid 3: Water Based Spacer

Displacement		Fluid Density:	8.34 lbm/gal
		Fluid Volume:	24.40 bbl

Job Procedure **9 5/8" Surface Casing Cement**

Detailed Pumping Schedule

Fluid #	Fluid Type	Fluid Name	Surface Density lbm/gal	Estimated Avg Rate bbl/min	Downhole Volume
1	Spacer	Spacer	8.3	3.0	20 bbl
2	Cement	Primary Cement	13.5	3.0	140 sks
3	Spacer	Displacement Fluid	8.3	3.0	24.40 bbl

Job Information 7" Production Casing Cement

7" Production Casing	0 - 2000 ft (MD)
Outer Diameter	7.000 in
Inner Diameter	6.366 in
Linear Weight	23 lbm/ft
8 3/4" Open Hole Section	350 - 2000 ft (MD)
Inner Diameter	8.750 in
Job Excess	100 %
9 5/8" Surface Casing	0 - 350 ft (MD)
Outer Diameter	9.625 in
Inner Diameter	9.001 in
Linear Weight	32.30 lbm

Calculations 7" Production Casing Cement

Spacer:

Total Spacer	= 112.29 ft ³
	= 20.00 bbl

Cement: (1500.00 ft fill)

350.00 ft * 0.1746 ft ³ /ft * 0 %	= 61.12 ft ³
1150.00 ft * 0.1503 ft ³ /ft * 100 %	= 345.76 ft ³
Total Lead Cement	= 406.88 ft ³
	= 72.47 bbl
Sacks of Cement	= 153 sks

Cement: (500.00 ft fill)

500.00 ft * 0.1503 ft ³ /ft * 100 %	= 150.33 ft ³
Tail Cement	= 150.33 ft ³
	= 26.77 bbl

Shoe Joint Volume: (40.00 ft fill)

40.00 ft * 0.221 ft ³ /ft	= 8.84 ft ³
	= 1.57 bbl
Tail plus shoe joint	= 159.17 ft ³
	= 28.35 bbl
Total Tail	= 85 sks

Total Pipe Capacity:

2000.00 ft * 0.221 ft ³ /ft	= 442.07 ft ³
	= 78.74 bbl

Displacement Volume to Shoe Joint:

Capacity of Pipe - Shoe Joint	= 78.74 bbl - 1.57 bbl
	= 77.16 bbl

Job Recommendation 7" Production Casing Cement

Fluid Instructions

Fluid 1: Water Based Spacer

Water Spacer		Fluid Density:	8.34 lbm/gal
42 gal/bbl	Fresh Water (Base Fluid)	Fluid Volume:	20 bbl

Fluid 2: RMCBM 3
Standard Cement

Fluid Weight	12 lbm/gal
Slurry Yield:	2.65 ft ³ /sk
Total Mixing Fluid:	15.58 Gal/sk
Top of Fluid:	0 ft
Calculated Fill:	1500 ft
Volume:	72.47 bbl
Calculated Sacks:	153.42 sks
Proposed Sacks:	160 sks

Fluid 3: RMCBM 3
Standard Cement

Fluid Weight	13.50 lbm/gal
Slurry Yield:	1.88 ft ³ /sk
Total Mixing Fluid:	9.82 Gal/sk
Top of Fluid:	1500 ft
Calculated Fill:	500 ft
Volume:	28.35 bbl
Calculated Sacks:	84.53 sks
Proposed Sacks:	90 sks

Fluid 4: Water Based Spacer
Displacement

Fluid Density:	8.34 lbm/gal
Fluid Volume:	77.16 bbl

Job Procedure 7" Production Casing Cement

Detailed Pumping Schedule

Fluid #	Fluid Type	Fluid Name	Surface Density lbm/gal	Estimated Avg Rate bbl/min	Downhole Volume
1	Spacer	Spacer	8.3	3.0	20 bbl
2	Cement	Lead Cement	12.0	3.0	160 sks
3	Cement	Tail Cement	13.5	3.0	90 sks
4	Spacer	Displacement Fluid	8.3	3.0	77.16 bbl

TOPIC AREA: WATER TREATMENT

CHAPTER 10:
Electrodialysis Process Development for the Demineralization of
Coalbed Methane Produced Water

Thomas Hayes¹
Paula Moon²

EXECUTIVE SUMMARY

The production of natural gas from dewatered coal is associated with large volumes of co-produced water that often exceeds brine generation rates observed with conventional natural gas wells. Technical problems of the management of CBM produced water include: 1) Lack of Class II injection well capacities (especially in basins of the Rocky Mountains); 2) Extreme hardness of the water (i.e. saturated with calcium and magnesium) and high carbonates that foul conventional membrane separation processes (such as reverse osmosis); and, 3) Generation of produced waters at remote and dispersed fields in CBM basins. Since much of this water is generated in arid areas, serious consideration is being given to the conditioning of CBM produced water for beneficial uses (e.g. irrigation, recharge of aquifers, etc.).

The objective of the effort in Task 2 of the Project was to develop a simplified, modular, electro dialysis-based, processing train for the conversion of coalbed methane produced water into a water stream suitable for beneficial use. This chapter describes Phase I of the effort: "Evaluation of a Laboratory Prototype." The general approach for Phase 1 involved the following steps: 1) Identify energy industry partners to provide access to active CBM production fields; 2) Characterize produced water samples taken from CBM fields in the Powder River Basin; 3) Determine treatment goals to achieve beneficial use criteria for water suitable for agricultural applications; 4) Design and construct a treatment train that will meet treatment goals and provide reliable operation; 5) Conduct testing on the electro dialysis process train addressing key issues related to performance and reliability to achieve the treatment goals. Energy industry partners (Marathon Oil and Anadarko) allowed access to selected CBM sites in the Powder River Basin and provided numerous water samples and water aliquots during the project. Based on the analysis of more than ten produced water samples taken from four locations in the Powder River Basin (PRB) of Wyoming, it was determined that PRB CBM produced water does not typically exhibit the problems of significant concentrations of oils and greases and high levels of soluble organic compounds (e.g. volatile acids). Based on the analysis of more than ten produced water samples taken from four regions in the Powder River Basin (PRB) of Wyoming, the following goals were established for achieving a quality of water suitable for agricultural beneficial use: 1) Product Water Recovery Efficiency > 90%; 2) Brine Volume Reduction > 90%; 3) Sodium Absorption Ratio (SAR) < 6; and, 4) Total Dissolved Solids levels reduced to the range of 1,000 to 2,000 mg/l (Conductivity < 1,500 μ S/cm).

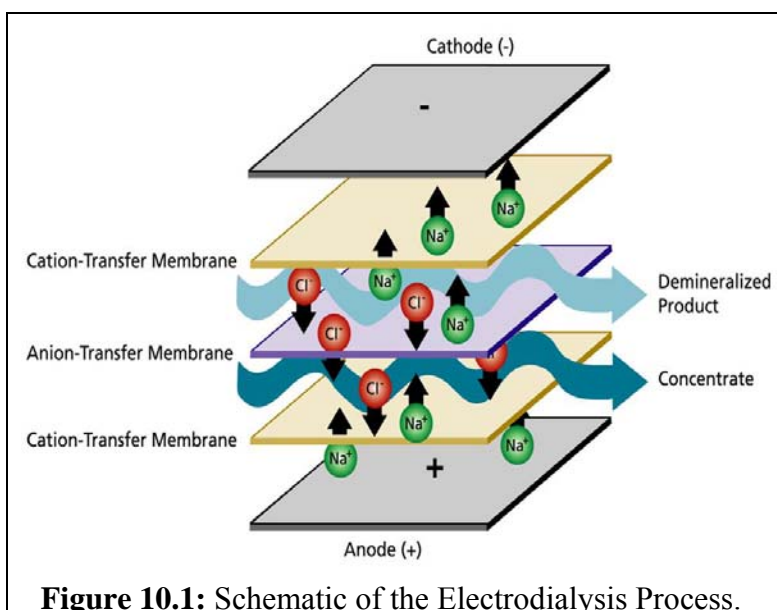
¹ Exploration and Production Center, Gas Technology Institute, 1700 S. Mount Prospect Rd, Des Plaines, IL 60018. Correspondence: tom.hayes@gastechnology.org.

² Energy Systems Division, Argonne National Laboratory, 9700 South Cass Ave., Argonne, IL 60439. Correspondence: moon@mcs.anl.gov.

The laboratory prototype that was constructed consisted of prefiltering for suspended solids removal, followed by electrodialysis (ED), followed by equilibration of the product water stream with a calcium-bearing mineral. Results indicated that a low-cost configuration for the ED system can consist of a non-selective membrane as the cation membrane, a sodium bicarbonate concentrate stream maintained at over 50,000 mg/l TDS, and a current density of 4.00 mAmps/cm². In a number of runs, approximately 90% desalination was achieved with modest energy inputs of 0.18 kWh/lb of NaCl removed or less; this was observed when the conductivity of the product water was reduced to very low levels (< 300 μS/cm). Where only partial desalination is required to achieve a treatment endpoint of 1,000 to 1,500 μS/cm, the required energy inputs can be reduced to levels as low as 0.11 kWh/lb of NaCl removed. Post treatment that employed passive equilibration with calcium carbonate in the form of powder or limestone was able to reduce SAR values from over 55 to below 6, without significantly raising the conductivity of the final water product. In terms of ease of use and cost effectiveness, passing the water stream over a bed of limestone is the recommended post treatment method. Using the simple pretreatment processing identified in this project, the laboratory ED unit operated on actual CBM produced water showed minimal degradation to the membranes of the stack cells over an extended 20 hour run before any cleaning was applied. In terms of overall performance, the laboratory ED process showed good stability in treating actual CBM produced waters; all performance goals were achieved. Based on these results, the ED technology can be considered a viable option for future scale-up and field piloting within the Powder River to achieve economical processing of CBM produced waters for the generation of beneficial use waters. Total breakeven system processing costs are estimated at less than 12 cents/bbl.

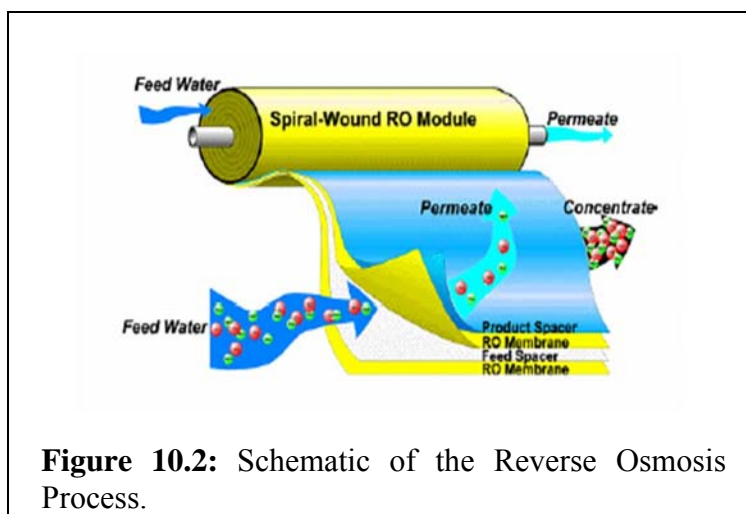
INTRODUCTION

Electrodialysis or ED is an electrically-driven membrane separation process that is capable of separating, concentrating, and purifying selected ions from aqueous solutions (as well as some organic solvents). In this process, ions are transferred through ion-selective membranes by means of a dc voltage as depicted in **Figure 10.1**.



ED is a well established process that has been used in the U.S. for decades. Electrodialysis was commercially available in the 1960's, about ten years before the introduction of RO. Over the past forty years, ED has provided separations for the manufacturing of many products in industry, including dairy foods, beverages, pharmaceuticals, metal finishing, and commodity biochemicals (such as organic acids). The development of the first generation of electrodialysis processing also represented a cost-effective way to desalt brackish water (AWWA, 2004).

The electrodialysis process is distinctly different from RO as shown in **Figure 10.2**. With RO, separation is achieved by size exclusion of molecules larger than water; water from a saline solution is passed under pressure through the membrane and is separated from the solutes (the dissolved material). Pressure drops across the membrane usually range from 17 to 27 bar (250 to 400 psi) for the treatment of brackish water and from 54 to 80 bar (800 to 1180 psi) in the treatment of concentrated salt water and seawater (above 30,000 mg/l TDS). The major energy required for this process is applied to the pressurization of the water (Doran and Leong, 2000; AWWA, 2004).



Electrodialysis, on the other hand, is an electrically-driven separation conducted at very low pressure drops across the process (usually less than 25 psi). The electrodialysis process, as applied to the treatment of salt water, depends on a number of principles. Soluble salts exist in water as ions, with positive and negative charges. This includes positively charged ions (cations) such as sodium, calcium, magnesium, and metals as well as negatively charged ions (anions) such as chloride, sulfide, sulfate, and bicarbonate. When electrodes are connected to an outside source of direct current, an electrical current is passed through the water and ions migrate to the electrode of the opposite charge as shown in **Figure 10.1**.

To achieve good separation, the movement of ions (TDS) is controlled by the addition of selectively permeable membranes that form watertight compartments that are arranged in a “stack”, as shown in **Figure 10.3**. Each anion transfer membrane allows only the transfer of negatively charged anions (e.g. chloride, sulfate, bicarbonate, nitrate, sulfide, etc.). The cation transfer membrane (C) allows only the passage of positively charged cations (calcium,

magnesium, sodium, potassium, metals, etc.). The membranes are electrically conductive and are impermeable to water flow, even under pressure.

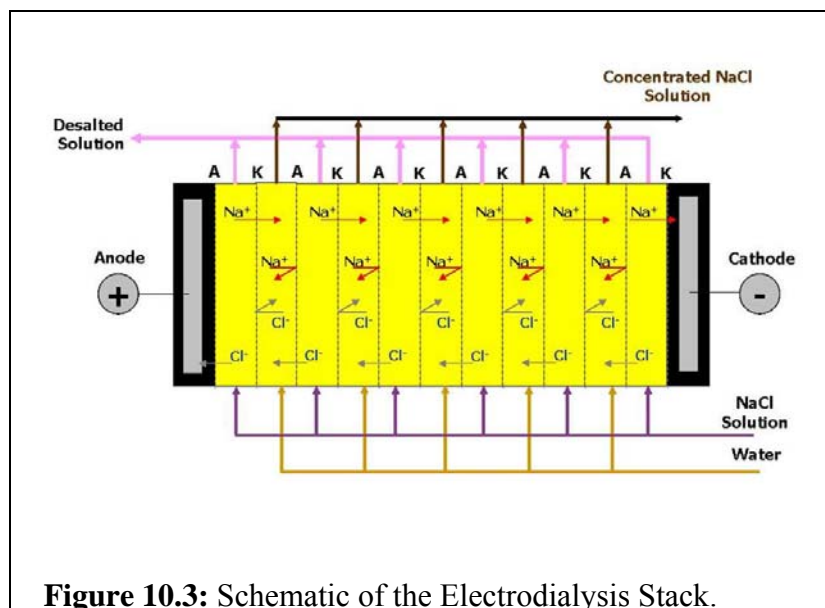


Figure 10.3: Schematic of the Electrodialysis Stack.

Using this arrangement, concentrated and diluted solutions are produced in the spaces between the alternating membranes. The spaces between the membranes are called cells and two adjacent cells are called a cell pair. The conventional electrodialysis process consists of several hundred cell pairs and is called a membrane stack. In practice, the electrodialysis system is composed of a series of stacks. Periodically, chemicals can be passed through the stack to achieve a clean-in-place operation.

A commercial electrodialysis system used in the demineralization of water is shown in **Figure 10.4**. An electrodialysis processing train usually includes the following components:

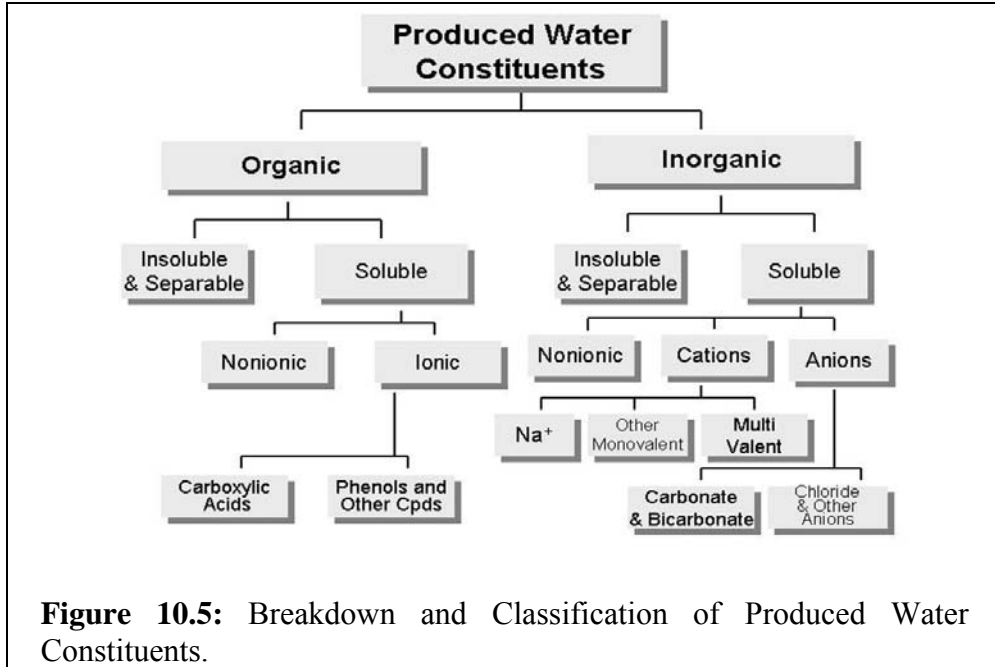
- Pretreatment
- Membrane Stack
- Low-pressure circulating pump
- Power supply for delivering direct current
- Post-treatment for water conditioning



Over the years, electrodesalination has been applied to the processing of brackish saline waters to achieve partial demineralization to meet criteria for surface discharge or for water supply uses. The past successful experience in applying conventional electrodesalination and EDR processes to the demineralization of brackish waters strongly suggests that these same processes could play a role in providing reliable separations of produced waters at a reasonable cost (Hayes, 2004).

The technical and economic feasibility of implementing treatment technologies for transforming produced water into beneficial use water streams will depend upon the initial composition of the produced waters, the type of processing to be used, and the quality of the finished effluent that is needed to meet regulatory criteria for the targeted end use for the product water.

Produced waters are highly varied in composition, a result that might be expected given that they arise from wide ranging formation characteristics, oil and gas hydrocarbon compositions, and a host of activities engaged by companies as a result of well development and maintenance. A breakdown of the categories of constituents of concern in produced water is shown in **Figure 10.5**; this breakdown is organized to illustrate the potential opportunities of using certain processes to achieve produced water separations. Constituents can be considered to be divided into organic and inorganic compounds. Inorganic constituents in produced water generated in the field are either insoluble (examples include scale, precipitates, grit, inorganic colloids, etc.) or soluble. Soluble salts are comprised of anions and cations. Some examples of cations in produced water include the monovalent cations of sodium and potassium and the multivalent cations of iron, calcium and magnesium. Major anions include chloride, sulfate, carbonate and bicarbonate. Non-charged soluble inorganic species may also present; examples of these include silicate (H_4SiO_2) and Borate (H_3BO_3).



In many cases, the conversion of produced water to a beneficial use water stream requires the removal of a number of classes of constituents to meet specifications for beneficial use waters. The concentrations and predominance of certain classes of constituents depends on the type of formation and natural gas system that is generating the water. The general characteristics of coalbed methane produced water compared to conventional natural gas produced water characteristics are shown in **Table 10.1** along with general criteria suggested for beneficial use according to targeted applications. The criteria, of course, are likely to vary from state to state and from basin to basin, depending upon environmental concerns and regulatory drivers associated with each proposed beneficial use. The most notable features that can be seen from the information in **Table 10.1** are that CBM produced water is by nature less concentrated in salt content than conventional produced water and that a far more modest reduction in total dissolved solids (TDS) content is required for the CBM waters to reach beneficial use quality than is the case for most conventional produced waters.

Table 10.1: Typical Values for Produced Water Quality Compared to Some Criteria (Lawrence, 1998; Hayes and Arthur, 2004)

Parameter	Suggested End Use Criteria			CBM Produced Water	Non-CBM (Conventional Gas Well) Water
	Drinking	Irrigation	Livestock		
pH	6.5 - 8	-	6.5 - 8	7 - 8	6.5 - 8
TDS, mg/l	< 500	< 2,000	< 5,000	3,000 - 10,000*	20,000 - 100,000
Benzene, ppb	< 5	< 5	< 5	< 100	1,000 - 4,000
SAR**	1.5-5	< 6	5-8	Highly Varied	Highly Varied
Na ⁺ , mg/l	< 200	See SAR	< 2,000	500 - 2000	6,000 - 35,000
Barium, mg/l				0.01 - 0.1	0.1 - 40
Cl ⁻ , mg/l	< 250	-	< 1,500	1,000 - 2,000	13,000 - 65,000
HCO ₃ ⁻ , mg/l	-	-	-	150 - 2,000	2,000 - 10,000

* Total Dissolved Solids (TDS) range estimated for the lower 50 percentile

** SAR = Sodium Absorption Ratio – a function of a ratio of Na to Ca and Mg Levels.

A produced water management parameter of growing importance among state regulatory agencies is the sodium absorption ratio or SAR. Sodium adsorption ratio (SAR) is a function of the ratio of sodium to the sum of calcium and magnesium cations; this parameter is defined by the following equation:

$$SAR = \frac{[Na^+]}{\sqrt{\frac{[Ca^{2+}] + [Mg^{2+}]}{2}}}$$

The SAR equation comes from the agronomy discipline and is used as a predictor for the response of clayey soils to exposure of water of various compositions involving sodium, calcium and magnesium. Concentrations for sodium, calcium and magnesium in the SAR equation are in meq/l. Highly “sodic” soils (those with SAR greater than 12) suffer from decreased water penetration; the specific SAR value at which soil damage begins depends on the nature of the soil itself. Optimum conductivity and SAR must be determined on a site-by-site basis. Using high SAR water for irrigation can affect soil permeability and water penetration, and therefore affect the survival of vegetation planted in that soil (Dallbauman and Sirivedhin, 2003). A SAR value below 6 is generally recommended for irrigation (Hergert and Knudsen, 1997). Another parameter used to regulate the quality of produced water is the total dissolved solids (TDS) which includes all soluble inorganic substances contained in a liquid.

As seen in **Table 10.1**, acceptable SAR values depend on the end use for the produced water; criteria for SAR values are also controlled to a high degree by each state. In many cases, SAR numbers less than 6 will be required for beneficial use water generated from treatment systems. From the equation, it can be seen that reducing the SAR from high values to acceptable levels can be accomplished through processes that either decrease sodium or increase calcium and magnesium.

In the conversion of CBM produced water to beneficial use water streams, it will be critical to develop processing that is capable of reliable demineralization capable of high efficiencies of

water recovery (> 90%) where the product water meets all of the criteria for beneficial water use, including the SAR criteria for agricultural applications. In the past, RO has not proven itself to be easily applied to CBM produced waters due to problems of membrane fouling due to precipitates and scale formation. On the other hand, field trials on conventional produced water conducted by GTI indicate that electrodialysis has the potential for fouling-resistant operation and predictable demineralization performance (Lawrence, et al., 1998).

The overall purpose of the work described in this chapter is to evaluate electrodialysis for potential application to the partial demineralization required to convert CBM produced water to a water stream suitable for beneficial use and to define the pretreatment and operating conditions that are necessary to maximize process reliability. This work was performed as a team effort between the Gas Technology Institute and Argonne National Laboratory.

APPROACH

The overall objective of this effort was to develop a simplified, small-footprint, processing train for the conversion of coalbed methane produced water into a water stream suitable for beneficial use. This work was to be conducted in two phases: Phase 1 - Evaluation of a laboratory prototype process train; and, Phase 2 - Pilot Unit Demonstration. This report covers the work performed in Phase 1.

The general approach for Phase 1 involved the following steps: 1) Identify energy industry partners to provide access to active CBM production fields; 2) Characterize produced water samples taken from CBM fields in the Powder River Basin; 3) Determine treatment goals to achieve beneficial use criteria for water suitable for agricultural applications; 4) Design and construct a treatment train that will meet treatment goals and provide reliable operation; 5) Conduct testing on the electrodialysis process train addressing key issues related to performance and reliability to achieve the treatment goals.

Energy industry collaborators in this effort included Marathon Oil Corporation and Anadarko Petroleum Corporation. Both of these companies operate numerous CBM well fields in the Powder River Basin. Information obtained from both companies indicated that in the majority of cases, agricultural application was the main beneficial use for the water generated from their CBM wells. Based on this feedback, and based on information obtained from other Principal Investigators in the CSM Program, agricultural end use was selected as the beneficial use of greatest impact for treated CBM produced water in the Powder River. Criteria for beneficial use water targeted for agricultural applications were, therefore, selected as the water quality specifications that needed to be achieved in laboratory prototype testing.

Goals for the prototype electrodialysis process train performance were based on the levels of treatment required to achieve good recoveries of demineralized water from CBM produced water that complied with criteria for beneficial use while exhibiting a level of operational stability that is consistent with economical processing. Specifically, the goals of this effort included the following:

- Achieve a product water recovery efficiency greater than 90%

- Brine volume reduction ratio > 10:1
- Maximize ED membrane lifespan:
 - Strict control of scale & suspended solids
 - Verify effectiveness of clean-in-place protocols
- Product water quality suitable for agricultural beneficial use
 - TDS < 1,000-2000 mg/l
 - SAR < 3-5 Depending on the drainage basin.
 - Address Chemicals of Potential Interest (if present in CBM produced water)
 - Benzene < 5 ppb
 - Barium, Ammonia, Iron, etc.

EXPERIMENTAL METHODS

Produced Water Characterization

With the assistance of the staff of energy industry collaborators, project investigators visited four production fields within the Powder River Basin and took samples at nine locations. The general locations of areas in the Powder River Basin where samples were taken are shown in **Figure 10.6**. Samples taken at each location were collected in a manner consistent with procedures specified for the analyses to be performed as defined by USEPA protocol. The analyses conducted on each sample and test methods that were employed are described in **Table 10.2**. Sample bottles filled with produced water from each field location were placed into coolers, packed with ice and sent by overnight mail to the Chicago-based, USEPA-certified laboratory (Stat Analysis Corporation) that performed the analyses.

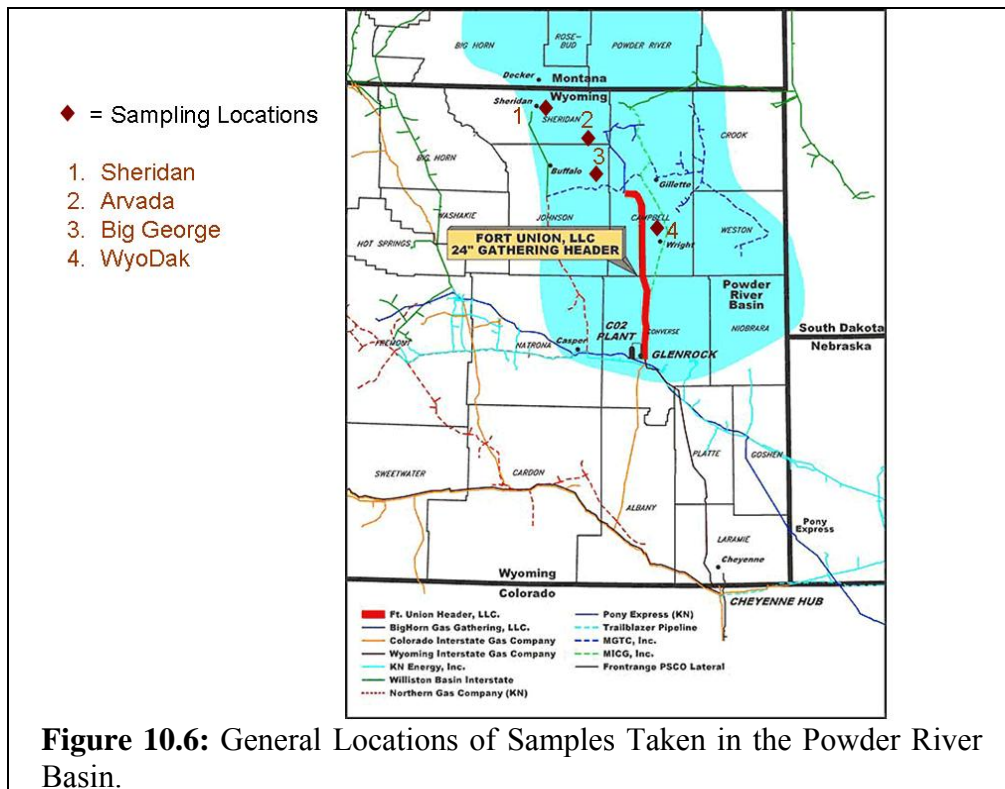


Figure 10.6: General Locations of Samples Taken in the Powder River Basin.

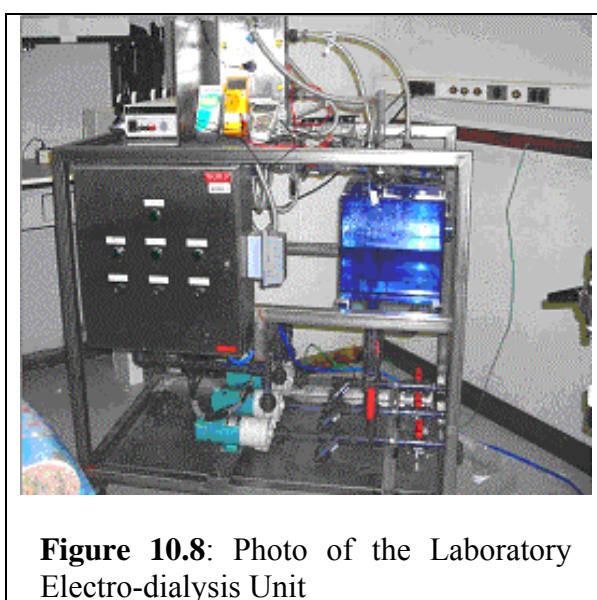
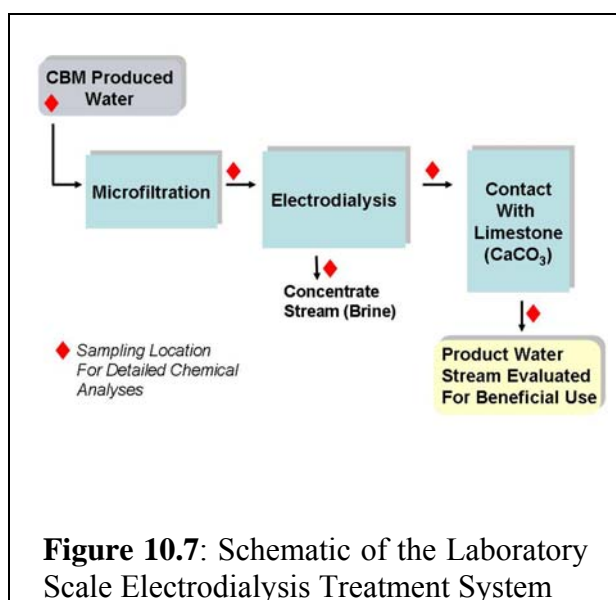
Using the results of the analyses performed on the nine grab samples, a location was identified for the collection of large aliquots of produced water that were collected in 55 gallon drums and shipped to Argonne National Laboratory in Illinois; this was done once in 2005 and once in 2006. Samples were collected from each aliquot and sent to STAT Analysis for detailed analysis. The CBM produced water from each aliquot was then used as feed water for testing the laboratory scale electro dialysis treatment prototype.

Table 10.2: Analytical Methods Used for Samples Collected from CBM Produced Water Sites.

Analysis	Method	Application Rules
Alkalinity, Total as CaCO ₃	EPA 310.1	All Samples
pH	EPA 9045C/150.1	All Samples
Benzene, Toluene, Ethylbenzene, Xylenes (BTEX)	EPA 8260B	Two samples per site (close to the well and at the end of the train)
Total Dissolved Solids (TDS)	EPA 160.1	All Samples
Total Suspended Solids (TSS)	EPA 160.2	Two samples per site (close to the well and at the end of the train)
Total Organic Carbon (TOC)	EPA 9060	Two samples per site (close to the well and at the end of the train)
Total Petroleum Hydrocarbons (TPH)	EPA 8015 Modified	Two Samples per site (close to the well and at the end of the train)
Chloride	EPA 325	All samples
Bicarbonate	EPA 310	All samples
Sulfate	EPA 375.2	One sample per site
Conductivity	EPA 120.1	All samples
Sodium	EPA 6020	All samples
Magnesium	EPA 6020	One sample per site
Calcium	EPA 6020	One sample per site
Potassium	EPA 6020	One sample per site
Nitrogen as Ammonia	EPA 350.1	All samples
Total Phosphorus	EPA 365.2	One sample per site

Laboratory Prototype Treatment Train

Based on the analyses performed on the above-collected samples, it was determined that oils & greases and soluble organic compounds were not present in the produced water at concentrations that could foul the membranes of the electro dialysis process. The process train selected for the laboratory treatment prototype consisted of the treatment scheme shown in **Figure 10.7**; this treatment train consisted of a simple combination of microfiltration to remove suspended solids followed by electro dialysis to recover demineralized product water and to concentrate salts into a far smaller volume of brine, followed by contact of the demineralized water with limestone to restore soluble calcium to the product water and thereby reduce the SAR parameter to very low levels. The principal factor that had the potential of degrading membrane performance was the suspended solids parameter. In order to control suspended solids to a very low level, the influent Wyoming Powder River Basin (PRB) CBM produced water was pretreated with microfiltration as simulated by passing the water through filter bags with 0.45 μm pores. A sample of this influent filtrate was sent to STAT Analysis Corporation to determine pH, conductivity, alkalinity and ion concentrations of Na^+ , Ca^{2+} , Mg^{2+} , K^+ , SO_4^{2-} and Cl^- . Samples were also taken at strategic points all along the entire process scheme as shown in **Figure 10.7**.



The ED laboratory skid system equipped with a two compartment ED stack EUR 2B-10 was designed by Eurodia Industries, France. A photo of this unit is shown in **Figure 10.8**. For all the experiments, the stack consisted of ten cell pairs and the ED unit was in batch configuration. The current and voltage were measured with a Xantrex XHR 40-25 instrument, a power supply manufactured by Xantrex Technology Inc., British Columbia, Canada. The optimum stack current density, determined by a limiting current density test, was kept constant at 4.00 mAmps/cm^2 . The average voltage drop per cell was maintained at less than 1.5 volts. All the membranes used with the ED system were Neosepta[®] membranes manufactured by ASTOM Corporation, Japan. Anion exchange membranes (AMX) were used for the anion membranes and cation exchange membranes (CMX) were used as the electrode rinse (ER) membranes. For the cation membranes, CMX or selective cation membranes (CMX-S) were used. The area of the

membranes used was 200 cm². The flow rates through the recirculation loops were kept at 0.9 gpm for the feed and concentrate and 1 gpm for the electrode rinse (ER) loops.

Laboratory Scale Electrodialysis Prototype Testing

For Experiments 1 through 4, the feed solution was PRB CBM produced water, and the ER solution was 30 g/L Na₂SO₄. The rest of the parameters for these experiments can be found in **Table 10.3**. Each treatment cycle was performed in batch mode where a feedstock was placed in a tank and the contents of the tank were recirculated through the ED stack and returned to the feed tank; periodic measurements and samples taken from this tank are labeled “feed” in **Table 10.3**. The conductivity and temperature of the feed and concentrate solutions were monitored throughout the experiments using a Cole-Parmer Instrument Company conductivity meter, and the pH was monitored using an Oakton pH meter. The runs were stopped when the percent of desalination of the feed tank solution reached around 90%. Percent desalination was calculated using the change in conductivity of the feed solution, unless it was specifically done for ions like Ca²⁺ and Mg²⁺, in which case the STAT Analysis results were used. Samples from all three tanks (feed, concentrate and ER) were taken throughout and at the end of the runs and sent to STAT Analysis Corporation to determine pH, conductivity, alkalinity and ion concentrations of Na⁺, Ca²⁺, Mg²⁺, K⁺, SO₄²⁻ and Cl⁻. The power consumption was calculated for the amount of NaCl removed from the feed solution.

Table 10.3: Parameters for Experiments 1 through 4

Experiment Number	Membrane Type	Volume (L)			Concentrate Solution
		Feed	ER*	Concentrate	
1	CMX	10	8	8	5 g/L NaCl
2	CMX-S	11	8	8	5 g/L NaCl
3	CMX	10	8	8	300 g/L NaCl
4	CMX	8	8	8	50 g/L NaHCO ₃

* *Electrode Rinse*

Testing and development of the laboratory scale prototype to determine its capability in meeting performance goals in treating CBM produced water for beneficial-use was conducted in three parts:

- Part I. Comparison of CMX versus CMX-S Membranes;
- Part II. Back-Diffusion Studies; and,
- Part III. Post Demineralization Treatment.
- Part IV Membrane Stability Testing

Part I: Comparison of CMX versus CMX-S membranes

Conventional cationic exchange membranes such as CMX are capable of allowing the passage of nearly all types of cations causing positively charged monovalent ions such as sodium (Na⁺) and multivalent ions such as calcium (Ca²⁺) to pass through the membrane. In this case, calcium and magnesium can be removed at efficiencies comparable to sodium, resulting in an elevated SAR

value for the product water even though total dissolved solids have been significantly reduced. Under normal conditions (as depicted in the schematic for the laboratory treatment system shown in **Figure 10.7**) the SAR value can be reduced to targeted levels by contacting the water with a calcium mineral – such as limestone (CaCO_3) – which restores soluble calcium to concentrations above 25 mg/l.

Alternatively, if calcium in the influent produced water stream is prevented from passing through the cationic exchange membrane, it might be possible to reach targeted SAR values without using the terminal limestone contactor step. This is technically possible through the use of CMX-S membranes in the place of CMX cation exchange membranes; CMX-S membranes are selective for the passage of monovalent cations (such as sodium) while excluding multivalent cations such as calcium and magnesium.

The tradeoff is, of course, whether the membranes are comparable in performance in terms of power use and efficiency of demineralization and whether the difference in cost is justified by the savings that could be realized by reducing or eliminating the terminal treatment step of equilibrating the product water with limestone. The purpose of Experiments 1 and 2 was to compare the CMX-S and CMX cation membranes in terms of power consumption and efficiency in desalting the produced water. The differences between vendor specs for CMX and for CMX-S membranes are described in **Table 10.4**.

Table 10.4: Comparison of CMX and CMX-S Membranes*

	CMX	CMX-S
Type of Membrane	Non-selective	Mono-selective
Transport Properties	Allows transport of monovalent and divalent cations	Only allows transport of monovalent cations Rejects over 90% of Mg^{2+} and Ca^{2+}
Mechanical Strength	Good	Good
Lifetime	2 years	2 years

* Based on Vendor Information Received from Ameridia Division of Eurodia.

Part II: Back-diffusion studies

The feasibility of achieving benefits of high efficiencies of product water recovery while generating a relatively small volume of brine depends upon the ability of the electro dialysis to move cations and anions through the membranes into the concentrate stream, even against high gradients of salts, with minimal back-diffusion. The purpose of Experiments 3 and 4 was to evaluate the electro dialysis selective and non-selective membranes' back diffusion effect of a dilute CBM produced water feed and a large salt solution concentrate. Back-diffusion studies were performed with both sodium chloride (NaCl) (Experiment 3) and sodium bicarbonate (NaHCO_3) (Experiment 4) as the concentrate. Sodium chloride was used to ensure that very high concentrations of sodium could be maintained on the concentrate side of the membrane without

the possibility of precipitation reactions; NaCl was chosen because it is a standard salt used for ED and produced water is known to contain NaCl. Sodium bicarbonate was chosen because, upon a detailed chemical composition analysis, it was determined that the PRB CBM produced water contained mostly NaHCO₃. The concentrations for both chemicals, 300 g/L NaCl and 50 g/L NaHCO₃, were chosen based on the fact that these values were close to the solubility limits in water of 359 g/L and 78 g/L for NaCl and NaHCO₃, respectively for standard conditions (25° C).

Part III: Post-demineralization treatment

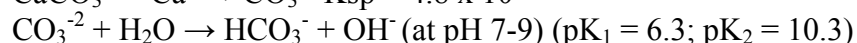
When demineralization is carried out using a non-selective cationic exchange membrane, such as CMX, calcium is removed simultaneously with sodium which causes the SAR value to remain higher than the levels required for targeted beneficial uses. The treatment strategy in this case is to restore the levels of soluble calcium in demineralized produced water (the effluent product water of ED) to levels sufficient to cause the calculated SAR value to fall to the desired range while avoiding a significant increase in TDS. The purpose of this effort was to test three calcium-bearing compounds in the use of passive equilibration treatment for restoring soluble calcium in demineralized CMB produced water.

Three different types of post-demineralization treatments were tested to adjust the SAR to levels suited to beneficial use (less than 6). This was done to identify the lowest cost approach for conditioning ED effluents to achieve SAR values suitable for beneficial use. The three different types of calcium bearing compounds that were used included powdered calcium sulfate (CaSO₄), powdered calcium carbonate (CaCO₃) and limestone rocks. Dissociation equations for the dissolution of calcium sulfate and calcium carbonate to restore calcium levels in CBM produced water are given below:

1) Calcium Sulfate Dissolution:



2) Calcium Carbonate (Powder or Limestone forms) Dissolution:



Approximately 5 g of each material was added to 500 mL of the demineralized CBM produced water (exhausted feed water) generated from the laboratory ED unit in Experiment 2. These mixtures were left to mix over night with a Palo Laboratory Supplies mixer. The water was then filtered using filter bags with 0.45 µm pores and the conductivity was measured. A sample of water from the three experiments was sent to STAT Analysis Corporation to determine pH, conductivity, alkalinity and ion concentrations of Na⁺, Ca²⁺, Mg²⁺, K⁺, SO₄²⁻ and Cl⁻.

Part IV: Membrane stability evaluation

The objective of this effort was to determine the performance stability of the ED membranes under the sodium bicarbonate concentrate conditions that reflect good brine concentration efficiencies during a 20-hour period of demineralization between membrane cleanings.

Measurements of conductivity were taken during each demineralization cycle as well as periodic water samples that were taken from the batch runs and analyzed for pH, sodium, calcium, magnesium, chloride, and alkalinity. During the sequence of batch runs, the level of sodium bicarbonate in the concentrate was maintained above 50,000 mg/l. Data collection was designed to allow detection of any deterioration of demineralization performance that might become apparent between successive ED batch treatments of the produced water.

The conductivity and temperature of the feed and concentrate solutions were monitored throughout the experiments with a Cole-Parmer Instrument Company conductivity meter and the pH was monitored with an Oakton pH meter. Multiple batches of produced water feed were processed for 30 hours and each was stopped when the percent of desalination of the feed was around 90%. Meanwhile, the concentrate was continuously recycled until all feed batches were processed and during this time the concentrate pH was not adjusted. The concentrate side initially contained 50 g/L of sodium bicarbonate. To simulate anticipated typical field conditions, a cleaning in place was carried out after 20 hours of processing; The feed consisted of actual CBM produced water from the Sheridan, WY site. Samples from all three tanks (feed, concentrate and ER) were collected for analysis at intermediate and final points.

RESULTS

Produced Water Characterization

Coalbed methane produced water characterization data from nine samples taken in the Powder River Basin in September and October of 2005 are tabulated in **Table 10.5**. The data indicate that for four locations across the Powder River basin, CMB produced water tends to be low in total dissolved solids, with a median value of about 1,400 mg/l. At one location, TDS values of 360 to 500 mg/l were recorded which are unusually low compared to most CBM produced waters. In all of the samples, anions were dominated by bicarbonate species (chlorides comprised less than 3% of the anion mass) and cations were dominated by sodium. The sodium median value approximated 700 mg/l while the calcium median value was about 15 mg/l and the magnesium median value was about 9 mg/l. In all cases, total suspended solids (particulates that filter out with glass fiber filters) were low, usually less than 10 mg/l. The SAR values for produced waters other than the two lowest TDS samples ranged from 23 to 60. Equally important, total organic carbon concentrations were at single-digits ppm levels, total petroleum concentrations were usually less than 0.5 mg/l and BTEX components were usually at or below detection levels.

Table 10.5: Analysis Results from Nine CBM Produced Water Samples Taken in the PRB.

Parameter	----- Sampling Locations -----								
	Arvada Jeff 7 Inflow	Arvada Jeff 7 Pond	Sheridan R Bull Inflow	Sheridan R Bull Pond	Sheridan Mooney Inflow	Big George Before Zeolite	Big George After Zeolite	Wyo- Dak Well Head	Wyo- Dak Outfall
pH	7.5	8.8	7.9	8.7	8.1	7.3	7.5	7.3	7.3
Sodium, mg/l	520	690	710	590	630	820	810	140	170
Calcium, mg/l	20	10	6.7	13	6.5	40	38	15	18
Magnesium, mg/l	11	9	2.2	8.5	2	23	22	6.5	9.3
Barium, mg/l	0.67	0.34	0.67	0.38	0.65	1.3	0.9	0.31	0.42
Potassium, mg/l	13	8.6	8.4	8.4	7.6	39	38	7.6	7.4
Alkalinity, mg/l as CaCO ₃	1,400	1,200	1,200	1,200	1,400	2,000	1,900	360	520
Chloride, mg/l	11	15	11	17	9	25	25	13	11
NH ₃ -N, mg/l as N	1.1	0.17	2.0	0.93	2.4	5.2	4.8	0.8	0.96
Total Organic Carbon, mg/l as C	6.2	6	1.6	7.2	2.8	9.1	7.6	6.7	5.6
Specific Conductance, μS/cm	1,850	2,130	2,170	2,170	1,960	2,620	2,580	488	673
Total Dissolved Solids, mg/l	1,200	1,400	1,400	1,400	1,500	2,000	2,000	360	500
Total Suspended Solids, mg/l	< 10	< 10	< 10	< 10	10	< 10	< 10	< 10	< 10
Sulfate, mg/l	< 15	< 15	< 15	< 15	< 15	< 15	< 15	< 15	< 15
Calculated SAR Value	23	38	60	31	55	25	26	7.5	8.0
Total Petroleum Hydrocarbon, mg/l	< 0.25	< 0.25	< 0.25	< 0.25	0.54	0.52	0.53	1.7	0.25
Benzene, mg/l	<0.005	<0.005	0.015	<0.005	0.012	<0.005	<0.005	<0.005	<0.005
Toluene, mg/l	<0.005	<0.005	<0.005	<0.005	<0.005	<0.005	<0.005	<0.005	<0.005
Ethylbenzene, mg/l	<0.005	<0.005	<0.005	<0.005	<0.005	<0.005	<0.005	<0.005	<0.005
Xylenes, mg/l	<0.015	<0.015	<0.015	<0.015	<0.015	<0.015	<0.015	<0.015	<0.015

Laboratory Scale Electrodialysis Prototype Testing

The properties and composition of the PRB CBM produced water, used as the feed for all experiments, can be found in **Table 10.6**. The feed water was collected from the Sheridan Wyoming site at the wellhead and is consistent in characteristics with the measurements taken on most of the Powder River Samples analyzed in this project. Because of the very low or non-detectable levels of oils and grease and BTEX in the water, the parameters of greatest interest in the conversion of the water to a beneficial use water stream is the SAR value which exceeded 56 and the conductivity which exceeded 2,600 $\mu\text{S}/\text{cm}$. As previously mentioned, prefiltration of the water ensured that the already low suspended solids ($<10 \text{ mg/l}$) would always remain in control. The overall strategy of the treatment system was to use electrodialysis to reduced sodium to low levels and to equilibrate the water with calcium compounds (if needed) to restore calcium concentrations.

Table 10.6: Properties and Composition of the Large PRB CBM Produced Water Aliquots Used as Feed for the Laboratory Treatment Unit.

Parameter	Units	Value
Sodium Concentration	mg/L	670
Calcium Concentration	mg/L	6.7
Magnesium Concentration	mg/L	2.3
Chloride Concentration	mg/L	140
Alkalinity	mg/L CaCO_3	1300
Conductivity	$\mu\text{S}/\text{cm}$	2650
pH	n/a	8.4
SAR	n/a	56.2

Part I: Comparison of CMX versus CMX-S membranes

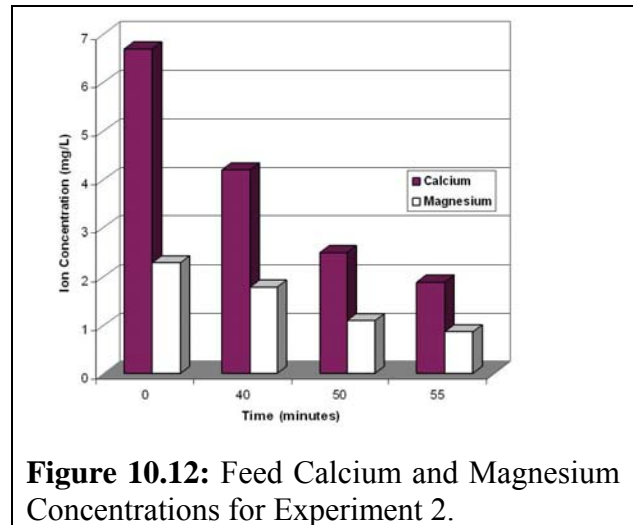
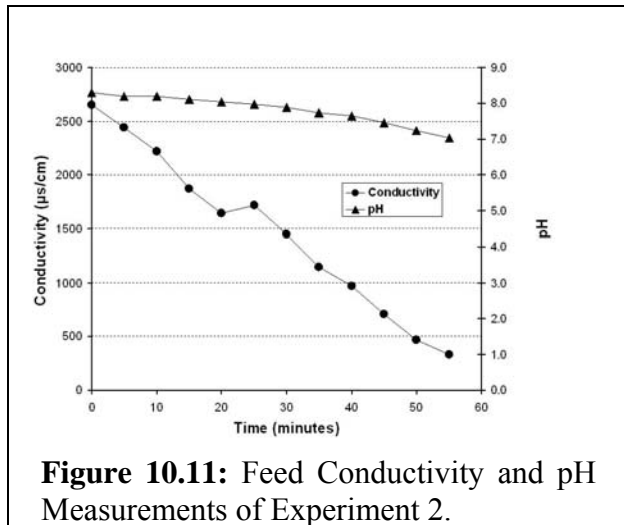
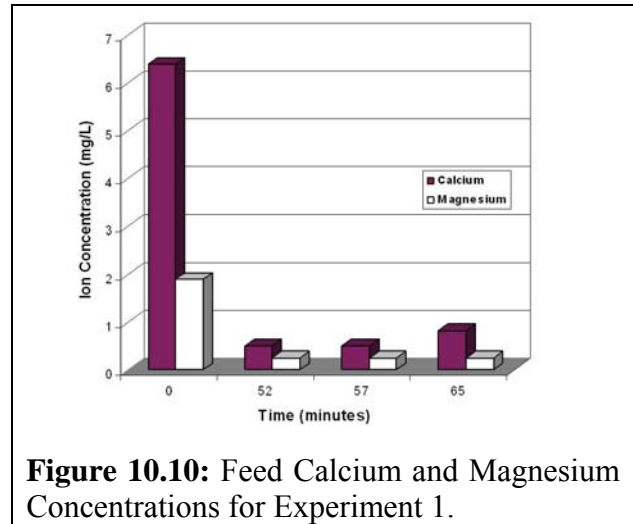
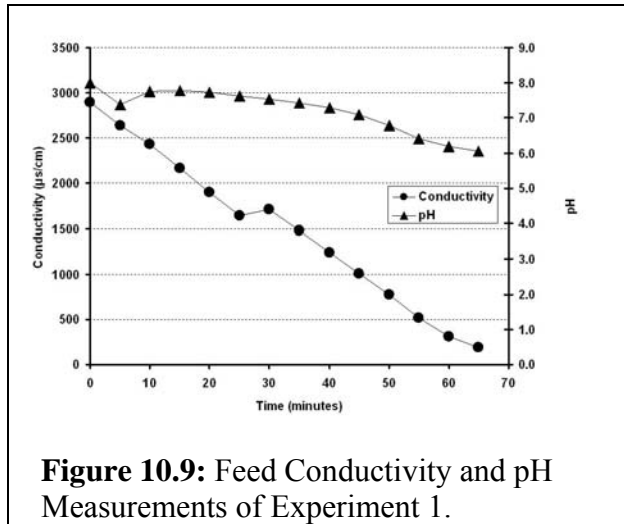
For Experiments 1 and 2, the conductivity and pH values over the range of the experiments can be found in **Figures 10.9 and 10.11**, respectively. **Figures 10.10 and 10.12** demonstrate the change in calcium and magnesium concentrations during the runs for Experiments 1 and 2, respectively. **Tables 10.7 and 10.8** contain the power consumption as a function of percent desalination and SAR for Experiments 1 and 2, respectively.

Table 10.7: Power Consumption as a Function of % Desalination and SAR Experiment 1: Non-Selective Membrane

Time (minutes)	% Desalination	Power Consumption (Kw-hr/lb NaCl removed)	SAR
55	82.1	0.14	10.2
65	93.5	0.20	9.3

Table 10.8: Power Consumption as a Function of % Desalination and SAR Experiment 2: Selective Membrane

Time (minutes)	% Desalination	Power Consumption (Kw-hr/lb NaCl removed)	SAR
50	82.3	0.20	10.9
55	87.5	0.21	8.3



Part II: Back-diffusion studies

For Experiments 3 and 4, the conductivity and pH values over the range of the experiments can be found in **Figures 10.13 and 10.14**, respectively. **Tables 10.9 and 10.10** contain the power consumption as a function of percent desalination and SAR for Experiments 3 and 4, respectively.

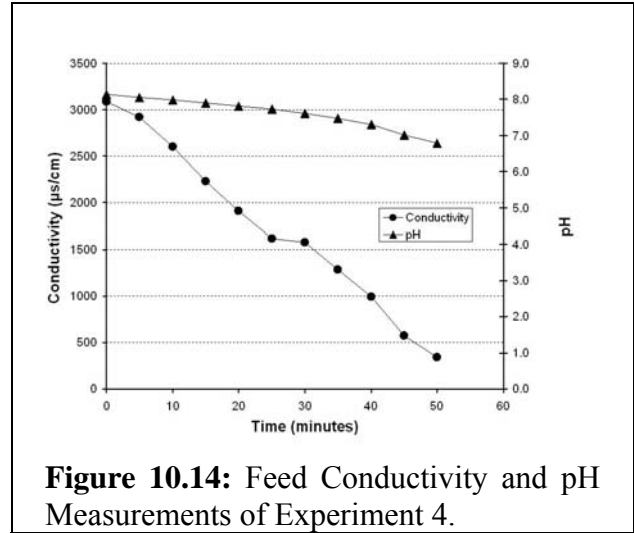
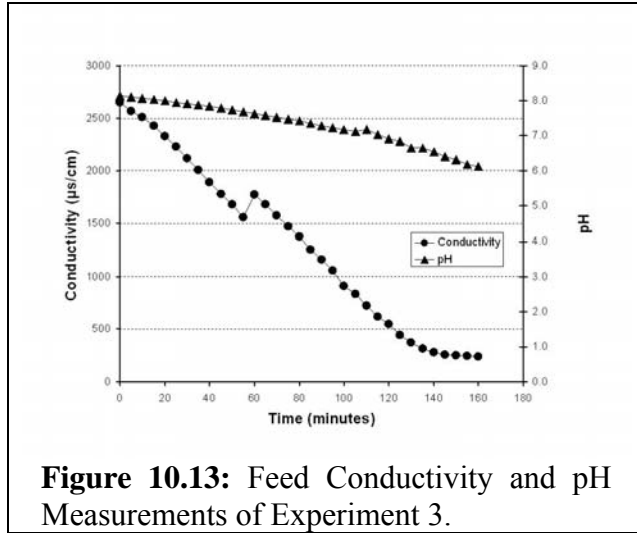


Table 10.9: Power Consumption as a Function of % Desalination and SAR Experiment 3: Back-Diffusion Study with NaCl

Time (minutes)	% Desalination	Power Consumption (Kw-hr/lb NaCl removed)
132	86.0	0.42
160	90.9	0.56

Table 10.10: Power Consumption as a Function of % Desalination and SAR Experiment 4: Back-Diffusion Study with NaHCO₃

Time (minutes)	% Desalination	Power Consumption (Kw-hr/lb NaCl* removed)
30	49.0	0.11
45	81.4	0.16
50	88.9	0.18

* That is: NaCl equivalent of sodium bicarbonate removed.

Part III: Post-demineralization treatment

The data set that summarizes the results of the post treatment of produced water employed in conjunction with Experiment 2 is shown in **Table 10.11**. The table contains the properties and composition of CBM produced water before treatment, after treatment with electro dialysis (ED) and following post-treatment comparing three modes of post treatment. The modes of post treatment that are compared in the table include equilibration with CaSO₄, powdered CaCO₃ (reagent grade) and limestone. Performance of the integrated laboratory ED treatment system that utilized limestone post treatment is described in **Figure 10.15**.

Table 10.11: Results of Post-Treatment of the ED Effluent Used in Conjunction with Experiment 2

Parameter	Units	CBM PW*	ED Treated**	Post Treatments		
				CaSO ₄	CaCO ₃	Limestone
Sodium Concentration	mg/L	670	56	57	56	55
Calcium Concentration	mg/L	6.7	1.9	690	17	18
Magnesium Concentration	mg/L	2.3	0.87	1.0	2.7	1.6
Chloride Concentration	mg/L	140	7	11	13	11
Alkalinity	mg/L CaCO ₃	1,300	350	140	210	180
Conductivity	μS/cm	2,650	331	2,820	324	333
pH	n/a	8.4	7.0	7.9	8.3	8.3
SAR	n/a	56.2	8.3	0.6	3.3	3.3

* Untreated CBM Produced Water Used in Experiment 2.

** Water from the laboratory ED unit after approximately 90% demineralization

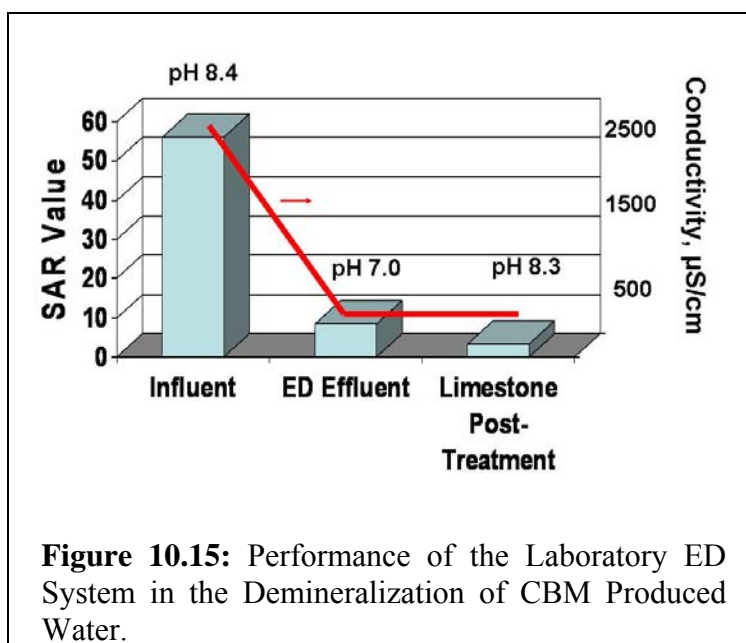
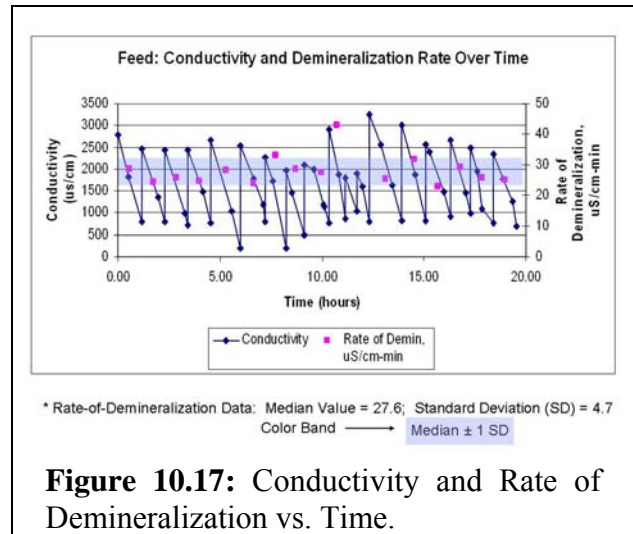
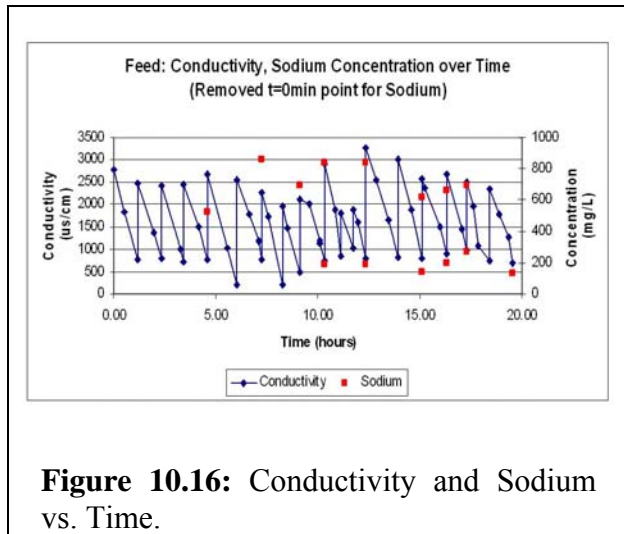


Figure 10.15: Performance of the Laboratory ED System in the Demineralization of CBM Produced Water.

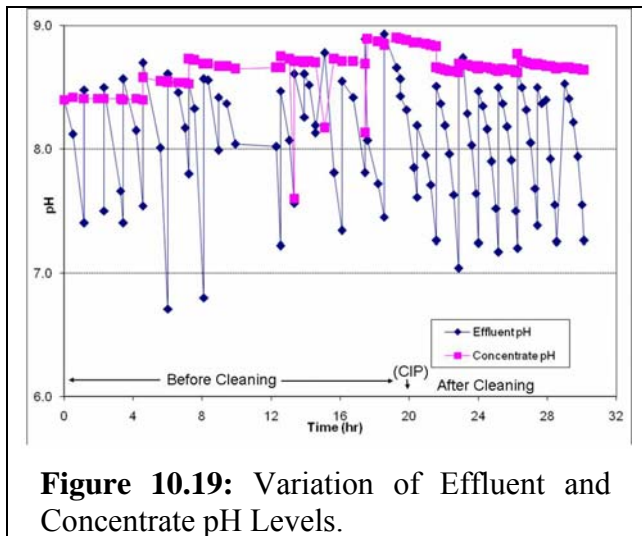
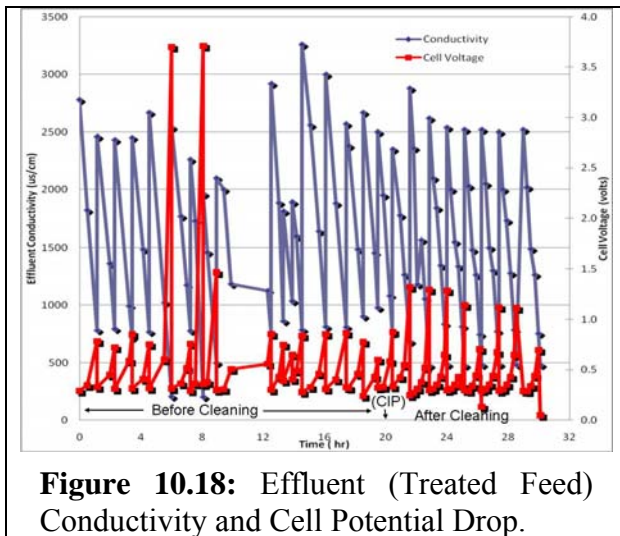
Part IV: Membrane stability evaluation

Demineralization data showing the decline in conductivity and sodium over the period of multi-cycle-batch operation is presented in **Figure 10.16** for the first 20 hours containing the initial 16 treatment batches. Samples for sodium analysis were taken at selected times during the initial 16 batches, usually at the very beginning of a batch cycle or at the end of a batch cycle as seen in the locations of sodium sample points in **Figure 10.16**. From the decrease of conductivity achieved by the membranes, a rate of demineralization (expressed as S/cm-min) was calculated for each of the batch cycles and these rates were plotted with time to determine if any deterioration of salt mass transfer performance occurred that would indicate deterioration of ED

membrane performance. This data is plotted in **Figure 10.17**. Taken together, the two figures provide a basis for assessing membrane integrity over the extended 20-hour run of the laboratory ED treatment system operating on actual CBM produced water.



Another graph that is useful in showing membrane stability is shown in the plots of effluent (treated feed) conductivity and cell voltage versus time as presented in **Figure 10.18**. Cyclical variations of effluent (treated feed) pH and concentrate pH values during the treatment run are shown in **Figure 10.19**. Finally, to estimate the precipitation or scale-deposition potential of the ED process, the concentrations of soluble calcium and magnesium in the concentrate solution before and after CIP are plotted in **Figure 10.20**.



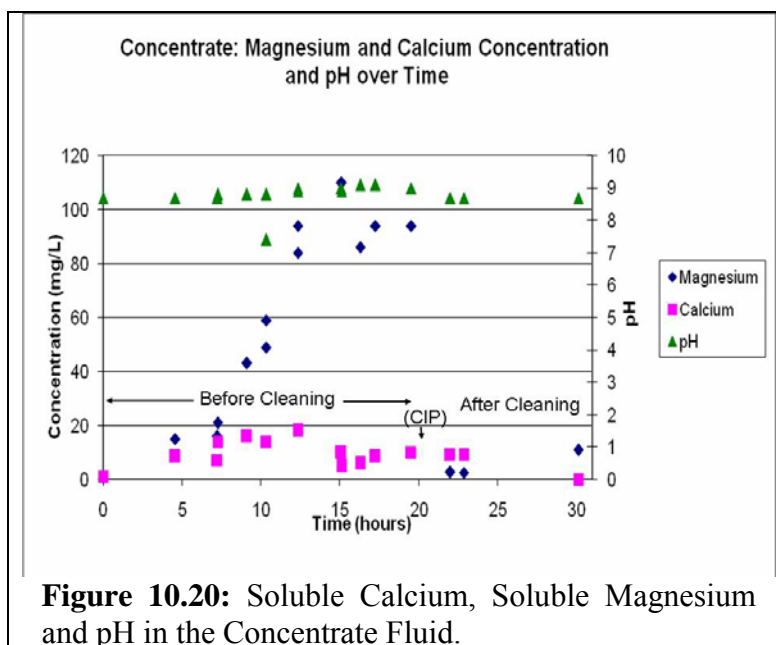


Figure 10.20: Soluble Calcium, Soluble Magnesium and pH in the Concentrate Fluid.

DISCUSSION

In general, the data indicate that electrodialysis is an effective process for the demineralization of CBM produced water. A water stream containing less than 1,000 mg/l total dissolved solids (TDS), having an SAR of less than 6 and containing virtually no organics would represent a high-quality produced water suitable for all agricultural beneficial uses. For the water aliquots that were used for testing the ED system in the lab, only partial demineralization with restoration of minor levels of calcium were required to convert CBM produced water into beneficial use water. Discussions of specific results from the experiments are given in the following sections.

Part I: Comparison of CMX versus CMX-S Membranes

For both Experiments 1 and 2, the pH values were lowered to values within the neutral pH bracket needed for beneficial use. For Experiment 1, the pH values went from 8.00 to 6.05 (**Figure 10.9**) and for Experiment 2, the values went from 8.30 to 7.03 (**Figure 10.10**). For both experiments, the conductivity steadily decreased, although more slowly in Experiment 2, as the water gradually became desalted. For Experiment 1, the conductivity went from 2900 $\mu\text{S}/\text{cm}$ to 189 $\mu\text{S}/\text{cm}$ (**Figure 10.9**), and for Experiment 2, it went from 2650 $\mu\text{S}/\text{cm}$ to 331 $\mu\text{S}/\text{cm}$. In terms of Ca^{2+} and Mg^{2+} concentrations, values for these cations dropped extremely rapidly in Experiment 1, and very slowly in Experiment 2. This was to be expected since the CMX-S membrane (used in Experiment 2) does not allow for the transport of divalent cations. In Experiment 1, the Ca^{2+} concentration was reduced by 92% in 52 minutes and the Mg^{2+} concentration was reduced by 87% in 52 minutes (**Figure 10.10**). In Experiment 2, the Ca^{2+} concentration was reduced by only 72% in 55 minutes and the Mg^{2+} concentration was reduced by only 62% in 55 minutes (**Figure 10.12**).

In comparing **Table 10.7 and 10.8**, it can be seen that a lot more power consumption per unit salt removed was needed when using a CMX-S membrane as opposed to a CMX membrane as

the cation membrane. In achieving desalination of approximately 82%, the selective CMX-S membrane required 0.20 Kw-hr/lb of NaCl removed while the non-selective CMX membrane required 0.14 Kw-hr/lb of NaCl removed, a 30% reduction in power demand. At the same power consumption, 0.20 Kw-hr/lb NaCl removed was sufficient to achieve 93.5% desalting (SAR of 9.3) with CMX membranes of Experiment 1 while the same power expenditure achieved only 82.3% desalting (SAR of 10.9) with CMX-S membranes of Experiment 2. Based on these observations, it would appear that CMX should be used as the cationic membrane of preference for future experiments. Because of the high jump in power consumption when using the non-selective membrane (CMX), e.g., 0.14 to 0.20 Kw-hr/lb NaCl removed when increasing the desalination from 82.1% to 93.5%, a different method should be sought to desalt up to 93% (see Part III).

Part II: Back-Diffusion Studies

For Experiment 3, back-diffusion occurred between 55 and 60 minutes, where a discontinuity in the decrease of conductivity could be seen as the value went from 1560 $\mu\text{S}/\text{cm}$ to 1773 $\mu\text{S}/\text{cm}$ (**Figure 10.13**). At that point, the concentrate had such a high concentration of NaCl (over 300,000 mg/l NaCl) that the ions moved along the concentration gradient, back into the feed, instead of moving along the electric field. Because of this back-diffusion, the power consumption needed to achieve over 90% desalination was much greater than in Experiment 1, which had the same conditions except for a lower concentration of NaCl in the concentrate (about 5,000 mg/l NaCl). For Experiment 1, 93.5% desalination was achieved with 0.20 Kw-hr/lb NaCl removed (**Table 10.7**), as opposed to 0.56 Kw-hr/lb NaCl removed for 90.9% desalination in Experiment 3 (**Table 10.9**). Notwithstanding the observation of back diffusion, Experiment 3 demonstrated that over 90% demineralization can be achieved under near-worse case conditions of moving ions from a feed water stream across the membranes into a concentrate solution against a salt concentration gradient approximating 300,000 mg/l (the difference between salt concentrations of the concentrate and the feed streams of the ED process) if sufficient energy input is applied to the process.

For Experiment 4, which maintained 50 g/l of sodium bicarbonate in the concentrate, no back-diffusion was observed; only a steady decrease in conductivity can be seen in **Figure 10.14**. In comparing results in **Tables 10.7 and 10.10**, it can be seen that less power consumption measured when using 50 g/l of NaHCO_3 in the concentrate was roughly comparable to the earlier run using only 5 g/l of NaCl in the concentrate. For Experiment 1, an energy input of 0.14 Kw-hr/lb removed (NaCl equivalent) was needed to achieve 82.1% desalination, while only 0.16 Kw-hr/lb removed (NaCl equivalent) was needed in Experiment 4 to achieve 81.4% desalination against a salt level in the concentrate that was more than 10 times higher than the level of Experiment 1.

When electrodialysis is implemented in the field to demineralize CBM produced water at Sheridan and at many other locations in the Powder River Basin, it is expected that the composition of the concentrate will most closely resemble that of Experiment 4 where the salts are mainly dominated by carbonate anions. If only half of the TDS needs to be removed to reach desalination goals for the ED unit, a fairly low power consumption would be required. This is

indicated by the results of Experiment 4 that show that 49% desalinization was achieved with a power input of 0.11 Kw-hr/lb removed (NaCl equiv.) (**Table 10.10**).

Part III: Post-Demineralization Treatment

Though showing excellent capability in reducing total dissolved solids and conductivity in CBM produced waters, it is apparent that in many cases electro dialysis alone will not be sufficient to generate a water product that consistently controls the SAR parameter to below the 4-6 levels required by regulations for agricultural uses. This is illustrated with the data of **Table 10.11** that show that electro dialysis was able to reduce the SAR of CBM produced water from over 56 to 8.3; at the same time, conductivity was reduced from 2,650 to approximately 330 S/cm. Further reductions in SAR levels to 3.3 were achieved through post treatment with calcium carbonate powder and limestone; equilibration with these forms of calcium mineral resulted in no significant increase in conductivity.

On the other hand, equilibration with calcium sulfate resulted in SAR value of 0.6, but the resultant conductivity increased to 2,820 S/cm which was higher than the initial salinity of the influent CBM produced water. This result is consistent with the higher solubility of calcium sulfate compared to the calcium carbonate compounds. This clearly indicates that equilibration with calcium carbonate in the form of powder or limestone would be a preferred strategy for adjustment of SAR if a passive equilibration system is used to restore calcium levels into the product water stream.

Based on data collected from the laboratory treatment train comprised of simple prefiltration, followed by electro dialysis demineralization, followed by passive equilibration of the product water with simple limestone, it would appear that all of the performance goals set forth at the beginning of the project have been met or exceeded. The ability to efficiently demineralize CBM produced water with up to 3,000 mg/l TDS against a sodium bicarbonate level exceeding 70,000 mg/l TDS in the concentrate stream is consistent with a product water recovery of over 90% and a brine reduction ratio greater than 11:1. Since only roughly 50% demineralization is required to achieve the TDS goal of 1,500 mg/l for beneficial use, the power consumption required for this level of treatment is approximately 0.11 Kw-hr/lb NaCl equivalent removed; this energy input is less than the goal of 0.14 Kw-hr/lb NaCl removed.

Part IV: Membrane Stability Evaluation

Fundamentally, the most important barometer of membrane stability is overall process performance during an extended period of operations without cleaning intervention. During the initial 20 hours of operation in the membrane stability experiment, 16 cycles of electro dialysis treatment were completed. The demineralization results throughout this initial period indicate that the last cycle was able to achieve the same excellent reductions in conductivity and sodium concentrations as observed in the initial cycles. A closer look at the demineralization rate that is calculated from the decrease in conductivity achieved in each treatment cycle and plotted at the midpoint of the time interval of each cycle provides a quantitative measure of the demineralization performance of the membranes through the first 20 hours of operation, as shown in **Figure 10.17**. Demineralization rates ($\mu\text{S}/\text{cm}\cdot\text{min}$) shown as points on the graph

indicate that the rate of salt transport through the membranes remained very consistent throughout the 20-hour treatment period; values stayed fairly close to the median rate of 27.6 $\mu\text{S}/\text{cm}\cdot\text{min}$ with a standard deviation of 4.7 $\mu\text{S}/\text{cm}\cdot\text{min}$. The shaded area of **Figure 10.17** encompasses the median rate plus or minus the standard deviation ($27.6 \pm 4.7 \mu\text{S}/\text{cm}\cdot\text{min}$). Nearly all of the demineralization rates (except one high value at 42 $\mu\text{S}/\text{cm}\cdot\text{min}$) fall within this narrow band of rates. It is note-worthy that the rates of the last several cycles were well within the shaded area, indicating that no statistically significant deterioration in membrane performance was detectable in the operation of the laboratory ED unit during the extended testing. These plots describing overall demineralization performance clearly indicate no deterioration of treatment capability of the ED system over the 20-hour operating period, providing evidence of good ED cell stability.

With regard to cell stability, the cyclic cell voltage before cleaning in place shows repeatability (a swing of about 0.5 volt) during the constant current (0.6 amp) operation over the 30 hours of testing. The repeatability of the cell voltage suggests membrane resistance remained stable during each recharging of the feed during the testing. Generally, a swing of less than one volt is considered well within desirable operating conditions. Following the cleaning in place (CIP), the voltage swing was also repeatable but ranged about 1 volt. The increase in voltage swing after the cleaning in place is likely a result of the operation of the concentrate without pH adjustment as shown in **Figure 10.19**, where the pH was maintained in a narrow range from about 8.5 to 8.8. Data analysis indicated that concentrations of soluble calcium remained below 20 mg/l, while soluble magnesium increased to above 90 mg/l until after the CIP event when magnesium concentrations fell to below 10 mg/l. The lack of continual increase in soluble calcium and the sudden decrease in magnesium observed after the cleaning event suggests some precipitation of these constituents may have occurred during the 30 hours of operation. More testing would be needed to determine whether these losses from the soluble phase led to any significant direct deposition of calcium or magnesium scales on the membrane. Whether or not this occurred did not affect the overall performance of the process during the testing period.

In general, the data from extended ED unit testing on CBM produced water indicated minimal evidence of process fouling; the ED unit exhibited no significant increase of cell resistance in the longer term experiments. The cell resistance in this 30-hour run exhibited a consistent pattern in each batch of 70 minutes duration. This suggests that membrane cleaning intervals can safely be extended to periods of much greater than 30 hours. The data also show that a field-scale system target voltage drop of less than 1.2 can be achieved so that power consumption can be kept at acceptable levels for a given product recovery. In addition, desalting (demineralization) efficiencies of greater than 70% were observed during the entire membrane-integrity test run.

ECONOMIC ANALYSIS

Using the levels of performance achieved with the integrated laboratory electro dialysis treatment system, the prototype testing information was submitted to Ameridia (Division of Eurodia Industrie), the manufacturer of commercial electro dialysis systems and the manufacturer of the laboratory ED unit used in this project. Also submitted to Ameridia were the detailed characteristics of the Sheridan CBM produced water and a list of recommended conditions related to field performance requirements and scale to use in the vendor estimation of costs. Pre-

treatment and post-treatment processes were sized and estimated using the GRI-ProWCalc™ produced water calculation cost model developed by GTI in previous produced water management projects (Lawrence, et al., 1995). The base case of treatment that was evaluated is described below:

Base Case Conditions

Components of the Integrated Process	<ul style="list-style-type: none">• Prefiltering• Continuous Flow Electrodialysis• Post Treatment – Equilibration with Limestone
Flow =	10,000 bbl/day
Influent TDS =	3,000 mg/l
Treated Water TDS =	1,000 mg/l
Water Recovery for Beneficial Use =	> 90%
Nature of ED Design	Modular, Mobile, Multi-site Use

Assumptions used in the economic analysis are as follows:

Interest Rate, %	6
Equipment Life, yrs	15
Stream Factor, %	90
Electricity Cost, \$/Kw-hr	0.06
Base Year	2007 Dollars (4Q)

Cost information that was obtained from Ameridia for a continuous flow commercial electrodialysis modular skid system applied to CBM produced water is described in **Table 10.12** for five cases (including the Base Case). In all cases, the commercial ED units were designed to achieve greater than 93% water recovery for beneficial use. In the Base Case, it was assumed that TDS levels would be reduced from 3,000 to 1,000 mg/l in the treated CBM produced water. Cases A1 and A2 represent variations in the influent and effluent levels of TDS handled by the ED system while Cases B1 and B2 represent varied scale (in terms of flow of produced water processed per day) in the commercial application of ED technology to CBM produced water streams. Capital requirements of skid-mounted modular ED units seem modest; for the Base Case, only \$1.3 million of capital expenditure would be required to treat 10,000 bbl/d.

Table 10.12: Costs for Commercial Scale Electrodialysis Units (Ameridia, 2007)

Parameter	Cases for Costing Commercial Scale Electrodialysis Units				
	A1	A2	Base	B1	B2
Flow, bbl/d	10,000	10,000	10,000	50,000	2,000
Flow, gpd	42,000	42,000	42,000	2,100,000	84,000
TDS Influent, mg/l	5,000	3,000	3,000	3,000	3,000
TDS Treated, mg/l	2,000	2,000	1,000	1,000	1,000
Recovered Water, gpd	393,000	404,700	393,000	1,965,000	78,600
Produced Brine, gpd	32,300	20,500	32,300	161,500	6,500
TDS Brine, mg/l	46,400	33,800	34,400	34,400	34,400
Water Recovery, %	93.6	96.4	93.6	93.6	93.6
Number of Stacks	2 EUR40B-500	1 EUR40B-732	2EUR40B-815	10EUR40B-822	2EUR40B-163
Capital Investment	\$720,000	\$670,000	\$870,000	\$3,720,000	\$450,000
Operating Costs, \$/day					
Electricity (@ 6 cents/kWh)	\$147	\$145.7	\$123.3	\$616.1	\$24.7
Sulfuric Acid (@ \$60/ton)	\$50.2	\$17.4	\$29.1	\$163.1	\$5.6
Membranes/ Electrodes Replacement	\$161.1	\$138.1	\$305.5	\$1,517	\$66.5
Antiscaling Agent (@ \$1,000/ton)	-	-	-	-	-
Total Operating Cost	\$358.3	\$301.2	\$457.9	\$2,296	\$96.8

A breakdown of costs calculated for the treatment system for the Base Case (10,000 barrels per day flow rate) are shown in **Table 10.13**; costs in this table are given in cents per barrel. For the Base Case, the total cost for the electrodialysis process is approximately 7 cents per barrel and the cost for the entire system (including prefiltering and post-treatment) is approximately 9 cents per barrel. As seen in the table, electrodialysis (ED) represents the bulk of the costs, amounting to nearly 80% of the total and the costs for ED seem to be mostly driven by operating costs, largely controlled by the cost of membrane and electrode replacement followed by electricity.

This cost is substantially less than the costs estimated for reverse osmosis (\$0.25 - \$0.50/bbl) and high efficiency vapor compression evaporation (\$1.50 – \$2.50/bbl) (Doran and Leong, 2001; Lawrence, et al., 1995).

Table 10.13: Cost Breakdown for Base Case Application of the CBM Produced Water Treatment System.

Component	Unit Costs, Cents per Barrel*		
	Capital	Operating**	Total
Prefiltration	0.6	0.4	1.0
Electrodialysis	2.4	4.6	7.0
Post Treatment (Equilibration with Limestone)	0.6	0.5	1.1
Total System	3.6	5.4	9.1

* Break even costs (without profit).

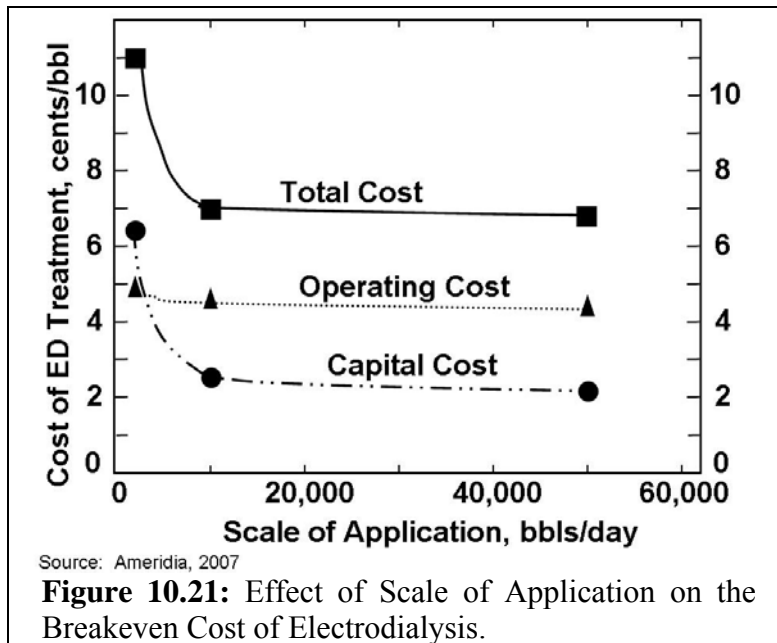
** Includes chemicals and electricity. Does not include labor provided by the host company.

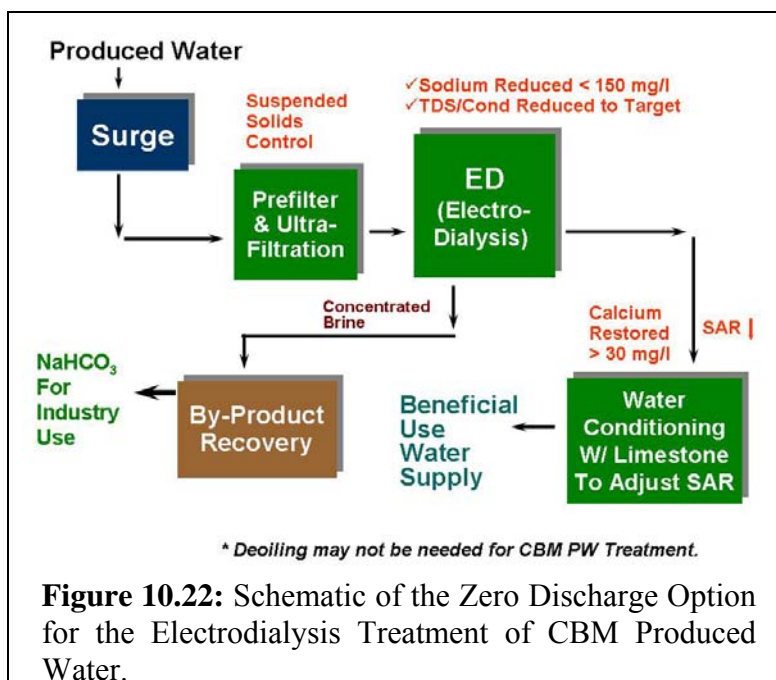
Analysis of cost of ED versus scale of application was also performed; results are shown in **Table 10.14**. Cost versus scale of application for the ED process component of the system is shown in **Figure 10.21**. This graph shows that the ED process reaches economy of scale at around 10,000 bbl/d flows. This will be highly useful since many CBM fields in the Powder River Basin have water gathering systems that approximate or exceed that level of flow. These estimates are for the ED process alone; costs of the water processing system would add about 2 cents for the pretreatment and post-treatment processing as shown in **Table 10.13** for the Base Case (10,000 bbl/d).

Table 10.14: Breakeven Commercial Costs Versus Commercial Scale of Application for Electrodialysis

Scale of Application, bbl/d	Total Capital, \$	Cents per Barrel		
		Capital	Operating	Total
2,000	450,000	6.2	4.8	11.0
10,000 (Base Case)	870,000	2.4	4.6	7.0
50,000	3,720,000	2.1	4.6	6.7

Calculation of the total cost of water management would have to include the disposal of the concentrate stream. Analysis of the concentrate stream generated from the laboratory ED unit treatment of actual produced water showed that the solids contained in this stream are comprised of sodium bicarbonate at a purity greater than 97% for the waters that were tested. The concentrate stream is also only 8% of the flow of the influent CBM produced water stream. If the concentrate stream is to be disposed of in commercial evaporation pits in the Powder River Basin, it is estimated that the cost per barrel of concentrate would be approximately \$2.00/bbl, including transportation (Boysen, 2002). When all costs are normalized for influent CBM produced water flow, concentrate disposal would add about 18 cents to amount to a total water management cost of approximately 27 cents per bbl. This cost may be reduced if the commercial evaporation of the concentrate stream leads to the by-product recovery of a high-purity sodium bicarbonate chemical that can be sold to nearby power plants or industry. If by-product recovery of sodium bicarbonate can be economically achieved, and if all of the product water is utilized as a beneficial use stream, the CBM produced water treatment system could be considered to be virtually zero-discharge as conceptually depicted in **Figure 10.22**. The technical and economic feasibility of this configuration would require testing at the pilot scale at several locations in the Powder River Basin to be properly evaluated.





CONCLUSIONS

Results from this work indicate that the electro dialysis process has the potential of providing a cost effective solution in the conversion of CBM produced water to beneficial use water streams in many areas of the Powder River Basin. Based on the performance of the integrated laboratory ED prototype, it was estimated that breakeven treatment costs could be as low as 11 cents per barrel for applications with produced water flows of 10,000 bbl/d or more.

Specific results from the lab show that all of the performance goals for prototype testing have been achieved. Analysis of the composition and properties of CBM produced water sampled from nine locations in the Powder River compared to the specifications required for beneficial use of treated water led to recommendations that the following treatment system be utilized: 1) Pretreatment with a cartridge filter to control suspended solids; 2) Partial demineralization of the water using electro dialysis; and, 3) Post treatment consisting of equilibration of the water with calcium carbonate to restore calcium concentrations to the water. Results indicated that a low-cost configuration for the ED system can consist of a non-selective membrane as the cation membrane, a sodium bicarbonate concentrate stream maintained at over 50,000 mg/l TDS, and a current density of 4.00 mAmps/cm². This setup seemed to provide good performance for the ED system. In a number of runs, approximately 90% desalination was achieved with modest energy inputs of 0.18 kWh/lb of NaCl removed or less; this was observed when the conductivity of the product water was reduced to very low levels (< 300 μS/cm). Where only partial desalination is required to a treatment endpoint of 1,000 to 1,500 μS/cm, the required energy inputs can be reduced to levels as low as 0.11 kWh/lb of NaCl removed. Post treatment that employed passive equilibration with calcium carbonate in the form of powder or limestone was able to reduce SAR values from 8.3 to 3.3, without significantly raising the conductivity of the final water product. In terms of ease of use and cost effectiveness, passing the water stream over a bed of limestone is the recommended post treatment method.

Using the simple pretreatment processing identified in this project, the laboratory ED unit was operated on actual CBM produced water showing minimal degradation to the membranes of the stack cells over an extended 20-hour run before any cleaning was applied. In terms of overall performance, the laboratory ED process showed good stability in treating actual CBM produced waters. Based on these results, the ED technology can be considered a viable option for future scale-up and field piloting within the Powder River to achieve economical processing of CBM produced waters for the generation of beneficial use waters.

RECOMMENDATIONS FOR FUTURE RESEARCH

This effort has shown that electro dialysis (ED) is potentially capable of achieving the levels of sodium removal and demineralization required for economical conditioning of CBM waters for beneficial use, including irrigation of clayey soils that often require reduction of SAR values in water from over 60 to less than 6. Preliminary costs appear reasonable, though the economic analysis extrapolated performance levels observed at the modest laboratory size to a conceptual commercial facility operated at full scale. Clearly, more development is required to verify performance at a commercial scale under actual field conditions. Specifically, a number of recommendations are offered by the investigators for future development of the ED treatment system for field application. First, it is recommended that a continuous-flow, hybrid ED process train (consisting of microfiltration, electro dialysis, and contact with limestone) be tested in the field over prolonged durations under actual field conditions to determine long term stability and to develop automatic controls to deal with variations in influent salts concentrations, pH, temperature, and other significant performance parameters. In the treatment of CBM produced waters with less than 3,000 mg/l TDS, it is suggested that only one ED stage may be needed to achieve the partial reductions in TDS to reach a suitable end use water quality. Prolonged field trials should also be accompanied by the development of clean-in-place (CIP) protocols to prevent premature fouling and maximize the performance and operational life of the ED membranes. Since the salt composition of the produced water is dominated by sodium bicarbonate, it is recommended that an engineering systems analysis be conducted on the combination of ED demineralization with further desalting and drying of the concentrate stream to produce a high-grade soda ash product that can potentially be reused by industry within the Rocky Mountain Region; such a hybrid process combination could result in a zero-discharge option for CBM produced water management. Lastly, it is recommended that research continue on the testing of the latest commercially-available membranes that achieve the greatest salt removals per unit of energy delivered with the goal of achieving the required demineralization at energy inputs at or less than 0.1 kWh/lb salts removed. This accomplishment would achieve further significant cost improvements in the application of membranes to the conditioning of CBM produced water for beneficial use purposes.

ACKNOWLEDGMENTS

In the performance of this project, a number of organizations and individuals contributed to the success of the laboratory research effort. Special recognition is extended to Mr. Danny Bar of the Ameridia Division of Eurodia Industries for his guidance in the design of the laboratory ED prototype and in the conceptual scaleup and costing of ED units envisioned for CBM produced

water demineralization. Appreciation is extended to Stephanie LeClair (currently at the University of Michigan at Ann Arbor) in running the long term stability tests. Dr. Seth Snyder of Argonne National Laboratory was project liaison. Appreciation is also extended to Dan Arthur and Heidi Kaiser of ALL Consulting for providing logistical support in collecting field samples and site information.

Special thanks go to Mr. Brian Hodgson of Marathon Oil and Dr. Jeffrey Cline of Anadarko for providing the industry support that was needed to collect samples, obtain information on the nature of CBM produced water management practices and procure large aliquots of water required to evaluate the laboratory electro dialysis prototype.

REFERENCES

- Ameridia, 2007.** Personal Communication to Obtain Cost Estimations from D. Bar of Ameridia, September – November.
- AWWA, 2004.** Water Desalting Planning Guide for Water Utilities, John Wiley & Sons Inc.
- Boysen, R., J. Boysen, J. Boysen, and D. Boysen. 2003.** Natural Gas Produced Water Management Decision Tree Model. GRI Report No. GRI-03/0072.
- Dallbauman, Liese and Sirivedhin, Tanita. 2003.** “Reclamation of Produced Water for Beneficial Use.” Separation Science and Technology, 40:1, 185-200.
- Doran, G. and L.Y.C. Leong. 2000.** Developing a Cost Effective Environmental Solution for Produced Water and Creating a “New” Water Resource. U.S. Department of Energy Report DOE/MT/95008-4.
- Hayes, T. 2004.** “The electro dialysis alternative for produced water management.” GasTIPS, 10(3):15-20.
- Hayes, T. and D. Arthur. Oct. 12, 2004.** “Overview of Emerging Produced Water Treatment Technologies.” 11th International Petroleum Environmental Conference, IPEC Proceedings.
- Hergert, G.W.; Knudsen, D., Aug. 1997.** Irrigation Water Quality Criteria, publication G77-328-A, Cooperative Extension, Institute of Agriculture and Natural Resources, University of Nebraska – Lincoln. <http://www.ianr.unl.edu/pubs/water/g328.htm> (accessed Sept 2003)
- Lawrence, A.W., et al. 1998.** Evaluation of Results from Lysite Wyoming Produced Water Treatment System Field Experiment. GRI Report No. GRI-07/0287.
- Lawrence, A.W., et al., 1995.** GRI ProWCalc : Produced Water Calculation Cost Model User’s Manual. GRI Report No. GRI-07/0287.

PUBLICATIONS TO DATE

- Hayes, T., P. Moon and S. Snyder. 2006.** “Integrated Electrodialysis for Cost Effective CBM Produced Water Demineralization.” Abstract Submitted to COGA-RMAG Conference. Denver, CO, August 7-9.
- Hayes, T., P. Moon, and S. Snyder. 2006.** “Transforming CBM Produced Water to Beneficial Use Through Electrodialysis Processing,” Technical Poster at the Colorado State University Produced Water Workshop, Fort Collins, CO, April 4-5.
- Moon, P., Hayes, T. and, LeClair S. 2008.** Electrodialysis Treatment of Produced Water from the Powder River Basin for Beneficial Use. To be submitted to Separation Science and Technology.
- Moon, P., Snyder, S., and Hayes, T., June 11-13, 2006.** Integrated Electrodialysis Process for CBM Produced Water Treatment, Paper # 107248, Rocky Mountain Section of American Association of Petroleum Geologists, Billings, Montana, <http://www.aapg.org/>, Rocky Mountain Section of AAPG Conference (June 2006).

CONFERENCES

- Hayes, T., D. Arthur, 2005.** Treatment Technologies for Coalbed Methane Produced Water Management. Rocky Mountain Section – AAPG, Jackson Hole, WY, September.
- Hayes, T., Gowell, S., Moon, P., and Snyder, S. Oct. 17-20, 2006.** Electrodialysis Treatment of Coal Bed Methane Produced Water: Application Issues and Projections of Costs, International Petroleum Environmental Conference, San Antonio, Texas.
- Hayes, T., Moon, P., and Snyder, S., April 4-5, 2006.** Transforming CBM Produced Water to Beneficial Use Through Electrodialysis Processing, Produced Water Workshop, Fort Collins, Co., <http://www.cwrri.colostate.edu>, Produced Water Workshop.
- Moon, P., S. Snyder, and Hayes, T., Aug. 8, 2006.** “Integrated Electrodialysis for Cost Effective CBM Produced Water Demineralization”, Presented at CERI Frontiers in Global Energy Session, RMAG Conference, Denver.
- Moon, P., Snyder, S., and Hayes, T., Oct. 17-20, 2006.** Integrated Electrodialysis Membrane Stability Results for Cost-Effective CBM Produced Water Demineralization, International Petroleum Environmental Conference, San Antonio, Texas.

CHAPTER 11: Standardized Testing of Coalbed Methane Water-Treatment Systems

John Wheaton and Shawn Kuzara¹

EXECUTIVE SUMMARY

One of the primary expenses incurred by coalbed methane (CBM) producers is disposal of production water. In the Powder River Basin, the production water is relatively good quality, and considered a resource for livestock operations (Wheaton and Donato, 2004). However, the high sodium content makes the water undesirable for discharge on ground surface or to surface-water bodies. If viable treatment systems can be designed and successfully deployed, operating costs for CBM producers will decrease, and options for utilization of the water resource will increase. Water-treatment technologies that are being proposed for reducing sodium concentrations in coalbed-methane production water include ion exchange, electro-dialysis, membrane filtration and distillation. Numerous techniques with varying claims for treatment of production water are currently being advertised, and additional systems will no doubt be introduced. However, given the high stakes, CBM operators need objective, comparable data to accurately evaluate and select an option and water-treatment companies need to be able to test and refine their methods under field conditions. The economics, energy requirements, and volume of waste water that must ultimately be disposed will vary according to treatment system and manufacturer specifications. Treatment methods will become a valuable option for CBM-production water management if they are economically viable, produce the target water quality, and create waste that is within acceptable limits. The actual performance of advertised treatment systems need to be documented to allow CBM operators to compare and choose the best option for their particular setting.

A field laboratory to test water-treatment systems has been designed and built under Task 8 and is ready for deployment. Originally intended to be an office trailer unit, the design has been altered and was built based on a pickup camper design with a small storage trailer. This will allow greater flexibility in applications. Several companies have voiced interest in using the unit. One company is preparing to test a high-pressure reverse osmosis system. Another company is ready to test an ion-exchange system and is planning to utilize this field laboratory for the first test. The electro-dialysis unit being designed by Argonne and GTI (Task 2 of this overall project) is intended to be tested using this unit for their field version. However, funding has not yet been received for field test of the ED unit.

Originally planned solely to evaluate water treatment systems, other water-management applications for the field laboratory are now apparent. The unit can be deployed to provide water-budget monitoring for irrigation applications (such as in Task 5 of this project) and for injection of CBM water if future funding of work initiated under Task 9 of this project is received. A company that has developed a downhole separator and pump has submitted a letter committing to test their system if funding becomes available.

¹ Montana Bureau of Mines and Geology, Montana Tech of The University of Montana, 1300 North 27th Street, Billings, MT 59101. Correspondence: jwheaton@mtech.edu.

PURPOSE

The purpose of Task 8 was to establish procedures and design and build a field laboratory for comparative evaluation of treatment technologies that are offered for reducing sodium content of coalbed-methane-production water.

To accomplish this goal a mobile facility was designed and constructed to test proposed treatment units under field conditions. The facility will allow correlation between performances of treatment units from different manufacturers, and during the testing phase allow manufacturers to fine tune their systems to the demands of coalbed methane. Basic longevity of treatment systems will also be documented to allow gas companies to choose performance based on comparable testing. Testing will involve beta units and final productions units would likely be improved versions.

This report describes the need for testing, approach that will be used in testing, and the operating procedures for the testing facility. The test method includes a list of the critical test parameters, as provided by the Montana Department of Environmental Quality.

This task was designed with 3 subtasks: 1) design and construct the mobile testing facility; 2) deploy the facility to a test site; and 3) apply the testing facility to treatment systems. The facility is completed and ready to be deployed to a test site. The first testing is currently scheduled for early spring, 2008.

The facility consists of a camper-style shell for a pickup truck, a small cargo trailer and instrumentation. The instrumentation allows continuous measuring and recording of water flow rates, specific conductivity, water temperature, sodium concentration, pH and oxidation/reduction potential. The facility is powered by a portable generator, solar panels and a power-take off from the pickup truck and it can be plugged in to a standard 120V outlet.

BACKGROUND

One of the primary expenses incurred by coalbed methane (CBM) operators is disposal of production water. In the Powder River Basin the production water is relatively good quality, and considered a resource for livestock operations. However, the high sodium content makes the water undesirable to discharge on ground surface or to surface-water bodies. If viable treatment systems can be designed and successfully deployed, operating costs for CBM producers will decrease, and options for utilization of the water resource will increase. Water-treatment technologies that are being proposed for reducing sodium concentrations in coalbed-methane production water include ion exchange, electro-dialysis, membrane filtration and distillation. Numerous techniques with varying claims for treatment of production water are currently being advertised, and additional systems will no doubt be introduced. However, given the high stakes, CBM operators need objective, comparable data to accurately evaluate and select an option. The treatment success and volume of waste water that must ultimately be disposed will vary according to treatment system and manufacturer specifications. Treatment methods will become a valuable option for CBM-production water management if they are economically viable, produce the target water quality, and create waste that is within acceptable limits. Providing

actual performance data from advertised treatment systems will allow CBM operators to compare and choose the best option for their particular setting. Providing a test facility including appropriate water supply will allow water-treatment companies to fine tune and improve their methods prior to putting them online in CBM-production.

In Montana, treatment facilities are permitted through the Department of Environmental Quality (MT DEQ). Staff from MT DEQ provided the following list of requirements that must be met in order to permit a CBM-water treatment plant.

- Expected discharge water quality
- Name of receiving water
- Ambient water-quality data of receiving water
- Volume of waste water from treatment plant and ultimate disposition
- Line drawing of water flow through plant with water balance values
- Reagent additions (type, purpose, volume)
- Monitoring equipment (type, location, purpose)
- Blending system and whether it is automatic or manual
- In-line sensors within the plant
- For a new facility, the sampling and monitoring plan
- Anticipated quality of effluent water from the plant

The primary water-quality parameters of interest are electrical (or specific) conductivity and sodium concentration. Secondary parameters include: fluoride, bicarbonate, ammonia, total dissolved solids, total nitrogen, total phosphorous, selenium, total and dissolved iron.

The field-testing laboratory is designed to continuously measure the primary water-quality parameters, water budget and additional water-quality parameters that are of interest in helping evaluate the treatment process. The secondary parameters will be measured in laboratory analyses of samples collected during the testing. During tests of treatment systems with the field laboratory, sodium concentration, specific conductivity, pH, ORP, water temperature and flow rates of the input or raw water supply and the output of treated water will be continuously measured. The quantity of waste water will be calculated as the difference and the quality of the waste water will be measured by laboratory analysis.

DESCRIPTION OF FIELD LABORATORY

The testing facility description is broken into three sections: 1) Laboratory and trailer; 2) flow measuring instruments; and 3) chemical instruments.

Laboratory and trailer

The field laboratory shell was specifically designed for this purpose and custom built in Kalispell, Montana. The field laboratory has been designed to maximize open space that can allow an enclosed lab/office and still provide ample secure storage for equipment (**Figures 11.1 and 11.2**). The field laboratory consists of a slide-in pickup truck camper shell equipped with counter space, work space, storage space for clean equipment such as computers, a simple

gravity water system for cleanup, heater and electrical hookups (**Figures 11.3, 11.4 and 11.5**). Jacks on each of the four corners allow the unit to be easily removed from the pickup, lowered to supports and left at the test site as needed. A single electrical plug connects the camper to the pickup when fully mounted. When removed from the pickup, the laboratory is self-contained and secure with propane, 12V and 120V (low amp) electrical outlets, wide walk-in door and numerous small access ports. All windows, ports and the walk-in door are locking.

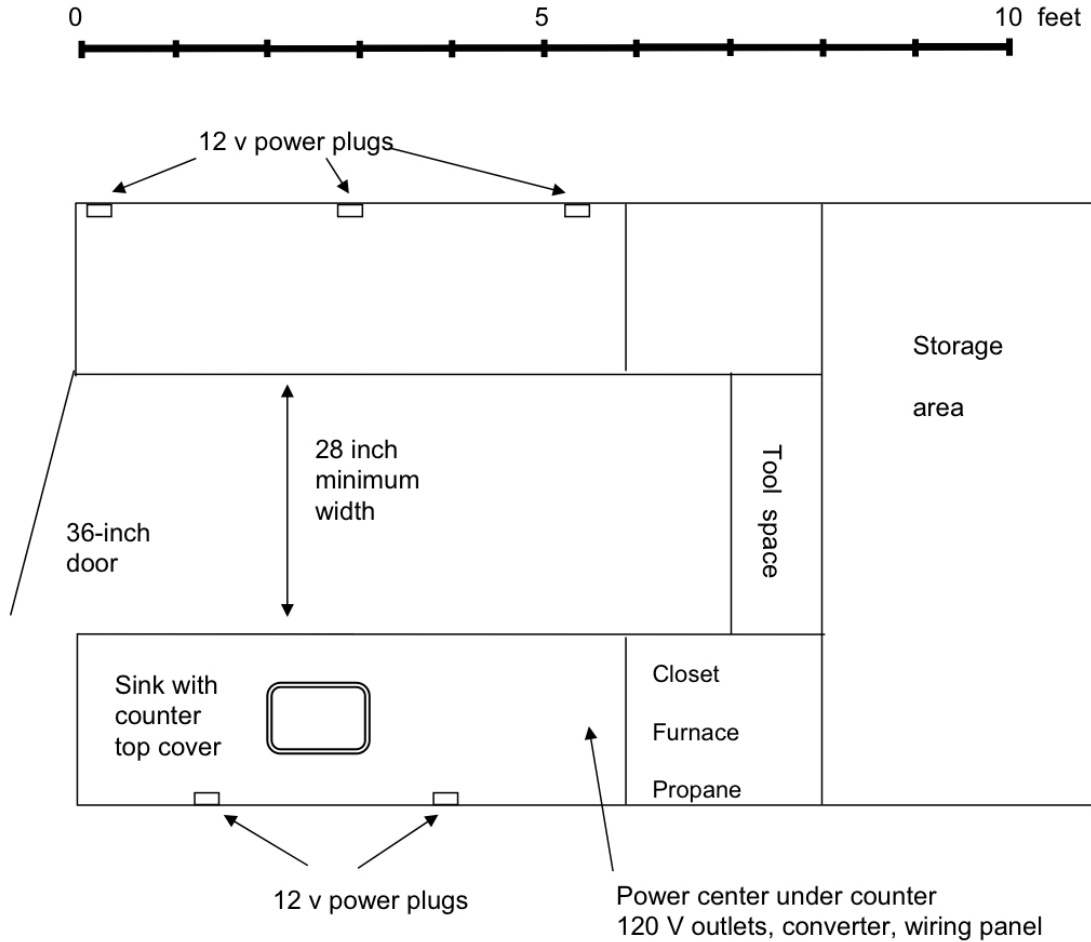


Figure 11.1: Floor plan for primary treatment testing facility.

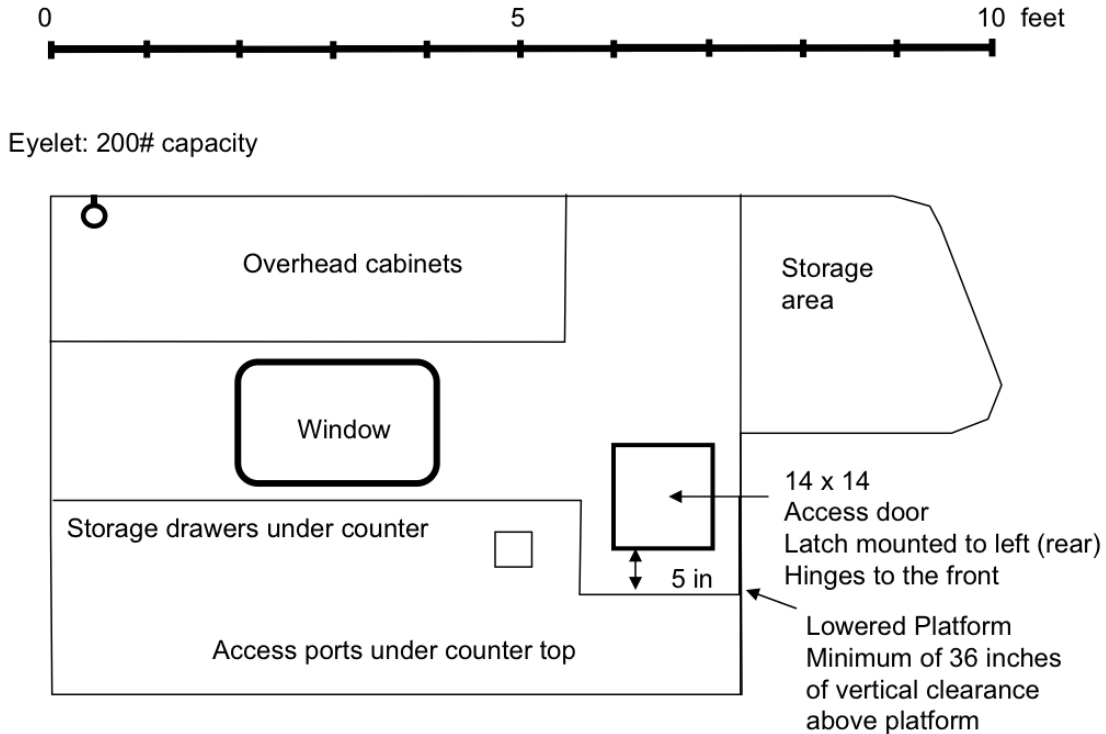


Figure 11.2: Schematic of interior, left (drivers) side of treatment testing facility.

The interior of the laboratory includes closets, drawers, open storage area and counters. Closed storage space allows tools to be stored in specific locations, office supplies in another, separated from testing and sampling equipment. Organization of the space allows efficient operation of the facility. The counter top on one side is used as a desk for computer and dataloggers (**Figure 11.4**). On the other side, the counter top (with sink) is used for processing water-quality samples (**Figure 11.5**). Water samples are filtered, acidified, and sealed for transport to the analytical laboratory. Alkalinity titrations, and other analyses appropriate for field laboratories can be performed as needed. Under field conditions, clean sample processing areas are crucial for successful analysis. The Powder River Basin is notoriously dusty and presents challenging conditions for water-quality sampling. Work space that is protected from the elements greatly improves data quality.

A small standard utility trailer was purchased and will be used for on-site storage as needed and will allow transportation of items that should not be transported in the laboratory space such as a gasoline generator. The trailer is equipped with a fold-down (or ramp) style rear door. Tie-down eyelets have been installed for securing cargo during transit. Small jack stands are used for stability and safety when loading and unloading the trailer. Like the field laboratory, the cargo trailer is fully locking, including an axle chain for security.

Flow measuring instruments

To evaluate a water-treatment unit, the quantity and quality of water coming into and out of the unit must be measured continuously. Water used to regenerate resins or flush membranes can be measured as the difference between inflow and outflow. Two full-pipe flow meters with data

loggers will be used to quantify the water flow rates. The sensors are GF Signet, Model 2536, Rotor-X, paddle-wheel meters providing a full range of flow measurement capability from 0.2 gallons per minute to 200 gallons per minute (**Table 11.1**). Pictures of a sensor being tested in the office are shown in **Figures 11.6 and 11.7**. The sensors mount in pressure-sealed fittings designed for pipe sizes of 0.5 inches, 1.0 inches and 2.0 inches.

The flow meters are connected to the pulse counting channels of a Campbell Scientific Inc. CR800 datalogger. The datalogger can collect data at intervals as closely spaced as 1 second. At normal data collection intervals of 1 per hour, the storage capacity is sufficient for several months. The treatment unit would not, however, be left unattended for durations longer than about 1 or 2 weeks, depending on the level of function. All dataloggers will be downloaded to the computer on each site visit. The datalogger and sensors are powered by a 12V battery mounted in the datalogger housing. The battery in turn is recharged either by a solar panel or from the field laboratory circuit.

The unit is stocked with a variety of plumbing supplies to allow connection of the sensors to the water flow streams.



Figure 11.3: Exterior photograph of testing facility.



Figure 11.4: Interior photograph of testing facility showing data logger bench.



Figure 11.5: Interior photograph of testing facility showing water-sample preparation area.

Table 11.1: Flow meter specifications

Flow meters

Rotor - X Low-Flow Paddle-Wheel Flow Sensor with Polypropylene body, titanium shaft 1/8"		Flow range (gpm)	Flow range (gpm)	Flow range (gpm)
Installation Fittings for 0.5 inch, 1 inch, 2 inch pipe		0.5 inch pipe	1 inch pipe	2 inch pipe
minimum velocity (ft/sec)	0.3	0.2	0.7	10
maximum velocity (ft/sec)	20	12	50	200
Repeatability	0.5% of full scale			
Datalogger: Campbell Scientific Inc, CR800				
Power supply: 12V, from datalogger with solar panel or take off from testing laboratory				

Manufactured by GF Signet, Model 2536



Figure 11.6: Assembly of flow meter.



Figure 11.7: Office testing of flow meter.

Field chemistry instrumentation

The effectiveness of water-treatment systems will be measured on a flow-dependent basis using field sensors mounted in the raw water supply and the treated water outflow. Water-quality sensors include, specific conductivity, water temperature, oxidation-reduction potential (ORP) and ion-specific electrodes for pH and sodium.

Access ports allow electrical leads from sensors and data loggers to run from the treatment unit into the field laboratory. A datalogger and a computer are housed within the laboratory. Monitored parameters include: source-water flow rates; clean treated-water flow rates; specific conductivity, temperature, pH, ORP and sodium concentration into and out of treatment system. All parameters will be monitored on a volumetric basis with time-date stamps on the data. Water-quality samples will be collected from the inflow water, treated outflow water and the waste stream.

The field sensor package and datalogger system were designed and manufactured specifically for this project by Eureka Environmental Engineering (Austin, TX). The measured parameters are listed in **Table 11.2**. The package includes two identical multiprobes (**Figures 11.8 and 11.9**). Each multiprobe has sensors to measure water temperature, specific conductivity, pH, ORP and sodium concentration. Sodium is measured using an ion-selective electrode. The multiprobes

contain an internal datalogger and control unit. Each has an external lead to allow connection to external power supplies and computer for downloading data.

During testing, the multiprobes will be installed in either a closed or open through-flow cell so one sensor is constantly submersed in the raw-water-supply stream and the other sensor in the treated-water-discharge stream. The electrical leads run through access ports in the laboratory facility and connect to the power supply and computer system. Instrument calibration will be performed prior to each tests and again during the regular visits to the test site. Calibration records will be maintained at the site and will be used in interpretation of test data.

PLANS FOR DEPLOYMENT

Subtasks 2 and 3 were intended for the purpose of deploying the facility to a test site followed by application and documentation of an experimental treatment system. Due to timing and weather challenges, the facility was not deployed during the duration of this project. One challenge, the ion selective sodium sensor, was manufactured in Great Britain and delivered in late October, 2007, just prior to the ending date of this project and at the beginning of winter in Montana. Plans have been made for deployment during the spring, 2008.

Several sites have been volunteered by landowners that are not CBM-production wells but that do have the same water quality. Laboratory data from three examples of private or research wells in the Powder River Basin are listed as **Appendix 11.A**. Additional data for these and other area wells are available from the Montana Ground Water Information Center (<http://mbmaggwic.mtech.edu/>). The three wells listed in **Appendix 11.A** have total dissolved solids (TDS) concentrations of less than 600 mg/L to nearly 1,800 mg/L, sodium adsorption ratios (SAR) of 34 to 62 and low concentrations of sulfate. These are typical values for CBM-produced water which has average TDS concentrations of 1200 mg/L, SAR values averaging 46, and the average sulfate concentration is 4.5 mg/L (Wheaton et al., 2007). Research and private water wells can be utilized for research purposes without putting a CBM producing company in dependence on a technology that is under primary field testing.

Table 11.2: Water quality instrumentation specifications.

Water quality parameters

Parameter	Range	Accuracy	Resolution
Temperature	-5°C – 50°C	±0.08°C	0.01°C
Specific Conductance	0 – 100 mS/cm	±0.5% of reading ± 0.001	4 digits
pH	2 – 12 units	±0.2 units	0.01 units
ORP	-999 - +999 mV	±20 mV	1 mV
Ion Selective Electrode (Sodium)	0.2-20,000 ppm		
Power supply: 12V, Solor Panel and Voltage Regulator, or take off from testing laboratory			
Nema 6 Enclosure, Waterproof/Corrosion Resistant			
Datalogger: Internal Eureka Manta			

Manufacturer: Eureka Environmental Engineering



Figure 11.8: Water quality multiprobe.



Figure 11.9: Office testing of water quality multiprobe.

The first deployment of the unit will be for a small-scale test designed by Montana Bureau of Mines and Geology (MBMG). This test will serve two purposes; to ensure the testing facility operates as designed and intended, and to give a preliminary test of a treatment medium of interest by MBMG. The test will be carried out at a well near Birney, Montana (site ID 198319 in **Appendix 11.A**).

CERI team members from Argonne National Laboratory have a treatment design that we hope will be the first system tested by this new facility. This design, using electro dialysis processing is innovative and if proven in a field test could make a significant improvement in water treatment options. This system is described in detail by Hayes and Moon in this volume.

Individual tests are expected to last for one month. During that time, treated water will be discharged for stock use and waste water will be collected in an evaporation pit. The above parameters will be monitored and data recorded continuously. During the tests, laboratory water-quality samples will be collected from the treated and waste streams and analyzed for major and minor ions.

An ion exchange system designed by Purotech is expected to be tested during the spring, 2008. Communication has been ongoing with staff of Puritech and Purolite to coordinate a test. To establish the testing facility, the testing costs for this first unit are included in this project budget. Thereafter, the facility is expected to be self-supporting based on user fees. The electro dialysis unit being designed by Tom Hayes and Paula Moon under this overall project is planned to be tested eventually.

In addition to standard water treatment research such as the ED unit being developed by Argonne and GTI (Task 2), we are looking at other water treatment approaches such as irrigation. This unit can be deployed and provide significant assistance to Dr. Terry Brown in his irrigation work under Task 5.

This unit was designed for long-term applications to CBM research. Future deployments are expected to include providing a clean work space and field laboratory for collecting methanogenic microbes for methane generation research. Funding for microbial research is being pursued by Argonne lab and others in hope of furthering methane reserves.

Once equipped, the unit will also be available to monitor CBM-produced water injection tests in Montana. Dr. David Lopez identified several key injection intervals (Task 9 of this project). Due to the nature and shape of these channels sandstone units, research in to the water-pressure response during injection will be critical to fully develop these zones.

REFERENCES

Wheaton, J., and Donato, T., 2004. Coalbed-methane basics: Powder River Basin, Montana: Montana Bureau of Mines and Geology, Informational Pamphlet 5, 25 pgs.

Wheaton, J., Redish-Kuzara, S., Donato, T.A., Hammer, L., 2007. 2006 Annual coalbed methane regional ground-water monitoring report: Northern portion of the Powder River Basin: Montana Bureau of Mines and Geology Open-File Report 556, 95 p., 3 sheets.

Final Report: Produced Water Management and Beneficial Use

Appendix 11.A

Ground-Water Information Center Water Quality Report
Report Date: 2/11/2008

Site Name: HC#20*ON DW RANCH LAND- KENDRICK CATTLE
[Compare to Water Quality Standards](#)

Location Information

Sample Id/Site Id: 1981Q1775 / 8130	Sample Date: 9/30/1981 5:00:00 PM
Location (TRS): 08S 43E 23 CDAA	Agency/Sampler: USGS / ARS
Latitude/Longitude: 45° 7' 21" N 106° 25' 43" W	Field Number: HC#20
Datum: NAD27	Lab Date: 11/5/1981
Altitude: 3605	Lab/Analyst: MBMG / FNA
County/State: BIG HORN / MT	Sample Method/Handling: PUMPED / 3120
Site Type: WELL	Procedure Type: DISSOLVED
Geology: 125TGRV	Total Depth (ft): 342
USGS 7.5' Quad: FORKS RANCH 7 1/2'	SWL-MP (ft): NR
PWS Id:	Depth Water Enters (ft): 306
Project:	

Major Ion Results

	mg/L	meq/L		mg/L	meq/L
Calcium (Ca)	5.900	0.294	Bicarbonate (HCO3)	1,949.600	31.954
Magnesium (Mg)	2.700	0.222	Carbonate (CO3)	0.000	0.000
Sodium (Na)	727.000	31.625	Chloride (Cl)	27.400	0.773
Potassium (K)	3.100	0.079	Sulfate (SO4)	15.700	0.327
Iron (Fe)	0.090	0.005	Nitrate (as N)	0.010	0.001
Manganese (Mn)	0.004	0.000	Fluoride (F)	3.670	0.193
Silica (SiO2)	9.900		Orthophosphate (OPO4)	NR	0.000
Total Cations		32.225	Total Anions		33.248

Trace Element Results (g/L)

Aluminum (Al): NR	Cesium (Cs): NR	Molybdenum (Mo): NR	Strontium (Sr): NR
Antimony (Sb): NR	Chromium (Cr): NR	Nickel (Ni): NR	Thallium (Tl): NR
Arsenic (As): NR	Cobalt (Co): NR	Niobium (Nb): NR	Thorium (Th): NR
Barium (Ba): NR	Copper (Cu): NR	Neodymium (Nd): NR	Tin (Sn): NR
Beryllium (Be): NR	Gallium (Ga): NR	Palladium (Pd): NR	Titanium (Ti): NR
Boron (B): NR	Lanthanum (La): NR	Praseodymium (Pr): NR	Tungsten (W): NR
Bromide (Br): NR	Lead (Pb): NR	Rubidium (Rb): NR	Uranium (U): NR
Cadmium (Cd): NR	Lithium (Li): 90.000	Silver (Ag): NR	Vanadium (V): NR
Cerium (Ce): NR	Mercury (Hg): NR	Selenium (Se): NR	Zinc (Zn): NR
			Zirconium (Zr): NR

Field Chemistry and Other Analytical Results

**Total Dissolved Solids (mg/L): 1,756.190	Field Hardness as CaCO3 (mg/L): NR	Ammonia (mg/L): NR
**Sum of Diss. Constituents (mg/L): 2,745.600	Hardness as CaCO3: 25.850	T.P. Hydrocarbons (g/L): NR
Field Conductivity (mhos): 2650	Field Alkalinity as CaCO3 (mg/L): NR	PCP (g/L): NR
Lab Conductivity (mhos): 2859	Akalinity as CaCO3 (mg/L): 1599.33	Phosphate, TD (mg/L as P): NR
Field pH: 8.01	Ryznar Stability Index: 7.010	Field Nitrate (mg/L): NR
Lab pH: 8.04	Sodium Adsorption Ratio: 62.225	Field Dissolved O2 (mg/L): NR
Water Temp (°C): 13.5	Langlier Saturation Index: 0.515	Field Chloride (mg/L): NR
Air Temp (°C): 14	Nitrite (mg/L as N): NR	Field Redox (mV): NR
	Hydroxide (mg/L as OH): NR	

Notes

Sample Condition: WATER IS SLIGHTLY MURKY * VERY FINE SAND *
 Field Remarks: FILTER WITH MODERATE GRAYISH-BROWN MUD * NO SILT * NO COAL * PUMPED WELL FOR 100 MIN
 * TEST DATA WITH USGS HELENA MT *
 Lab Remarks: FU NA 752 MG/L GIVES -.1 SIGMA AND 33.3 TOTAL CATION MEQVS

Explanation: mg/L = milligrams per Liter; g/L = micrograms per Liter; ft = feet; NR = No Reading in GWIC

Qualifiers: **A** = Hydride atomic absorption; **E** = Estimated due to interference; **H** = Exceeded holding time; **K** = Na+K combined; **N** = Spiked sample recovery not within control limits; **P** = Preserved sample; **S** = Method of standard additions; * = Duplicate analysis not within control limits; ** = Sum of Dissolved Constituents is the sum of major cations (Na, Ca, K, Mg, Mn, Fe) and anions (HCO3, CO3, SO4, Cl, SiO2, NO3, F) in mg/L. Total Dissolved Solids is reported as equivalent weight of evaporation residue.

Disclaimer

These data represent the contents of the GWIC databases at the Montana Bureau of Mines and Geology at the time and date of the retrieval. The information is considered unpublished and is subject to correction and review on a daily basis. The Bureau warrants the accurate transmission of the data to the original end user. Retransmission of the data to other users is discouraged and the Bureau claims no responsibility if the material is retransmitted.

Final Report: Produced Water Management and Beneficial Use

Ground-Water Information Center Water Quality Report

Site Name: IP-06 ART HAYES

Report Date: 2/11/2008

[Compare to Water Quality Standards](#)

Location Information

Sample Id/Site Id: 2004Q0287 / 198319	Sample Date: 11/5/2003 4:30:00 PM
Location (TRS): 05S 42E 34 ABCB	Agency/Sampler: MBMG / JRW
Latitude/Longitude: 45° 21' 49" N 106° 32' 0" W	Field Number: IP-6
Datum: NAD27	Lab Date: 1/7/2004
Altitude: 3190	Lab/Analyst: MBMG / KTH
County/State: ROSEBUD / MT	Sample Method/Handling: FLOW COMPOSITE / 4230
Site Type: WELL	Procedure Type: DISSOLVED
Geology: 125TGRV	Total Depth (ft): NR
USGS 7.5' Quad: BIRNEY	SWL-MP (ft): NR
PWS Id:	Depth Water Enters (ft): NR
Project: CBMINV, CBMIP	

Major Ion Results

	mg/L	meq/L		mg/L	meq/L
Calcium (Ca)	1.480	0.074	Bicarbonate (HCO ₃)	462.100	7.574
Magnesium (Mg)	0.304	0.025	Carbonate (CO ₃)	20.100	1.080
Sodium (Na)	226.000	9.831	Chloride (Cl)	3.980	0.112
Potassium (K)	1.210	0.031	Sulfate (SO ₄)	94.500	1.968
Iron (Fe)	0.014	0.001	Nitrate (as N)	<0.5 P	0.000
Manganese (Mn)	0.005	0.000	Fluoride (F)	0.133	0.007
Silica (SiO ₂)	9.700		Orthophosphate (OPO ₄)	0.260	0.008
Total Cations		9.973	Total Anions		10.750

Trace Element Results (g/L)

Aluminum (Al):	<30	Cesium (Cs):	NR	Molybdenum (Mo):	<10	Strontium (Sr):	93.100
Antimony (Sb):	<2	Chromium (Cr):	<2	Nickel (Ni):	<2	Thallium (Tl):	<5
Arsenic (As):	<1	Cobalt (Co):	<2	Niobium (Nb):	NR	Thorium (Th):	NR
Barium (Ba):	68.400	Copper (Cu):	<2	Neodymium (Nd):	NR	Tin (Sn):	NR
Beryllium (Be):	<2	Gallium (Ga):	NR	Palladium (Pd):	NR	Titanium (Ti):	<5
Boron (B):	93.700	Lanthanum (La):	NR	Praseodymium (Pr):	NR	Tungsten (W):	NR
Bromide (Br):	95.000	Lead (Pb):	<2	Rubidium (Rb):	NR	Uranium (U):	<0.5
Cadmium (Cd):	<1	Lithium (Li):	8.640	Silver (Ag):	<1	Vanadium (V):	<5
Cerium (Ce):	NR	Mercury (Hg):	NR	Selenium (Se):	<1	Zinc (Zn):	2.620
						Zirconium (Zr):	<2

Field Chemistry and Other Analytical Results

**Total Dissolved Solids (mg/L):	585.370	Field Hardness as CaCO ₃ (mg/L):	NR	Ammonia (mg/L):	NR
**Sum of Diss. Constituents (mg/L):	819.790	Hardness as CaCO ₃ :	4.950	T.P. Hydrocarbons (g/L):	NR
Field Conductivity (mhos):	899	Field Alkalinity as CaCO ₃ (mg/L):	NR	PCP (g/L):	NR
Lab Conductivity (mhos):	965	Akalinity as CaCO ₃ (mg/L):	412.28	Phosphate, TD (mg/L as P):	0.054
Field pH:	8.66	Ryznar Stability Index:	8.669	Field Nitrate (mg/L):	NR
Lab pH:	8.76	Sodium Adsorption Ratio:	44.217	Field Dissolved O ₂ (mg/L):	NR
Water Temp (°C):	16.8	Langlier Saturation Index:	0.045	Field Chloride (mg/L):	NR
Air Temp (°C):	-10	Nitrite (mg/L as N):	NR	Field Redox (mV):	NR
		Hydroxide (mg/L as OH):	NR		

Notes

Sample Condition: CLEAR, FLOWING WELL.

Field Remarks: DRILLED IN MID 1980S.

Lab Remarks:

Explanation: mg/L = milligrams per Liter; g/L = micrograms per Liter; ft = feet; NR = No Reading in GWIC

Qualifiers: A = Hydride atomic absorption; E = Estimated due to interference; H = Exceeded holding time; K = Na+K combined; N = Spiked sample recovery not within control limits; P = Preserved sample; S = Method of standard additions; * = Duplicate analysis not within control limits; ** = Sum of Dissolved Constituents is the sum of major cations (Na, Ca, K, Mg, Mn, Fe) and anions (HCO₃, CO₃, SO₄, Cl, SiO₂, NO₃, F) in mg/L. Total Dissolved Solids is reported as equivalent weight of evaporation residue.

Disclaimer

These data represent the contents of the GWIC databases at the Montana Bureau of Mines and Geology at the time and date of the retrieval. The information is considered unpublished and is subject to correction and review on a daily basis. The Bureau warrants the accurate transmission of the data to the original end user. Retransmission of the data to other users is discouraged and the Bureau claims no responsibility if the material is retransmitted.

Final Report: Produced Water Management and Beneficial Use

Ground-Water Information Center Water Quality Report

Report Date: 2/11/2008

Site Name: IP-20 GLEN GAY

[Compare to Water Quality Standards](#)

Location Information

Sample Id/Site Id: 2005Q0296 / 105056	Sample Date: 10/27/2004 11:59:00 AM
Location (TRS): 07S 49E 16 CD	Agency/Sampler: MBMG / CWS
Latitude/Longitude: 45° 13' 11" N 105° 43' 41" W	Field Number: IP-20
Datum: NAD83	Lab Date: 12/1/2004
Altitude: 3225	Lab/Analyst: MBMG / WO
County/State: POWDER RIVER / MT	Sample Method/Handling: PUMPED /
Site Type: WELL	Procedure Type: DISSOLVED
Geology: 211LHUD	Total Depth (ft): 880
USGS 7.5' Quad:	SWL-MP (ft): NR
PWS Id:	Depth Water Enters (ft): NR
Project: CBMIP	

Major Ion Results

	mg/L	meq/L		mg/L	meq/L
Calcium (Ca)	6.300	0.314	Bicarbonate (HCO3)	778.500	12.760
Magnesium (Mg)	1.860	0.153	Carbonate (CO3)	0.000	0.000
Sodium (Na)	377.000	16.400	Chloride (Cl)	86.500	2.440
Potassium (K)	2.610	0.067	Sulfate (SO4)	<12.5	0.000
Iron (Fe)	0.050	0.003	Nitrate (as N)	<0.25 P	0.000
Manganese (Mn)	0.010	0.000	Fluoride (F)	2.140	0.113
Silica (SiO2)	8.900		Orthophosphate (OPO4)	<0.25	0.000
Total Cations		16.956	Total Anions		15.312

Trace Element Results (g/L)

Aluminum (Al):	<50	Cesium (Cs):	NR	Molybdenum (Mo):	<10	Strontium (Sr):	243.000
Antimony (Sb):	<10	Chromium (Cr):	<10	Nickel (Ni):	<2	Thallium (Tl):	<20
Arsenic (As):	<5	Cobalt (Co):	<2	Niobium (Nb):	NR	Thorium (Th):	NR
Barium (Ba):	252.000	Copper (Cu):	<5	Neodymium (Nd):	NR	Tin (Sn):	NR
Beryllium (Be):	<2	Gallium (Ga):	NR	Palladium (Pd):	NR	Titanium (Ti):	<1
Boron (B):	126.000	Lanthanum (La):	NR	Praseodymium (Pr):	NR	Tungsten (W):	NR
Bromide (Br):	487.000	Lead (Pb):	<10	Rubidium (Rb):	NR	Uranium (U):	<3
Cadmium (Cd):	<1	Lithium (Li):	10.800	Silver (Ag):	<5	Vanadium (V):	<10
Cerium (Ce):	NR	Mercury (Hg):	NR	Selenium (Se):	<5	Zinc (Zn):	67.800
						Zirconium (Zr):	<2

Field Chemistry and Other Analytical Results

**Total Dissolved Solids (mg/L):	869.970	Field Hardness as CaCO3 (mg/L):	NR	Ammonia (mg/L):	NR
**Sum of Diss. Constituents (mg/L):	1,265.230	Hardness as CaCO3:	23.390	T.P. Hydrocarbons (g/L):	NR
Field Conductivity (mhos):	1470	Field Alkalinity as CaCO3 (mg/L):	NR	PCP (g/L):	NR
Lab Conductivity (mhos):	1439	Akalinity as CaCO3 (mg/L):	638.91	Phosphate, TD (mg/L as P):	0.055
Field pH:	8.05	Ryznar Stability Index:	7.660	Field Nitrate (mg/L):	0.000
Lab pH:	8.13	Sodium Adsorption Ratio:	33.922	Field Dissolved O2 (mg/L):	NR
Water Temp (°C):	11.1	Langlier Saturation Index:	0.235	Field Chloride (mg/L):	NR
Air Temp (°C):	12	Nitrite (mg/L as N):	NR	Field Redox (mV):	NR
		Hydroxide (mg/L as OH):	NR		

Notes

Sample Condition: CLEAR

Field Remarks:

Lab Remarks:

Explanation: **mg/L** = milligrams per Liter; **g/L** = micrograms per Liter; **ft** = feet; **NR** = No Reading in GWIC

Qualifiers: **A** = Hydride atomic absorption; **E** = Estimated due to interference; **H** = Exceeded holding time; **K** = Na+K combined; **N** = Spiked sample recovery not within control limits; **P** = Preserved sample; **S** = Method of standard additions; * = Duplicate analysis not within control limits; ** = Sum of Dissolved Constituents is the sum of major cations (Na, Ca, K, Mg, Mn, Fe) and anions (HCO3, CO3, SO4, Cl, SiO2, NO3, F) in mg/L. Total Dissolved Solids is reported as equivalent weight of evaporation residue.

Disclaimer

These data represent the contents of the GWIC databases at the Montana Bureau of Mines and Geology at the time and date of the retrieval. The information is considered unpublished and is subject to correction and review on a daily basis. The Bureau warrants the accurate transmission of the data to the original end user. Retransmission of the data to other users is discouraged and the Bureau claims no responsibility if the material is retransmitted.

APPENDIX

APPENDIX A: Statement of Tasks Performed*

- Task 1 Membrane-Enhanced CBM to Minimize Produced Water
- Subtask 1.1: Perform membrane study to determine the mass transfer characteristics of various gas permeable membranes.
 - Subtask 1.2: Perform lysimeter study to determine the rate of methane transport in coal as facilitated by carbon dioxide (CO₂) injection.
 - Subtask 1.3: Develop a model to evaluate the feasibility of the membrane enhanced coal bed methane approach.
- Task 2 Electrodialysis Treatment of Produced Water
- Subtask 2.1: Select candidate sites or settings and the targeted beneficial end use for the produced water treatment in consultation with the DOE project manager.
 - Subtask 2.2: Characterize the produced water of up to three candidate production field sites or “settings” (oil & grease, TOC, volatile acids, and inorganic salts).
 - Subtask 2.3: Construct a laboratory scale processing train including de-oiling, filtration, process train that includes de-oiling, filtration, electrodialysis and reversible sorbents for purposes of treatability testing of produced water samples collected from candidate “settings.”
 - Subtask 2.4: Conduct tests in semi-batch mode on the laboratory process train using synthetic and actual produced water streams that represent the candidate settings.
 - Subtask 2.5: Determine the performance of each unit process and the potential for improved operation. Determine the technical feasibility of the treatment train to economically achieve treatment criteria for the targeted beneficial end uses. Develop a preliminary plan for follow-on piloting of the electrodialysis system.
- Task 3 Isotopic Evaluation of CBM-Produced Waters
- Subtask 3.1: Monitor Sr isotopic composition of CBM-produced water at Beaver Creek and Coal Creek in the Powder River Basin to determine variations between coal seams and spatially across the basin. Sr isotopic monitoring of infiltration and dispersion of produced water into the shallow subsurface.
 - Subtask 3.2: Characterize water-rock interactions involving Sr along flow path using instrumented field sites and laboratory studies.
 - Subtask 3.3: Document changes in Sr isotopic composition of produced water along flow path using data from the Beaver Creek and Coal Creek monitoring sites. To increase geographic coverage, conduct Sr isotopic studies at two new sites in Montana, near Moorhead and Birney, respectively. Conduct laboratory studies in which produced water is tumbled with alluvial and Wasatch samples collected from each study site to relate changes in Sr isotopic ratio to specific exchange or dissolution reactions. Conduct step-wise leaching experiments to identify the reactions taking place.

* Administrative tasks have not been included.

- Task 4 Reservoir Geomechanics and the Effectiveness of Wellbore Completion Methods in Coalbed Methane Wells in the Powder River Basin
- Subtask 4.1: Synthesize data regarding inadvertent hydraulic fracturing during wellbore completion and its effect on water production and gas production. Analyze data to develop a comprehensive database, a set of maps and correlations between topography, geology, depth, coals seams, etc. that lead to development of appropriate completion methods.
 - Subtask 4.2: Acquire data from operating companies with interest in the project and state and federal data bases. Compile measurements of S_{hmin} in both the coal seams and overlaying shales to predict vertical growth of hydrofracs which could possibly allow the communication between sand layers and the coal seams. Collect coal pore pressure data; data from coals south of Gillette indicate significant under pressure.
 - Subtask 4.3: Determine geologic factors controlling horizontal and vertical hydraulic fracture growth.
 - Subtask 4.4: Develop best practices guidelines to assure optimal gas production with minimal water production.
- Task 5 Evaluating the Use of Produced Water Generated During Coal Bed Methane Extraction for Land Application in the Powder River Basin
- Subtask 5.1: Collect soil samples from treatment plots to establish baseline chemistry and to determine treatment rates for gypsum and elemental sulfur. Evaluate chemistry of produced water to establish treatment rates for bicarbonate removal and gypsum injection. Install wick lysimeters in irrigation and soil treatment areas to support characterization of drainage water and determination of leaching fraction.
 - Subtask 5.2: Install of additional wick lysimeters (Gee passive capillary lysimeter) and shallow monitoring wells. Apply gypsum and elemental sulfur treatments to treatment plots. Apply irrigation to the site throughout the growing season.
 - Subtask 5.3: Conduct soil amendment applications, water treatment activities and irrigation activities. Collect soils samples for chemical and physical properties both midway and at the end of the irrigation season. Analyze soil samples for pH, EC, major cations, major anions, and SAR. Analyze soil hydraulic properties by tension infiltrometer. Analyze produce water chemistry month throughout the irrigation season to evaluate treatment rates. Analyze drainage water chemistry from wick lysimeters.
 - Subtask 5.4: Monitor soil chemical and physical properties during ongoing irrigation activities. Monitor the chemistry of produced water throughout the irrigation season to evaluate treatment rates. Develop geochemical modeling to characterize chemistry of soils by treatment. Use HYDRUS 1D model to estimate solute transport into alluvial aquifer.
 - Subtask 5.5: Complete geochemical modeling to characterize the chemistry of soils by treatment. Use data collected from the field site to calibrate the geochemical model. Use the UNSATCHM and/or HYDRUS models to estimate solute transport below the plant root zone into alluvial aquifer.

- Task 6 Regional Siting Criteria for CBM Infiltration Ponds
- Subtask 6.1: Verify and improve methods to streamline assessments of proposed infiltration pond sites in the Powder River Basin. Use preliminary site-assessment methods that include saturated paste extracts and computer modeling. Verify and improve predictive methods by comparison to longer-term field investigations. Use existing study sites (15 in Montana and 3 in Wyoming) to provide core data. Identify and add additional sites as needed to provide additional solid phase samples. Collect water-quality samples twice per year at selected sites in discharge areas, down gradient wells and surface water sites.
 - Subtask 6.2: Evaluate concepts for sequestering sodium and controlling salt migration from infiltration ponds using site data from Task 1 and the MODFLOW and PHREEQEC1 computer models. Analyze Leonardite, used as a sodic-soil amendment, as a potential pond-based sequestration medium at the laboratory scale using leach columns.
 - Subtask 6.3: Test several remote-sensing techniques for potential use in mapping areas where infiltration ponds might be likely to cause serious water-quality damage. Analyze the results using site data from Task 1 and the MODFLOW and PHREEQEC1 computer models.
 - Subtask 6.4: Use multispectral imaging, cross-referenced to field mapping to identify candidate areas for infiltration ponds. Evaluate application of multispectral analysis of Powder River Basin.
- Task 7 Controls on the Fate of CBM Co-Produced Waters and Impacts to Shallow Aquifer Groundwater Quality
- Subtask 7.1: Evaluate and quantify the factors controlling the exchange of CBM discharge and shallow groundwater. Compare infiltration capacity from field measurements with values from water budget analyses. Conduct slug and pump tests at monitoring wells to characterize streambed hydraulic conductivity. Continue watershed monitoring. Conduct sampling and testing of pond sediments to evaluate the effects of silting on long-term infiltration rates.
 - Subtask 7.2: Calibrate numerical models of groundwater flow (and chemical transport) and surface runoff at the local (km) scale using field observations. Analyze hydrologic data to determine both time-averaged and time series of water budgets. Develop a 3-dimensional model of groundwater flow. Calibrate models using infiltration data and history matching of water levels in monitoring wells and by field monitoring of stream-flow. Use models to project runoff and infiltration in (a) undeveloped watersheds and (b) for additional development scenarios in a given watershed. Use models for water management while minimizing aquifer impacts.
 - Subtask 7.3: Develop viable proxies and evaluation tools (numerical models) from well-documented case study(ies), which will be transferable to other regions and ultimately to a basin-wide scale. Undertake numerical modeling of surface water-groundwater flow to calibrate models and test viability of proxies for infiltration. Undertake coupled fluid flow-solute transport modeling to integrate geochemical tracer data (Sr isotopic data) with physical hydrologic data.

- Task 8 Field Laboratory and Standard Method of Testing Performance of Water Quality Treatment Systems
- Subtask 8.1: Design a small office-style trailer to house testing equipment. Include in the design needed plumbing, data logger sensors sampling ports and a computer system. Locate the testing equipment between the water supply well and the treatment unit being tested. Include as monitoring parameters: flow from source, clean treated flow, waste stream flow, specific conductance and temperature in and out of treatment system and energy consumption by treatment system. Monitor on a time and volumetric basis. Collect water quality samples from inflow, outflow and the waste stream.
 - Subtask 8.2: Deploy the testing equipment to selected test site(s).
 - Subtask 8.3: Once the testing equipment is on site, test up to three treatment systems.
- Task 9 Water Treatment by Injection
- Subtask 9.1: Identify potential zones for disposal in the Tongue River Member of the Fort Union Formation (above the Lebo Shale Member), particularly in thick porous and permeable channel sandstone units and in the immediate area of CBM developments with high SAR produced water. Apply techniques developed during a previous DOE-funded research project that successfully identified, correlated and mapped channel sandstones in the Tongue River Member of the Fort Union Formation in the area of the Northern Cheyenne Reservation of eastern Montana. Include:
 - Subsurface correlation of Tongue River Member channel sandstones and coal beds, using available well logs from oil and gas exploration wells.
 - Isopach mapping of channel sandstones to determine trends and paleo-drainage patterns.
 - Known fault zones from published geologic maps.
 - Fracture system map from interpretation of ASTER satellite imagery.
 - Identification of potential water injection sites based on presence of thick porous sandstones and other potential zones such as deep coal beds not subject to CBM development, the likely occurrence of natural fractures and proximity to CBM development.
 - Subtask 9.2: Identify areas where permeability may be naturally enhanced in regional fracture systems.
 - Subtask 9.3: Develop an engineering method to separate the water and gas streams down-hole, followed by injection into appropriate permeable zones. Alternatively, develop a method of disposal of larger volumes of water into a separate injection well in zones that are most likely water saturated above the Lebo Shale Member. Attempt to overcome the complication of using water-saturated injection zones by using multiple zones for injection. For well bores dedicated to water re-injection:
 - Develop injector-well plans based on volume and pressure requirements.
 - Determine required completion efficiency programs to achieve required injection rates (i.e. perforation design, stimulation design, etc.)
 - Design a monitoring and control system to meter the volumes of water

injected down-hole and to prevent exceeding the hydraulic fracture gradients.

- Design surface equipment for handling, treating, and pressurizing various volumes of water for injection.

For well bores designed for CBM production and water re-injection:

- Research mechanisms and feasibility of existing down-hole gas-water separation equipment.
- If down-hole gas-water separation is feasible, research methods for down-hole pressurization of the water for re-injection into zones hydraulically isolated from the CBM-producing intervals.
- Develop an economic feasibility study for down-hole separation and re-injection, consistent with CBM development plans.

Task 10 Regulations/Technology Consistency (Argonne National Laboratory)

- Subtask 10.1: Inform and advise the rest of the project team regarding the produced water regulatory requirements in effect at the start of the project and the directions in which water policy is moving throughout the duration of the project. Provide an initial briefing with the technology developers as well as periodic written or oral updates as regulatory requirements evolve.
- Subtask 10.2: Interact with state and federal agencies that are likely to establish additional water management controls to keep them informed of the technology developments made by the other project team members and to watch for potential regulatory barriers. Maintain up-to-date expertise through regular review of state and EPA water regulations, periodic contacts with key agency officials and participation in national and international water quality and produced water management conferences and workshops.

National Energy Technology Laboratory

626 Cochrans Mill Road
P.O. Box 10940
Pittsburgh, PA 15236-0940

3610 Collins Ferry Road
P.O. Box 880
Morgantown, WV 26507-0880

One West Third Street, Suite 1400
Tulsa, OK 74103-3519

1450 Queen Avenue SW
Albany, OR 97321-2198

539 Duckering Bldg./UAF Campus
P.O. Box 750172
Fairbanks, AK 99775-0172

Visit the NETL website at:
www.netl.doe.gov

Customer Service:
1-800-553-7681

